NASA Conference Publication 2355

Landsat-4 Science Characterization Early Results

Volume II—Thematic Mapper (TM), Part 1

John L. Barker, *Editor*
NASA Goddard Space Flight Center
Greenbelt, Maryland

Proceedings of the Landsat-4 Science Characterization
Early Results Symposium, February 22–24, 1983
held at NASA Goddard Space Flight Center
Greenbelt, Maryland

NASA
**National Aeronautics
and Space Administration**

**Scientific and Technical
Information Branch**

1985

LANDSAT-4 SCIENCE CHARACTERIZATION EARLY RESULTS

CONTENTS

Volume I: MULTISPECTRAL SCANNER

Page

FOREWORD iii

SUMMARY OF MSS CHARACTERIZATION INVESTIGATIONS
William L. Alford and Marc L. Imhoff
NASA/Goddard Space Flight Center I-1

RADIOMETRIC ACCURACY ASSESSMENT OF LANDSAT-4 MULTISPECTRAL SCANNER DATA
William L. Alford and Marc L. Imhoff
NASA/Goddard Space Flight Center I-9

SPECTRAL CHARACTERIZATION OF THE LANDSAT-4 MSS SENSORS
Brian L. Markham and John L. Barker
NASA/Goddard Space Flight Center I-23

INVESTIGATION OF RADIOMETRIC PROPERTIES OF LANDSAT-4 MSS
Daniel P. Rice and William A. Malila
Environmental Research Institute of Michigan I-57

RADIOMETRIC CALIBRATION AND GEOCODED PRECISION PROCESSING OF LANDSAT-4 MULTISPECTRAL SCANNER PRODUCTS BY THE CANADA CENTRE FOR REMOTE SENSING
J. Murphy, D. Bennett and F. Guertin
Canada Centre for Remote Sensing I-77

LANDSAT SCENE-TO-SCENE REGISTRATION ACCURACY ASSESSMENT
James E. Anderson
NASA/National Space Technology Laboratories I-119

GEOMETRIC ACCURACY OF LANDSAT-4 MSS IMAGE DATA
R. Welch and E. Lynn Usery
University of Georgia I-123

GEODETIC ACCURACY OF LANDSAT-4 MULTISPECTRAL SCANNER AND THEMATIC MAPPER DATA
J. M. Thormodsgard and D. J. DeVries
U.S. Geological Survey, EROS Data Center I-133

GEOMETRIC ACCURACY ASSESSMENT OF LANDSAT-4 MULTISPECTRAL SCANNER (MSS) DATA
Marc L. Imhoff and William L. Alford
NASA/Goddard Space Flight Center I-143

IMPACT OF LANDSAT MSS SENSOR DIFFERENCES ON CHANGE DETECTION ANALYSIS
William C. Likens and Robert C. Wrigley
NASA/Ames Research Center I-159

PRECEDING PAGE BLANK NOT FILMED

CONTENTS (Continued)

Page

LANDSAT-4 MSS GEOMETRIC CORRECTION: METHODS AND RESULTS
J. Brooks, E. Kimmer and J. Su
General Electric Company I-177

INDEX OF AUTHORS I-201

Volume II: THEMATIC MAPPER

INTRODUCTION TO THEMATIC MAPPER INVESTIGATIONS
John L. Barker and Brian L. Markham
NASA/Goddard Space Flight Center II-1

AN OVERVIEW OF LANDSAT-4 AND THE THEMATIC MAPPER
James R. Irons
NASA/Goddard Space Flight Center II-15

RADIOMETRIC CALIBRATION AND PROCESSING PROCEDURE FOR REFLECTIVE BANDS ON LANDSAT-4 PROTOFLIGHT THEMATIC MAPPER
John L. Barker
NASA/Goddard Space Flight Center

R. B. Abrams, D. L. Ball and K. C. Leung
Computer Sciences Corporation II-47

AN OVERVIEW OF THE THEMATIC MAPPER GEOMETRIC CORRECTION SYSTEM
Eric P. Beyer
General Electric Company II-87

TM DIGITAL IMAGE PRODUCTS FOR APPLICATIONS
John L. Barker
NASA/Goddard Space Flight Center

Fred J. Gunther, Rochelle B. Abrams and Dave Ball
Computer Sciences Corporation II-147

CANADIAN PLANS FOR THEMATIC MAPPER DATA
W. M. Strome, F. E. Guertin, A. B. Collins and D. G. Goodenough
Canada Centre for Remote Sensing II-221

SPECTRAL CHARACTERIZATION OF THE LANDSAT THEMATIC MAPPER SENSORS
Brian L. Markham and John L. Barker
NASA/Goddard Space Flight Center II-235

PRELAUNCH ABSOLUTE RADIOMETRIC CALIBRATION OF THE REFLECTIVE BANDS ON THE LANDSAT-4 PROTOFLIGHT THEMATIC MAPPER
John L. Barker
NASA/Goddard Space Flight Center

D. L. Ball and K. C. Leung
Computer Sciences Corporation

J. A. Walker
Santa Barbara Research Center II-277

CONTENTS (Continued)

Page

CHARACTERIZATION OF RADIOMETRIC CALIBRATION OF LANDSAT-4 THEMATIC MAPPER REFLECTIVE BANDS
John L. Barker
NASA/Goddard Space Flight Center

R. B. Abrams, D. L. Ball and K. C. Leung
Computer Sciences Corporation II-373

INDEX OF AUTHORS II-475

VOLUME III: THEMATIC MAPPER (Continued)

RELATIVE RADIOMETRIC CALIBRATION OF LANDSAT TM REFLECTIVE BANDS
John L. Barker
NASA/Goddard Space Flight Center III-1

EVALUATION OF THE RADIOMETRIC INTEGRITY OF LANDSAT-4 THEMATIC MAPPER BAND 6 DATA
John R. Schott
Rochester Institute of Technology III-221

THERMAL BAND CHARACTERIZATION OF THE LANDSAT-4 THEMATIC MAPPER
Jack C. Lansing
Santa Barbara Research Center

John L. Barker
NASA/Goddard Space Flight Center III-233

A PRELIMINARY ASSESSMENT OF LANDSAT-4 THEMATIC MAPPER DATA
D. G. Goodenough, E. A. Fleming and K. Dickinson
Department of Energy, Mines and Resources, Canada III-257

PRELIMINARY EVALUATION OF THE RADIOMETRIC CALIBRATION OF LANDSAT-4 THEMATIC MAPPER DATA BY THE CANADA CENTRE FOR REMOTE SENSING
J. Murphy, W. Park and A. Fitzgerald
Canada Centre for Remote Sensing III-275

A PRELIMINARY ANALYSIS OF LANDSAT-4 THEMATIC MAPPER RADIOMETRIC PERFORMANCE
C. Justice and L. Fusco
European Space Agency/EPO, Frascati, Italy

W. Mehl
Commission of the European Communities/JRC, Ispra, Italy III-309

EVALUATION OF THE RADIOMETRIC QUALITY OF THE TM DATA USING CLUSTERING, LINEAR TRANSFORMATIONS AND MULTISPECTRAL DISTANCE MEASURES
L. A. Bartolucci, M. E. Dean and P. E. Anuta
Purdue University III-321

CONTENTS (Continued)

Page

TM GEOMETRIC PERFORMANCE: LINE-TO-LINE DISPLACEMENT ANALYSIS (LLDA)
L. Fusco
European Space Agency/EPO, Frascati, Italy

W. Mehl
Commission of the European Communities/JRC, Ispra, Italy III-359

IN-PROGRESS ABSOLUTE RADIOMETRIC INFLIGHT CALIBRATION OF THE LANDSAT-4 SENSORS
R. G. Holm, K. R. Castle, C. J. Kastner, J. M. Palmer and P. N. Slater
University of Arizona

M. Dinguirard
Centre d'Etudes et de Recherches de Toulouse

C. E. Ezra and R. D. Jackson
USDA/Agricultural Research Service

R. Savage
Atmospheric Sciences Laboratory, White Sands Missile Range III-389

LANDSAT-4 THEMATIC MAPPER CALIBRATION AND ATMOSPHERIC CORRECTION
Warren A. Hovis
NOAA/National Environmental Satellite, Data,
and Information Service III-411

SCAN ANGLE AND DETECTOR EFFECTS IN THEMATIC MAPPER RADIOMETRY
Michael D. Metzler and William A. Malila
Environmental Research Institute of Michigan III-421

THEMATIC MAPPER SPECTRAL DIMENSIONALITY AND DATA STRUCTURE
E. P. Crist and R. C. Cicone
Environmental Research Institute of Michigan III-443

MTF ANALYSIS OF LANDSAT-4 THEMATIC MAPPER
Robert Schowengerdt
University of Arizona III-467

INTRABAND RADIOMETRIC PERFORMANCE OF THE LANDSAT-4 THEMATIC MAPPER
Hugh H. Kieffer, Eric M. Eliason and Pat S. Chavez, Jr.
U.S. Geological Survey III-471

A PRELIMINARY EVALUATION OF LANDSAT-4 THEMATIC MAPPER DATA FOR THEIR GEOMETRIC AND RADIOMETRIC ACCURACIES
M. H. Podwysocki, N. Falcone, L. U. Bender and O. D. Jones
U.S. Geological Survey III-497

THE USE OF LINEAR FEATURE DETECTION TO INVESTIGATE THEMATIC MAPPER DATA PERFORMANCE AND PROCESSING
Charlotte M. Gurney
Systems and Applied Sciences Corporation III-513

CONTENTS (Continued)

Page

SPATIAL RESOLUTION ESTIMATION OF LANDSAT-4 THEMATIC MAPPER DATA
Clare D. McGillem, Paul E. Anuta and Erick Malaret
Purdue University III-527

AN ANALYSIS OF THE HIGH FREQUENCY VIBRATIONS IN EARLY THEMATIC MAPPER SCENES
John Kogut and Eliane Larduinat
Research and Data Systems, Inc. III-537

ASSESSMENT OF THEMATIC MAPPER BAND-TO-BAND REGISTRATION BY THE BLOCK CORRELATION METHOD
Don H. Card and Robert C. Wrigley
NASA/Ames Research Center

Frederick C. Mertz and Jeff R. Hall
Technicolor Government Services, Inc. III-553

TESTS OF LOW-FREQUENCY GEOMETRIC DISTORTIONS IN LANDSAT-4 IMAGES
R. M. Batson and W. T. Borgeson
U.S. Geological Survey III-565

INVESTIGATION OF TM BAND-TO-BAND REGISTRATION USING THE JSC REGISTRATION PROCESSOR
S. S. Yao and M. L. Amis
Lockheed Engineering and Management Service Company, Inc. III-571

GEODETIC ACCURACY OF LANDSAT-4 MULTISPECTRAL SCANNER AND THEMATIC MAPPER DATA
J. M. Thormodsgard and D. J. DeVries
U.S. Geological Survey, EROS Data Center III-581

INDEX OF AUTHORS III-591

Volume IV: APPLICATIONS

OVERVIEW OF TM "APPLICATIONS" RESEARCH REPORTS
Darrel L. Williams
NASA/Goddard Space Flight Center IV-1

IMPACT OF THEMATIC MAPPER SENSOR CHARACTERISTICS ON CLASSIFICATION ACCURACY
Darrel L. Williams, James R. Irons, Brian L. Markham, Ross F. Nelson and David L. Toll
NASA/Goddard Space Flight Center

Richard S. Latty
University of Maryland

Mark L. Stauffer
Computer Sciences Corporation IV-7

CONTENTS (Continued)

Page

ANALYSIS AND EVALUATION OF THE LANDSAT-4 MSS AND TM SENSORS AND GROUND DATA PROCESSING SYSTEMS -- EARLY RESULTS
Ralph Bernstein and Jeffrey B. Lotspiech
IBM Palo Alto Scientific Center IV-25

CHARACTERIZATION OF LANDSAT-4 TM AND MSS IMAGE QUALITY FOR THE INTERPRETATION OF CALIFORNIA'S AGRICULTURAL RESOURCES
Stephen D. DeGloria and Robert N. Colwell
University of California, Berkeley IV-91

EVALUATION OF THEMATIC MAPPER PERFORMANCE AS APPLIED TO HYDROCARBON EXPLORATION
John R. Everett, Charles Sheffield and Jon Dykstra
Earth Satellite Corporation IV-119

GEOLOGIC UTILITY OF LANDSAT-4 TM DATA
Michael Abrams, Anne Kahle, Alan Gillespie, James Conel and Harold Lang
Jet Propulsion Laboratory IV-127

AN INITIAL ANALYSIS OF LANDSAT-4 THEMATIC MAPPER DATA FOR THE DISCRIMINATION OF AGRICULTURAL, FORESTED WETLANDS, AND URBAN LAND COVERS
Dale A. Quattrochi
NASA/National Space Technology Laboratories IV-131

PRELIMINARY EVALUATION OF THEMATIC MAPPER IMAGE DATA QUALITY
R. B. MacDonald, F. G. Hall, D. E. Pitts and R. M. Bizzell
NASA/Johnson Space Center

S. Yao, C. Sorensen, E. Reyna and J. Carnes
Lockheed Engineering and Management Services Company, Inc. IV-153

ASSESSMENT OF COMPUTER-BASED GEOLOGIC MAPPING OF ROCK UNITS IN THE LANDSAT-4 SCENE OF NORTHERN DEATH VALLEY, CALIFORNIA
Nicholas M. Short
NASA/Goddard Space Flight Center IV-163

A CONCEPT FOR THE PROCESSING AND DISPLAY OF THEMATIC MAPPER DATA
Rupert Haydn
University of Munich IV-217

QUICK LOOK ANALYSIS OF TM DATA OF THE WASHINGTON, D.C. AREA
Darrel L. Williams, James R. Irons, Brian L. Markham, Ross F. Nelson and David L. Toll
NASA/Goddard Space Flight Center

Richard S. Latty
University of Maryland

Mark L. Stauffer
Computer Sciences Corporation IV-237

CONTENTS (Continued)

Page

REMOTE SENSING OF COASTAL WETLANDS BIOMASS USING THEMATIC MAPPER WAVEBANDS
Michael A. Hardisky and Vytautas Klemas
University of Delaware IV-251

A PRELIMINARY COMPARISON OF THE INFORMATION CONTENT OF DATA FROM THE LANDSAT-4 THEMATIC MAPPER AND MULTISPECTRAL SCANNER
John C. Price
USDA/Agricultural Research Service Hydrology Laboratory IV-271

EARLY RESULTS OF INVESTIGATIONS OF LANDSAT-4 THEMATIC MAPPER AND MULTISPECTRAL SCANNER APPLICATIONS
F. G. Sadowski, J. A. Sturdevant, W. H. Anderson, P. M. Seevers,
J. W. Feuquay, L. K. Balick and F. A. Waltz
Technicolor Government Services, Inc.

D. T. Lauer
U.S. Geological Survey, EROS Data Center IV-281

THEMATIC MAPPER DATA QUALITY AND PERFORMANCE ASSESSMENT IN RENEWABLE RESOURCES/AGRICULTURE/REMOTE SENSING
R. M. Bizzell and H. L. Prior
NASA/Johnson Space Center IV-299

PRELIMINARY COMPARISONS OF THE INFORMATION CONTENT AND UTILITY OF TM VERSUS MSS DATA
Brian L. Markham
NASA/Goddard Space Flight Center IV-313

ASSESSING LANDSAT TM AND MSS DATA FOR DETECTING SUBMERGED PLANT COMMUNITIES
Steven G. Ackleson and Vytautas Klemas
University of Delaware IV-325

A FIRST EVALUATION OF LANDSAT TM DATA TO MONITOR SUSPENDED SEDIMENTS IN LAKES
F. R. Schiebe, J. C. Ritchie and G. O. Boatwright
USDA/Agricultural Research Service IV-337

SNOW REFLECTANCE FROM THEMATIC MAPPER
Jeff Dozier
University of California, Santa Barbara IV-349

PRELIMINARY EVALUATION OF TM FOR SOILS INFORMATION
David R. Thompson, Keith E. Henderson, A. Glen Houston and
David E. Pitts
NASA/Johnson Space Center IV-359

CONTENTS (Continued)

Page

THE USE OF THEMATIC MAPPER DATA FOR LAND COVER DISCRIMINATION - PRELIMINARY RESULTS FROM THE UK SATMAP PROGRAMME
M. J. Jackson and J. R. Baker
Natural Environment Research Council, UK

J. R. G. Townshend, J. E. Gayler and J. R. Hardy
Reading University, UK IV-369

PRELIMINARY STUDY OF INFORMATION EXTRACTION OF LANDSAT TM DATA FOR A SUBURBAN/REGIONAL TEST SITE
David L. Toll
NASA/Goddard Space Flight Center IV-387

COMPARATIVE TECHNIQUES USED TO EVALUATE THEMATIC MAPPER DATA FOR LAND COVER CLASSIFICATION IN LOGAN COUNTY, WEST VIRGINIA
J. O. Brumfield
Marshall University

R. G. Witt and H. W. Blodget
NASA/Goddard Space Flight Center

R. F. Marcell
Computer Sciences Corporation IV-403

COMPARISON OF MSS AND TM DATA FOR LANDCOVER CLASSIFICATION IN THE CHESAPEAKE BAY AREA - A PRELIMINARY REPORT
P. J. Mulligan and J. C. Gervin
NASA/Goddard Space Flight Center

Y. C. Lu
Computer Sciences Corporation IV-415

COMPARISON OF LAND COVER INFORMATION FROM LANDSAT MULTISPECTRAL SCANNER (MSS) AND AIRBORNE THEMATIC MAPPER SIMULATOR (TMS) DATA FOR HYDROLOGIC APPLICATIONS
J. C. Gervin
NASA/Goddard Space Flight Center

Y. C. Lu and R. F. Marcell
Computer Sciences Corporation IV-421

RELATIVE ACCURACY ASSESSMENT OF LANDSAT-4 MSS AND TM DATA FOR LEVEL I LAND COVER INVENTORY
E. M. Middleton and R. G. Witt
NASA/Goddard Space Flight Center

Y. C. Lu and R. S. Sekhon
Computer Sciences Corporation IV-431

INDEX OF AUTHORS IV-447

omit to
p II-15

INTRODUCTION TO THEMATIC MAPPER INVESTIGATIONS

SECTION I: RADIOMETRY
John L. Barker
NASA/Goddard Space Flight Center

SECTION II: GEOMETRY
Brian L. Markham
NASA/Goddard Space Flight Center

SECTION I: RADIOMETRY

This section of the Introduction to Thematic Mapper (TM) Investigations is an overview of papers which deal with radiometric characterization of the TM sensor. Spectral characteristics are summarized in the paper by Markham and Barker. Papers dealing primarily with geometric characteristics of TM are overviewed in Section 2 of this introduction by Brian Markham.

References in this introduction will be in one of four forms:

- P:Author (Example: P:Bernstein)
  "P" refers to a paper in one of the two TM volumes in these February, 1983 Proceedings, and the name of the author is the first author. If there is more than one paper by the same first author, the name of the second author will also be included.

- S:Author, p (Example: S:Barker, Ball et al., Vol. I, 130-139)
  "S" refers to a summary in one of the two volumes of abstracts in NASA Conference Publication 2326 (1984) entitled "Landsat-4 Science Investigations Summary including December 1983 Workshop Results." The page location in the publication is given by "p". In almost all cases there will be a reference to either the summary or to the papers in the proceedings, but not to both.

- I:Author (Example: I:Malila)
  "I" refers to one of the papers in the May, 1984 issue of IEEE Transactions on Geoscience and Remote Sensing entitled "Special Issue on Landsat-4." The table of contents of this issue is given at the end of this report.

- Author, Year (Example: Engel, 1980)
  References to other papers are given by first author and year of publication, with the complete citation being at the end of this report. There is no intention to provide more than a few such references to other papers since this is a report on the radiometric and geometric activities of the Landsat Image Data Quality Assessment (LIDQA) investigators (Table 1).

For most users, the primary scientific requirement is to convert digital numbers (DN) on computer compatible tapes (CCT) to radiance or spectral radiance units. Minimum and maximum spectral radiances for the six reflective bands are given for radiometrically calibrated tapes for two periods of time:

Scrounge-Era prior to August 1983 (S:Barker and Ball, Vol. I, 130-139, Table 3)

TIPS-Era after 15 January 1984 (S:Barker, Vol. I, 140-180, Table 1; and P:Barker, Appendix 9.1).

For both the reflective bands and the emissive thermal band, TM6, the actual dynamic range used in calibrating the digital imagery is contained in one of the fields of the CCT. For perfectly calibrated noise-free data, these post-calibration dynamic ranges are all the radiometric information needed.

Investigations reported here, and still in progress, are characterizing and monitoring the radiometric performance of the TM sensor on both Landsat-4 (TM/PF) and on Landsat-5 (TM/F). These efforts include pre-launch calibration and in-orbit calibration of sensors. There has not yet been an opportunity to characterize the performance or optimize the parameters used in the radiometric ground processing of TM imagery. This section is divided into three topics: characterizing pre-launch sensor performance, characterizing in-orbit sensor performance, and characterizing calibrated digital image data quality.

Pre-Launch Sensor Performance

Summary charts on the TM sensor description and characteristics are given here (S:Engel, Vol. 1, 41-61) and in a previous paper (Engel and Weinstein, 1983). Details of the absolute radiometric calibration using an integrating sphere are given for Landsat-4 TM/PF (P:Barker and Ball) along with summary results on gains and offsets for Landsat-5 TM/PF (P:Barker, Appendices 9.3 and 9.4). Many special tests were performed before launch, especially on Landsat-5 TM/F, and tapes from these tests provide an option for future re-calibration based on a knowledge of how to reduce certain systematic sources of variability that were not characterized until after launch. Re-calibration of the integrating sphere may also result in a further updating of the post-calibration dynamic range in the parameter file of the TM Image Processing System (TIPS). Independent measurement of absolute radiometric calibration is being attempted by comparing in-orbit imagery with simultaneous

TABLE 1. LANDSAT SCIENTIFIC CHARACTERIZATION - LIDQA INVESTIGATORS

University (U.S.)	Private Industry	Government Agencies	Outside U.S.
Anuta (Purdue/LARS)	Bernstein (IBM)	Anderson (NASA/ERL)	Begni (France)
Colwell (California/Berkley)	Everett (EARTHSAT)	Bender (USGS/Reston)	Fusco (ESA)
Dozier (California/Santa Barbara)	Gurney (SASC)	Erickson (NASA/JSC)	Jackson (England)
Duggin (State U. New York)	Malila (ERIM)	Hill (NASA/ERL)	Parada (Brazil)
Ford (California/Davis)	Wukelic (Battelle)	Hovis (NOAA/NESS)	Rasool (France)
Khorram (N. Carolina)		Kahle (NASA/JPL)	Strome (Canada)
Klemas (Delaware)		Kieffer (USGS/Flagstaff)	
Schott (Rochester inst. Tech.)		Lauer (USGS/EDC)	
Slater (Arizona)		MacDonald (NASA/JSC)	
Welch (Georgia)		Price (USDA/ARS)	
		Thormodsgard (USGS/EDC)	
		Wrigley (NASA/Ames)	
		Zobrist (NASA/JPL)	

observations from the ground (S:Castle, Vol. II, 15-19; S:Hovis, Vol. I, 181-185). Absolute calibration had a specified accuracy requirement of 10% of full scale in each band.

In-Orbit Sensor Performance

As part of the investigations program, several scientific teams have had access to raw uncalibrated TM digital imagery on engineering tapes, including foreign ground stations with direct access to TM transmission from Landsat. Several radiometric studies have used uncalibrated digital imagery, either CCT-BT tapes produced during the Scrounge-era or "unity" CCT-AT tapes from TIPS, in conjunction with the background shutter and internal calibration data provided either on CCT-ADDS tapes in the Scrounge-era or on CCT-CALDUMP tapes in the TIPS-era. These studies characterize the in-orbit sensor performance, prior to ground processing. Scrounge-era digital products are described (P:Barker and Gunther).

Background on radiometric procedures used in the Scrounge-era processing of the reflective bands is provided (P:Barker, Abrams; (procedure paper)). Processing of Landsat-4 data during Scrounge-era was done one scene at a time. Results for approximately fifty Landsat-4 scenes are summarized in terms of within-scene types of systematic variability and between-scene apparent changes in gain or sensitivity (S:Barker, Vol. I, 140-180, and P:Barker). Emphasis in these studies is placed on characterizing precision, or relative radiometry, rather than on absolute accuracy. The most significant types of within-scene systematic variabliy on the order of 1-2 DN, are:

- Bin-Radiance Dependence
- Scan-Corrleated Shifts
- Coherent Noise
- Bright-Target Saturation.

There may also be some variability, less than 0.5 DN, from:

- Within-Line Droop
- Forward/Reverse Scan Differences.

The following papers deal with the radiometric characterization of in-orbit TM sensor performance from raw data:

- P:Barker and Abrams, Characterization Paper
    - Stability of Internal Calibration System
    - Pre-Launch Sensor Performance (Vacuum Shift)
    - Post-Launch Sensor Performance
    - Stability with Time
    - Noise (Coherent)
    - Location of Calibration Collect Window
    - Non-Uniformity in the A/D Converter (Bin-Radiance Dependence)
    - Recommendations for Operating and Processing

- P:Lansing
  - Thermal Band Characterization
- P:Murphy
  - Raw Data from the Canada Centre fo Remote Sensing (CCRS)
  - Gains and Offsets
  - Histograms (Bin-Radiance Dependence)
  - Striping
- I:Murphy
  - Background in Shutter Region (Scan-Correlated Shift)
  - Internal Calibration Region
- P:Justice
  - Band-to-Band Correlations
- P:Metzler and I:Malila
  - Scan Angle Effects (Within-Line Droop)
  - Quantization-Level Histograms (Bin-Radiance Dependence)
  - Down-Track Trace of Scan-Line Mean Signal (Scan-Correlated Shift)
  - Correlation of Scan-Line Means
- P:Kieffer
  - Variation of Response with Scan Direction (Forward/Reverse Scan Differences)
  - Level Shift (Scan-Correlated Shift)
  - Overshoot
  - Gain Sag
  - High Frequency Noise (Coherent Noise)
- P:Barker ("R and R Paper")
  - Table of Contents, as listed in Table 2.

The characterization of possible within-line droop and foward-reverse-scan differences is currently limited by an inadequate quantification of the effects of bright target saturation (P:Barker).

It is assumed that between-scene variability of detector sensitivity or electronics will be calibrated out by adjustment in gain and offset to the raw data. One method to check the reasonableness of this assumption is to monitor the apparent change in gain, and offset, with time and if it is changing significantly, to see if that change can be accounted for by expected changes in a channel within a band, rather than a change in characteristics of the internal calibration system. Results for Landsat-4 TM/PF apparent gain changes with time are presented and analyzed in the "R and R" paper (P:Barker).

Image Data Quality

If the sensor and calibration were perfect and unaffected by geometric resampling, then a user of TM digital imagery need only acquire a calibrated and geometrically corrected CCT-PT tape and apply it directly to their information extraction requirements. That is the ideal objective for the product of ground processing. This section identifies the radiometric

TABLE 2

TABLE OF CONTENTS FOR RELATIVE RADIOMETRIC CALIBRATION OF LANDSAT TM REFLECTIVE BANDS

Section 1 - Introduction. III-9

1.1 Radiometric Characterization III-10
1.2 Post-Calibration Dynamic Range III-11
1.3 Sources of Radiometric Variability III-11
1.4 Research Objectives III-13
1.5 TM Radiometric Calibration III-14
1.6 Approach to Radiometric Characterization III-16

Section 2 - Between-Scene Changes in TM/PF Gain . . . III-19

Section 3 - Between-Band Changes in TM/PF Gain. . . . III-26

Section 4 - Within-Scene Variability in TM Radiometry. III-31

4.1 Bin-Radiance Dependence. III-32
4.2 Within-Line Droop. III-35
4.3 Bright-Target Saturation III-37
4.4 Coherent Noise III-43
4.5 Scan-Correlated Shifts III-48
4.6 Forward/Reverse-Scan Differences III-55
4.7 Total Noise. III-57
4.8 Within-Scene Error Models. III-57
4.9 Summary of Within-Scene Variability III-65

Section 5 - Processing Effects on Radiometry. III-76

5.1 Calibration with Internal Calibrator III-76

  5.1.1 Background Calculation. III-77
  5.1.2 Pulse Window Locations. III-79
  5.1.3 Pulse Integration Parameters. III-80
  5.1.4 Pulse Averaging Parameters. III-83
  5.1.5 Regression Strategy III-86
  5.1.6 Within-Scene Smoothing. III-87
  5.1.7 Within-Path Smoothing III-88
  5.1.8 Between-Date Smoothing. III-89

5.2 Image Calibration. III-89

  5.2.1 Histogram Equalization. III-89
  5.2.2 Replacement of Channels III-92
  5.2.3 Post-Calibration Dynamic Range. III-94
  5.2.4 Unbiased Pixel Calibration. III-95
  5.2.5 Geometric Resampling. III-96

TABLE 2. (Cont'd)

TABLE OF CONTENTS (Cont'd)

Section 5 (Cont'd)

5.3 Radiance-To-Reflectance Conversion III-98

- 5.3.1 Irradiance Normalization. III-98
- 5.3.2 Atmospheric Peeling III-99

5.4 Information Extraction III-103

- 5.4.1 Spectrometry. III-105
- 5.4.2 Radiometry. III-108
- 5.4.3 Geometry. III-109

Section 6 - Recommendations III-111

6.1 Engineering Characterization III-111

- 6.1.1 Absolute Radiometric Calibration. . . . III-111
- 6.1.2 Relative Radiometric Calibration. . . . III-112
- 6.1.3 Modeling of Systematic Variabilities. . III-113
- 6.1.4 TM Sensor Report. III-114

6.2 Flight Segment Operations. III-115

- 6.2.1 Changes in Operational Procedures . . . III-115
- 6.2.2 In-Orbit Calibration Tests. III-117
- 6.2.3 In-Orbit Characterization Tests III-117
- 6.2.4 In-Orbit Scientific Mission Tests . . . III-118

6.3 TIPS Ground Processing III-120

- 6.3.1 Radiometric Calibration Parameters. . . III-121
- 6.3.2 IC Systematic Radiometric Corrections . III-122
- 6.3.3 Histograms Equalization III-125
- 6.3.4 Geometric Processing. III-128
- 6.3.5 Three-Sectioned Post-Calibration Dynamic Range III-129
- 6.3.6 Image Calibration III-130
- 6.3.7 Products. III-130
- 6.3.8 Research and Development. III-134

6.4 Contingency Experiments. III-135

- 6.4.1 Scientific Experiments. III-135
- 6.4.2 Engineering Experiments III-135

Section 7 - Acknowledgments III-137

TABLE 2. (Cont'd)

TABLE OF CONTENTS (Cont'd)

Section 8 - Selected Bibliography III-139

Section 9 - Appendices. III-144

9.1 TIPS Post-Calibration Dynamic Range. III-144
9.2 Integrating Sphere Spectral Radiances. III-147
9.3 TM/F Gains III-148
9.4 TM/F Offsets III-149
9.5 TM/PF Apparant Gain Change With Time III-150
9.6 Landsat-4 Images Processed by TRAPP. III-157
9.7 TM/PF Plots of "Shifted" Background Versus Scan III-159
9.8 TM/PF Tables of Scan-Correlated Shifts III-167
9.9 TM/PF Plots of Shutter background Versus Scan III-174
9.10 TM/F Plots of "Shifted" Background Versus Scan. III-187
9.11 TM/F Tables of Scan-Correlated Shifts. III-196
9.12 Shutter Backgrounds. III-203
9.13 Recommendations. III-209
9.14 Key Words. III-215

investigations of the final CCT-PT, and more generally, its immediate pre-cursor, the radiometrically unresampled CCT-AT. Both of these tapes are available to the public. To the extent that these investigations of image data quality find the radiometry within required tolerances, there is no need to proceed backwards to determine whether or not the observed radiometric variability, or uncertainty, can be reduced by alternative ground processing procedures, or calibration, or whether it is an uncorrectable, innate characteristic of the sensor. Within the specifications of the system, it was the design objective of TIPS to produce a CCT-PT that would require no further calibration by the user. Specifications call for a post-calibration radiometric precision of ± 1 DN. In the absence of both a line-by-line calibration and an as yet undemonstrated capability for within-line removal of effects of bright-target saturation, it will not be possible to obtain the objective in all scenes. Suggestions have been made for possible correction of known sources of systematic errors.

The following papers report on the radiometric characteristics of radiometrically calibrated TM digital image products:

- P:Irons
  - TM Data Processing (During Scrounge-Era)
- P:Lyons
  - Scrounge-Era Processing
- I:Fischel
  - TM Radiometric Correction Algorithms (During Scrounge-Era)
- P:Barker and Abrams, Procedure Paper
  - Ground Processing (During Scrounge-Era)
- P:Barker and Gunther
  - TM Image Products (Format and Characteristics of Tapes)
- P:Murphy and I:Murphy
  - Radiometric Processing at CCRS
- P:Bernstein and I:Bernstein
  - Sensor Data Entropy
  - Histograms
  - A/D Converter Non-Linearity (Bin-Radiance Dependence)
  - Failed Detectors (Landsat-) and Compensation
  - Sensor Noise (32 KHz) and Reduction
  - Radiometric Correction Processing
  - Striping Removal
  - Probabilistic Calibration
- P:Bartolucci
  - Classification
  - Clustering
  - Principal Components
  - Covariance
  - Correlation Matrices
  - Water Temperature Mapping

- I:Anuta
    - Coherent Noise (3.12 and 17 pixel/cycle)
    - Scan Angle Response
    - Principal Components
    - Temperature Mapping

- P:Metzler
    - Qauntization Level Histograms (Bin-Radiance Dependence)
    - Down-Track Means (Scan-Correlated Shifts)

- P:Kieffer
    - Detector-to-Detector Variations (Striping)
    - Scan-to-Scan Variations (Banding)
    - Forward/Reverse Scan Differences
    - Level Shifts (Scan-Correlated Shifts)
    - Dynamic Response
    - Gain Sag
    - Coherent Noise
    - Between-Band Correlation

- P:Podwysocki
    - Striping.

SECTION II: GEOMETRY

The TM geometric analyses/discussions can be divided into four categories: (1) pre-launch characterization of the sensor geometry, (2) discussions of the geometrical processing algorithms, (3) post-launch characterization of the geometrical behavior of the TM instrument and (4) post-launch geometrical characterization of fully corrected (P-type) TM data. Under the first category, the geometry and geometrical measures of the TM sensor are discussed. The TM geometric correction operations and the differences between the interim TM processing system (Scrounge) and the final system (TIPS) are presented in the second section. Under the third category, the emphasis is on characterizing the magnitude of satellite vibrations (jitter) and the modulation transfer functions. In the fourth category, analyses have concentrated on evaluating band-to-band registration accuracy and the internal geometric consistency of the TM data. The referencing convention followed by Barker in the first section of this introduction will also be followed here.

Stringent specifications on the radiometric and geometric performance of the TM instrument necessitated greater complexity in the instrument than in previous MSS instruments. Key new TM geometric features include (S:Engel, Vol. I, 41-61): (1) two focal planes, one containing the silicon detectors of bands 1-4 and the second containing the cooled detectors (InSb and HgCdTe) of bands 5-7, (2) nominally 30 meter IFOV's in bands 1-5, 7 with 16 detectors per bands, (3) bi-directional cross-tracking scanning with a scan line corrector to maintain a perpendicular scan, and (4) an angular displacement sensor to record vibrations at the sensor. A summary of the pre-launch geometrical data collected on the TM instrument is presented (S:Engel, Vol I, 65-89): (1) measured instantaneous fields of view (line spread function half widths), without electronics effects, (2) focal plane step response characteristics (rise-time, overshoot, settling times), (3) square wave responses, (4) band-to-band registration, and (5) mirror scan profiles. These pre-launch measurements have been used (Schueler, 1983; Markham, 1984) to provide estimates of the line spread functions and transfer functions for the Thematic Mapper. Along-scan estimates of the line spread function half-widths were approximately 36 meters for bands 1-5, 7 and 137 meters for band 6.

The TM geometric ground processing was initially performed by the Scrounge system (P:Lyon) and transferred to the operational Thematic Mapper Image Processing System (TIPS) (P:Beyer) in the Fall of 1983. Both of these systems use spacecraft attitude, ephemeris, and mirror scan correction data transmitted from the satellite, combined with pre-launch sensor data (e.g., band-to-band spacing and detector electronic delays) to generate systematic correction data (SCD). In addition in TIPS, control point processing is being used to remove bias and drift errors in the SCD, generating Geodetic Correction Data (GCD). Then, using the GCD or SCD the data are geometrically corrected, registered to a map projection and resampled by a cubic interpolation algorithm to 28.5 by 28.5 meter pixels. The standard cubic convolution weights were used in the Scrounge resampling process until 1 April 1983. New weights, as recommended by Park, 1983 which result in a smaller overshoot near edges in images were then implemented (I:Fischel). The TIPS system will also use the revised weights.

Due to the pre-launch concern with high frequency vibrations of the spacecraft, especially due to the scan mirrors, the post-launch TM instrument geometrical analyses were concentrated on jitter. Most of the observed jitter was at 7KHz in the along-scan direction and can be easily corrected. The along-track effect of this jitter is to produce underlap or overlap between adjacent scans. Analyses conducted (S:Kogut, Vol II., 54; P:Kogut) indicated that the range of underlap and overlap was in the neighborhood of 0.7 pixels.

Several investigators are examining the spatial resolution characteristics of the TM P-data (P:Schowengerdt, P:McGillem). Although this does not correspond to the spatial resolution of the TM instrument due to resampling and atmospheric degradations, it provides an overall system measure. These analyses are concentrating on estimating the sensor Line Spread Functions (LSF), or modulation transfer functions (MTF) based on the rendition of step-like or line-like features on the Earth's surface that intersect the scan pattern at oblique angles. Early results pointed to a system resolution (LSF half-power points) of 39 meters in a Webster Co., Iowa scene (P:McGillem) which is consistent with sensor characteristics and a moderate degradation due to atmospheric and resampling effects. Later estimates indicated LSF half-widths of 39-45 meters (I:Anuta). The forward and reverse scan MTF's have also been compared as well as the MTF of the interpolation/ resampling processing (I:Wrigley). Results indicated little, if any, difference in the system MTF from forward to reverse and a resampling MTF that was as expected.

Band-to-band registration accuracy was the most intensively studied geometric characteristic of TM P-data (P:Card, P:Fusco, P:Gurney, P:Podwysocki, P:Yao, I:Bernstein, I:Walker). Registration between the four primary focal plane bands (1-4) was reported to be well within specifications (<.2 pixels) as was the registration between bands 5 and 7. Between the prime focal plane and the secondary focal plane, a misregistration of 0.5 to

0.8 pixels along scan and 0.2 to 0.3 pixels across-scan was reported. In addition, band 6 data was found to be misregistered by approximately 3 resampled pixels. Shifts in the locations of the focal planes due to launch stress and vibration testing (bands 1-4 versus 5 and 7) and software errors (band 6) were deemed responsible for the misregistrations. Software changes were incorporated to account for the shifts and errors in early 1983 (I:Fischel).

The lack of geodetically corrected data has limited the ability of investigators to characterize the geodetic accuracy of processed TM P-data. Early results found that the discrepancy between systematically corrected data and the ground is largely translational (S:Thormodsgard, Vol. II, 62-63) indicating that the internal geometry is quite good and that the images can be corrected with only a low-order mapping to a projection. Later results (I:Walker; I:Welch) have confirmed the high internal accuracy of TM data.

Additional geometrically related analyses of TM data included (1) an analysis of the geometric accuracy of the GSFC filmwriter used for TM images, which showed that TM low frequency distortions are likely to be less than the distortions introduced by the filmwriter (P:Batson) and (2) a linear feature detection analysis which confirmed the resampled pixel size as 28.5 meters and showed linear feature detection capabilities to as small as 6 meters (P:Gurney).

Overall, the TM instrument and ground processing techniques appear to be functioning properly and to within specification to the extent tested. Pre-launch concerns of excessive jitter did not materialize. Post-launch estimates of the system's spatial resolution are consistent with pre-launch estimates. In the initial Scrounge tapes there were band-to-band misregistrations. The source of these errors has been located and apparently corrected. The Scrounge system did not geodetically correct the data, however, systematically corrected data is internally consistent and the discrepancy with ground projections appears to be primarily translational and/or rotational. The TIPS processing system currently in use is under evaluation for its geometric properties: band-to-band registration and geodetic accuracy in particular.

GENERAL REFERENCES

1983 Engel, J.L. and O. Weinstein, "The Thematic Mapper - An Overview," IEEE Transactions on Geoscience and Remote Sensing, Vol. GE-21, No. 3, pp. 258-265.

1984 Markham, B., "Characterization of the Landsat Sensor's Spatial Responses, "NASA TM-86130, NASA/Goddard Space Flight Center, Greenbelt, Maryland 20771, July.

1983 Park, S.K. and R.A. Schowengerdt, "Image Reconstruction by Parametric Cubic Convolution," Computer Vision, Graphics, and Image Processing, Vol. 23, pp. 258-272.

1983 Schueler, C., "Thematic Mapper Protoflight Model Line Spread Function," in Proc. 17th Int. Symp. on Remote Sensing of Environment, May 9-13.

"I" REFERENCES

1984 IEEE Transactions on Geoscience and Remote Sensing, Volume GE-22, No. 3, May, Special Issue on Landsat-4.

CHARACTERIZATION OF LANDSAT-4 MSS AND TM DIGITAL IMAGE DATA
W.A. Malila, M.D. Metzler, D.P. Rice and R.P. Crist

ANALYSIS AND PROCESSING OF LANDSAT-4 SENSOR DATA USING ADVANCED IMAGE PROCESSING TECHNIQUES AND TECHNOLOGIES
R.Bernstein, J.B. Lotspiech, H .J. Myers, H.G. Kolsky, and R.D. Lees

LANDSAT-4 MSS AND THEMATIC MAPPER DATA QUALITY AND INFORMATION CONTENT ANALYSIS
P.E. Anuta, L.A. Bartolucci, M.E. Dean, D.F.Lozano, E. Malaret, C.D. McGillem, J.A. Valdes, and C.R. Valenzuela

VALIDATION OF THE THEMATIC MAPPER RADIOMETRIC AND GEOMETRIC CORRECTION ALGORITHMS
D. Fischel

REVISED RADIOMETRIC CALIBRATION TECHINQUE FOR LANDSAT-4 THEMATIC MAPPER DATA
J.M. Murphy, T. Butlin, P.F. Duff, and A.J. Fitzgerald

IN-FLIGHT ABSOLUTE RADIOMETRIC CALIBRATION OF THE THEMATIC MAPPER
K.R. Castle, R.G. Holm, C.J. Kastner, J.M. Palmer, P.N. Slater, M. Dingirard, C.E. Ezra, R.D. Jackson and R.K. Savage

A PHYSICALLY-BASED TRANSFORMATION OF THEMATIC MAPPER DATA
E.P. Crist and R.C. Cicone

"I" REFERENCES (Cont)

THEMATIC MAPPER IMAGE QUALITY: REGISTRATION, NOISE AND RESOLUTION
R.C. Wrigley, D.H. Card, C.A. Hlavka, J.R. Hall, F.C. Mertz, C. Archwamety, and R.A. Schowengerdt

COMPARISON OF THE INFORMATION CONTENT OF DATA FROM THE LANDSAT-4 THEMATIC MAPPER AND THE MULTISPECTRAL SCANNER
J.C. Price

CARTOGRAPHIC ACCURACY OF LANDSAT-4 MSS AND TM IMAGE DATA
R. Welch and E.L. Usery

AN ANALYSIS OF LANDSAT-4 THEMATIC MAPPER GEOMETRIC PROPERTIES
R.E. Walker, A.L. Zobrist, N.A. Bryant, B. Gokhman, S.Z. Friedman, and T.L. Logan

A STATISTICAL EVALUATION OF THE ADVANTAGES OF LANDSAT THEMATIC MAPPER DATA IN COMPARISON TO MULTISPECTRAL SCANNER DATA
D.L. Williams, J.R. Irons, B.L. Markham, R.F. Nelson, D.L.Toll, R.S. Latty, and M.L. Stauffer

SPECTRAL VARIABILITY OF LANDSAT-4 THEMATIC MAPPER AND MULTISPECTRAL SCANNER DATA FOR SELECTED CROP AND FOREST COVER TYPES
S.D. DeGloria

EVALUATION OF CORN/SOYBEAN SEPARABILITY USING THEMATIC MAPPER AND THEMATIC MAPPER SIMULATOR DATA
D.E. Pitts, G.D. Badhwar, D.R. Thompson, K.E. Henderson, S.S. Shen, C.T. Sorensen, and J.G. Carnes

EVALUATION OF THEMATIC MAPPER FOR DETECTING SOIL PROPERTIES UNDER GRASSLAND VEGETATION
D.R. Thompson and K.E. Henderson

SNOW REFLECTANCE FROM LANDSAT-4 THEMATIC MAPPER
J.Dozier

THEMATIC MAPPER: THE ESA-EARTHNET GROUND SEGMENT AND PROCESSING EXPERIENCE
L. Fusco

EFFECTIVE BANDWIDTHS FOR LANDSAT-4 AND LANDSAT-D' MULTISPECTRAL SCANNER AND THEMATIC MAPPER SUBSYSTEMS
J.M. Palmer

N85-20509

AN OVERVIEW OF LANDSAT-4 AND THE THEMATIC MAPPER

James R. Irons

NASA/Goddard Space Flight Center
Earth Resources Branch
Greenbelt, MD 20771

ABSTRACT

Descriptions of the Landsat-4 satellite, its sensor payload, its orbit, and the acquisition and processing of Thematic Mapper (TM) data are provided to aid investigators in the effective utilization of TM data. Landsat-4 was launched into a near polar, sun-synchronous orbit on July 16, 1982. This satellite is the first in the Landsat series to conform to NASA's Multimission Modular Spacecraft design. The new design permits three-axis control of attitude and improved stability and pointing accuracy. The sensor payload consists of a familiar Multispectral Scanner (MSS) and the new TM. The TM offers advancements over the MSS with respect to spatial, spectral, and radiometric resolutions.

Landsat-4 is designed to use the Tracking and Data Relay Satellite (TDRS) system to transmit both MSS and TM data to a ground station. The capability to transmit the data directly to ground stations is provided for the interim between the launch of Landsat-4 and the initiation of TDRS operations. Unfortunately, after transmitting approximately 6000 TM scenes, the transmitter for TM data failed and additional TM data will not often be received until routine TDRS operations begin during the autumn of 1983. The available TM data are undergoing radiometric and geometric corrections to provide TM investigators with pictorial and digital image data. Early analyses of TM data indicate that the geometric and radiometric characteristics of the data exceed or are comparable to prelaunch specifications.

INTRODUCTION

Knowledge of satellite and sensor characteristics is essential to the effective utilization of Thematic Mapper data. This paper provides a detailed description of the Landsat-4 satellite, its instrument payload, its orbit, and the reception, processing, and dissemination of TM data on the ground. Preliminary information on sensor performance and data quality is also presented.

THE SPACECRAFT

The Landsat-4 satellite conforms to NASA's standard design for a Multimission Modular Spacecraft (MMS). The standard support structure consists of two connected frames (Figure 1). One frame, the universal MMS structure, supports modules for satellite propulsion, attitude control, power, and data communications. The other frame, the mission-specific Instrument Module Structure, carries the instrument and sensor payload. For Landsat-4, a large mast supporting an antenna and a single-wing array of solar panels are attached to this supporting structure. The antenna will be used for data communications with the Tracking and Data Relay Satellite (TDRS) system and the mast minimizes interference by the solar panel array. The array consists of four 1.5-m by 2.3-m panels which can generate up to two kilowatts of power. Landsat-4 is the first of the Landsat satellites to utilize the MMS design.

The MMS offers improved attitude control capabilities over the previous Landsat satellites. The MMS permits three-axis control of attitude. The pointing accuracy is specified to be within 0.01 degree (one sigma) and the stability is specified to be within 10^{-6} degree/second (one sigma). The first three Landsat satellites only provide one-axis control of attitude resulting in a 0.7 degree pointing accuracy and a stability value of 0.01 degree/second (Salomonson et al., 1980). The improved attitude control facilitates the cartographic and multitemporal registration of image data and should produce higher registration accuracies.

THE SENSOR PAYLOAD

The remote sensing instruments aboard Landsat-4 are the Multispectral Scanner (MSS) and the Thematic Mapper (TM). Both are object-space line scanners which use moving mirror assemblies to scan across the spacecraft ground track and the orbital motion of the spacecraft to scan the perpendicular (i.e., along-track) direction. Both sensors generate multispectral image data in a digital format.

The Landsat-4 MSS is nearly identical to the MSS's aboard the previous Landsat satellites. The MSS mirror reflects radiance from the earth through a Ritchey-Chretein telescope onto a single focal plane. At the focal plane, optical filters separate the incident electromagnetic energy into the familiar four MSS spectral bands (Table 1). Fiber optic bundles relay the separated energy from the focal plane to detectors which convert the energy to electronic signals (Figure 2). Six detectors are used for each spectral band; photo-

ORIGINAL PAGE IS
OF POOR QUALITY

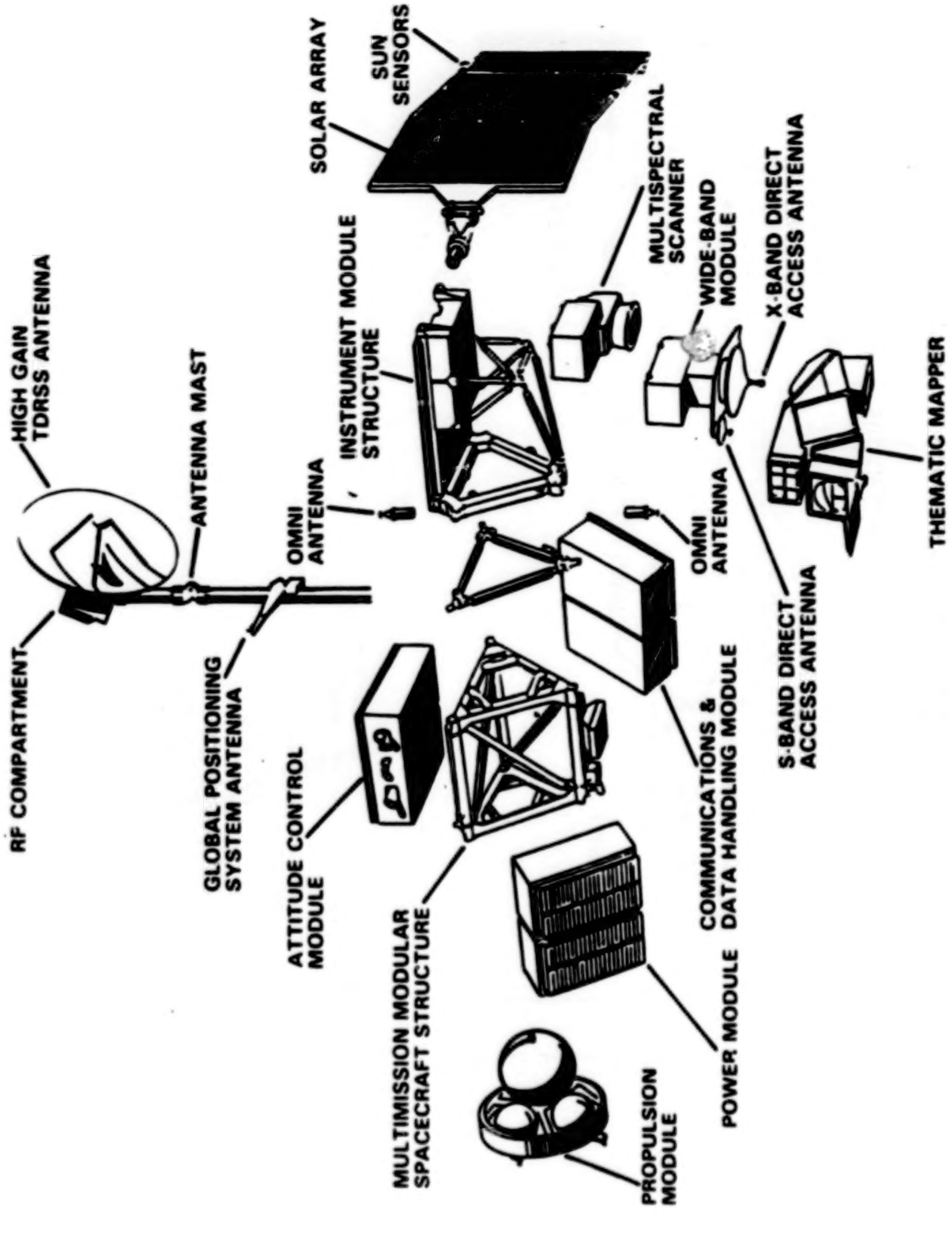
HIGH GAIN TDRSS ANTENNA
RF COMPARTMENT
ANTENNA MAST
GLOBAL POSITIONING SYSTEM ANTENNA
OMNI ANTENNA
ATTITUDE CONTROL MODULE
MULTIMISSION MODULAR SPACECRAFT STRUCTURE
INSTRUMENT MODULE STRUCTURE
SOLAR ARRAY
SUN SENSORS
MULTISPECTRAL SCANNER
WIDE-BAND MODULE
X-BAND DIRECT ACCESS ANTENNA
OMNI ANTENNA
COMMUNICATIONS & DATA HANDLING MODULE
POWER MODULE
PROPULSION MODULE
S-BAND DIRECT ACCESS ANTENNA
THEMATIC MAPPER

Figure 1. Exploded View of Landsat-4

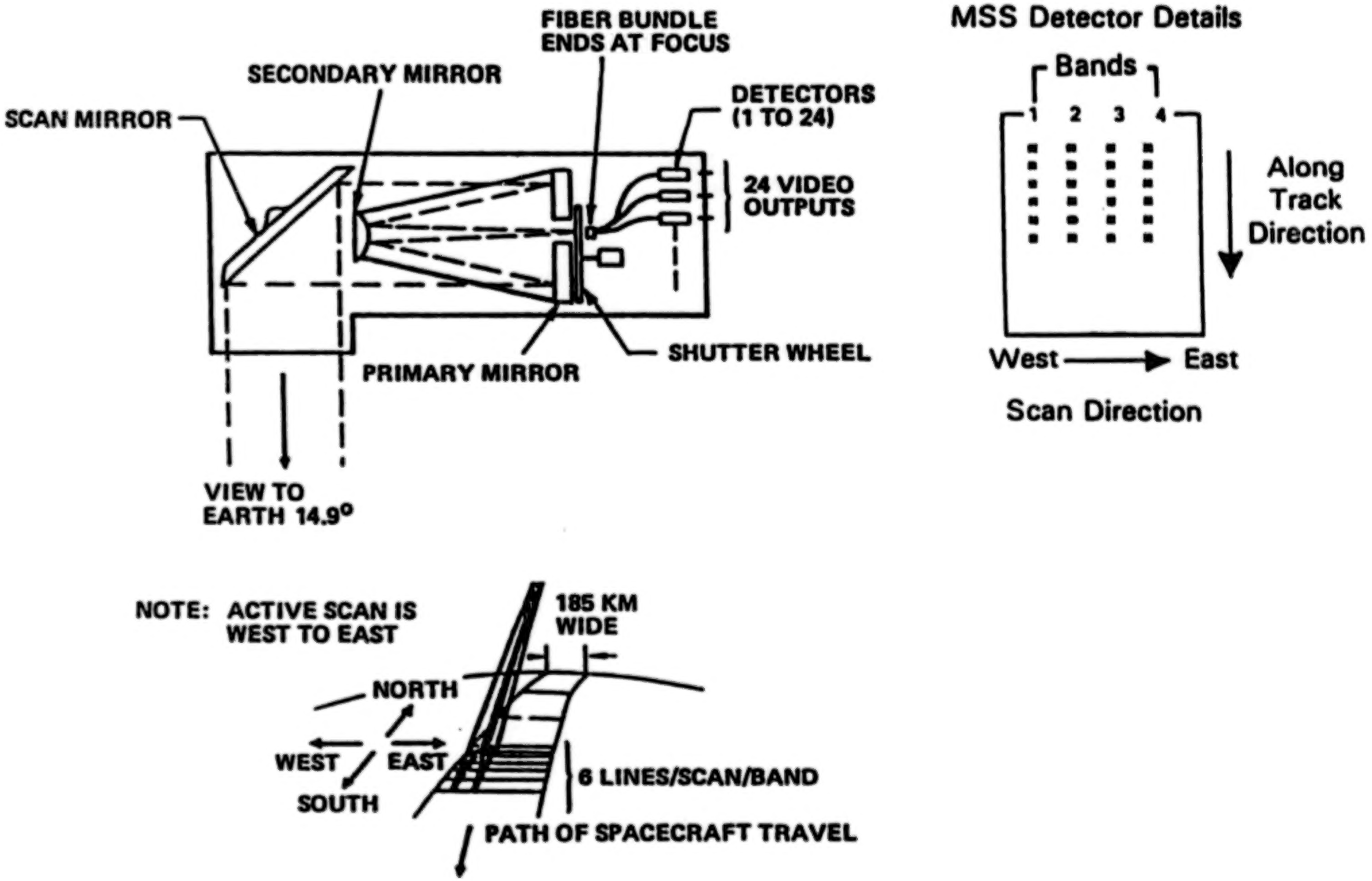
FIBER BUNDLE ENDS AT FOCUS
SECONDARY MIRROR
SCAN MIRROR
DETECTORS (1 TO 24)
24 VIDEO OUTPUTS
PRIMARY MIRROR
SHUTTER WHEEL
VIEW TO EARTH 14.9°
MSS Detector Details
Bands
1
2
3
4
Along Track Direction
West
East
Scan Direction
NOTE: ACTIVE SCAN IS WEST TO EAST
185 KM WIDE
NORTH
WEST
EAST
SOUTH
6 LINES/SCAN/BAND
PATH OF SPACECRAFT TRAVEL

Figure 2. Schematic of the Landsat-4 Multispectral Scanner

multiplier tubes are used for spectral bands MSS1 through MSS3 and silicon photodiodes are employed for band MSS4. The detectors' signals are quantized to six bits (64 digital counts) before the image data are transmitted to the ground. With six detectors per band, the MSS generates six scan lines of data per scan mirror sweep.

Table 1. Landsat-4 Multispectral Scanner Spectral Bands (Salomonson et al., 1980)

Band Designation	Specified Band Width (μm)	Specified Radiometric Sensitivity (NEΔρ)*
MSS1	0.5 - 0.6	0.57%
MSS2	0.6 - 0.7	0.57%
MSS3	0.7 - 0.8	0.65%
MSS4	0.8 - 1.1	0.70%

* NEΔρ - noise equivalent change in surface reflectance

Both the across-track swath (185 km) viewed by the newest MSS and the new sensor's instantaneous-field-of-view (80 m) also remain nearly equal to the swath width and IFOV of the earlier MSS's. Since the earlier Landsat satellites all flew at a higher altitude (920 km) than Landsat-4 (705 km), the optics and the active scan angle of the Landsat-4 MSS were adjusted to compensate for the difference in altitude. The earlier sensors employed a 11.56° scan angle and the new MSS employs a scan angle of 14.92°.

Several major differences exist between the basic design of the MSS and the design of the TM. First, the TM acquires data during both the forward (west-to-east) and reverse (east-to-west) sweeps of its scan mirror. The MSS collects data in only one scan direction (west-to-east). The bidirectional approach was adopted to reduce the scan rate and to increase detector dwell time. The TM scan mirror oscillates at a rate of approximately seven cycles (one cycle consists of both a forward and a reverse scan mirror sweep) per second and actively scans the surface through an angle of 15.4° (plus-or-minus 7.7° from nadir).

As another example of design differences, the TM does not rely on fiber optics, as does the MSS, to direct incoming electromagnetic energy onto photosensitive detectors. Fiber optics are incapable of transmitting 100 percent of the incident energy from a focal plane to detectors. Instead of using fiber optics, the TM focuses incident radiation through its own Ritchey-Chretein telescope directly onto detectors within a prime focal plane assembly and through a set of relay mirrors to the detectors of a cooled focal plane assembly (Figure 3). The prime focal plane assembly contains four sets of 16 monolithic silicon detectors for four spectral bands in the visible and near infrared portions of the spectrum. The 16 detectors for each band are mounted in a common module with a spectral filter and preamplifier electronics. The

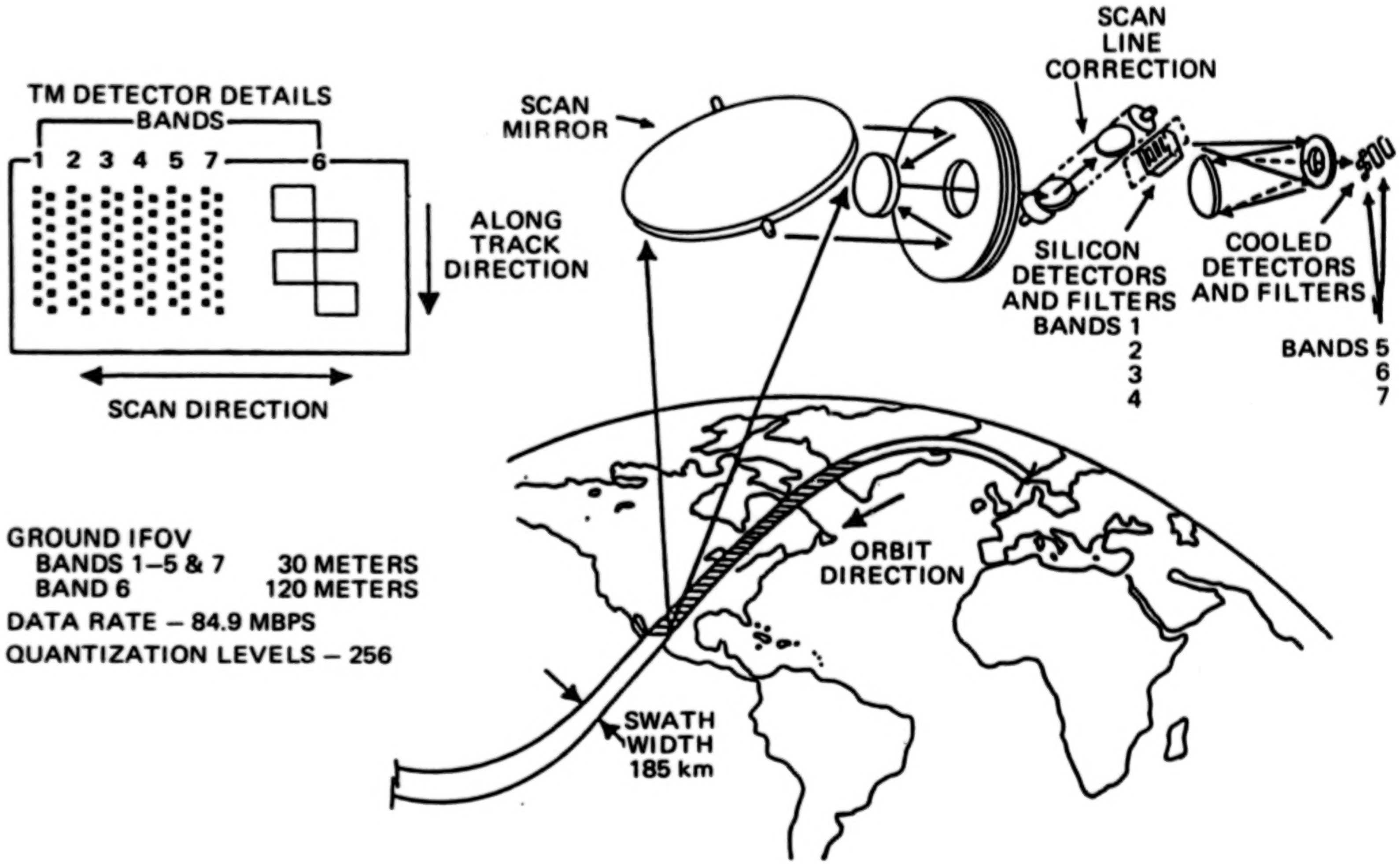
TM DETECTOR DETAILS
BANDS
1 2 3 4 5 7
6
ALONG TRACK DIRECTION
SCAN DIRECTION
SCAN MIRROR
SCAN LINE CORRECTION
SILICON DETECTORS AND FILTERS BANDS 1 2 3 4
COOLED DETECTORS AND FILTERS
BANDS 5 6 7
ORBIT DIRECTION
SWATH WIDTH 185 km
GROUND IFOV
BANDS 1–5 & 7 30 METERS
BAND 6 120 METERS
DATA RATE – 84.9 MBPS
QUANTIZATION LEVELS – 256

Figure 3. Schematic of the Thematic Mapper

cooled focal plane assembly contains two sets of 16 indium antimonide (InSb) photodiodes for two middle infrared spectral bands and four mercury cadmium telluride (HgCdTe) detectors for a thermal band along with spectral filters and electronics. The cooled focal plane assembly is mounted in a dewar assembly on the second stage of a passive radiative cooler. The use of multiple detectors for each spectral band results in the generation of 16 scan lines of data for the six reflective bands and four lines of data for the thermal band during each sweep of the scan mirror. At any one instant, surface radiance is sensed by a total of 100 TM detectors.

Due to the necessary spacing of the detector modules on the focal planes, an area on the surface is not simultaneously scanned in all seven TM spectral bands. Accurate band-to-band registration thus requires precise time registration and scan mirror profile (scan angle versus time) linearity and repeatability. A scan angle monitor on the mirror generates signals indicating the scan mirror's angular position as a function of time. These signals are called mirror scan correction data and are transmitted to the ground for geometric processing of TM image data.

Signals from the scan angle monitor also initiate the motions of the scan angle corrector located in front of the primary focal plane (Figure 3). During each scan mirror sweep, the scan line corrector rotates the TM line-of-sight backward along the ground track to compensate for the forward motion of the satellite. The compensation prevents the overlap and underlap of scan lines and produces straight scan lines which are perpendicular to the ground track (Figure 4). Also located within the Thematic Mapper is a three-axis angular displacement sensor. This sensor provides data to the ground data processing system to compensate for any high-frequency displacements of the TM optical axis caused by the vibrations of the TM and MSS scan mirrors.

The TM also contains an internal radiometric calibration source located behind the primary mirror and in front of the primary focal plane. The calibration source consists of three small tungsten filament lamps (each operating at a different intensity), a blackbody for the thermal band, and a flex pivot mounted resonant shutter. A fiber optics bundle relays energy from the stationary lamps to the moving shutter. The shutter oscillates in a manner which causes it to introduce the calibration source energy and a direct current (dc) restore surface into the detectors' fields of view during the turnaround time of each scan mirror sweep (Engel, 1980). For the thermal band (TM6), a small concave mirror on the shutter reflects energy from the stationary blackbody into the thermal detectors' fields of view.

The lamps are turned on-and-off to provide eight different calibration levels (seven energy levels plus a dark level). The calibration level remains constant for 20 scan cycles (i.e., 20 forward plus 20 reverse scan mirror sweeps). After each 20 cycle interval, a single lamp is turned either on or off to change the level. Since 16 detectors are used for each band, a total of 5120 scan lines of image data are generated during the time interval required to view all eight levels (eight calibration levels, 40 scan mirror sweeps per level, 16 lines of data per mirror sweep). For the thermal band, both the temperature of the blackbody and of the shutter's dc restore surface are known to provide a two-level calibration of the four thermal detectors.

Figure 5 provides an overview of the Thematic Mapper design. The TM is horizontally mounted in the satellite with the sun shade pointing toward earth. The scan mirror is located directly above the sun shade aperture along with the mirror's drive mechanism, control electronics, and scan angle monitor. The primary mirror is secured approximately in the center of the telescope and is preceded by the secondary mirror and optical baffles. The scan line corrector, the internal calibrator, and the primary focal plane are directly behind the primary mirror. The back end of the instrument contains the relay optics and the cooled focal plane within the radiative cooler. The electronics package sits in a wedge-shaped box above the telescope and contains the multiplexer, power supplies, signal amplifiers, and electronic filters.

The complex design of the TM affords advanced sensor attributes in comparison to the MSS. For instance, the TM will acquire data for seven spectral bands of which four bands are located in portions of the spectrum not sensed by the MSS. The location and width of the seven bands were carefully chosen for sensitivity to certain natural phenomena and to minimize the attenuation of energy within the bands by atmospheric water. Table 2 lists the spectral bands along with the rationale for selecting each band.

Another major advancement by the TM involves spatial resolution. The TM instantaneous-field-of-view (IFOV) is 30 m-by-30 m for the six reflective spectral bands and 120 m-by-120 m for the thermal band. The MSS provides a resolution of approximately 80 m-by-80 m for all four of the MSS bands. Table 3 lists the TM optical characteristics which effect the surface spatial resolution.

The TM also offers improved radiometric sensitivity over the MSS, even though the TM spectral bands are more narrow and the TM IFOV is smaller. Sensitivity specifications in terms of noise equivalent change in surface reflectance (NE$\Delta\rho$) are presented in Table 1 for the MSS and Table 2 for the TM. In conjunction with the improved sensitivity, TM data are quantized to eight bits (256 digital counts) while MSS data are quantized to six bits (64 digital counts).

In summary, the TM's improved sensor capabilities relative to the MSS are a result of the advanced design of the TM. Design factors which significantly effect capabilities include: the detectors' angular IFOV which is a function of detector size and telescope focal length; the optics of the scan mirror and telescope which minimize diffraction and blur and thus enhance radiometric sensitivity and spatial resolution; the use of the bidirectional active scan approach which increases detector dwell time and thus enhances radiometric sensitivity; the internal calibrator which permits eight level, in-flight radiometric calibration; the relay optics and cooled focal plane which enable sensing of energy within middle infrared and thermal infrared spectral bands; and the scan angle monitor and the scan line corrector which facilitate the precise geographic registration of the fine resolution image data. The rationale for creating this advanced design is to generate data which can be better exploited for scientific research.

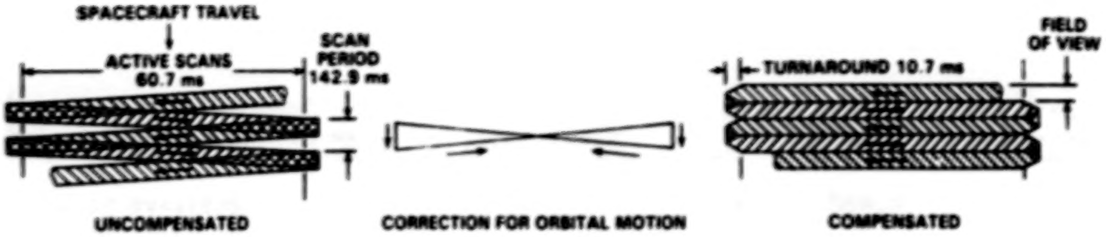
SPACECRAFT TRAVEL
ACTIVE SCANS 60.7 ms
SCAN PERIOD 142.9 ms
TURNAROUND 10.7 ms
FIELD OF VIEW
UNCOMPENSATED
CORRECTION FOR ORBITAL MOTION
COMPENSATED

Figure 4. Scan Line Corrector Compensation

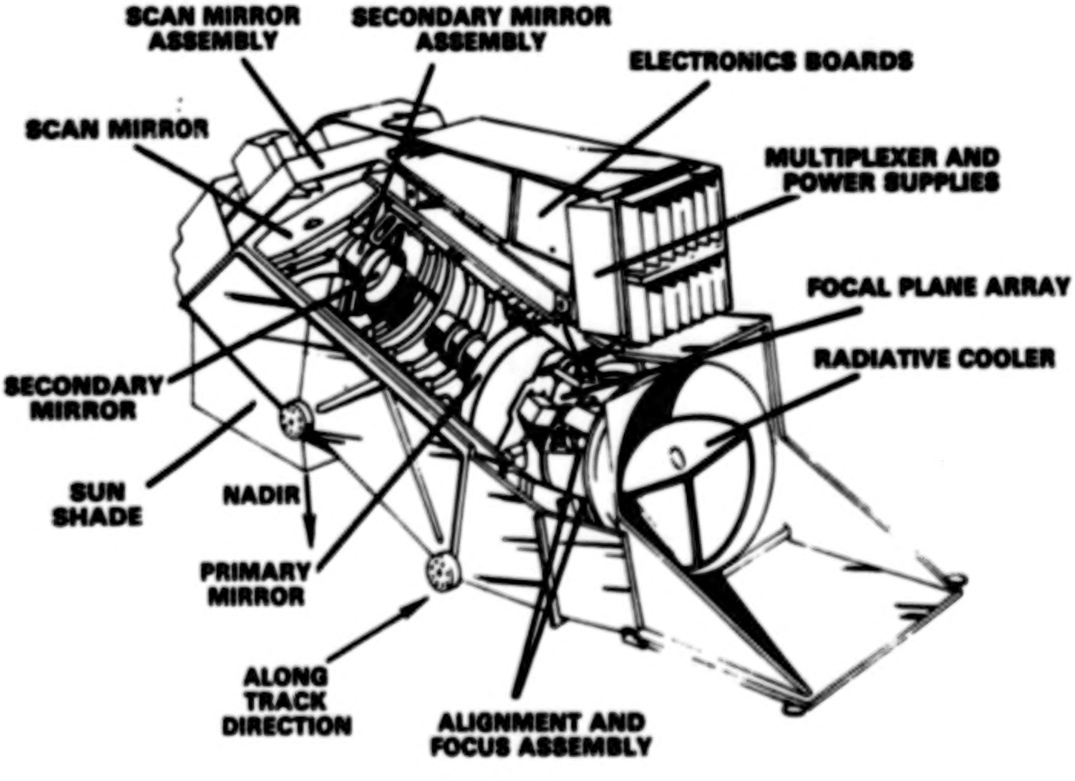
SCAN MIRROR ASSEMBLY
SECONDARY MIRROR ASSEMBLY
ELECTRONICS BOARDS
SCAN MIRROR
MULTIPLEXER AND POWER SUPPLIES
FOCAL PLANE ARRAY
RADIATIVE COOLER
SECONDARY MIRROR
SUN SHADE
NADIR
PRIMARY MIRROR
ALONG TRACK DIRECTION
ALIGNMENT AND FOCUS ASSEMBLY

Figure 5. Cut-a-Way View of the Thematic Mapper

Table 2. Thematic Mapper Spectral Bands (Salomonson et al., 1980)

Band Designation	*Band Width (μm)	Specified Radiometric Sensitivity (NEΔρ)**	Selection Rationale
TM1	0.452 - 0.518	0.8%	Sensitive to chlorophyll and carotinoid concentrations for soil/vegetation differentiation, deciduous/coniferous differentiation. Coastal water mapping.
TM2	0.529 - 0.610	0.5%	Sensitive to green reflectance by healthy vegetation.
TM3	0.624 - 0.693	0.5%	Sensitive to chlorophyll absorption for plant species differentiation.
TM4	0.776 - 0.905	0.5%	Sensitive to near infrared reflectance of healthy vegetation for biomass surveys.
TM5	1.568 - 1.784	1.0%	Sensitive to vegetation moisture and snow/cloud reflectance differences.
TM6	10.42 - 11.66	0.5 K NETD***	Thermal mapping.
TM7	2.10 - 2.35	2.4%	Sensitive to vegetation moisture and to hydroxyl ions in minerals for geological mapping.

*Band edges at half maximum (Markham and Barker, 1983).

**NEΔρ - noise equivalent change in surface reflectance

***NETD - noise equivalent temperature difference

Table 3. Thematic Mapper Optical Characteristics (Engel, 1980)

40.6 cm. Aperature
f/6 at Prime Focus
42.5 μrad Angular IFOV, Bands TM1 through TM4
f/3 at Relay Focus
43.8 μrad Angular IFOV, Bands TM5 and TM7
170 μrad Angular IFOV, Band TM6

THE ORBIT AND COVERAGE

Landsat-4 travels in repetitive, circular, sun-synchronous, near-polar orbits at a nominal altitude of 705 km. The orbits have an inclination angle of 98.2 degrees with respect to the equator, and the satellite crosses the equator at approximately 9:45 a.m. local solar time during the descending (north-to-south) portion of each orbit. The TM can acquire thermal data during the satellite's ascending (south-to-north) node in which the satellite crosses the equator at 9:45 p.m. local solar time. Each orbit takes almost 99 minutes, and the spacecraft completes just over 14.5 orbits each day. Due to the Earth's rotation, the distance between ground tracks for two consecutive orbits is 2752km at the equator. Figure 6 illustrates the orbital characteristics of Landsat-4.

The orbital configuration described above creates a 16 day repeat cycle for Landsat-4. In other words, the satellite will travel along a particular ground track once every 16 days. The time interval between an orbit over a specific ground track and an adjacent track is seven days (Figure 7). This arrangement contrasts with the 18-day orbital cycles of the first three Landsat satellites which resulted in a one day interval between orbits over adjacent tracks.

The altitude, optics, and 15.4 degree scan of the TM enable the instrument to view a 185 km swath across the ground track of the satellite. At the equator, adjacent swaths overlap by 7.6 percent. The overlap increases as the ground tracks move away from the equator toward either pole. At 40 degrees north or south latitude, the overlap is 18.5 percent.

The Landat-4 orbital repeat cycle requires 233 orbits, rendering the system incompatible with the 251-orbit Worldwide Reference System (WRS) used to index MSS data from the previous Landsat satellites. A new system of path and row indices has been designed for both Landsat-4 MSS and TM data. A path index number is assigned to the ground track of each orbit. The new system consists of 233 orbital paths numbered east-to-west with path 001 crossing the equator at 64.95 degrees west longitude. The data acquired along each path are divided into consecutive scenes where each scene consists of the data acquired during a 25.87-second increment of the orbit. Both the MSS data and the TM data for each scene cover a 185-by-185 km surface area. A row index is assigned to each scene center. Row one

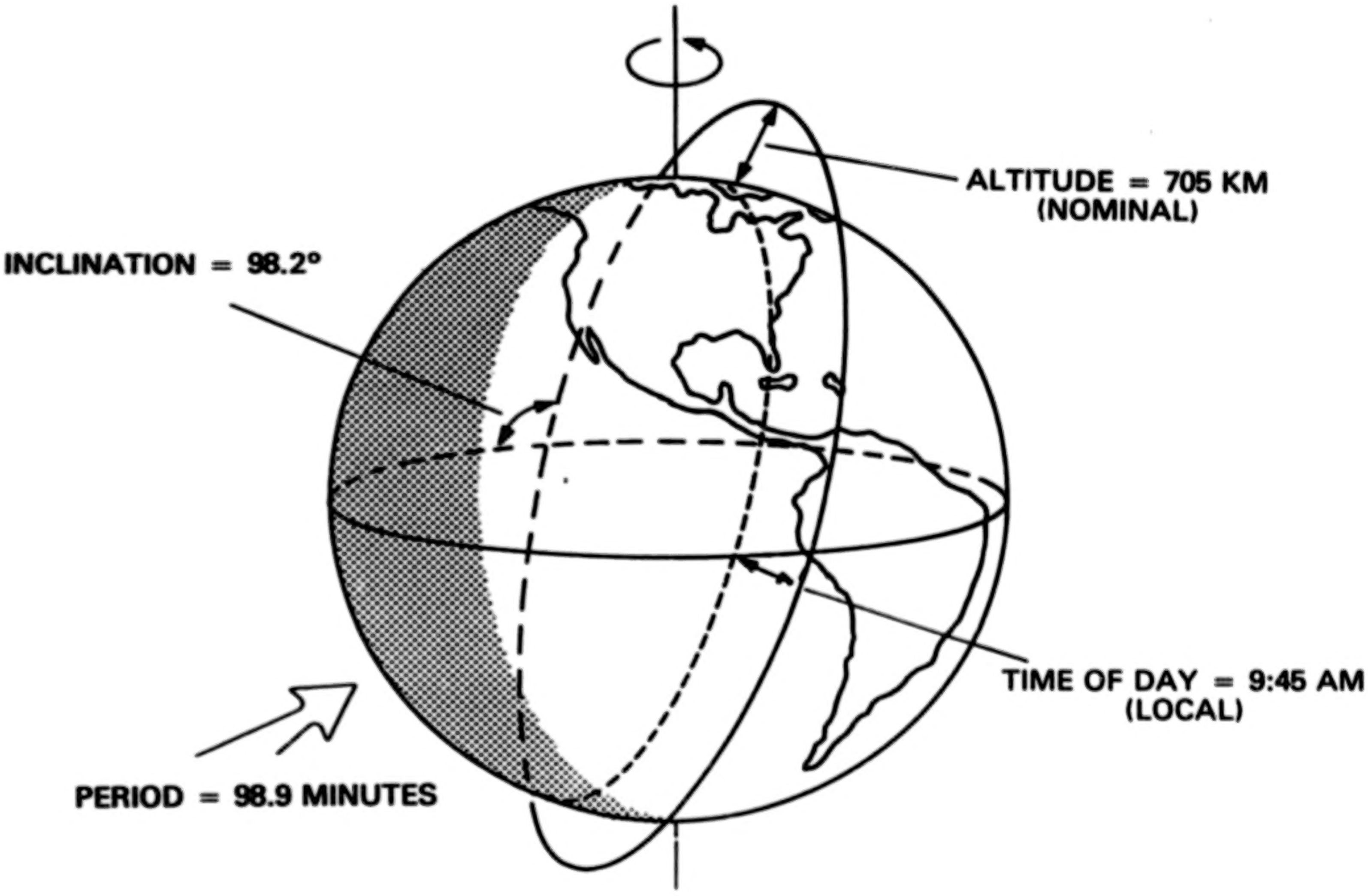
ALTITUDE = 705 KM
(NOMINAL)
INCLINATION = 98.2°
TIME OF DAY = 9:45 AM
(LOCAL)
PERIOD = 98.9 MINUTES

Figure 6. The Sun-Synchronous Orbit of Landsat-4

ORIGINAL PAGE IS
OF POOR QUALITY

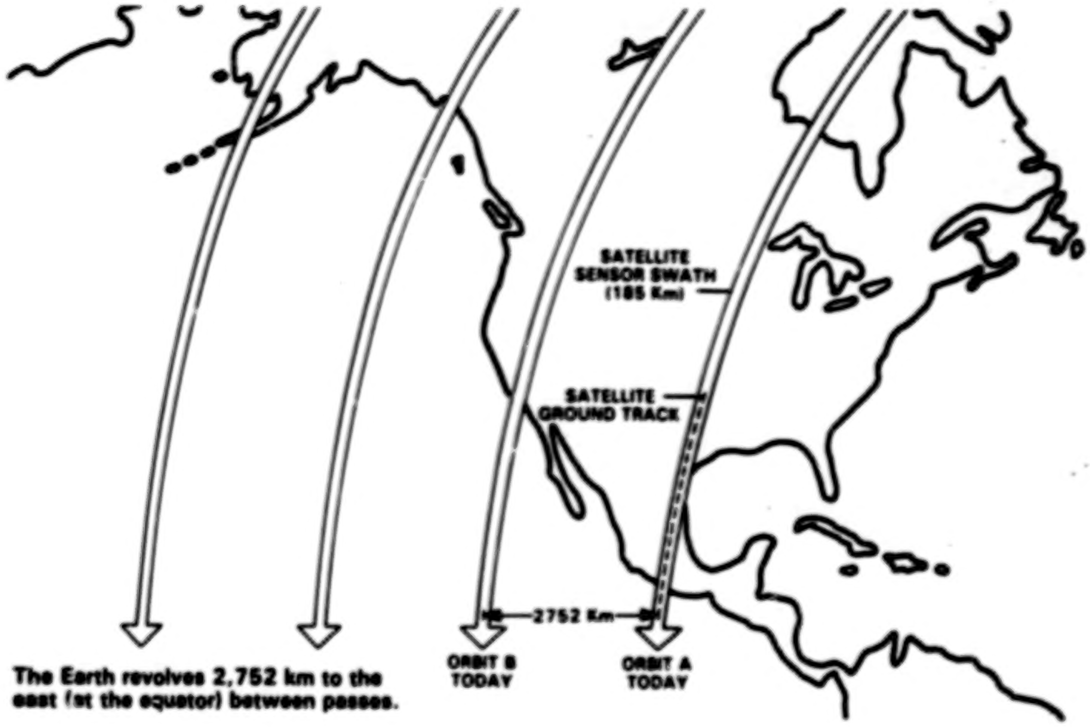
SATELLITE
SENSOR SWATH
(185 Km)
SATELLITE
GROUND TRACK
2752 Km
ORBIT B
TODAY
ORBIT A
TODAY

The Earth revolves 2,752 km to the east (at the equator) between passes.

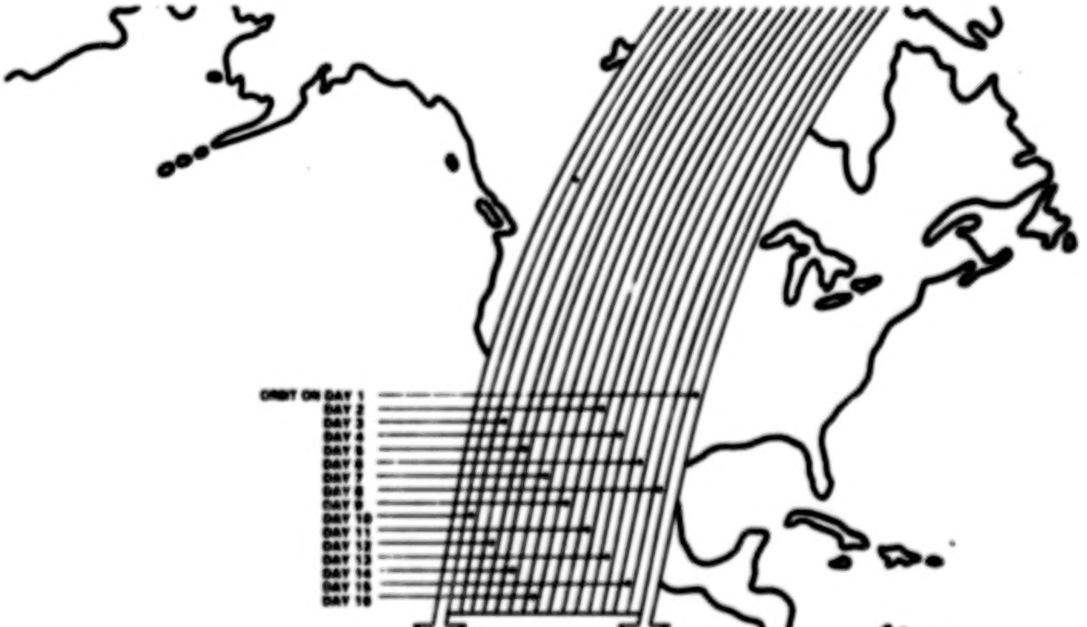
ORBIT ON DAY 1
DAY 2
DAY 3
DAY 4
DAY 5
DAY 6
DAY 7
DAY 8
DAY 9
DAY 10
DAY 11
DAY 12
DAY 13
DAY 14
DAY 15
DAY 16

Adjacent swaths (moving westward) are imaged 7 days apart.

Figure 7. The Landsat-4 Orbital Repeat Cycle

of each path starts at 80°51' north latitude and the numbering increases southward through the equator (row 60) to 81°51' south latitude (row 122). The satellite then travels northward for the ascending (nighttime) portion of the orbit, and row numbers increase from south-to-north through the equator (row 184) to 81°51' north latitude (row 246). Thus, row indices 123 through 246 refer to scenes of nighttime TM thermal data which are not acquired on a routine basis. Maps delineating paths and rows can be obtained from the EROS Data Center, Mundt Federal Building, Sioux Falls, South Dakota.

TM DATA COMMUNICATIONS

As the scan mirror sweeps back-and-forth seven times per second, the incoming energy is focused onto the photosensitive detectors The detectors translate the energy into low-level electrical signals which are amplified, quantized to eight-bit digital words, and then multiplexed into an 84.9 megabits-per-second (Mbps) data stream. The digital image data are then transmitted to the ground along with additional data for radiometric and geometric corrections.

The previous Landsat satellites relied upon onboard tape recorders to store data until the satellite flew within range of a ground receiving station. These recorders were often the first component to fail. Landsat-4 can use a new communications system, called the Tracking and Data Relay Satellite (TDRS) system, which eliminates the need for onboard recorders. The system will consist of two satellites (plus an in-orbit spare satellite) in geosynchronous orbits and a ground station at White Sands, New Mexico. The first TDRS satellite was launched on April 4, 1983 aboard NASA's space shuttle Challenger. After overcoming problems caused by a malfunction of the satellite's Inertial Upper Stage (IUS), the satellite was placed in a geosynchronous orbit over the equator at 67° west longitude and at an altitude of 35,890km. The satellite will be placed in its final position at 41° west longitude during the autumn of 1983. The schedule for the launch of the second TDRS satellite is uncertain until the problems with the IUS can be thoroughly evaluated. When launched, the second TDRS satellite will be located 35,890km over the equator at 171° west longitude.

The TDRS satellites will not routinely relay TM data until both satellites are placed in their proper orbits and their operations tested. Some TM data has been relayed to the ground station to test and demonstrate the system before routine operations begin. When the system becomes fully operational, the TDRS satellites will enable the acquisition and transmission of TM and MSS data for nearly all of the Earth's surface. With both satellites in their final positions, only a small area over the Indian Ocean between 67° east and 82° east longitude and between 50° north and 50° south latitude will be excluded from coverage by the system's geometry.

To handle the high data rates from Landsat-4, as well as data from other spacecraft served by TDRS, the TDRS system will employ a Ku-band (approximately 15 Gigahertz) frequency for data communications. This frequency will be transmitted from Landsat-4's TDRS antenna (Fig. 1) and then relayed through one or the other TDRS satellite to the ground receiving station at White Sands, New Mexico. The data received by the White Sands facility will be demodulated, separated, and recorded on wide-band digital data tapes. Once every eight-hours, the compacted raw data will be read from the tapes and then transmitted, by way of a domestic communications satellite (DOMSAT), to a data processing facility at NASA's Goddard Space Flight Center (GSFC) in Greenbelt, Maryland. This scheme ensures the reception of data at the GSFC facility within eight hours of data generation by the sensor. After geometric and radiometric corrections are performed at GSFC (described below), the processed TM data, on film and on computer compatible tapes, are sent by air shipment to the EROS Data Center for public dissemination. Figure 8 traces the TM data pathway.

Arrangements were also made for the transmission and reception of TM data during the interim between the launch of Landsat-4 and the deployment of the TDRS satellites. Until recently, TM image data and associated ancillary data were transmitted on an X-band (8.025 to 8.4 Gigahertz) frequency directly to a Transportable Ground Station located at GSFC or to a Canadian facility in Prince Albert, Saskatchewan. Together, the two stations enabled coverage of most of the North American Continent by the TM, and over 6000 scenes of data were received. Unfortunately, the X-band transmitter aboard Landsat-4 failed on February 15, 1983. No additional TM data will be received until the TDRS satellites are able to relay data using the Ku-band frequency. Reception of Landsat-4 MSS data continues by way of an S-band (2206 to 2300 megahertz) frequency antenna and the worldwide network of ground stations used to receive MSS data from the previous Landsat satellites. The S-band frequency cannot support data transmission at the rate which the TM generates data.

Along with the TM image data of the surface scene, Landsat-4 also transmits data required for the radiometric and geometric correction of the image data. This additional data includes: radiometric calibration data consisting of the quantized responses of the photosensitive detectors to energy from the internal calibrator; mirror scan correction data, from the scan angle monitor, describing the angular position of the scan mirror as a function of time; and payload correction data describing the attitude and the ephemeris of the sensor. These additional data are integrated with the TM image data aboard the spacecraft, and the integrated data are collectively called wideband data. Wideband data are transmitted by the X-band antenna or the Ku-band antenna.

Payload correction data are also transmitted separately from the other wideband data. Payload correction data consist of data from the angular displacement sensor, data from the satellite's attitude control system, earth-centered ephemeris, and housekeeping information such as timing codes and Thematic Mapper internal temperatures. The ephemeris is computed by Landsat4's on-board computer which receives information on the satellite's position from ground stations of the NASA communications network (NASCOM). Landsat-4 is also capable of receiving information from the Global Positioning System (GPS) satellites, but this system is not complete and Landsat-4 has not yet utilized ephemeris information from the GPS. A multiplexer aboard Landsat-4 places all of the payload correction data into a standard format and sends the data to the TM for incorporation with the other wideband data. The payload correction data are also sent separately by S-band

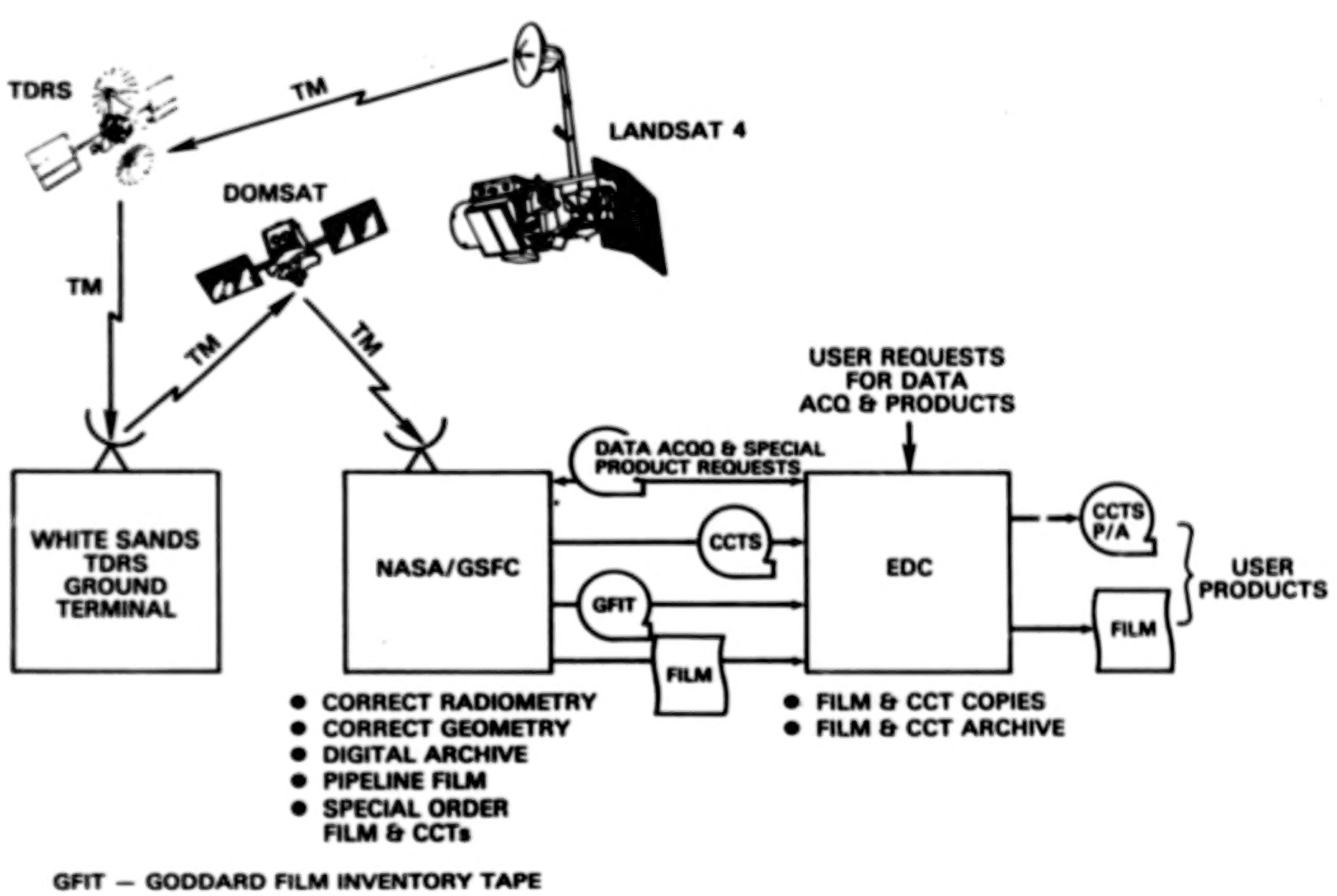
TDRS
TM
LANDSAT 4
DOMSAT
TM
TM
TM
USER REQUESTS FOR DATA ACQ & PRODUCTS
DATA ACQQ & SPECIAL PRODUCT REQUESTS
WHITE SANDS TDRS GROUND TERMINAL
NASA/GSFC
CCTS
GFIT
FILM
EDC
CCTS P/A
FILM
USER PRODUCTS
● CORRECT RADIOMETRY
● CORRECT GEOMETRY
● DIGITAL ARCHIVE
● PIPELINE FILM
● SPECIAL ORDER FILM & CCTs
● FILM & CCT COPIES
● FILM & CCT ARCHIVE
GFIT — GODDARD FILM INVENTORY TAPE

Figure 8. Thematic Mapper Data Flow

telemetry to NASCOM ground stations. NASCOM then forwards the data to GSFC.

TM DATA PROCESSING

Following reception by a ground station, raw MSS data and raw TM data are sent to GSFC for processing to produce film and digital image products for investigators. The GSFC facilities, referred to as the Landat-4 Ground Segment, consist of the Mission Management Facility (MMF), the Control and Simulation Facility (CSF), and the Image Generation Facility (IGF). The MMF receives and processes user requests for data covering specific ground locations and is responsible for data archival. Data requests are then sent to the CSF which commands, controls, and monitors the satellite and also schedules TDRS, DOMSAT, and NASCOM support. Processing of MSS and TM image data is performed by separate systems in the IGF.

The IGF system for TM data is called the Thematic Mapper Image Processing System (TIPS). The development of TIPS was delayed by past uncertainty in the delivery of the TM in time for the Landsat-4 launch. TIPS commenced operations in July, 1983. Before then, TM data were processed for research activities by an improvised system popularly known as the "Scrounge System."

The Scrounge System was put together from available pieces of computer hardware when the timely delivery of the TM became apparent. The system consisted of the Applications Development Data System (ADDS), the Landsat Assessment System (LAS), and elements of the Mission Management Facility (MMF). ADDS is primarily a test system designed to develop the use of array processors for the efficient processing of digital image data. The central processing unit of ADDS is a minicomputer which serves as a host for two array processors. The original intent of the LAS was to expedite the scientific utilization of TM data by providing investigators with an advanced image analysis facility. The sytem supports three interactive image analysis stations, and each station includes multiple cathode ray tubes for the video display of image data. The LAS central processing unit is a minicomputer supported by an array processor (Fischel, 1983). Another two computers within the MMF are used to process payload correction data for both the Scrounge System and TIPS. ADDS and LAS were pressed into service for TM data processing until TIPS began operations.

TIPS consists of two identical systems operating in parallel. The central processing unit of each system is a minicomputer interfaced to an advanced, high-speed array processor. The advanced array processors enables TIPS to process an entire TM scene in under 15 minutes (Fischel, 1983).

The main functions of both TIPS and the Scrounge System are the radiometric and geometric correction of TM image data. The Scrounge System correction algorithms emulated the procedures implemented by TIPS, and experience gained during Scrounge System processing was incorporated into the final development of TIPS. The Scrounge System, however, operated at a much slower rate than the specified rate for TIPS processing. The Scrounge System processed data at an approximate rate of one scene per day. TIPS processes data at a rate of seven scenes per day. This rate will increase to 50 completely processed scenes per day plus 100 radiometrically corrected scenes per day when TIPS is turned over to NOAA in January, 1985.

Data processing begins with the reception of a scene of TM wideband data at the Data Receive Record Transmit System (DRRTS) within the Image Generation Facility and the reception of the associated, but separated, payload correction data (PCD) by the Control and Simulation Facility. DRRTS sends the mirror scan correction data to the Mission Management Facility (MMF) for geometric processing (described below) and passes the rest of the wideband data to ADDs or to TIPS.

The first function performed by either ADDS or TIPS is alternate-sweep scan line reversal. Recall that the TM generates 16 scan lines of data (four scan lines of thermal band data) per scan mirror sweep and that data are generated during both the forward and reverse sweeps of the mirror. To orient all of the raw image data in the same direction, the order of the pixels from each east-to-west (reverse) sweep is reversed to a west-to-east orientation. In ADDS, the raw TM image data were stored on computer compatible tape (CCT) after scan line reversal for shipment to the LAS. These data were called B-data.

After achieving a consistent pixel orientation over a TM scene, the data are radiometrically corrected. The primary objective of radiometric correction is to remove detector-to-detector striping. The TM employs 16 detectors per spectral band and striping is caused by variation in the radiometric response (the function relating detector output to incident spectral radiance) between these detectors. The correction creates data which appears to be generated by detectors of nearly equal responses.

The radiometric correction of TM data requires several steps. The first step replaces the data from two malfunctioning detectors. The next step involves the computation of parameters which define the radiometric response of each detector for a spectral band and the average response of all 16 detectors (four detectors for the thermal band). The final step is the application of the parameters to the correction of the image data.

The third detector of band TM5 produces no photometric response and the response of the fourth detector of band TM2 is considered unreliable. The data from each bad detector is replaced by the raw data from an adjacent detector in the band. The replacement data are then treated in the same manner as the original data from the functioning detectors during subsequent processing.

The computation of radiometric parameters is an iterative process which uses both calibration data and the statistical distribution of TM data in a scene. A nominal response function for the detectors of each band was derived from the pre-launch calibration of the TM. The nominal response functions express digital output as a linear function of incident spectral radiance. These linear functions can be derived directly from the nominal dynamic ranges of the spectral bands (Table 4). The radiance generated by each internal calibration lamp level was also measured prior to launch, and therefore, for each spectral band, nominal digital response to each calibration level can be derived from the nominal response function. To characterize the response of an individual detector in operation, the internal calibration data for a TM scene are used to express the observed digital responses to the calibration lamps as a function of nominal response by way of linear regression analysis. The slope and intercept of the regression line, referred to as gain and bias, respectively, characterize the observed response of each detector.

Table 4. Nominal Dynamic Ranges of Thematic Mapper Radiometric Responses (Barker et al., 1983)

	Dynamic Range	
Band	RMIN	RMAX
	$(mWcm^{-2}sr^{-1}\mu m^{-1})$	
TM1	-0.152	15.842
TM2	-0.284	30.817
TM3	-0.117	23.463
TM4	-0.151	22.432
TM5	-0.037	3.242
TM7	-0.015	1.700
TM6	0.200	1.560

RMIN is the spectral radiance corresponding to a detector response of zero digital counts.

RMAX is the minimum radiance required to saturate detector response (i.e. produce a response of 255 digital counts).

Each detector's gain and bias are modified by a histogram normalization process. The purpose of normalization is to further minimize detector-to-detector striping by compensating for limits in the accuracy of internal calibration data and for the statistical uncertainty in the derivation of the detector gains and biases. The process assumes that each detector senses an equal distribution of radiance over a scene.

To accomplish the normalization, a frequency histogram of the data from each detector is created by sampling every fourth digital count generated by the detector. Each histogram is adjusted by application of the detector's gain and bias to the new data values. The adjustment alters the mean and standard deviation of the raw data in a manner which is mathematically equivalent to the following equations:

(1) $M_i^a = (M_i - B_i)/G_i$

(2) $S_i^a = S_i/G_i$

where:

G_i is the gain for detector i in terms of observed digital counts per nominal digital count;

B_i is the bias for detector i in units of observed digital counts;

M_i is the mean of raw data generated by detector i;

S_i is the standard deviation of raw data generated by detector i;

M_i^a is the altered mean; and

S_i^a is the altered standard deviation.

After the alterations, the average altered mean and the average altered standard deviation are computed for the 16 detectors of each spectral band (four detectors for the thermal band):

(3) $M^a = (\sum_{i=1}^{16} M_i^a)/16$

(4) $S^a = (\sum_{i=1}^{16} S_i^a)/16$

The averaged parameters are then used to normalize each detector's gain and bias:

(5) $G_i^a = G_i \ S_i^a/S^a$

(6) $B_i^a = B_i + G_i \ [M_i^a - (S^a M^a/S_i^a)]$

where:

G_i^a is the normalized gain for detector i; and

B_i^a is the normalized bias for detector i.

The normalization is an iterative process, and the new gains and biases are used to continue the adjustment:

(7) $M_i^b = (M_i - B_i^a)/G_i^a$

(8) $S_i^b = S_i/G_i^a$

$$(9)\quad M^b = (\sum_{i=1}^{16} M_i^b)/16$$

$$(10)\quad S^b = (\sum_{i=1}^{16} S_i^b)/16$$

$$(11)\quad G_i^b = G_i^a \, S_i^b/S^b$$

$$(12)\quad B_i^b = B_i^a + G_i^a[M_i^B - (S^b M^b/S_i^b)]$$

Both the Scrounge System and TIPS halt the normalization procedure after this second iteration on the basis of early normalization efforts in which additional iterations did not significantly modify the gains and biases.

The last step in the radiometric correction process is to apply the normalized gains and biases, G_i^b and B_i^b, to the correction of the image data:

$$(13)\quad H_i = (I_i - B_i^b)/G_i^b$$

where:

I_i is a raw datum generated by detector i; and

H_i is the corrected datum.

To expedite computer processing, equation 13 is used to derive radiometric look up tables (RLUT's) which map raw digital counts to the corrected values. One look up table is generated for each detector, and the tables are used to conduct the correction.

TM data which have undergone alternate-sweep scan line reversal and which have been radiometrically corrected are referred to as A-data. The Scrounge System stored A-data on either computer compatible tapes (nine track, 6250 bits per inch on each track) or a high density tape (28 tracks, 33.3 kilobits per inch on each track) in a band sequential format. Within the Scrounge System, ADDS performed the scan line reversal and computed the initial detector gains and biases. The image data and detector parameters were then passed to LAS which performed the histogram normalization, corrected the image data, and stored the A-data on tape.

TIPS performs all of the radiometric processing internally. A-data is stored on either computer compatible tapes (CCT's) or high density tapes (HDT's) in a band-interleaved-by-line format. TIPS is able to complete the radiometric correction of the data for all seven spectral bands from an entire TM scene in less than five minutes (Fischel, 1983).

Geometric correction is performed after radiometric correction. The purpose of geometric correction is to create a nearly conformal representation of the surface consisting of TM multispectral digital image data in which the data for each spectral band are precisely registered to the data from every other spectral band. To this end, the data from each band are registered to either the Space Oblique Mercator (SOM) or the Universal Transverse Mercator (UTM) cartographic projections. The geometric processing begins in the Mission Management Facility (MMF) with the payload correction data and the mirror scan correction data.

Within the MMF, geometric correction matrices are derived from the payload correction data and the mirror scan correction data. These matrices define the location of all TM samples on the output coordinate system. The output coordinate system consists of a 28.5-by-28.5 m grid registered to either the SOM or UTM projection. Collectively, the correction matrices are referred to as systematic correction data (SCD) (Beyer, 1983).

By use of the payload correction data, the derivation of the systematic correction data takes into account the following factors: sensor and satellite attitude; satellite ephemeris; high frequency structural disturbances, commonly called jitter, caused by operation of the instruments aboard the satellite; the TM optics and the location of the detectors on the focal planes; nonlinearities in the scan mirror profile and the operation of the scan line corrector; and the desired cartographic representation of the three-dimensional surface viewed by the sensor. Errors, however, may remain in the spatial transformation defined by the systematic correction data due to limits in the accuracy of the data. To minimize low-frequency bias and drift errors, TIPS is capable of using ground control points to adjust the sytematic correction data. The adjusted data are called geodetic correction data (GCD). The derivation of the GCD is described in detail by Beyer (1983).

For each spectral band, the spatial transformation defined by the SCD or the GCD is used to digitally overlay the registered, 28.5-by-28.5 m, output grid onto the input image which consists of A-data. A digital count is then assigned to each output grid cell by a cubic convolution resampling of the input image data. Figure 9 illustrates the resampling procedure. The pixels along each input scan line are first resampled to assign digital counts to temporary pixels located at the intersection of the output columns and the input scan lines. The temporary pixels are then resampled to assign digital counts to the grid cells of the output image.

The resampling procedures also compensates for spatial gaps which often occur between the last scan line generated during a mirror sweep and the first scan line of the subsequent sweep. The gaps are caused by small fluctuations in the sensor's viewing geometry as measured by the payload correction data. To fill in the gaps with data, pixels are generated for locations on synthetic scan lines which extend into the spatial gap and run parallel to the scan lines of the upper mirror sweep (Figure 10). The extension pixels are derived from a resampling of the temporary pixels of both the upper and lower sweeps and are located at the intersection of the output image columns and the synthetic scan lines. The extension pixels are then resampled to

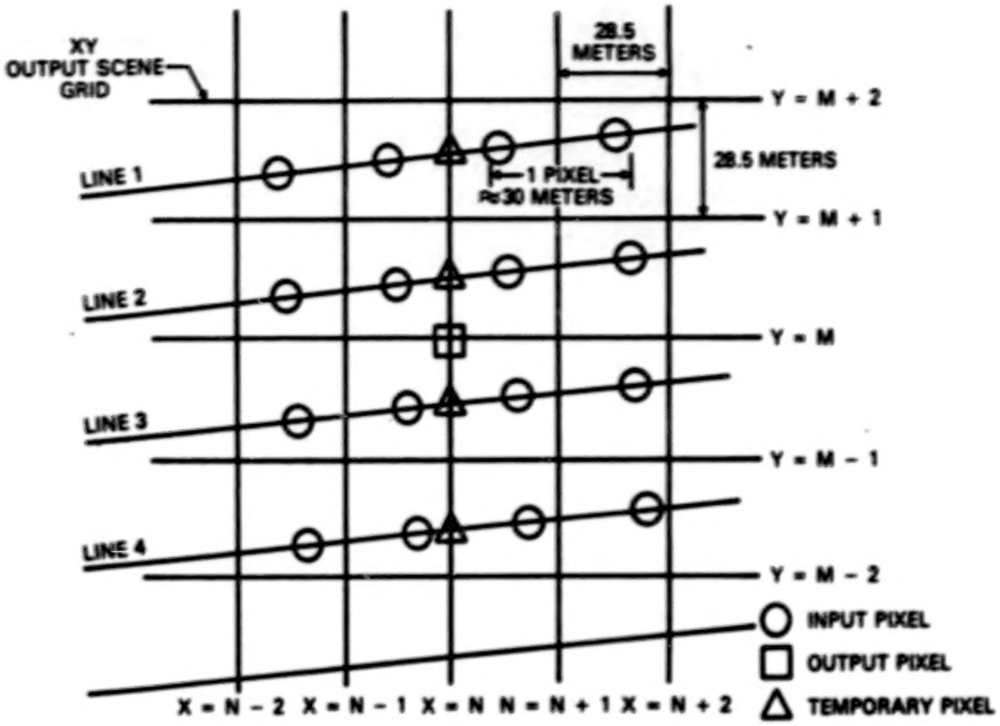
XY OUTPUT SCENE GRID
28.5 METERS
Y = M + 2
LINE 1
28.5 METERS
1 PIXEL ≈30 METERS
Y = M + 1
LINE 2
Y = M
LINE 3
Y = M - 1
LINE 4
Y = M - 2
INPUT PIXEL
OUTPUT PIXEL
X = N - 2
X = N - 1
X = N
N = N + 1
X = N + 2
TEMPORARY PIXEL

Figure 9. Resampling of Thematic Mapper Data for Geometric Correction (Lyon et al., 1983)

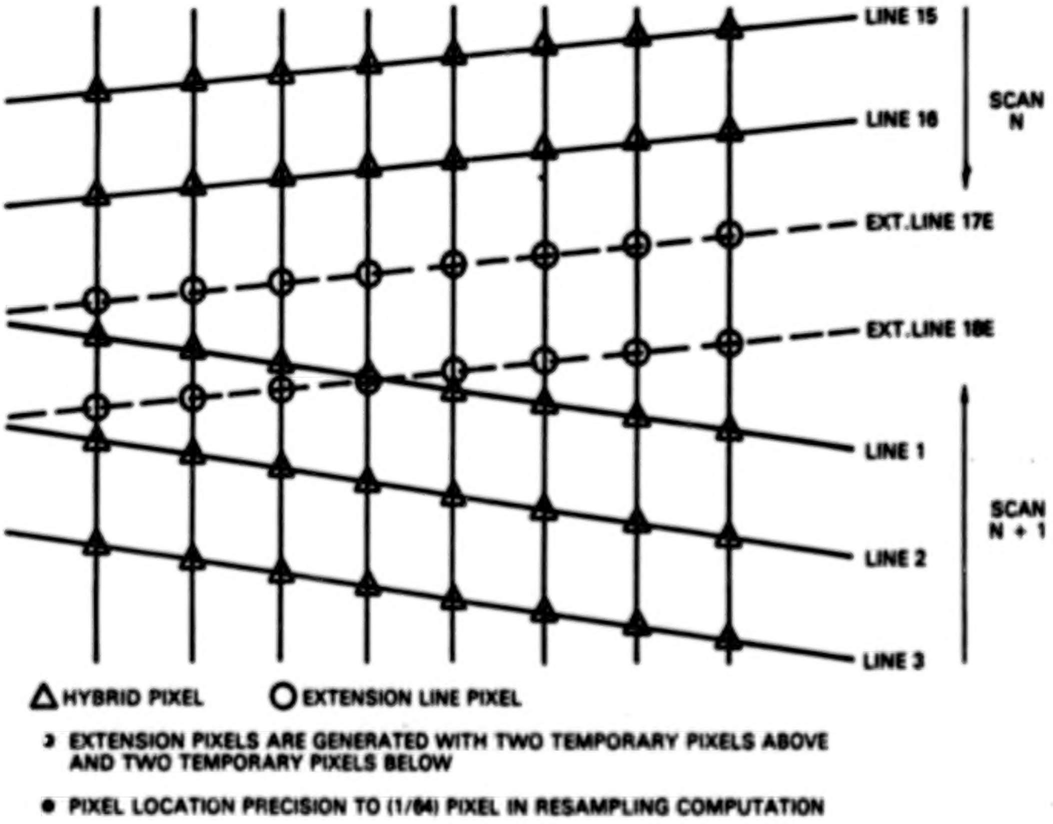
LINE 15
LINE 16
SCAN N
EXT.LINE 17E
EXT.LINE 18E
LINE 1
LINE 2
LINE 3
SCAN N + 1
HYBRID PIXEL
EXTENSION LINE PIXEL

- EXTENSION PIXELS ARE GENERATED WITH TWO TEMPORARY PIXELS ABOVE AND TWO TEMPORARY PIXELS BELOW
- PIXEL LOCATION PRECISION TO (1/64) PIXEL IN RESAMPLING COMPUTATION

Figure 10. Scan Line Extension for Geometric Correction (Lyon et al., 1983)

derive digital counts for output grid cells falling in the gaps of the input image. This resampling procedure is rather complex and is described in more detail by Beyer (1983).

Geometric correction of the TM thermal data requires special consideration. Recall that only four detectors are used to acquire thermal data, and one pixel of raw thermal data represents an area equivalent to four pixels from any of the reflective bands. To facilitate multispectral analyses of TM data, the coarse resolution thermal data is also resampled to form a registered grid of 28.5m-by-28.5m pixels. Thus, all bands of geometrically correct TM data contain the same number of pixels per unit area.

The Scrounge System did not use ground control points for geometric corrections. The SCD were passed from the Mission Management Facility (MMF) to ADDS. The SCD were then attached to the TM image data (B-data) and sent to LAS. After radiometric corrections, LAS used the SCD for the resampling of the A-data and creation of a registered output image (Lyon et al., 1983). TM digital image data which have undergone both the radiometric and geometric corrections are referred to as P-data. The LAS stored P-data on CCT's in a band sequential format.

A ground control point library is being developed for TIPS. If points are available for the area represented by a particular TM scene, TIPS accepts the systematic correction data (SCD) from the MMF and then derives geodetic correction data from the SCD by use of ground control point processing. TIPS then uses the GCD for resampling of A-data to create P-data. TIPS stores the P-data on both HDT's and CCT's in a band-sequential format. TIPS completes the geometric processing of one TM scene in less than eight minutes (Fischel, 1983).

In summary, raw TM data undergoes extensive processing before image products are generated for investigators. Figure 11 provides an overview of TM data processing by the TM Ground Segment at GSFC and Figure 12 illustrates the flow of the data through the Ground Segment hardware. The intention of this processing is to enhance data utility for scientific research.

The standard data products from the Scrounge System are digital P-data on CCT's and pictorial imagery derived from P-data by use of a film recorder. All P-data generated to date have been registered to the SOM cartographic projection, but if requested, P-data registered to the UTM system can be produced. Investigators can also obtain A-data and, if requested before processing begins, B-data on CCT's. In addition to image data, the Scrounge System CCT's contain Header, Ancillary, Annotation, and Trailer (HAAT) files which include scene path and row indices, date of data acquisition, and the radiometric look up tables and correction data used for geometric correction. The Scrounge System required approximately seven hours to complete both the radiometric and geometric processing of one, seven-band TM scene. Scrounge System products were shipped to the EROS Data Center for public dissemination.

TIPS is able to complete the processing of an entire TM scene in less than 15 minutes. The image products from TIPS include digital A-data and P-

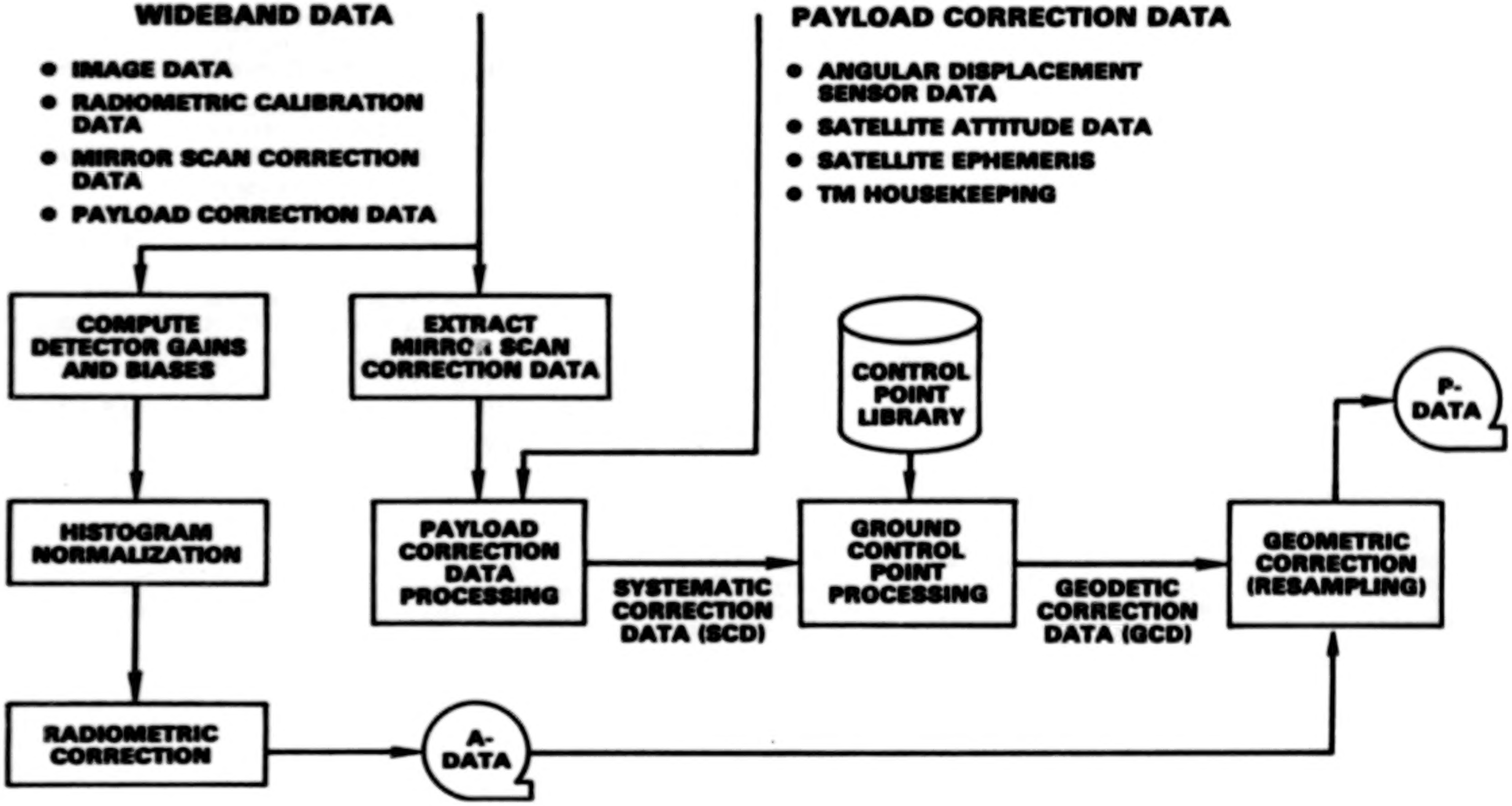
WIDEBAND DATA
● IMAGE DATA
● RADIOMETRIC CALIBRATION DATA
● MIRROR SCAN CORRECTION DATA
● PAYLOAD CORRECTION DATA
PAYLOAD CORRECTION DATA
● ANGULAR DISPLACEMENT SENSOR DATA
● SATELLITE ATTITUDE DATA
● SATELLITE EPHEMERIS
● TM HOUSEKEEPING
COMPUTE DETECTOR GAINS AND BIASES
EXTRACT MIRROR SCAN CORRECTION DATA
CONTROL POINT LIBRARY
P-DATA
HISTOGRAM NORMALIZATION
PAYLOAD CORRECTION DATA PROCESSING
SYSTEMATIC CORRECTION DATA (SCD)
GROUND CONTROL POINT PROCESSING
GEODETIC CORRECTION DATA (GCD)
GEOMETRIC CORRECTION (RESAMPLING)
RADIOMETRIC CORRECTION
A-DATA

Figure 11. Overview of Thematic Mapper Data Processing (Lyon et al., 1983)

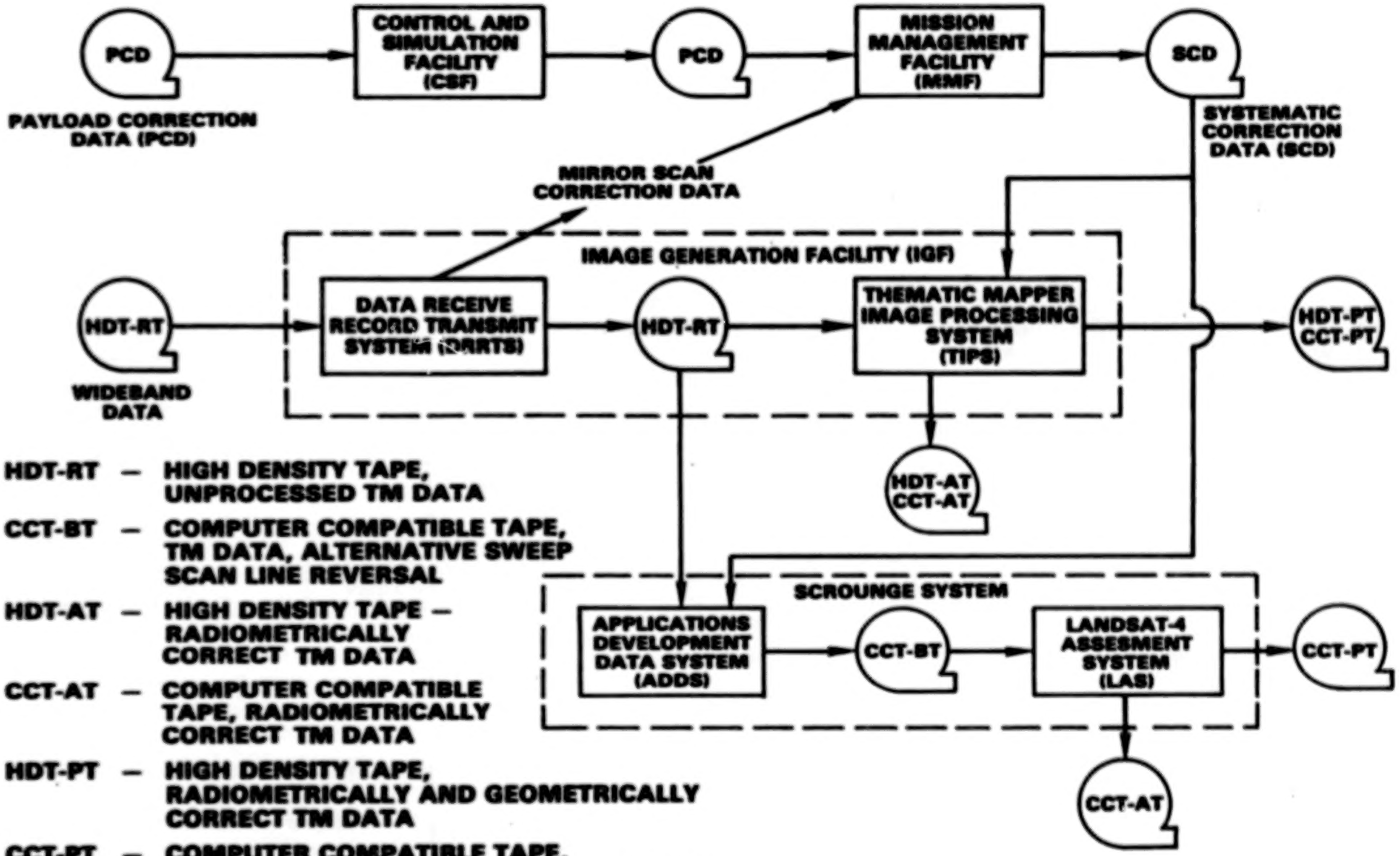
PCD
PAYLOAD CORRECTION DATA (PCD)
CONTROL AND SIMULATION FACILITY (CSF)
PCD
MISSION MANAGEMENT FACILITY (MMF)
SCD
SYSTEMATIC CORRECTION DATA (SCD)
MIRROR SCAN CORRECTION DATA
IMAGE GENERATION FACILITY (IGF)
HDT-RT
WIDEBAND DATA
DATA RECEIVE RECORD TRANSMIT SYSTEM (DRRTS)
HDT-RT
THEMATIC MAPPER IMAGE PROCESSING SYSTEM (TIPS)
HDT-PT CCT-PT
HDT-AT CCT-AT
SCROUNGE SYSTEM
APPLICATIONS DEVELOPMENT DATA SYSTEM (ADDS)
CCT-BT
LANDSAT-4 ASSESMENT SYSTEM (LAS)
CCT-PT
CCT-AT

HDT-RT — HIGH DENSITY TAPE, UNPROCESSED TM DATA

CCT-BT — COMPUTER COMPATIBLE TAPE, TM DATA, ALTERNATIVE SWEEP SCAN LINE REVERSAL

HDT-AT — HIGH DENSITY TAPE — RADIOMETRICALLY CORRECT TM DATA

CCT-AT — COMPUTER COMPATIBLE TAPE, RADIOMETRICALLY CORRECT TM DATA

HDT-PT — HIGH DENSITY TAPE, RADIOMETRICALLY AND GEOMETRICALLY CORRECT TM DATA

CCT-PT — COMPUTER COMPATIBLE TAPE, RADIOMETRICALLY AND GEOMETRICALLY CORRECT TM DATA

Figure 12. Thematic Mapper Data Flow Through the Ground Segment Facilities

data, along with the associated HAAT files, stored on both HDT's and CCT's. The A-data is stored in a band-interleaved-by-line format and the P-data is stored in a band sequential format. Pictorial imagery is also derived from the TIPS P-data using the film recorder. TIPS products are also shipped to the EROS Data Center. Specifications for TIPS operations call for the complete processing of a TM scene within 48 hours of the reception of the raw data at GSFC.

TM SENSOR PERFORMANCE AND IMAGE DATA QUALITY

Preliminary results of the Landsat-4 Image Data Quality Analysis (LIDQA) investigations were presented at a symposium held at GSFC in February, 1983. Results indicate that the sensor was performing quite well, and the quality of data processed by the Scrounge System is excellent. Most indicators of geometric and radiometric quality are comparable to or exceed prelaunch specifications.

Current evaluations of geometric correction results focus on band-to-band registration accuracy. Specifications call for registration errors of less than 0.2 pixels (6m) between bands. On the basis of the preliminary reports, the bands of the primary focal plane (TM1 to TM4) are registered to within 0.1 pixels. The registration errors between the middle-infrared bands (TM5 and TM7) of the cold focal plane are also less than 0.1 pixels. Misregistration of approximately 0.75 pixels along-scan and 0.20 pixels across-scan, however, has been found between the bands of the cold focal plane and the bands of the primary focal plane. The misregistration is attributed to small changes in the relative locations of the two focal planes resulting from vibration testing and launch stress. The thermal band detectors (TM6) are also located on the cold focal plane, and three pixel misregistration was observed between thermal band data and data from the other spectral bands. A Scrounge System software error was discovered as the cause of the thermal band misregistration. This error has been corrected and other software changes have been made to account for the shift in the relative location of the focal planes.

Ground segment performance specifications require temporal (scene-to-scene) registration errors of less than 0.3 pixels and geodetic (scene-to-map) registration errors of less than 0.5 pixels. Neither the temporal nor the geodetic registration of TM data, however, have been thoroughly assessed. Sufficient multitemporal data sets have not yet been processed for evaluations of temporal registration. Studies of geodetic registration are awaiting the incorporation of ground control points into the correction process.

Before launch, much concern was directed towards the potential effects of high frequency spacecraft vibrations, commonly called jitter, on image geometric quality. These concerns have been alleviated by post launch analyses of TM data. The most noticeable effect of jitter is spatial overlap or underlap between the last scan lines generated during a particular scan mirror sweep and the first several scan lines of the next sweep. An analysis of 20 TM scenes (Kogut and Larduinat, 1983) demonstrated that the maximum overlap or underlap in a scene is, on average, much less than one pixel (Table 5). This overlap is effectively removed by the geometric processing of TM data (Lyon et al., 1983).

Some small geometric problems are caused by the replacement of data from the third detector of band TM5 and the fourth detector of band TM2. The replacements cause the appearance of small discontinuities in images of some smooth, narrow features.

Table 5. TM Maximum Overlap/Underlap Statistics for 20 Scenes from Day 15 to Day 50 After Launch (Kogut and Larduinat, 1982).

	OVERLAP (PIXELS)		UNDERLAP (PIXELS)	
BAND	MEAN	STD. DEV.	MEAN	STD. DEV.
1	-0.326	0.046	0.356	0.019
2	-0.332	0.046	0.358	0.017
3	-0.337	0.047	0.360	0.017
4	-0.340	0.047	0.360	0.017
5	-0.345	0.049	0.358	0.018
6	-0.034	0.012	0.141	0.004
7	-0.344	0.049	0.359	0.017

The radiometric quality of processed TM data appears good, but not perfect. Minor detector-to-detector striping, on the order of one or two digital counts, remains within the data for the reflective spectral bands. This striping becomes visually apparent only when TM imagery is subjected to extreme contrast enhancement. The striping is attributed primarily to variation in detector bias from scan-to-scan and, possibly, variation along a scan. More dramatic striping has been observed in thermal band data. Much of the thermal striping was caused by a software problem which has been corrected.

Sweep-to-sweep striping is also found between groups of 16 scan lines in processed TM data. This striping is attributed to direct current restore circuitry which does not perform identically for the two scan directions employed by the TM. The circuitry apparently creates a different bias in each direction for each detector. The calculation of biases as a function of scan direction is under investigation for improved radiometric corrections.

Another radiometric problem is caused by the TM analog-to-digital (A/D) converter aboard the satellite. The A/D converter does not distribute an equal increment of signal into each digital count bin. In other words, the increment of radiance represented by a specific digital count is not necessarily the same as the increment represented by another count. Fortunately, the digital response of the detectors over the full eight-bit range has remained linear.

The effect of the A/D converter performance is apparent in A-data given frequency histograms of data from each detector. A particular digital value will occur much more or much less frequently than neighboring values. This effect is masked in P-data by the resampling procedure used to geometrically correct the data.

The radiometric responses of the thermal band detectors vary over time (Lansing and Barker, 1983). Data were not acquired from the cold focal plane detectors until the focal plane was outgassed in August, 1982. A gradual build up of water vapor condensation on the cold focal plane caused the detectors' gains to slowly decrease until outgassing was again performed in January, 1983. Table 6 presents the average dynamic ranges for the thermal band detectors after outgassing and just prior to the second outgassing. Apparently, periodic outgassing is needed to return the response of the thermal detectors to their initial levels of performance.

The absolute calibration for the reflective spectral bands has not yet been extensively evaluated. Calibration assessments will be provided by ongoing LIDQA studies which are comparing TM observations of uniform surface features to ground measurements of reflected radiance.

The TM detectors are performing very well with respect to noise. Signal-to-noise ratios have been derived for each detector from calibration studies made prior to launch. Almost all detectors have greater ratios than specified before instrument fabrication. Table 7 lists the average signal-to-noise ratio for the 16 detectors of each reflective band given the minimum spectral radiance required to saturate the detectors' responses (i.e., produce a response of 255 digital counts).

CURRENT STATUS OF TM DATA COLLECTION

Before the failure of the X-band transmitter aboard Landsat-4, over 6,000 scenes of TM data were received by the two ground stations. Approximately 1,000 of these scenes contain less than 20% cloud cover and were acquired while the solar elevation was greater than 20°. Current plans call for the processing of these 1,000 scenes by either the Scrounge System or TIPS. Some additional scenes with lower solar elevations or greater cloud cover may also be processed. As of July 6, 1983, the Scrounge

Table 6. Average Dynamic Range of Thermal Band Detectors (Lansing and Barker, 1983)

	RMIN (mW/cm^2·sr·μm)	RMAX
Prior to second outgassing	-0.05	2.13
After first and second outgassing	0.20	1.56

RMIN is the spectral radiance corresponding to zero counts.

RMAX is the minimum spectral radiance required for saturation (255 counts).

Table 7. Signal-to-Noise Ratios for the Detectors of the TM Reflective Bands (Barker et al., 1983).

	Signal-to-Noise Ratios at the RMAX*	
Band	Specified	Observed
TM1	85	152
TM2	170	281
TM3	143	235
TM4	240	341
TM5	75	180
TM7	45	175

RMAX is the minimum spectral radiance required for saturation (255 counts).

System had completed processing of 224 scenes and forwarded the P-data to the EROS Data Center. Figure 13 shows the location of the processed scenes and Table 8 lists EROS Data Center prices for TM image products. Eight of the TM scenes at the EROS Data Center are nighttime scenes.

Table 8. EROS Data Center Prices for TM Image Products

	Present	Effective 10/1/83	Effective 2/1/84
Pictorial Imagery			
10 in film (B & W; Pos)	$38	$50	$75
10 in film (B & W; Neg)	42	60	80
10 in paper (B & W)	33	50	75
20 in paper (B & W)	70	95	140
40 in paper (B & W)	115	50	200
10 in paper (color)	105	140	190
10 in paper (color)	75	115	170
20 in paper (color)	135	200	235
40 in paper (color)	235	275	290
Digital Products			
TM CCT full scene (9 track, 6250 bpi, 4 tapes)	2800	3400	4400
TM CCT, quarter-scene (9-track, 6250 bpi, 1 tape)	750	925	1350

References Cited

Barker, J. L., D. L. Ball, K. C. Leung, and J. A. Walker. 1983. Prelaunch Absolute Radiometric Calibration of the Reflective Bands on Landsat-4 Protoflight Thematic Mapper. presented at the Landsat-4 Scientific Characterization Early Results Symposium, February 22-24, 1983, NASA/Goddard Space Flight Center, Greenbelt, MD.

Beyer, E. P. 1983. An Overview of the Thematic Mapper Geometric Correction System. Landsat-4 Reference Document TI.01, Science Office Library, Code 902, Goddard Space Flight Center, Greenbelt, MD.

Engel, J. L. 1980. Thematic Mapper - An Interim Report on Anticipated Performance. Proceedings of the AIAA Sensor Systems for the 80's Conference, Colorado Spring, CO: pp. 25-37.

Fischel, D. 1983. Some Current Uses of Array Processors for Preprocessing of Remote Sensing Data. presented at the Seventeenth International Symposium on Remote Sensing of Environment, May 9-13, 1983, Ann Arbor, MI.

Kogut, J., and E. Larduinat. 1982. A Preliminary Analysis of the High Frequency Vibrations in Early Landsat-4 Thematic Mapper Scenes. (Contractor Report. Research and Data Systems, Inc., Lanham, MD).

Lansing, J. C., and J. L. Barker. 1983. Thermal Band Characterization of Landsat-4 Thematic Mapper. presented at the Landsat-4 Scientific Characterization Early Results Symposium, February 22-24, 1983, NASA/Goddard Space Flight Center, Greenbelt, MD.

Lyon, J. C., D. Fischel, and E. Beyer. 1983. Production and Analyses of Output Data Products for Landsat-4 in the Engineering Check-Out Phase. presented at the Twenty-First Goddard Memorial Symposium, March 24-25, 1983, NASA/Goddard Space Flight Center, Greenbelt, MD.

Markham, B. L., and J. Barker. 1983. Spectral Characterization of the Landsat Thematic Mapper Sensors. presented at the Landat-4 Scientific Characterization Early Results Symposium, February 22-24, 1983, NASA/Goddard Space Flight Center, Greenbelt, MD.

Salomonson, V. V., P. L. Smith, Jr., A. B. Park, W. C. Webb, and T. L. Lynch. 1980. An Overview of Progress in the Design and Implementation of Landsat-D Systems. IEEE Transactions on Geoscience and Remote Sensing, Vol. GE-18, No. 2: pp. 137-146.

N85-20510 D2

RADIOMETRIC CALIBRATION AND PROCESSING PROCEDURE FOR REFLECTIVE BANDS ON LANDSAT-4 PROTOFLIGHT THEMATIC MAPPER

J. L. Barker

NASA/Goddard Space Flight Center
Greenbelt, Maryland 20771

R. B. Abrams, D. L. Ball, and K. C. Leung

Computer Sciences Corporation
8728 Colesville Road
Silver Spring, Maryland 20910

RADIOMETRIC CALIBRATION AND PROCESSING PROCEDURES FOR REFLECTIVE BANDS ON LANDSAT-4 PROTOFLIGHT THEMATIC MAPPER

ABSTRACT

This paper provides descriptive and procedural background material for understanding results that are given in the following papers by Barker et al. appearing in these Proceedings: "Prelaunch Absolute Radiometric Calibration of the Reflective Bands on the Landsat-4 Protoflight Thematic Mapper," "Characterization of Radiometric Calibration of Landsat-4 TM Reflective Bands," "TM Digital Image Products for Applications," and "Relative Radiometric Calibration of Landsat-4 TM Reflective Bands."

The radiometric subsystem of NASA's Landsat-4 Thematic Mapper (TM) sensor is described. Special emphasis is placed on the internal calibrator (IC) pulse shapes and timing cycle. The procedures for the absolute radiometric calibration of the TM channels with a 122-centimeter integrating sphere and the transfer of radiometric calibration from the channels to the IC are reviewed.

The use of the IC to calibrate TM data in the ground processing system consists of pulse integration, pulse averaging, IC state identification, linear regression analysis, and histogram equalization. An overview of the SCROUNGE-era (before August 1983) method is presented. Procedural differences between SCROUNGE and the TIPS-era (after July 1983) and the implications of these differences are discussed.

KEY WORDS: absolute calibration, relative calibration, band-to-band calibration, internal calibration system, SCROUNGE, TIPS, scan cycle timeline, Thematic Mapper, Landsat-4

INTRODUCTION

Absolute calibration is essential for a variety of scientific studies and image analysis applications. Arithmetic spectral transformations, such as those used to determine path radiance for removal or normalization of atmospheric effects, require absolute radiometric data. To extend signatures, based on averages or moments, beyond a scene, to data collected in different scenes or at different times under different atmospheric conditions, or even to data collected by different satellites, requires both an absolute measure of radiance and correction for atmospheric effects.

PRECEDING PAGE BLANK NOT FILMED

PAGE II-48 INTENTIONALLY BLANK

Understanding the innate bidirection reflectance characteristics of the target depends on exact knowledge of reflected radiance. To evaluate theoretical models that relate spectral radiance to ground and/or atmospheric parameters, numerical values for radiance are necessary.

To achieve absolute radiometric accuracy, frequent in-orbit recalibration of the sensor system is necessary. The Landsat-4 Thematic Mapper (TM) meets this need with an internal calibration (IC) system based on incandescent lamps controlled by photodiode incandescent circuits. The IC system itself, however, is not immune to changes with time. Frequent recalibration by a constant external source, such as the Sun, would increase the absolute radiometric accuracy. Use of the IC can provide relative radiometric accuracy, which is essential to eliminate striping and to delineate boundaries.

This paper describes the prelaunch absolute radiometric calibration procedures and the relative radiometric calibration procedures in the postlaunch ground processing of the six reflective bands. Both SCROUNGE and TIPS (TM Image Processing System) methodologies are discussed. Lyons et al. (1984) present an overview of the entire SCOUNGE system, with special emphasis on geometric correction procedures. Lansing and Barker (1984) describe the calibration procedures for the thermal band (band 6).

THEMATIC MAPPER RADIOMETRIC SUBSYSTEM

This section briefly reviews background essential to this paper and characterizes raw data obtained from the IC system. Engel (1980) describes the TM in detail.

The TM observes radiance reflected from the Earth's surface in six bands of the following wavelengths: 0.45 to 0.52 µm, 0.52 to 0.60 µm, 0.63 to 0.69 µm, 0.76 to 0.90 µm, 1.55 to 1.75 µm, and 2.08 to 2.35 µm. Each band comprises 16 detectors that create 16 raster lines as the ground is scanned in a cross-track direction. Data are collected during the full cycle of the scan mirror rotation resulting in both west-to-east and east-to-west scans. In descending orbits (daytime), west-to-east scans are known as forward scans and east-to-west scans, as reverse scans; in ascending orbits, the converse occurs. The 64 silicon detectors that form the first four bands reside in the primary focal plane. The indium antimonide detectors used for the remaining two reflective bands, bands 5 and 7, reside in a cooled focal plane. On each band, the eight even-numbered detectors lie in a separate row, staggered from the odd-numbered detectors, and have separate electronic connections. Figures 1 and 2 show the path that light travels within the TM.

The IC consists of three miniature tungsten filament lamps for the reflective bands, a blackbody for the thermal band, and a flex pivot-mounted resonant shutter. The IC inserts reference radiance levels just ahead of the spectral filters of each band at the prime focal plane while obscuring the Earth view of the detector array. To do this correctly, the IC shutter flag motion must be synchronized with that of the scan mirror assembly and the scan line corrector. (Engel (1980) gives a description of these subsystems.) Figure 3 is an overview of the IC shutter flag and transfer optics. Figure 4 illustrates the optics for the three lamps.

Figure 5 is a scaled schematic timeline of a TM scan cycle showing the time periods during which the detectors observe the target image and during which the shutter flag obscures the image during scan mirror turnaround. It should be noted that the image obscuration time is subdivided into a dark period for the collection of background data and a period during which the radiance from the calibration lamps is in view. During 3 milliseconds of the dark period, the background radiation is adjusted to approach preset values. Tables 1 and 2 show all events on the TM scan timeline for a forward and a reverse scan.

The lamps in the IC operate at 1900 K, with the amplitude of each lamp in the normal mode controlled by a silicon photodiode in a feedback circuit to maintain a constant radiance level. (A backup mode that does not maintain the lamp radiance level is also available; with lamp aging, the backup mode will not provide stable lamp levels). The IC lamps, with energy balance filters and masks, output at levels reduced by 0, 25, and 50 percent (see Figure 4). A bundle of six fiber optic threads delivers the combined lamp output to the shutter flag. This method of transmitting radiation to the moving calibration shutter allows the lamps to provide radiation independently and to contribute proportionately toward illuminating all detectors. When in the automatic sequencing mode, the three lamps are cycled automatically to provide eight calibration levels (seven plus dark) to all detectors of bands 1 through 5 and 7. Each level is on for approximately 40 scans. In this paper, lamp configuration is indicated by three binary digits (that is, 100 means lamp A is on and B and C are off, 011 means only B and C are on, and so on).

The shape of the pulse output by the internal calibration system depends on the physical location of the detector with respect to the calibration light source. Detectors are

Landsat-4 Thematic Mapper (TM) Optical Path

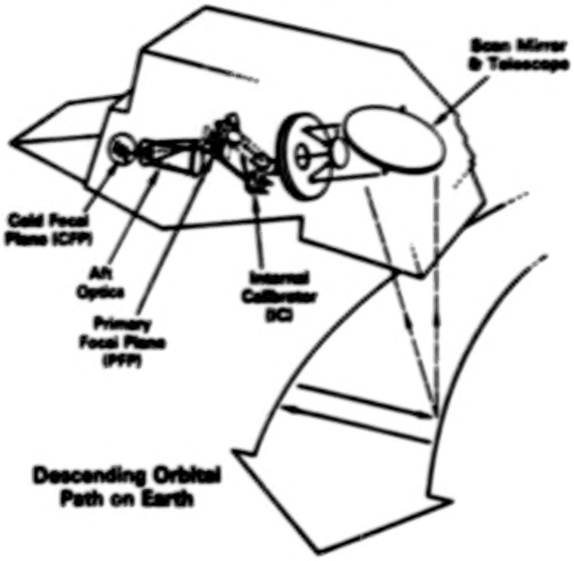
Scan Mirror & Telescope
Cold Focal Plane (CFP)
Aft Optics
Primary Focal Plane (PFP)
Internal Calibrator (IC)
Descending Orbital Path on Earth

FIGURE 1

TM Optical Path
Landsat-4 Thematic Mapper

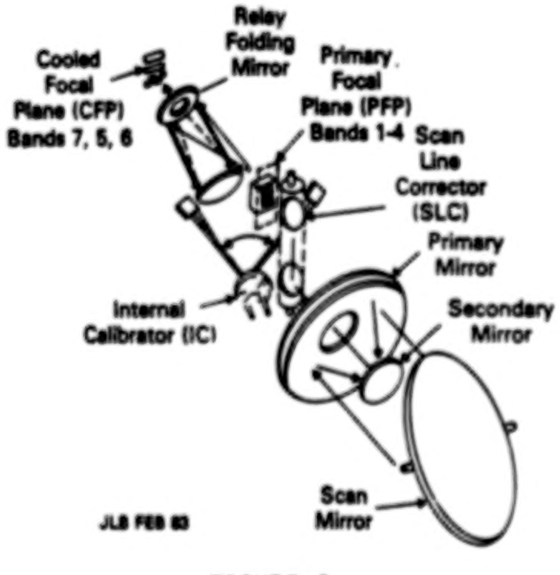
Cooled Focal Plane (CFP) Bands 7, 5, 6
Relay Folding Mirror
Primary Focal Plane (PFP) Bands 1-4
Scan Line Corrector (SLC)
Primary Mirror
Internal Calibrator (IC)
Secondary Mirror
Scan Mirror
JLB FEB 83

FIGURE 2

LANDSAT-4 THEMATIC MAPPER INTERNAL CALIBRATION TRANSFER OPTICS

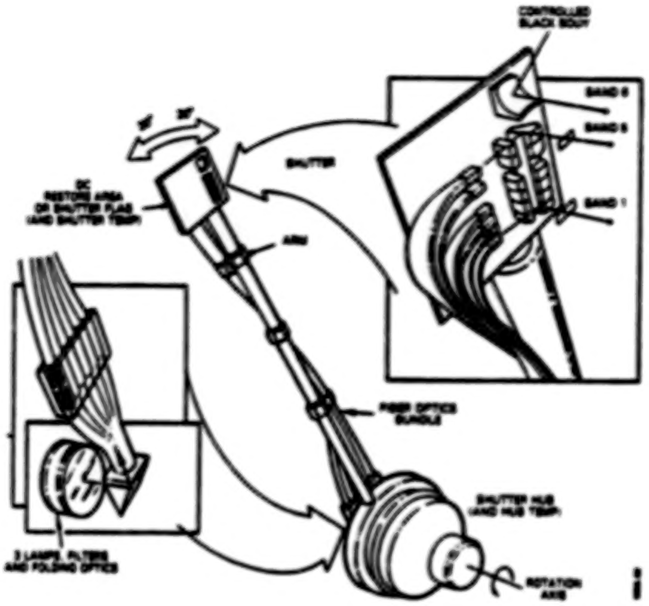
CONTROLLED BLACK BODY
BAND 6
BAND 5
BAND 1
SHUTTER
DC RESTORE AREA OR SHUTTER FLAG (AND SHUTTER TEMP)
ARM
FIBER OPTICS BUNDLE
SHUTTER HUB (AND HUB TEMP)
3 LAMPS, FILTERS AND FOLDING OPTICS
ROTATION AXIS

FIGURE 3

LANDSAT-4 THEMATIC MAPPER INTERNAL CALIBRATION THREE LAMP OPTICS

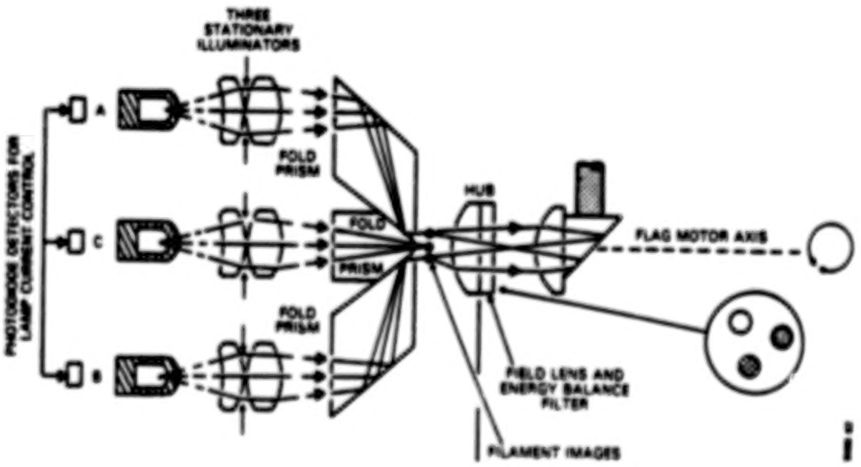
THREE STATIONARY ILLUMINATORS
PHOTODIODE DETECTORS FOR LAMP CURRENT CONTROL
A
C
B
FOLD PRISM
FOLD
PRISM
FOLD PRISM
HUB
FLAG MOTOR AXIS
FIELD LENS AND ENERGY BALANCE FILTER
FILAMENT IMAGES

FIGURE 4

DIGITAL MINOR FRAME LOCATIONS FOR SUCCESSIVE TM SCANS

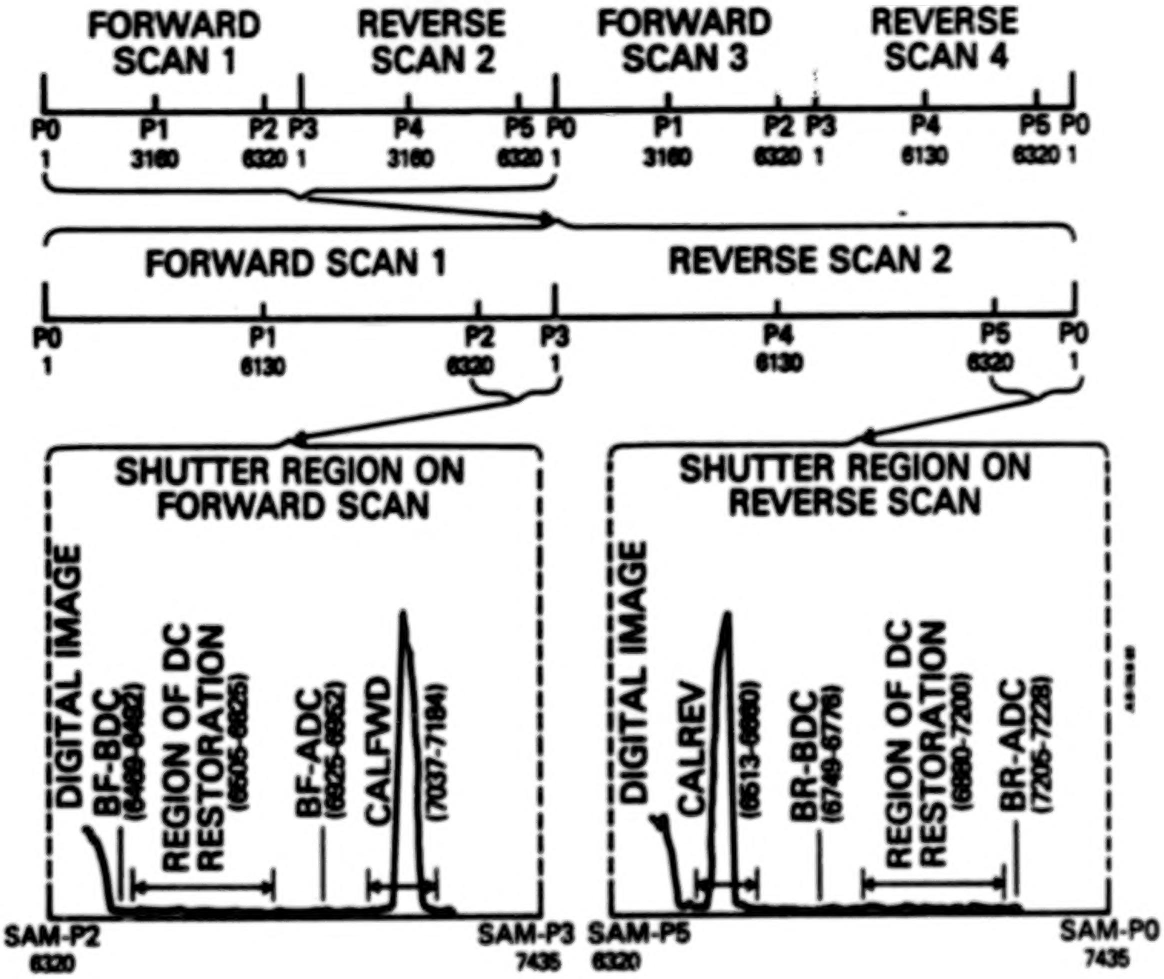
FORWARD SCAN 1
REVERSE SCAN 2
FORWARD SCAN 3
REVERSE SCAN 4
P0 1
P1 3160
P2 6320
P3 1
P4 3160
P5 6320
P0 1
P1 3160
P2 6320
P3 1
P4 6130
P5 6320
P0 1
FORWARD SCAN 1
REVERSE SCAN 2
P0 1
P1 6130
P2 6320
P3 1
P4 6130
P5 6320
P0 1
SHUTTER REGION ON FORWARD SCAN
DIGITAL IMAGE
BF-BDC (6469-6482)
REGION OF DC RESTORATION (6505-6825)
BF-ADC (6825-6852)
CALFWD (7037-7184)
SAM-P2 6320
SAM-P3 7435
SHUTTER REGION ON REVERSE SCAN
DIGITAL IMAGE
CALREV (6513-6660)
BR-BDC (6749-6776)
REGION OF DC RESTORATION (6880-7200)
BR-ADC (7205-7228)
SAM-P5 6320
SAM-P0 7435

FIGURE 5

]

Table 1
Timing Locations on Main Shutter during Odd Numbered (Forward) Scans of Internal Calibrator (IC) on Landsat-4 Thematic Mapper and Scrounge-ERA (1982-1983) Ground Processing IC Collect Windows

Collect Window Label	Location From Start of Line (mf)	Location From Start of Line (msec)	Minor Frame Label	Description of Label	Method of Calculating Location (2)	
(1)	(2)	(3)				
	1	0.00	P0	SAM SOL (Scan Angle Monitor FWD Start)	DEF	Start of mf Counting in ADDS
	3160	30.37	P1	SAM Midpoint of Active FWD Scan	NOM	From Scan Mirror Frequency
	6320	60.74	P2	SAM EOL End of Active FWD Scan	NOM	From Scan Mirror Frequency
	6383	61.35	EOIF16	End of Image (FWD) for CH 16	CALC	SOSF16-16= SOSF1-70
	6399	61.50	SOSF16	Start of IC Shutter (FWD) for CH 16	CALC	SOSF1-[(CALF1-CALF16) -54]
	6407	61.58	SADDSF	Start of 824mf ADDS FWD "MAP1" Buffer	DEF	
	6437	61.87	EOIF1	End of Image (FWD) for CH 1	CALC	SOSF1-16
	6453	62.02	SOSF1	Start of Shutter (FWD) for CH 1	OBS	ADDS Comtal of 2 NOV 82 Data
BF-BDC	6469	62.17	SBFBDC	Start of 24mf ADDS FWD BKGD Before DC	CALC	(Multiple of 4) +1 of(MBFBDC-12)
BF-BDC	6479	62.27	MBFBDC	Middle of ADDS FWD BKGD Before DC	CALC	(SOSF1 + SODCF) / 2
BF-BDC	6492	62.39	EBFBDC	End of 24mf ADDS FWD BDGD Before DC	CALC	SBFBDC + 24-1
	6505	62.52	SODCF	Start of DC Restore Region for FWD Scan	CALC	1.023 msec (106mf) to SOSF16
	6825	65.60	EODCF	End of DC Restore Region for FWD Scan	CALC	3.075 msec (320mf) to SODCF
BF-ADC	6925	66.56	SBFADC	Start of 28mf ADDS FWD BKGD After DC	CALC	(Multiple of 4)+1 of(MBFADC-14)
BF-ADC	6938	66.68	MBFADC	Middle of ADDS FWD BKGD After DC	CALC	(CALF16-32+EODCF) / 2
BF-ADC	6952	66.82	EBFADC	End of 28mf ADDS FWD BKGD After DC	CALC	SBFADC + 28 - 1
CALFWD	7037	67.63	SCALF	Start of 148mf ADDS CAL FWD Collect	DEF	Starting 20 May 83
CALFWD	7084	68.08	CALF16	Center of CAL FWD Pulse for CH 16	OBS	TRAPP (4) for 2 NOV 82 Scene
CALFWD	7109	68.32	CALF9	Center of CAL FWD Pulse for CH 9	OBS	TRAPP (4) for 2 NOV 82 Scene
CALFWD	7111	68.34	MCALF	Middle of CAL FWD Region	CALC	(CALF16 + CALF1) / 2
CALFWD	7112	68.35	CALF8	Center of CAL FWD Pulse For CH 8	OBS	TRAPP (4) for 2 NOV 82 Scene
CALFWD	7138	68.60	CALF1	Center of CAL FWD Pulse for CH 1	OBS	TRAPP (4) for 2 NOV 82 Scene
CALFWD	7184	69.05	ECALF	End of 148mf ADDS CAL FWD Collect	CALC	SCALF + 148-1
	7182	69.03	EOSF16	End of IC Shutter (FWD) for CH 16	OBS	ADDS Comtal of 2 NOV 82 Data
	7198	69.18	SOIR16	Start of Image Before REV Scan for CH 1	CALC	EOSF16 + 16
	7230	69.49	EADDSF	End of 824mf ADDS FWD "MAP1" BUFFER	DEF	
	7236	69.55	EOSF1	End of Shutter (FWD) for CH 1	CALC	EOSF16 + 54
	7252	69.70	SOIR1	Start of Image Before REV Scan for CH 1	CALC	EOSF1 + 16
	7435	71.46	P3	SAM SOL (Scan Angle Monitor REV Start)	CALC	71.46 msec/.009611 msec/mf

FOOTNOTES FOR TABLE 1
MF LOCATIONS FOR ODD-NUMBERED (FORWARD) SCANS

(1) Collection of digital data for radiometric calibration of TM during the Scrounge-Era preprocessing by ADDS, 824mf (minor frames) of IC (Internal Calibrator) data are temporarily put in a buffer of a Macro Array Processor (MAP1). These calibration data are collected starting at minor frame 6407, which is close to the end of the scene video data and the beginning of shutter obscuration. 200 of the 824mf are sent on to a Vax computer for use in radiometric calibration.

For odd-numbered scans (forward sweeps of the TM scan mirror), these 200mf from the IC shutter are collected from three separate regions (windows). Labels and descriptions for the three collect windows from each forward scan are given below:

BF-BDC	This is a 24mf region of dark level background (BKG) taken on a forward scan before DC restoration begins. Prior to May 20, 1983, there was a single 52mf ADDS BKG collect window which started before DC restoration, at MF 6543.
BF-ADC	28mf BKG taken after DC forward restoration ends.
CALFWD	This is a 148mf forward scan calibration (CAL) region containing the TM responses to light from the current configuration of the three IC lamps. Prior to December 22, 1982, the 148mf CAL collect window started at MF 7009. It then began at MF 7029 until May 20, 1983, when it was changed to MF 7037.

(2) MF (Minor Frame) locations were arrived at one of four ways:

DEF	By Definition
NOM	From nominal value of another variable
OBS	Observed from in-orbit digital data
CALC	Calculated from values of other MF locations and defined, nominal or observed relative differences

(3) MSEC (Milliseconds) locations were calculated from MF locations assuming a nominal 9.611 microseconds per minor frame.

(4) TRAPP is a TM Radiometric and Algorithmic Performance software program run on pre and postlaunch tapes at the LAS Facility.

Revised 25 MAY 83/JLB

Table 2
Timing Locations on Main Shutter during Even Numbered(Reverse) Scans of Internal Calibrator (IC) on Landsat-4 Thematic Mapper and Scrounge-ERA (1982-1983) Ground Processing IC Collect Windows

Collect Window Label	Location From Start of Line (mf)	Location From Start of Line (msec)	Minor Frame Label	Description of Label	Method of Calculating Location (2)	
(1)	(2)	(3)				
	1	0.00	P3	SAM SOL (Scan Angle Monitor REV Start)	DEF	Start of mf Count
	3160	30.37	P4	SAM Midpoint of Active REV Scan	NOM	From Scan Mirror Frequency
	6320	60.74	P5	SAM EOL (End of Active REV Scan)	NOM	From Scan Mirror Frequency
	6407	61.58	SADDSR	Start of 824mf ADDS REV "MAP1" Buffer	DEF	
	6453	62.02	EOIR1	End of Image (REV) for CH 1	CALC	(SOSR1-12); also OBS Comtal
	6465	62.14	SOSR1	Start of IC Shutter (REV) for CH 1	OBS	ADDS Comtal of 2 NOV 82 Data
	6507	62.54	EOIR16	End of Image (REV) for CH 16	CALC	(SOSR16-12); also OBS Comtal
CALREV	6513	62.60	SCALR	Start of 148mf ADDS CAL REV Collect	DEF	Starting 20 MAY 83
CALREV	6519	62.65	SOSR16	Start of IC Shutter (REV) for CH 16	OBS	ADDS Comtal of 2 NOV 82 Data
CALREV	6560	63.05	CALR1	Center of CAL REV Pulse for CH 1	OBS	TRAPP (4) Data for 2 NOV 82 Scene
CALREV	6580	63.24	CALR8	Center of CAL REV Pulse for CH 8	OBS	TRAPP (4) Data for 2 NOV 82 Scene
CALREV	6587	63.31	MCALR	Middle of CAL REV Region	CALC	(CALR1 + CALR16) / 2
CALREV	6614	63.57	CALR16	Center of CAL REV Pulse for CH 16	OBS	TRAPP (4) Data for 2 NOV 82 Scene
CALREV	6660	64.01	ECALR	End of 148mf ADDS CAL REV Collect	CALC	SCALR + 148-1
BR-BDC	6749	64.86	SBRBDC	Start of 28mf ADDS REV BKGD Before DC	CALC	(Multiple of 4)+1 of (MBRBDC-14)
BR-BDC	6763	65.00	MBRBDC	Middle of REV BKGD Before DC	CALC	(CALR16 + 32 + SODCR) / 2
BR-BDC	6776	65.12	EBRBDC	End of 28mf ADDS REV BKGD Before DC	CALC	SBRBDC + 28-1
	6880	66.12	SODCR	Start of DC Restore Region for REV Scan	CALC	4.098msec (426mf) to EOSR16
	7200	69.20	EODCR	End of DC Restore Region for REV Scan	CALC	3.075msec (320mf) to SODCR
BR-ADC	7205	69.25	SBRADC	Start of 24mf ADDS REV BKGD After DC	CALC	EBRADC - 24 + 1
BR-ADC	7226	69.45	MBRADC	Middle of REV BKGD After DC	CALC	(EODCR + EOSR1) / 2
BR-ADC	7228	69.47	EBRADC	End of 24mf ADDS REV BKGD After DC	CALC	First Multiple of 4 below EADDSR
	7230	69.49	EADDSR	End of 824mf ADDS REV "MAP1" Buffer	DEF	
	7252	69.70	EOSR1	End of IC Shutter (REV) for CH 1	CALC	SOSR1 + 787
	7264	69.81	SOIF1	Start of Image Before FWD Scan for CH 1	CALC	EOSR1 + 12
	7306	70.22	EOSR16	End of IC Shutter (REV) for CH 16	CALC	SOSR16 + 787
	7318	70.33	SOIF16	Start of Image Before FWD Scan for CH 16	CALC	EOSR16 + 12
	7435	71.46	P0	SAM SOL (Scan Angle Monitor FWD Start)	CALC	71.46 msec/.009611 msec/mf

FOOTNOTES FOR TABLE 2
MF LOCATIONS FOR EVEN-NUMBERED (REVERSE) SCANS

(1) Collection of digital data for radiometric calibration of TM during the Scrounge-Era preprocessing by ADDS, 824mf (minor frames) of IC (Internal Calibrator) data are temporarily put in a buffer of a Macro Array Processor (MAP1). These calibration data are collected starting at minor frame 6407, which is close to the end of the scene video data and the beginning of shutter obscuration. 200 of the 824mf are sent on to a Vax computer for use in radiometric calibration.

For even-numbered scans (reverse sweeps of the TM scan mirror), these 200 mf from the IC shutter are collected from three separate regions (windows). Labels and descriptions for the three collect windows from each reverse scan are given below:

CALREV	This is a 148mf reverse scan calibration (CAL) region containing the TM responses to light from the current configuration of the three IC lamps. Prior to December 22, 1982, the 148mf CAL collect window started at MF 6525. It then began at MF 6517 intil May 20, 1983, when it was changed to MF 6513.
BR-BDC	This is a 28mf region of dark level background (BKG) taken on a reverse scan before DC restoration begins.
BR-ADC	24mf BKG taken after DC reverse restoration ends. This is the same shutter location as the 24mf forward BKG. Prior to May 20, 1983, there was a single 52mf ADDS BKG collect window which started after DC restoration, at MF 7089.

(2) MF (Minor Frame) locations were arrived at one of four ways:

DEF	By definition
NOM	From nominal value of another variable
OBS	Observed from in-orbit digital data
CALC	Calculated from values of other MF locations and defined, nominal or observed relative differences.

(3) MSEC (milliseconds) locations were calculated from MF locations assuming a nominal 9.611 microseconds per minor frame.

(4) TRAPP is a TM Radiometric and Algorithmic Performance software program run on pre and postlaunch tapes at the LAS Facility.

Revised 25 May 83/JLB

stored by band number in even-numbered and odd-numbered rows; thus even (or odd) numbered channels of a given band have the same pulse shape. Sample pulses are provided in Appendix A (Figures A-1 through A-18); Figure 6 shows a typical pulse. Pulse shape is independent of scan direction. If the pulse from a reverse scan is overlaid on a forward scan pulse, the difference in counts for corresponding positions is at most two digital numbers (DN) (Figures 7 and 8).

Within a given band, the location of the pulse center progresses to higher numbered minor frames as the channel number decreases. Bands 1 and 4 have sharp asymmetric peaks; bands 2 and 3 have rounder, less asymmetric peaks. Bands 1 and 2 have peaks to the right of the pulse center in the forward scan; bands 3 and 4 have peaks to the left of the pulse center. In bands 1 and 2, the odd channels have larger pulses, about 6 counts higher in band 1 and 20 counts higher in band 2. The even channels in bands 3 and 4 have slightly larger pulses than the odd channels, about five counts in band 3 and two counts in band 4. Band 5 even pulses are 38 counts higher than odd pulses. For both even and odd channels, the pulse is asymmetric, peaking to the right of the center, but the odd-channel pulses are much rounder. Although even-channel pulses in bands 6 and 7 are only eight counts greater than odd-channel pulses, the pulse shapes are qualitatively different in the two cases. The even channels have nearly symmetrical rounded pulses, peaking slightly to the right of center. The odd channels have a flat plateau to the left of center, and then a peak to the right.

Figure 9 shows pulse averages, as determined by the Hughes method discussed below, versus scan number for a post-launch scene. It should be noted that transitions involving the turning on of a lamp result in approximately 15-percent overshoot. In mid-IR bands, bands 5 and 7, blackbody heat radiation from the newly turned off lamp contributes to the pulse height for approximately eight scans (four forward and four reverse).

ABSOLUTE RADIOMETRIC CALIBRATION PROCEDURE

Prelaunch absolute radiometric calibration of the TM sensor channels and the IC is critical because the TM does not observe the Sun or other extraterrestrial bodies of known radiance while in orbit. This section presents an overview of prelaunch absolute calibration procedures used on the Landsat-4 TM. A detailed discussion of the results of absolute calibration is presented in Barker et al. (1984a).

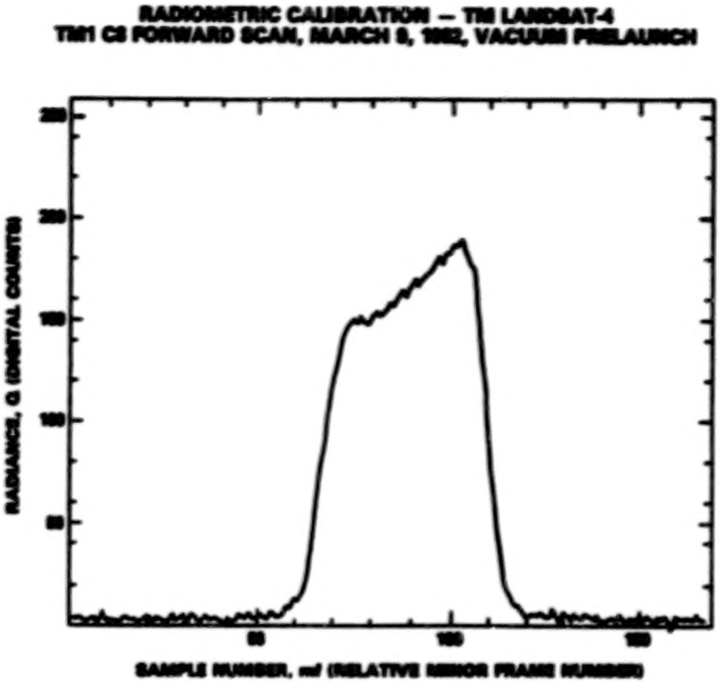
RADIOMETRIC CALIBRATION — TM LANDSAT-4
TM1 C8 FORWARD SCAN, MARCH 9, 1982, VACUUM PRELAUNCH

FIGURE 6

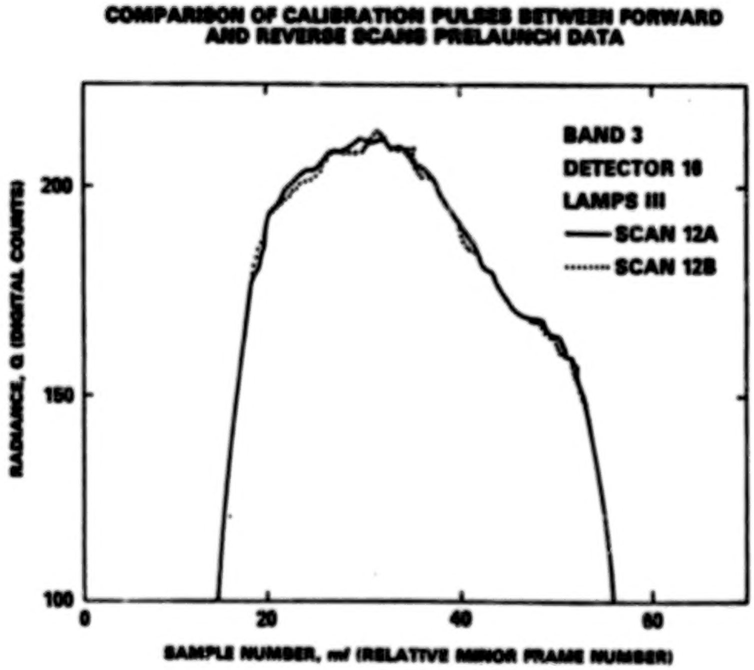
COMPARISON OF CALIBRATION PULSES BETWEEN FORWARD
AND REVERSE SCANS PRELAUNCH DATA

FIGURE 7

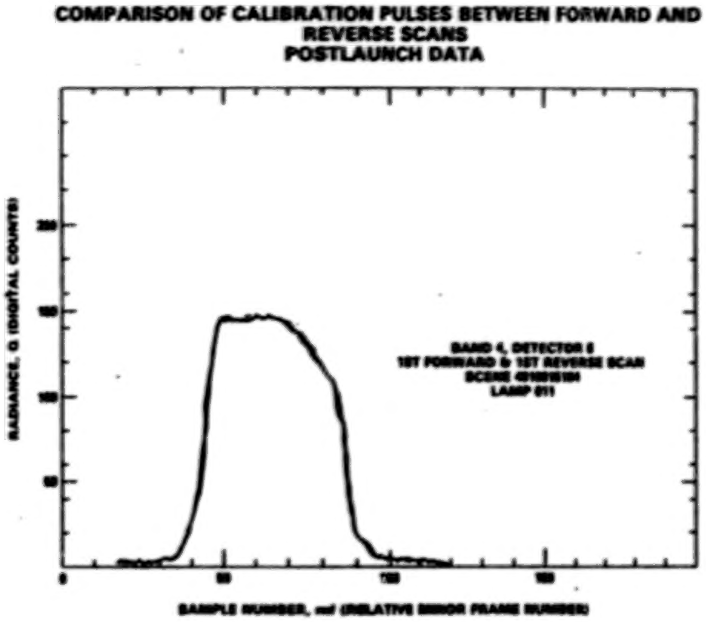
COMPARISON OF CALIBRATION PULSES BETWEEN FORWARD AND REVERSE SCANS
POSTLAUNCH DATA

FIGURE 8

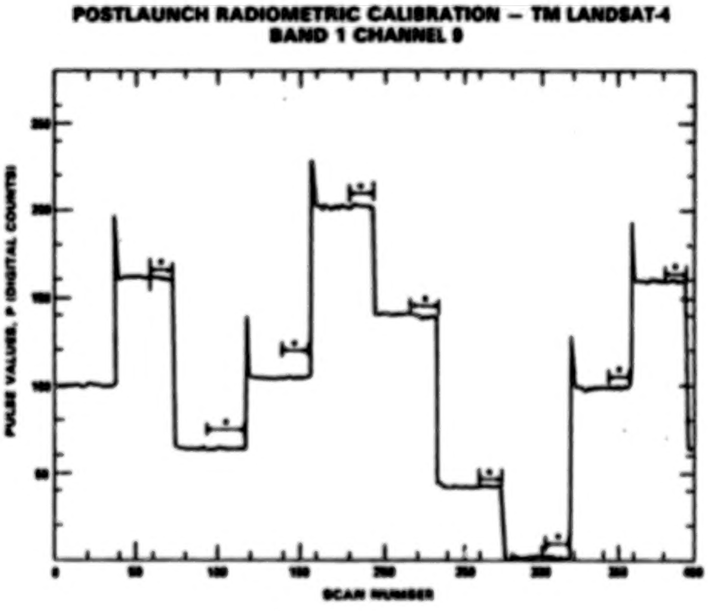
POSTLAUNCH RADIOMETRIC CALIBRATION – TM LANDSAT-4
BAND 1 CHANNEL 9

* PULSE VALUES USED IN COMPUTING PULSE AVERAGE, $\bar{P}$, IN THE SCROUNGE SYSTEM.

FIGURE 9

The prelaunch radiometric calibration procedures are designed to ensure that the TM meets its performance requirements. The radiometric specifications can be divided into three groups: dynamic range, sensitivity, and accuracy.

The TM is designed for land observations; the reflective bands are therefore designed for maximum dynamic range for the expected land radiance levels (Fraser, 1975; Duck, 1977). This range can be tested using a well-calibrated external source. The radiometric sensitivity is expressed in terms of signal-to-noise ratio (SNR) for reflective bands. Radiometric accuracy is one of the most important issues to be addressed. The relative accuracy requirements are quite stringent: about 1 quantum level for between-detector accuracy and 2 percent for between-band accuracy. The overall absolute accuracy specified for the TM is 10 percent. Obtaining absolute calibration accuracy for spaceborne instruments has traditionally been a very difficult task.

The calibration procedure used was developed by Hughes Aircraft Company (HAC) to test the performance of the TM channels; to determine the end-to-end radiometric transfer function with 10-percent accuracy; and to verify that the relative radiometric accuracy is better than 2 percent, the within-band accuracy is 1 DN, the SNR is within specification, and the IC is accurate and has the correct range.

CALIBRATION EQUIPMENT

The usual approach to the prelaunch calibration of visible and near-infrared sensors is by comparing them to a secondary source that has been calibrated with a National Bureau of Standards (NBS) standard lamp. The secondary standard used with the TM is a 122-centimeter (diameter) Integrating Sphere (IS(122)) maintained by the National Aeronautics and Space Administration/Goddard Space Flight Center (NASA/GSFC) and HAC Santa Barbara Research Center (SBRC) personnel. SBRC has maintained the IS(122) and has periodically recalibrated it by comparison with a secondary standard lamp using a monochromator. These tests were performed in June 1979 and February 1982 at NASA/GSFC and in June 1980 and May 1982 at SBRC and are discussed by Walker (1982a, 1982b). The secondary standard is related to an NBS standard by a similar calibration procedure.

The IS(122) is a hollow sphere with an inside diameter of 122 centimeters. It consists of two aluminum hemispheres mounted in a framework that allows easy access to the interior for bulb and surface maintenance. A 46-centimeter-diameter aperture allows reflected light from the

12 quartz-halogen standard lamps out of the interior to calibrate the sensor. The inside surface of the sphere is coated with a white diffusely reflecting barium sulfate-based paint (McCullough et al., 1969).

The lamps in the IS(122) have different wattages. There are six 200-watt lamps, two 100-watt lamps, and four 25-watt lamps, for a maximum of 1500 watts. The lamps are operated at derated wattages to prolong their useful lifetimes. During the calibration tests, the lamps are all lighted initially for each test sequence, as shown in Table 3. The lamps are then sequenced off to reach the next lower radiance level. Twenty levels are used in all. The responses of all 96 detectors in the reflective bands (bands 1 through 5 and 7) are noted at each level, and the detector gains, offsets, and SNRs are calculated.

The IS(122) is directly calibrated against a secondary standard lamp that has in turn been calibrated by a standard lamp of similar design and is directly related to an NBS standard. The standard and the secondary lamps are both quartz-halogen 1000-watt lamps. The overall accuracy of these lamps and the complete calibration sequence are discussed in Barker et al. (1984a).

CALIBRATION PROCEDURES FOR THE TM WITH THE IS(122)

Calibration of the TM with a known source, the IS(122), consists of comparing the TM output with the series of known radiances input to the TM from the source. This procedure is designed to determine the overall response of the TM under known conditions.

Each calibration of the IS(122) results in a series of spectral radiance values at intervals of 50 nanometers in wavelength from 400 to 2500 nanometers for each sphere-lamp configuration (combination of particular lamps on) (Walker, 1982b). This spectral radiance output from the IS(122) is then combined with the measured wavelength response of the TM (Markham and Barker, 1984) in each band to obtain the spectral radiance that each TM detector would see in a particular band and for a particular IS(122) lamp configuration.

These radiance levels by band are the known input to the TM for calibration. During each test, the digital output response of the TM to each input level is collected, averaged, and then compared to the known radiance input to obtain the calibration parameters (gain and offset). Figure 10 illustrates a linear fit of digital counts to radiance to determine channel gain (G(C)) and offset (O(C)).

TABLE 3

INTEGRATING SPHERE LAMP CONFIGURATIONS BY RADIANCE LEVEL

TEST SEQUENCE I			TEST SEQUENCE II		
SEQUENCE NUMBER[b]	LAMP CONFIGURATION[a]	NOMINAL LAMP POWER (W)	SEQUENCE NUMBER[b]	LAMP CONFIGURATION[a]	NOMINAL LAMP POWER (W)
1(1)	624	1500	1(6)	224	700
2(2)	524	1300	2(7)	214	600
3(3)	424	1100	3(9)	114	400
4(4)	324	900	4(13)	014	200
5(5)	224	700	5(17)	004	100
6(8)	124	500	6(18)	003	75
7(10)	024	300	7(19)	002	50
8(11)	023	275	8(20)	001	25
9(12)	022	250			
10(14)	012	150			
11(15)	011	125			
12(16)	010	100			

[a] ABC WHERE A = NUMBER OF 200-W LAMPS, B = NUMBER OF 100-W LAMPS, AND C = NUMBER OF 25-W LAMPS. LAMPS 1 THROUGH 6 ARE 200 W EACH, 7 AND 8 ARE 100 W EACH, AND 9 THROUGH 12 ARE 25 W EACH.

[b] NUMBER IN PARENTHESES IS RANK OF SEQUENCE LEVEL FROM 1 (BRIGHTEST) TO 20 (FAINTEST) FOR ALL 20 TEST LEVELS.

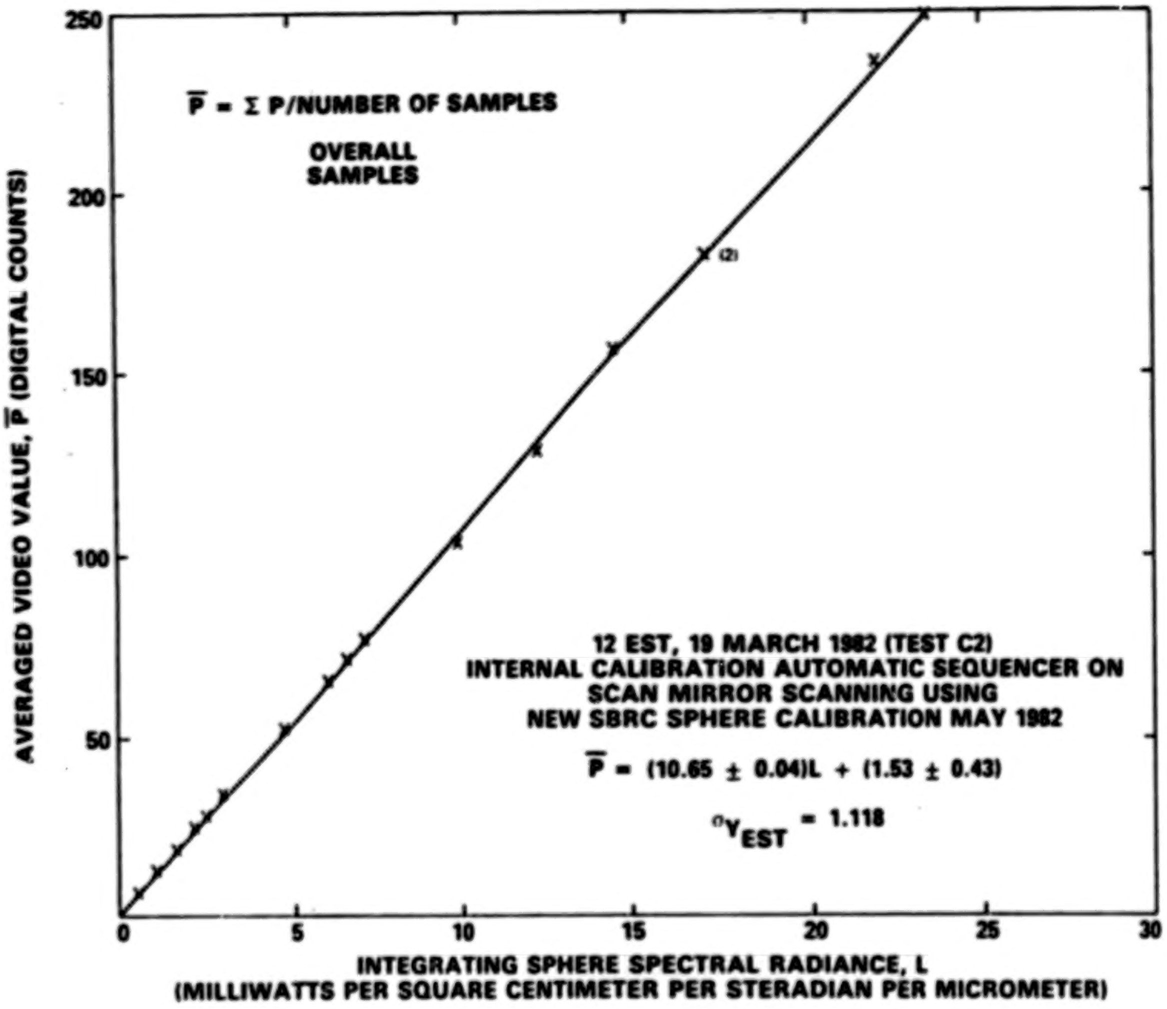

ILLUSTRATIVE TM/PF RADICMETRIC ABSOLUTE DETECTOR CALIBRATION FOR CHANNEL 9 OF BAND 3 (624-693 nm)

$\overline{P} = \Sigma$ P/NUMBER OF SAMPLES

OVERALL
SAMPLES

12 EST, 19 MARCH 1982 (TEST C2)
INTERNAL CALIBRATION AUTOMATIC SEQUENCER ON
SCAN MIRROR SCANNING USING
NEW SBRC SPHERE CALIBRATION MAY 1982

$\overline{P} = (10.65 \pm 0.04)L + (1.53 \pm 0.43)$

$\sigma_{Y_{EST}} = 1.118$

FIGURE 10

The SNR at each level (k) is also computed from the averaged digital count ($\overline{P}_k$) and the standard deviation (σ_k):

$$SNR_k = \frac{\overline{P}_k}{\sigma_k}$$

A least-square linear regression is used to obtain SNR as a function of $\overline{P}$.

The input radiance to the TM is computed by combining the output of the IS(122) for a given configuration of lamps (radiance level) with the measured response of the TM in each band. This is given by

$$L_\lambda(B) = \frac{\int_{\lambda_1}^{\lambda_2} L^j_{sphere}(\lambda) \cdot R(\lambda)\, d\lambda}{\int_{\lambda_1}^{\lambda_2} R(\lambda)\, d\lambda}$$

where

$L_\lambda(B)$ = spectral radiance in a particular TM band

$L^j_{sphere}(\lambda)$ = output of the sphere at radiance level j

$R(\lambda)$ = spectral response of the TM band as a function of wavelength

The integration is done from wavelength λ_1 to λ_2 for a particular TM band. The critical parameters in the calibration are alignment and separation between the IS(122) and the TM, the TM scan mirror operating mode (locked or scanning), and the sphere output to the TM in each band at each radiance level ($L_\lambda(B)$ above). The alignment of the TM with the IS(122) is shown schematically in Figure 11. The distance marked A in the figure has varied widely in the different tests performed to calibrate the TM. Table 4 gives

PLACEMENT OF THE TM AND THE IS(122) ILLUSTRATING THE NEED FOR GOOD ALIGNMENT WHEN THE DISTANCE OF A IS LARGE

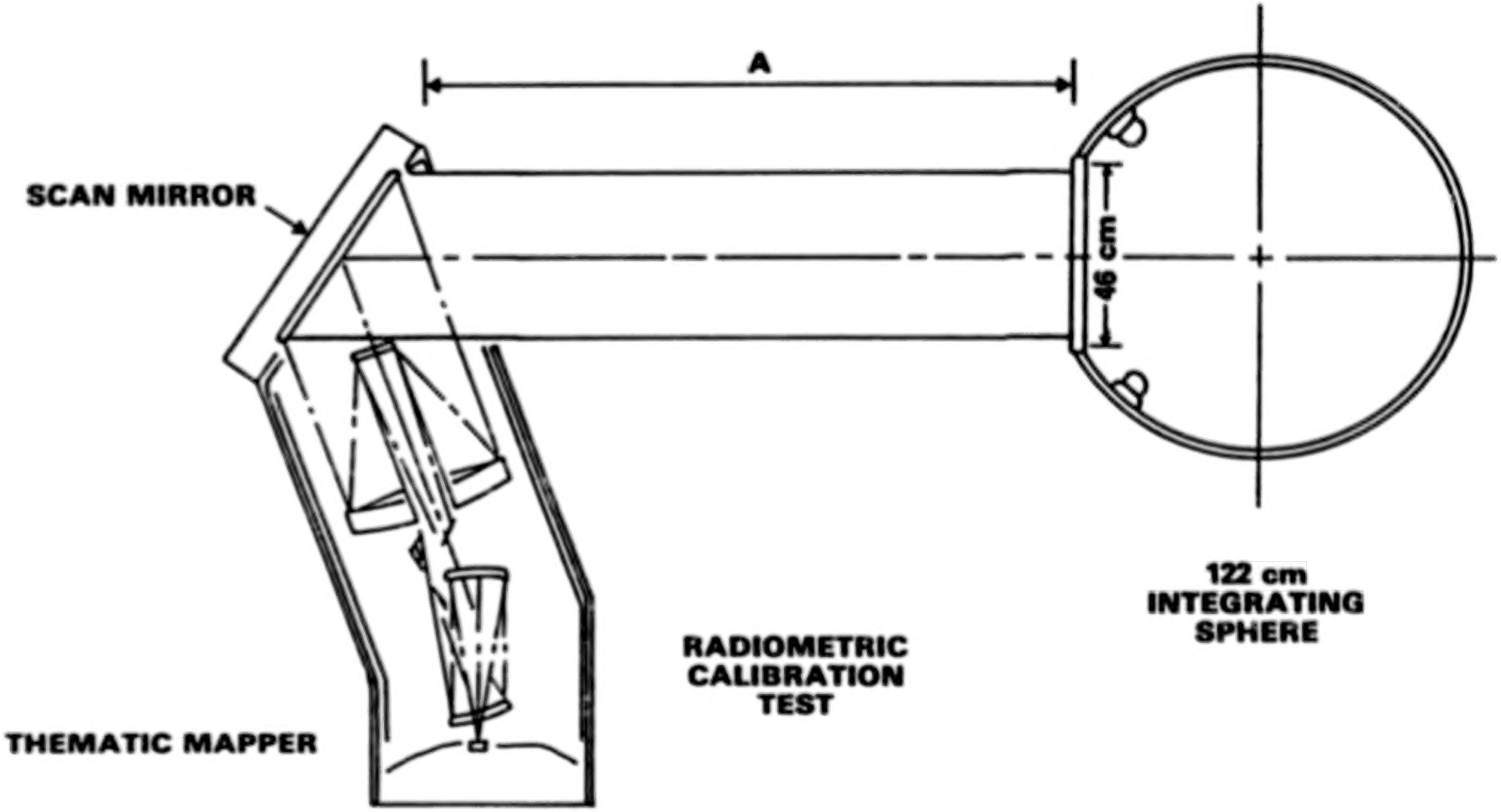
A
SCAN MIRROR
46 cm
122 cm INTEGRATING SPHERE
RADIOMETRIC CALIBRATION TEST
THEMATIC MAPPER

FIGURE 11

TABLE 4

DATES OF CALIBRATION OF THE TM WITH THE IS(122)

TEST[a] DESIGNATION	TEST DATE	SEPARATION DISTANCE (METERS)	LOCATION[c]
A	29 AND 30 JUNE, 1981	5.2	HAC/SBRC
B[b, d]	3 NOVEMBER, 1981	7.6—9.1	GE/VF
C[d]	19 MARCH, 1982	3.7—4.3	GE/VF

[a] ALL HAC AND GE DOCUMENTS HAVE USED THE HUGHES "AC02" DESIGNATION FOR IS TESTS. REFERENCES: TEST A, OSGOOD AND LANSING (1981); TEST B, YOUNG (1982); AND TEST C, UNDOCUMENTED.

[b] BANDS 1 THROUGH 4 ONLY.

[c] HAC/SBRC, HUGHES AIRCRAFT COMPANY, SANTA BARBARA RESEARCH CENTER, SANTA BARBARA, CA; GE/VF, GENERAL ELECTRIC, VALLEY FORGE, PA.

[d] SCAN MIRROR WAS ALLOWED TO SCAN THE SPHERE APERTURE. DURING TEST A, THE SCAN MIRROR WAS LOCKED.

NOTE: TEST A CONSISTED OF TWO SEPARATE CALIBRATION RUNS WITH THE CFPA TEMPERATURE AT −179.8° AND −168.5°C (TESTS A1 AND A2, RESPECTIVELY). TEST C CONSISTED OF THREE SEPARATE RUNS ($T_{CFPA} \sim -177°C$): SCAN MIRROR LOCKED (TEST C1) IC AUTOMATIC SEQUENCER ON, SCAN MIRROR SCANNING (IC A.S. ON) (TEST C2), AND MIRROR SCANNING (IC IN BACKUP MODE) (TEST C3). NEW SBRC SPHERE CALIBRATION (MAY 1982) USED FOR ALL C TESTS.

the dates, the separation distances (A) between the TM and the IS(122), and a letter designation for each test. Table 5 shows the variability in the measured channel gain in each test. The alignment of the TM with the IS(122) is particularly important at the larger separations if the scan mirror is locked in place. The IS(122) aperture is 46 centimeters, which is illuminating the 41-centimeter TM aperture; at a separation of 5.2 meters, the spread of the TM spectral bands along the scan is 3 centimeters at the prime focal plane. This leaves a maximum travel of 2 centimeters during which all detectors of each band (1 through 5 and 7) may simultaneously see the same part of the IS(122). If the scan mirror is locked in place, the alignment thus becomes critical. This is not the case if the scan mirror is allowed to move. Test procedures originally required the scan mirror to be locked at midscan; these were changed after the June 1981 test. Both locked and scanning modes were used in March 1982. To ensure that the peak response is actually measured, the test procedures with the scan mirror operating may also require that the raw output from the sphere be searched for the largest response and then fitted by a second-order polynomial. This has not been a part of the calibration procedure, however, and may have to be included to reduce the error if it is found that the output of the IS(122) as seen by the TM is not sufficiently flat. The test procedure may thus be summarized as follows:

1. Select an external radiance source as standard (IS(122))

2. Determine the characteristics and output of the external standard

3. Adjust trim resistors for each detector in the TM to obtain the correct dynamic range

4. Measure the TM performance at various external radiance levels and cooled focal plane temperatures

5. Determine the gain, offset, dynamic range, and SNR of each detector

6. Transfer the calibration from the detectors to the IC

7. Use the TM to calibrate other external calibrators for use when the IS(122) is unavailable (as in vacuum chamber testing)

8. Conduct spectral matching tests for band-to-band comparisons

TABLE 5

SUMMARY OF AVERAGE GAIN CHANGES IN PERCENT BY TEST REFERENCED TO TEST C2

BAND		TEST					
		A1	A2	B	C1	C2	C3
1	ODD	5.28	5.22	1.17	0.82	—	−0.03
	EVEN	4.91	4.83	1.13	0.91	—	−0.02
	ALL	5.09	5.03	1.15	0.86	—	−0.02
2	ODD	0.48	0.24	−1.95	−0.29	—	−0.63
	EVEN	0.45	0.21	−2.01	−0.32	—	−0.67
	ALL	0.47	0.22	−1.98	−0.30	—	−0.65
3	ODD	0.45	0.20	−2.22	−0.32	—	−0.55
	EVEN	0.23	−0.01	−2.29	−0.23	—	−0.51
	ALL	0.34	−0.09	−2.25	−0.28	—	−0.53
4	ODD	3.91	4.00	3.75	0.62	—	0.08
	EVEN	3.78	3.88	3.69	0.61	—	0.06
	ALL	3.85	3.94	3.72	0.62	—	0.07
5	ODD	5.45	4.75	—[b]	−0.17	—	−0.02
	EVEN	5.45	4.78	—	−0.28	—	−0.18
	ALL	5.45	4.77	—	−0.23	—	−0.11
7	ODD	3.59	3.09	—[b]	0.01	—	−0.12
	EVEN	3.47	4.77	—	0.06	—	−0.09
	ALL	3.53	3.93	—	0.03	—	−0.11

[a] GAIN CHANGE DEFINED AS: VALUE = 100%x(CURRENT − REFERENCE) + REFERENCE.

[b] NO BANDS 5 AND 7 DATA TAKEN DURING TEST B.

CALIBRATION TRANSFER TO THE IC

The IC is used mainly for measuring relative performance in flight. External calibrators can be used only on the ground. To maintain good radiometric accuracy, it is important to carefully calibrate the IC using a known standard. Furthermore, the behavior of the TM as a function of temperature and age should be well understood so that IC measurements can be corrected, because there is no way to obtain absolute calibration in flight.

The function of the calibration transfer is to provide reference radiance levels for the IC in different operating modes. These reference data are then used to calibrate in-orbit scene data and to monitor the health of the detectors during postlaunch operation. The procedures used to process the raw transfer data should be the same as those proposed for operational postlaunch ground processing. To transfer the absolute IS(122) calibration from the TM detectors to the IC, the raw IC calibration pulse must be extracted from the telemetry stream; a suitable pulse integration method must be applied to all detector data; and all integrated values for a particular lamp configuration must be averaged, excluding certain scans near lamp state changes. The actual algorithms used are the same as the SCROUNGE ground radiometric processing procedures discussed in the next section. The lamp state values may then be converted from averaged digital counts ($\bar{P}$) (output from the TM) to effective spectral radiance using the calibration parameters (G and O) determined from the IS(122) calibration (Barker, 1984).

Regardless of the IC operational mode, all eight lamp states for all detectors must be processed through the eight steps mentioned previously.

GROUND RADIOMETRIC PROCESSING PROCEDURES

From launch through July 1983, TM image data were processed using the IC with the SCROUNGE processing algorithms. In July 1983, an early version of TIPS became available. The important features of the SCROUNGE algorithms will be described here, and the resulting products will be mentioned. TIPS will be discussed only in terms of its differences from SCROUNGE.

The use of the IC to radiometrically calibrate image data from the reflective bands involves six steps:

1. Extracting calibration minor frames

2. Integrating a pulse to obtain a pulse height

3. Averaging pulse heights belonging to a state and identifying the IC state

4. Obtaining detector gains and offsets by regression analysis of observed pulse averages versus nominal values

5. Adjusting gains and offsets of channels within a band to achieve a common radiance range

6. Balancing relative grey levels using histogram normalization (optional)

During the SCROUNGE era, only the minor frames (mf) falling within a 148-mf window are examined for pulse extraction. If part of the pulse falls outside the window, the integrated pulse value is reduced. The pulse extraction window is located at a fixed distance from the start of the line. The distance is the same for all channels but different for forward and reverse scans. A detailed history of the location of calibration windows is given in Barker et al. (1984b). SCROUNGE integrates pulses by using the Hughes algorithm (Figure 12), which consists of the following steps:

1. Locate pulse maximum

2. Move outward from the maximum to locate pulse edges that are 40 percent of the maximum value

3. Define pulse center as the midpoint of the line segment defined by the pulse edges

4. Average 31 points (pulse integration width) about the pulse center to obtain the pulse height

Pulse averaging involves identifying an IC state transition, determining which scans between transitions to include in the average, averaging the pulses from selected scans to obtain the averaged pulses $\bar{P}(\ell,C)$, and associating $\bar{P}(\ell,C)$ with an IC state. In SCROUNGE, pulse heights from forward and reverse scans are averaged together. A transition occurs when the pulse height of a scan differs from the pulse height of the previous scan by more than three digital counts. The first 25 scans following a transition are ignored (Figure 9); the remaining scans, preceding the next transition, are averaged to determine $\bar{Q}$. The average pulse is associated with the IC state having the closest nominal averaged pulse value. Data from each of the 96 reflective channels are processed separately. When

POSTLAUNCH RADIOMETRIC CALIBRATION — TM LANDSAT-4 HUGHES ALGORITHM

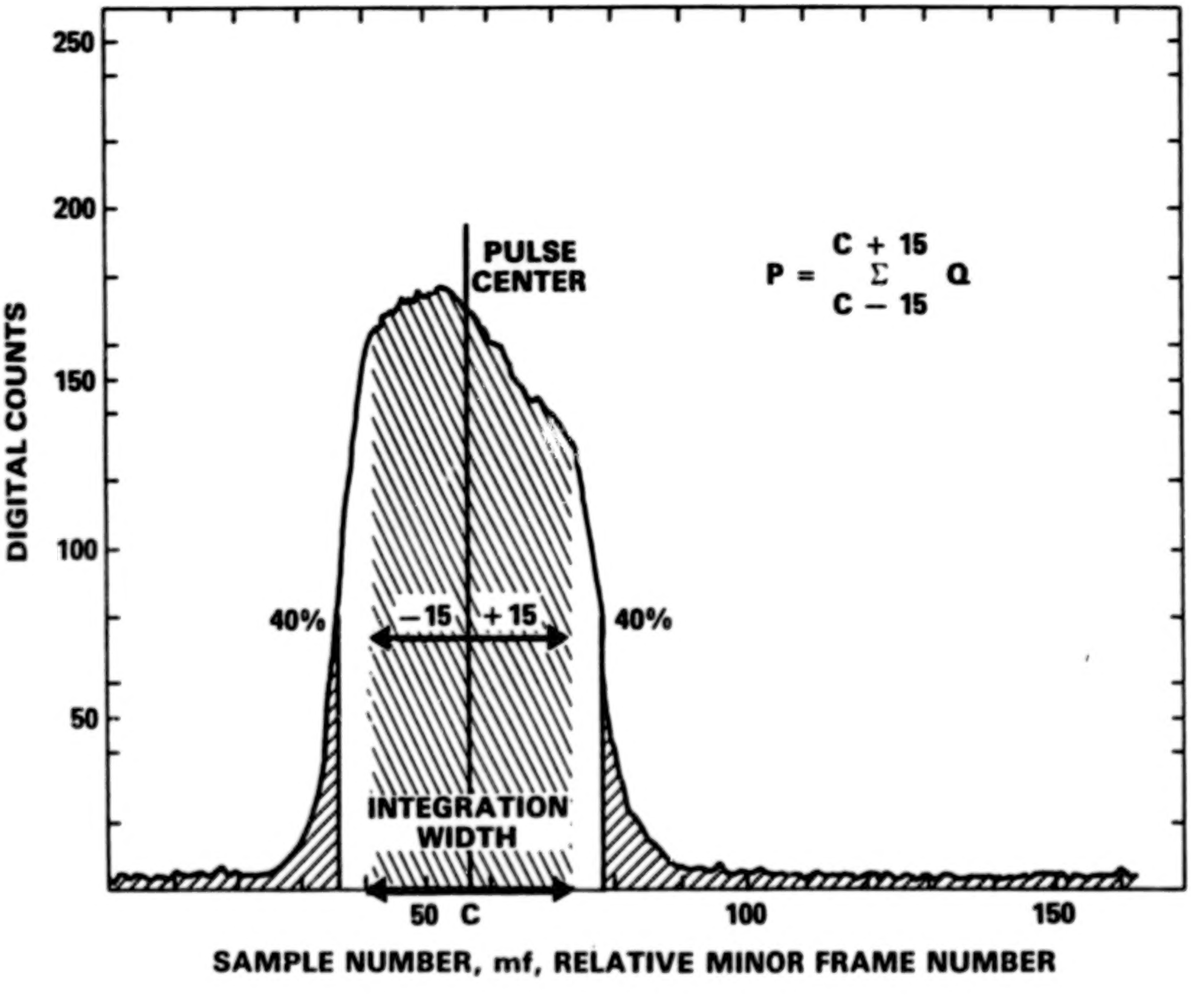

FIGURE 12

51 channels agree on an IC state, the IC state is considered identified and is assigned to all channels.

Gain (G(C)) and offset (O(C)) are determined for each channel by a linear unweighted regression of counts versus nominal counts using all eight IC states. A radiance range in digital counts common to all the channels within the band (RMAX-RMIN) is determined for each band. Gains and offsets are then normalized so that values obtained for each channel lie within the common range.

First RMAX and RMIN are used to determine postcalibration gain ($G^o(B)$) and offset ($O^o(B)$):

$$G^o(B) = \frac{QMAX}{RMAX-RMIN}$$

$$O^o(B) = \frac{QMIN - QMAX*RMIN}{(RMAX-RMIN)}$$

where QMAX is the full-scale digital value (255) and QMIN is the minimum digital value (0). Normalized gain $NG_{IC}(C)$ and normalized offset ($NO_{IC}(C)$) for each channel (C) in the band are then determined as follows:

$$NG_{IC}(C) = G(C)/G^o(B)$$

$$NO_{IC}(C) = O(C) - NG_{IC}(C) * O^o(B)$$

As a result of this approach, adjusted count values for particular channels that lie outside the common range are simply set to lie at the maximum or minimum of the range as appropriate.

Histogram normalization involves the following steps for each band:

1. Histograms are obtained for each channel.
2. The histograms for all the channels in the band are combined to form an average histogram.

3. A new gain (N'G) and a new offset (N'O) for each channel are derived by adjusting $NG_{IC}(C)$ and $NO_{IC}(C)$ so that the channel histogram will have the same average (μ) and standard deviation (σ) as the band average histogram:

$$N'G = NG_{IC}(C) * \frac{\sigma_i}{\bar{\sigma}}$$

and

$$N'O = NO_{IC}(C) - N'G * \bar{\mu} - \frac{\bar{\sigma} * \mu_i}{\sigma_i}$$

where μ_i and σ_i are the respective mean and standard deviation for the histogram for channel i before normalization.

4. The new gains and offsets are then used to produce a radiometric lookup table (RLUT) for each channel:

$$RLUT_{ij} = \frac{P_j - N'O}{N'G}$$

where $RLUT_{ij}$ is the value in the lookup table corresponding to an initial value P_j in channel C.

5. The image is radiometrically corrected using the RLUT.

Uncalibrated image data are available on a computer-compatible tape (CCT) known as the CCT-BT tape. This tape also contains the initial gains and offsets (prior to range adjustment and histogram normalization) for each channel. CCT-BT tapes generated after April 1983 also contain the histogram-normalized gains and offsets. The CCT-AT tapes contain the radiometrically corrected image. A final product containing radiometrically and geometrically corrected resampled data is also available. These digital products are described in detail in Barker and Gunther (1984).

TIPS is a flexible system that provides three options: the use of nominal gains and offsets, the use of nominal gains and scene-specific background for offsets, and the use of the IC to determine gains and offsets. In each case, the use of histogram normalization is optional. Differences between the SCROUNGE and TIPS processing algorithms are highlighted below.

In general, the TIPS algorithms produce more stable results and handle noise in the calibration data better. Specifically, TIPS will examine the entire shutter flag part of the scan to extract the calibration pulse, thereby eliminating the risk of clipped pulses. The TIPS pulse integration method, THRESH, uses a wider pulse integration width of 65 minor frames. The pulse averaging algorithm uses information from several scans (currently 10) to locate IC state transitions. Out-of-range scans (deviating by a predefined amount from the average of the stable part of the current data) as well as scans on both sides of a transition are not included in the averaged pulse value $\bar{P}$. In the regression analysis, background data from each scan as well as the 000 IC state value are used. Each pulse average used in the regression is weighted based on the number of scans contributing to the pulse average and the standard deviation of the average. The one aspect of SCROUNGE that is probably safer than TIPS is in IC state identification. Unlike SCROUNGE, TIPS uses only one or a small number of channels to identify the IC state.

SUMMARY

The TM radiometric subsystem observes radiance reflected from the Earth in six reflective bands: 0.45 to 52 μm, 0.52 to 0.60 μm, 0.63 to 0.69 μm, 0.76 to 0.90 μm, 1.55 to 1.75 μm, and 2.08 to 2.35 μm and one thermal band at 10.4 to 11.6 μm. Each band comprises 16 detectors that create 16 raster lines as the ground is scanned in both forward and reverse directions along the crosstrack. The IC consists of three miniature tungsten filament lamps for the reflective bands, a blackbody for the thermal band, and a flex pivot-mounted resonant shutter. The IC inserts reference radiance levels just ahead of the spectral filters of each band at the prime focal plane while obscuring the Earth from the detectors.

Prior to launch, the TM channels were absolutely calibrated with a secondary standard 122-centimeter integrating sphere. The objectives of the calibration procedure were to determine absolute channel gain and to characterize relative radiometric accuracy, within-band accuracy, SNR, and dynamic range. The TM channels were used to calibrate the IC.

The use of the IC to calibrate TM data in the ground processing system consists of pulse extraction, pulse integration, pulse averaging, IC state identification, linear regression analysis, adjustment of the detectors within a band to a common range, and histogram equalization. The important features of the SCROUNGE radiometric calibration system, which was operative through July 1983, are as follows:

- Pulse integration width is 31 minor frames wide.
- Forward and reverse scans are processed together.
- The first 25 scans following an IC state transition are excluded from the pulse average. No scans are skipped before a lamp transition.
- IC state identification is made through comparison with nominal values. All channels are checked with the results determined by agreement of the majority.
- Linear regression analysis is unweighted and includes all eight IC states.
- In histogram equalization, the mean and standard deviation of each channel are adjusted to conform with the band average.

The TIPS radiometric calibration process, which replaced SCROUNGE in July 1983, differs from SCROUNGE as follows:

- Pulse integration width is 65 minor frames.
- In pulse averaging, scans on both sides of an IC state transition are skipped.
- Only a small preselected group of channels are checked to identify the IC state.
- Linear regression is weighted. Background data from each scan are used as well as the eight IC states. In band 4, the 111 state, which is saturated, is not used in the calibration.

RECOMMENDATIONS

Brief recommendations are given below; expanded recommendations are given in Barker (1984). An improvement in both relative and absolute accuracy of the radiometric calibration can be achieved by modifying the calibration procedure. Of course, any change in the postlaunch procedure would require a reprocessing of the prelaunch absolute calibration data using the modified algorithms. From the results presented in Barker et al. (1984b), it is clear that forward and reverse scan data should be processed separately. A wider pulse integration width would reduce the noise in the averaged pulse values. A wider pulse extraction window or a pulse extraction window that shifted with channel number would eliminate pulse truncation and permit the use of a wider integration width. The use of background data from each scan line for calibration of that scan would probably be preferable to applying the average background observed during the lamps-off (000) state to all the scans in a scene. When applying background data to an image line, however, care must be taken to use background data that have not been altered by dark current (DC) restore subsequent to the time the image was taken. Barker et al., 1984, presents additional recommendations for postlaunch procedures; Barker et al., 1984a, recommends improvements for the absolute calibration procedures.

REFERENCES

Barker, John L., "Relative Radiometric Calibration of Landsat TM Reflective Bands," PROCEEDINGS, LANDSAT-4 SCIENTIFIC CHARACTERIZATION EARLY RESULTS SYMPOSIUM, Goddard Space Flight Center, Greenbelt, Maryland, April 1984

Barker, J. L., D. L. Ball, K. C. Leung, and J. A. Walker, "Prelaunch Absolute Radiometric Calibration of the Reflective Band on Landsat-4 Protoflight Thematic Mapper," PROCEEDINGS, LANDSAT-4 SCIENTIFIC CHARACTERIZATION EARLY RESULTS SYMPOSIUM Goddard Space Flight Center, Greenbelt, Maryland, April, 1984a

--, R. B. Abrams, D. L. Ball, and K. C. Leung, "Characterization of Radiometric Calibration of Landsat-4 TM Reflective Bands," PROCEEDINGS, LANDSAT-4 SCIENTIFIC CHARACTERIZATION EARLY RESULTS SYMPOSIUM, Goddard Space Flight Center, Greenbelt, Maryland, April 1984b

--, F. J. Gunther, R. B. Abrams, and D. L. Ball, "TM Digital Image Products for Applications," PROCEEDINGS, LANDSAT-4 SCIENTIFIC CHARACTERIZATION EARLY RESULTS SYMPOSIUM, Goddard Space Flight Center, Greenbelt, Maryland, April 1984

Duck, K. I., "Revised Thematic Mapper Radiometric Assessment," Goddard Space Flight Center, Greenbelt, Maryland, Internal Memorandum, 1977

Engel, J. C., "Thematic Mapper: An Interim Report on Anticipated Performance" (paper presented at AIAA Sensor Systems for the 80's Conference, Colorado Springs, Colorado, 1980)

Fraser, R. S., "Radiances for Thematic Mapper," Goddard Space Flight Center, Internal Memorandum, 1975

Lansing, J. C., and J. L. Barker, "Thermal Band Characterization of Landsat-4 Thematic Mapper," PROCEEDINGS, LANDSAT-4 SCIENTIFIC CHARACTERIZATION EARLY RESULTS SYMPOSIUM, Goddard Space Flight Center, Greenbelt, Maryland, April 1984.

Lyons, J., D. Fischel, and E. Beyer, "Production and Analysis of the Output Data Products for Landsat-4 in the Engineering Checkout Phase," PROCEEDINGS, LANDSAT-4 SCIENTIFIC CHARACTERIZATION EARLY RESULTS SYMPOSIUM, Goddard Space Flight Center, Greenbelt, Maryland, April 1983

Markham, B., and J. L. Barker, "Spectral Characterization of the Landsat Thematic Mapper Sensors," PROCEEDINGS, LANDSAT-4 SCIENTIFIC CHARACTERIZATION EARLY RESULTS SYMPOSIUM, Goddard Space Flight Center, Greenbelt, Maryland, April 1984

McCullough, A. W., J. T. McLean,, and E. I. Mohr, "Evaluation and Calibration of Some Energy Sources for the Visible and Near Infrared Regions of the Electromagnetic Spectrum," NASA/GSFC, X-622-69-195, 1969

Walker, J. A., "Comparisons of 48SIS Calibrations--NASA and SBRC," Santa Barbara Research Center, HS236-8160, 1982a

--, "48 SIS Calibration Data for GE Post T.V. Test Configuration," Santa Barbara Research Center, HS236-7995, 1982b

APPENDIX - CALIBRATION PULSES

Figures A-1 through A-18 are calibration pulses taken from the March 9, 1982, prelaunch vacuum data. Samples are included for forward and reverse scans, even and odd channels.

FIGURE A-1
RADIOMETRIC CALIBRATION — TM LANDSAT-4
TM1 C8 FORWARD SCAN, MARCH 9, 1982, VACUUM PRELAUNCH

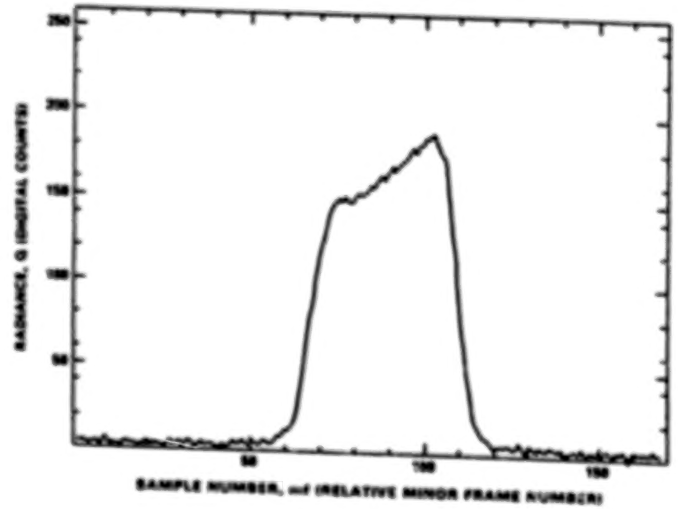

FIGURE A-2
RADIOMETRIC CALIBRATION — TM LANDSAT-4
TM1 C8 FORWARD SCAN, MARCH 9, 1982, VACUUM

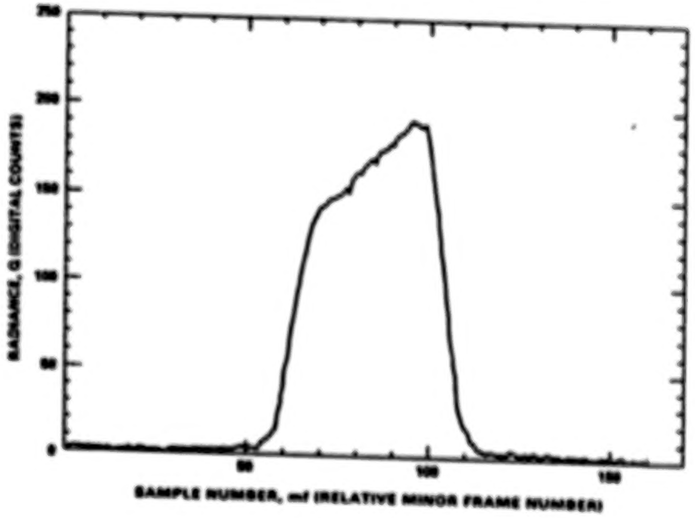

FIGURE A-3
RADIOMETRIC CALIBRATION — TM LANDSAT-4
TM1 C8 REVERSE SCAN, MARCH 9, 1982, VACUUM

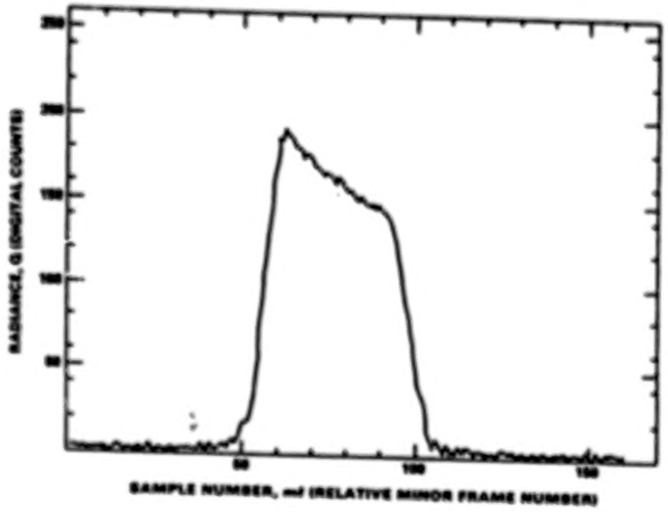

FIGURE A-4

RADIOMETRIC CALIBRATION — TM LANDSAT-4
TM2 CHANNEL 8 FORWARD SCAN, MARCH 9, 1982, VACUUM

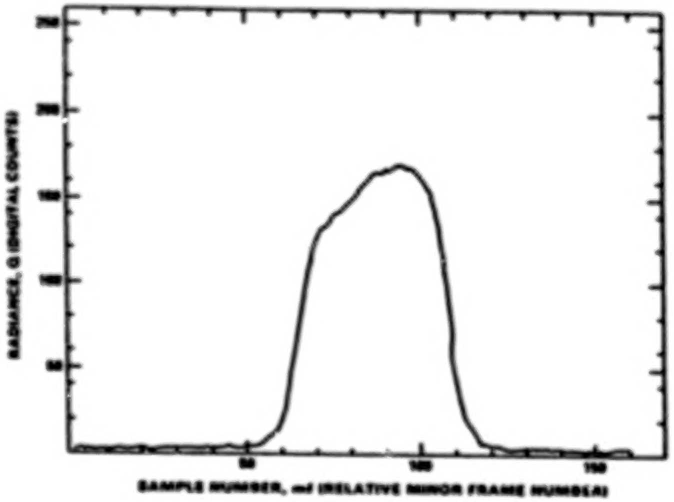

FIGURE A-5

RADIOMETRIC CALIBRATION — TM LANDSAT-4
TM2 C9 FORWARD SCAN, MARCH 9, 1982, VACUUM

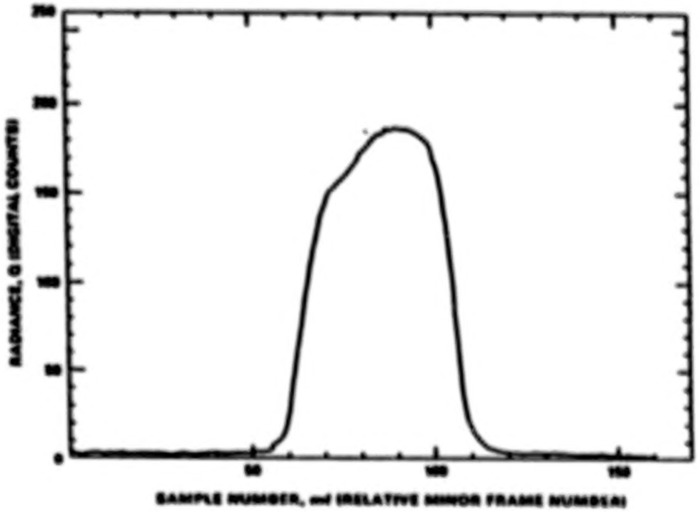

FIGURE A-6

RADIOMETRIC CALIBRATION — TM LANDSAT-4
TM2 C8 REVERSE SCAN, MARCH 9, 1982, VACUUM

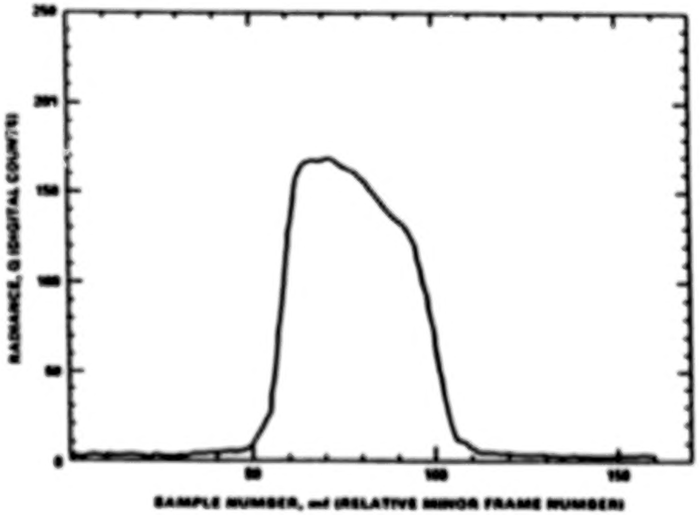

FIGURE A-7
RADIOMETRIC CALIBRATION — TM LANDSAT-4
TM3 CHANNEL 8 FORWARD SCAN, MARCH 9, 1982, VACUUM

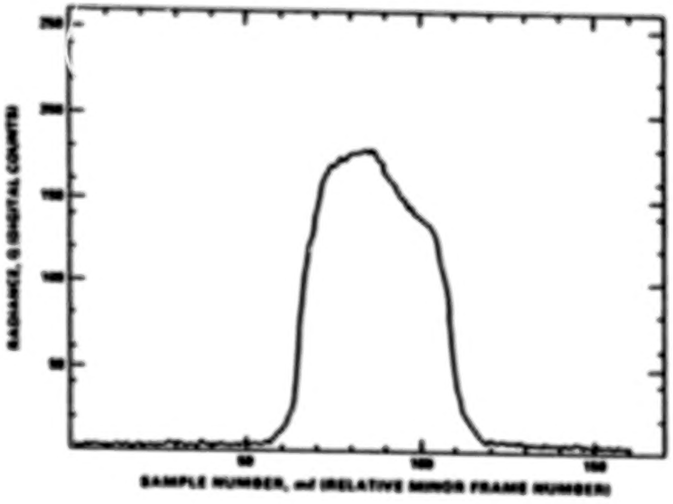

FIGURE A-8
RADIOMETRIC CALIBRATION — TM LANDSAT-4
TM3 C8 FORWARD SCAN, MARCH 9, 1982, VACUUM

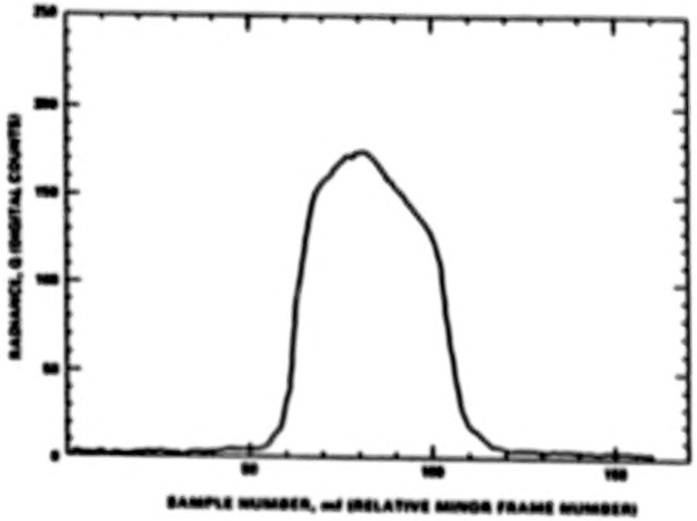

FIGURE A-9
RADIOMETRIC CALIBRATION — TM LANDSAT-4
TM3 C8 REVERSE SCAN, MARCH 9, 1982, VACUUM

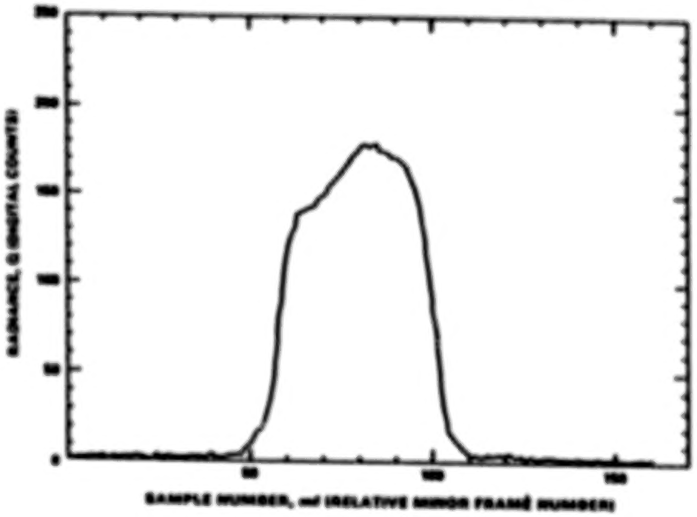

FIGURE A-10
RADIOMETRIC CALIBRATION — TM LANDSAT-4
TM4 CHANNEL 8 FORWARD SCAN, MARCH 8, 1982, VACUUM

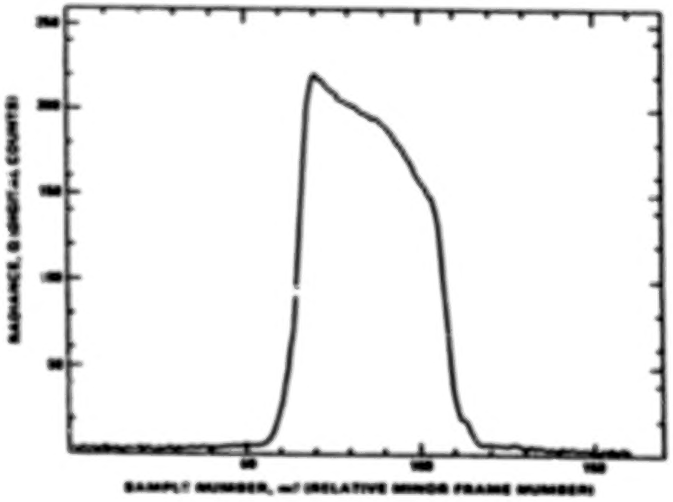

FIGURE A-11
RADIOMETRIC CALIBRATION — TM LANDSAT-4
TM4 C8 FORWARD SCAN, MARCH 8, 1982, VACUUM

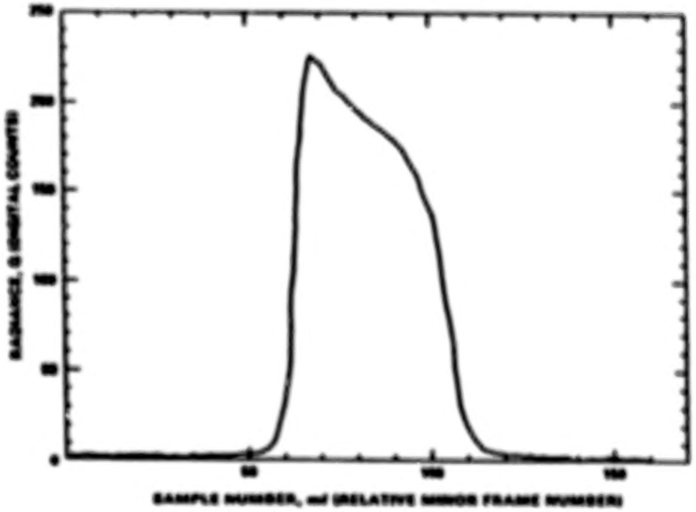

FIGURE A-12
RADIOMETRIC CALIBRATION — TM LANDSAT-4
TM4 C8 REVERSE SCAN, MARCH 8, 1982, VACUUM

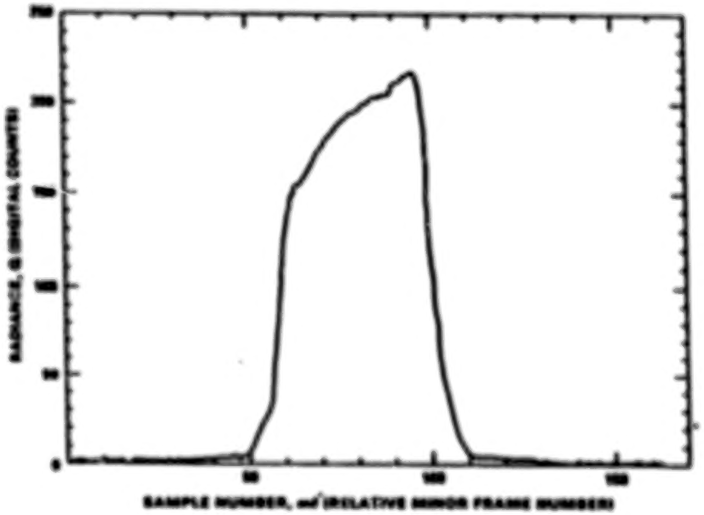

FIGURE A-13
RADIOMETRIC CALIBRATION — TM LANDSAT-4
TMS CHANNEL 9 FORWARD SCAN, MARCH 9, 1982, VACUUM

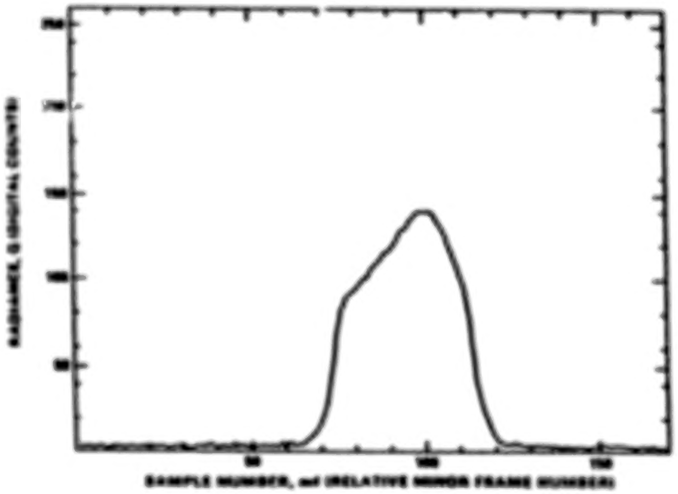

FIGURE A-14
RADIOMETRIC CALIBRATION — TM LANDSAT-4
TMS C9 FORWARD SCAN, MARCH 9, 1982, VACUUM

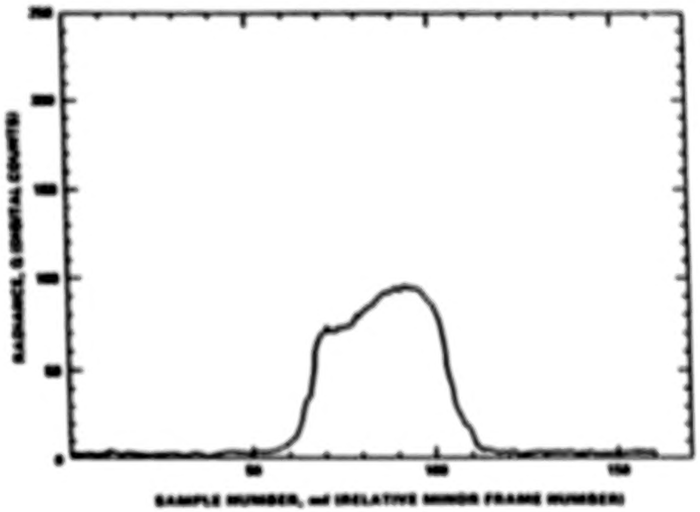

FIGURE A-15
RADIOMETRIC CALIBRATION — TM LANDSAT-4
TMS C9 REVERSE SCAN, MARCH 9, 1982, VACUUM

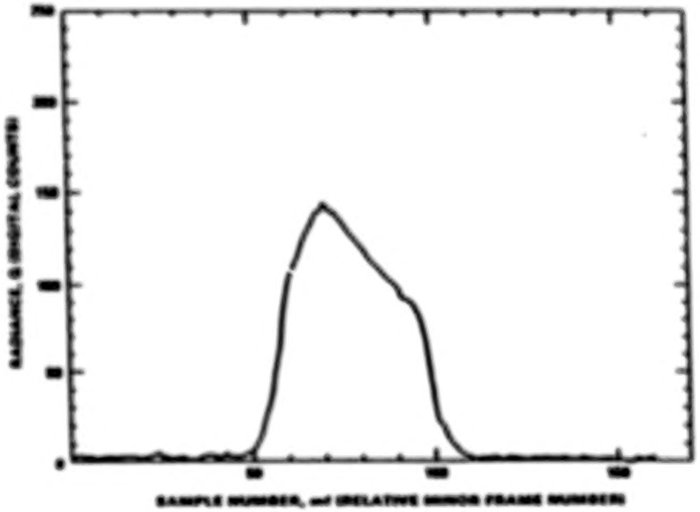

FIGURE A-16
RADIOMETRIC CALIBRATION — TM LANDSAT-4
TM7 CHANNEL 8 FORWARD SCAN, MARCH 8, 1982, VACUUM

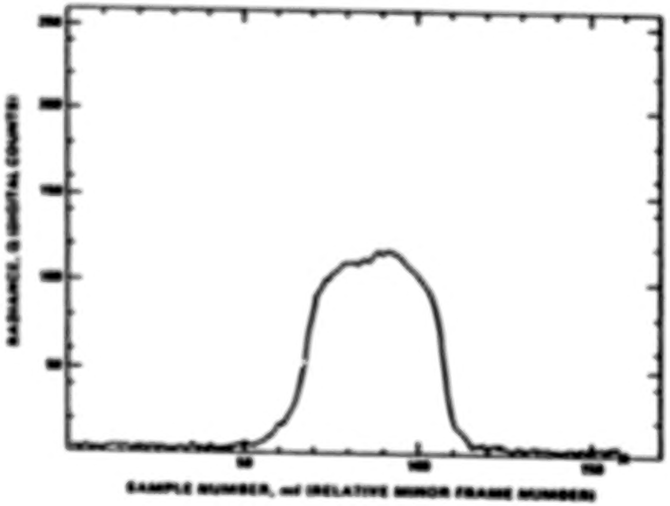

FIGURE A-17
RADIOMETRIC CALIBRATION — TM LANDSAT-4
TM7 C8 FORWARD SCAN, MARCH 8, 1982, VACUUM

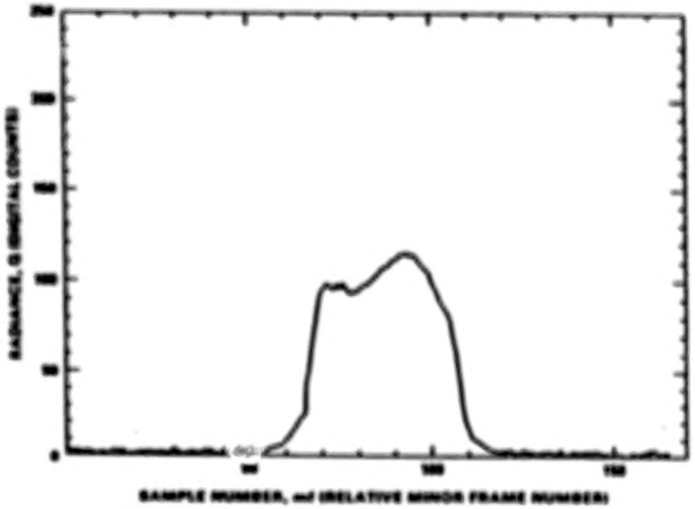

FIGURE A-18
RADIOMETRIC CALIBRATION — TM LANDSAT-4
TM7 C8 REVERSE SCAN, MARCH 8, 1982, VACUUM

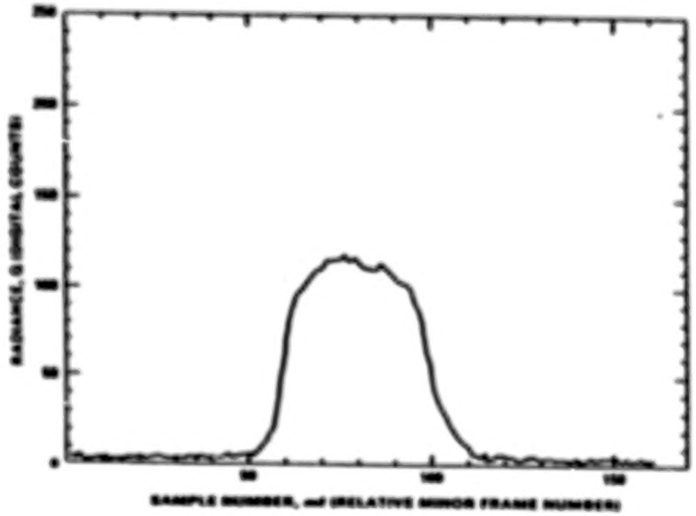

D3

N85-20511

AN OVERVIEW OF THE THEMATIC MAPPER GEOMETRIC CORRECTION SYSTEM

Eric P. Beyer
General Electric Company
Philadelphia, PA 19101

1.0 INTRODUCTION

This paper summarizes the processing concepts which form the basis of the NASA Thematic Mapper (TM) Geometric Correction System.

TM geometric correction is a system process which includes both the Flight and Ground Segments. The principle Flight Segment subsystems are:

Thematic Mapper,
Attitude Control,
Attitude Measurement,
On-Board Computer.

The principle Ground Segment processes are:

Payload Correction,
Control Point Processing,
Geometric Correction (Resampling).

1.1 Purpose and Fundamental Concept of Geometric Correction

The overall purpose of Geometric Correction is to place TM image samples onto an output coordinate system which is related to a map projection. This output product simplifies the data processing for subsequent applications. Conceptually, the geometric correction is accomplished in two phases: First, correction data is generated and then the raw TM image data is resampled using the correction data.

Figure 1-1 illustrates correction data generation. The spacecraft position, TM frame attitude, position of the TM scanning mirrors and detector sampling are known as a function of time, through a combination of Flight Segment measurements, Ground Segment modeling and control point information. This information, along with an earth geoid model, is used to determine the geoid location for each TM image sample (geoid look point). Then, using map projections, correction data can be generated which defines the location of each TM sample on the output coordinate system.

As with previous Landsats, products will be provided on an output grid system known as a World Reference System (WRS). The WRS is defined by a nominal orbit path. Each of the nominal 233 orbit paths of the sun synchronous Landsat-D orbit is divided into 248 WRS scenes. Including overlap with adjacent scenes in the same orbit, a scene is approximately 170 km along-track by 185 km across-track. A WRS scene is identified by a scene center latitude and longitude and a map rotation angle for each map projection. Output products can be provided in either of two map projections:

C 2

1. Space Oblique Mercator (SOM).
2. Universal Transverse Mercator when scene center is between 65 degrees South latitude and 65 degrees North latitude or Polar Stereographic when scene center is below 65 degrees South latitude and above 65 degrees North latitude.

The output coordinate system for all satellite passes over the WRS scene is the map projection coordinate system rotated about the WRS scene center location by the map rotation angle.

Figure 1-2 illustrates the resampling concept. The correction data is used to locate TM detector samples on the output coordinate system, and TM detector samples are then interpolated to the desired output grid locations.

1.2 Geometric Accuracy

An overview of the Landsat-D geometric accuracy specifications are shown in Figure 1-3. Effectively, a reference interval (set of consecutively imaged scenes) is geodetically rectified to a set of maps. Registration control points are then extracted from the reference interval and stored in a control point library. Subsequently imaged intervals are registered to the reference interval using the control point library. There are three geometric accuracy requirements: Band-to-band registration, temporal registration and geodetic rectification.

Band-to-band registration is the ability to overlay spectral bands within a single scene. It is considered the most important accuracy requirement. The Thematic Mapper band-to-band requirements are 0.2 pixel (90% of the time) between spectral bands on the same focal plane and 0.3 pixel (90% of the time) between spectral bands on primary and cold focal planes. A TM pixel is 42.5 microradians. Bands 1 to 4 are on the primary focal plane and Bands 5 to 7 are on the cold focal plane. With ground processing, these band-to-band accuracy requirements are expected to be easily satisfied.

Temporal registration is the ability to overlay a band of the registrant scene with the corresponding band of the reference scene. The accuracy requirement is 0.3 pixel (90% of the time). The temporal registration requirement is the most challenging system accuracy requirement. The following simplified calculation illustrates this point:

$$\text{0.3 pixel temporal (90\%)} \times \frac{42.5\ \mu\text{rad}}{\text{pixel}} \times \frac{(1\sigma)}{1.645\ (90\%)} \times \frac{\text{Single scene}}{\sqrt{2}\ \text{temporal}}$$

$$= 5.48\ \mu\text{rad}\ (1\sigma)\ \text{single scene}$$
$$= 1.13\ \text{arc-sec}\ (1\sigma)\ \text{single scene}$$
$$= 3.87\ \text{meter (at 705.3 km)}\ (1\sigma)\ \text{single scene}$$

That is, the 0.3 pixel 90% of the time accuracy between two scenes allows no more than 3.87 meters (1σ) total system error for one scene. This simplified calculation assumes that the error is Gaussian (the factor of 1/1.645 converts 90% to 1σ) and that the errors in the two scenes are uncorrelated (the factor of $1/\sqrt{2}$). The temporal registration accuracy requires an adequate number of ground control points. This may be as large as 18 control points when a single scene is processed, but can be reduced to 3 to 4 control points per scene when consecutive scenes from one orbit (an interval) are processed. This requirement excludes the error effects caused by interaction of earth topology and orbit non-repeatability (see Section 2.1).

Geodetic rectification is the ability to overlay a band of the registrant scene with the original maps. The accuracy requirement is 0.5 pixel (90% of the time). This accuracy is to be met when the maps have no geometric errors, over regions without topological variations and given sufficient numbers of geodetic control points. To the extent that these conditions are not satisfied in actual operation, the geodetic accuracy of output products will degrade.

1.3 System Overview

An overview of NASA's Landsat-D TM Geometric Correction System is shown in Figure 1-4. The Flight Segment includes the TM instrument, attitude measurement devices, attitude control and ephemeris processing. The Flight Segment inertial attitude estimates are made using an extended Kalman Filter process, which corrects integrated gyro measurements using star tracker information. Attitude is controlled using reaction wheels. Ephemeris, used for attitude control and ground processing, is uplinked from the ground or determined using the on-board Global Positioning System. Attitude control and ephemeris processing are implemented in the On-Board Computer.

The spacecraft attitude is downlinked for ground processing but at a rate of (4.096 seconds) that cannot follow all TM attitude deviations. Low frequency (0 to 2 Hz) attitude deviations are measured by gyro samples supplied every 0.064 seconds per axis. Higher frequency (2 to 125 Hz) attitude deviations are measured using Angular Displacement Sensors (ADS) which are sampled every 0.002 seconds per axis. The Angular Displacement Sensor is mounted directly on the Thematic Mapper.

A spacecraft formatter combines the necessary On-Board Computer information and the ADS samples into a 32 kilobit per second telemetry stream called Payload Correction Data (PCD). PCD contains all Flight Segment information needed to perform TM data processing. It is both downlinked on a telemtry channel and included with the TM wideband data. Also imbedded into TM wideband data is Mirror Scan Correction Data (MSCD) from which the scan mirror position is determined as a function of time. This data includes scan start time, scan direction, first half scan time error, and second half scan time error.

The NASA TM ground processing extracts the Mirror Scan Correction Data (MSCD) from the TM wideband data. The PCD is received using the telemetry path. Payload Correction Processing then combines the MSCD and PCD to generate Systematic Correction Data (SCD). The Systematic Correction Data is a complete set of correction data except that large bias and slow drift errors exist due to time, ephemeris. gyro measurement, attitude control and TM alignment uncertainty. These bias and drift errors are removed by Control Point Processing. Control Point Processing uses the mislocation between features in reference interval and the same features in the registrant interval to estimate these SCD errors. The SCD is then modified to remove the error effects and the result is called Geodetic Correction Data.

The payload correction and control point processing are performed over an interval or number of consecutively images scenes in an orbit path. This results in improved accuracy and fewer control points than processes that operate on individual scenes.

The final steps in geometric correction system involve resampling the TM image samples to place them onto the output coordinate system. The TM wideband data is first reformatted into Archive imagery in which reverse scan data has been reordered to correspond to the forward scan data, and integer detector and band offsets have been removed. The Archive imagery is then resampled during Geometric Correction Processing. The resampling is performed using the Geodetic Correction Data and it results in product imagery.

A more detailed description of the Flight Segment contributions to geometric correction is given in Section 2.0, the Ground Segment Processing is described in Section 3.0.

2.0 FLIGHT SEGMENT

The Landsat-D Flight Segment is shown in Figure 2-1. It is configured in two modules: Multimission Modular Spacecraft (MMS) and Instrument Module (IM). The MMS provides standard spacecraft subsystems such as Attitude Control (ACS), Propulsion Module for orbit adjust, a Collection and Data Handling (C&DH) Module which includes an On-Board Computer (OBC), and a Power Module. The Instrument Module includes the mission unique subsystems such as Thematic Mapper, Multispectral Scanner (MSS), Wideband Communications, High Gain Antenna and RF Compartment, Global Positioning (GPS) and Solar Array.

The Flight Segment contributions to geometric correction will be described in terms of TM position (ephemeris), TM attitude, TM scanning operation and associated Flight Segment correction information which is used in the Ground Segment Processing.

2.1 Position

TM inertial position is a factor in determining the TM sample location on the output coordinate system. Before describing how this knowledge is obtained (Section 2.1.2), the basic orbital parameters will be described.

Landsat-D Orbit

As shown in Figure 2-2, the Landsat-D orbit is sun synchronous, nominally crossing the equator at 9:45 a.m. local time. The orbit inclination is nominally 98.21 degrees with periodic orbit adjust maintaining this inclination to ±.045 degrees. The nominal equatorial altitude is 705.3 kilometers and due to a combination of periodic orbital eccentricity and earth oblateness the altitude will vary from 696 to 741 kilometers. The ground track repeats on a 16-day cycle and the equatorial crossing is maintained to within ±10 kilometers by periodic orbit adjust. The 16-day cycle generates 233 ground paths with a seven-day skip-cycle between adjacent paths.

The orbit inclination drifts, orbit altitude variation and ground track variation have significant geometric impacts. Orbit inclination drift is a factor affecting image rotation requirements. Altitude variation effects ground sample distance, inter-scan gap and scan line skew (see Section 2.3). Ground track and altitude variations interact with earth topology to create temporal registration errors.

Ephemeris

Ephemeris is data which describes the position and velocity of the TM as a function of time. Landsat-D ephemeris data is obtained directly from downlinked Payload Correction Data (PCD) telemetry. A more detailed description of Payload Correction Data is given in Section 2.4.

A system level ephemeris data flow is given in Figure 2-3. There are two possible sources of ephemeris data: NASA Goddard Orbit Support Computing Division (OSCD) and the Global Positioning System (GPS). OSCD generates predicted Earth Centered Inertial (ECI) ephemeris, then converts it to a highly compressed Fourier power series and residuals representation. The compressed data is uplinked to the Flight Segment where the on-board computer reconstructs the ECI ephemeris.

A GPS receiver/processor assembly (R/PA) is an experimental subsystem which is part of the Flight Segment. The receiver/processor assembly uses ranging information from GPS satellites to estimate Landsat-D ephemeris. The GPS ephemeris is computed in Earth Centered Earth Fixed coordinates, then sampled, converted to ECI and extrapolated by the On-Board Computer.

Independent of the ephemeris source, the resulting ECI ephemeris is used for attitude control and pointing the TDRSS Antenna. The ephemeris is sampled every 8.192 seconds and formatted for downlink by the On-Board Computer. Once on the ground, the received ephemeris data is fitted with a J2 orbit model. This is done to remove GPS data discontinuities or processing errors caused by the compression and decompression of OSCD ephemeris. The ground ephemeris processing is discussed in Section 3.1 (Payload Correction Processing).

The downlinked OSCD ephemeris may be a two-day old prediction. After ground processing, the error standard deviation of such data is given below:

	Position (Meters)	Velocity (Meters/Second)
Along-Track	500	.163
Cross-Track	100	.065
Radial	33	.650

The error standard deviation of GPS ephemeris is difficult to predict because it depends upon the number of operational GPS satellites and the length of time since the last GPS observation. GPS accuracy is expected to be considerably better than OSCD two-day predicts.

A ±20 millisecond uncertainty in spacecraft time will result in an additional ±140 meter along-track positional uncertainty.

The geometric effect of ephemeris and time errors are estimated and corrected during control point processing. This processing is described in Section 3.2.

2.2 Attitude

The TM attitude (orientation in an inertial frame of reference) is another factor used in determining the TM sample location on the output coordinate system. There are three dominant components which effect TM attitude: the Attitude Control Subsystem (ACS), higher frequency attitude deviations, and TM alignment with the Attitude Control Subsystem.

For discussion purposes, the instrument coordinate system is shown below:

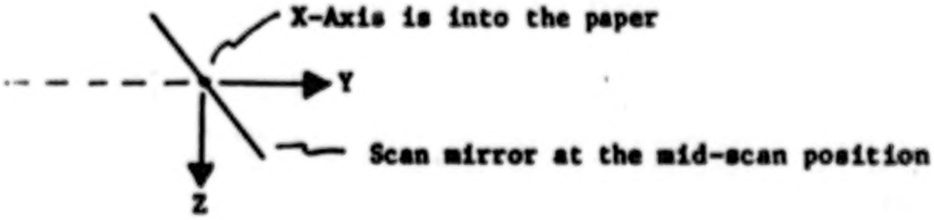

The X-axis is along the scan mirror pivot axis, the Z-axis is the telescope optical axis reflected through scan mirror at midscan, and the Y-axis completes the right hand coordinate system. Rotation about the X, Y and Z axes are called roll, pitch and yaw, respectively.

Such coordinate systems are defined for the TM and Multispectral Scanner (MSS) instruments. The instruments are mounted onto the Flight Segment such that the difference between the TM and MSS axes is less than 0.15 degrees in roll, 0.5 degrees in pitch, and 0.5 degrees in yaw. The alignments between the ACS axes and the TM axes and between the TM axes and MSS axes are then measured. Based on the available ECI ephemeris, the ACS controls the mean axes between the TM and MSS such that the mean Z-axis points to the earth center and the mean X-axis points along the instantaneous ephemeris velocity vector.

The ACS is a low frequency control system with bandwidths less than 0.01 Hz. Any higher frequency attitude deviations, which arise from the TDRSS antenna drive, the solar array drive, and TM or MSS mirror impacts, are not compensated by the ACS. Such disturbances must be measured and corrected in ground processing.

The ACS, alignments and high frequency attitude deviations are now described in more detail.

Attitude Control System (ACS)

Figure 2-4 shows a simplified functional block diagram of the Landsat-D Attitude Control System. The DRIRU (gyros) and Fixed Head Star Trackers constitute the attitude measurement devices. The reaction wheels are used to effect attitude control. In ACS operation the DRIRU measures change in inertial attitude about each of its three axes every 0.064 seconds. Gyro Data Processing removes gyro drift and low pass filters the samples to a 0.5 Hz bandwidth. The Euler Parameter Integration propagates the ACS Attitude using the processed DRIRU increments every 0.512 seconds. The Update Filter implements an extended Kalman filter process which uses the attitude error between the propagated ACS attitude estimate and star tracker measurements to compute gyro drift and an attitude correction. Star tracker measurements are made every minute under the best conditions and under the worst conditions tens of minutes may elapse between star measurements. Based on ECI ephemeris (see Section 2.1) and the alignment between the ACS axes and mean instrument axes, the desired ACS attitude is computed. The desired attitude has the mean TM & MSS instrument Z-axis pointed to the earth center and the mean instrument X-axis along the instantaneous velocity vector. An attitude error is computed and the reaction wheels are appropriately commanded every 0.512 seconds.

The ACS is a closed loop system because the attitude changes effected by the reaction wheels are sensed by the DRIRU. The ACS control bandwidth is 0.01 Hz about the pitch axis and 0.005 Hz about the roll and yaw axes. Exclusive of ephemeris error and disturbances caused by the TM and MSS, the ACS is required to control its pointed axes to within 0.01 degrees (1σ) with an attitude rate error of less than 10^{-6} degree/second (measured over a 100 minute interval). The dominant source of ACS error arises from Star Tracker measurement error.

As Figure 2-4 indicates, the DRIRU data (every .064 seconds), gyro drift estimate (every 4.096 seconds) and ACS attitude estimate (every 4.096 seconds) are downlinked for ground processing. Significant low frequency error exists in this data and their error effects must be removed during control point processing. These errors result from Star Tracker measurement errors, gyro drift estimation errors and propagated DRIRU Measurement Errors, and could be as large as 0.01 degrees (1σ) about the roll, pitch and yaw axes.

Alignment

The alignment between the ACS and the TM axes is a factor is determining the TM sample locations on the output coordinate system. ACS to TM alignment uncertainty results from error in the alignment measurement process in which eight separate alignment measurements are required. These measured alignments change as a result of launch structural stress, difference in thermal conditions between alignment measurements and orbital conditions, and spacecraft reassembly at the launch site. The ACS to TM alignment uncertainty will be 125 arc-sec (1σ) in roll and 250 arc-sec (1σ) in pitch and yaw. These alignment uncertainties will be substantially reduced by ground measurements using control points.

Under orbital conditions, a dynamic alignment error is expected to result from temperature variations within the spacecraft structure. The dominant source of these temperature variations is the operation of TM, MSS, Wideband Communications Subsystem and Multimission Spacecraft Modules. The thermal alignment rate error can be expected to be as large as 0.167 arc-second (1σ) and this error effect will be removed by control point processing (Section 3.2).

High Frequency Attitude Disturbances

There are four dominant sources of high frequency (greater than 0.01 Hz) mechanical disturbances: TDRSS Antenna drive, solar array drives, MSS scan mirror, and TM scan mirror. Interaction of these disturbances with the spacecraft structure causes attitude deviations. An extensive effort involving structural testing, modeling and simulation analysis characterized these interactions. A brief summary of these results will be given.

The TDRSS antenna is driven around the spacecraft z-axis (azimuth) and an elevation axis to follow the relative motions between Landsat-D and the earth synchronous TDRSS. A stepper motor drives the antenna. Under normal operating conditions, there are between 0 and 3 steps per second required to exactly follow TDRSS in elevation. The rate depends upon the relative position between Landsat-D and TDRSS. A randomizing antenna control system is implemented in the On-Board Computer that avoids dwelling on large structural resonances in the 0-3 Hz frequency region.

The solar array is driven open loop to follow the sun by a stepper motor (19.66 steps/second). The resultant spacecraft disturbance is estimated to be 0.2 arc-second (RMS). When the solar array position is adjusted to compensate for misalignment with the sun, much larger disturbances will occur. Solar array adjustment will not occur immediately before or during TM instrument operation.

The low level of attitude deviation due to the TDRSS antenna has been achieved through design of their control systems. No such control could be exercised for the TM and MSS instruments. The bumper impacts of the MSS and TM scan mirrors will create attitude deviations. MSS and TM scan mirrors operate at 13.62 and approximately 7 Hz, respectively. The alternating direction and impulsive impact of the scan mirrors produce significant torque amplitudes at odd harmonics (see Table 2.1). Minor differences in spacecraft manufacture can significantly affect the structural response to these excitations. The ground processing is conservatively designed to meet temporal registration specifications with roll, pitch and yaw attitude deviations of 20.0, 2.2 and 16.3 arc-seconds, respectively.

High Frequency Attitude Measurements

The High frequency attitude disturbances cannot be reduced to an acceptable level through structural design. It was shown in Section 1.2 that 1.13 arc-second (1σ) constituted the entire temporal registration error budget for a single scene. The actual allocation to high frequency attitude error is 0.5 arc-second (1σ). This situation requires measuring the attitude deviations of the spacecraft and providing a companion correction capability in the ground processing. After consideration of available measurement devices, structural flexibility, accuracy. and size and power requirements, it was decided to use a combination of the existing ACS gyro package (DRIRU) and a small three axis Angular Displacement Sensor Assembly (ADSA) to measure TM attitude deviations. The DRIRU measures angular displacements in the 0 to 2 Hz band and the ADSA measures angular displacements in the 2 to 125 Hz band. Their data is combined in ground processing (See Section 3.1) to yield angular displacements in the 0 to 125 Hz band.

The DRIRU is a NASA Standard. It contains 3 two-degree-of-freedom dry tuned gyros operating in a strapdown mode. The gyros are oriented such that redundant measurements are provided along three orthogonal axes. The output of each gyro channel is an asynchronous pulse train in which each pulse represents an incremental angular rotation about the gyro input axis. The pulses are accumulated in a register which is sampled every 0.064 seconds by the On-Board Computer. The key DRIRU performance parameters per axis are:

Drift Rate: 0.05 arc-second/second (1σ)
Drift Rate Stability: 0.003 arc-second/second (1σ) over 6 hours of operation
Noise: 1 arc-second (0 to peak) after linear drift removal
Bandwidth (3 dB): between 1.5 and 2.5 Hz
Quantization: 0.05 arc-second/pulse
Sample Time: 0.064 second

The Angular Displacement Sensor Assembly consists of three independent angular displacement sensors (ADS) oriented along orthogonal axes. As shown in Figure 2.5, the ADS uses a fluid-rotor inertia element which remains inertially fixed as the case is rotated about its input axis. A vane assembly is immersed in the fluid and its position with respect to the case is sensed with a low noise differential inductive pickoff. The pickoff system produces an analog signal output which is directly proportioned to the deviation of the vane assembly from its null position. To maintain the vane assembly at the desired null position, an electrical auto-null system is used to feed back a torque to the moving vane assembly. The feedback is in part proportional to the integral of the output signal, keeping the average vane position at a fixed output value. This in turn keeps the vane assembly average position at the null position of the pick-off and the ADS does not respond to low frequency inputs. Since the auto-zero feedback loop contributes torque proportional to position as well as the integral of position, it produces a low natural frequency second-order system response in combination with the inertia of the rotor, with a nominal loop closure at 2 Hz. This provides an overall amplitude frequency response for the unit which rises at 18 dB/octave to 0.05 Hz, at 12 dB/octave from 0.05 to 2 Hz and is nominally flat from 2 Hz to 2000 Hz. Significant phase shift exists below 30 Hz.

Three ADS sensors are mounted in the ADSA along with presample low pass filter and A/D electronics. Key ADSA performance parameters per axis are:

Noise: 0.01 microradian (RMS)
Bandwidth (3 dB): 2 to 125 Hz (nominal)
Threshold: Not measurable
Quantization: 0.122 microradians
Full scal reading: 250 microradians
Sample time: 0.002 seconds

2.3 Thematic Mapper

TM Geometric characteristics have impacts on the ground processing. While the TM and MSS both employ object plane scanning, certain TM geometric characteristics differentiate the two instruments. In general, these characteristics are related to the TM bidirectional scanning, the relatively wide focal plane separation of TM spectral bands, the decreased TM field-of-view size, and the availability of good performance data. A brief review of significant TM geometric characteristics follows.

Focal Plane Layout and Detector Sampling

A geometric overview of TM is shown in Figure 2-6. The TM detectors are arranged in two focal plane assemblies: primary and cold. The primary focal plane assembly (PFPA) consists of four high resolution spectral bands each having 16 detectors, and an instantaneous field-of-view (IFOV) of 42.5 microradians. The odd numbered detectors are arranged in a row normal to the scan direction. The even detectors are arranged in a parallel row, offset 1 IFOV in the cross-scan direction and 2.5 IFOV's in the along-scan direction. The cold focal plane assembly (CFPA) consists of two high resolution bands each of which is arranged similarly to the high resolution bands of the PFPA. The cold focal plane assembly also consists of a thermal band which has only four detectors with a 170 microradian IFOV. Figure 2-7 shows the overall layout of the focal plane assemblies with the cold focal plane projected to the prime focal plane location.

The detector arrays are swept back-and-forth approximately normal to the ground track by the scan mirror. A West-to-East scan (on a daytime descending orbit pass) is called a forward scan. The East-to-West scan is called a reverse scan. Each high resolution band detector is sampled every 9.611 microseconds which correponds to one IFOV (42.5 microradians) of nominal object space mirror motion. All odd numbered detector outputs are held at one time and all even number detector outputs are held one half sample time later. With the nominal 2.5 IFOV spacing between odd and even numbered detectors, this creates a 2 IFOV odd-to-even detector spacing on forward scans and a 3 IFOV spacing on reverse scans.

Scanning Mechanisms

The TM has two scanning mirrors: the Scan Mirror and the Scan Line Corrector. The Scan Mirror rotates about (approximately) the spacecraft X-axis and thus scans the detector arrays normal to the direction of flight. The scan mirror scan cycle is 7 ± .01 Hz. Nominally, the active scan time (imaging time) in one direction is 0.060743 seconds with 0.010719 seconds of turnaround time. The forward scan start and end are marked relative to the TM frame by an optical sensor called the Scan Angle Monitor (SAM). The SAM similarly marks the reverse scan start and end with nominal co-location between forward scan start and reverse scan end and between forward scan end and reverse scan start. The SAM also identifies scan mirror mid-scan position.

The scan line corrector (SLC) scans about the spacecraft Y-axis and sweeps the detector arrays to oppose the spacecraft ground track motion during the active portion of the scan. The SLC is reset during the forward the reverse scan mirror turnarounds. This generates an approximately parallel forward and reverse scan pattern on the earth.

Ideal TM scanning is illustrated in Figure 2-8. The 16 x 42.5 = 680 microradian wideband arrays are swept across the spacecraft ground track by the scan mirror. The increase in array ground width from the scan center to the extreme scan positions is a 5 meter "bow-tie" effect. The SLC scans against the along-track ground velocity at a fixed rate which will cancel the in track earth velocity and the small in track earth rotational velocity component at the 712.8 km design altitude. The composite scan is illustrated in the lower part of Figure 2-8. At spacecraft position (1), the scan mirror is in its start scan position for a forward scan, and the SLC points the 680 microradian band arrays ahead of the sub-satellite point. The scan mirror moves the band arrays normal to the paper's plane, for nominally 0.060743 seconds, until the end of forward scan is reached. During that time, imagery is acquired, the spacecraft advances along its orbit, the SLC pushes the scan back along the ground track and the band arrays scanned normal to the ground track. At the end of forward scan (spacecraft position (2)), the SLC reset command is issued. During the nominal .010719 second scan mirror turnaround, the SLC is reset to its initial pointing angle, the spacecraft advances to position (3) and the scan mirror has moved to the start of reverse scan. The process is then repeated for the reverse scan.

The TM band array width, active scan time, scan mirror turnaround time and SLC active scan rates are fixed. They have been designed for an altitude of 712.8 km and an effective ground velocity of 6.821 km/second (the nominal condition at 40° Latitude) with the effect of bow-tie split, creating an equally small scan gap at scan center and overlap at scan end. However, spacecraft altitude varies between 696 and 741 km while velocity variations are small. As shown in Figure 2-9 at altitudes above the TM design point the scan width widens causing scan overlap and the SLC over-compensates the spacecraft ground track velocity causing scan skew. The actual scan error pattern is a composite of scan overlap, scan skew and bow-tie effects. The result is that the 16 detectors within a scan are always evenly spaced but the detector spacing between scans varies. The difference in ground spacing for detector spacing within a scan and for detectors 1 and 16 of two consecutive scans is called scan gap. Scan gap is positive when the spacing between scans is greater than the spacing within a scan. In general, scan gap varies across the scan and is usually greatest at the end of scans. Figure 2-10 shows the worst case end scan gap from altitude variation (as a function of Latitude), spacecraft atttitude deviation, and TM overlap/underlap. The composite worst case range of scan gap is -2.8 IFOV to 2.0 IFOV. The altitude deviation scan gap error results from scan width, SLC skew and bow-tie effects. Spacecraft attitude deviation is caused by pitch and yaw axis motions and the one IFOV scan gap is a spacecraft structural design requirement. The TM underlap/overlap is the specified limit imposed on the instrument. It is expected that the attitude deviation effects will be substantially less than shown and that scan gaps due to altitude variation will dominate.

Scan Profiles

Ideally, the scan mirror has a constant angular rate over the active scan time (from scan start to scan end). As Figure 2-11 indicates, small rate variations will occur in scan mirror motion. The deviation in angular position from linear motion is called nonlinearity or profile. The profile results from small torques acting on the scan mirror. Magnetic compensators have been incorporated into the TM design that have the effect of significantly reducing the residual flex pivot torque. This results in an extremely linear mirror motion with worst case nonlinearity less than 200 microradians (object space). This low nonlinearity is required for good instrument level band-to-band registration due to the relatively wide geometric spacing between band arrays. It has been shown that the profile can be described by a fifth order polynomial and that different polynomials are required for forward and reverse scans.

After extensive scan mirror unit level testing, it was learned that the scan mirror profiles were not stable over time. They slowly "wander" about ±20 microradians (object space) after days of operation. Wander is limited to the second order profile component and this can be estimated (see Section 3.1) by using information about first half scan and second half scan times. This data is supplied in the TM wideband data.

Nonlinearities in the cross axis scan mirror motion and in the SLC motions must also be compensated during ground processing.

Scan Line Length Control

Active scan time (the time from scan start to scan end) is also known as line length. The TM actively controls line length by measuring scan times and appropriately adjusting the torque magnitudes applied to the scan mirror during turnaround. The scan mirror is free running during the active scan time with no applied torque. This control scheme differs from that of the MSS which essentially controls scans cycle time (start to start time). The TM scan control is insensitive to attitude deviations which are self induced. Under such conditions, line length variations of 1 microsecond (1σ) are typical. However, it is extremely sensitive to externally induced attitude deviations. For example, one microradian of MSS excitation at 68.1 Hz is capable of creating line length variations of 16 microseconds or about 70 microradians in geometric effect. Line length variations as large as 400 microseconds are accommodated in ground processing design.

Forward to Reverse Scan Discontinuity

The bi-directional TM scanning introduces a number of significant factors that were not present with the MSS design. The different forward-to-reverse profiles have already been mentioned. Detector amplifier delays (typically 10 microseconds) and SAM electronic delays act in the opposite directions for the forward and reverse scans. The result is a forward-to-reverse scan discontinuity which must be corrected during ground processing.

2.4 Flight Segment Correction Data

There are two sources of Flight Segment data needed for geometric correction ground processing: Mirror Scan Correction Data (MSCD) and Payload Correction Data (PCD). The Mirror Scan Correction Data is imbedded into the TM wideband data. It includes the spacecraft time at scan start (scan time), the first half scan time error, the second half scan time error and the scan direction (forward to reverse) indicator. The scan time is the spacecraft time, with 0.0625 millisecond precision, at the scan mirror start position. This time is used to relate scan mirror position to the ephemeris, ADSA and DRIRU data. The time at any TM detector sample is obtained by adding 9.611 microseconds times the sample number to the scan time. The first half and second half scan time errors define the time error from a nominal scan time. These errors are known to a 0.188 microsecond precision and are determined from the TM oscillator.

Payload Correction Data includes ADSA angular samples every 0.002 seconds per axis, DRIRU output register samples every 0.064 seconds per axis, DRIRU drift estimates every 16.384 seconds per axis, ephemeris data every 8.192 seconds, spacecraft time, and TM housekeeping telemetry data. PCD is transmitted via a 32 kilobit/second telemetry link and is also imbedded into the TM wideband data. Figure 2-12 shows the PCD attitude data and scan start timing. All PCD data collection is driven by the spacecraft oscillator. This oscillator generates time code which is imbedded into the PCD telemetry cycle and identifies the TM start scan time. The spacecraft oscillator synchronizes ADSA sampling and synchronizes on-board computer (OBC) operation. The OBC executive scheduler in turn drives DRIRU sampling.

The ADSA samples and OBC data are supplied to the PCD Formatter which constructs the PCD Telemetry Cycle Data. This is a fixed format telemetry data package occurring every 16.384 seconds. For each occurrance of a given data item in the PCD telemetry cycle, its occurrence time relative to the imbedded time code is known. For example, as indicated in Figure 2-13, the first ADSA X-axis sample was taken 3/8 milliseconds after the telemetry time code and each subsequent X-axis ample in the PCD cycle occurs every 0.002 seconds.

3.0 GROUND SEGMENT

With respect to geometric correction, the Thematic Mapper Ground Segment uses Mirror Scan Correction Data, Payload Correction Data and control point information to determine where TM detector samples fall on output map projection systems. Then the raw imagery is reformatted and resampled to produce image samples on a selected output projection grid system.

Figure 1-4 shows the TM geometric correction functions performed by the ground processing. These functions were briefly described in Section 1.0 and will now be discussed in more detail.

3.1 Payload Correction Processing

Payload Correction Processing uses Payload Correction Data (PCD) and Mirror Scan Correction Data (MSCD) to generate Systematic Correction Data (SCD). All subsequent processing uses the relatively simple SCD to determine TM imagery geometric distortions. SCD provides a means of locating TM detector samples on the output projection system. Large bias and relatively slowly varying drift errors are contained in the available attitude, ephemeris, time and TM alignment information used in generating the SCD. These errors remain in the SCD but their effect is removed during control point processing. A set of SCD applies to World Reference System scene and consists of four data groups: Benchmark Matrices, High Frequency Matrices, Focal Plane Geometry Matrices, and Processing Parameters.

Benchmark Matrices define the location of the TM optical axis assuming perfect attitude, linear scan mirror motions, linear SLC motions and nominal active scan times. Ephemeris, TM alignment, actual scan start times and map projections are used in generating the Benchmark Matrices. These matrices include only slowly varying distortion information and thus are defined on a relatively sparce grid system consisting of 256 data items per WRS scene. Any given detector sample is located by interpolating the grids. The Benchmark Matrices provide the basic geometric distortion information. All other distortions resulting from attitude deviations, scan profiles or actual detector location on the focal plane assemblies are small additive errors.

High Frequency Matrices define the attitude deviations, scan profile error and line length variations of each scan in the WRS scene. These matrices are time based and define the high frequency optical axis deviations from the Benchmark Matrices. This data is considerably more dense and consists of 26180 data items per WRS scene.

Focal Plane Geometry Matrices define the geometric adjustments needed to move from the optical axis location to that of any TM detector. These adjustments include actual focal plane detector location and the geometric effect of electronic time delays. The data quantity is relatively small consisting of 240 data items per WRS scene.

Processing parameters are data items, such as scan line length and detector offset adjustments made during image reformatting. They are needed during image resampling processing.

As shown in Figure 3-1, Payload Correction Processing consists of three major functions: Payload Correction Data Processing, Mirror Scan Correction Data Processing and Systematic Correction Data Generation.

Payload Correction Data Processing

Payload Correction Data Processing operates on the ephemeris information and attitude deviation measurements (ADSA and DRIRU Data) from the spacecraft Payload Correction Data (PCD). This processing synchronizes all attitude and ephemeris data to a common PCD telemetry start time for ease of subsequent processing.

The ephemeris data from PCD arrives as Earth Centered Inertial position and velocity estimates every 8.192 seconds. This received ephemeris is not directly suitable for precision image processing due to on-board computer processing errors, potential Global Positioning System data discontinuities and telemetry errors. The control point processing (Section 3.2) requires a smooth analytic ephemeris with known error dynamics. This is provided by fitting the initial conditions of a second zonal harmonic (J2) orbit model to the received ephemeris. The fit error is a data quality indicator for the received ephemeris data. Ephemeris processing uses the fitted initial conditions to synchronize the ephemeris data with the PCD telemetry start time and regenerates the smoothed ECI ephemeris data every 2.048 seconds using the J2 model.

Attitude Data Processing (ADP) combines and synchronizes the ADSA and DRIRU attitude deviation information to yield TM optical axis roll, pitch and yaw attitude deviations in a zero to 125 Hz bandwidth. ADS and DRIRU data are first processed to replace bad values and are logically extended through missing data that may occur due to telemetry link errors. Figure 3-2 shows the functions performed in ADP. The 0.002 second ADSA roll, pitch and yaw axis samples are converted to microradian units, and synchronized to the PCD telemetry start time. The coordinate axes are then rotated to align with the TM optical axis.

The 0.064 second roll, pitch and yaw DRIRU angles are similarly converted to microradian angular change units, the on-board computer gyro drift estimates are applied, the data is rotated to align with the spacecraft pointed axis, nominal body rates derived from ephemeris data are removed, the data is then aligned with the TM optical axis, and digitally pre-filtered. The processed DRIRU angular increments are then synchronized to the PCD telemetry start time and interpolated to 0.002 second samples.

The processed ADSA and DRIRU data are now in a common coordinate system and time synchronized. The data sets are then summed and digitally filtered to remove phase and amplitude distortions. The processing has been designed to provide less than 1% error.

Provisions have been made that allow modification of DRIRU pre-filter and final combined digital filter coefficients based on ADS temperature information. The need for this capability has not been demonstrated by ADSA testing and this filter coefficient processing is not being used.

Mirror Scan Correction Data Processing

Mirror Scan Correction Data Processing generates along-scan profile deviations and cross-scan profile deviations for each scan. The profile deviations are relative to the TM body axes and are time synchronized with the Attitude Data Processing outputs. The start scan times are also adjusted to use the PCD start time as their reference.

The Mirror Scan Correction Data (MSCD) Processing inputs (scan start time, first half scan time error, second half scan time error and scan direction) are imbedded by the TM into its wideband data. This data is extracted from the wideband data and checked for self consistency. That is, proper scan time advancement, within tolerance variation in estimated nonlinearity at midscan, and scan direction changes are evaluated. Front end processing hardware also provides independent measures of total line length and start-scan to start-scan time. The number of 8 bit TM words between scan start and end codes imbedded in the TM wideband data are counted. Due to the critical need for proper MSCD, it is also checked for consistency against these independent measures. Errors are reported and best estimates are substituted for rejected MSCD values. The first half scan time errors and second half scan time errors are converted to mid-scan time interval and end-scan time interval for subsequent processing.

Figure 3-3 shows the MSCD Processing functional flow. Telemetry-Imagery Synchronization adjusts the scan start times to reference the PCD start time and computes the line length processing parameters needed during resampling. Scan Mirror Data Processing uses the relative scan start times, mid-scan interval time and end-scan time interval to interpolate the roll axis attitude deviations at scan start, mid-scan and end-scan times. These roll axis deviations along with the static first half and second half scan angles, and the mid-scan and end-scan interval times are used to estimate the second order scan mirror profile adjustment. The scan profile is estimated for each scan. A linear correction factor, based on end-scan interval time, is then used to modify the adjusted profile and generate along-scan profile deviations at the same times as the ADP output samples.

Scan Line Corrector Data Processing generates cross-scan profile deviations which arise from the Scan Line Correction (SLC) profile and the cross-axis scan mirror profile. The SLC position is reset by the end-scan Scan Angle Monitor (SAM) position and it initiates active scanning independent of the SAM start. Thus, mirror turnaround variation effects the coordination between SLC and the scan mirror. The nominal SLC profile is, therefore, adjusted based upon mirror turnaround time. A linear correction factor, based on end-scan interval time, is also applied to adjust the cross-axis scan mirror profile. The composite adjusted cross-axis Scan Mirror and SLC profiles are then used to generate cross axis profile deivations at the same times as the ADP output samples.

Systematic Correction Data Generation

PCD Processing and MSCD Processing have both compensated and time synchronized the ephemeris, attitude deviation and scan profile data. The final function of Payload Correction Processing is Systematic Correction Data (SCD) Generation. Figure 3-4 shows the SCD Generation Processing flow. An overview of SCD content is shown in Figures 3-5, 6 and 7.

Image framing determines the WRS scene parameters. Scene center time, scene center scan, and output coordinate system scene center X-shift are determined from World Reference System path and row identification. The output projection scene center location is always X=0, Y=0 with output grid points spaced every 28.5 meters in X and Y.

The benchmark matrix calculation generates a grid of geometric distortion information for each output map projection. Figure 3-8 illustrates the benchmark matrix concept. This Figure shows an example of the optical axis path on a portion of the X,Y output coordinate system. The circles along the optical axis path represent sample times (every 9.611 microseconds) of odd numbered high resolution band detectors. The i value is the sample number relative to scan start. The benchmark value, P_0, indicates the fractional sample number and the benchmark value, Y_0, indicates the output projection Y coordinate where the optical axis path crosses a specific output projection X coordinate (X = 43.776 km for this example). The computation is also performed for a point on the focal plane shifted $\sigma = 318.75$ microradian cross-scan from the optical axis. These benchmark values are called P_1 and Y_1.

There are 374 scans identified with each WRS scene. The first scan is always a forward scan. The benchmarks are calculated at 4 pairs of forward and reverse scans: 1 and 2, 125 and 126, 249 and 250, 373 and 374. For each scan, P_0, Y_0 and P_1, Y_1 values are determined for X coordinates: -102.144 km, -72.96 km, -43.776 km, -14.592 km, 14.592 km, 43.776 km, 72.96 km, and 102.144 km.

Benchmark values can be determined for other scans of X-coordinates by interpolating the benchmark matrix data. Actual scan times must be used during this interpolation process.

The benchmark matrices are generated using WRS scene center parameters, map projections, TM alignment, smoothed ephemeris data, and scan start times for the evaluated scans. The processing assumes that the attitude control maintains perfect pointing of its controlled axes and that the scan mirrors have linear angular motion with nominal active scan time. These assumptions are removed when high frequency matrices are combined with the benchmark matrices.

High Frequency Matrices combine the ADP altitude deviation data and the Mirror Scan deviation data. There are two high frequency matrices: along-scan and cross-scan. The along-scan High Frequency Matrix has 35 data values with 0.002 second spacing for each of the 374 scans comprising a WRS scene. These high frequency values are created by summing the scan mirror deviations and the ADP roll data. Figure 3-9 illustrates which high frequency values are used for a given scan. For each scan, 35 high frequency values (0.068 seconds) are supplied. The scan start time is within 0.001 second of the second value's time.

The Cross-Scan High Frequency Matrix is generated by combining cross-scan mirror deviations (σ_E), pitch (θ_{pitch}) and yaw (θ_{yaw}) attitude deviations:

$$\theta_{HF} = \sigma_E - \theta_{pitch} \cdot \cos\theta - \theta_{yaw} \cdot \mathrm{SIN}\theta$$

where θ is the scan mirror point angle relative to mid-scan. The matrix has 35 entries, evaluated every 0.002 sec, for each of the 374 scans comprising the WRS scene. The selection of the 35 points is performed analogously to the Along-Scan High Frequency Matrix.

Detector focal plane location parameters define the along-scan and cross-scan off-axis location of the detector elements. These parameters include the effective geometric error due to TM timing delays. These data items are fixed in a static data base and include the nominal pointing vector scan rate across the output projection, nominal along scan focal plane band locations, along scan focal plane detector locations, nominal cross scan focal plane band location and the cross-scan focal plane detector spacing.

The Data Formatter-Processor (DFP) performs the function of nominally aligning odd-even detectors and spectral bands arrays within a scan. This operation is performed on an integer detector sample basis while the TM archive imagery is being formatted. The DFP odd detector shifts indicate the magnitude of this shift for each scan direction.

3.2 Control Point Processing

Control point processing estimates the low frequency errors due to uncertainties in the input data that was used to generate the SCD. Measurements for estimating the SCD errors are provided by control point mislocations in the imagery generated by resampling TM data using the SCD.

The SCD geometric errors fall into two broad categories: (1) High frequency errors and (2) Bias and drift errors. High frequency errors cannot be removed using control points. These errors are principally caused by:

- High frequency (greater than 0.01 Hz) attitude deviation measurement and processing errors
- TM scan repeatability errors
- Computational and linearization errors made in generating and using SCD

The effect of bias and drift errors can be substantially reduced through control point processing. These errors are caused by data uncertainties in:

- Ephemeris
- Low frequency attitude
- TM alignment

The basic approach used in estimating these errors is to model their variation over time and then use control point mislocation measurements to estimate state variable parameters of these models. In this manner, significant reduction to the number of needed control points can be achieved, especially when a group of consecutively imaged scenes are processed. This approach also provides reduced sensitivity to control point location distribution over simple polynomial error models which have been used in previous Landsat processing systems. Information from regions with large numbers of control points can be propagated to image regions with few control points.

Drift and Bias Errors in SCD

The spacecraft ephemeris data has been smoothed with a J2 orbit model during Payload Correction Processing. This process does not significantly increase the ephemeris uncertainty described in Section 2-1. It does provide a smoothed analytic ephemeris with known error dynamics with respect to true ephemeris. Thus, dynamic equations can be written defining ephemeris error propagation in time.

The relative timing between scan data and attitude deviation data is tightly controlled by the spacecraft oscillator. However, time errors effectively create additional uncertainty in ephemeris, especially in the rapidly changing along-track component. Time errors present no additional processing complexity over those of the ephemeris uncertainty.

The spacecraft attitude control system has an inertial attitude uncertainty (0.01 degrees (1σ)) due to star tracker uncertainty, star tracker misalignment, non-linear gyro drift and ephemeris uncertainty. The gyros measure any attitude deviations below 2 Hz and attitude control stability is not a significant factor. The dynamics of the pointing uncertainty are well understood and can be accurately modeled as shown in Figure 3-10.

The alignment between the TM and the Attitude Control Systems reference axis is uncertain due to alignment measurement error, differing structural temperatures at time of alignment measurement and during orbital conditions, reassembly of the Multimission Spacecraft and Instrument Module at the launch site, and structural stresses during launch. In addition to this unknown alignment bias, structural temperature variation from cyclic operation of spacecraft subsystems will cause the alignment to vary over time. A good characterization of dynamic alignment is difficult to obtain. The system level design approach has been to estimate alignment effects during control point processing. The processing has been parametrically exercised with flexible correlated noise models such as that shown in Figure 3-11.

Landsat-D Control Point Concept

The Landsat-D concept underlying the use of control points is shown in Figure 3-12. The Landsat spacecraft is maintained in an orbit which generates a repeatable ground track. An orbital ground track is repeated every 16 days. Each time a World Reference System scene is imaged, the output product should be temporally registered to previous output products.

If Systematic Correction Data were used to generate output products, the resulting imagery would be internally consistent (with the exception of high frequency and drift errors), but would exhibit large offsets when compared temporally. Control points are used to establish temporal registration by estimating the spacecraft errors (ephemeris, time, low frequency attitude and alignment errors) needed to force each overflight to register with the reference interval imagery.

In order to establish a Geodetic basis for output products, the reference interval is first rectified to a geodetic reference. Landsat-D uses available maps (called Standard Maps) as the geodetic reference. This rectification is accomplished during a Control Point Library Build process. The reference interval imagery is corrected using SCD's. Then mislocations between the corrected reference interval and geodetic control point locations from the Standard Maps are used to estimate the spacecraft errors. All Landsat-D TM processing is performed using a standard geoid. Thus, Geodetic Control Point information from the Standard Maps are converted to latitude, longitude and elevation relative to the standard geoid. The elevation is needed so that spacecraft errors can be properly estimated. The spacecraft error effects are removed from the benchmark matrices of the SCD's creating Geodetic Correction Data (GCD). Although the elevations of Geodetic Control points were used in estimating spacecraft errors, during resampling it is assumed that all TM detector samples fall on the standard geoid and earth topographical effects are not considered.

The control point library for the reference interval can now be constructed. It consists of registration control point chips which are 32 pixel by 32 line sections of SCD corrected reference interval imagery. At a defined location on the control point chip, the latitude and longitude and elevation are defined relative to the standard geoid. The elevation information is derived from the standard maps. The latitude and longitude are derived using the GCD's for the reference interval, the elevation information, and map projection equations. These registration control points are used to determine the mislocations between the reference interval and all subsequent passes over the reference interval.

Control Point Processing Flow

An overview of the Control Point Processing Flow is shown in Figure 3-13. Payload Correction Processing has generated a set of SCD's for scenes comprising the interval to be processed. The SCD along with the control point latitude, longitude and elevation information from the control point library are used to determine the expected control point location in the unprocessed TM imagery. Control point search neighborhoods are then extracted from the unprocessed imagery. The extracted neighborhood is sufficiently large to generate a 128 pixel by 256 line section of product imagery which is centered on the expected control point location. With this sizing, the 32 pixel by 32 line control point chip can be found in the control point neighborhood even for three sigma ephemeris, time, attitude, and alignment errors. The extracted search neighborhood imagery is first radiometrically corrected using look-up tables (RLUT) and then geometrically corrected using the SCD.

The resultant control point search neighborhood is then digitally correlated with the corresponding control point chip from the control point library. This correlation involves gradient enhancement of edge features in both the control point chip and neighborhood to reduce temporal changes; a rejection criteria which examines the correlation peak and surrounding correlation values; and a subpixel location routine. To meet the specified temporal registration performance, the control point location procedure must be capable of finding chip to neighborhood match points with an error of less than 0.1 pixel (1σ).

Next, the control point mislocation is determined. This is the error on the output projection between the expected control point location (determined from the latitude, longitude and elevation) and the actual observed control point location in the SCD processed control point neighborhood.

The Geodetic Error Determinator (GED) software uses the control point mislocation information to update the SCD's in the interval. GED processing has three basic steps: Filtering, smoothing, SCD to GCD conversion. During filtering, the mislocation results are used to estimate state variables of a spacecraft error model. The spacecraft error state variables are position error (x,y,z), velocity error $(\dot{x},\dot{y},\dot{z})$, attitude error (R,P,Y) and attitude rate error $(\dot{R},\dot{P},\dot{Y})$. After simulation analysis, it was discovered that alignment and attitude errors could be combined into a single set of six attitude variables. The filtering proceeds by propagating the spacecraft error state to a control point time. The spacecraft state is estimated as a weighted average of the state measured using the mislocation information and the propagated state. The smoother adjusts the spacecraft error state using the control point information over the entire interval. The SCD to GCD conversion processing applies the spacecraft error states to adjust the benchmark matrix values of the SCD's. The adjustments remove the measured error effects from the SCD and the result is called Geodetic Correction Data (GCD).

3.3 Geometric Correction Processing

Geodetic Correction Data locates TM detector samples on the output projection system. This information is used during Geometric Correction Processing to resample the detector samples, placing them on the output grid locations as indicated in Figure 3-14.

An output scene may be generated using either of two resampling methods: Nearest Neighbor and Cubic Convolution. Both resampling types are implemented in a two step process which is illustrated for cubic convolution in Figure 3-15. This Figure shows the resampling process without consideration of scan gap problems. First, samples of a given detector (input pixels) are resampled to output projection column locations. This resampling occurs in one dimension along a line of detector samples (called a scan line). Such resampled values are called hybrid pixels and the process that generates the hybrid pixels is called X-resampling. Next, single dimension resampling is performed along each output projection column using the hybrid pixels. This is called Y-resampling and the result is a resampled value called an output pixel. Cubic convolution uses four pixels in the resampling process. The applied weights are those of a cubic spline and are shown in Figure 3-16. Nearest Neighbor interpolation chooses the closest pixel value for each resampling step.

The TM scan gap error, described in Section 2.3, causes additional complexity for the resampling process. With MSS processing, acceptable geometric error results from assuming that the line spacing within a scan is equal to the line spacing between scans over a limited region of imagery. With TM processing the gap spacing must be considered. The system throughput requirements place severe limitations on the resampling process implementation. There are nearly 3 x 10^8 output pixels in a TM scene. The ground processing requirements translate to an average processing rate of 750,000 pixels/second for resampling. Generation of every pixel requires at least eight integer multiplies and six adds when using cubic convolution. To meet these high rates, a dedicated processor is used to implement the arithmetic pipeline resampling procedure. The processor is called a Geometric Correction Operator (GCO). Figure 3-17 defines the scan parameters of gap size, gap skew and scan line skew. These parameters specify the geometry between scans and between a scan and the output grid. The GCO generates output segments of 128 pixels (detector samples) by approximately 17 lines and Table 3-1 shows the GCO capability and worst case conditions for the scan parameters.

When cubic convolution resampling is used, the GCO implements a three-pass process to resample the gap region between two scans. The first pass is call X-resampling. It generates hybrid pixels aligned along output grid columns by using cubic convolution resampling along input lines as previously described. Figure 3-18 shows the hybrid pixel locations for two scans after X-resampling. The generation of samples at grid locations requires the use of four unevenly spaced hybrid pixels between 15 and 18. The resampling weights to be applied in this gap region are a function of two parameters: the distance between the grid point and scan line 16 and the gap size. Note that the line spacing within scan N and scan N+1 may be assumed equal.

When performing high speed resampling, it is necessary to use precomputed sets of four weights. This avoids the significant overhead of generating the weights during processing. The weight sets are calculated every 1/32 pixel. In order to reduce the number of weight sets and to simplify the processing, an intermediate resampling pass called sweep extension (or E-resampling) is used. Starting with the hybrid pixels from scans N and N+1, scan N is extended (lines 17E, 18E, etc.) using a spline interpolation along output columns as shown in Figure 3-18. This extension continues until output grid pixels can be generated using cubic convolution with the hybrid pixels of scan N+1 alone. The extension pass requires weight sets which are a function of one parameter, the gap size, because the extension lines are spaced at an integer number of line spacings below line 16.

The last resampling pass (Y-resampling) is then performed after sweep extension. The output grid pixels can be generated using cubic convolution along the output grid columns as with the zero gap case. The hybrid pixels from scan N and the extension pixels are used in this pass.

The gap region between scans N+1 and N+2 is similarly processed by extending scan N+1 and performing Y-resampling starting from the point at which processing of scan N was terminated.

By appropriately defined weight sets, both positive and negative gaps can be accommodated using sweep extension. This approach reduces into standard cubic convolution when the gap size is zero. The sweep extension resampling is implemented with cubic spline interpolations which are defined in Figure 3-19.

4.0 ACKNOWLEDGEMENT

This work was supported by NASA Goddard Space Flight Center under Contract NAS5-25300.

CORRECTION DATA GENERATION CONCEPT

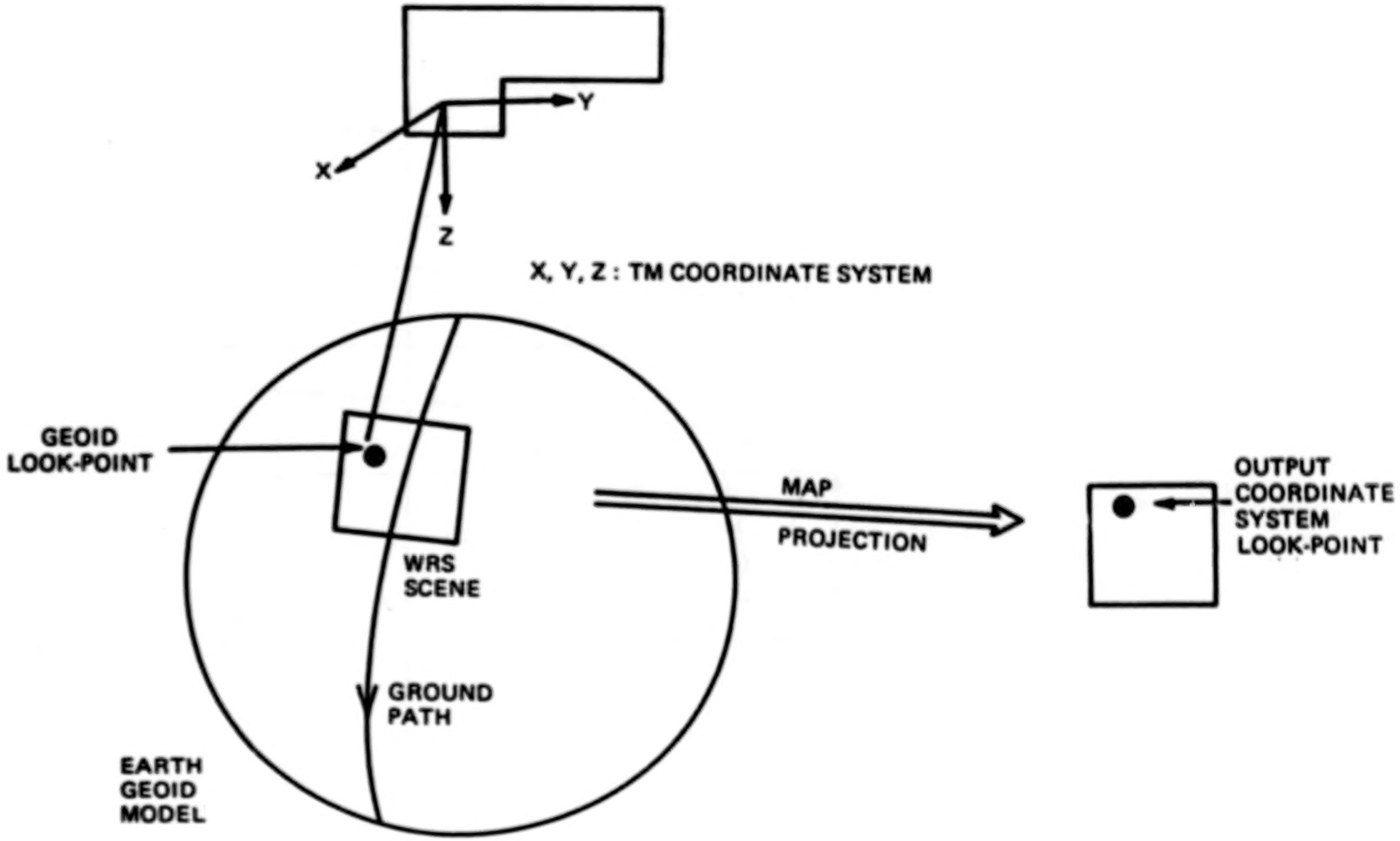
Y
X
Z
X, Y, Z : TM COORDINATE SYSTEM
GEOID LOOK-POINT
WRS SCENE
GROUND PATH
EARTH GEOID MODEL
MAP
PROJECTION
OUTPUT COORDINATE SYSTEM LOOK-POINT

FIGURE 1-1

RESAMPLING CONCEPT

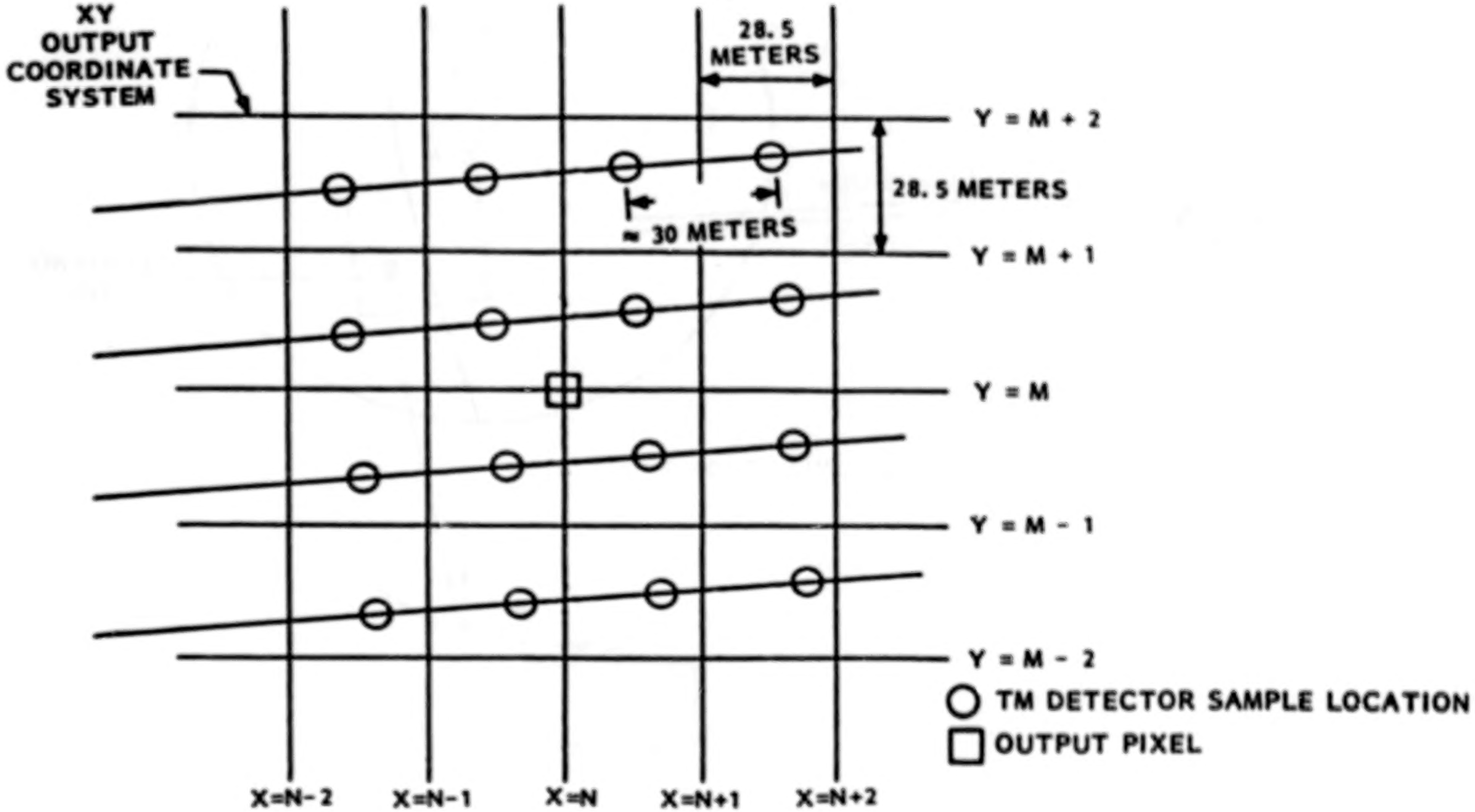
XY
OUTPUT
COORDINATE
SYSTEM
28.5
METERS
28.5 METERS
≈ 30 METERS
Y = M + 2
Y = M + 1
Y = M
Y = M - 1
Y = M - 2
○ TM DETECTOR SAMPLE LOCATION
□ OUTPUT PIXEL
X=N-2
X=N-1
X=N
X=N+1
X=N+2

FIGURE 1-2

GEOMETRIC ACCURACY SPECIFICATIONS

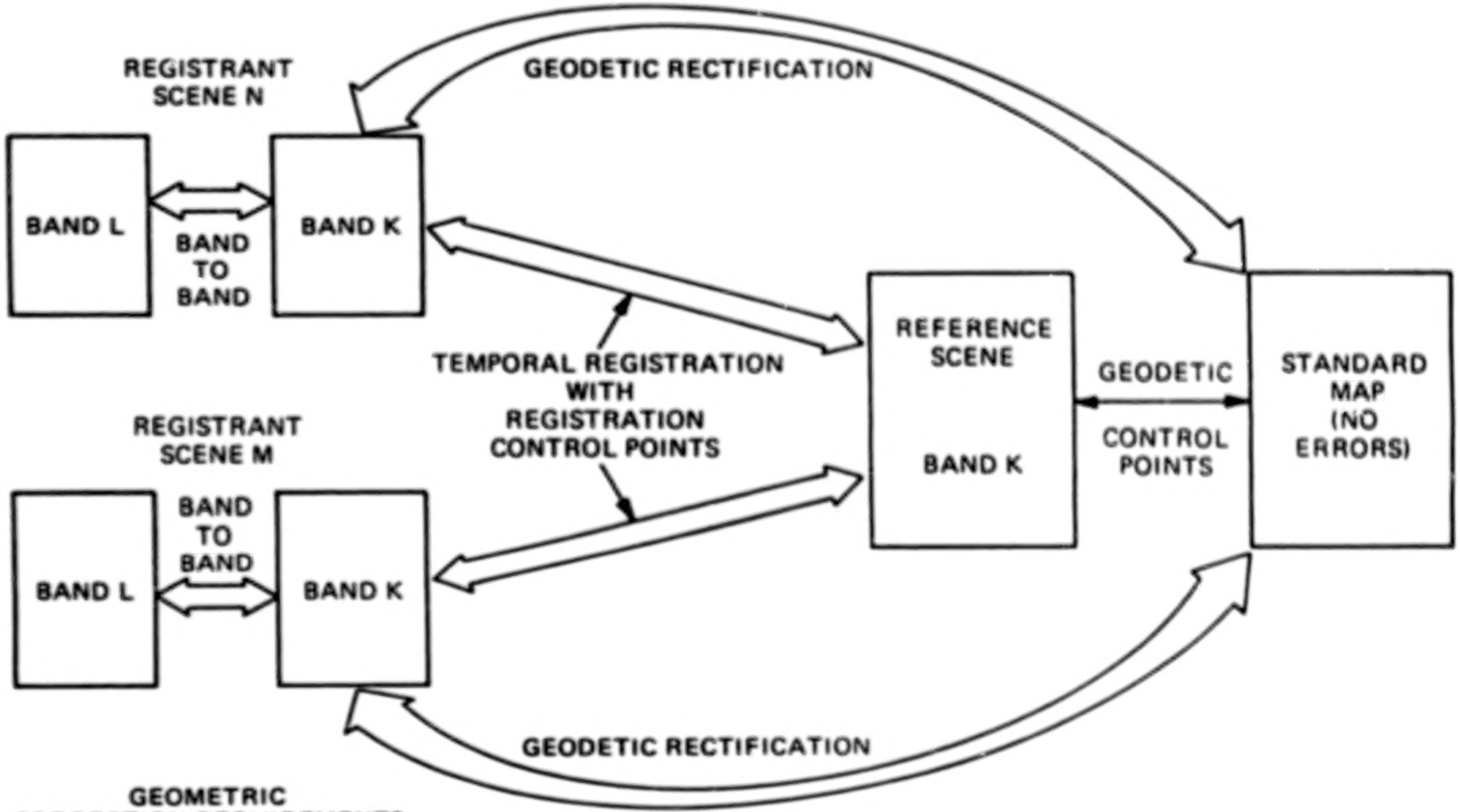
REGISTRANT SCENE N
BAND L
BAND TO BAND
BAND K
GEODETIC RECTIFICATION
REGISTRANT SCENE M
BAND L
BAND TO BAND
BAND K
TEMPORAL REGISTRATION WITH REGISTRATION CONTROL POINTS
REFERENCE SCENE
BAND K
GEODETIC
CONTROL POINTS
STANDARD MAP (NO ERRORS)
GEODETIC RECTIFICATION

GEOMETRIC
CORRECTION REQUIREMENTS
90% OF THE TIME

GEODETIC	0.5 PIXEL
TEMPORAL	0.3 PIXEL (REGISTRANT TO REFERENCE)
BAND-TO-BAND	0.3 PIXEL (BETWEEN PRIMARY AND COLD FOCAL PLANES) 0.2 PIXEL (WITHIN EACH FOCAL PLANE)

FIGURE 1-3

LANDSAT D TM GEOMETRIC CORRECTION SYSTEM OVERVIEW

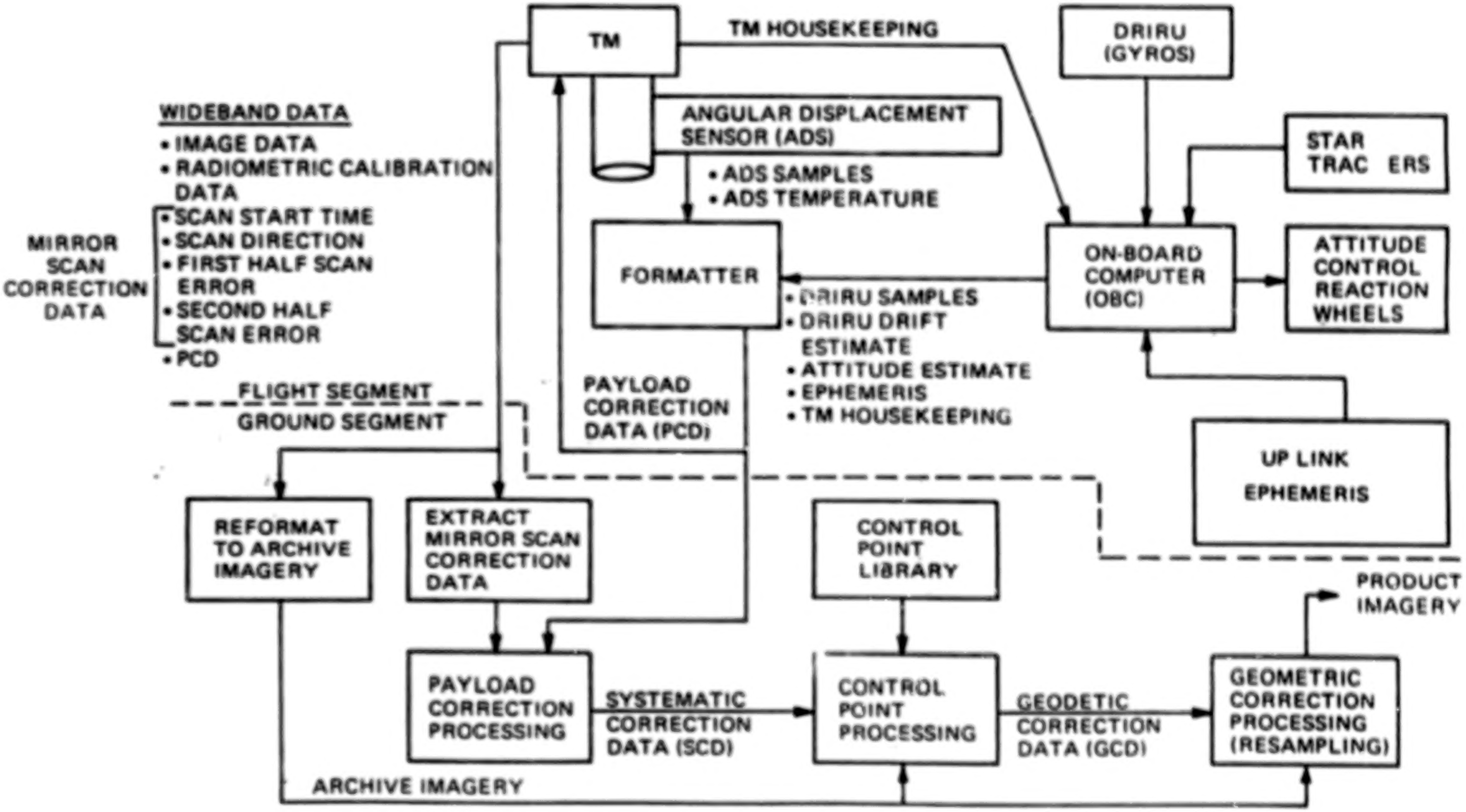
TM
TM HOUSEKEEPING
DRIRU
(GYROS)
WIDEBAND DATA
• IMAGE DATA
• RADIOMETRIC CALIBRATION DATA
• SCAN START TIME
• SCAN DIRECTION
• FIRST HALF SCAN ERROR
• SECOND HALF SCAN ERROR
• PCD
MIRROR SCAN CORRECTION DATA
ANGULAR DISPLACEMENT SENSOR (ADS)
• ADS SAMPLES
• ADS TEMPERATURE
STAR TRAC ERS
FORMATTER
ON-BOARD COMPUTER (OBC)
ATTITUDE CONTROL REACTION WHEELS
• DRIRU SAMPLES
• DRIRU DRIFT ESTIMATE
• ATTITUDE ESTIMATE
• EPHEMERIS
• TM HOUSEKEEPING
FLIGHT SEGMENT
GROUND SEGMENT
PAYLOAD CORRECTION DATA (PCD)
UP LINK EPHEMERIS
REFORMAT TO ARCHIVE IMAGERY
EXTRACT MIRROR SCAN CORRECTION DATA
CONTROL POINT LIBRARY
PRODUCT IMAGERY
PAYLOAD CORRECTION PROCESSING
SYSTEMATIC CORRECTION DATA (SCD)
CONTROL POINT PROCESSING
GEODETIC CORRECTION DATA (GCD)
GEOMETRIC CORRECTION PROCESSING (RESAMPLING)
ARCHIVE IMAGERY

FIGURE 1-4

LANDSAT D FLIGHT SEGMENT

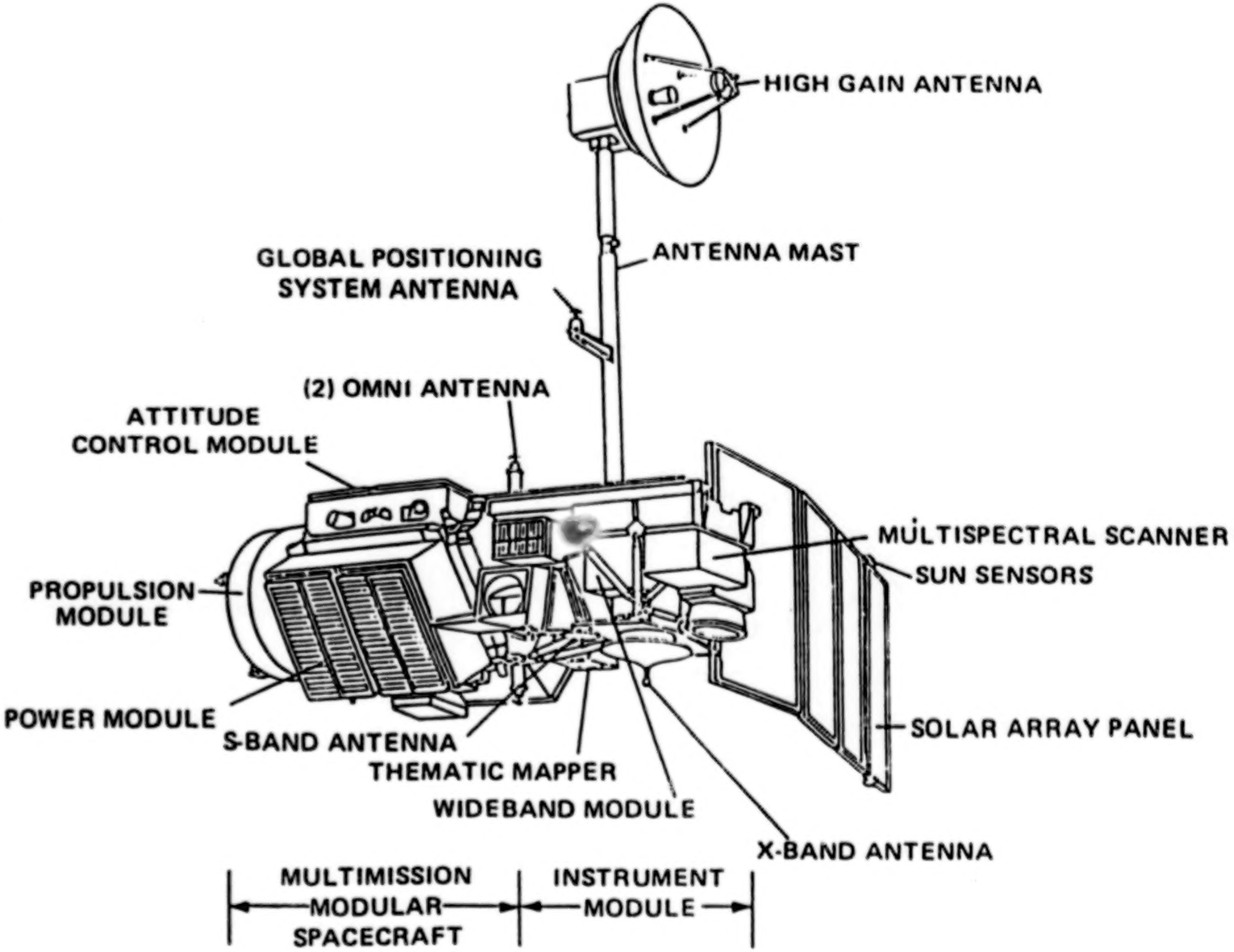
HIGH GAIN ANTENNA
ANTENNA MAST
GLOBAL POSITIONING SYSTEM ANTENNA
(2) OMNI ANTENNA
ATTITUDE CONTROL MODULE
MULTISPECTRAL SCANNER
SUN SENSORS
PROPULSION MODULE
POWER MODULE
S-BAND ANTENNA
THEMATIC MAPPER
WIDEBAND MODULE
SOLAR ARRAY PANEL
X-BAND ANTENNA
MULTIMISSION MODULAR SPACECRAFT
INSTRUMENT MODULE

FIGURE 2-1

LANDSAT-D ORBIT

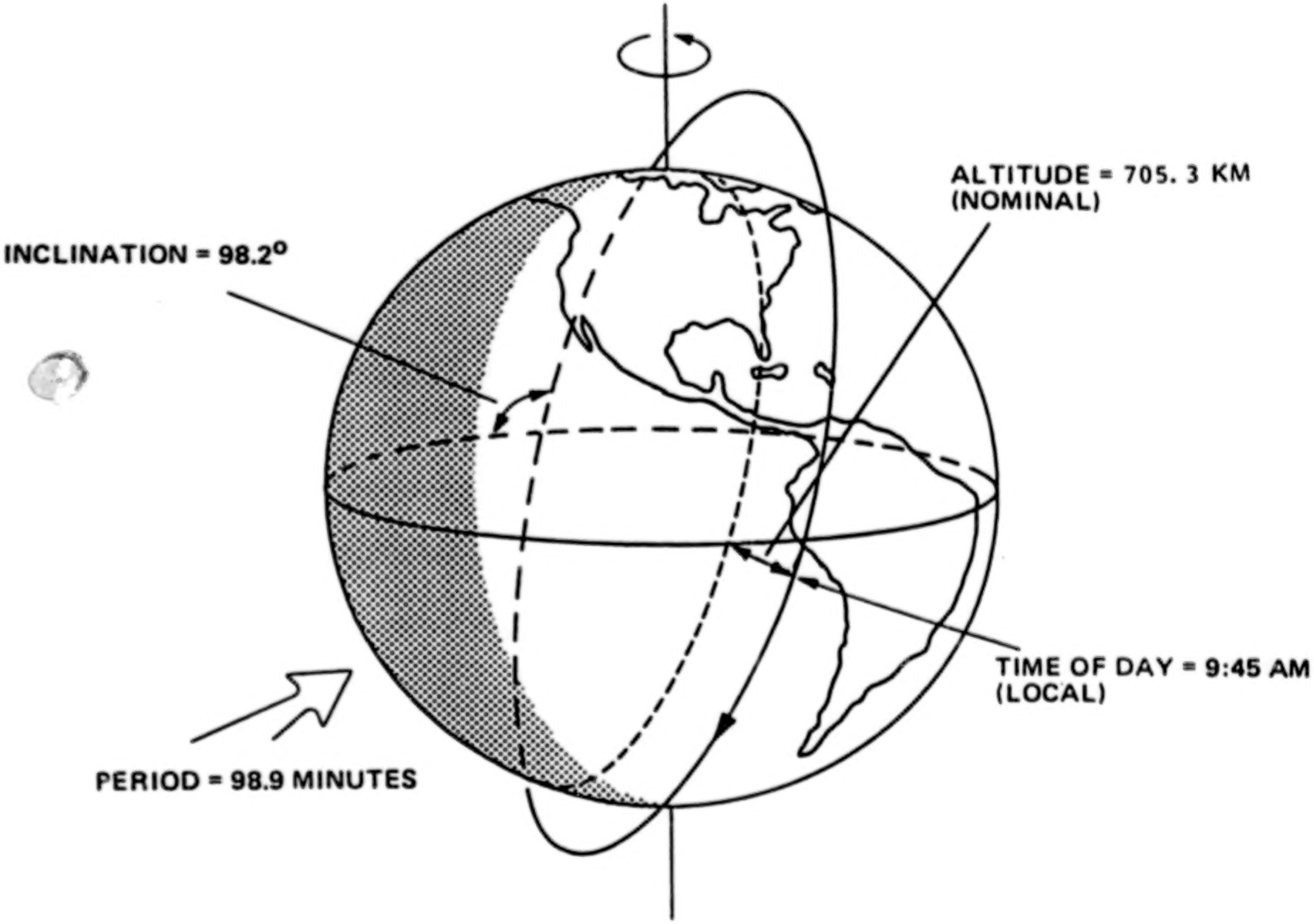
ALTITUDE = 705. 3 KM
(NOMINAL)
INCLINATION = 98.2°
TIME OF DAY = 9:45 AM
(LOCAL)
PERIOD = 98.9 MINUTES

FIGURE 2-2

SYSTEM EPHEMERIS DATA FLOW FOR TM GEOMETRIC CORRECTION

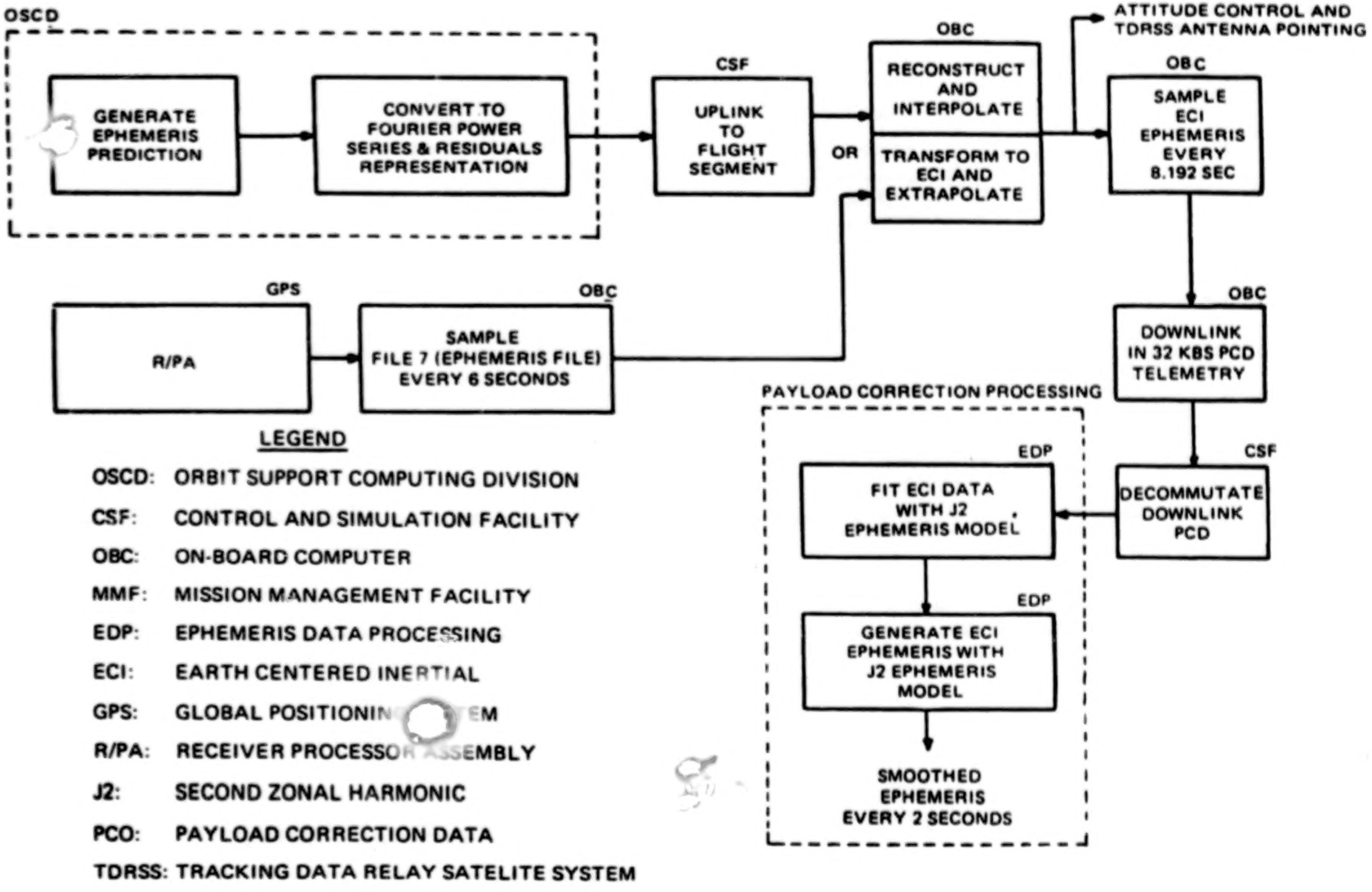
OSCD
GENERATE EPHEMERIS PREDICTION
CONVERT TO FOURIER POWER SERIES & RESIDUALS REPRESENTATION
CSF
UPLINK TO FLIGHT SEGMENT
OR
OBC
RECONSTRUCT AND INTERPOLATE
TRANSFORM TO ECI AND EXTRAPOLATE
ATTITUDE CONTROL AND TDRSS ANTENNA POINTING
OBC
SAMPLE ECI EPHEMERIS EVERY 8.192 SEC
GPS
R/PA
OBC
SAMPLE FILE 7 (EPHEMERIS FILE) EVERY 6 SECONDS
OBC
DOWNLINK IN 32 KBS PCD TELEMETRY
CSF
DECOMMUTATE DOWNLINK PCD
PAYLOAD CORRECTION PROCESSING
EDP
FIT ECI DATA WITH J2 EPHEMERIS MODEL
EDP
GENERATE ECI EPHEMERIS WITH J2 EPHEMERIS MODEL
SMOOTHED EPHEMERIS EVERY 2 SECONDS

LEGEND

OSCD: ORBIT SUPPORT COMPUTING DIVISION
CSF: CONTROL AND SIMULATION FACILITY
OBC: ON-BOARD COMPUTER
MMF: MISSION MANAGEMENT FACILITY
EDP: EPHEMERIS DATA PROCESSING
ECI: EARTH CENTERED INERTIAL
GPS: GLOBAL POSITIONIN[illegible]TEM
R/PA: RECEIVER PROCESSOR ASSEMBLY
J2: SECOND ZONAL HARMONIC
PCO: PAYLOAD CORRECTION DATA
TDRSS: TRACKING DATA RELAY SATELITE SYSTEM

FIGURE 2-3

ATTITUDE CONTROL SUBSYSTEM (ACS)
NORMAL OPERATING MODE FUNCTIONAL BLOCK DIAGRAM

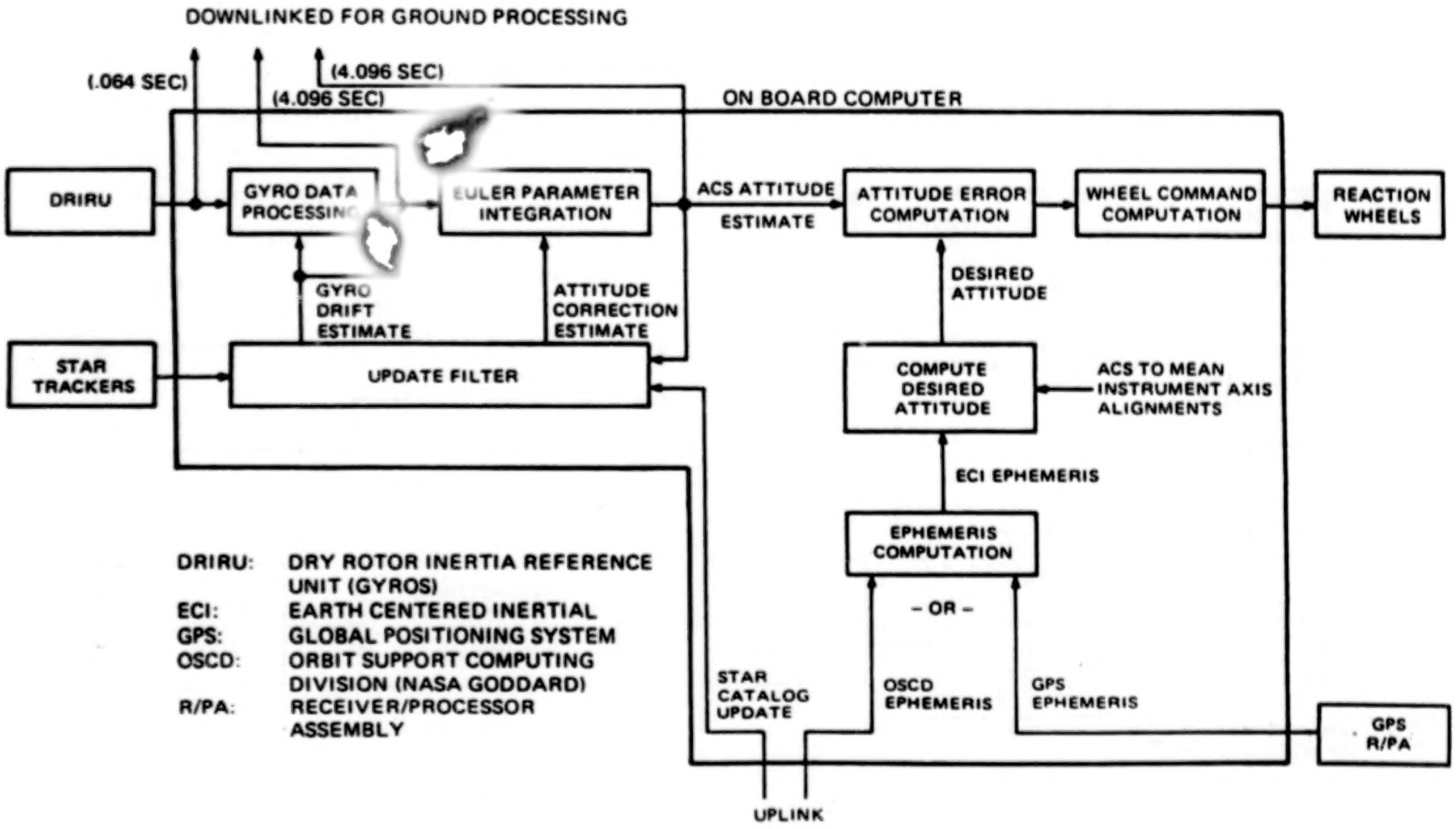
DOWNLINKED FOR GROUND PROCESSING
(.064 SEC)
(4.096 SEC)
(4.096 SEC)
ON BOARD COMPUTER
DRIRU
GYRO DATA PROCESSING
EULER PARAMETER INTEGRATION
ACS ATTITUDE ESTIMATE
ATTITUDE ERROR COMPUTATION
WHEEL COMMAND COMPUTATION
REACTION WHEELS
GYRO DRIFT ESTIMATE
ATTITUDE CORRECTION ESTIMATE
DESIRED ATTITUDE
STAR TRACKERS
UPDATE FILTER
COMPUTE DESIRED ATTITUDE
ACS TO MEAN INSTRUMENT AXIS ALIGNMENTS
ECI EPHEMERIS
EPHEMERIS COMPUTATION
– OR –
STAR CATALOG UPDATE
OSCD EPHEMERIS
GPS EPHEMERIS
GPS R/PA
UPLINK

DRIRU:	DRY ROTOR INERTIA REFERENCE UNIT (GYROS)
ECI:	EARTH CENTERED INERTIAL
GPS:	GLOBAL POSITIONING SYSTEM
OSCD:	ORBIT SUPPORT COMPUTING DIVISION (NASA GODDARD)
R/PA:	RECEIVER/PROCESSOR ASSEMBLY

FIGURE 2-4

TABLE 2-1

AMPLITUDES OF TM AND MSS SCAN MIRROR TORQUE COMPONENTS

TM		MSS	
FREQUENCY (Hz)	AMPLITUDE (IN-LBS)	FREQUENCY (Hz)	AMPLITUDE (IN-LBS)
7	43.343	13.620	40.398
21	41.543	40.860	39.507
35	39.106	68.100	37.770
49	33.341	95.340	35.269
63	27.663	122.580	32.122
77	21.547	149.820	28.476
91	15.476	177.060	24.494
105	9.8845	204.300	20.351
119	5.1200	231.540	16.217
		258.780	12.253
		286.020	8.601
		313.260	5.373
		340.50	2.651

ANGULAR DISPLACEMENT SENSOR

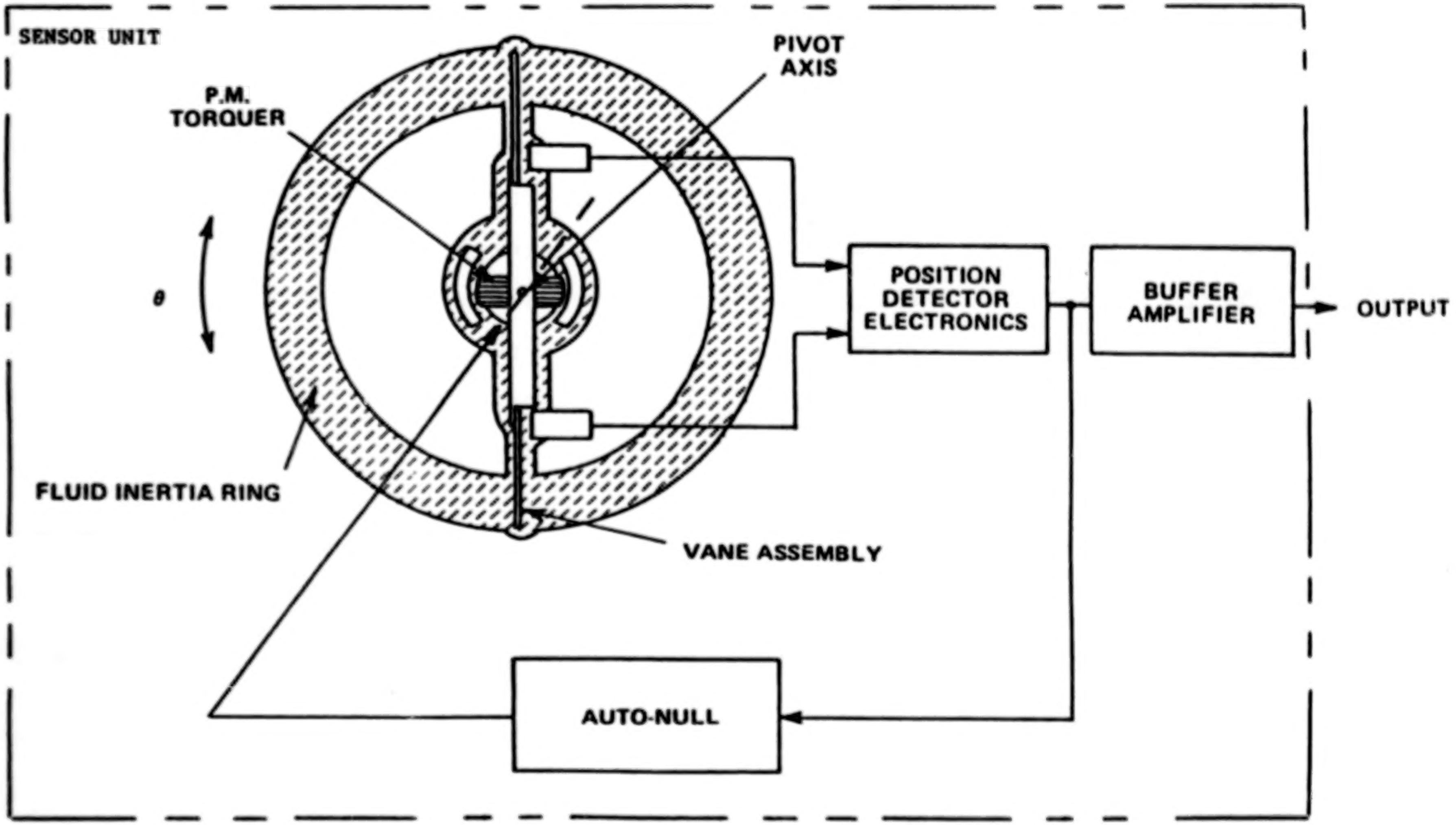
SENSOR UNIT
P.M. TORQUER
PIVOT AXIS
θ
FLUID INERTIA RING
VANE ASSEMBLY
POSITION DETECTOR ELECTRONICS
BUFFER AMPLIFIER
OUTPUT
AUTO-NULL

FIGURE 2-5

THEMATIC MAPPER GEOMETRY

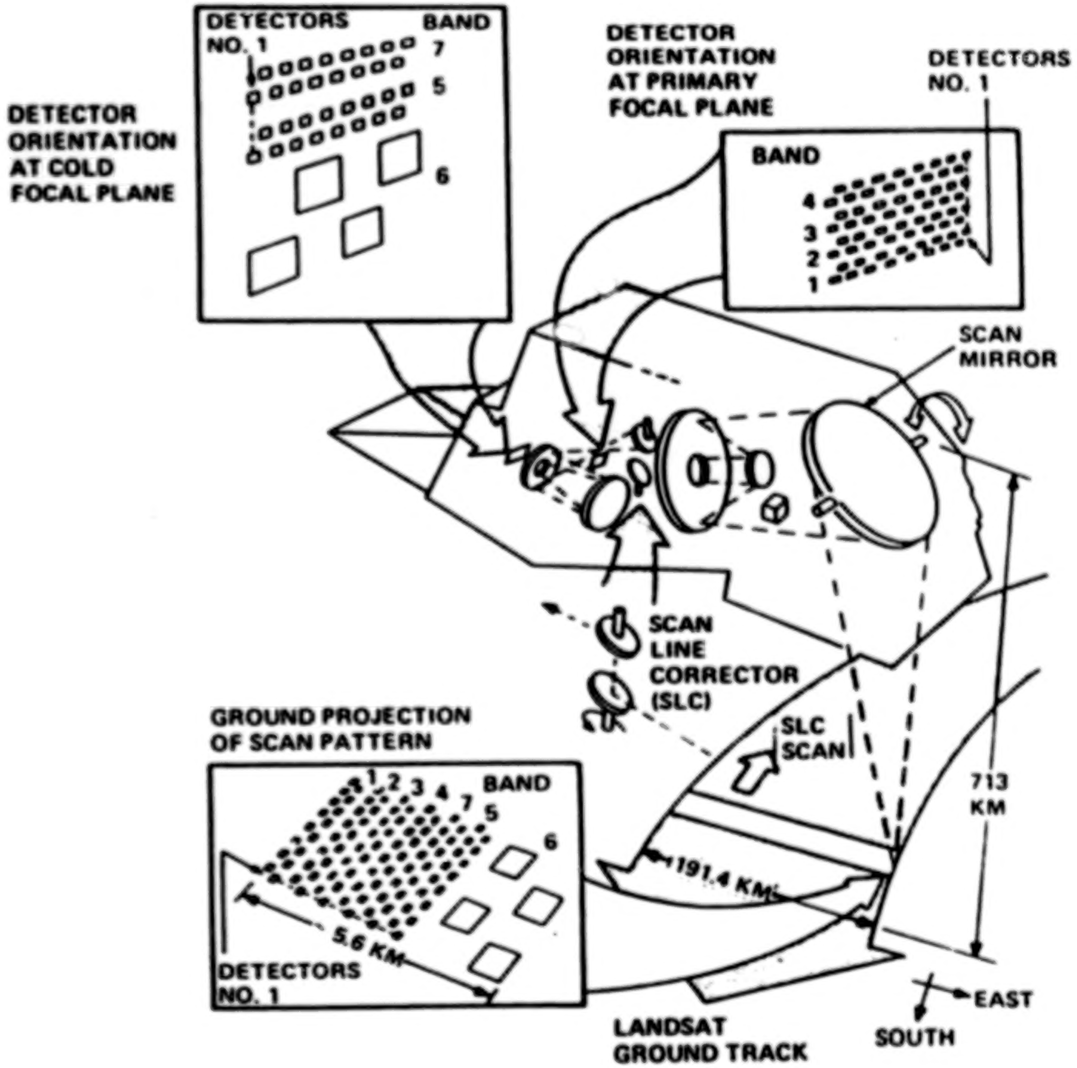
DETECTOR ORIENTATION AT COLD FOCAL PLANE
DETECTORS NO. 1
BAND
7
5
6
DETECTOR ORIENTATION AT PRIMARY FOCAL PLANE
DETECTORS NO. 1
BAND
4
3
2
1
SCAN MIRROR
SCAN LINE CORRECTOR (SLC)
SLC SCAN
713 KM
GROUND PROJECTION OF SCAN PATTERN
1 2 3 4 7
BAND
5
6
5.6 KM
DETECTORS NO. 1
191.4 KM
LANDSAT GROUND TRACK
EAST
SOUTH

FIGURE 2-6

KEY GEOMETRIC FEATURES

- SCAN MIRROR
  - BI-DIRECTIONAL CROSS TRACK SCANNING
  - DATA AVAILABLE TO GROUND:
    - SCAN START TIME
    - SCAN DIRECTION
    - FIRST HALF SCAN TIME ERROR
    - SECOND HALF SCAN TIME ERROR
- SCAN LINE CORRECTOR
  - PROVIDES IN TRACK SCANNING
- TWO FOCAL PLANE ASSEMBLIES
- INSTANTANEOUS FIELD OF VIEW (IFOV)
  - BANDS 1-5, 7: 42.5 μrad (30 METERS)
  - BAND 6: 170 μrad (120 METERS)

DETECTOR PROJECTION AT PRIME FOCAL PLANE

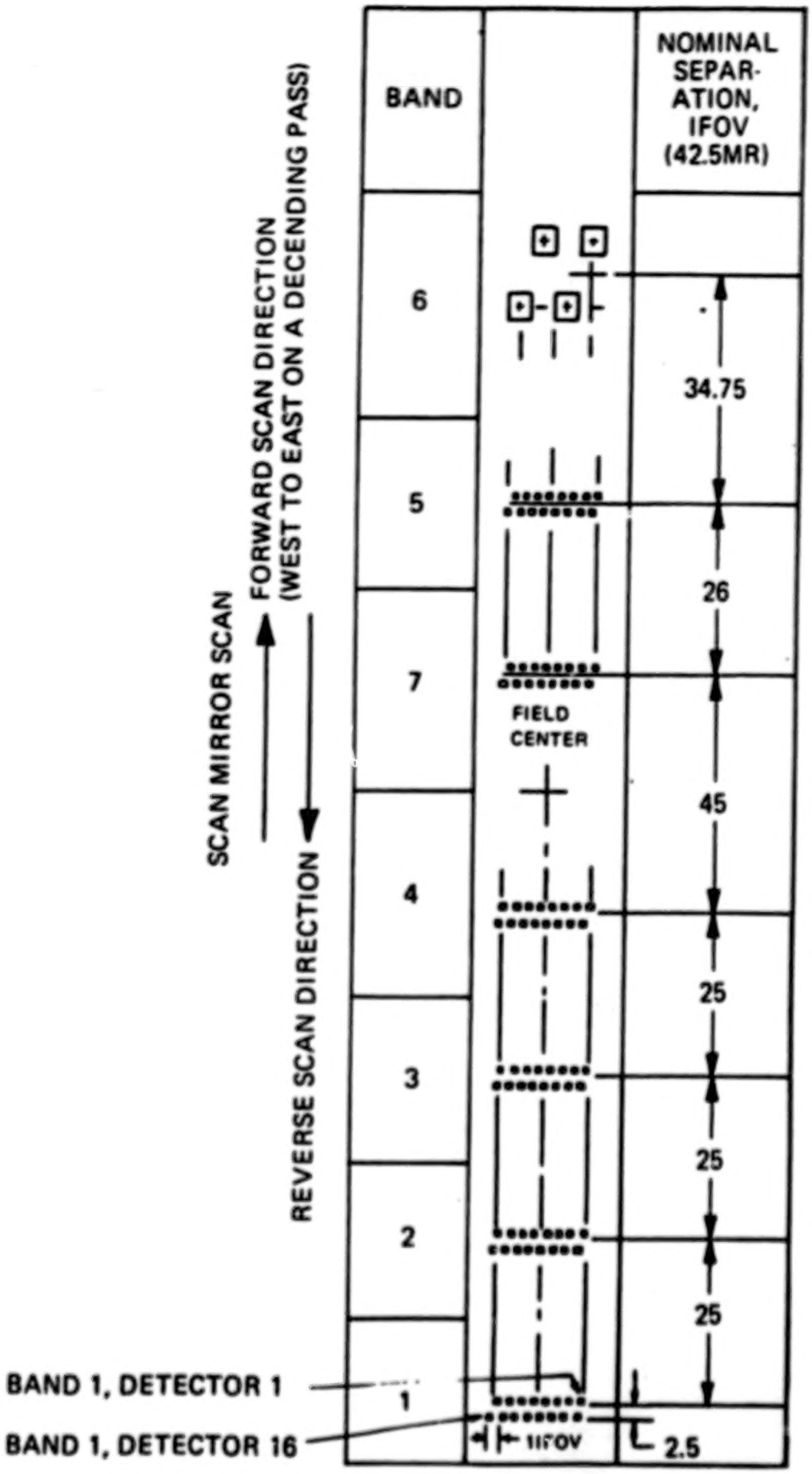
BAND
NOMINAL SEPARATION, IFOV (42.5MR)
6
5
7
4
3
2
1
34.75
26
45
25
25
25
2.5
FIELD CENTER
1IFOV
SCAN MIRROR SCAN
FORWARD SCAN DIRECTION (WEST TO EAST ON A DECENDING PASS)
REVERSE SCAN DIRECTION
BAND 1, DETECTOR 1
BAND 1, DETECTOR 16

FIGURE 2-7

THEMATIC MAPPER SCANNING

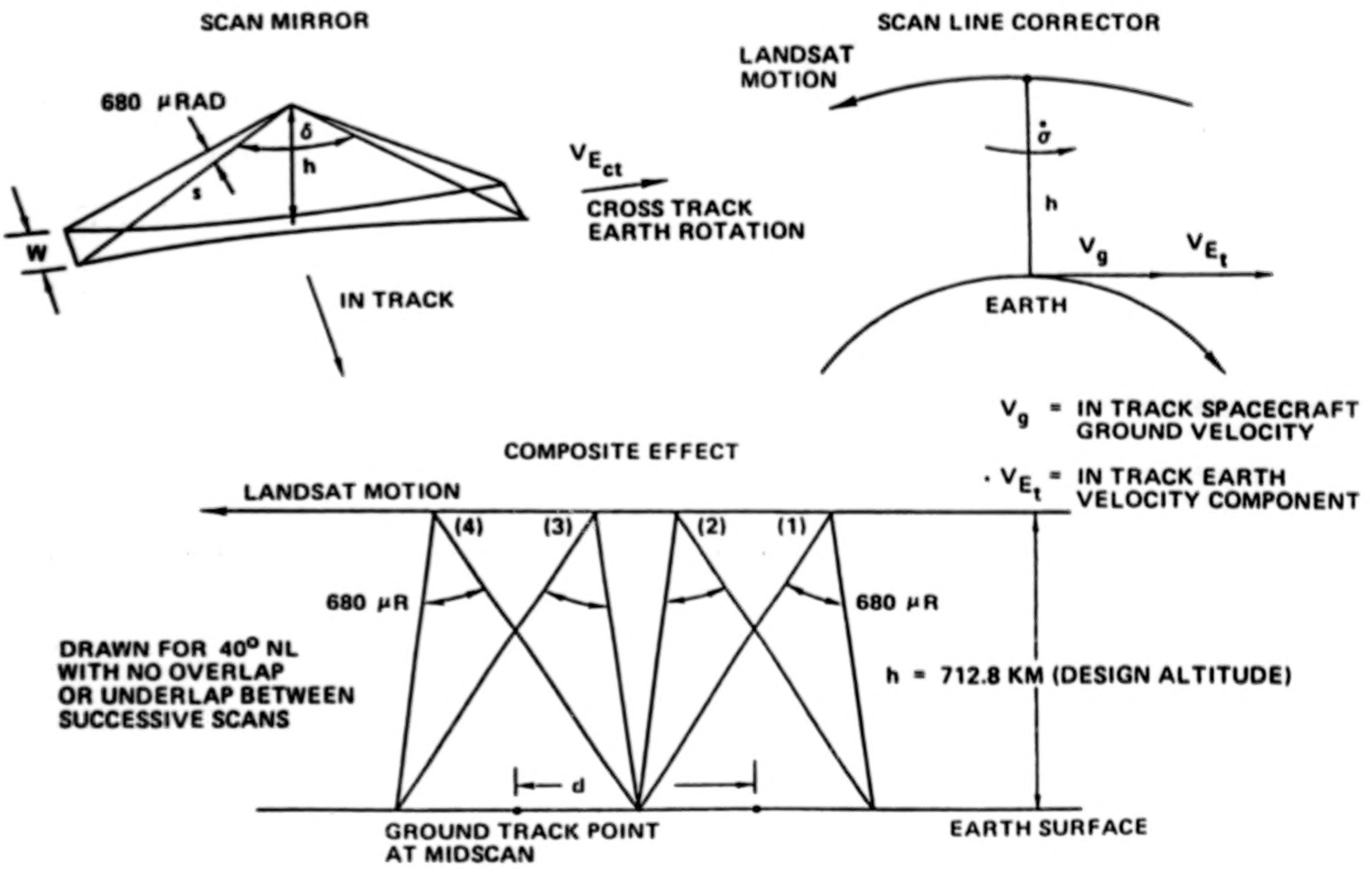
SCAN MIRROR
680 μRAD
δ
h
s
W
$V_{E_{ct}}$
CROSS TRACK EARTH ROTATION
IN TRACK
SCAN LINE CORRECTOR
LANDSAT MOTION
$\dot{\sigma}$
h
V_g
V_{E_t}
EARTH
V_g = IN TRACK SPACECRAFT GROUND VELOCITY
$\cdot V_{E_t}$ = IN TRACK EARTH VELOCITY COMPONENT
COMPOSITE EFFECT
LANDSAT MOTION
(4)
(3)
(2)
(1)
680 μR
680 μR
DRAWN FOR 40° NL WITH NO OVERLAP OR UNDERLAP BETWEEN SUCCESSIVE SCANS
h = 712.8 KM (DESIGN ALTITUDE)
d
GROUND TRACK POINT AT MIDSCAN
EARTH SURFACE

FIGURE 2-8

THEMATIC MAPPER SCAN
IS AFFECTED BY ALTITUDE DEVIATION

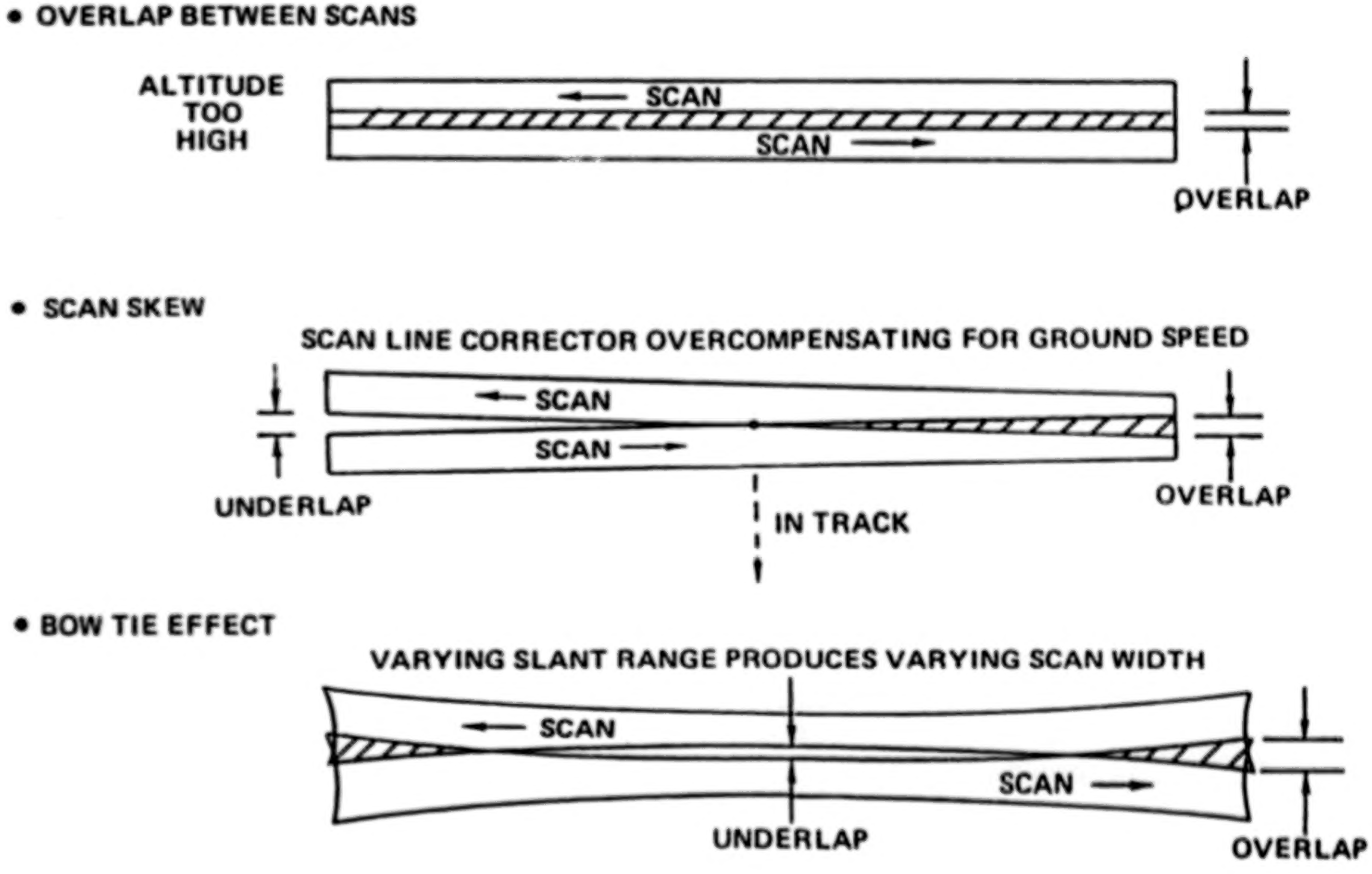

- OVERLAP BETWEEN SCANS
- SCAN SKEW
- BOW TIE EFFECT

ALTITUDE TOO HIGH
SCAN
SCAN
OVERLAP
SCAN LINE CORRECTOR OVERCOMPENSATING FOR GROUND SPEED
SCAN
SCAN
UNDERLAP
OVERLAP
IN TRACK
VARYING SLANT RANGE PRODUCES VARYING SCAN WIDTH
SCAN
SCAN
UNDERLAP
OVERLAP

FIGURE 2-9

SCAN GAP** ERROR

ALTITUDE VARIATION	SPACECRAFT ATTITUDE DEVIATION	TM UNDERLAP/OVERLAP
696 – 741 KM FOR 705.3 ORBIT 713 KM TM DESIGN ALTITUDE	LESS THAN 1 PIXEL	0.2 PIXEL (SPEC)

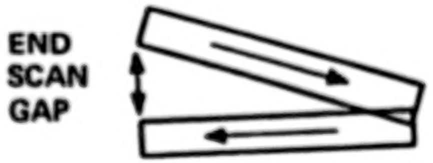

EARTH LOCATION	WORST CASE END SCAN GAP IN PIXELS*
NORTHERN HEMISPHERE	-0.7 TO 0.8
45°N	-0.4 TO 0.6
EQUATOR	-0.2 TO 0.8
45°S	-0.9 TO 0.1
SOUTHERN HEMISPHERE	-1.6 TO 0.8

WORST CASE GAP RANGE

-2.8 TO 2.0

(WORST CASE TOTAL OF ALTITUDE VARIATION, JITTER, TM UNDERLAP/OVERLAP EFFECTS)

*INCLUDES SCAN WIDTH, SCAN LINE CORRECTOR SKEW AND BOWTIE EFFECTS

**GAP < 0 : OVERLAP
= 0 : NOMINAL
> 0 : UNDERLAP

FIGURE 2-10

TM SCAN MIRROR PROFILE

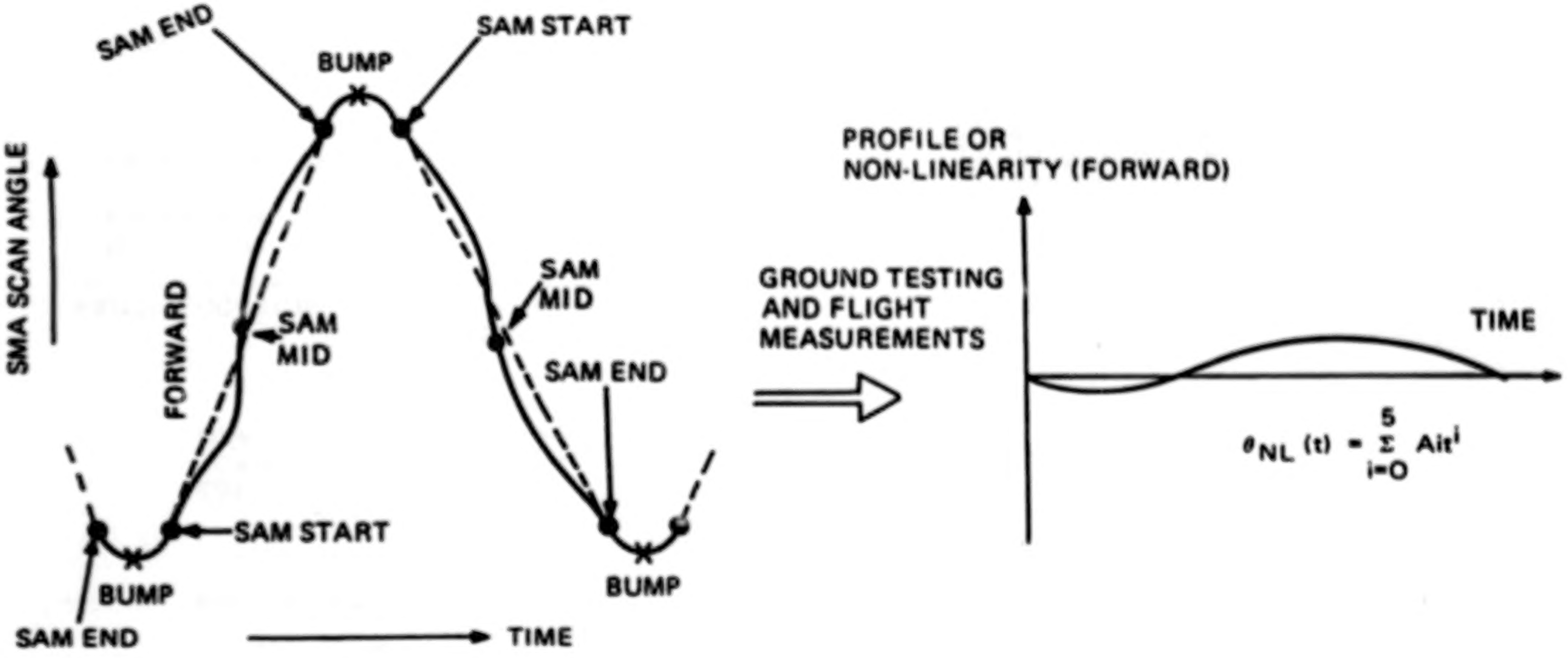
SAM END
BUMP
SAM START
SMA SCAN ANGLE
FORWARD
SAM MID
SAM MID
SAM END
SAM START
BUMP
SAM END
BUMP
TIME
GROUND TESTING AND FLIGHT MEASUREMENTS
PROFILE OR NON-LINEARITY (FORWARD)
TIME
$\theta_{NL}(t) = \sum_{i=0}^{5} A_i t^i$

SAM: SCAN ANGLE MONITOR

FIGURE 2-11

ATTITUDE DATA AND SCAN START TIMING

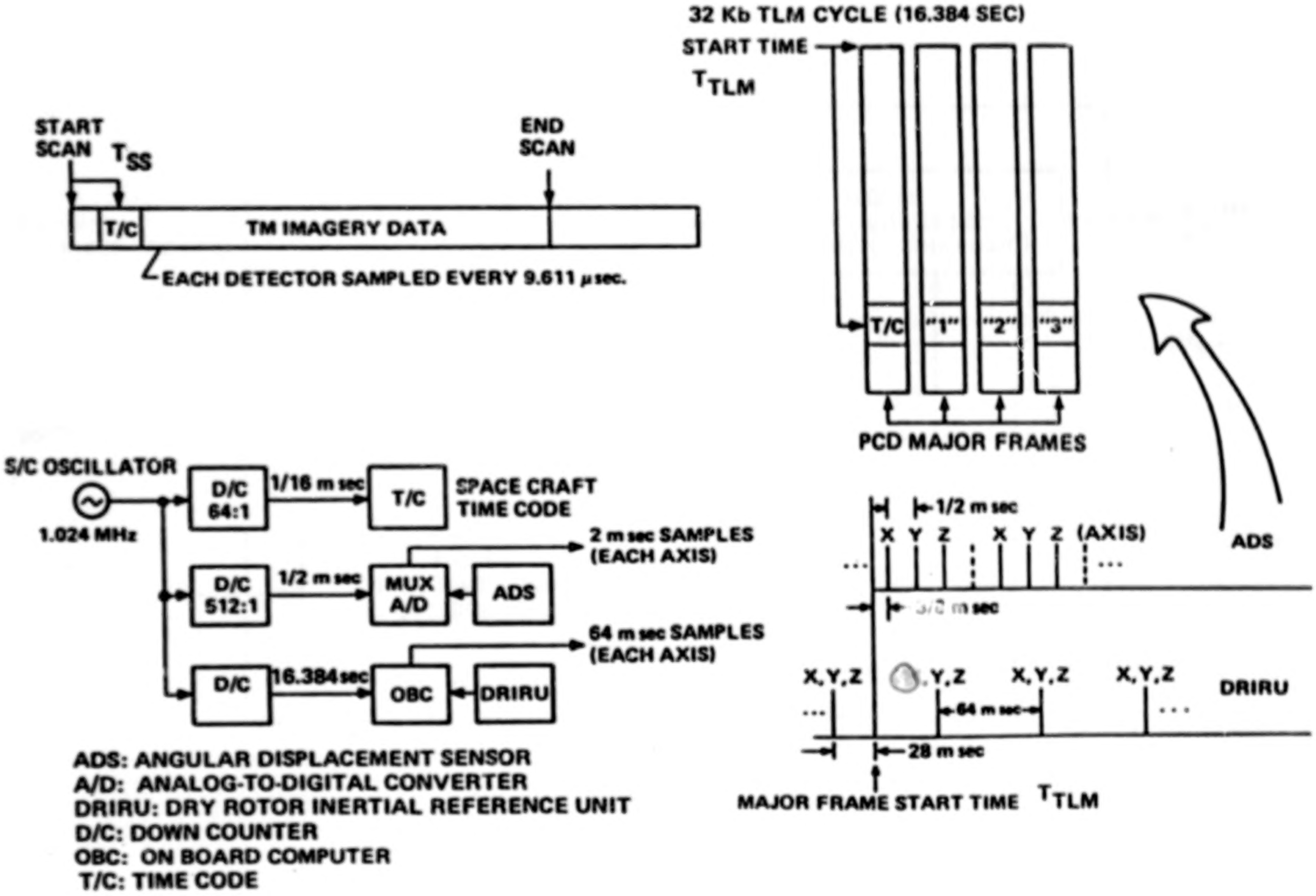
32 Kb TLM CYCLE (16.384 SEC)
START TIME
T_{TLM}
T/C
"1"
"2"
"3"
PCD MAJOR FRAMES
START SCAN
T_{SS}
END SCAN
T/C
TM IMAGERY DATA
EACH DETECTOR SAMPLED EVERY 9.611 μsec.
S/C OSCILLATOR
1.024 MHz
D/C 64:1
1/16 m sec
T/C
SPACE CRAFT TIME CODE
D/C 512:1
1/2 m sec
MUX A/D
ADS
2 m sec SAMPLES (EACH AXIS)
D/C
16.384 sec
OBC
DRIRU
64 m sec SAMPLES (EACH AXIS)
1/2 m sec
X Y Z X Y Z (AXIS)
ADS
3/8 m sec
X,Y,Z
Y,Z
X,Y,Z
X,Y,Z
DRIRU
64 m sec
28 m sec
MAJOR FRAME START TIME
T_{TLM}

ADS: ANGULAR DISPLACEMENT SENSOR
A/D: ANALOG-TO-DIGITAL CONVERTER
DRIRU: DRY ROTOR INERTIAL REFERENCE UNIT
D/C: DOWN COUNTER
OBC: ON BOARD COMPUTER
T/C: TIME CODE

FIGURE 2-12

PAYLOAD CORRECTION PROCESSING

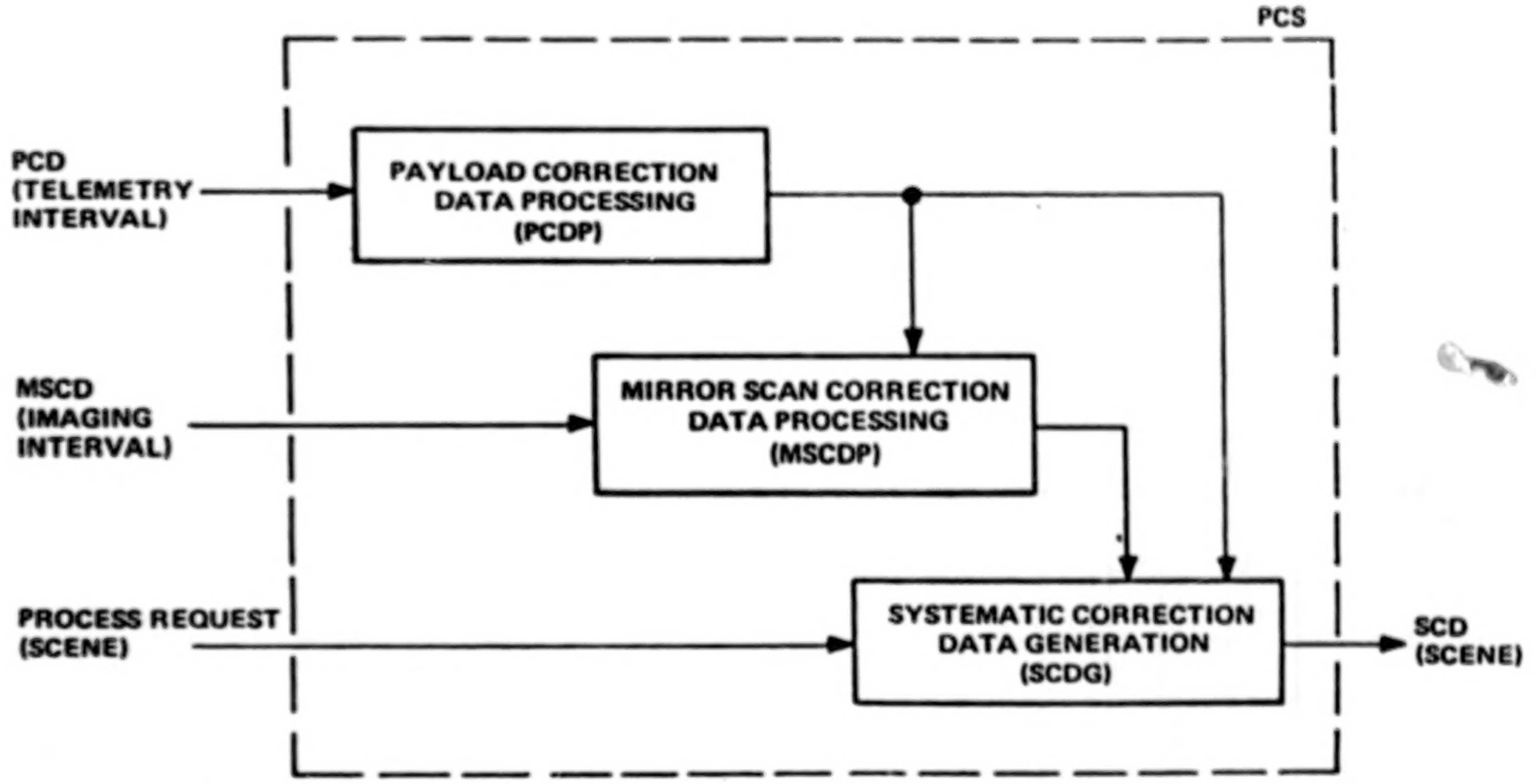
PCS
PCD (TELEMETRY INTERVAL)
PAYLOAD CORRECTION DATA PROCESSING (PCDP)
MSCD (IMAGING INTERVAL)
MIRROR SCAN CORRECTION DATA PROCESSING (MSCDP)
PROCESS REQUEST (SCENE)
SYSTEMATIC CORRECTION DATA GENERATION (SCDG)
SCD (SCENE)

MSCD: MIRROR SCAN CORRECTION DATA
PCD: PAYLOAD CORRECTION DATA
SCD: SYSTEMATIC CORRECTION DATA

FIGURE 3-1

ATTITUDE DATA PROCESSING

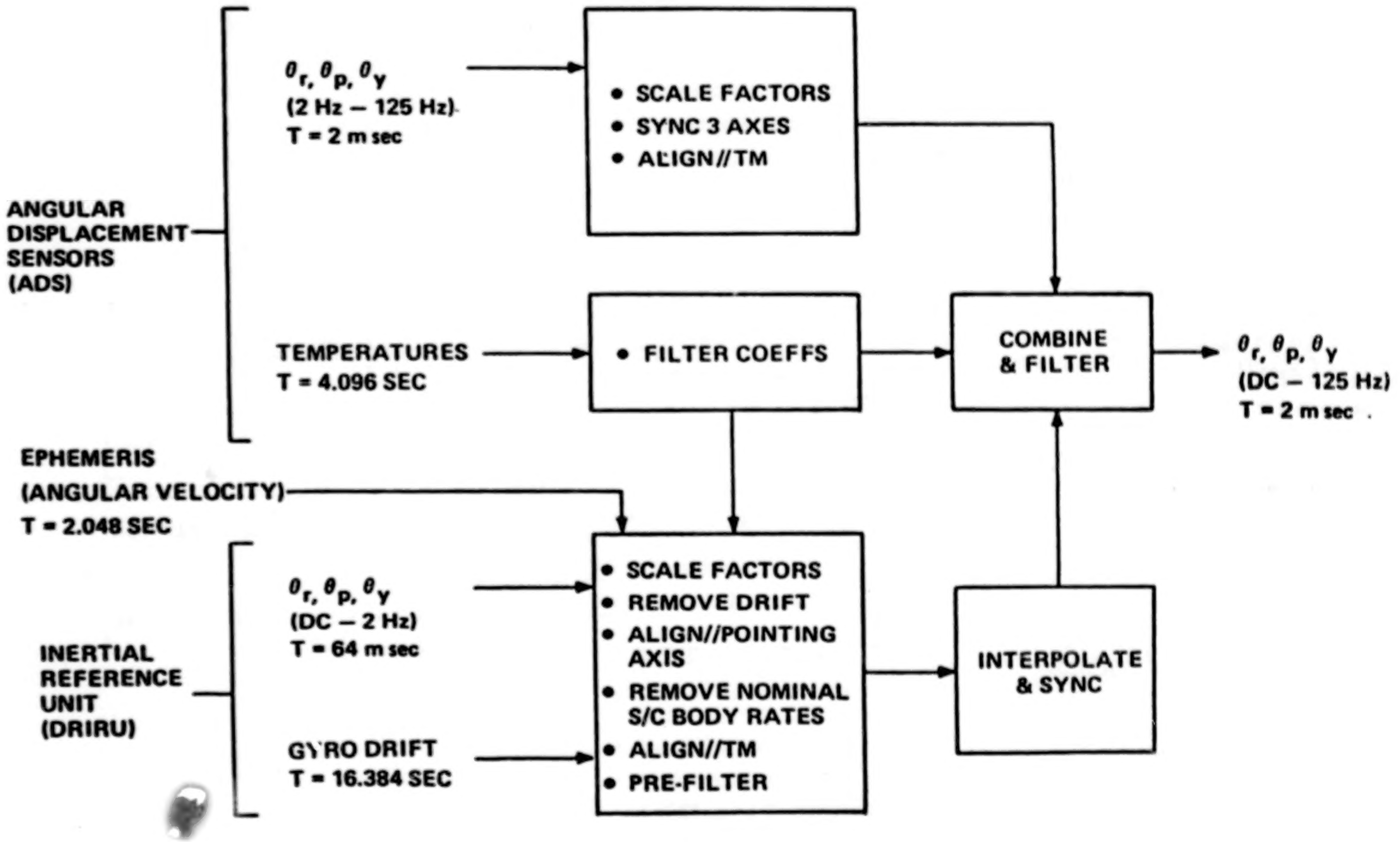
ANGULAR DISPLACEMENT SENSORS (ADS)
$\theta_r, \theta_p, \theta_y$ (2 Hz – 125 Hz) T = 2 m sec
• SCALE FACTORS
• SYNC 3 AXES
• ALIGN//TM
TEMPERATURES T = 4.096 SEC
• FILTER COEFFS
COMBINE & FILTER
$\theta_r, \theta_p, \theta_y$ (DC – 125 Hz) T = 2 m sec
EPHEMERIS (ANGULAR VELOCITY) T = 2.048 SEC
INERTIAL REFERENCE UNIT (DRIRU)
$\theta_r, \theta_p, \theta_y$ (DC – 2 Hz) T = 64 m sec
GYRO DRIFT T = 16.384 SEC
• SCALE FACTORS
• REMOVE DRIFT
• ALIGN//POINTING AXIS
• REMOVE NOMINAL S/C BODY RATES
• ALIGN//TM
• PRE-FILTER
INTERPOLATE & SYNC

FIGURE 3-2

MIRROR SCAN CORRECTION DATA PROCESSING

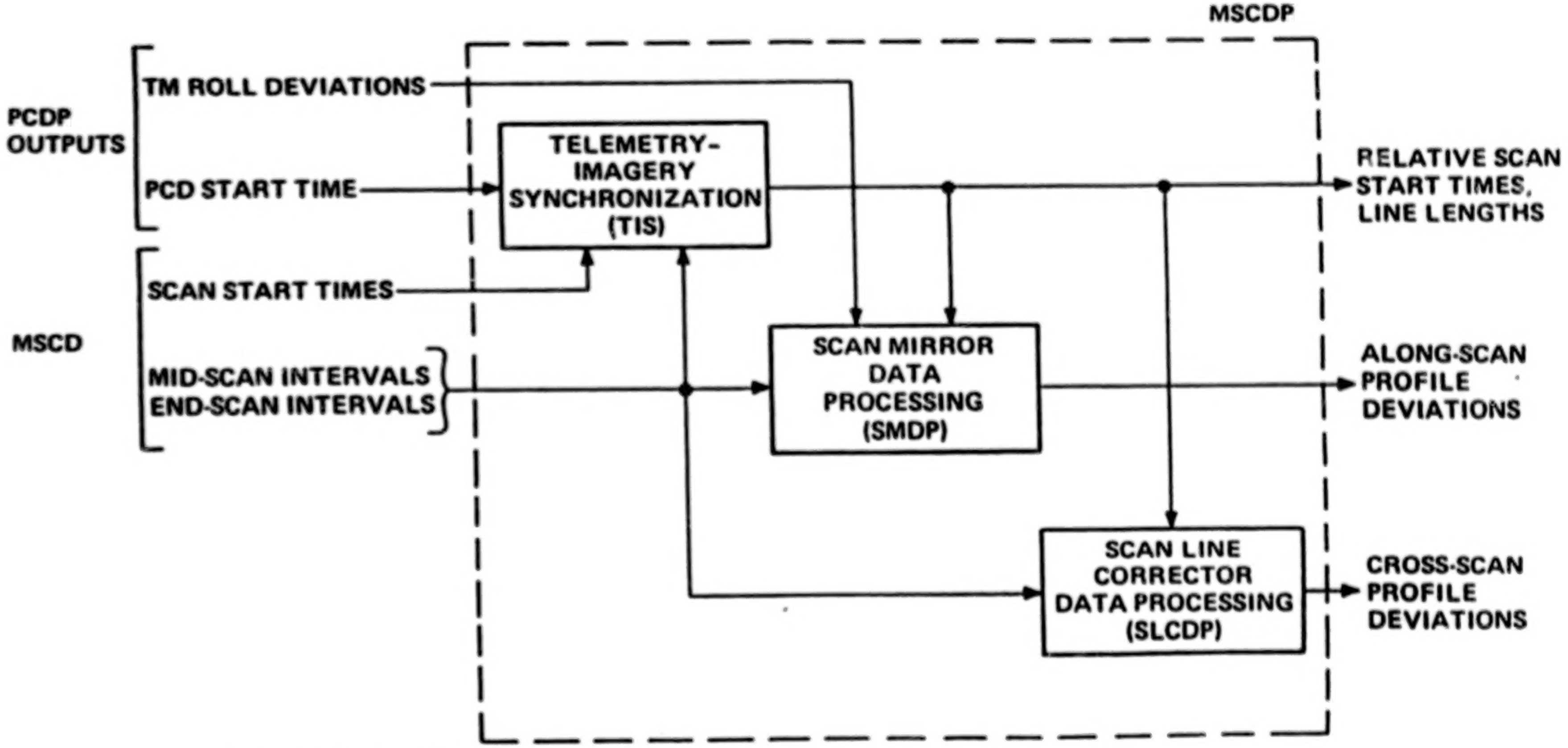
MSCDP
PCDP OUTPUTS
TM ROLL DEVIATIONS
PCD START TIME
MSCD
SCAN START TIMES
MID-SCAN INTERVALS
END-SCAN INTERVALS
TELEMETRY-IMAGERY SYNCHRONIZATION (TIS)
SCAN MIRROR DATA PROCESSING (SMDP)
SCAN LINE CORRECTOR DATA PROCESSING (SLCDP)
RELATIVE SCAN START TIMES, LINE LENGTHS
ALONG-SCAN PROFILE DEVIATIONS
CROSS-SCAN PROFILE DEVIATIONS

PCDP: PAYLOAD CORRECTION DATA PROCESSING
MSCD: MIRROR SCAN CORRECTION DATA PROCESSING

FIGURE 3-3

SYSTEMATIC CORRECTION DATA GENERATION

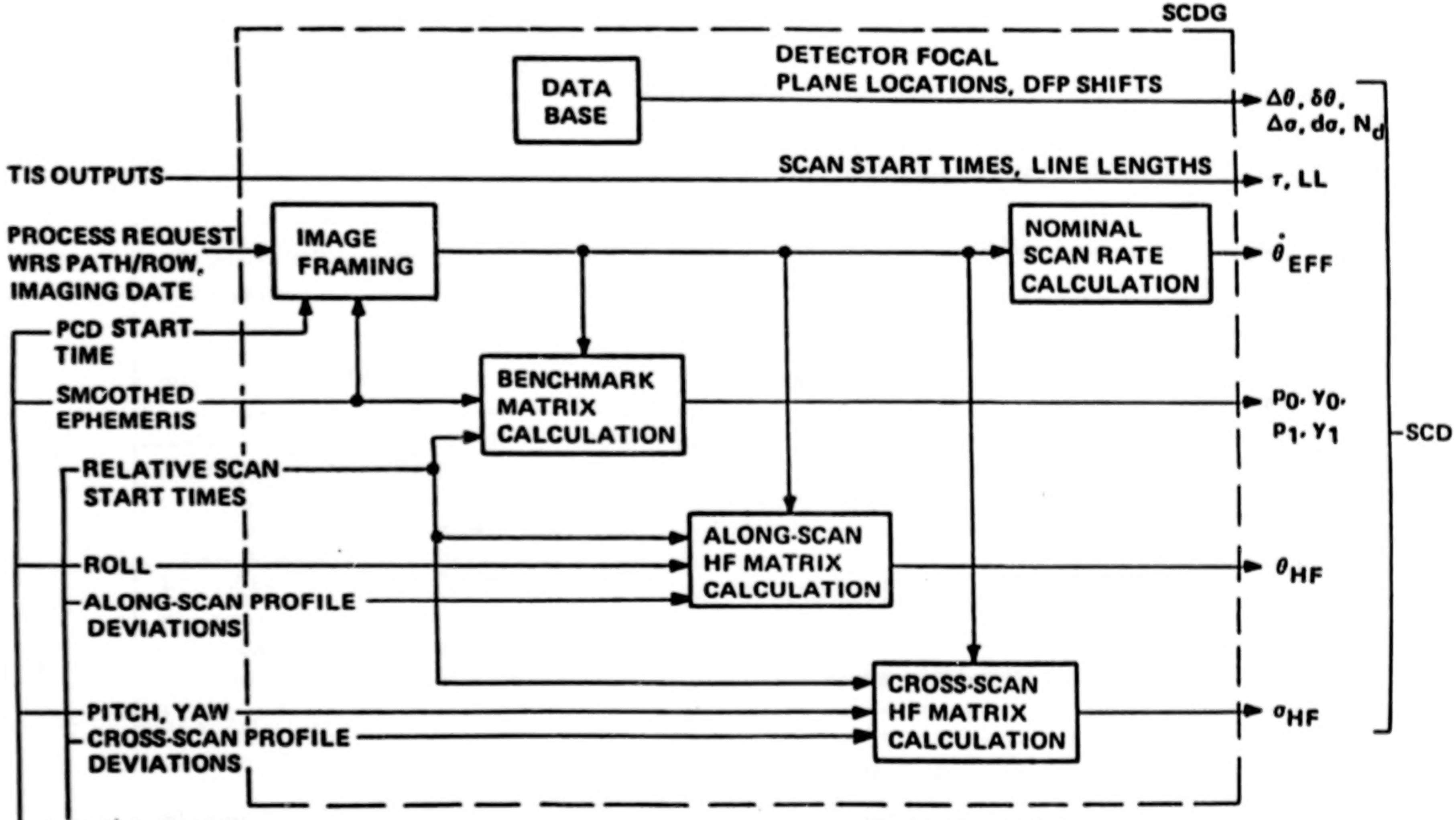
SCDG
DATA BASE
DETECTOR FOCAL PLANE LOCATIONS, DFP SHIFTS
$\Delta\theta, \delta\theta, \Delta\sigma, d\sigma, N_d$
TIS OUTPUTS
SCAN START TIMES, LINE LENGTHS
τ, LL
PROCESS REQUEST WRS PATH/ROW, IMAGING DATE
IMAGE FRAMING
NOMINAL SCAN RATE CALCULATION
$\dot{\theta}_{EFF}$
PCD START TIME
SMOOTHED EPHEMERIS
BENCHMARK MATRIX CALCULATION
p_0, y_0, p_1, y_1
SCD
RELATIVE SCAN START TIMES
ROLL
ALONG-SCAN PROFILE DEVIATIONS
ALONG-SCAN HF MATRIX CALCULATION
θ_{HF}
PITCH, YAW
CROSS-SCAN PROFILE DEVIATIONS
CROSS-SCAN HF MATRIX CALCULATION
σ_{HF}
MSCDP OUTPUTS
PCDP OUTPUTS

TIS: TELEMETRY-IMAGERY SYNCHRONIZATION
DFP: DATA FORMATTER-PROCESSOR
WRS: WORLD REFERENCE SYSTEM
HF: HIGH FREQUENCY

TLM: TELEMETRY
MSCDP: MIRROR SCAN CORRECTION DATA PROCESSING
PCDP: PAYLOAD CORRECTION DATA PROCESSING

FIGURE 3-4

SCD: OPTICAL AXIS POSITION ON THE OUTPUT COORDINATE SYSTEM

BENCHMARK MATRICES

p_0 (i,j,k), y_0 (i,j,k)

p_1 (i,j,k), y_1 (i,j,k)

i = x coordinate index = 1, . . . ,8

j = sweep index = 1, . . . ,4

k = scan direction index = 1,2

INCLUDES: EPHEMERIS, NOMINAL LINEAR TM ACTIVE SCAN, PERFECT ACS, KNOWN INSTRUMENT ALIGNMENT, MAP PROJECTION

(ONE SET FOR EACH PROJECTION)

ALONG SCAN

HIGH FREQUENCY MATRIX

θ_{HF} (i,j)

i = sample number index = 1, . . . ,35

j = scan number = 1, . . . ,374

INCLUDES: SMA ALONG SCAN PROFILE, SMA LINE LENGTH, S/C ROLL JITTER

MIRROR SCAN START TIMES

τ (j)

j = scan number = 1, . . ., 374

RELATIVE START TIME FOR EACH SCAN

CROSS SCAN

HIGH FREQUENCY MATRIX

σ_{HF} (i,j)

i = sample number index = 1, . . . ,35

j = scan number = 1, . . . ,374

INCLUDES: SMA CROSS SCAN PROFILE, SMA LINE LENGTH, SLC PROFILE, SLC DELAY, S/C PITCH AND YAW JITTER

SMA: SCAN MIRROR ASSEMBLY
SLC: SCAN LINE CORRECTOR
S/C: SPACECRAFT

FIGURE 3-5

SCD: OPTICAL AXIS TO DETECTOR SAMPLE LOCATION

NOMINAL POINTING VECTOR SCAN RATE ACROSS OUTPUT COORDINATES

$\dot{\theta}_{EFF}(k)$

k = scan direction index = 1,2

NOMINAL ALONG SCAN FOCAL PLANE BAND LOCATION

$\Delta\theta\ (m)$

m = band number = 1, . . . ,7

ALONG SCAN ANGULAR DISTANCE FROM OPTICAL AXIS TO BAND CENTER

NOMINAL CROSS-SCAN FOCAL PLANE BAND LOCATION

$\Delta\sigma\ (m)$

m = band number = 1, . . . ,7

CROSS SCAN ANGULAR DISTANCE FROM OPTICAL AXIS TO BAND CENTER

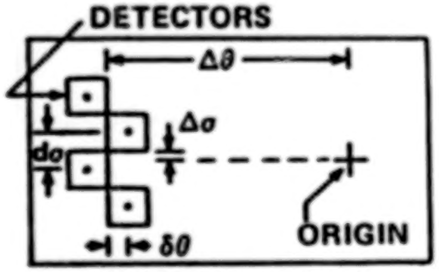

TM FOCAL PLANE

ALONG SCAN FOCAL PLANE DETECTOR LOCATIONS

$\delta\theta\ (m,n,k)$

m = band number = 1, . . . ,7
n = detector number = 1, . . . ,16
k = scan direction index = 1,2

INCLUDES: ALONG SCAN ANGULAR DISTANCE BETWEEN BAND CENTER AND DETECTOR LOCATION, DETECTOR CHANNEL DELAYS, SAM PULSE DELAYS

CROSS SCAN FOCAL PLANE DETECTOR SPACING

$d\sigma\ (m)$

m = band number = 1, . . . ,7

AVERAGE INTER-DETECTOR CROSS SCAN FOCAL PLANE SPACING

SAM: SCAN ANGLE MONITOR

FIGURE 3-6

SCD: PROCESSING PARAMETERS

SCAN LINE LENGTH

LL (j)

j = scan number = 1, . . . ,374

NUMBER OF COMPLETE IMAGING MINOR FRAMES

DATA FORMATTER – PROCESSOR ODD DETECTOR SAMPLE SHIFTS

N_d (m,k)

m = band number = 1, . . . ,7

k = scan direction index = 1,2

LINE SHIFT INTRODUCED BY THE DFP FOR ODD NUMBERED DETECTORS

FIGURE 3-7

BENCHMARK MATRIX CONCEPT
(AN EXAMPLE)

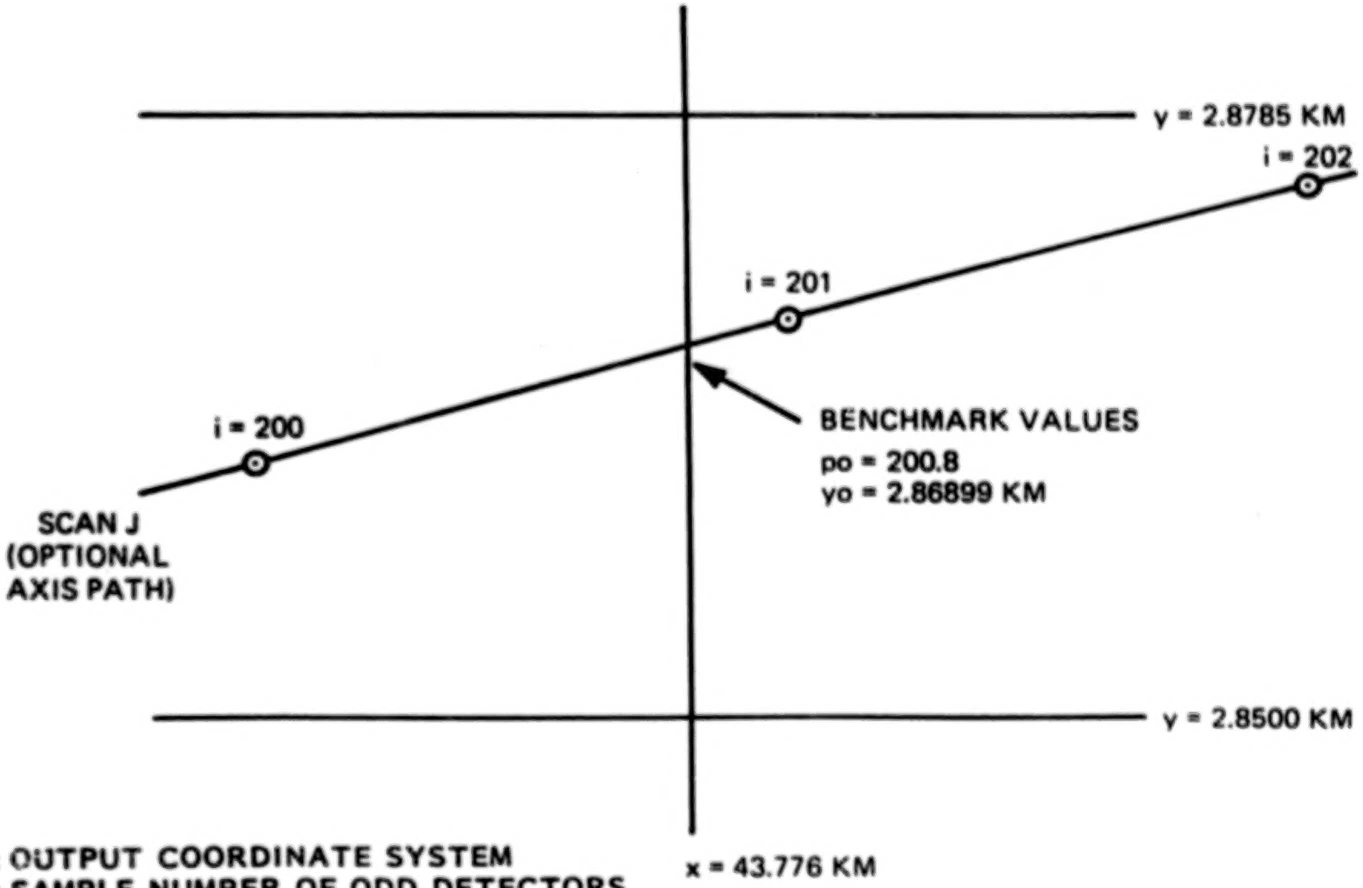
y = 2.8785 KM
i = 202
i = 201
i = 200
BENCHMARK VALUES
po = 200.8
yo = 2.86899 KM
SCAN J
(OPTIONAL
AXIS PATH)
y = 2.8500 KM
x = 43.776 KM

X, Y : OUTPUT COORDINATE SYSTEM
i : SAMPLE NUMBER OF ODD DETECTORS RELATIVE TO SCAN START

FIGURE 3-8

ALONG SCAN HIGH-FREQUENCY MATRICES

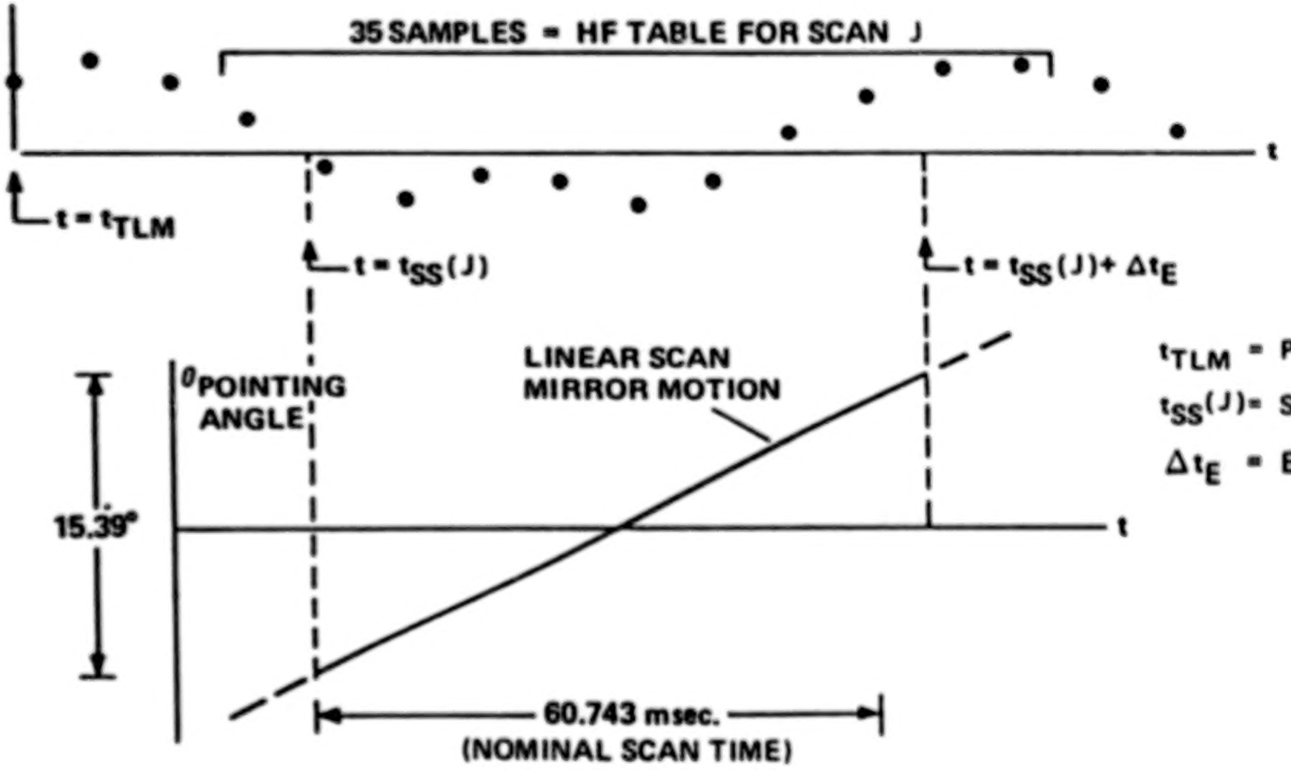
35 SAMPLES = HF TABLE FOR SCAN J
t
t = tTLM
t = tSS(J)
t = tSS(J) + ΔtE
θ POINTING ANGLE
LINEAR SCAN MIRROR MOTION
15.39°
t
60.743 msec.
(NOMINAL SCAN TIME)

t_{TLM} = PCD TELEMETRY START TIME

$t_{SS}(J)$ = START SCAN TIME, SCAN J

Δt_E = END SCAN TIME INTERVAL

ALONG-SCAN $\theta_{HF} = \theta_\epsilon + \theta_{ROLL}$; θ_ϵ = **SCAN MIRROR NONLINEARITY**

HF: HIGH FREQUENCY

FIGURE 3-9

LOW FREQUENCY ATTITUDE ERROR DYNAMICS

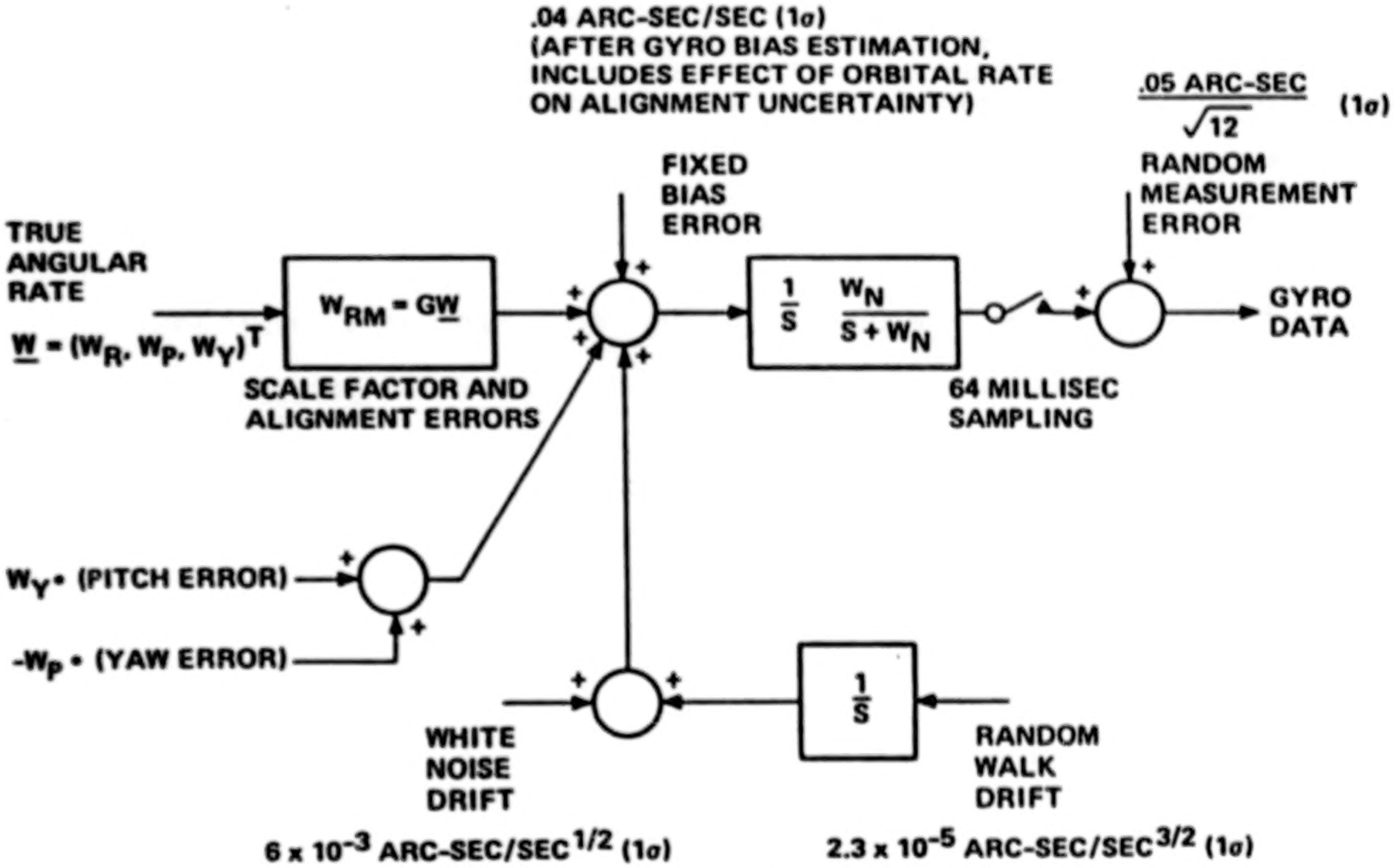
.04 ARC-SEC/SEC (1σ)
(AFTER GYRO BIAS ESTIMATION, INCLUDES EFFECT OF ORBITAL RATE ON ALIGNMENT UNCERTAINTY)
$\frac{.05 \text{ ARC-SEC}}{\sqrt{12}}$ (1σ)
RANDOM MEASUREMENT ERROR
FIXED BIAS ERROR
TRUE ANGULAR RATE
$\underline{W} = (W_R, W_P, W_Y)^T$
$W_{RM} = G\underline{W}$
SCALE FACTOR AND ALIGNMENT ERRORS
$\frac{1}{S} \quad \frac{W_N}{S + W_N}$
64 MILLISEC SAMPLING
GYRO DATA
$W_Y \cdot$ (PITCH ERROR)
$-W_P \cdot$ (YAW ERROR)
+
$\frac{1}{S}$
WHITE NOISE DRIFT
RANDOM WALK DRIFT
6×10^{-3} ARC-SEC/SEC$^{1/2}$ (1σ)
2.3×10^{-5} ARC-SEC/SEC$^{3/2}$ (1σ)

(ONLY ROLL AXIS MODEL SHOWN)

W_R, W_P, W_Y: ROLL, PITCH YAW ANGULAR RATES

FIGURE 3-10

SPACECRAFT ALIGNMENT DYNAMICS
(ACS TO TM OPTICAL AXIS)

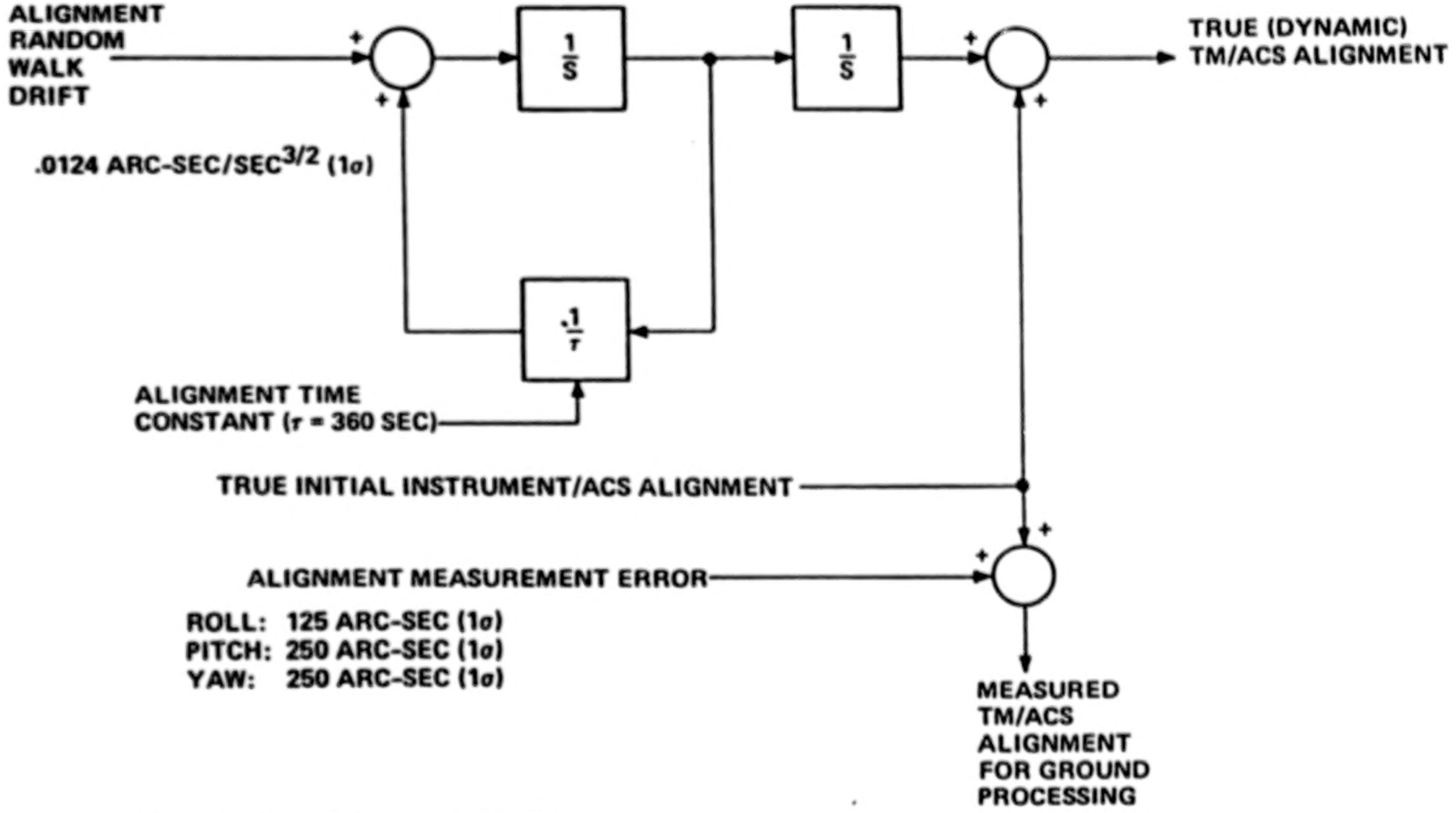
ALIGNMENT RANDOM WALK DRIFT
.0124 ARC-SEC/SEC$^{3/2}$ (1σ)
+
+
$\frac{1}{S}$
$\frac{1}{S}$
$-\frac{1}{\tau}$
ALIGNMENT TIME CONSTANT (τ = 360 SEC)
TRUE (DYNAMIC) TM/ACS ALIGNMENT
TRUE INITIAL INSTRUMENT/ACS ALIGNMENT
ALIGNMENT MEASUREMENT ERROR
ROLL: 125 ARC-SEC (1σ)
PITCH: 250 ARC-SEC (1σ)
YAW: 250 ARC-SEC (1σ)
MEASURED TM/ACS ALIGNMENT FOR GROUND PROCESSING

ACS: ATTITUDE CONTROL SYSTEM

FIGURE 3-11

CONTROL POINT CONCEPT

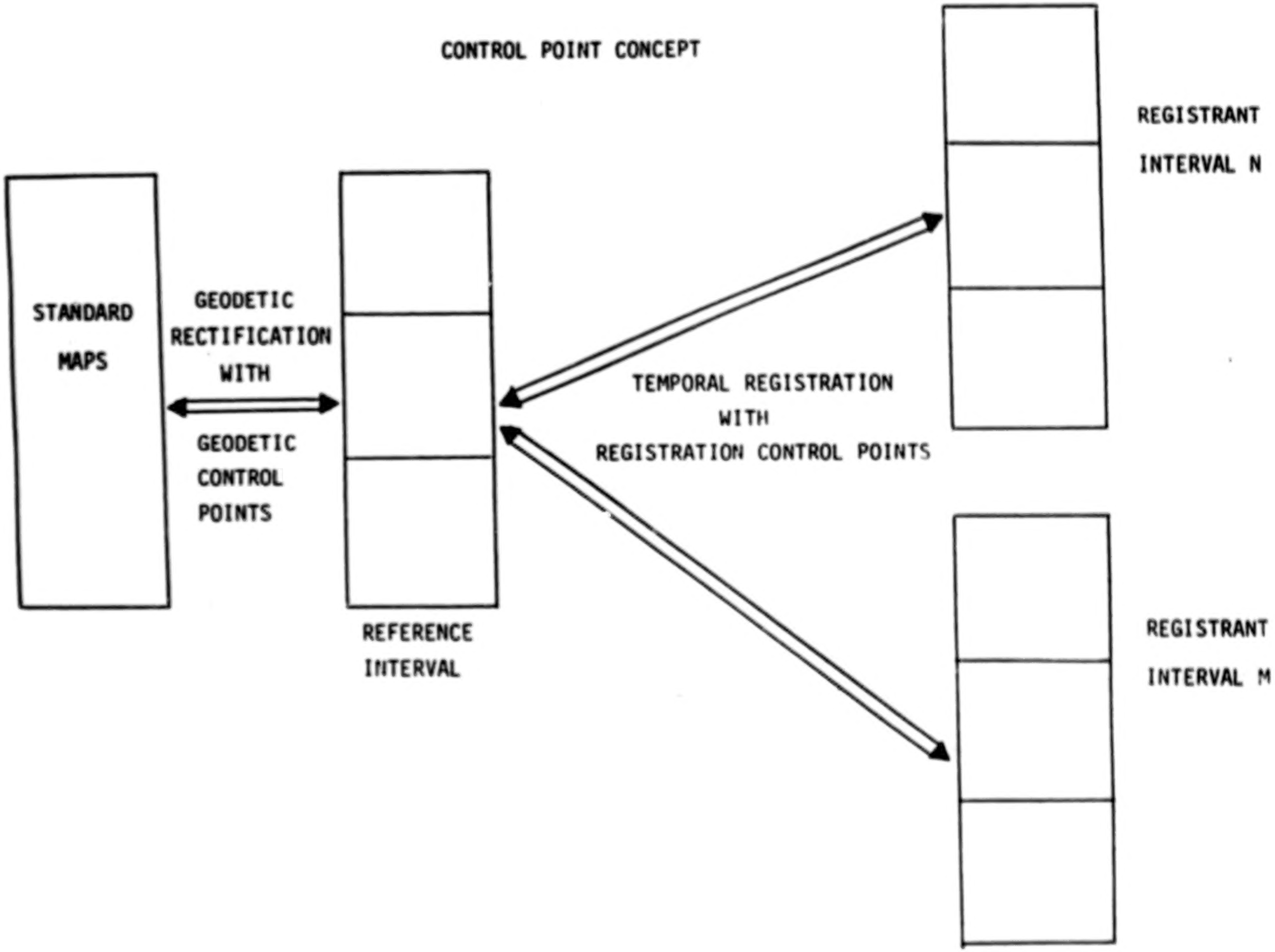
REGISTRANT
INTERVAL N
STANDARD
MAPS
GEODETIC
RECTIFICATION
WITH
GEODETIC
CONTROL
POINTS
TEMPORAL REGISTRATION
WITH
REGISTRATION CONTROL POINTS
REFERENCE
INTERVAL
REGISTRANT
INTERVAL M

FIGURE 3-12

CONTROL POINT PROCESSING FLOW

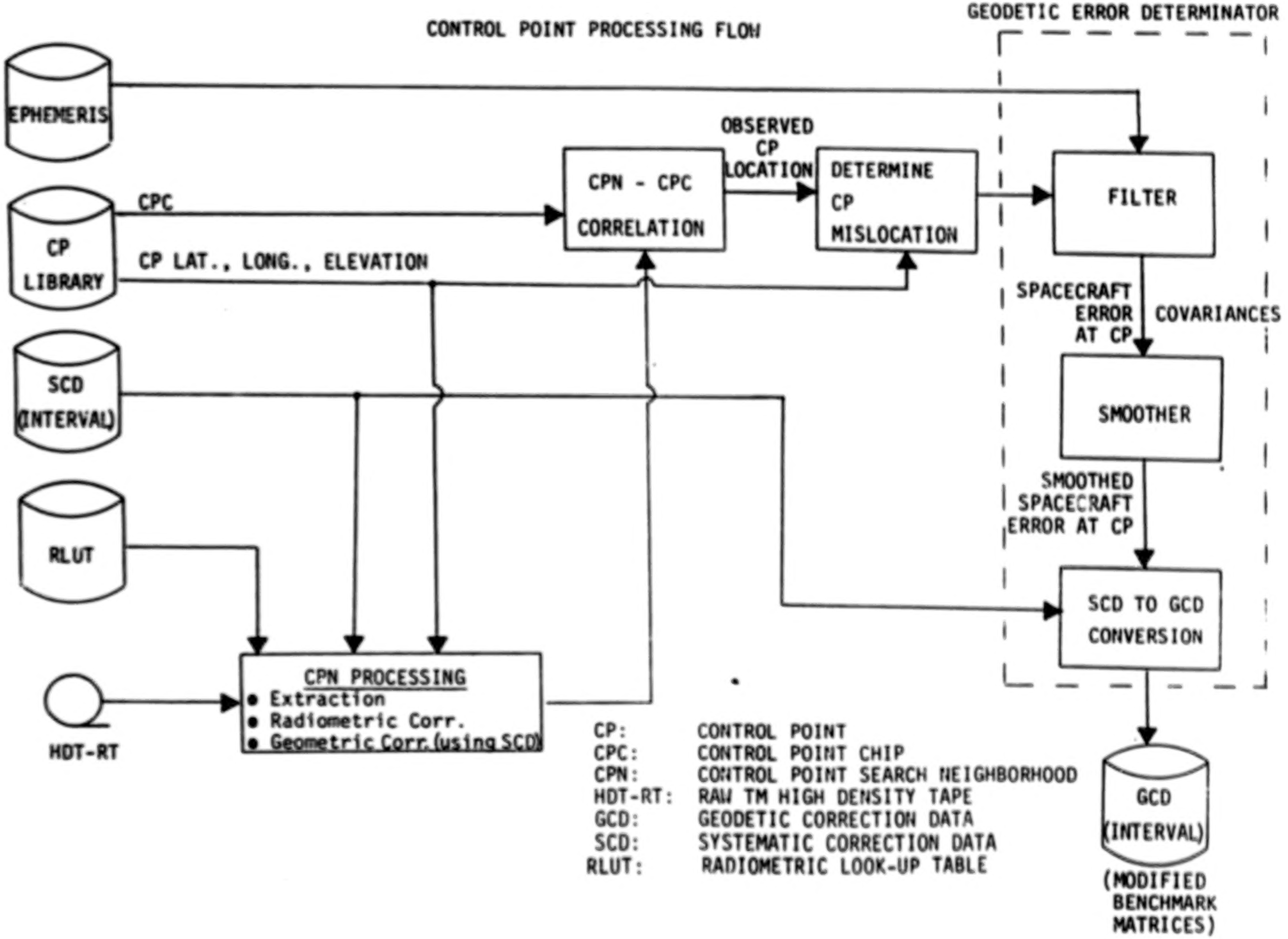
GEODETIC ERROR DETERMINATOR
EPHEMERIS
CP LIBRARY
CPC
CP LAT., LONG., ELEVATION
SCD (INTERVAL)
RLUT
HDT-RT
CPN PROCESSING
• Extraction
• Radiometric Corr.
• Geometric Corr. (using SCD)
CPN - CPC CORRELATION
OBSERVED CP LOCATION
DETERMINE CP MISLOCATION
FILTER
SPACECRAFT ERROR AT CP
COVARIANCES
SMOOTHER
SMOOTHED SPACECRAFT ERROR AT CP
SCD TO GCD CONVERSION
GCD (INTERVAL)
(MODIFIED BENCHMARK MATRICES)

CP: CONTROL POINT
CPC: CONTROL POINT CHIP
CPN: CONTROL POINT SEARCH NEIGHBORHOOD
HDT-RT: RAW TM HIGH DENSITY TAPE
GCD: GEODETIC CORRECTION DATA
SCD: SYSTEMATIC CORRECTION DATA
RLUT: RADIOMETRIC LOOK-UP TABLE

FIGURE 3-13

TM GEOMETRIC CORRECTION PROCESS OVERVIEW

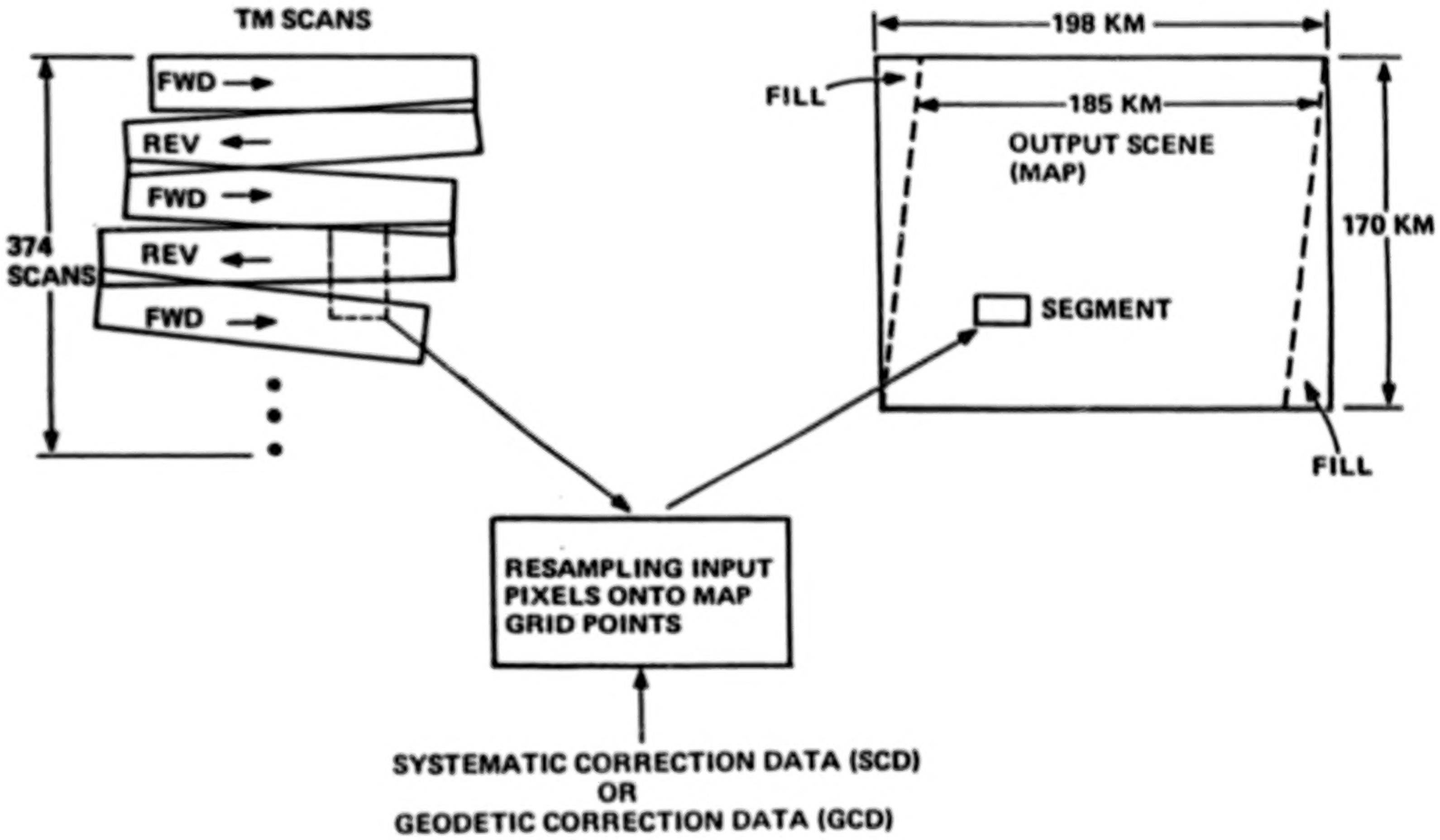
TM SCANS
FWD
REV
FWD
REV
FWD
374 SCANS
198 KM
FILL
185 KM
OUTPUT SCENE (MAP)
170 KM
SEGMENT
FILL
RESAMPLING INPUT PIXELS ONTO MAP GRID POINTS
SYSTEMATIC CORRECTION DATA (SCD)
OR
GEODETIC CORRECTION DATA (GCD)

FIGURE 3-14

TWO-DIMENSIONAL CUBIC CONVOLUTION RESAMPLING

- X-RESAMPLING: GENERATE HYBRID PIXELS
- Y-RESAMPLING: GENERATE OUTPUT PIXELS

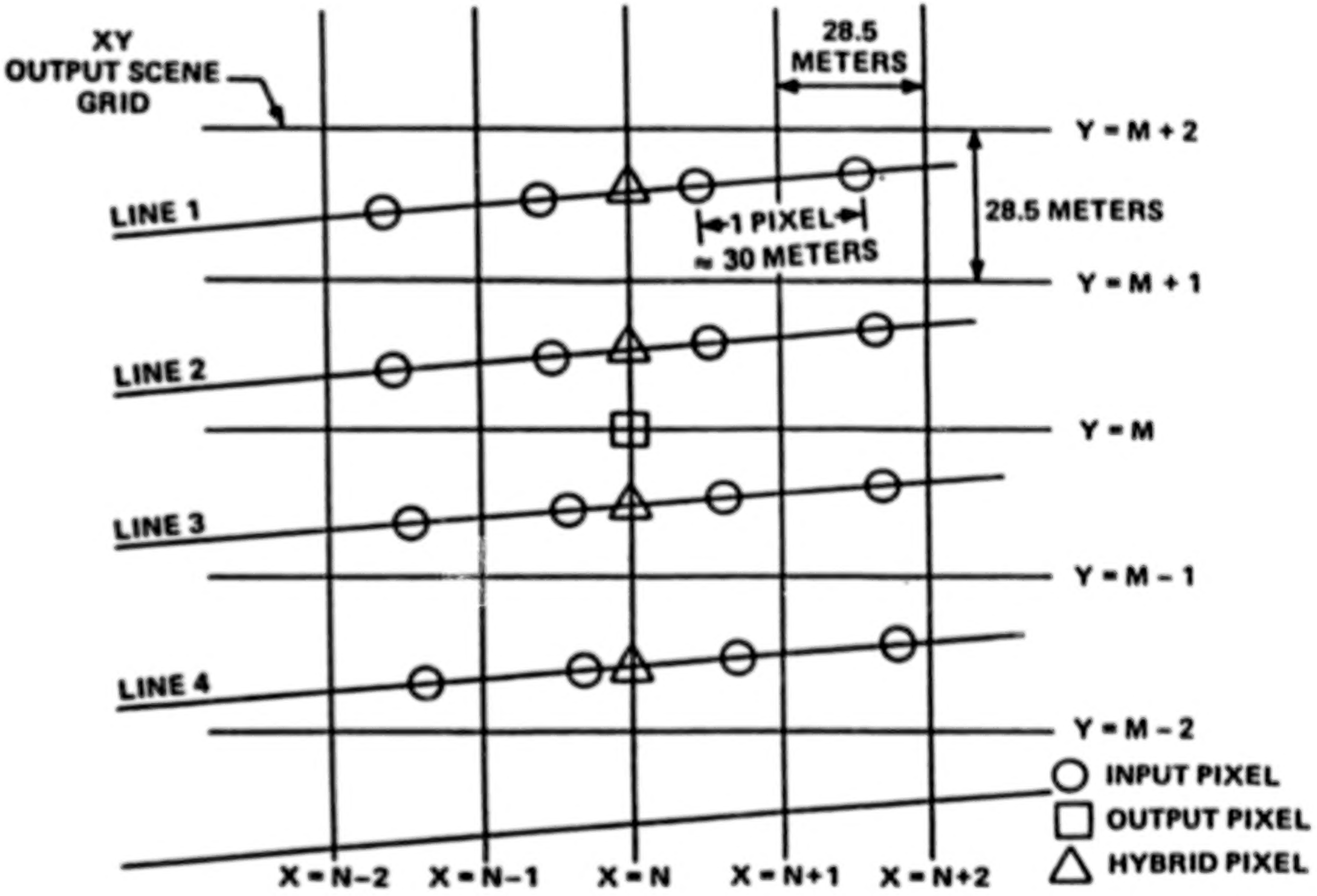
XY
OUTPUT SCENE
GRID
28.5
METERS
28.5 METERS
1 PIXEL
≈ 30 METERS
LINE 1
LINE 2
LINE 3
LINE 4
Y = M + 2
Y = M + 1
Y = M
Y = M − 1
Y = M − 2
X = N−2
X = N−1
X = N
X = N+1
X = N+2
○ INPUT PIXEL
□ OUTPUT PIXEL
△ HYBRID PIXEL

FIGURE 3-15

ONE-DIMENSIONAL CUBIC CONVOLUTION RESAMPLING

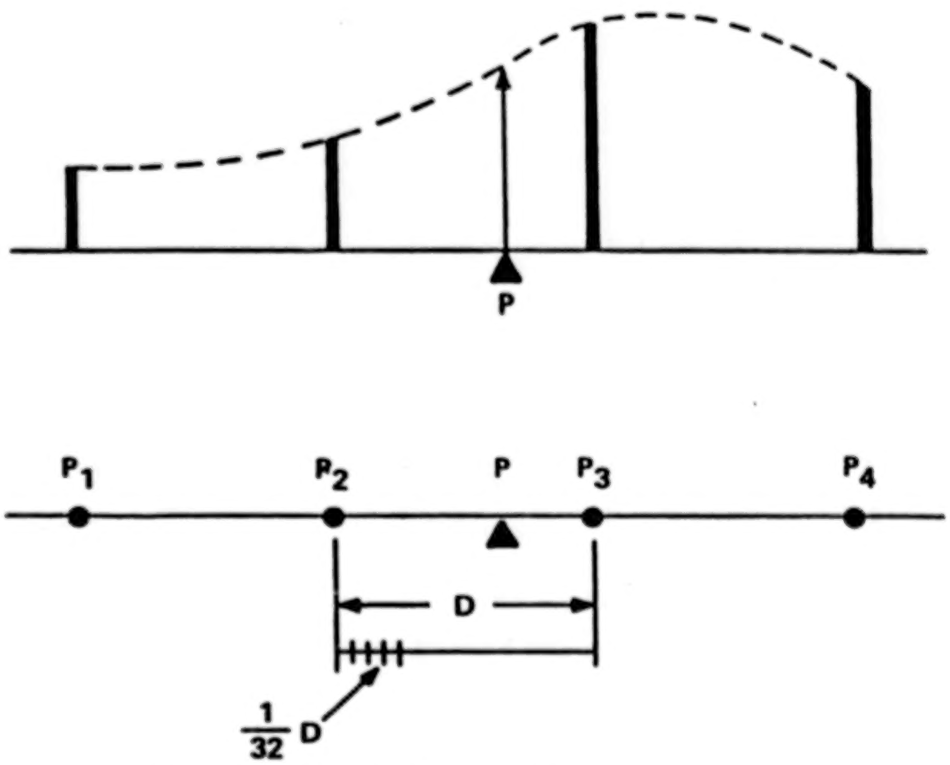

- $P = P_1W_1 + P_2W_2 + P_3W_3 + P_4W_4$
- 32 SETS OF WEIGHTING COEFFICIENTS (W_1, W_2, W_3, W_4) FOR 32 SUB-INTERVALS
- OUTPUT PIXEL LOCATION PRECISION TO (1/64) PIXEL IN RESAMPLING COMPUTATION
- INPUT PIXELS MUST BE EQUALLY SPACED

FIGURE 3-16

SCAN GAP, GAP SKEW AND SCAN LINE SKEW

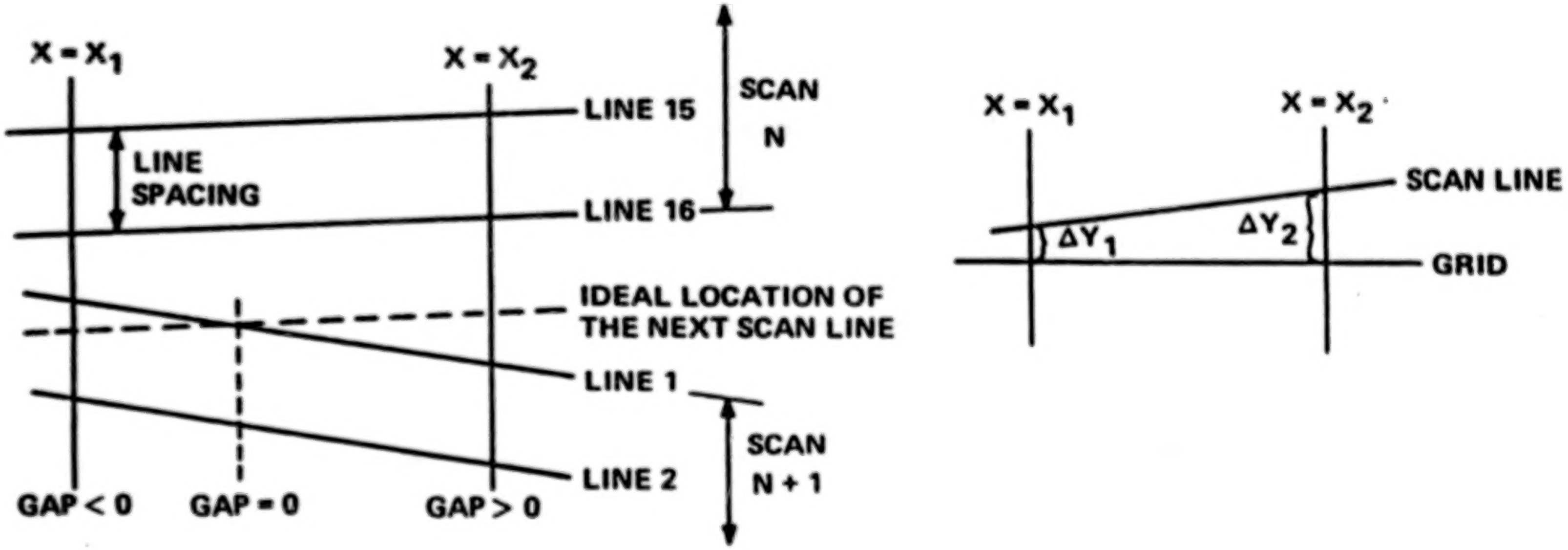
$X = X_1$
$X = X_2$
LINE 15
LINE 16
SCAN N
LINE SPACING
IDEAL LOCATION OF THE NEXT SCAN LINE
LINE 1
LINE 2
SCAN N + 1
GAP < 0
GAP = 0
GAP > 0
$X = X_1$
$X = X_2$
SCAN LINE
GRID
ΔY_1
ΔY_2

- SCAN GAP IS CAUSED PRIMARILY BY ALTITUDE VARIATION, SCAN LINE CORRECTOR SCAN RATE, SPACECRAFT PITCH AND YAW JITTER.
- GAP SIZE = (SPACING BETWEEN LINE 16 AND LINE 1) – LINE SPACING
- GAP SKEW $= \dfrac{\text{GAP SIZE }(X_2) - \text{GAP SIZE }(X_1)}{X_2 - X_1}$
- SCAN LINE SKEW $= \dfrac{\Delta Y_2 - \Delta Y_1}{X_2 - X_1}$
- X_1, X_2 = LEFT, RIGHT SIDE OF OUTPUT SEGMENT
- $X_2 = X_1 + 128$

FIGURE 3-17

TABLE 3-1

GEOMETRIC CORRECTION OPERATOR (GCO) GAP HANDLING CAPABILITY

	WORST CASE (IN PIXELS)	GCO CAPABILITY (IN PIXELS)
GAP SIZE	–2.8 TO 2.0	-5 TO 3
GAP SKEW OVER 128 OUTPUT PIXELS	–0.42 TO 0.42	-2 TO 2
TM SCAN LINE SKEW OVER 128 OUTPUT PIXELS	–1.0 TO 1.0	-2 TO 2

GENERATE SCAN EXTENSION LINE PIXELS

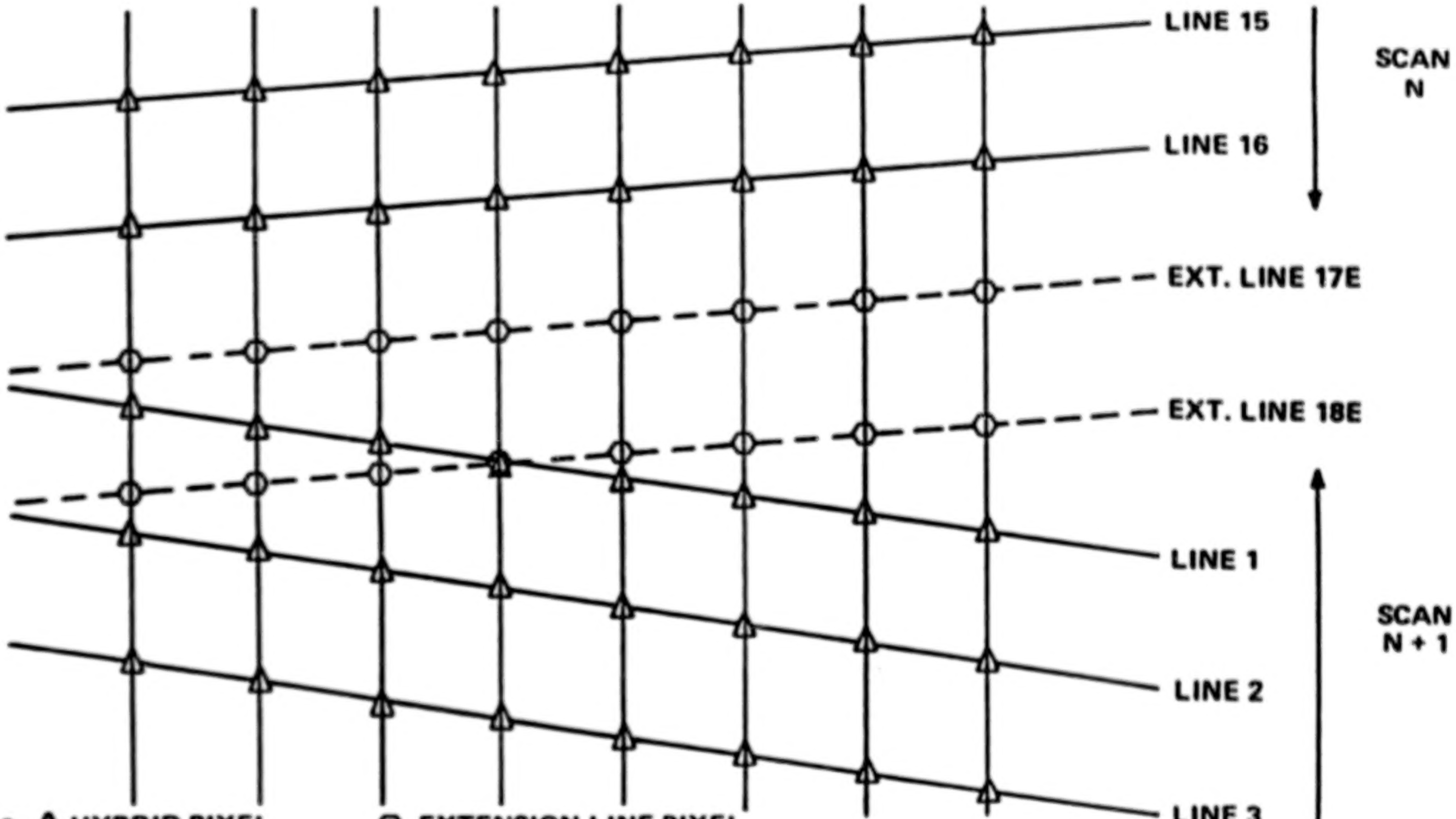
LINE 15
LINE 16
EXT. LINE 17E
EXT. LINE 18E
LINE 1
LINE 2
LINE 3
SCAN
N
SCAN
N + 1

- Δ HYBRID PIXEL ○ EXTENSION LINE PIXEL
- EXTENSION PIXELS ARE GENERATED WITH TWO HYBRID PIXELS ABOVE AND TWO HYBRID PIXELS BELOW
- PIXEL LOCATION PRECISION TO (1/64) PIXEL IN RESAMPLING COMPUTATION

FIGURE 3-18

SPLINE INTERPOLATION FORMULA

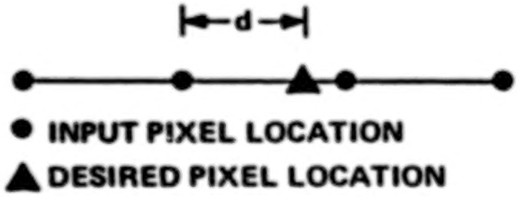

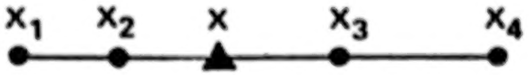

	CUBIC CONVOLUTION WEIGHT FORMULAS	CUBIC SPLINE WEIGHT FORMULAS
W_1	$-d(1-d)^2$	$\frac{2a_1}{ch_1h_2} f_1f_2f_3 - \frac{1}{ch_1} g_1g_2g_3$
W_2	$(1-d)(1+d-d^2)$	$-\frac{1}{ch_1} f_1f_2f_3 \left(1+\frac{2a_1}{h_2}+\frac{2a_1}{h_1}\right)+\frac{f_3}{h_2}+\frac{1}{c} g_1g_2g_3\left(\frac{2a_0}{h^2_2}+\frac{1}{h_1}+\frac{1}{h_2}\right)$
W_3	$d(1+d-d^2)$	$\frac{1}{c} f_1f_2f_3\left(\frac{2a_1}{h^2_2}+\frac{1}{h_2}+\frac{1}{h_3}\right)-\frac{1}{ch_2}\left(g_1g_2g_3\right)\left(1+\frac{2a_0}{h_2}+\frac{2a_0}{h_3}\right)+\frac{g_3}{h_2}$
W_4	$-d^2(1-d)$	$-\frac{1}{ch_3} f_1f_2f_3+\frac{2a_0}{ch_2h_3} g_1g_2g_3$

$f_1 = X_3 - X - h_2$
$f_2 = X_3 - X + h_2$
$f_3 = X_3 - X$

$g_1 = X - X_2 - h_2$
$g_2 = X - X_2 + h_2$
$g_3 = X - X_2$

$h_1 = X_2 - X_1$
$h_2 = X_3 - X_2$
$h_3 = X_4 - X_3$

$a_0 = h_1 + h_2$
$a_1 = h_2 + h_3$
$c = 4a_0a_1 - h^2_2$

FIGURE 3-19

N85-20512 D4

TM DIGITAL IMAGE PRODUCTS FOR APPLICATIONS

by

John L. Barker
Landsat-4 Associate Project Scientist
Code 923, Earth Resources Branch
GODDARD SPACE FLIGHT CENTER
Greenbelt MD 20771

Fred J. Gunther
Staff Scientist

Rochelle B. Abrams
Staff Scientist

and Dave Ball
Computer Scientist

Earth Observation Systems Department
COMPUTER SCIENCES CORPORATION
8728 Colesville Road
Silver Spring MD 20910

Original photography may be purchased
from EROS Data Center
Sioux Falls, SD 57198

PRECEDING PAGE BLANK NOT FILMED

[illegible] II-146 INTENTIONALLY BLANK

ABSTRACT

Landsat-4 Thematic Mapper (TM) images recorded on computer compatible tapes (CCTs) are currently available from the SCROUNGE image processing system of the Landsat-4 Assessment System (LAS) project of the National Aeronautics and Space Administration (NASA) at Goddard Space Flight Center (GSFC) in the following tape formats: 1) raw rectified data (CCT-BT); 2) calibrated data (CCT-AT); and 3) geometrically corrected data (CCT-PT). These formats represent different steps in the process of producing fully-corrected TM data. CCT-BT images are rectified from telemetry format to image format, but are uncorrected radiometrically and geometrically; they are generally used for internal transportation of data from one ground processing system to another. CCT-AT images have had data from faulty channels replaced and all data radiometrically calibrated to produce an archive image; they are available to researchers for radiometric characterization. The final products, the CCT-PT images, have been resampled by cubic convolution procedures to provide a geometrically corrected image using satellite ephemeris data. The CCT-PT image is the one to which all of the various radiometric and geometric corrections have been applied; this is the product that is available to all users.

Image files on the three tapes of the CCT-PT set are blocked four image lines per tape record, yielding a blocksize of 28672 bytes. The CCT-AT images also has a blocking factor of four but a blocksize of 26624 bytes; the equivalent values for the CCT-BT images are five and 32000 bytes.

Forward and reverse scans on all products are properly oriented east-west, but the CCT-BT and CCT-AT images have an alignment offset between scans. Original band-6 120m IFOV pixels have been replicated to four 30m IFOV pixels along a line in CCT-BT images, but the lines are not replicated to yield a full 4x4 block of 30m IFOV pixels that are array compatible with the other bands until the CCT-AT image is produced.

Saturated or very bright isolated pixels occurring in all bands result from apparent specular reflection of small objects on the ground. The pixels have proven to be useful in calculating interband registration coefficients for all CCT formats. The coefficients indicate that the bands are registered to each other within a small fraction of a pixel.

Author recommendations call for 1) better documentation, including that on tape files; 2) better calibration procedures and calibrated images; 3) nearest-neighbor resampling option in addition to cubic convolution; 4) computer processing using real-number formats for all intermediate products, to eliminate the effects of integer roundoff; and 5) the use of video laser disk media for recording archival and browse images. Areas for future research are indicated.

PAGE II-148 INTENTIONALLY BLANK

PRECEDING PAGE BLANK NOT FILMED

KEYWORDS: Remote Sensing, Landsat-4, Thematic Mapper, Digital Image Processing, Calibration, Geometric Correction, Interband Registration, Computer Compatible Tapes, Data Formats, CCT-BT, CCT-AT, CCT-PT.

CONTENTS

SECTION Page

1.0 INTRODUCTION II-156

2.0 DIGITAL IMAGE PROCESSING II-157

2.1 Raw Digital Image (CCT-BT) II-159

2.1.1 Blocking Factor II-159

2.1.2 Scan Shift II-160

2.1.3 Defective Detectors II-160

2.1.4 Band-6 Format II-161

2.1.5 Ancillary Data II-161

2.2 Radiometrically Calibrated Image (CCT-AT) . . II-163

2.2.1 Blocking Factor II-164

2.2.2 Scan Shift II-164

2.2.3 Defective Detectors II-164

2.2.4 Band-6 Format II-164

2.2.5 Calibration II-164

2.2.6 Ancillary Data II-166

2.3 Geocorrected Image (CCT-PT) II-167

2.3.1 Blocking Factor II-167

2.3.2 Geometric Corrections Applied II-167

2.3.3 Earth Rotation Correction II-168

3.0 RESULTS II-169

3.1 Specular Reflectance II-169

3.2 Registration II-169

3.2.1 Prime Focal Plane, Internal II-170

3.2.2 Cold Focal Plane, Internal II-170

3.2.3 Prime-Cold Comparisons II-171

3.3 Striping II-171

3.4 CCT-AT Radiometric Abnormalities II-172

3.5 CCT-PT Radiometric Abnormalities II-173

3.6 Pseudocolor Pixel Prints II-173

4.0 DISCUSSION II-174

4.1 Summary II-174

4.2 Research Areas II-174

4.2.1 Overshoot and Undershoot II-175

4.2.2 Bright-Spot Recovery II-175

4.2.3 Light Leaks II-175

4.2.4 Out-of-Band Spectral Response II-176

4.2.5 Specifications II-176

4.2.6 Odd-Even Difference II-176

4.2.7 Within-Scan Droop II-176

4.2.8 Spectral Calibration II-177

4.2.9 Autocorrelation II-177

5.0 CONCLUSIONS II-178

5.1 Definitely True Conclusions II-178

5.2 Probably True Conclusions II-178

5.3 Possibly True Conclusions II-179

6.0 RECOMMENDATIONS II-180

6.1 Spacecraft Management II-180

6.2 Landsat-4 SCROUNGE II-180

6.3 Landsat-4 TIPS II-180

6.4 Landsat-4 NOAA II-181

6.5 Landsat-D' II-181

7.0 REFERENCES CITED II-183

ILLUSTRATIONS

All figures follow the text, starting at page II-158.

FIGURES

Figure 2-1. File organization of TM data and images on the two CCT-BT tapes used for data exchange between ADDS and LAS.

Figure 2-2. An example of data and organization of TM images in unblocked CCT-BT format.

Figure 2-3. An example of data and organization of TM images in blocked CCT-BT format.

Figure 2-4. An example of a Band 5 image in CCT-AT format.

Figure 2-5. An example of a Band 5 image in A' format.

Figure 2-6. An example of a Pseudocolor Pixel Print image for TM data in B' format.

Figure 2-7. An example of data for TM band 5, showing the defective channel #3.

Figure 2-8. An example of data and organization for TM band 6, in unblocked CCT-BT format.

Figure 2-9. An Example of a Pseudocolor Pixel Print image for TM Band 6 in B' format.

Figure 2-10. File organization of TM data and images on the two CCT-AT tapes used by LAS for data archive.

Figure 2-11. Image file contents for the CCT-AT.

Figure 2-12. An example of data and ogranization for TM images in unblocked CCT-AT format.

Figure 2-13. An example of TM data for spectral band 4 in CCT-AT format, unblocked, nominal calibration.

Figure 2-14. An example of TM data for spectral band 2 in CCT-AT format, unblocked, nominal calibration.

Figure 2-15. An example of TM data for spectral band 5 in CCT-AT format, unblocked, nominal calibration.

Figure 2-16. An example of TM data for spectral band 6 in CCT-AT format, unblocked, nominal calibration.

Figure 2-17. Diagram of LAS calibration options for TM data.

Figure 2-18. An example of TM data for spectral band 2 in CCT-AT format, unblocked, internal calibration.

Figure 2-19. An example of TM data in CCT-AT format, unblocked, internal calibration.

Figure 2-20. An example of TM data for spectral band 5 in CCT-AT format, unblocked, internal calibration.

Figure 2-21. An example of TM data for spectral band 6 in CCT-AT format, unblocked, internal calibration.

Figure 2-22. The difference image between TM band 2 data processed using two different calibration options.

Figure 2-23. The difference image between TM band 4 data processed using two different calibration options.

Figure 2-24. The difference image between TM band 7 data processed using two different calibration options.

Figure 2-25. The difference image between TM band 5 data processed using two different calibration options.

Figure 2-26. Histograms showing the frequency of differences between images produced by two different TM calibration options.

Figure 2-27. Histograms for each channel showing the different frequency of differences between band-7 images produced by two different calibration options.

Figure 2-28. File organization of TM data and images on the three CCT-PT tapes produced by LAS as final products.

Figure 2-29. Image file contents of Landsat-4 TM data in CCT-PT format.

Figure 3-1. An example of spectral reflectivity.

Figure 3-2. Interband registration for the primary focal plane.

Figure 3-3. Interband registration for a 7-band TM image.

Figure 3-4. An example of a histogram for one data channel showing empty bins.

Figure 3-5. An example of empty bin locations and periodicity for data from detector 1, all 7 TM spectral bands.

SECTION Page

Table 2-1. General Comparison among Landsat-4 Thematic Mapper Digital Products II-158

Table 2-2. File Contents for the TAPE ID file II-162

SECTION 1 -- INTRODUCTION

The Landsat Thematic Mapper (TM) remote sensing team includes people with varied fields of interest and experience. There are the engineers, the scientists, the managers and the users, to name a few of the major groups. From a different perspective, there are the people who designed the system, those who built it (Covault, 1982a), those who tested it to see who th hardware and software lived up to expectations, and those who want to use the resulting images (Covault, 1982b; 1983) and digital products to solve problems (Williams, 1983; Everett et al., 1983; Abrams et al., 1983; and Quattrochi, 1983). The firs three groups talk common languages in engineering, mathematics and computer programming. The fourth group, the users, in many cases may not be acquainted with or understand the technical documentation produced by the engineers, scientists and computer professionals.

This document provides a transition. It is intended to provide a scientific characterization of the images, and information on the means by which the various images are being produced for the benefit of TM investigators, especially those who are concerned with radiometry. It assists users in information extraction by presenting some of the features and characteristics of the various digital image products used to produce the generally available final digitalimage product, the CCT-PT. It points to more detailed treatments of image characteristics o data formats in other documents.

Evaluation of TM image data will be the subject of another paper. Preliminary results by other investigators indicate that TM data have "... an image resolution and quality beyond expectations,..." (Covault, 1982b; 1983), due to performance at the optimum-expectation level of spacecraft and groundprocessing systems (Salomonson & Koffler, 1983). Others have concluded "...the TM data exhibits very good data quality and reliability, and can be used for accurate mensuration studies ..." (Bernstein & Lotspiech, 1983).

Other papers in this symposium cover technical details of the Landsat-4 system (Barker, 1983). Calibration procedures are presented in Barker, Abrams, et al. (1984a). Absolute calibration and engineering test results are in Barker, Abrams, et al. (1984b) while Barker, Ball, et al. (1984) describes post-launch calibration results for the TM reflective bands and studies improvements in the ground processing procedure. A discussion of sensor radiometry for the thermal band appears in Lansing & Barker (1984). Detailed discussion of results and recommendations is given in Barker (1984). This document will concentrate on the characterization of digital products.

SECTION 2 -- DIGITAL IMAGE PROCESSING

Thematic Mapper (TM) in-orbit data is now available for general use (Covault, 1982b; 1983; Williams, 1983). The SCROUNGE system, which comprised the Mission Management Facility (MMF), the Data Receive, Record, and Transmit Subsystem (DRRTS), the Applications Development Data System (ADDS), and the Landsat-D Assessment System (LAS) has processed TM images on a research and development basis at Goddard Space Flight Center (GSFC), of the National Aeronautics and Space Administration (NASA). SCROUNGE provided intermediate and/or final products directly to principal investigators (PIs) of TM assessment projects, and indirectly to the general public through the EROS Data Center (EDC) at Sioux Falls SD. SCROUNGE processing at NASA/GSFC provided images at the rate of one TM image per day. In July 1983, one year after launch, the TM Image Processing System (TIPS) took over image processing at a rate of 102 images per day.

SCROUNGE-era computer-assisted (digital) image processing resulted in photoproducts and computer-compatible tapes (CCTs) representing different levels of processing. Most people will work with the images and CCTs at the final-product stage, but intermediate products are available as an engineering tool. TM data in final-product form has geometric and radiometric corrections applied and is ready to be used in image analysis; the intermediate products have different levels of corrections applied (Table 2-1). This section discusses the characteristics of the different types of digital products.

In addition to the several high-density (HDT) tape formats used internally by NASA (Jai, 1982), SCROUNGE-era digital TM data exist in three formats (Table 2-1). The three formats are:

- Raw rectified data (CCT-BT)(Anon., 1982a) is generally used only for internal transportation of digital data from one ground processing system to another.
- Calibrated data (CCT-AT)(Baker & Gilson, 1982) should be used only by investigators doing radiometric characterization.
- Geometrically corrected data (CCT-PT) (Baker & Gilson, 1982) is the final product. The final product, the CCT-PT, is the one to which all of the various radiometric and geometric corrections have been applied; this is the product that is ideal for image analysis for applications.

General Comparisons among Landsat-4 Thematic Mapper Digital Products.

CCT SCROUNGE-ERA FORMATS (1982-1983)
LANDSAT-4 TM DIGITAL DATA

	CCT-BT	CCT-AT	CCT-PT
TAPES	2	2	3
DENSITY	6250 bpi	6250 bpi	6250 bpi
BAND FORMAT	BSQ	BSQ	BSQ
IMAGE RECORDS/FILE	1197 (300—B6)	1497	1483
RECORD LENGTH	32000 BYTES	26624 BYTES	28672 BYTES
LINE LENGTH (FILLED)	6400 (6400)	6176 (6656)	6967 (7168)
BLOCKING FACTOR	5	4	4
PREPROCESSING			
RADIOMETRIC	NONE	YES	RESAMPLED
GEOMETRIC	FLIP REVERSE SCANS	NONE	RESAMPLED
EROS DATA CENTER AVAILABILITY	NO	YES	YES

Table 2-1. General Comparison among Landsat-4 Thematic Mapper Digital Products.

2.1 Raw Digital Image (CCT-BT)

SCROUNGE-era partially processed TM data was produced in a format (CCT-BT) used for data exchange between the ADDS and LAS (Anon., 1982a). CCT-BT tapes are not ready for general applications digital image processing. They are available through the NASA Science Office only to TM principal investigators (PIs). Radiometric correction and geometric registration procedures have not been applied to the image data. Start-line pulses and initial image pixels, not present in all channels of the telemetry data, have been trimmed before writing the image to the CCT-BT. Reverse scans have been flipped so that east and west ends of each scan are properly oriented. The interleaved minor-frame format used in the telemetry was sorted into band-sequential format (Figure 2-1).

The images were written as 8-bit byte data on two standard 6250 bpi CCTs in band sequential (BSQ) format. Four image files are on the first CCT-BT, and three image files are on the second (Figure 2-1). Tape identification files are also placed on both tapes. In addition, the first tape contains a special data file with housekeeping, ephemeris, attitude, and minor scan data plus data quality information (Section 2.1.5).

Each image line follows a particular format (Anon., 1982a). The first 10 bytes of each image line provide support data, including the scan number for that TM scene. The next 6176 pixels are image data, with the first pixel at the western edge of the scene. The image data are followed by 64 bytes of zero fill, by 64 bytes of support data containing channel gain and offset information, and by a final 64 bytes of zero fill (Figure 2-2). This yields an image line of 6400 bytes. Five such lines make a record on the tape (Section 2.1.1).

2.1.1 Blocking Factor

To save space on the tapes, image lines were not written as separate records to tape files, but were blocked five (5) lines per tape record. If an image is copied from the tape without taking into consideration the blocking factor, the image is compressed by having only one line out of five in the vertical direction and five lines across in the horizontal direction (Figure 2-3). The image has a line length (logical record length = LRECL in IBM terminology) of 6400 bytes; the physical record length (= BLKSIZE) on the tape is 32000 bytes. Some minicomputers are unable to read blocks of this size.

The image must be unblocked to be useful (Figure 2-2). The unblocking may be a preprocessing step on an auxillary computer where the image is copied from one tape to another by a utility program or unblocking may be performed automatically by the computer program that puts the image or a portion of it on a disk file for computer access.

2.1.2 Scan Shift

TM image data in B format is not aligned between forward scans and reverse scans (Engel, 1980). A linear feature is properly recorded within each scan, but between scans there is a large offset (Kieffer, Abrams, et al., 1983) (Figure 2-4).

The offset of the image in B format can be corrected to yield a nominal alignment of pixel columns, a B' format (Figures 2-5 and 2-6). To do this, an analyst makes repeated runs of a "mosaic" program; one run for each 16 image lines. The number of pixels offset is variable, dependent upon scene latitude. An offset that appears ideal for Mississippi does not appear to be appropriate for Maryland nor for New Mexico.

The offset applied to the B format image corrects the alignment between forescan and backscan, but does not take into account all factors. It is necessary to correct the B format image for the rotation of the earth. The correction for the rotation of the earth is applied by moving the start sample for each mosaic of 16 lines to the east (i.e., by increasing the value of the start sample by a constant). The value of the constant used is a function of angular distance from the equator. Operationally, it is easiest to produce an intermediate image, to determine the correction for the rotation of the earth, and then to apply that correction to the image to be studied. The application of both scan-offset and earth-rotation corrections produces a B'' format image.

The image in B format is available through the NASA Science Office to TM PIs only. The image in B' and B'' formats must be produced by the individual investigator doing his own digital image processing; the B' and B'' image formats are not standard Landsat-4 digital products.

Note that the B'' image format is close to being geometrically correct, without any resampling. It is not a precision-registered, geometrically-correct image. This format is useful for radiometric studies that require ground truth. It is also useful for other studies where lack of ancillary data prohibit the construction of a final-product image.

2.1.3 Defective Channels

Before launch, four channels were found to be defective. Because of construction difficulties, the sensor was launched with the known defects, and ground-processing software was adjusted to replace defective data. In the B format image, these corrections have not been applied.

Detector 3 of band 5 does not respond to radiance input (Barker, Ball, et al., 1984). Instead of valid data, the instrument counts or data numbers (DNs) in that data channel are at least one order of magnitude lower than that recorded in the previous channel and the following channel (Figure 2-7).

Channel 2 of band 2 and channel 7 of band 7 have twice as much noise as the average for all channels for the respective band (Barker, 1983 and Barker, Ball, et al., 1984). Channel 4 of band 2 has a smaller modular transfer function (MTF) than desired (Barker, 1983 and Barker, Ball, et al., 1984).

2.1.4 Band-6 Format

Band 6 is the thermal band, with a larger instantaneous field of view (IFOV) than the reflected-light bands (Engel, 1980; Covault, 1982a). The "footprint" for band 6 is 120m by 120m rather than 30m by 30m; this results in an array of numbers for the image that is 1/16 the size of the array for the other bands. For digital image processing purposes, the array size of each band should be the same. To accomplish this, processing software replicates each band-6 pixel to produce four pixels along a line and four identical lines.

In the B format image, the replication process is only half done. The pixel values are replicated in the scan direction, but the scan line has not been replicated (Figure 2-8). As a result, in the B format data, the band 6 image file has only 1/4 as many records as the other files (Figure 2-1). In the B' (Figure 2-9) image format, the scan lines have been duplicated by the user so that the band-6 file has the same number of records.

2.1.5 Ancillary Data

In addition to the image files that are characterized in the above sections, each tape produced in SCROUNGE-era B format contains data files that have useful ancillary data.

The first ancillary data file is the TAPE ID file (Anon., 1982a), found as the first file on both tapes. The ID file is one physical record, or five logical records (Section 2.1.1). A detailed description of the information and format of the ID file appears in Table 2-2.

The second ancillary data file is the Header Ancillary Annotation Trailer (HAAT) file, found as the second file on the first tape only (Anon., 1982a). The HAAT file is seven physical blocks in length; each logical record is 6400 bytes. HAAT file internal head and tail records contain general timing and location information; other records contain detailed housekeeping, ephemeris and attitude data. The general information is described below; characterization of the detailed information can be found in the "Interface Control Document" (Anon., 1982a).

Table 2-2. File Contents for the TAPE ID file.

Label	Location (bytes)	Example	Note
SYSTEM ID & DATE	1-12	L4TCC8230801	1
IMAGE FORMAT & VOLUME	15-22	CCT-BT 1	2
IMAGE SCENE ID.	23-38	0109 015-033	3
SOFTWARE VERSION	41-52	ADDS0 102.00	

Notes:
1. Landsat-4, Thematic Mapper, Computer Compatible Tape, created on day 308 (4 November) of 1982, tape #1.
2. First tape of data in B format.
3. Image taken on Launch Day + 109 days, for World Reference System (WRS) Path=015, Row=033.

The first record in the HAAT file contains general timing information as literal or alphanumeric fields. The times at which the first scan and the last scan lines for this scene were taken are given in bytes 21-36 and 37-52 in YYDDDHHMMSSTTTFF format. In this format "YY" is the year, ignoring the century numbers, "DDD" is the Julian day of the year, "HH" is the hour of the day and "MM" is the minute of the hour. The seconds are reported by "SS" and the thousandths of a second by "TTT"; "FF" values are the 16ths of a millisecond (Jai, 1982). The start and stop Payload Correction Data (PCD) times are given in bytes 53-68 and 69-84 in the same format.

The seventh or last record in the HAAT file contains general location information as literal fields. The date of acquisition is given in bytes 5-11. The latitude and longitude for the image center are given in bytes 13-28, and the same for the NW corner in bytes 39-54. The World Reference System (WRS) path-row coordinates are given in bytes 31-37. Bytes 66-78 contain solar elevation data. The full scene identification code may be found in bytes 92-117.

2.2 Radiometrically Calibrated Image (CCT-AT)

The intermediate digital-data product during the SCROUNGE-era was the CCT-AT. In producing the CCT-AT digital product, some of the imperfections of the CCT-BT images are removed, and the images are written on the tapes in a general user format (Anon., 1979). The images are not yet suitable for general applications analyses.

Radiometric correction procedures have been applied to the image data (Barker, Abrams, et al., 1984a), but not geometric registration procedures. CCT-AT tapes, which are generated by NASA-GSFC for archival purposes, are available through EDC to researchers interested in radiometry.

The images were written in band sequential format (BSQ) as 8-bit byte data on two standard 6250 bpi CCTs. Three image files are on the first CCT-AT, and four image files are on the second (Figure 2-10). Tape identification files and other data files are also placed on both tapes. Identification files, data files and image files are packaged in the manner recommended by the Landsat Ground Station Operators Working Group (LGSOWG) (Anon., 1979; Baker, et al., 1983).

The formats for the image file and for the image lines are different for a CCT-BT (Section 2.1) and a CCT-AT (Figure 2-11). The image file for a CCT-AT has prefixed one internal header record to the image data. In the A format image, the image lines do not have the initial 10 bytes of labeling information, but they do have an appendage of 480 bytes (Section 2.2.1); the first image pixel is at byte #1.

2.2.1 Blocking Factor

CCT-AT image data during the SCROUNGE-era were blocked 4 lines per tape record (Baker, et al., 1983). In addition, hardware efficiency demands in LAS require that the 6176 data pixels per line be padded so that the line length is an even multiple of 512. This results in an additional 480 bytes per line, for a total line length of 6656 bytes and a physical record length (= BLKSIZE) of 26624 bytes (Figure 2-11).

The one-line internal header record for the image file is in a separate record the same length as the image line. Most of that record is blank. When the internal header record is reblocked along with the true image lines, it produces one line with alphanumeric header data and three lines with "spaces" (ASCII code = 32) (Figure 2-12).

The resulting image array does not have its start line and start sample at location 1,1 but rather at line=5, sample=1.

2.2.2 Scan Shift

The scan shift is the same in both A format and B format images. Since the transformation from B to A does not involve geometric corrections (Figures 2-13 to 2-16), A' and A'' products are derived by the user from an A format image in the same way as B' and B'' images were derived from a B format image (Section 2.1.2).

2.2.3 Defective Detectors

In the A format image, a software "quick fix" was applied by SCROUNGE to two of the channels of data produced by defective detectors (Section 2.1.3). Data from band 5, channel 3, is replaced with data from channel 4, and data from band 2, channel 4, is replaced with data from channel 5. This results in two identical lines out of every 16, in both forward and reverse scans in images from bands 2 and 5 (Figures 2-14 and 2-15).

2.2.4 Band-6 Format

Unlike the band 6 image in B format, the band 6 image file in A format has the same structure as the other bands (Figures 2-10 and 2-16). The size of the image array was enlarged to provide array compatibility with that of the other bands.

2.2.5 Calibration

TM image data in A format is produced by radiometric calibration (Barker, Abrams, et al., 1984a) of images in B format.

Prior to launch, the channels were calibrated against a National Bureau of Standards integrating sphere (Engel, 1980; Anon., 1982b; Barker, Abrams, et al., 1984a; Barker, Ball, et al., 1984). The calibrated channels were used to calibrate the on-board Internal Calibration (IC) system (Barker, Abrams, et al., 1984a; Barker, Ball, et al., 1984). Since launch, data from the IC was used to determine gain and offset for each channel (Barker, Abrams, et al., 1984a; 1984b). The application of sensor-specific calibration factors provided by the IC to the reflectance data allows production of high-quality images containing accurate radiometric data (Barker, Abrams, et al., 1984a). The actual application of calibration data proceeds at high speed through the use of a radiometric look up table (RLUT).

A B-format image can be calibrated in several ways (Figure 2-17) to produce an A-format image. For example, the authors placed a special order for a particular image to be calibrated by using pre-launch nominal values, without use of the IC, plus histogram equalization procedures to produce one set (Figures 2-13 to 2-16) of A format images, and by the IC plus histogram equalization procedures to produce another set (Figures 2-18 to 2-21) of A format images. An investigator interested in radiometry can make special requests for image calibration in A format:

- An image that has received nominal calibration only; this requires special processing by the ADDS portion of the SCROUNGE system.
- An image that has received IC calibration only, without histogram normalization.
- An image that has received the nominal calibration, followed by histogram equalization; this requires special processing by the ADDS portion of the SCROUNGE system.
- An image that has received IC calibration, followed by histogram equalization. Under the SCROUNGE system, this is the option used if there is no special request.
- An image that has received histogram equalization processing only.

The authors found differences between the products of the two types of calibration, IC followed by histogram equalization and nominal followed by histogram equalization. These differences were investigated by producing difference images for corresponding bands between the IC calibration and nominal calibration A format images. Examples of the difference images (Figures 2-22 to 2-25) show that: 1) differences between the two calibration techniques are almost always less than 2 DN levels (see below); 2) changes in calibration tend to be autocorrelated along scan lines, since the corrections have the same calibration offset for all data produced by a given channel, and since the calibration gain for similar pixels is similar; 3) each scan line tends to have changes in calibration that are independent of what happens in neighboring lines; and 4) each TM band has its own pattern of changes in calibration.

Histograms have been produced for calibration difference images for all TM bands (Figure 2-26). These histograms show that for all TM bands except band 4, most pixel DNs are not changed by the change in calibration procedure. TM band 4 has a 1-DN change between the two calibration procedures for 86.5% of the sampled image pixels and a 2-DN change of 5.2%. This could arise from the unusual IC pulse shape for band 4 channels (Barker et al, 1983b). TM band 1 has a 1-DN change for 33.2% of the pixels. TM band 3 has a 1-DN change between the two calibration procedures for 16.4% of the image pixels. Band 2 has a 1-DN change for 15.4% and band 5 has a 1-DN change for 8.7% of the pixels. Band 7 has 2-DN changes for 0.1%. Other DN changes involve trivial percentages.

Histograms were also produced for each of the 16 channels for each spectral band (Figure 2-27). These show that the two types of calibration produce different results for each channel.

A word of caution. Instrument variability with time (Barker, Abrams, et al., 1984b) has placed constraints on the several calibration procedure options available (Figure 2-17). Radiometric image analysis (Barker, 1983; Barker, Abrams, et al., 1984b) has indicated that it is essential to apply IC radiometric correction before other calibration corrections to preserve the radiometric accuracy needed for applications analyses.

2.2.6 Ancillary Data

In addition to the image files that are characterized in the above sections, each tape in A format contains data files that are not in image format. These data files contain information that may be necessary or very useful to the individual interested in information extraction.

The first ancillary data file is the LGSOWG VOLUME DIRECTORY file (Anon., 1979; Baker & Gilson, 1982), found as the first file on both tapes. The file has 17 physical records, or 68 logical records (Section 2.2.1). The first logical record contains the LGSWOG Volume Descriptor Record. The next 16 records contain pointers to various files on that tape. Details of file contents may be obtained from Baker & Gilson (1982).

The second ancillary file is the LAS label file for HAAT data. This label file contains a record describing the HAAT data file and optional history records.

The third ancillary data file is the HAAT file, found as the third file on the first tape only (Baker & Gilson, 1982). HAAT file records contain detailed housekeeping, ephemeris and attitude data. The general information is found on records #2 and #32, which are copies of records #1 and #7 from the HAAT file of the CCT-BT tape (Section 2.1.5). Characterization of the detailed information may be obtained in Baker & Gilson (1982).

The fourth ancillary data file is the LAS label file for image data, band 1. The general contents of the label file are the same as that described above for the HAAT label file. Files with this same format and data are found as external labels in front of each image file on both tapes (Figure 2-10).

2.3 Geocorrected Image (CCT-PT)

The final and finished digital-data product is the CCT-PT. The radiometrically fully-corrected images were written on the tapes in a user format (Anon., 1979) and are suitable for general applications analyses.

Completely processed TM data generated by SCROUNGE (Baker & Gilson, 1982) is available in the CCT-PT format used for product data. Radiometric and geometric correction procedures have been applied to the image data. This is the format for the image data on tape that NASA/GSFC supplied during the SCROUNGE era to the EROS Data Center (EDC).

The images were written as 8-bit byte data in BSQ format on three standard 6250 bpi CCTs (Figure 2-28). Two image files are on the first and second CCT-PT, and three image files are on the third. Tape identification files and other data files are also placed on the tapes. Identification files, data files and image files are packaged in the manner recommended by LGSOWG (see Baker & Gilson, 1982a).

2.3.1 Blocking Factor

To save space on the tapes, image lines were not written separately to tape files, but were blocked 4 lines per tape record (Baker & Gilson, 1982). In addition, hardware efficiency demands within the LAS computer required that the 6967 data pixels per line be padded so that the line length was an even multiple of 512. This padding resulted in an additional 201 bytes per line, for a total line length of 7168 bytes and a blocksize of 28672 bytes (Figure 2-29).

The one-line internal header record for the image file is in a separate record in front of the image data. The situation is nearly identical to that for A format images (Section 2.2.1).

The resulting image array does not have its start line and start sample at location 1,1 but rather at line=5, byte=1.

2.3.2 Geometric Corrections Applied

Geometric correction places TM image samples into a map coordinate system. This simplifies subsequent applications data processing (Beyer, MS), but does not affect the spectral response of ground cover types (Bartolucci et al., 1983).

During the SCROUNGE-era, ground processing produced geometrically corrected images using resampling based on systematic correction data (SCD), derived from payload correction data (PCD) (Anon., 1982b) and mirror scan correction data (MSCD). During this processing, flight segment telemetry was converted into a geometric projection of the scan pattern (Beyer, 1983). A transformation was generated between the geoid location of each pixel and the appropriate coordinates for any output grid system. The output grid was filled with data using a resampling technique. SCROUNGE used cubic convolution procedures rather than nearest neighbor or bilinear interpolation for resampling. The original 30 m IFOV of the pixels in the B and A format images was resampled to a grid interval of 28.5 m.

Precision geometric correction using the known locations of ground control points was not available during the SCROUNGE-era. The nominal corrections produced from satellite ephemeris data provide images that closely correspond to maps. Working with a CCT-PT image of Death Valley CA, registered to a topographic base, Abrams et al. (1983) found a registration error of less than two pixels, for terraine with 7000 feet of local relief. McDonald (1983), working with a CCT-PT image of flat farmland in Arkansas, reported an error in geometric accuracy of about 0.1 pixel. Goodenough (1983) found that ground registration errors along a scan were greater than across a scan (32m versus 40m). Bryant et al. (1983) calculated an average vector offset of 132.77m using 75 ground control points for a full scene.

Some apparent errors in geometric precision in film products result from imperfect geometric fidelity of filmwriters. Kiefer et al. (1983) found scale errors corresponding to 4 pixels and skew errors of 3 pixels. Large errors reported (68-72m) were attributed at least in part to "highly significant skewness" in the rotary-drum, film-writing device (Bender, et al., 1983).

2.3.3 Earth Rotation Correction

A consequence of applying geometric corrections is the correction for the rotation of the earth under the orbiting satellite. This correction results in the two black wedges found in full-scene or near-edge photoproducts and the corresponding fields of zero values found in the digital image files as "fill" pixels (Figure 2-29). These two fill fields have caused problems in image enhancement procedures that expand the dynamic range of raw or transformed data by thresholding selected percentages at the high and low ends of the frequency distribution.

Because the effects of the earth's rotation are corrected by using fill pixels, the first image pixel will be found in tape record line 5, but at a sample number some distance in from the start of the line. The distance is a variable depending upon latitude north or south. If it is necessary to locate the first image pixel on any line, the analyst or a computer program must search for the first non-zero pixel in that line, and then move three pixels to the right, to avoid edge effects caused by cubic convolution resampling of image data and fill data (Baker & Gilson, 1982).

SECTION 3 -- RESULTS

The authors employed a number of digital image analysis tools to examine particular features of Landsat-4 TM images. Preliminary results from these investigations are presented below.

3.1 Specular Reflectance

Statistically-based image evaluation procedures commonly show the presence of a few very high values, often reaching saturation levels (DN=255). Line and sample location data and printouts of pixel values show (Figure 3-1) that the same pixels are involved in each band. This indicates that the high DN values result from specular reflectance from some object within the scene and are not noise.

In a few cases, the source of specular reflectance was determined. In a Goddard Space Flight Center (GSFC) TM scene, curved surfaces (the inflated warehouse near Bldg. 20, the water tower at Bldg. 16, and the pressure dome for Bldg. 15) show specular reflectance. In the same scene, some flat roof areas also show specular reflectance. Specular reflectance could be obtained from silo tops, from covered stadiums, from cars parked in alignment in a parking lot, from pitched roofs, etc.

The specular-reflectance pixele provided an opportunity to look for instrument lag. It is important to know if the TM sensors are slow to recover from a bright reflectance reading. Examination of the DN values around several specular-reflectance pixels indicates that the next pixel in the scan line is at least 100 DN values lower. Any adjacent pixel with DN values above those of its neighboring pixels can easily be explained as a mixed pixel from a large bright source. Statistical studies of large numbers of specular-reflectance pixels are being considered, but at present there is no clear evidence for instrument lag.

3.2 Registration

Two aspects of registration can be considered: 1) the band-to-band registration that provides an accurate multispectral image array; and 2) the image to ground registration that allows the image to be used as a map. The latter aspect was not investigated by the authors; it is discussed in Section 2.3.2.

Investigation of specular radiometric responses (Section 3.1) has shown that there is close interband registration in both the B and A format images, which have the same image geometry, and in the P format images. Identification of specular reflectance pixels is complicated by the different sensitivities of the different spectral bands (see also Bryant et al., 1983a). In some bands, notably bands 1 and 4, the spectral reflectance pixels are saturated; saturated pixels record a maximum DN of 255. In other bands, notably 2 and 3, the spectral reflectance provides a peak DN value considerably above that of its neighbors, but not at saturation. The same peak can almost always be identified in all spectral bands (Figures 3-2 and 3-3).

3.2.1 Prime Focal Plane, Internal

The two early, 4-band TM scenes for Detroit, MI (scene ID = 40004-15401 and 40009-15413) in CCT-BT format, and one 7-band scene for Memphis, TN (ID = 40037-16033) in CCT-AT format have have been examined for interband registration as indicated by spectral reflectance. Each scene was treated separately. In some cases, specular reflectance pixels for large areas such as quarries occupy too large and diverse an area for registration evaluation. In most cases, specular reflectance involves only one or two pixels, and these locations are suitable for interband registration evaluation.

The authors have made center-of-gravity calculations for small image segments centered on isolated specular reflectance pixels. The assumption is that the weighted-average line and sample values for each band in the multispectral small image segment will have the same value if the bands are corrected. The data for each Detroit scene taken separately indicates that the bands on the primary focal plane (Engel, 1980) are registered to a fraction of a pixel in both line and sample directions (Figure 3-2). The Detroit-1 image had a registration error of up to 0.14 pixels in the scan direction and up to 0.28 pixels across scan; the equivalent values for the Detroit-2 image are 0.22 and 0.48. Errors of up to 0.45 pixels in scan and up to 0.15 pixels across scan were obtained for a comparison of bands 1-4 for the Memphis scene (Figure 3-3).

Other authors have reported similar results. Using a different procedure, that of line-to-line displacement, Fusco and Mehl (1983) found a misregistration that measured less than 0.1 pixel. The same value was determined by Bryant et al. (1983a; 1983b). Visual comparison of contrasting targets using an interactive video display on a part of the Washington D.C. scene (ID = 40109-15140) found that bands 1-4 were perfectly coregistered (Bender et al., 1983).

3.2.2 Cold Focal Plane, Internal

Center-of-gravity calculations for specular reflectance pixels for a subimage from the Memphis scene (ID = 40037-16033) in CCT-AT format indicates that bands 5 and 7 on the cold focal plane (Engel, 1980) are registered to 0.04 pixels in scan and

0.05 pixels across scan directions (Figure 3-3). Band 6 was not investigated at this time because it senses emitted rather than reflected light.

Band-to-band registration error of bands 5 and 7 was reported to be less than 0.1 pixel (Bryant et al., 1983a; 1983b).

3.2.3 Prime-Cold Comparisons

Most studies indicate that the reflected-light bands on the two focal planes are only slightly misregistered. The authors' center-of-gravity (Section 3.2.1) comparison between the two focal planes using a part of the Memphis scene (ID = 40037-16033) in CCT-AT format indicates that the error in registration of the reflected-light bands to each other is 0.2 pixels in the scan direction and 0.3 pixels across scan (Figure 3-3). Card et al. (1983), using a moving-block correlation method on the Arkansas scene (ID = 40037-16031), reported errors of 0.25 and 0.50 pixels along and across scan. Using the phase correlation image alignment method on the 2 November 1982 Washington D.C. scene (ID = 40109-15140), Bryant et al. (1983a; 1983b) found between 0.1 and 0.35 pixels error in registration.

Other authors, using different images and techniques, have reported larger registration errors. Fusco and Mehl (1983) reported a displacement of 0.5 pixels between focal planes for the Arkansas scene (ID = 40037-16031), as measured by correlation profile maxima. Bender et al. (1983) found a displacement of 1-2 pixels by interactive video display analysis of the Washington D.C. scene (ID = 40109-15140). Barker (1983) reported an apparent misregistration of about 0.75 pixels along scan and 0.2 pixels across scan. Using an analysis of linear features, Gurney & Eng (1983) reported error values of 0.75 pixels and 0.5 pixels along and across scans respectively.

3.3 Striping

Digital image processing for image segments that are very uniform shows the presence of light and dark stripes (Metzler & Malila, 1983). Some images have forward and reverse scans that are consistantly different by up to 4 DNs (Barker, 1983; Metzler & Malila, 1983). Other images show only minor differences between forward and reverse scans; Kiefer et al. (1983) reported a difference of about 0.1 DN in the mean for a CCT-AT image segment from the Washington D.C. scene (ID = 40109-15140), and Bender et al. (1983) reported DN differences with a range of 0.3-0.9 for a different part of the same scene.

Another type of striping is found within each scan. Some image lines have DNs that are consistantly higher or lower than those of neighboring lines for the same scan; Kiefer, Abrams, et al. (1983) found a typical 0.8 DN difference in the mean among the 16 channels in each band.

In photoproducts, the range in DN values results in line-parallel stripes by line and by scan, seen in water bodies, ice and snow fields, and other large uniform areas. Striping is present in 3-band color composite images, 1-band pseudocolor images, and black and white images.

The sensor pecularities that produce the striping are also present in data from heterogenous areas, but in these cases, the image signal variability overpowers the striping noise.

Striping is evident in B, A, and P format images. Because of the difficulties of making sensors exactly alike, it is not suprising that striping is found in B format images. Striping in A format images indicates that sensor calibration is not yet able to remove all of the differences in sensitivity of neighboring detectors. Striping in P format images indicates that cubic convolution resampling does not remove the effect.

Photointerpretation of the image data is only slightly hampered by the striping, but striping poses major problems for digital image processing. Image enhancement procedures will enhance the striping. Image classification mapping procedures will produce incorrect classifications; most classification procedures work one pixel at a time and are unable to compensate for the radiometric changes that produce light or dark stripes.

3.4 CCT-AT Radiometric Abnormalities

One consequence of applying radiometric corrections to byte data is the phenomenon of empty bins in frequency histograms (Bartolucci et al., 1983; Bender et al., 1983). A histogram of a large area in a TM scene (Figure 3-4) in A format has occasional DN values in the middle of a gradational sequence with no frequency counts. This is especially true if the histogram is otained for a single channel of data.

This is an effect of integer arithmetic. Calibration corrections are not integer numbers, but numbers with decimal fractions. Image DN numbers are integers, ranging from zero to to 255. When an integer is multiplied by a decimal value, and the result is stored as an integer value, there will be certain DN values in the resulting calibrated image that can not be generated. A histogram of the calibrated data will have a zero tally for these particular DNs.

The cubic convolution resampling procedure used to produce the final product image produces new DN values (Section 2.3.2), so that empty bins do not exist in P format images (Metzler & Malila, 1983).

In a histogram for any data channel, the empty bins occur with a constant periodicity (Figure 3-5). The period of occurrence is different for each channel and each spectral band. The difference in the reoccurrence period arises from the different calibration factors applied to data from each detector of each band. The periodicity results from the linear calibration correction procedures used.

The periodicity in the data for a given channel can be used to back-calculate one of the calibration factors used for that channel. For example, data channel 1 of band 7 for Memphis (scene ID = 40037-16033) has a period of 33 for the presence of empty bins. This means that a range of 32 DNs in the uncalibrated image is placed into a range of 33 DNs in the calibrated image. Thus

$$33/32 = 1.03125$$

is calculated to be the relative calibration gain factor, for original digital counts to calibrated digital counts. Neither the calibration offset factor nor the original radiance values can be determined in this manner.

3.5 CCT-PT Radiometric Abnormalities

An artifact is created by applying cubic convolution resampling methods to digital TM data. At each end of a scan of 16 lines, the CCT-PT image has fill pixels with zero DNs (Section 2.3.3). The resampling procedure operates in such a manner that the near-edge combination of zero DNs and real-data DNs produces intermediate DNs along a 3-pixel border zone (Baker & Gilson, 1982). These "fuzzy frame edges" (Kiefer et al., 1983) result in erroneous histograms and misclassified pixels when the image is processed for applications analyses.

3.6 Pseudocolor Pixel Prints

The authors have devised a new tool for the radiometric evaluation of TM images that takes advantage of color graphics and human response to changes in color. The pseudocolor pixel print (PsCPP) product is produced by applying a custom color look up table to an image. Standard pseudocolor (Ps) look up tables span the range of 0-255 in a gradient that allows gross structure to be easily detected but that masks fine structure. The PsCPP look up table was designed to show differences in DN values of one count as color differences, over a repeating cycle of 32 colors. PsCPP uses eight cycles of colors to span the entire range of 0-255; this masks coarse structure, but the combination of Ps and PsCPP processing permits analysis of both levels of structure.

PsCPP products show dramatically the fine structure in TM single-band images (Figures 2-6 and 2-9). Banding becomes very obvious, especially that caused by dead detectors (Section 2.1.3) rather than by minor variation in detector response and calibration (Section 3.2).

SECTION 4 -- DISCUSSION

4.1 Summary

Thematic mapper (TM) digital data has characteristics of tape files, image format and image radiometry that are important to the applications scientist. First of all, the data resides in different tape files at initial (Figure 2-1), intermediate (Figure 2-10), and final (Figure 2-28) stages of SCROUNGE processing at LAS. Within each image data file, the image lines are blocked by a factor of either 5 for a CCT-BT or 4 for a CCT-AT and CCT-PT (Sections 2.1.1, 2.2.1, and 2.3.1); access to a mainframe or large minicomputer is needed because of the large block sizes involved (i.e., up to 32,000 bytes). On each set of tapes, the image data files are in correct spectral sequence, but not in correct number sequence; band 7 is located before band 6 because band 7 was added to the sensor package late in the program, and is thus the 7th set of sensors (Covault, 1982a). Within each CCT format, the image file has a different format; support data are provided in the CCT-BT format (Section 2.1, Figure 2-2) and internal header records are provided in the CCT-AT and CCT-PT formats (Sections 2.2 and 2.3, Figure 2-12). Channels with defective data have been repaired in a manner that substitutes a minor image defect for a major one (Section 2.1.3). The cubic convolution resampling used to produce the CCT-PT images masks but does not eliminate the effects of duplicating lines. TM calibration on the intermediate CCT-AT product and the final CCT-PT product does not perfectly compensate for all problems, with the result that currently-available TM images show striping both by line and by scan (Section 2.2.5). Nominal geometric corrections which provide proper geodetic relationships between different parts of the image are available only for the final product image, the CCT-PT (Sections 2.3.2 and 2.3.3). Special user processing of the intermediate TM image formats can yield an image with approximate geometric alignment without resampling (Section 2.1.2); this special product, a CCT-B'' or a CCT-A'' image, is useful for radiometric studies, but does not otherwise take the place of the CCT-PT image.

4.2 Research Areas

During their investigation of TM image characteristics, the authors have noted many image or sensor characteristics that need to be determined and quantified. For this Early Results Symposium, not all could be done; many interesting characteristics of TM images remain to be explored.

4.2.1 Overshoot & Undershoot

The absence, or the presence and characterization, of undershoot and overshoot need to be determined for TM data. Kieffer et al. (1983) reported erratic overshoot and undershoot for a portion of the Washington D.C. scene (ID = 40109-15140). Since both cases represent the response lag of the sensors in crossing a sharp boundary in reflectivity, scenes featuring land-water or snow/ice-water boundaries need to be examined. Overshoot would exist if the scan, in passing from a uniform bright area to a uniform dark area, exhibits a gradational transition rather than a sharp transition. Undershoot would exist in the case of a gradational transition from a uniform dark area to a uniform bright area.

It is necessary to distinguish two cases. A gradational transition in the real world that is accurately recorded by TM sensors must be distinguished from a sharp transition in the real world that is inaccurately recorded by TM sensors as a gradational transition. For large areas, the boundary between bright and dark areas will be traversed by both forward and reverse TM scans. If the same gradational boundary is found in both scan directions, it should be a real-world event and not a sensor artifact.

Another consideration is the type of image product involved. Undershoot and overshoot on an image in B or A formats could be a characteristic of the sensor. The same effect on an image in P format could be a characteristic of the cubic convolution resampling procedure; this would be independent of forward and reverse scans, but should involve a narrow boundary zone.

4.2.2 Bright-Spot Recovery

Closely linked to the problem of overshoot and undershoot is the problem of bright-spot recovery. In the latter case, the item of concern is how quickly do TM detectors return to low reflectance conditions after sensing an individual pixel of high reflectivity.

The evaluation done to date using specular reflectance pixels (Section 3.1) evaluated by printouts of DNs for small areas within an image indicates that the recovery from bright spots is sufficiently rapid. However, statistical studies using large numbers of specular reflectance pixels are needed to determine how fast the TM detectors recover.

4.2.3 Light Leaks

The presence of internal reflections affecting the primary focal plane sensors was reported (Markham & Barker, 1984). Preliminary analysis indicates that the sensor receives light comming from two directions; from the front (towards the telescope) and from the back. Light that has passed through filters and sensors for band 1 has the greatest effect on other bands. In this case, there is a 15-pixel lag between sensing a bright spot in band 1 and the effect of internally reflected light producing a 1.2% increase in DN value in band 4 (e.g., a 255 DN pixel in band 1 adds 3 DNs to what is sensed in band 4. The lag results from the different physical locations of the sensor array within the TM. There appear to be interactions among other bands, but at much lower percentages.

The internal reflection will have to be completely characterized so that the effect can be eliminated before attempting to calculate the absolute radiometric data needed for a variety of research projects (Barker, Abrams, et al., 1984a).

4.2.4 Out-of-Band Spectral Response

Another possible phenomenon to be characterized is the response of the sensors to light with a wavelength outside the band width (Markham & Barker, 1983). In other words, the filters are not completely opaque outside of spectral window. Of concern is not only the light with wavelengths just outside the 50% shoulder that defines the spectral window for the filter, but also the light sensed that is at some wavelength distant from the filter window. How much light is sensed and at what wavelength location, both in absolute terms and relative to the filter window, are the questions for which answers need to be sought.

4.2.5 Specifications

How the TM system meets specifications (Anon., 1982b) will be discussed in a later document. This research is still ongoing.

4.2.6 Odd-Even Difference

Examination of image statistics has shown that there is an odd-even difference in detectors which is not removed by calibration. This results from a difference in physical location in the sensor array between even-numbered detectors and odd-numbered detectors (Anon., 1982b) and/or different electronics. This effect needs to be quantified and characterized using multiple images, so that it can be removed by improved radiometric calibrations.

4.2.7 Within-Scan Droop

A possible problem is a change in the electronically-induced offset (Barker, Abrams, et al., 1984b; Metzler & Malila, 1983) during a scan. If the offset changes between the start and end of the individual scan, the usefulness of TM data for radiometric and digital-image classification-mapping purposes could be reduced. It should be possible to detect the effects of this condition, if it takes place, by the analysis of uniform bright and dark scenes. The effect, if present, would follow the direction of scan, and therefore could be separated from atmospheric and illumination effects. It should be possible to remove the effects of this drift during radiometric calibration.

4.2.8 Spectral Calibration

It is necessary to test the assumption of homogeneity of filters. The filters were cut out of a single piece of "uniform" filter material (Markham & Barker, 1984), so that different filter chips came from different microlocations and small, detectable nonuniformities could be present. For characterization of the spectral calibration among data channels, it is necessary to look at the microscale heterogeneity of the filter material used. In addition, by comparing relative gains in each channel over several scenes, spectral differences between the channels can be characterized (Engel et al., 1983; Markham & Barker, 1984).

4.2.9 Autocorrelation

The examination of the differences between nominal and IC calibration procedures has shown (Section 2.2.5) that changes in DNs between the two calibration procedures applied often occur in scan lines. Printouts of the difference images give ample visual evidence of autocorrelation (Figures 2-22 to 2-25). This needs to be tested statistically, and characterized so that autocorrelation effects can be removed by those that consider it necessary to do so (Basu & Odell, 1974; Irons & Labovitz, 1982).

SECTION 5 -- CONCLUSIONS

5.1 Definitely True Conclusions

Without any reservations or qualifications, we can make the following conclusions at this time about the Landsat-4 TM sensor system and its digital-data products:

- Detector 3 of band 5 does not respond. In any image processing software system, this channel of data will need to be replaced (Section 2.1.3).
- The "empty-bin" phenomenon in CCT-AT images results from integer truncations of mixed-mode arithmetic operations (Section 3.4).

5.2 Probably True Conclusions

With only minor reservations or qualifications, we can conclude:

- TM final-product digital data (CCT-PT) is very useful data with high radiometric and geometric quality (Salomonson & Koffler, 1983; Bernstein et al., 1983) that will open new avenues of Earth-related research (Williams, 1983).
- Interband registration, calculated from apparent spectral-response pixels for small, reflective objects on the ground, is within 0.5 pixel accuracy in both line and sample directions (Section 3.2), both within and between each focal plane.
- Ancillary data files, residing on the same tapes as the image files, contain useful information in character format. This data can be printed in easy-to-read forms by utility "TAPEDUMP" programs that read and print character format.

5.3 Possibly True Conclusions

With reservations and qualifications, we can make the following conclusions at this time:

- The SCROUNGE-era fixup employed for the various defective data channels (Section 2.1.3), that of replacing the defective line with a duplicate of the previous good line, is acceptable. This conclusion should be tested by a study that compares accuracy against computer processing cost for these alternate methods: 1) complete line replacement using the previous line; 2) alternate pixel replacement from previous and following lines; 3) replacement with the average of neighboring lines; and 4) calculation of missing scan lines from data in the same and neighboring lines in the different bands once band adjustments are made for differing spectral responses.

SECION 6 -- RECOMMENDATIONS

6.1 Landsat-4 Spacecraft Management

As part of the continuing improvements and changes to the operational procedures for spacecraft control, maintenance, and sensor operation, we recommend that:

- repeated lamp turn-ons be avoided when using manual-mode internal calibration in order to extend the life of the lamp (Barker, Abrams, et al., 1984b).

6.2 Landsat-4 SCROUNGE

As part of the continuing improvements and changes to the SCROUNGE system, we recommend that:

- Better documentation accompany the digital products. This includes not only documentation on paper but also internal documentation on magnetic tape files. More parameter values should be recorded in literal (character) fields so that a simple tape dump can provide the user with the data.
- Better calibration be applied to remove channel and scan differences that result in striping (see also Bernstein & Lotspeich, 1983). This would involve treating forward and reverse scans separately rather than averaging pulse heights from forward and reverse scans (Barker, Abrams, et al., 1984b) and using drive-specific background average data rather than scene-wide averages to determine offset (Barker, Ball, et al., 1984).
- Data from bad channels be handled better. For channel 4 of band 2, the "bad" data should be used, not replaced. For channel 3 of band 5, a more appropriate substitution should be used (see also Bernstein & Lotspiech, 1983).

6.3 Landsat-4 TIPS

In the development of the TM Image Processing System (TIPS), we recommend that:

- In addition to the SCROUNGE-era resampling by cubic convolution procedures to produce the CCT-PT image

(Section 2.3.2), the optional capability be developed to produce a CCT-PT product using the nearest neighbor resampling procedure. The latter procedure has the advantage of not changing the DNs of the pixels. Pixel values that are unchanged after radiometric calibration are needed to allow radiometric characterization and evaluation of TM scenes.

- In addition to the SCROUNGE-era geodetic correction to produce a CCT-PT product, TIPS apply corrections based upon known locations of ground-control points. Research into registration requirements for accuracy (Boyd et al., 1981) has shown that an even distribution of ground-control points is more important than the total number.

6.4 Landsat-4 NOAA

We recommend that:

- Ground processing computer programs have the ability to go directly to CCT-PT geocorrected images. This would eliminate integer arithmetic problems with intermediate products, thus providing higher radiometric accuracy.
- Images be made available to the user community both on a full scene basis and on a partial scene basis. Such a partial scene basis could produce images that correspond to 1x2-degree topographic quadrangles, or to 15-minute quadrangles. Partial scene images could be made available on CCTs or on 8-inch floppy disks.
- Archival, browse, and product images be recorded on video laser disk media. Low cost, random access, multiple scene storage, and ease of distribution are the obvious advantages (Goldstein, 1982; Mobery & Laefsky, 1982; Moussy, 1983). Remote sensing has been described as a "write-once, read often" process.

6.5 Landsat-D'

In preparing the TM sensor system before the launch of Landsat-D', we recommend that:

- The dynamic range be expanded. Alternately, high-gain / normal-gain options should be added to the analog-digital converter to permit a normal scene to more nearly fill the available DN range of 0-255. TM bands 2 and 3 do not reach saturation levels, even when recording light reflected from snow.

- An opaque light-trap be placed behind the sensors to eliminate internally reflected light which is affecting the TM sensors of Landsat-4.
- An opaque light-mask be placed around filter mounts on the prime focal plane to eliminate light passing between the detector assemblies (Barker, Abrams, et al., 1984b).

REFERENCES CITED

Anon., "LGSOWG CCT Format CCB Document: The Standard CCT Family of Tape Formats," CCB-CCT-002D, NASA/GODDARD SPACE FLIGHT CENTER, GREENBELT, MARYLAND, August 1979.

Anon., "Landsat-D Project, ADDS/LAS. SCROUNGE Interface Control Document," ADDS, NASA/GODDARD SPACE FLIGHT CENTER, Greenbelt, MARYLAND, February 1982.

Anon., "Landsat-D to Ground Station Interface Description," NASA/GODDARD SPACE FLIGHT CENTER, Greenbelt, Maryland, February 1982.

Abrams, M., A. Kahle, A. Gillespie, J. Conel, & H. Long, "Geologic Utility of Landsat-4 TM Data: Death Valley, California," ABSTRACTS, LANDSAT-4 SCIENTIFIC CHARACTERIZATION, EARLY RESULTS SYMPOSIUM. Greenbelt, Maryland. February 1983.

Baker P., & B. Gilson, "Landsat-D Assessment System Library. Computer Compatible Tape (LASLIB-CCT/LAS-CCT). Tape Format Document for Thematic Mapper," WBS no. 10T031, NASA/GODDARD SPACE FLIGHT CENTER, Greenbelt, Maryland. February 1982.

Barker, J. L., "TM Report," ABSTRACTS, LANDSAT-4 SCIENTIFIC CHARACTERIZATION, EARLY RESULTS SYMPOSIUM. Greenbelt, Maryland. February 1983.

Barker, J. L., "Relative Radiometric Calibration of Landsat TM Reflective Bands," PROCEEDINGS, LANDSAT-4 SCIENTIFIC CHARACTERIZATION, EARLY RESULTS SYMPOSIUM. Greenbelt, Maryland. April 1984.

Barker, J. L., R. B. Abrams, D. L. Ball, & K. C. Leung, "Radiometric Calibration and Processing Procedures for Reflective Bands on Landsat-4 Protoflight Thematic Mapper," PROCEEDINGS, LANDSAT-4 SCIENTIFIC CHARACTERIZATION, EARLY RESULTS SYMPOSIUM. Greenbelt, Maryland. April 1984a.

Barker, J. L., R. B. Abrams, D. L. Ball, & K. C. Leung, "Characterization of Radiometric Calibration of Landsat-4 TM Reflective Bands," PROCEEDINGS, LANDSAT-4 SCIENTIFIC CHARACTERIZATION, EARLY RESULTS SYMPOSIUM. Greenbelt, Maryland. April 1984b.

Barker, J. L., D. L. Ball, K. C. Leung, & J. A. Walker, "Prelaunch Absolute Radiometric Calibration of the Reflective Bands on Landsat-4 Protoflight Thematic Mapper," PROCEEDINGS, LANDSAT-4 SCIENTIFIC CHARACTERIZATION, EARLY RESULTS SYMPOSIUM. Greenbelt, Maryland. April 1984.

Bartolucci, L. A., M. E. Dean & P. E. Anuta, "Evaluation of the Radiometric Quality of the TM Data Using Clustering and Multispectral Distance Measures," ABSTRACTS, LANDSAT-4 SCIENTIFIC CHARACTERIZATION, EARLY RESULTS SYMPOSIUM. Greenbelt, Maryland. February 1983.

Basu, J. P., & P. L. Odell, "Effect of Intraclass Correlation among Training Samples on the Misclassification Probabilities of Bayes' Procedure," PATTERN RECOGNITION, Vol. 6, no. 1. 1974. Pages 13-16.

Bender, L. U., M. H. Podwysocki, L. C. Rowan, & J. W. Salisbury, "An Evaluation of Landsat-4 Thematic Mapper Data for their Geometric and Radiometric Occurrences and their Relevances to Geologic Mapping," ABSTRACTS, LANDSAT-4 SCIENTIFIC CHARACTERIZATION, EARLY RESULTS SYMPOSIUM. Greenbelt, Maryland. February 1983.

Bernstein,R., & J. B. Lotspiech, "Analysis and Evaluation of Landsat-4 MSS and TM Sensors and Ground Data Processing -- Early Results," ABSTRACTS, LANDSAT-4 SCIENTIFIC CHARACTERIZATION, EARLY RESULTS SYMPOSIUM. Greenbelt, Maryland. February 1983.

Beyer, E. P., "An Overview of the Thematic Mapper Geometric Correction System," GENERAL ELECTRIC COMPANY, VALLEY FORGE SPACE CENTER, VALLEY FORGE PA. (undated draft manuscript)

Beyer, E. P., "Geometric Processing," ABSTRACTS, LANDSAT-4 SCIENTIFIC CHARACTERIZATION, EARLY RESULTS SYMPOSIUM. Greenbelt, Maryland. February 1983.

Boyd, R. K., F. J. Gunther, & Y. C. Lu, "Information Systems Accuracy Needs Evaluation," CSC/TM-81/6089, COMPUTER SCIENCES CORPORATION, SYSTEM SCIENCES DIVISION, Silver Spring, MD. April 1981.

Bryant, N. A., A. L. Zobrist, F. C. Billingsley, S. Z. Friedman, B. Gokhman & T. L. Logan, "Evaluation of Landsat-4 Thematic Mapper Ground Segment Performance without Ground Control," ABSTRACTS, LANDSAT-4 SCIENTIFIC CHARACTERIZATION, EARLY RESULTS SYMPOSIUM. Greenbelt, Maryland. February 1983.

Bryant, N. A., A. L. Zobrist, & B. Gokhman, "Geometric Accuracy Assessment of Landsat-4 Thematic Mapper P-Tapes," SUMMARIES, 17 INTERNATIONAL SYMPOSIUM ON REMOTE SENSING OF THE ENVIRONMENT, ENVIRONMENTAL RESEARCH INSTITUTE OF MICHIGAN, Ann Arbor, Michigan. May 1983.

Card, D. H., R. C. Wrigley, F. C. Metz & J. R. Hall, "Assessment of Thematic Mapper Band to Band Registration by the Block Correlation Method: Preliminary Results," ABSTRACTS, LANDSAT-4 SCIENTIFIC CHARACTERIZATION, EARLY RESULTS SYMPOSIUM. Greenbelt, Maryland. February 1983.

C-3

Covault, C., "Landsat D to yield More Precise Data," AVIATION WEEK & SPACE TECHNOLOGY, 5 July 1982, Pages 40ff.

Covault, C., "Images from Space Reshape NASA Plans," AVIATION WEEK & SPACE TECHNOLOGY, 7 August 1982. Pages 16-18.

Covault, C., "Landsat-4 Boosts Remote Sensing Uses," AVIATION WEEK & SPACE TECHNOLOGY, 7 February 1983. Pages 77-78.

Engel, J. L., "Thematic Mapper -- An Interim Report on Anticipated Performance," CONFERENCE ON SENSOR SYSTEMS FOR THE 80S, AMERICAN INSTITUTE OF AERONAUTICS & ASTRONAUTICS, Colorado Springs CO. December 1980. 13 Pages.

Engel, J. C., J. C. Lansing, Jr., and D. G. Brandshaft, "Thematic Mapper Performance," SUMMARIES, 17 INTERNATIONAL SYMPOSIUM ON REMOTE SENSING OF THE ENVIRONMENT, ENVIRONMENTAL RESEARCH INSTITUTE OF MICHIGAN, Ann Arbor, Michigan. May 1983.

Everett, J. R., C Sheffield, & J. Rykstra, "Evaluation of Thematic Mapper Performance as applied to Hydrocarbon Exploration," ABSTRACTS, LANDSAT-4 SCIENTIFIC CHARACTERIZATION, EARLY RESULTS SYMPOSIUM. Greenbelt, Maryland. February 1983.

Fusco, L., & W. Mel, "TM Geometric Performance: Line to Line Displacement Analysis (LLDA)," ABSTRACTS, LANDSAT-4 SCIENTIFIC CHARACTERIZATION, EARLY RESULTS SYMPOSIUM. Greenbelt, Maryland. February 1983.

Goldstein, C. M., "Optical Disk Technology and Information," SCIENCE, Vol. 215, no. 4534. 12 February 1982. Pages 862-868.

Goodenough, D., "A Preliminary Assessment of Landsat-4 TM Data Processing by NASA," ABSTRACTS, LANDSAT-4 SCIENTIFIC CHARACTERIZATION, EARLY RESULTS SYMPOSIUM. Greenbelt, Maryland. February 1983.

Gurney, C., & K. Eng, "The Use of Linear Feature Detection to Investigate Thematic Mapper Data Performance and Processing," ABSTRACTS, LANDSAT-4 SCIENTIFIC CHARACTERIZATION, EARLY RESULTS SYMPOSIUM. Greenbelt, Maryland. February 1983.

Irons, J. R., & M. L. Labovitz, "A Data Analytic Approach to Look-Angle Radiance Adjustment," JOURNAL OF APPLIED PHOTOGRAPHIC ENGINEERING, Vol. 8, no. 3. June 1982. Pages 128-137.

Jai, A., "Landsat-D Data Format Control Book. Volume VI. Appendix A. Partially Processed Thematic Mapper High Density Tape (HDT-AT)," GES 10033, Revision B, GENERAL ELECTRIC COMPANY, SPACE SYSTEMS DIVISION, Lanham, Maryland. June 1982.

Kieffer, H. H., E. Eliason, P. Chavez, R. Batson, & W. Borgeson, "Thematic Mapper Interband Radiometric Performance," ABSTRACTS, LANDSAT-4 SCIENTIFIC CHARACTERIZATION, EARLY RESULTS SYMPOSIUM. Greenbelt, Maryland. February 1983.

Lansing, J. C., & J. L. Barker, "Thermal Band Characterization of Landsat-4 Thematic Mapper," PROCEEDINGS, LANDSAT-4 SCIENTIFIC CHARACTERIZATION, EARLY RESULTS SYMPOSIUM. Greenbelt, Maryland. April 1984.

MacDonald, R. B., "Landsat-4 Image Analysis," ABSTRACTS, LANDSAT-4 SCIENTIFIC CHARACTERIZATION, EARLY RESULTS SYMPOSIUM. Greenbelt, Maryland. February 1983.

Markham, B. L., & J. L., Barker, "Spectral Characterization of the Landsat Thematic Mapper Sensor," PROCEEDINGS, LANDSAT-4 SCIENTIFIC CHARACTERIZATION, EARLY RESULTS SYMPOSIUM. Greenbelt, Maryland. April 1984.

Metzler, M. D., and W. A. Malila, "Scan-Angle and Detector Effects in Thematic Mapper Radiometry," ABSTRACTS, LANDSAT-4 SCIENTIFIC CHARACTERIZATION, EARLY RESULTS SYMPOSIUM. Greenbelt, Maryland. February 1983.

Moberg, D. , & I. M. Laefsky, "Videodisks and Optical Data Storage," BYTE, Vol. 7, no. 6. June 1982. Pages 142ff.

Moussy, L., "The Digital Optical Disk: The Data Processing Storage Medium of the Comming Years," SUMMARIES, 17 INTERNATIONAL SYMPOSIUM ON REMOTE SENSING OF THE ENVIRONMENT, ENVIRONMENTAL RESEARCH INSTITUTE OF MICHIGAN, Ann Arbor, Michigan. May 1983.

Salomonson, V. V., & R. Koffler, "An Overview of Landsat-4 Status and Results from Thematic Mapper Data Analyses," SUMMARIES, 17 INTERNATIONAL SYMPOSIUM ON REMOTE SENSING OF THE ENVIRONMENT, ENVIRONMENTAL RESEARCH INSTITUTE OF MICHIGAN, Ann Arbor, Michigan. May 1983.

Quattrochi, D. A., "An Initial Analysis of Landsat-4 Thematic Mapper Data for the Discrimination of Agricultural, Forested Wetlands, and Urban Land Covers," ABSTRACTS, LANDSAT-4 SCIENTIFIC CHARACTERIZATION, EARLY RESULTS SYMPOSIUM. Greenbelt, Maryland. February 1983.

Williams, D., "Landsat-4 Highlights," ABSTRACTS, LANDSAT-4 SCIENTIFIC CHARACTERIZATION, EARLY RESULTS SYMPOSIUM. Greenbelt, Maryland. February 1983.

LANDSAT-4 TM – DIGITAL TAPE CONTENTS – CCT-BT (5X BLOCKING)

SCROUNGE-ERA (1982-1983)

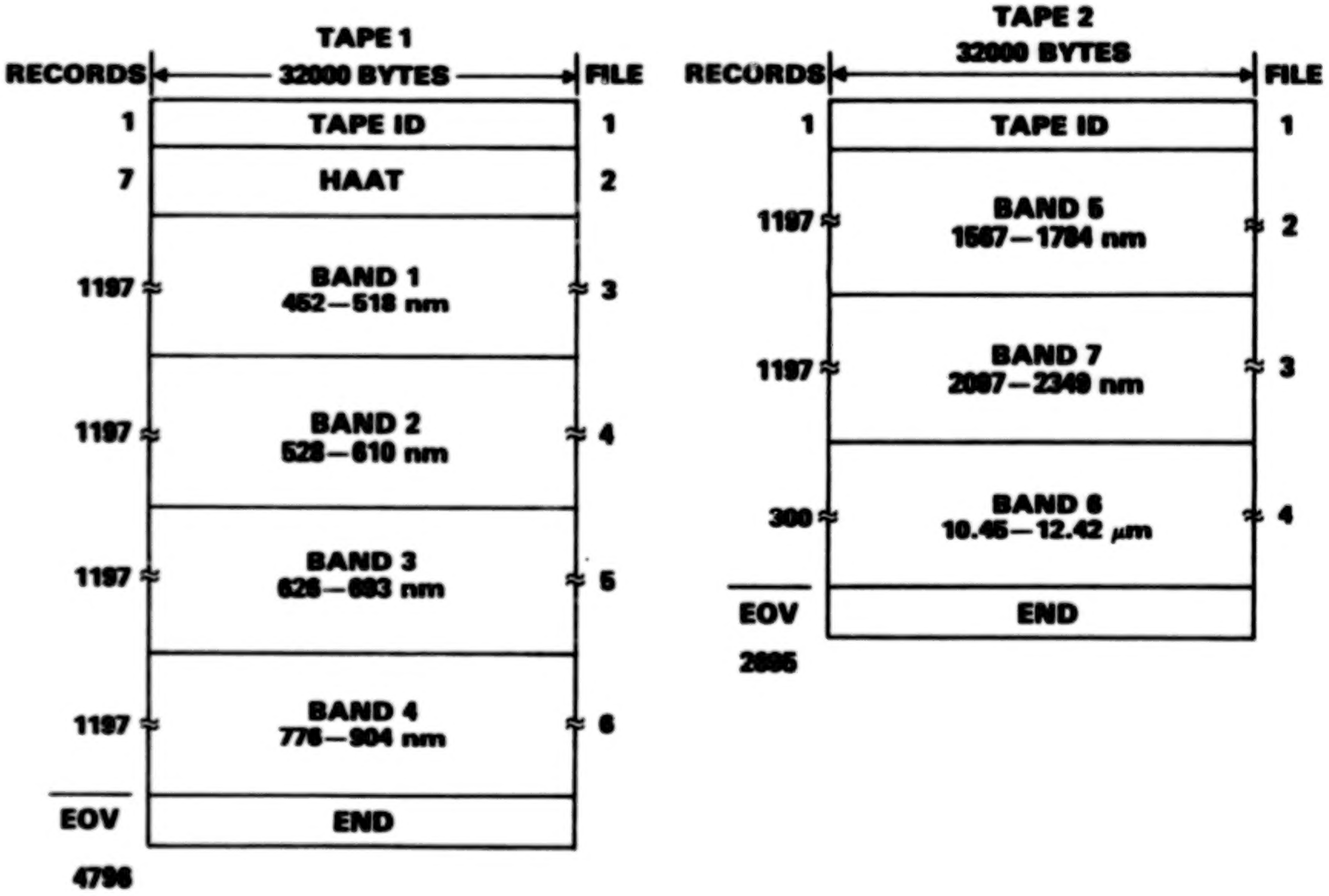

TAPE 1
RECORDS
32000 BYTES
FILE
1
TAPE ID
1
7
HAAT
2
1197
BAND 1
452—518 nm
3
1197
BAND 2
528—610 nm
4
1197
BAND 3
626—693 nm
5
1197
BAND 4
776—904 nm
6
EOV
END
4796
TAPE 2
RECORDS
32000 BYTES
FILE
1
TAPE ID
1
1197
BAND 5
1567—1784 nm
2
1197
BAND 7
2097—2349 nm
3
300
BAND 6
10.45—12.42 μm
4
EOV
END
2695

Figure 2-1. File organization of TM data and images on the two CCT-BT tapes used for data exchange between ADDS and LAS. Note that TM band 6 follows band 7 in correct spectral sequence.

LANDSAT-4 TM — CCT-BT — INITIAL PORTION OF DATA MATRIX (UNBLOCKED)

WASHINGTON DC (ID = 40109-15140) 2 NOV 1982

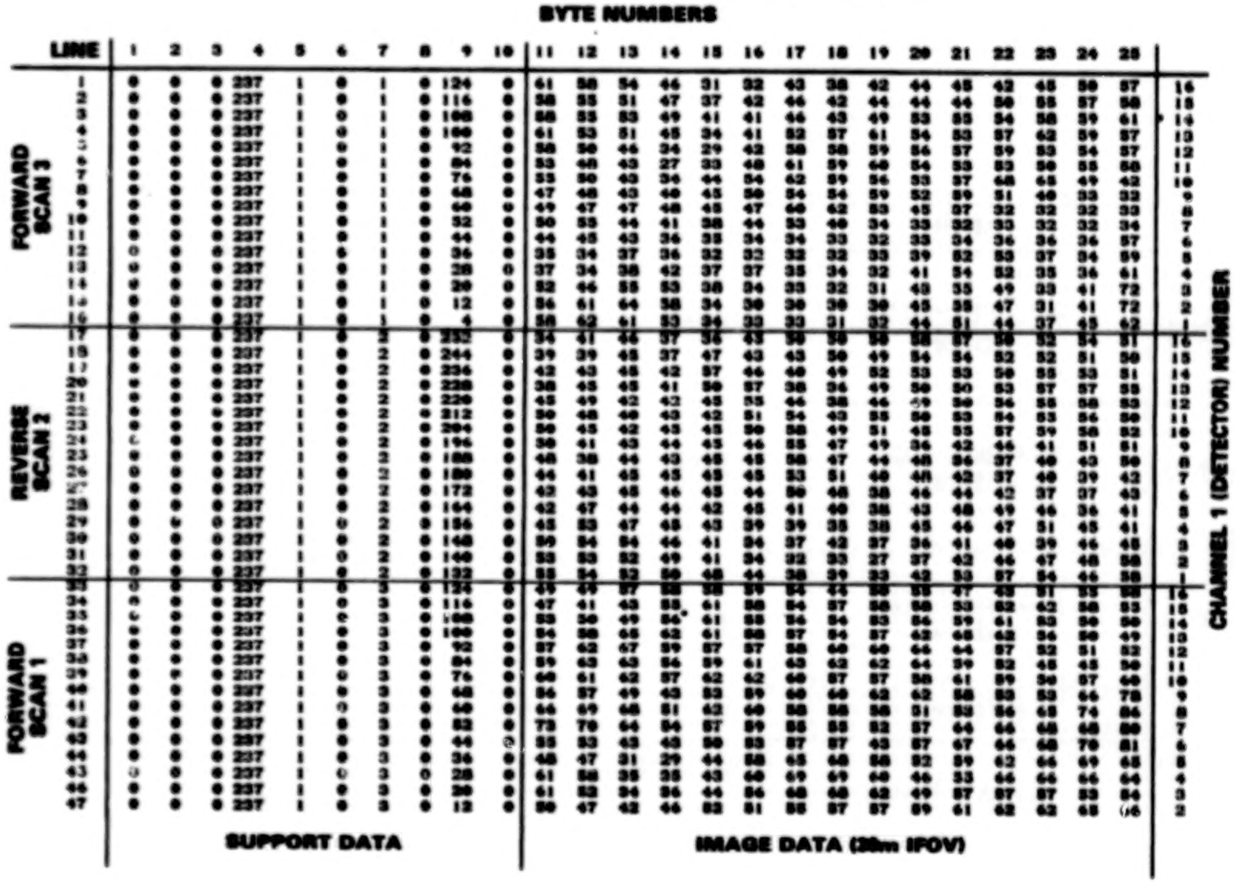
BYTE NUMBERS
LINE
1 2 3 4 5 6 7 8 9 10 11 12 13 14 15 16 17 18 19 20 21 22 23 24 25
FORWARD SCAN 3
REVERSE SCAN 2
FORWARD SCAN 1
SUPPORT DATA
IMAGE DATA (30m IFOV)
CHANNEL 1 (DETECTOR) NUMBER

Figure 2-2. An example of data and organization of TM images in CCT-BT format, as unblocked when written onto a copy tape or a disk file. The example shows the initial portion of each image line, which is now also a data record. Note the scan number in Column 7. Compare with Figure 2-4. Note that the grey wedge in column 9 is complete for a reverse scan (even numbered line) followed by a forward scan (odd numbered line).

LANDSAT-4 TM — CCT-BT (ORIGINAL 5X BLOCKING)

WASHINGTON DC (ID = 40109-15140) 2 NOV 1982

BYTE NUMBERS

SAMPLE LINE	1	2	3	4	5	6	7	8	9	10	11	12	13	14	15	16	17	18	19	20	21	22	23	24	25
1	0	0	0	237	1	0	1	0	124	0	61	58	54	46	31	32	43	38	42	44	45	42	45	50	57
2	0	0	0	237	1	0	1	0	84	0	53	48	43	27	33	48	61	59	60	54	53	53	50	55	58
3	0	0	0	237	1	0	1	0	44	0	44	45	45	36	35	34	34	33	32	33	34	36	36	36	57
4	0	0	0	237	1	0	1	0	4	0	58	62	61	53	34	33	33	31	32	44	51	44	37	45	62
5	0	0	0	237	1	0	2	0	220	0	45	49	42	42	45	55	46	38	46	49	50	56	55	58	53
6	0	0	0	237	1	0	2	0	180	0	44	41	45	45	45	45	53	51	40	48	42	37	40	39	42
7	0	0	0	237	1	0	2	0	140	0	53	53	52	49	41	34	32	33	27	37	42	46	47	48	58
8	0	0	0	237	1	0	3	0	100	0	54	58	65	62	61	58	57	54	57	62	65	62	56	50	49
9	0	0	0	237	1	0	3	0	60	0	66	69	68	51	62	60	58	58	58	51	53	56	65	74	86
10	0	0	0	237	1	0	3	0	20	0	61	52	34	36	44	56	68	68	62	49	57	57	57	53	54
11	0	0	0	237	1	0	4	0	236	0	54	56	56	52	56	58	57	55	59	60	61	45	49	44	40
12	0	0	0	237	1	0	4	0	196	0	61	54	52	57	57	58	59	61	64	54	49	55	50	55	60
13	0	0	0	237	1	0	4	0	156	0	52	57	59	56	55	59	61	59	48	46	45	48	51	58	62
14	0	0	0	237	1	0	5	0	116	0	33	50	47	46	47	49	48	45	45	46	47	49	49	50	54
15	0	0	0	237	1	0	5	0	76	0	52	63	75	83	80	70	61	55	48	38	26	23	27	33	38
16	0	0	0	237	1	0	5	0	36	0	61	55	45	39	30	33	36	36	39	43	52	59	52	40	37
17	0	0	0	237	1	0	6	0	252	0	68	73	69	57	51	53	52	52	55	60	55	53	57	51	57
18	0	0	0	237	1	0	6	0	212	0	56	54	50	55	54	62	68	69	70	70	57	46	49	49	52
19	0	0	0	237	1	0	6	0	172	0	54	65	69	69	76	73	77	75	53	32	39	33	45	51	46
20	0	0	0	237	1	0	6	0	132	0	72	69	74	74	72	68	57	49	61	69	65	61	62	62	63

SUPPORT DATA

IMAGE DATA (30m IFOV)

Figure 2-3. An example of data and organization of TM images in CCT-BT format, as blocked on the tape. The example shows the initial portion of each tape record. Because of the blocking factor, five (5) image lines make up one record on the tape. Note the scan number in column 7. Compare with Figure 2-3.

ORIGINAL PAGE IS
OF POOR QUALITY

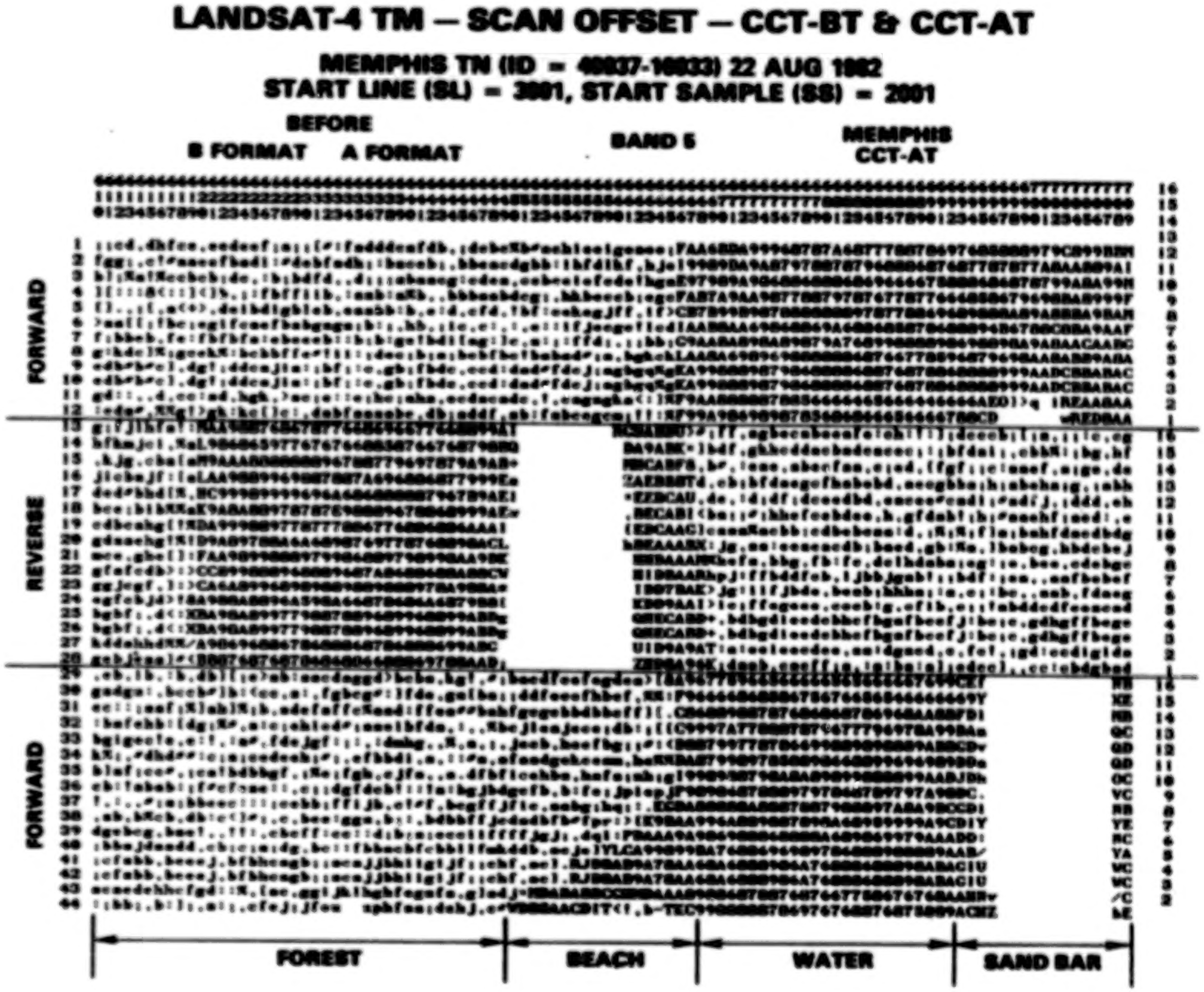

Figure 2-4. An example of a Band 5 image in CCT-AT format. The "before" image demonstrates the existing scan shift between forward and reverse scans (See Figure 2-5).

ORIGINAL PAGE IS
OF POOR QUALITY

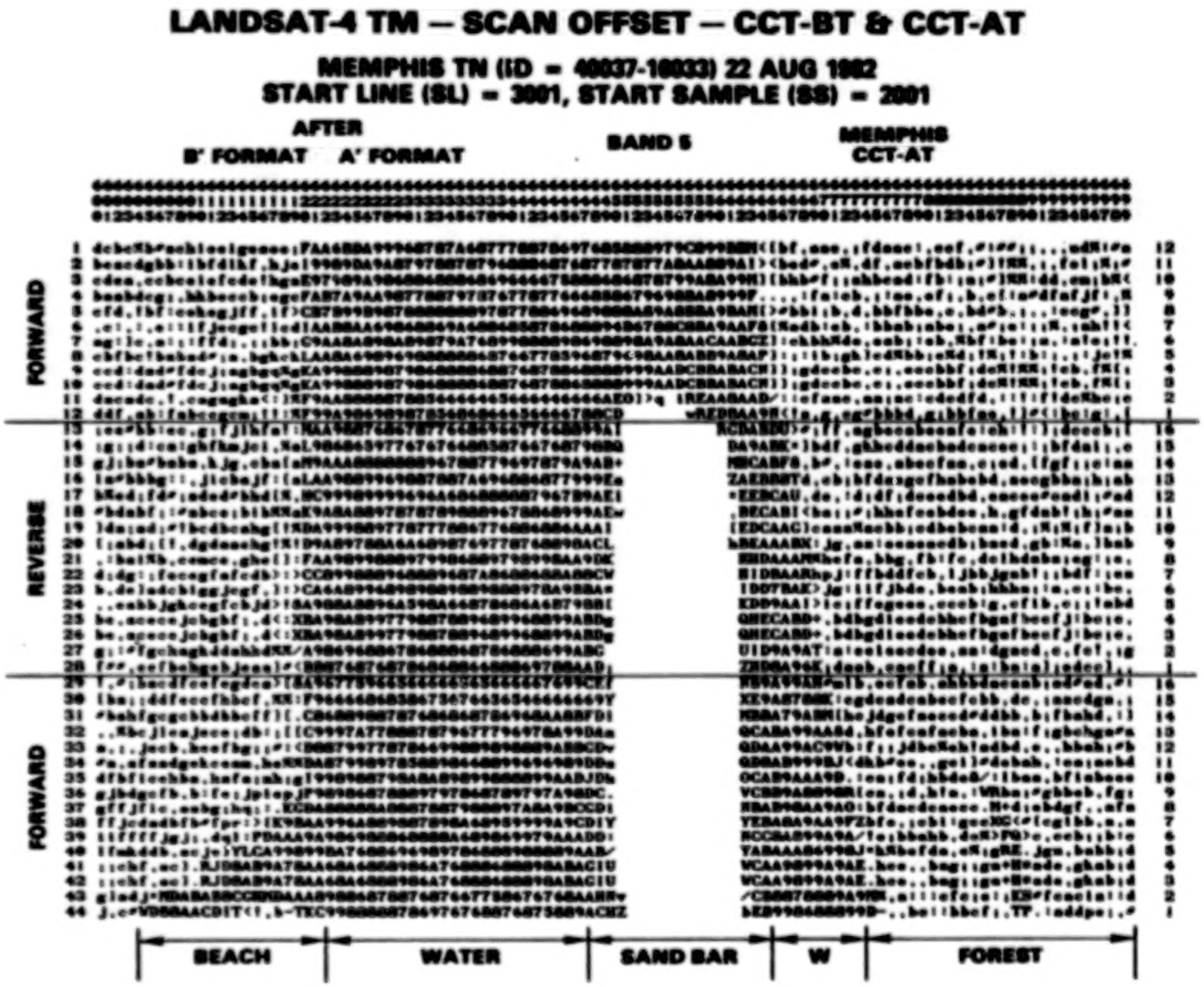
LANDSAT-4 TM — SCAN OFFSET — CCT-BT & CCT-AT
MEMPHIS TN (ID = 40037-16033) 22 AUG 1982
START LINE (SL) = 3001, START SAMPLE (SS) = 2001
AFTER
B' FORMAT
A' FORMAT
BAND 5
MEMPHIS
CCT-AT
FORWARD
REVERSE
FORWARD
BEACH
WATER
SAND BAR
W
FOREST

Figure 2-5. An example of a Band 5 image in A' format. The "after" image demonstrates the results of digital image processing to remove alignment offset and to produce an A' or B' format image. The area demonstrated is a 3.0 km wide by 1.32 km high portion of the Mississippi River near Memphis TN; DNs are represented by an alphanumeric code allowing evaluation of both gross and fine structure. Compare with Figure 2-4.

ORIGINAL PAGE IS
OF POOR QUALITY

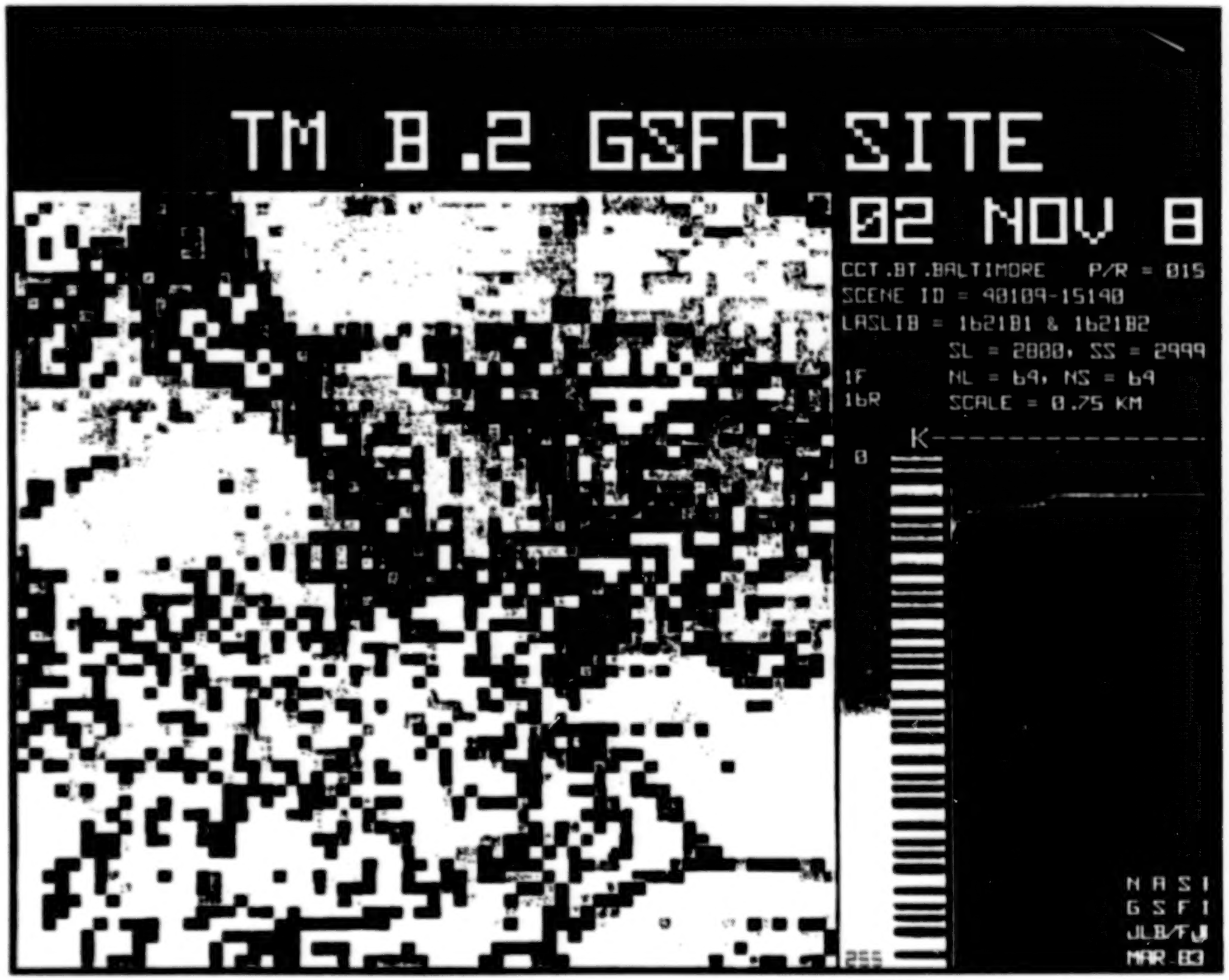
TM B.2 GSFC SITE
02 NOV 8
CCT.BT.BALTIMORE P/R = 015
SCENE ID = 40109-15140
LASLIB = 162181 & 162182
SL = 2800, SS = 2999
1F NL = 64, NS = 64
16R SCALE = 0.75 KM
K
0
255
N A S I
G S F I
JLB/FJ
MAR 83

Figure 2-6. An example of a Pseudocolor Pixel Print image for TM data in B' format. The sensor scans have been adjusted right and left to produce a nominally geometrically correct alignment. The area demonstrated is an image segment centered on NASA-GSFC. The ragged histogram is due to unequal bin size in the Analog-Digital (A-D) Converter in the sensor system.

LANDSAT-4 TM — CCT-AT — BAND 5 (UNBLOCKED)

WASHINGTON DC (ID = 40109-15140) 2 NOV 1982
BYTE NUMBERS

	SAMPLE LINE	61	62	63	64	65	66	67	68	69	70	71	72	73	74	75	76	77	78	79	80	81	82	83	84	85	CHANNEL (DETECTOR) NUMBER
FORWARD SCAN 1	1	100	110	119	115	110	92	78	86	78	53	63	82	94	90	77	50	56	58	58	57	71	68	65	54	54	16
	2	92	104	108	110	102	83	77	89	75	56	56	73	93	89	73	38	48	56	62	62	64	62	63	56	54	15
	3	97	109	111	109	100	79	79	82	81	65	58	68	92	83	61	46	42	47	61	61	66	60	61	57	69	14
	4	101	112	104	93	86	77	76	77	69	71	67	66	78	73	61	56	51	49	53	50	51	59	69	76	78	13
	5	74	78	76	72	70	76	86	84	82	76	73	70	76	78	68	65	57	57	54	61	65	72	73	90	102	12
	6	83	81	77	74	74	84	98	98	93	90	78	73	78	81	77	66	69	66	61	70	78	78	83	91	106	11
	7	77	77	73	72	78	86	92	90	87	87	77	68	79	83	77	53	64	70	61	69	74	81	78	79	97	10
	8	77	75	76	86	85	84	89	92	90	85	82	71	73	79	73	54	69	71	60	57	68	79	79	74	76	9
	9	84	86	93	94	95	95	93	91	91	91	84	74	73	78	70	54	61	66	66	55	58	73	76	82	82	8
	10	97	94	98	94	98	92	93	93	90	92	83	68	70	80	71	58	70	77	67	55	61	74	80	89	91	7
	11	82	83	77	73	74	73	72	71	68	68	67	66	62	74	74	60	70	72	62	57	59	69	83	91	87	6
	12	67	65	61	66	67	69	66	66	62	62	58	65	58	63	74	65	72	66	57	55	50	55	81	91	84	5
	13	67	66	66	74	70	67	67	68	66	64	58	57	61	66	62	62	72	66	64	54	46	46	77	88	84	4
	14	2	3	3	2	4	2	3	3	3	3	3	3	2	3	4	2	3	3	3	3	2	3	3	2	3	3 ←
	15	70	71	72	72	69	64	65	66	65	[illegible]	61	65	48	66	68	60	65	64	58	52	44	43	68	85	85	2
	16	76	70	72	74	70	60	67	69	65	63	67	73	66	63	70	68	70	60	57	47	30	38	42	66	70	1
REVERSE SCAN 2	17	94	93	82	70	68	61	66	62	53	56	54	63	63	68	69	73	74	75	76	78	72	68	69	78	86	16
	18	94	90	87	79	80	78	78	80	65	59	58	68	72	74	77	76	79	76	76	73	66	63	67	68	82	15
	19	91	90	90	82	77	74	79	78	64	57	57	69	73	80	83	85	88	83	76	74	70	70	70	72	87	14
	20	90	92	90	83	79	74	77	79	65	58	57	68	83	83	85	84	86	88	85	85	70	76	78	90	100	13
	21	94	93	91	87	81	77	77	79	66	61	64	70	85	84	82	82	77	77	74	82	90	94	102	105	110	12
	22	93	92	90	89	84	78	77	81	73	63	64	67	69	68	68	66	68	67	69	71	93	104	109	109	109	11
	23	85	84	86	85	84	76	73	81	74	63	63	65	65	64	64	62	64	64	65	66	86	101	105	104	104	10
	24	82	82	80	85	86	80	76	82	80	65	68	66	68	63	61	65	62	66	66	65	72	99	106	105	100	9
	25	67	76	83	84	88	82	78	79	79	66	67	66	68	65	66	66	69	72	70	73	76	93	99	94	90	8
	26	53	67	73	75	74	73	73	69	65	66	62	60	76	78	77	76	78	83	82	83	82	85	88	88	83	7
	27	57	66	62	59	61	59	60	61	59	57	58	59	74	74	74	70	78	75	76	77	76	78	82	85	89	6
	28	59	65	59	56	57	58	58	58	59	57	58	58	66	72	72	70	72	71	72	73	72	67	73	81	82	5
	29	61	68	76	73	73	77	75	76	80	80	79	76	74	62	57	58	59	60	61	59	61	59	62	76	73	4
	30	2	4	3	3	3	2	3	2	3	3	3	3	3	3	3	3	3	3	2	3	2	4	3	3	3	3 ←
	31	56	74	77	74	77	77	77	76	75	76	72	72	74	66	60	61	60	55	51	46	42	34	20	32	28	2
	32	33	73	80	74	60	61	34	37	73	74	[illegible]	64	58	53	31	30	34	49	34	20	24	27	26	43	37	1
FORWARD SCAN 3	33	70	69	78	95	100	104	101	98	100	100	100	98	87	78	65	78	72	65	51	48	30	41	37	59	75	16
	34	79	81	88	99	102	101	101	98	96	94	92	90	82	77	62	65	68	56	39	46	51	47	40	38	57	15
	35	89	88	89	96	95	96	93	92	90	93	93	89	85	72	39	67	68	59	47	43	44	41	32	56	55	14
	36	85	87	91	94	94	96	96	97	91	93	91	89	82	78	62	67	66	66	69	59	44	45	59	55	61	13
	37	69	75	76	78	77	82	90	96	92	90	82	78	83	88	68	72	71	75	73	62	60	70	68	68	60	12
	38	69	70	71	69	73	76	78	86	81	79	77	81	80	74	74	83	82	85	74	58	70	69	67	67	70	11
	39	68	74	80	78	81	74	75	85	84	82	71	81	75	66	68	70	70	73	59	52	65	67	70	70	73	10
	40	78	73	66	59	60	63	67	73	77	78	71	82	85	84	65	72	72	72	64	87	69	77	77	82	73	9
	41	87	85	79	77	68	63	61	58	54	66	60	61	62	82	67	67	72	67	60	50	59	57	52	70	74	8
	42	82	81	82	83	79	83	81	79	76	78	100	62	62	76	70	60	70	66	51	51	68	68	62	79	70	7
	43	74	76	76	78	75	77	73	78	78	82	89	78	66	73	68	61	68	62	47	49	64	71	74	78	67	6
	44	72	70	69	66	66	68	71	71	73	77	76	70	60	71	69	60	62	62	44	52	53	58	66	54	50	5
	45	85	87	91	87	82	72	36	60	64	68	66	68	66	71	67	64	59	64	61	46	46	62	55	56	58	4
	46	3	3	3	3	4	3	3	3	2	3	3	4	4	3	3	3	3	3	3	2	3	4	4	2	3	3 ←
	47	89	89	92	86	87	81	76	76	73	72	73	73	74	73	73	64	62	53	38	36	39	42	58	68	74	2

Figure 2-7. An example of data for TM band 5, showing the defective channel 3. The scan organization is the same shown in Figure 2-3.

ORIGINAL PAGE IS
OF POOR QUALITY

BAND 6
LANDSAT-4 TM — CCT-BT — INITIAL PORTION OF DATA MATRIX (UNBLOCKED)

WASHINGTON DC (ID = 40109-15140) 2 NOV 1982
BYTE NUMBERS

SAMPLE LINE	1	2	3	4	5	6	7	8	9	10	11	12	13	14	15	16	17	18	19	20	21	22	23	24	25	
1	0	0	0	237	1	0	1	0	30	0	117	117	117	117	116	116	116	116	117	117	117	117	118	118	118	4
2	0	0	0	237	1	0	1	0	22	0	114	114	114	114	114	114	114	114	116	116	116	116	116	116	116	3
3	0	0	0	237	1	0	1	0	14	0	117	117	117	117	119	119	119	119	118	118	118	118	117	117	117	2
4	0	0	0	237	1	0	1	0	6	0	115	115	115	115	116	116	116	116	115	115	115	115	114	114	114	1
5	0	0	0	237	1	0	2	0	158	0	118	118	118	118	117	117	117	117	117	117	117	117	118	118	118	4
6	0	0	0	237	1	0	2	0	150	0	116	116	116	116	114	114	114	114	114	114	114	114	115	115	115	3
7	0	0	0	237	1	0	2	0	142	0	119	119	119	119	118	118	118	118	119	119	119	119	119	119	119	2
8	0	0	0	237	1	0	2	0	134	0	116	116	116	116	115	115	115	115	115	115	115	115	116	116	116	1
9	0	0	0	237	1	0	3	0	30	0	118	118	118	118	118	118	118	118	118	118	118	118	118	118	118	4
10	0	0	0	237	1	0	3	0	22	0	115	115	115	115	114	114	114	114	115	115	115	115	114	114	114	3
11	0	0	0	237	1	0	3	0	14	0	118	118	118	118	117	117	117	117	117	117	117	117	118	118	118	2
12	0	0	0	237	1	0	3	0	6	0	114	114	114	114	114	114	114	114	116	116	116	116	116	116	116	1

SUPPORT DATA

IMAGE DATA (120m IFOV + 4)

Figure 2-8. An example of data and organization for TM band 6, in unblocked CCT-BT format. Note that raw 120m IFOV pixels from the sensor were repeated four (4) times along a line by the ADDS preprocessing to produce the B format image. Compare with Figures 2-3 and 2-16.

ORIGINAL PAGE IS
OF POOR QUALITY

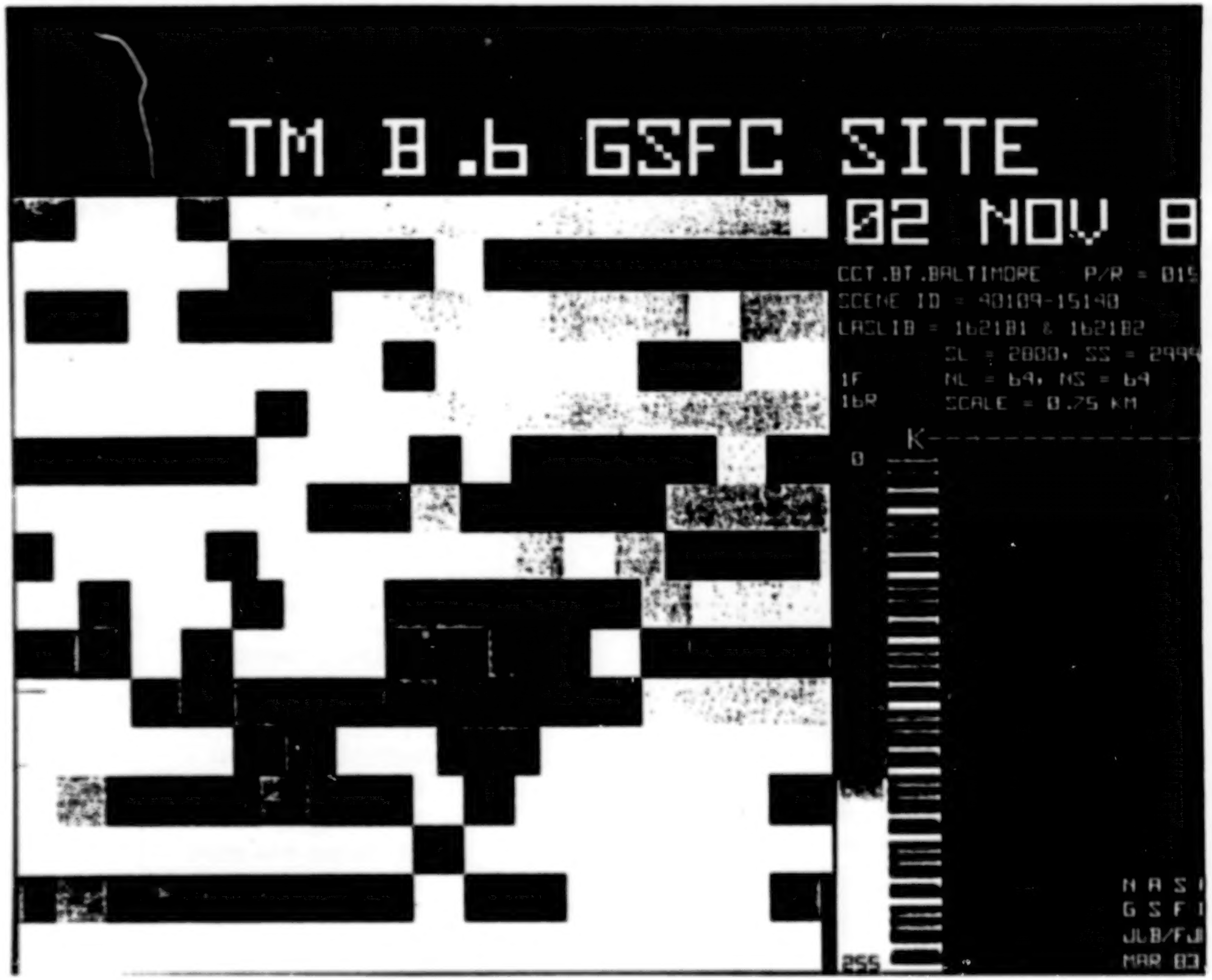
TM B.6 GSFC SITE
02 NOV 8
CCT.BT.BALTIMORE P/R = 015
SCENE ID = 40109-15140
LASLIB = 162181 & 162182
SL = 2800, SS = 299
1F NL = 64, NS = 64
16R SCALE = 0.75 KM
K
0
255
N A S
G S F
JLB/FJ
MAR 83

Figure 2-9. An Example of a Pseudocolor Pixel Print image for TM Band 6 in B' format. Compare with Figure 2-6; notice the 120 m IFOV pixel size. In the histogram, the unequal bin size resulting in a minimum between two modes is a result of the A-D converter in the sensor system.

LANDSAT-4 TM — DIGITAL TAPE CONTENTS — CCT-AT
(4X BLOCKING)

SCROUNGE-ERA (1982-1983)

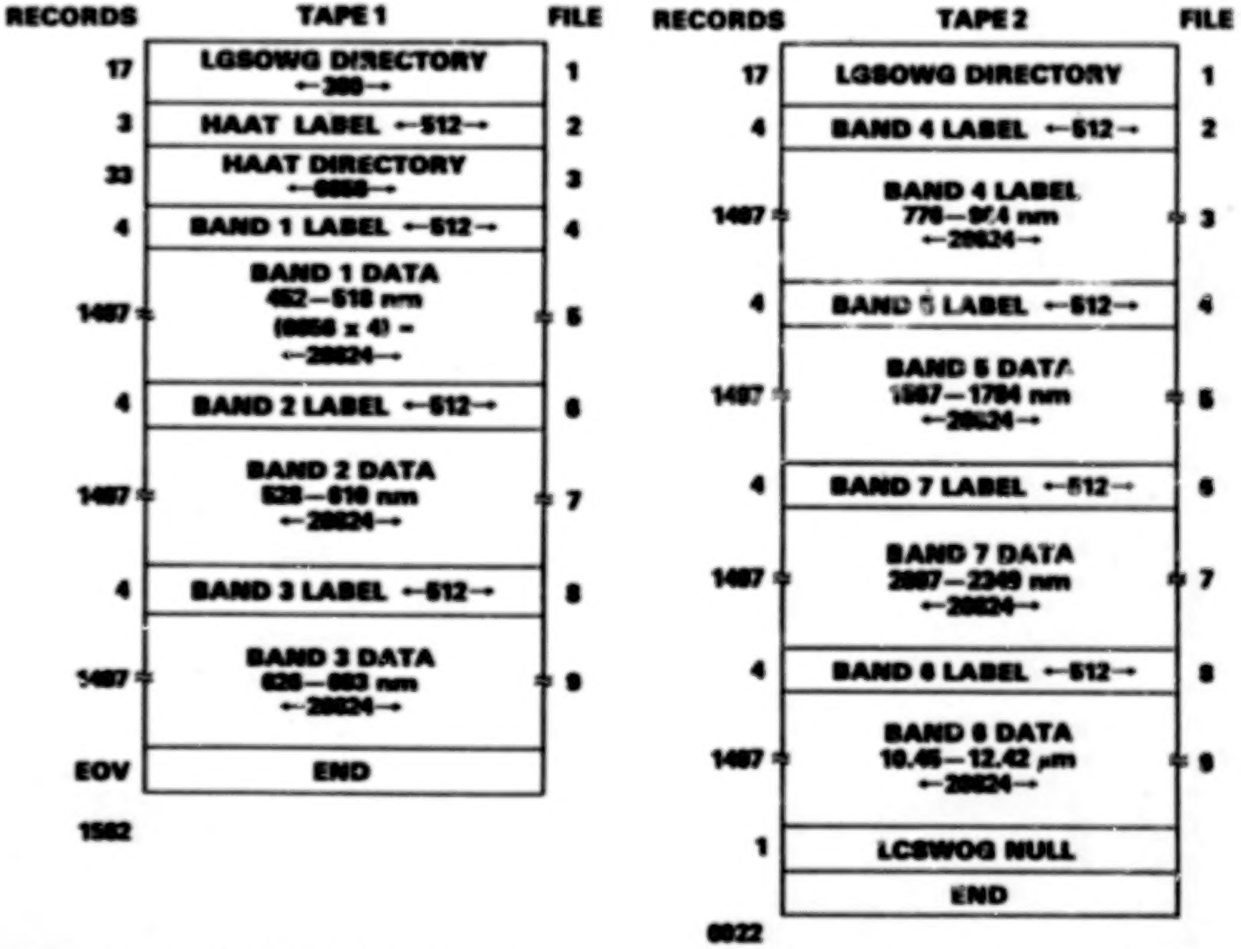
RECORDS
TAPE 1
FILE
17
LGSOWG DIRECTORY ←360→
1
3
HAAT LABEL ←512→
2
33
HAAT DIRECTORY ←6956→
3
4
BAND 1 LABEL ←512→
4
1497
BAND 1 DATA 452—518 nm (6956 x 4) = ←28624→
5
4
BAND 2 LABEL ←512→
6
1497
BAND 2 DATA 528—609 nm ←28624→
7
4
BAND 3 LABEL ←512→
8
1497
BAND 3 DATA 626—693 nm ←28624→
9
EOV
END
1582
RECORDS
TAPE 2
FILE
17
LGSOWG DIRECTORY
1
4
BAND 4 LABEL ←512→
2
1497
BAND 4 LABEL 776—904 nm ←28624→
3
4
BAND 5 LABEL ←512→
4
1497
BAND 5 DATA 1567—1784 nm ←28624→
5
4
BAND 7 LABEL ←512→
6
1497
BAND 7 DATA 2097—2349 nm ←28624→
7
4
BAND 6 LABEL ←512→
8
1497
BAND 6 DATA 10.45—12.42 μm ←28624→
9
1
LGSWOG NULL
END
6022

Figure 2-10. File organization of TM data and images on the two CCT-AT tapes used by LAS for data archive.

LANDSAT-4 TM CCT-AT IMAGE FILE CONTENTS

SCROUNGE ERA (1982—1983)

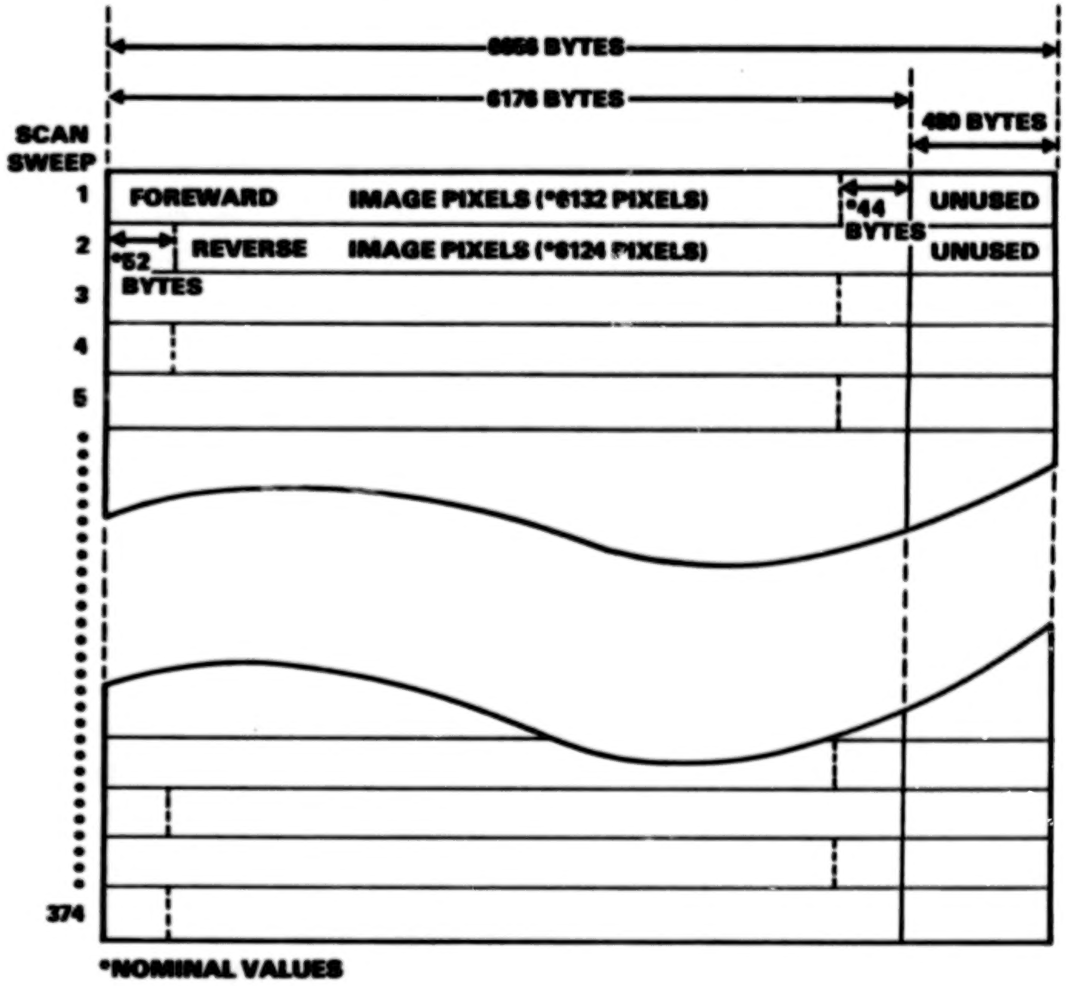
6656 BYTES
6176 BYTES
480 BYTES
SCAN SWEEP
1
2
3
4
5
374
FOREWARD
IMAGE PIXELS (*6132 PIXELS)
*44 BYTES
UNUSED
*52 BYTES
REVERSE
IMAGE PIXELS (*6124 PIXELS)
UNUSED
*NOMINAL VALUES

Figure 2-11. Image file contents for the CCT-AT.

LANDSAT-4 TM — CCT—AT — INITIAL PORTION OF DATA MATRIX (UNBLOCKED)

MEMPHIS TN (ID = 40037-16033) 22 AUG 1982
SCROUNGE ERA (1982-1983)

	SAMPLE LINE	1	2	3	4	5	6	7	8	9	10	11	12	13	14	15	16	17	18	19	20	21	22	23	24	25	CHANNEL NUMBER
HEADER	1	0	0	0	1	63	192	18	18	0	0	104	0	65	32	32	32	67	67	66	45	67	67	84	45	48	
	2	32	32	32	32	32	32	32	32	32	32	32	32	32	32	32	32	32	32	32	32	32	32	32	32	32	
	3	32	32	32	32	32	32	32	32	32	32	32	32	32	32	32	32	32	32	32	32	32	32	32	32	32	
	4	32	32	32	32	32	32	32	32	32	32	32	32	32	32	32	32	32	32	32	32	32	32	32	32	32	
IMAGE DATA	5	96	87	86	88	77	77	75	75	74	74	75	71	69	67	70	71	71	65	61	62	61	55	55	57	59	16
	6	91	85	84	87	74	72	71	70	70	72	71	71	68	64	67	68	72	66	64	66	66	60	60	60	57	15
	7	88	89	82	88	79	74	71	69	73	75	75	76	76	72	77	72	67	66	65	67	71	67	62	57	58	14
	8	90	105	86	88	89	83	83	74	78	80	79	79	79	74	75	77	71	67	66	65	67	67	68	69	67	13
	9	79	84	87	100	100	97	100	89	82	80	74	75	74	76	75	77	74	70	68	70	76	84	90	90	90	12
	10	76	87	85	87	95	94	90	84	84	86	81	74	70	72	72	75	74	85	92	89	88	87	90	89	90	11
	11	79	97	93	88	85	81	85	84	85	84	84	80	77	75	75	75	77	89	88	88	88	89	88	91	87	10
	12	76	88	99	93	92	86	84	84	85	84	83	84	80	79	79	76	78	86	89	90	90	92	90	88	88	9
	13	76	83	93	101	95	89	86	85	84	86	81	85	83	81	79	80	82	79	86	86	91	91	89	90	96	8
	14	73	77	99	118	95	86	87	87	85	85	84	83	83	79	81	80	80	82	86	87	87	90	90	99	110	7
	15	72	76	95	127	105	86	84	85	85	80	84	78	78	81	84	81	80	82	88	91	88	91	89	93	96	6
	16	71	77	86	114	94	86	76	78	78	82	78	78	79	80	80	82	83	83	94	92	89	90	89	93	95	5
	17	72	77	80	103	101	86	78	78	83	80	78	80	76	81	82	80	83	83	96	96	88	90	89	89	96	4
	18	72	77	80	103	101	86	78	78	83	80	78	80	76	81	82	80	83	83	96	96	88	90	89	89	96	3
	19	70	71	78	99	102	77	76	81	87	84	83	80	77	78	78	79	78	81	81	89	90	90	89	91	90	2
	20	71	70	75	88	104	82	84	82	87	85	84	84	83	80	80	80	79	80	80	87	92	90	90	92	92	1

Figure 2-12. An example of data and ogranization for TM images in CCT-AT format, as unblocked when written to a copy tape or a disk file. The three lines of "32" values represent blanks padding the internal header record before the data is unblocked.

LANDSAT-4 TM — CCT-AT—NOMINAL CALIBRATION — BAND 4

MEMPHIS TN (ID = 40037-16033) 22 AUG 1982
START LINE (SL) = 3001, START SAMPLE (SS) = 2001
SCROUNGE ERA (1982-1983)

SWEEP	SAMPLE LINE	641	642	643	644	645	646	647	648	649	650	651	652	653	654	655	656	657	658	659	660	661	662	663	664	665	
FORWARD	13	29	29	29	29	28	29	29	30	31	49	88	89	90	92	91	89	87	75	47	30	30	30	29	30	39	16
	14	28	29	28	28	28	29	28	29	30	57	89	89	90	92	92	89	90	88	81	43	28	30	28	29	32	15
	15	28	29	29	29	29	29	30	30	34	68	89	91	93	93	93	93	92	90	85	50	30	31	28	29	30	14
	16	29	29	30	28	29	30	29	30	35	74	89	91	92	93	93	92	92	92	88	59	30	32	30	30	30	13
	17	29	28	28	28	30	29	30	30	38	80	92	93	93	94	93	93	93	92	88	63	27	30	29	30	29	12
	18	28	29	29	28	29	29	30	30	43	83	89	90	93	93	93	93	93	93	90	64	30	31	30	30	28	11
	19	29	29	29	29	29	29	29	31	48	88	90	93	93	93	92	93	92	92	90	64	29	29	29	28	29	10
	20	28	29	28	29	29	30	29	30	52	87	89	92	92	92	93	91	92	92	88	68	30	30	29	28	28	9
	21	29	28	29	28	28	30	30	31	54	94	90	94	94	94	94	92	91	94	94	76	28	28	27	28	29	8
	22	29	30	29	29	29	30	30	32	63	91	91	92	92	92	93	93	93	92	92	82	35	30	30	29	29	7
	23	30	29	30	30	29	30	30	34	71	93	93	93	93	93	94	94	93	93	92	85	37	27	30	28	29	6
	24	28	29	29	28	29	29	29	34	72	92	93	93	93	94	94	94	94	93	92	88	44	28	29	28	28	5
	25	28	28	28	28	29	30	30	36	78	93	93	94	93	95	94	95	95	94	93	87	48	25	28	28	28	4
	26	28	29	28	28	29	29	29	39	82	91	92	93	93	93	94	93	95	93	91	87	50	26	29	29	29	3
	27	29	28	29	29	29	30	30	39	85	95	93	93	94	94	94	94	94	95	93	89	49	24	27	28	29	2
	28	29	29	29	29	30	30	30	37	78	92	92	93	93	93	94	95	95	95	93	90	45	27	30	29	29	1
REVERSE	29	75	72	78	83	76	68	73	71	68	75	73	77	77	73	73	78	80	77	77	77	84	78	72	89	53	16
	30	80	76	80	78	66	67	73	72	75	79	74	78	79	75	75	76	85	79	76	75	75	73	73	93	56	15
	31	78	74	77	68	71	70	71	77	85	78	77	76	78	74	75	80	81	79	78	79	78	81	77	89	53	14
	32	76	76	72	69	74	75	74	77	79	80	94	84	74	78	79	83	78	76	76	81	72	78	71	91	51	13
	33	75	71	71	68	80	83	78	77	84	88	83	78	76	76	78	81	76	71	78	84	77	88	81	89	51	12
	34	71	72	70	73	76	86	76	78	81	80	77	76	86	76	78	80	77	73	84	86	81	91	78	88	54	11
	35	75	71	74	73	79	86	85	84	88	85	76	86	85	74	70	76	78	78	80	78	86	100	89	90	66	10
	36	71	75	73	84	88	94	87	84	80	77	77	80	76	77	71	77	82	78	84	104	97	89	75	60	54	9
	37	79	77	73	79	86	83	84	85	81	80	82	72	76	78	74	77	86	84	104	99	85	83	48	31	30	8
	38	74	77	80	73	82	79	83	80	79	75	77	78	80	80	71	80	96	105	95	80	82	46	31	29	28	7
	39	73	78	79	81	87	83	81	85	79	83	77	79	83	86	72	82	93	108	94	67	38	30	29	28	28	6
	40	79	73	76	84	91	82	86	90	84	75	77	73	80	80	88	93	73	62	44	31	29	29	28	29	28	5
	41	80	83	86	84	73	71	74	81	80	79	78	83	82	70	55	36	32	30	29	30	28	28	30	28	28	4
	42	75	79	75	70	73	82	76	74	79	91	85	72	44	31	30	29	28	27	29	29	29	29	29	29	28	3
	43	72	79	80	79	80	69	76	89	93	84	48	34	30	29	28	28	28	28	33	43	43	43	34	30	29	2
	44	70	79	83	77	80	66	83	81	69	39	29	28	28	28	29	32	33	47	63	81	75	72	65	53	42	1
FORWARD	45	29	30	30	29	30	29	29	29	30	30	31	43	85	93	93	93	93	95	93	92	95	92	78	33	29	16
	46	28	29	28	28	29	28	29	29	29	29	30	35	71	94	92	93	94	93	93	93	93	92	82	37	29	15
	47	28	30	29	29	30	29	29	29	30	30	30	32	59	92	92	93	94	94	94	93	93	93	86	43	30	14
	48	29	29	29	30	30	28	30	30	29	30	30	30	48	89	92	93	95	94	92	92	93	92	88	50	30	13
	49	30	29	28	29	29	28	29	29	29	30	30	30	41	85	94	94	94	93	92	92	92	91	90	56	27	12
	50	28	30	29	30	29	28	28	29	29	29	29	29	34	71	92	92	93	94	93	91	93	93	92	68	31	11
	51	29	29	29	29	29	29	29	29	29	29	29	30	32	58	92	93	94	94	93	91	91	92	90	77	33	10
	52	29	29	28	28	28	28	28	28	29	29	29	29	30	43	85	92	93	93	92	92	90	90	92	83	37	9
	53	29	30	30	29	29	30	29	29	30	28	29	30	30	33	69	96	92	95	94	91	92	92	91	88	47	8
	54	28	30	29	29	29	29	28	29	29	29	30	30	29	31	54	91	93	92	92	92	91	93	93	92	60	7
	55	29	30	30	29	29	29	28	29	29	29	29	30	30	31	39	80	94	94	94	92	92	92	93	93	75	6
	56	29	30	29	28	29	28	28	28	28	28	29	29	29	30	32	62	92	93	94	93	93	93	93	93	86	5
	57	28	29	29	28	29	29	28	29	29	28	28	30	28	30	31	39	80	97	94	93	93	94	93	93	91	4
	58	28	29	28	28	28	28	27	28	29	28	29	29	28	29	29	33	60	92	92	92	93	92	92	92	92	3
	59	29	30	29	28	30	28	28	29	29	28	28	29	29	29	30	31	44	86	96	94	94	93	93	94	93	2

Figure 2-13. An example of TM data in CCT-AT format, unblocked. Note the changes in DNs between forward and reverse scans. Compare with Figures 2-14 to 2-16 to see the same pattern in other multispectral bands for this same image segment.

LANDSAT-4 TM — CCT-AT — NOMINAL CALIBRATION — BAND 2

MEMPHIS TN (ID = 40037-16033) 22 AUG 1982
START LINE (SL) = 3001, START SAMPLE (SS) = 2001
SCROUNGE ERA (1982-1983)

SWEEP	SAMPLE LINE	641	642	643	644	645	646	647	648	649	650	651	652	653	654	655	656	657	658	659	660	661	662	663	664	665	CHANNEL
FORWARD	13	38	38	38	38	38	39	39	39	39	49	71	71	72	72	72	70	68	61	44	38	39	37	37	37	33	16
	14	38	38	38	38	38	38	39	39	40	53	72	72	74	74	73	72	73	70	66	46	38	40	38	37	35	15
	15	39	39	39	38	39	39	39	39	42	60	76	75	74	75	74	75	74	72	67	49	38	39	38	37	36	14
	16	39	38	39	39	39	39	39	39	43	63	76	75	74	76	76	75	74	72	71	55	38	40	39	38	37	13
	17	38	38	38	39	38	38	39	39	43	66	72	75	74	75	73	74	74	72	71	56	38	38	37	38	35	12
	18	38	38	38	38	38	39	38	39	45	67	72	72	75	74	74	73	75	74	72	58	38	39	39	37	38	11
	19	38	38	39	39	38	39	41	41	51	73	74	75	76	75	74	75	75	73	72	58	37	39	38	37	37	10
	20	39	39	39	39	39	39	39	41	51	72	74	74	74	73	74	74	74	74	71	60	40	39	39	38	38	9
	21	39	39	39	39	39	39	39	41	55	72	73	75	76	75	73	75	75	75	72	64	40	40	39	38	37	8
	22	38	37	37	37	38	38	38	41	56	73	72	73	74	72	73	73	73	71	71	69	42	37	40	37	37	7
	23	38	39	38	38	39	38	41	42	61	72	74	74	73	74	74	74	74	74	72	67	45	39	38	38	37	6
	24	38	38	38	39	39	39	39	41	61	73	73	73	74	74	74	73	74	73	72	70	50	37	39	39	38	5 ←
	25	38	38	38	39	39	39	39	41	61	73	73	73	74	74	74	73	74	73	72	70	50	37	39	39	38	4
	26	39	39	39	39	39	39	39	45	67	72	73	72	74	74	73	74	75	73	73	70	50	36	39	39	36	3
	27	39	38	41	38	40	41	42	42	60	69	72	75	74	75	77	76	75	75	74	75	61	46	41	42	39	2
	28	40	39	39	40	40	39	41	43	66	75	74	75	76	76	77	77	77	77	76	74	52	39	42	40	39	1
REVERSE	29	27	27	28	28	27	27	27	27	27	28	28	28	28	28	27	28	28	29	28	28	29	31	30	30	38	16
	30	27	27	26	27	27	26	27	27	27	27	27	27	28	27	28	27	29	29	28	28	29	29	29	30	38	15
	31	28	29	28	27	27	27	28	28	30	28	28	28	28	28	28	29	30	28	29	29	30	32	31	31	39	14
	32	27	30	27	27	27	27	27	28	30	30	31	28	28	28	28	28	28	28	28	30	30	31	31	31	38	13
	33	28	28	27	27	27	27	27	27	27	28	28	27	27	28	28	29	28	28	29	30	28	30	30	32	38	12
	34	27	28	27	27	27	28	28	27	28	29	28	28	29	28	28	30	30	28	30	30	28	30	30	31	38	11
	35	28	28	28	28	27	28	28	28	30	28	28	28	28	29	27	28	29	30	30	28	29	31	32	31	41	10
	36	27	28	28	27	28	30	30	28	28	28	28	29	30	28	28	28	30	28	28	31	31	31	35	42	43	9
	37	28	28	28	28	28	30	29	29	29	30	30	28	28	28	28	29	30	29	30	33	30	34	40	45	45	8
	38	26	27	27	27	27	28	28	27	28	27	27	27	28	28	27	28	29	31	30	27	34	43	45	46	46	7
	39	27	28	29	27	28	30	29	28	27	29	27	29	28	29	27	29	30	33	33	37	43	47	45	46	47	6
	40	28	27	27	29	29	30	29	30	29	29	28	28	29	29	30	33	35	38	42	45	45	45	42	41	44	5 ←
	41	28	27	27	29	29	30	29	30	29	29	28	28	29	29	30	33	35	38	42	45	45	45	42	41	44	4
	42	27	27	27	28	27	28	27	27	28	29	29	35	42	44	45	45	44	44	46	45	46	43	41	39	40	3
	43	28	30	28	30	28	29	30	31	33	39	39	43	46	46	45	46	43	44	40	39	40	41	39	39	40	2
	44	27	27	29	28	30	29	30	30	33	42	45	45	45	45	45	42	38	34	31	30	33	34	35	38	41	1
FORWARD	45	38	39	37	39	39	38	39	39	39	39	42	46	71	75	76	76	76	78	76	76	75	72	66	42	39	16
	46	39	38	38	39	40	39	41	39	39	41	41	42	61	75	74	75	77	77	76	75	75	74	70	45	40	15
	47	39	39	39	39	39	39	40	40	39	39	42	42	58	76	75	77	77	79	78	76	75	75	71	47	39	14
	48	39	39	39	39	39	39	39	39	39	41	40	41	50	75	76	76	79	79	77	78	76	76	74	52	40	13
	49	38	38	39	39	39	39	39	38	39	40	40	40	46	70	75	75	76	77	76	77	75	74	72	54	38	12
	50	39	39	39	38	39	38	39	38	39	39	41	39	42	62	76	76	76	76	77	76	75	73	74	62	39	11
	51	38	38	39	39	39	38	39	39	39	41	42	41	41	56	77	77	77	78	79	76	75	74	75	66	42	10
	52	39	39	39	39	39	39	39	39	39	40	40	40	40	47	72	77	75	77	78	77	75	73	74	71	46	9
	53	38	39	39	39	39	39	39	39	38	39	39	40	40	43	63	78	76	77	78	77	76	75	75	72	50	8
	54	37	38	38	38	38	40	37	38	38	38	38	40	40	42	52	75	75	75	75	74	74	74	72	74	58	7
	55	39	38	38	38	38	38	38	38	39	39	40	40	40	41	45	67	77	77	76	76	75	75	75	74	65	6
	56	38	39	39	38	37	38	39	38	38	40	40	39	40	41	40	54	77	76	76	76	75	74	73	75	72	5 ←
	57	38	39	39	38	37	38	39	38	38	40	40	39	40	41	40	54	77	76	76	76	75	74	73	75	72	4
	58	40	38	39	39	39	38	38	39	40	39	39	39	39	39	41	41	55	76	75	76	74	75	74	75	73	3
	59	39	40	38	38	38	40	39	40	39	38	39	40	38	41	40	41	45	63	70	72	77	75	76	77	75	2

Figure 2-14. An example of TM data for spectral band 2 in CCT-AT format, unblocked. Note the duplication of DNs for channel 5 to replace defective data in channel 4. Note also the difference in DNs between forward and reverse scans resulting from the scan offset.

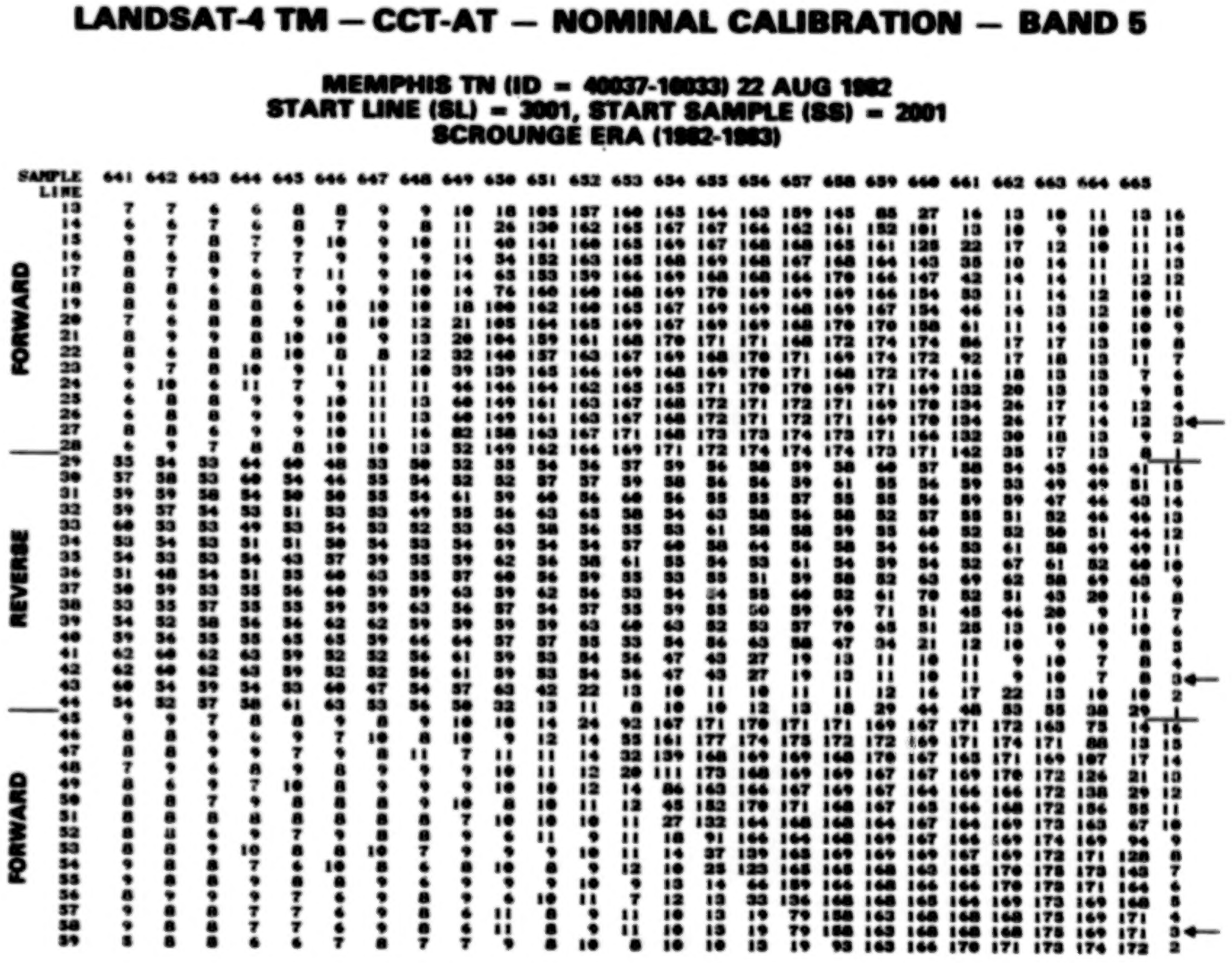

LANDSAT-4 TM — CCT-AT — NOMINAL CALIBRATION — BAND 5

MEMPHIS TN (ID = 40037-16033) 22 AUG 1982
START LINE (SL) = 3001, START SAMPLE (SS) = 2001
SCROUNGE ERA (1982-1983)

	SAMPLE LINE	641	642	643	644	645	646	647	648	649	650	651	652	653	654	655	656	657	658	659	660	661	662	663	664	665	
FORWARD	13	7	7	6	6	8	8	9	9	10	18	105	157	160	165	164	163	159	145	85	27	16	13	10	11	13	16
	14	6	6	7	6	8	7	9	8	11	26	130	162	165	167	167	166	162	161	152	101	13	10	9	10	11	15
	15	9	7	8	7	9	10	9	10	11	40	141	160	165	169	167	168	168	165	161	128	22	17	12	10	11	14
	16	8	6	8	7	7	9	9	9	14	34	152	163	165	168	169	168	167	168	164	143	35	10	14	11	11	13
	17	8	7	9	6	7	11	9	10	14	65	153	159	166	169	168	168	166	170	166	147	42	14	14	11	12	12
	18	8	8	6	8	9	9	9	10	14	76	160	160	168	169	170	169	169	169	166	154	53	11	14	12	10	11
	19	8	6	8	8	6	10	10	10	18	100	162	160	165	167	169	169	168	169	167	154	46	14	13	12	10	10
	20	7	6	8	8	9	8	10	12	21	105	164	165	169	167	169	169	168	170	170	158	61	11	14	10	10	9
	21	8	9	9	8	10	10	9	13	20	104	159	161	168	170	171	171	168	172	174	174	86	17	17	13	10	8
	22	8	6	8	8	10	8	8	12	32	140	157	163	167	169	168	170	171	169	174	172	92	17	18	13	11	7
	23	9	7	8	10	9	11	11	10	39	139	165	166	169	168	169	170	171	168	172	174	116	18	13	13	7	6
	24	6	10	6	11	7	9	11	11	46	146	164	162	165	165	171	170	170	169	171	169	132	20	13	13	9	5
	25	6	8	8	9	9	10	11	13	60	149	161	163	167	168	172	171	172	171	169	170	134	26	17	14	12	4
	26	6	8	8	9	9	10	11	13	60	149	161	163	167	168	172	171	172	171	169	170	134	26	17	14	12	3
	27	8	8	6	9	9	10	11	16	82	158	163	167	171	168	173	173	174	173	171	166	132	30	18	13	9	2
	28	6	9	7	8	8	10	10	13	52	149	162	166	169	171	172	174	174	174	173	171	142	35	17	13	8	1
REVERSE	29	55	54	53	64	60	48	53	50	52	55	56	56	57	59	56	58	59	58	60	57	58	54	45	46	41	16
	30	57	58	53	60	54	46	55	54	52	52	57	57	59	58	56	56	39	61	55	56	59	53	49	49	51	15
	31	59	59	58	54	50	50	55	54	61	59	60	56	60	56	55	55	57	55	55	56	59	59	47	46	43	14
	32	59	57	54	53	51	53	53	49	55	56	63	65	58	54	63	58	56	58	52	57	55	51	52	46	46	13
	33	60	53	53	49	53	54	53	52	53	63	58	56	55	53	61	58	58	59	55	60	52	52	50	51	44	12
	34	53	54	53	51	51	50	54	53	54	59	54	54	57	60	58	64	56	58	54	66	53	61	58	49	49	11
	35	54	53	53	54	43	57	59	55	59	62	56	58	61	55	54	53	61	54	59	54	52	67	61	52	60	10
	36	51	48	54	51	55	60	63	55	57	60	56	59	55	53	55	51	59	58	52	63	69	62	58	69	65	9
	37	50	59	53	55	56	60	59	59	63	59	62	56	53	54	54	55	60	52	61	70	52	51	43	20	16	8
	38	53	55	57	55	55	59	59	63	56	57	54	57	55	59	55	50	59	69	71	51	45	46	20	9	11	7
	39	54	52	58	56	56	62	62	59	59	59	59	63	60	63	52	53	57	70	65	51	25	13	10	10	10	6
	40	59	56	55	55	65	65	59	66	64	57	57	55	33	54	56	63	58	47	34	21	12	10	9	9	8	5
	41	62	60	62	63	59	52	52	56	61	59	53	54	56	47	43	27	19	13	11	10	11	9	10	7	8	4
	42	62	60	62	63	59	52	52	56	61	59	53	54	56	47	43	27	19	13	11	10	11	9	10	7	8	3
	43	60	54	59	54	53	60	47	54	57	63	42	22	13	10	11	10	11	11	12	16	17	22	13	10	10	2
	44	54	52	57	58	61	63	53	56	50	32	13	11	8	10	10	12	13	18	29	44	48	53	55	38	29	1
FORWARD	45	9	9	7	8	8	9	8	9	10	10	14	24	92	167	171	170	171	171	169	167	171	172	163	75	14	16
	46	8	8	9	6	9	7	10	8	10	9	12	14	55	161	177	174	175	172	172	169	171	174	171	88	13	15
	47	8	8	9	9	7	9	8	11	7	11	11	14	32	139	168	169	169	168	170	167	165	171	169	107	17	14
	48	7	9	6	8	9	8	9	9	9	10	11	12	20	111	173	168	169	169	167	167	169	170	172	126	21	13
	49	8	6	9	7	10	8	9	9	9	10	10	12	14	86	163	166	167	169	167	164	166	166	172	138	29	12
	50	8	8	7	9	8	8	8	9	10	8	10	11	12	45	152	170	171	168	167	165	166	168	172	156	55	11
	51	8	8	8	8	8	8	8	8	7	10	10	10	11	27	132	164	168	168	164	167	164	169	173	163	67	10
	52	8	8	6	9	7	9	8	8	9	6	11	9	11	18	91	166	164	168	169	167	166	169	174	169	94	9
	53	8	8	9	10	8	8	10	7	9	9	9	10	11	14	37	139	165	169	169	169	167	169	172	171	128	8
	54	9	8	8	7	6	10	8	6	8	10	8	9	12	10	25	123	165	165	168	162	165	170	175	173	143	7
	55	9	8	8	9	8	8	9	6	9	9	9	10	9	13	14	66	159	166	168	166	166	170	175	171	164	6
	56	8	9	9	9	7	6	9	8	9	6	10	11	7	12	13	33	136	168	168	165	164	169	173	169	160	5
	57	9	8	8	7	7	6	9	8	6	11	8	9	11	10	13	19	79	158	163	168	168	168	175	169	171	4
	58	9	8	8	7	7	6	9	8	6	11	8	9	11	10	13	19	79	158	163	168	168	168	175	169	171	3
	59	5	8	8	6	6	7	8	7	7	9	8	10	8	10	10	13	19	93	163	166	170	171	173	174	172	2

Figure 2-15. An example of TM data for spectral band 5 in CCT-AT format, unblocked. Note the duplication of DNs for channel 4 to replace defective data in channel 3. Note also the difference in DNs between forward and reverse scans resulting from the scan offset.

LANDSAT-4 TM — CCT-AT — NOMINAL CALIBRATION — BAND 6

MEMPHIS TN (ID = 40037-16033) 22 AUG 1982
START LINE (SL) = 3001, START SAMPLE (SS) = 2001
SCROUNGE ERA (1982-1983)

SWEEP	SAMPLE LINE	641	642	643	644	645	646	647	648	649	650	651	652	653	654	655	656	657	658	659	660	661	662	663	664	665	CHANNEL
FORWARD	13	135	135	135	135	136	136	136	136	137	137	137	137	157	157	157	157	166	166	166	166	155	155	155	155	137	4
	14	135	135	135	135	136	136	136	136	137	137	137	137	157	157	157	157	166	166	166	166	155	155	155	155	137	
	15	135	135	135	135	136	136	136	136	137	137	137	137	157	157	157	157	166	166	166	166	155	155	155	155	137	
	16	135	135	135	135	136	136	136	136	137	137	137	137	157	157	157	157	166	166	166	166	155	155	155	155	137	
	17	134	134	134	134	135	135	135	135	138	138	138	138	159	159	159	159	168	168	168	168	159	159	159	159	137	3
	18	134	134	134	134	135	135	135	135	138	138	138	138	159	159	159	159	168	168	168	168	159	159	159	159	137	
	19	134	134	134	134	135	135	135	135	138	138	138	138	159	159	159	159	168	168	168	168	159	159	159	159	137	
	20	134	134	134	134	135	135	135	135	138	138	138	138	159	159	159	159	168	168	168	168	159	159	159	159	137	
	21	136	136	136	136	136	136	136	136	140	140	140	140	163	163	163	163	168	168	168	168	161	161	161	161	139	2
	22	136	136	136	136	136	136	136	136	140	140	140	140	163	163	163	163	168	168	168	168	161	161	161	161	139	
	23	136	136	136	136	136	136	136	136	140	140	140	140	163	163	163	163	168	168	168	168	161	161	161	161	139	
	24	136	136	136	136	136	136	136	136	140	140	140	140	163	163	163	163	168	168	168	168	161	161	161	161	139	
	25	134	134	134	134	134	134	134	134	140	140	140	140	162	162	162	162	168	168	168	168	164	164	164	164	141	1
	26	134	134	134	134	134	134	134	134	140	140	140	140	162	162	162	162	168	168	168	168	164	164	164	164	141	
	27	134	134	134	134	134	134	134	134	140	140	140	140	162	162	162	162	168	168	168	168	164	164	164	164	141	
	28	134	134	134	134	134	134	134	134	140	140	140	140	162	162	162	162	168	168	168	168	164	164	164	164	141	
REVERSE	29	136	136	136	136	136	136	136	136	136	136	136	136	137	137	137	137	136	136	136	136	136	136	136	136	136	4
	30	136	136	136	136	136	136	136	136	136	136	136	136	137	137	137	137	136	136	136	136	136	136	136	136	136	
	31	136	136	136	136	136	136	136	136	136	136	136	136	137	137	137	137	136	136	136	136	136	136	136	136	136	
	32	136	136	136	136	136	136	136	136	136	136	136	136	137	137	137	137	136	136	136	136	136	136	136	136	136	
	33	135	135	135	135	135	135	135	135	135	135	135	135	136	136	136	136	136	136	136	136	136	136	136	136	135	3
	34	135	135	135	135	135	135	135	135	135	135	135	135	136	136	136	136	136	136	136	136	136	136	136	136	135	
	35	135	135	135	135	135	135	135	135	135	135	135	135	136	136	136	136	136	136	136	136	136	136	136	136	135	
	36	135	135	135	135	135	135	135	135	135	135	135	135	136	136	136	136	136	136	136	136	136	136	136	136	135	
	37	137	137	137	137	137	137	137	137	136	136	136	136	136	136	136	136	136	136	136	136	136	136	136	136	135	2
	38	137	137	137	137	137	137	137	137	136	136	136	136	136	136	136	136	136	136	136	136	136	136	136	136	135	
	39	137	137	137	137	137	137	137	137	136	136	136	136	136	136	136	136	136	136	136	136	136	136	136	136	135	
	40	137	137	137	137	137	137	137	137	136	136	136	136	136	136	136	136	136	136	136	136	136	136	136	136	135	
	41	136	136	136	136	136	136	136	136	137	137	137	137	136	136	136	136	135	135	135	135	135	135	135	135	134	1
	42	136	136	136	136	136	136	136	136	137	137	137	137	136	136	136	136	135	135	135	135	135	135	135	135	134	
	43	136	136	136	136	136	136	136	136	137	137	137	137	136	136	136	136	135	135	135	135	135	135	135	135	134	
	44	136	136	136	136	136	136	136	136	137	137	137	137	136	136	136	136	135	135	135	135	135	135	135	135	134	
FORWARD	45	136	136	136	136	136	136	136	136	136	136	136	136	140	140	140	140	161	161	161	161	166	166	166	166	155	4
	46	136	136	136	136	136	136	136	136	136	136	136	136	140	140	140	140	161	161	161	161	166	166	166	166	155	
	47	136	136	136	136	136	136	136	136	136	136	136	136	140	140	140	140	161	161	161	161	166	166	166	166	155	
	48	136	136	136	136	136	136	136	136	136	136	136	136	140	140	140	140	161	161	161	161	166	166	166	166	155	
	49	134	134	134	134	135	135	135	135	135	135	135	135	137	137	137	137	154	154	154	154	166	166	166	166	160	3
	50	134	134	134	134	135	135	135	135	135	135	135	135	137	137	137	137	154	154	154	154	166	166	166	166	160	
	51	134	134	134	134	135	135	135	135	135	135	135	135	137	137	137	137	154	154	154	154	166	166	166	166	160	
	52	134	134	134	134	135	135	135	135	135	135	135	135	137	137	137	137	154	154	154	154	166	166	166	166	160	
	53	135	135	135	135	136	136	136	136	136	136	136	136	137	137	137	137	147	147	147	147	166	166	166	166	163	2
	54	135	135	135	135	136	136	136	136	136	136	136	136	137	137	137	137	147	147	147	147	166	166	166	166	163	
	55	135	135	135	135	136	136	136	136	136	136	136	136	137	137	137	137	147	147	147	147	166	166	166	166	163	
	56	135	135	135	135	136	136	136	136	136	136	136	136	137	137	137	137	147	147	147	147	166	166	166	166	163	
	57	134	134	134	134	134	134	134	134	135	135	135	135	135	135	135	135	138	138	138	138	158	158	158	158	165	1
	58	134	134	134	134	134	134	134	134	135	135	135	135	135	135	135	135	138	138	138	138	158	158	158	158	165	
	59	134	134	134	134	134	134	134	134	135	135	135	135	135	135	135	135	138	138	138	138	158	158	158	158	165	

Figure 2-16. An example of TM data for spectral band 6 in CCT-AT format, unblocked. Note the blocks of 16 pixels representing the 120-meter IFOV of the band-6 detectors. Note also the effects of the scan offset as seen previously in Figures 2-13 to 2-15.

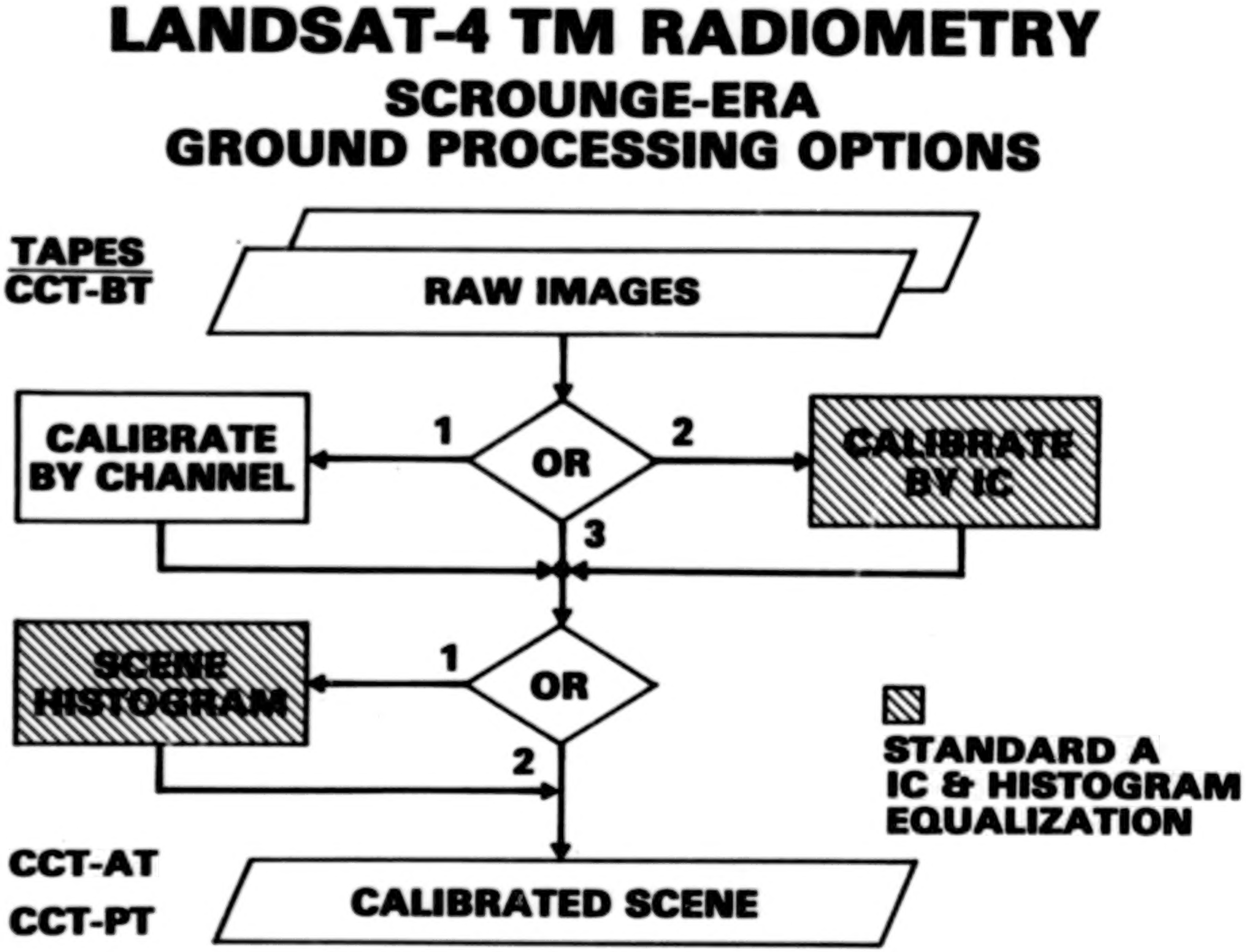

LANDSAT-4 TM RADIOMETRY

SCROUNGE-ERA
GROUND PROCESSING OPTIONS

TAPES
CCT-BT

RAW IMAGES

1 CALIBRATE BY CHANNEL

2 CALIBRATE BY IC

3

1 SCENE HISTOGRAM

2

CCT-AT
CCT-PT

CALIBRATED SCENE

▨ STANDARD A IC & HISTOGRAM EQUALIZATION

Figure 2-17. Diagram of LAS calibration options for TM data.

LANDSAT-4 TM — CCT-AT— IC BAND 2

MEMPHIS TN (ID = 40037-16033) 22 AUG 1982
START LINE (SL) = 3001, START SAMPLE (SS) = 2001
SCROUNGE ERA (1982-1983)

```
SAMPLE  641 642 643 644 645 646 647 648 649 650 651 652 653 654 655 656 657 658 659 660 661 662 663 664 665
  LINE
    13   38  38  38  38  38  39  39  39  39  50  72  72  73  73  73  71  69  61  45  50  39  37  37  37  33
    14   38  38  38  38  38  38  39  39  40  53  72  72  74  74  73  72  73  70  66  46  38  40  38  37  38
    15   39  39  39  38  39  39  39  39  42  61  76  75  74  75  74  75  74  72  60  49  38  39  38  37  36
    16   39  38  39  39  39  39  39  39  43  63  76  75  73  76  76  75  73  72  71  55  38  40  39  38  37
    17   38  38  38  39  38  38  39  39  44  66  73  76  75  76  74  75  75  73  72  56  38  38  37  38  35
    18   38  38  38  38  38  39  38  39  45  68  72  72  75  74  74  73  75  74  72  59  38  39  39  37  38
    19   39  39  40  40  39  40  41  41  51  73  74  75  76  75  74  75  75  73  72  58  38  40  39  38  38
    20   39  39  39  39  39  39  39  41  52  72  74  74  74  73  74  74  74  74  71  60  40  39  39  38  38
    21   40  40  40  40  40  40  40  42  55  73  74  75  76  75  74  75  75  75  73  65  41  41  40  38  37
    22   39  38  38  38  39  39  39  41  57  74  73  74  75  73  74  74  74  73  72  70  42  38  40  38  38
    23   38  39  38  38  39  38  41  42  61  72  74  74  73  74  74  74  74  74  72  67  45  39  38  38  37
    24   38  38  38  39  39  39  39  41  61  73  73  73  74  74  74  73  74  73  72  70  50  37  39  39  38
    25   38  38  38  39  39  39  39  41  61  73  73  73  74  74  74  73  74  73  72  70  50  37  39  39  38
    26   39  39  39  39  39  39  39  45  60  73  74  73  75  75  74  75  76  74  74  71  51  37  39  39  37
    27   39  38  41  38  40  41  42  42  60  69  72  76  74  76  78  77  76  76  74  76  61  46  41  42  39
    28   40  39  39  40  40  39  41  43  65  75  74  75  74  76  77  77  77  77  76  74  82  39  42  40  39
    29   27  27  28  28  27  27  27  27  27  28  28  28  28  28  27  28  28  29  28  28  29  31  30  30  30
    30   27  27  26  27  27  26  27  27  27  27  27  27  28  27  28  27  29  29  28  28  29  29  29  30  38
    31   27  28  27  26  26  26  27  27  30  27  27  27  27  27  27  28  30  27  28  28  30  32  31  31  39
    32   26  30  26  26  26  26  26  27  30  30  31  27  27  27  27  27  27  27  27  30  30  31  31  31  38
    33   28  28  27  27  27  27  27  27  27  28  28  27  27  28  28  29  28  28  29  30  28  30  30  32  38
    34   27  28  27  27  27  28  28  27  28  29  28  28  29  28  28  30  30  28  30  30  28  30  30  31  38
    35   28  28  28  28  27  28  28  28  30  28  28  28  28  29  27  28  29  30  30  28  29  31  32  31  41
    36   27  28  28  27  28  30  30  28  28  28  28  29  30  28  30  28  30  28  28  31  31  31  35  42  43
    37   28  28  28  28  28  30  29  29  29  30  30  28  28  28  28  29  30  29  30  33  30  34  41  46  46
    38   27  28  28  28  28  29  29  28  29  28  28  28  29  29  28  29  39  32  31  28  35  43  45  46  46
    39   27  28  29  27  28  30  29  28  27  29  27  29  28  29  27  29  30  33  33  37  43  47  45  46  47
    40   28  27  27  29  29  30  29  30  29  29  28  28  29  29  30  32  33  38  42  45  45  45  42  41  44
    41   28  27  27  29  29  30  29  30  29  29  28  28  29  29  30  33  35  38  42  45  45  45  42  41  44
    42   28  28  28  29  28  29  28  28  29  30  30  36  42  44  46  46  46  44  46  45  44  43  41  39  40
    43   28  30  28  30  28  29  30  31  33  39  39  43  46  46  45  46  45  46  40  39  40  41  39  39  40
    44   27  27  29  28  30  29  30  30  33  42  46  45  45  45  45  42  50  34  31  30  33  34  35  38  41
    45   38  39  37  39  39  38  39  39  39  39  43  47  72  76  77  77  77  79  77  77  76  73  67  43  39
    46   39  38  38  39  40  39  41  39  39  41  41  42  61  75  74  75  77  77  76  75  75  74  70  45  40
    47   39  39  39  39  39  39  40  40  39  39  42  42  58  76  78  77  77  79  78  76  75  75  71  47  39
    48   39  39  39  39  39  39  39  39  39  41  40  41  50  75  76  76  79  79  77  78  76  76  73  52  40
    49   38  38  39  39  39  39  39  38  39  40  40  40  47  71  76  76  77  78  77  78  76  75  73  55  38
    50   39  39  39  38  39  38  39  38  39  39  41  39  42  65  76  76  76  76  78  76  75  73  74  63  39
    51   39  39  40  40  40  39  40  40  40  41  42  41  41  56  77  77  77  78  79  76  75  74  75  67  42
    52   39  39  39  39  39  39  39  39  39  40  40  40  40  47  72  77  75  77  78  77  75  73  74  71  46
    53   38  40  40  40  40  40  40  40  38  40  40  41  41  44  64  78  76  77  78  77  76  75  75  73  50
    54   38  39  39  39  39  40  38  39  39  39  39  40  40  42  53  76  74  76  76  75  75  75  73  75  59
    55   39  38  38  38  38  38  38  38  39  39  40  40  40  41  45  67  78  78  76  76  75  75  75  74  65
    56   38  39  39  38  37  38  39  38  38  40  40  39  40  41  40  54  77  76  76  76  75  74  73  75  72
    57   38  39  39  38  37  38  39  38  38  40  40  39  40  41  40  54  77  76  76  76  75  74  73  75  72
    58   40  38  39  39  39  38  38  39  40  39  39  39  39  39  41  41  56  77  76  77  75  76  75  76  74
    59   39  40  38  38  38  40  39  40  39  38  39  40  38  41  40  41  45  63  70  72  78  76  77  78  76
```

Figure 2-18. An example of TM data for spectral band 2 in CCT-AT format, unblocked, internal calibration. Note the duplication of DNs for channel 5 to replace defective data in channel 4. Note also the difference in DNs between forward and reverse scans resulting from the scan offset. Compare with Figures 2-14 and 2-22.

LANDSAT-4 TM — CCT-AT — IC — BAND 4

MEMPHIS TN (ID = 40037-16033) 22 AUG 1982
START LINE (SL) = 3001, START SAMPLE (SS) = 2001
SCROUNGE ERA (1982-1983)

SAMPLE LINE	641	642	643	644	645	646	647	648	649	650	651	652	653	654	655	656	657	658	659	660	661	662	663	664	665
13	28	28	28	28	27	28	28	29	30	48	87	88	89	92	91	88	86	74	46	29	29	29	28	29	39
14	28	29	28	28	28	29	28	29	30	36	88	88	89	91	91	88	89	87	88	43	28	30	28	29	32
15	27	28	28	28	28	28	29	29	33	67	88	90	92	92	92	92	91	89	84	49	29	30	27	28	29
16	28	28	29	27	28	29	28	29	34	73	88	90	91	92	92	91	91	91	87	59	29	31	29	29	29
17	28	27	27	27	29	28	29	29	38	79	91	92	92	93	92	92	92	91	87	62	26	29	28	29	28
18	28	29	29	28	29	29	30	30	42	82	88	89	92	92	92	92	92	92	89	63	30	31	30	30	28
19	28	28	28	28	28	28	28	30	47	87	89	92	92	92	91	92	91	91	89	63	28	28	28	27	28
20	27	28	27	28	28	30	28	30	51	86	88	91	91	91	93	90	91	91	87	68	30	30	28	27	27
21	28	27	28	27	27	29	29	30	53	93	90	93	93	93	93	92	91	93	93	75	27	27	26	27	28
22	28	29	28	28	28	29	29	31	62	90	90	91	91	91	92	92	92	91	91	81	34	29	29	28	28
23	29	28	29	29	30	29	29	33	70	92	92	92	92	92	93	93	92	92	91	84	36	26	29	27	28
24	28	29	29	28	29	29	29	34	71	91	92	92	92	93	93	93	93	92	91	87	43	28	29	28	28
25	27	27	27	27	28	29	29	36	77	92	92	93	92	94	93	94	94	93	92	87	47	24	27	27	27
26	28	29	28	28	29	29	29	38	81	90	91	92	92	92	93	92	94	92	90	86	49	26	29	29	29
27	28	27	28	28	28	29	29	39	85	94	92	92	93	93	93	93	93	94	92	88	48	23	26	27	28
28	28	28	28	28	30	30	30	37	77	91	91	92	92	92	93	94	94	94	92	89	45	26	30	28	28
29	74	71	77	82	75	68	72	70	68	74	72	76	76	72	72	77	79	76	76	76	83	77	71	88	52
30	79	76	79	77	65	66	73	72	75	78	74	77	78	75	75	76	84	78	76	75	75	73	73	92	55
31	77	73	76	67	71	70	71	76	84	77	76	75	77	73	74	79	80	70	77	78	77	80	76	88	52
32	75	75	71	68	73	74	73	76	78	79	93	83	73	77	78	82	77	75	75	80	71	77	70	90	51
33	74	71	71	68	79	82	77	76	83	87	82	77	75	75	77	80	75	71	77	83	76	87	80	88	50
34	70	71	69	72	75	83	75	78	81	80	76	75	85	75	78	80	76	72	83	85	81	90	78	87	54
35	74	70	73	72	78	85	84	83	87	84	75	85	84	73	69	75	77	77	79	77	85	99	88	89	65
36	70	74	72	83	87	94	86	83	79	76	76	79	75	76	70	76	81	77	83	103	96	80	74	59	53
37	78	76	72	78	85	82	83	84	80	79	81	71	75	77	73	76	85	83	103	98	84	82	47	30	29
38	74	76	79	73	81	78	82	79	78	75	76	77	79	79	71	79	95	104	94	79	81	46	30	28	27
39	72	77	78	81	86	83	81	84	78	83	76	78	83	85	71	82	92	107	93	66	37	29	28	27	27
40	78	72	73	84	90	82	85	89	84	74	76	72	79	79	87	92	72	61	43	31	29	29	28	29	28
41	79	82	86	84	72	70	73	80	79	78	77	82	81	69	54	36	32	29	28	29	27	27	29	27	27
42	75	78	75	70	73	81	76	74	78	90	84	72	43	31	30	29	28	27	29	29	29	29	29	29	28
43	71	78	79	78	79	68	73	88	92	84	47	34	29	28	27	27	27	27	33	42	42	42	34	29	28
44	69	78	83	76	80	65	83	81	68	39	28	27	27	27	28	32	33	47	62	81	74	71	64	52	42
45	28	29	29	28	29	28	28	28	29	29	30	43	84	93	93	93	93	94	93	92	94	92	77	32	28
46	28	29	28	28	29	28	29	29	29	29	30	34	71	93	91	92	93	92	92	93	92	91	81	36	29
47	27	29	28	28	29	28	28	28	29	29	29	31	58	91	91	92	93	93	93	92	92	92	85	43	29
48	28	28	28	29	29	27	29	29	28	29	29	29	48	88	91	92	94	93	91	91	92	91	87	50	29
49	29	28	27	28	28	27	28	28	28	29	29	29	41	84	93	93	93	92	91	91	91	90	89	55	26
50	28	30	29	30	29	28	28	29	29	29	29	29	34	70	91	91	92	93	92	90	92	92	91	67	31
51	28	28	28	28	28	28	28	28	28	28	28	29	31	57	91	92	93	93	92	90	90	91	89	76	32
52	28	28	27	27	27	27	27	27	28	28	28	28	30	43	84	91	93	93	91	91	89	89	91	82	37
53	28	29	29	28	28	29	28	28	29	27	28	29	29	32	68	95	92	94	93	91	92	92	91	87	46
54	27	29	28	28	28	28	27	28	28	28	29	29	28	30	53	90	92	91	91	91	90	92	92	91	59
55	28	29	29	28	28	28	27	28	28	28	28	29	29	30	38	79	93	93	93	91	91	91	92	92	74
56	29	30	29	28	29	28	28	28	28	28	29	29	29	30	32	61	91	92	93	92	92	92	92	92	85
57	27	28	28	27	28	28	27	28	28	27	27	29	27	29	31	39	79	96	93	92	92	93	92	92	90
58	28	29	28	28	28	28	27	28	29	28	29	29	28	29	29	33	59	91	91	91	92	91	91	91	91
59	28	29	28	27	29	27	27	28	28	27	27	28	28	28	29	31	43	86	95	93	93	92	92	93	92

Figure 2-19. An example of TM data in CCT-AT format, unblocked, internal calibration. Note the changes in DNs between forward and reverse scans. Compare with Figures 2-14 to 2-16 to see the same pattern in other multispectral bands for this same image segment. Compare with Figures 2-13 and 2-23.

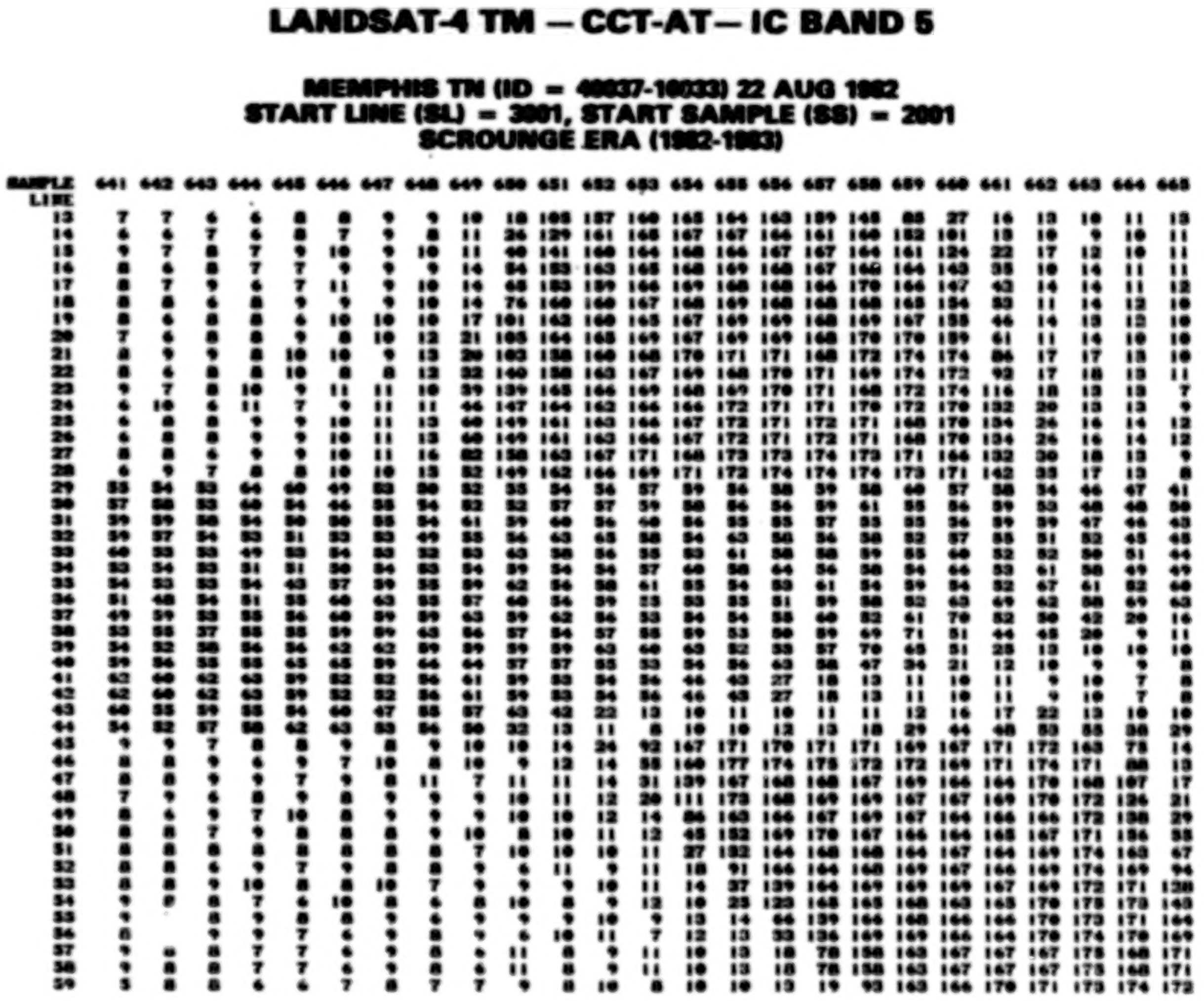

LANDSAT-4 TM — CCT-AT— IC BAND 5

MEMPHIS TN (ID = 40037-16033) 22 AUG 1982
START LINE (SL) = 3001, START SAMPLE (SS) = 2001
SCROUNGE ERA (1982-1983)

```
SAMPLE  641 642 643 644 645 646 647 648 649 650 651 652 653 654 655 656 657 658 659 660 661 662 663 664 665
  LINE
    13    7   7   6   6   8   8   9   9  10  10 105 157 160 165 164 163 159 148  85  27  16  13  10  11  13
    14    6   6   7   6   8   7   9   8  11  26 129 161 165 167 167 166 161 160 152 101  13  10   9  10  11
    15    9   7   8   7   9  10   9  10  11  40 141 160 164 168 166 167 167 164 161 124  22  17  12  10  11
    16    8   6   8   7   7   9   9   9  14  54 153 163 165 168 169 168 167 166 164 143  35  10  14  11  11
    17    8   7   9   6   7  11   9  10  14  65 153 159 166 169 168 168 166 170 166 147  43  14  14  11  12
    18    8   8   6   8   9   9   9  10  14  76 160 160 167 168 169 168 168 168 165 134  53  11  14  12  10
    19    8   6   8   8   6  10  10  10  17 101 162 160 165 167 169 169 168 169 167 135  46  14  13  12  10
    20    7   6   8   8   9   8  10  12  21 105 164 165 169 167 169 169 168 170 170 159  61  11  14  10  10
    21    8   9   9   8  10  10   9  13  20 103 158 160 168 170 171 171 168 172 174 174  86  17  17  13  10
    22    8   6   8   8  10   8   8  13  32 140 158 163 167 169 168 170 171 169 174 172  92  17  18  13  11
    23    9   7   8  10   9  11  11  10  39 139 165 166 169 168 169 170 171 168 172 174 116  18  13  13   7
    24    6  10   6  11   7   9  11  11  46 147 164 162 166 166 172 171 171 170 172 170 132  20  13  13   9
    25    6   8   8   9   9  10  11  13  60 149 161 163 166 167 172 171 172 171 168 170 134  26  16  14  12
    26    6   8   8   9   9  10  11  13  60 149 161 163 166 167 172 171 172 171 168 170 134  26  16  14  12
    27    8   8   6   9   9  10  11  16  82 150 163 167 171 168 173 173 174 173 171 166 132  30  18  13   9
    28    6   9   7   8   8  10  10  13  52 149 162 166 169 171 172 174 174 174 173 171 142  33  17  13   8
    29   55  54  53  64  60  49  53  50  52  55  54  56  57  59  56  58  59  58  60  57  58  34  46  47  41
    30   57  58  53  60  54  46  55  54  52  52  57  57  59  58  56  56  59  61  55  56  59  53  48  48  50
    31   59  59  58  54  50  50  55  54  61  59  60  56  48  56  55  55  57  53  53  36  59  39  47  46  43
    32   59  57  54  53  51  53  53  49  55  56  63  65  58  54  63  58  56  58  52  57  55  51  52  45  45
    33   60  53  53  49  53  54  53  32  53  63  58  56  55  53  61  58  58  59  55  60  52  52  50  51  44
    34   53  54  53  51  51  50  54  53  54  59  54  54  57  60  58  64  56  58  54  64  53  61  58  49  49
    35   54  53  53  54  43  57  59  55  59  62  56  58  61  55  54  53  61  54  59  54  52  67  61  52  60
    36   51  48  54  51  55  60  63  55  57  60  54  59  53  53  55  51  59  58  52  63  69  62  58  69  63
    37   49  59  53  55  56  60  59  59  63  59  62  56  53  54  54  55  60  52  61  70  52  50  42  20  16
    38   53  55  37  55  55  59  59  65  56  57  54  57  55  59  53  50  59  69  71  51  44  45  20   9  11
    39   54  52  58  56  56  62  62  59  59  59  59  63  60  63  52  55  57  70  65  51  25  13  10  10  10
    40   59  56  55  55  65  65  59  66  64  57  57  55  33  56  56  63  58  47  34  21  12  10   9   9   8
    41   62  60  62  63  59  52  52  56  61  59  53  54  56  46  43  27  18  13  11  10  11   9  10   7   8
    42   62  60  62  63  59  52  52  56  61  59  53  54  56  46  43  27  18  13  11  10  11   9  10   7   8
    43   60  55  59  55  54  60  47  55  57  63  42  22  13  10  11  10  11  11  12  16  17  22  13  10  10
    44   54  52  57  58  62  63  53  56  50  32  13  11   8  10  10  12  13  18  29  44  48  53  55  38  29
    45    9   9   7   8   8   9   8   9  10  10  14  24  92 167 171 170 171 171 169 167 171 172 163  73  14
    46    8   8   9   6   9   7  10   8  10   9  12  14  55 160 177 174 175 172 172 169 171 174 171  88  13
    47    8   8   9   9   7   9   8  11   7  11  11  14  31 139 167 168 168 167 169 166 164 170 168 107  17
    48    7   9   6   8   9   8   9   9   9  10  11  12  20 111 173 168 169 169 167 167 169 170 172 126  21
    49    8   6   9   7  10   8   9   9   9  10  10  12  14  86 163 166 167 169 167 164 166 166 172 138  29
    50    8   8   7   9   8   8   8   9  10   8  10  11  12  45 152 169 170 167 166 164 165 167 171 136  35
    51    8   8   8   8   8   8   8   8   7  10  10  10  11  27 132 164 168 168 164 167 164 169 174 163  67
    52    8   8   6   9   7   9   8   8   9   6  11   9  11  18  91 166 164 168 169 167 166 169 174 169  94
    53    8   8   9  10   8   8  10   7   9   9   9  10  11  14  37 139 166 169 169 169 167 169 172 171 128
    54    9   8   8   7   6  10   8   6   8  10   8   9  12  10  25 123 168 165 168 163 165 170 175 173 143
    55    9       8   9   8   8   9   6   9   9   9  10   9  13  14  66 139 166 168 166 166 170 173 171 164
    56    8       9   9   7   6   9   8   9   6  10  11   7  12  13  33 136 169 169 166 164 170 174 170 169
    57    9   8   8   7   7   6   9   8   6  11   8   9  11  10  13  18  78 158 163 167 167 167 175 168 171
    58    9   8   8   7   7   6   9   8   6  11   8   9  11  10  13  18  78 158 163 167 167 167 175 168 171
    59    5   8   8   6   6   7   8   7   7   9   8  10   8  10  10  13  19  93 163 166 170 171 173 174 172
```

Figure 2-20. An example of TM data for spectral band 5 in CCT-AT format, unblocked, internal calibration. Note the duplication of DNs for channel 4 to replace defective data in channel 3. Note also the difference in DNs between forward and reverse scans resulting from the scan offset. Compare with Figures 2-15 and 2-24.

LANDSAT-4 TM — CCT-AT — IC BAND 6

MEMPHIS TN (ID = 40037-16033) 22 AUG 1982
START LINE (SL) = 3001, START SAMPLE (SS) = 2001
SCROUNGE ERA (1982-1983)

SAMPLE LINE	641	642	643	644	645	646	647	648	649	650	651	652	653	654	655	656	657	658	659	660	661	662	663	664	665
13	135	135	135	135	136	136	136	136	137	137	137	137	157	157	157	157	166	166	166	166	155	155	155	155	137
14	135	135	135	135	136	136	136	136	137	137	137	137	157	157	157	157	165	166	166	166	155	155	155	155	137
15	135	135	135	135	136	136	136	136	137	137	137	137	157	157	157	157	166	166	166	166	155	155	155	155	137
16	135	135	135	135	136	136	136	136	137	137	137	137	157	157	157	157	166	166	166	166	155	155	155	155	137
17	134	134	134	134	135	135	135	135	138	138	138	138	159	159	159	159	168	168	168	168	159	159	159	159	137
18	134	134	134	134	135	135	135	135	138	138	138	138	159	159	159	159	168	168	168	168	159	159	159	159	137
19	134	134	134	134	135	135	135	135	138	138	138	138	159	159	159	159	168	168	168	168	159	159	159	159	137
20	134	134	134	134	135	135	135	135	138	138	138	138	159	159	159	159	168	168	168	168	159	159	159	159	137
21	136	136	136	136	136	136	136	136	140	140	140	140	163	163	163	163	168	168	168	168	161	161	161	161	139
22	136	136	136	136	136	136	136	136	140	140	140	140	163	163	163	163	168	168	168	168	161	161	161	161	139
23	136	136	136	136	136	136	136	136	140	140	140	140	163	163	163	163	168	168	168	168	161	161	161	161	139
24	134	136	136	136	136	136	136	136	140	140	140	140	163	163	163	163	168	168	168	168	161	161	161	161	139
25	134	134	134	134	134	134	134	134	140	140	140	140	162	162	162	162	168	168	168	168	164	164	164	164	141
26	134	134	134	134	134	134	134	134	140	140	140	140	162	162	162	162	168	168	168	168	164	164	164	164	141
27	134	134	134	134	134	134	134	134	140	140	140	140	162	162	162	162	168	168	168	168	164	164	164	164	141
28	134	134	134	134	134	134	134	134	140	140	140	140	162	162	162	162	168	168	168	168	164	164	164	164	141
29	136	136	136	136	136	136	136	136	136	136	136	136	137	137	137	137	136	136	136	136	136	136	136	136	136
30	136	136	136	136	136	136	136	136	136	136	136	136	137	137	137	137	136	136	136	136	136	136	136	136	136
31	136	136	136	136	136	136	136	136	136	136	136	136	137	137	137	137	136	136	136	136	136	136	136	136	136
32	136	136	136	136	136	136	136	136	136	136	136	136	137	137	137	137	136	136	136	136	136	136	136	136	136
33	135	135	133	135	135	135	135	135	135	135	135	135	136	136	136	136	136	136	136	136	136	136	136	136	135
34	135	135	135	135	135	135	135	135	135	135	135	135	136	136	136	136	136	136	136	136	136	136	136	136	135
35	135	135	135	135	135	135	135	135	135	135	135	135	136	136	136	136	136	136	136	136	136	136	136	136	135
36	135	135	135	135	135	135	135	135	135	135	135	135	136	136	136	136	136	136	136	136	136	136	136	136	135
37	137	137	137	137	137	137	137	137	136	136	136	136	136	136	136	136	136	136	136	136	136	136	136	136	135
38	137	137	137	137	137	137	137	137	136	136	136	136	136	136	136	136	136	136	136	136	136	136	136	136	135
39	137	137	137	137	137	137	137	137	136	136	136	136	136	136	136	136	136	136	136	136	136	136	136	136	135
40	137	137	137	137	137	137	137	137	136	136	136	136	136	136	136	136	136	136	136	136	136	136	136	136	135
41	136	136	136	136	136	136	136	136	137	137	137	137	136	136	136	136	135	135	135	135	135	135	135	135	134
42	136	136	136	136	136	136	136	136	137	137	137	137	136	136	136	136	135	135	135	135	135	135	135	135	134
43	136	136	136	136	136	136	136	136	137	137	137	137	136	136	136	136	135	135	135	135	135	135	135	135	134
44	136	136	136	136	136	136	136	136	137	137	137	137	136	136	136	136	135	135	135	135	135	135	135	135	134
45	136	136	136	136	136	136	136	136	136	136	136	136	140	140	140	140	161	161	161	161	166	166	166	166	155
46	136	136	136	136	136	136	136	136	136	136	136	136	140	140	140	140	161	161	161	161	166	166	166	166	155
47	136	136	136	136	136	136	136	136	136	136	136	136	140	140	140	140	161	161	161	161	166	166	166	166	155
48	136	136	136	136	136	136	136	136	136	136	136	136	140	140	140	140	161	161	161	161	166	166	166	166	155
49	134	134	134	134	135	135	135	135	135	135	135	135	137	137	137	137	154	154	154	154	166	166	166	166	160
50	134	134	134	134	135	135	135	135	135	135	135	135	137	137	137	137	154	154	154	154	166	166	166	166	160
51	134	134	134	134	135	135	135	135	135	135	135	135	137	137	137	137	154	154	154	154	166	166	166	166	160
52	134	134	134	134	135	135	135	135	135	135	135	135	137	137	137	137	154	154	154	154	166	166	166	166	160
53	135	135	135	135	136	136	136	136	136	136	136	136	137	137	137	137	147	147	147	147	166	166	166	166	163
54	135	135	135	135	136	136	136	136	136	136	136	136	137	137	137	137	147	147	147	147	166	166	166	166	163
55	135	135	135	135	136	136	136	136	136	136	136	136	137	137	137	137	147	147	147	147	166	166	166	166	163
56	133	135	135	135	136	136	136	136	136	136	136	136	137	137	137	137	147	147	147	147	166	166	166	166	163
57	134	134	134	134	134	134	134	134	135	135	135	135	135	135	135	135	136	136	136	136	158	158	158	158	163
58	134	134	134	134	134	134	134	134	135	135	135	135	135	135	135	135	136	136	136	136	158	158	158	158	163
59	134	134	134	134	134	134	134	134	135	135	135	135	135	135	135	135	136	136	136	136	158	158	158	158	163

Figure 2-21. An example of TM data for spectral band 6 in CCT-AT format, unblocked, internal calibration. Note the blocks of 16 pixels representing the 120-meter IFOV of the band-6 detectors. Note also the effects of the scan offset as seen previously in Figures 2-13 to 2-15. Compare with Figure 2-16.

LANDSAT-4 TM — CCT-AT — NOMINAL MINUS IC — BAND 2

MEMPHIS TN (ID = 40037-16033) 22 AUG 1982
START LINE (SL) = 3001, START SAMPLE (SS) = 2001
SCROUNGE ERA (1982-1983)

SAMPLE LINE	641	642	643	644	645	646	647	648	649	650	651	652	653	654	655	656	657	658	659	660	661	662	663	664	665
13	●	●	●	●	●	●	●	●	●	-1	-1	-1	-1	-1	-1	-1	-1	●	-1	●	●	●	●	●	●
14	●	●	●	●	●	●	●	●	●	●	●	●	●	●	●	●	●	●	●	●	●	●	●	●	●
15	●	●	●	●	●	●	●	●	●	-1	●	●	●	●	●	●	●	●	-1	●	●	●	●	●	●
16	●	●	●	●	●	●	●	●	●	●	●	●	1	●	●	●	1	●	●	●	●	●	●	●	●
17	●	●	●	●	●	●	●	●	-1	●	-1	-1	-1	-1	-1	-1	-1	-1	-1	●	●	●	●	●	●
18	●	●	●	●	●	●	●	●	●	-1	●	●	●	●	●	●	●	●	●	-1	●	●	●	●	●
19	-1	-1	-1	-1	-1	-1	●	●	●	●	●	●	●	●	●	●	●	●	●	●	-1	-1	-1	-1	-1
20	●	●	●	●	●	●	●	●	-1	●	●	●	●	●	●	●	●	●	●	●	●	●	●	●	●
21	-1	-1	-1	-1	-1	-1	-1	-1	●	-1	-1	●	●	●	-1	●	●	●	-1	-1	-1	-1	-1	●	●
22	-1	-1	-1	-1	-1	-1	-1	●	-1	-1	-1	-1	-1	-1	-1	-1	-1	-1	-1	-1	●	-1	●	-1	-1
23	●	●	●	●	●	●	●	●	●	●	●	●	●	●	●	●	●	●	●	●	●	●	●	●	●
24	●	●	●	●	●	●	●	●	●	●	●	●	●	●	●	●	●	●	●	●	●	●	●	●	●
25	●	●	●	●	●	●	●	●	●	●	●	●	●	●	●	●	●	●	●	●	●	●	●	●	●
26	●	●	●	●	●	●	●	●	-1	-1	-1	-1	-1	-1	-1	-1	-1	-1	-1	-1	-1	-1	●	●	-1
27	●	●	●	●	●	●	●	●	●	●	●	-1	●	-1	-1	-1	-1	-1	●	-1	●	●	●	●	●
28	●	●	●	●	●	●	●	●	1	●	●	●	●	●	●	●	●	●	●	●	●	●	●	●	●
29	●	●	●	●	●	●	●	●	●	●	●	●	●	●	●	●	●	●	●	●	●	●	●	●	●
30	●	●	●	●	●	●	●	●	●	●	●	●	●	●	●	●	●	●	●	●	●	●	●	●	●
31	1	1	1	1	1	1	1	1	●	1	1	1	1	1	1	1	●	1	1	1	●	●	●	●	●
32	1	●	1	1	1	1	1	1	●	●	●	1	1	1	1	1	1	1	1	●	●	●	●	●	●
33	●	●	●	●	●	●	●	●	●	●	●	●	●	●	●	●	●	●	●	●	●	●	●	●	●
34	●	●	●	●	●	●	●	●	●	●	●	●	●	●	●	●	●	●	●	●	●	●	●	●	●
35	●	●	●	●	●	●	●	●	●	●	●	●	●	●	●	●	●	●	●	●	●	●	●	●	●
36	●	●	●	●	●	●	●	●	●	●	●	●	●	●	●	●	●	●	●	●	●	●	●	●	●
37	●	●	●	●	●	●	●	●	●	●	●	●	●	●	●	●	●	●	●	●	●	●	-1	-1	-1
38	-1	-1	-1	-1	-1	-1	-1	-1	-1	-1	-1	-1	-1	-1	-1	-1	-1	-1	-1	-1	-1	●	●	●	●
39	●	●	●	●	●	●	●	●	●	●	●	●	●	●	●	●	●	●	●	●	●	●	●	●	●
40	●	●	●	●	●	●	●	●	●	●	●	●	●	●	●	●	●	●	●	●	●	●	●	●	●
41	●	●	●	●	●	●	●	●	●	●	●	●	●	●	●	●	●	●	●	●	●	●	●	●	●
42	-1	-1	-1	-1	-1	-1	-1	-1	-1	-1	-1	-1	●	●	●	●	●	●	●	●	●	●	●	●	●
43	●	●	●	●	●	●	●	●	●	●	●	●	●	●	●	●	●	●	●	●	●	●	●	●	●
44	●	●	●	●	●	●	●	●	●	●	●	●	●	●	●	●	●	●	●	●	●	●	●	●	●
45	●	●	●	●	●	●	●	●	●	●	-1	-1	-1	-1	-1	-1	-1	-1	-1	-1	-1	-1	-1	-1	●
46	●	●	●	●	●	●	●	●	●	●	●	●	●	●	●	●	●	●	●	●	●	●	●	●	●
47	●	●	●	●	●	●	●	●	●	●	●	●	●	●	●	●	●	●	●	●	●	●	●	●	●
48	●	●	●	●	●	●	●	●	●	●	●	●	●	●	●	●	●	●	●	●	●	●	1	●	●
49	●	●	●	●	●	●	●	●	●	●	●	●	-1	-1	-1	-1	-1	-1	-1	-1	-1	-1	-1	-1	●
50	●	●	●	●	●	●	●	●	●	●	●	●	●	-1	●	●	●	●	-1	●	●	●	●	-1	●
51	-1	-1	-1	-1	-1	-1	-1	-1	-1	●	●	●	●	●	●	●	●	●	●	●	●	●	●	-1	●
52	●	●	●	●	●	●	●	●	●	●	●	●	●	●	●	●	●	●	●	●	●	●	●	●	●
53	●	-1	-1	-1	-1	-1	-1	-1	●	-1	-1	-1	-1	-1	-1	●	●	●	●	●	●	●	●	-1	●
54	-1	-1	-1	-1	-1	●	-1	-1	-1	-1	-1	●	●	●	-1	-1	-1	-1	-1	-1	-1	-1	-1	-1	-1
55	●	●	●	●	●	●	●	●	●	●	●	●	●	●	●	●	-1	-1	●	●	●	●	●	●	●
56	●	●	●	●	●	●	●	●	●	●	●	●	●	●	●	●	●	●	●	●	●	●	●	●	●
57	●	●	●	●	●	●	●	●	●	●	●	●	●	●	●	●	●	●	●	●	●	●	●	●	●
58	●	●	●	●	●	●	●	●	●	●	●	●	●	●	●	●	-1	-1	-1	-1	-1	-1	-1	-1	-1
59	●	●	●	●	●	●	●	●	●	●	●	●	●	●	●	●	●	●	●	●	-1	-1	-1	-1	-1

Figure 2-22. An example of the difference image between TM data processed using two different calibration options. Compare with Figures 2-14 and 2-18.

LANDSAT-4 TM — CCT-AT — NOMINAL MINUS IC — BAND 4

MEMPHIS TN (ID = 40037-16033) 22 AUG 1982
START LINE (SL) = 3001, START SAMPLE (SS) = 2001
SCROUNGE ERA (1982-1983)

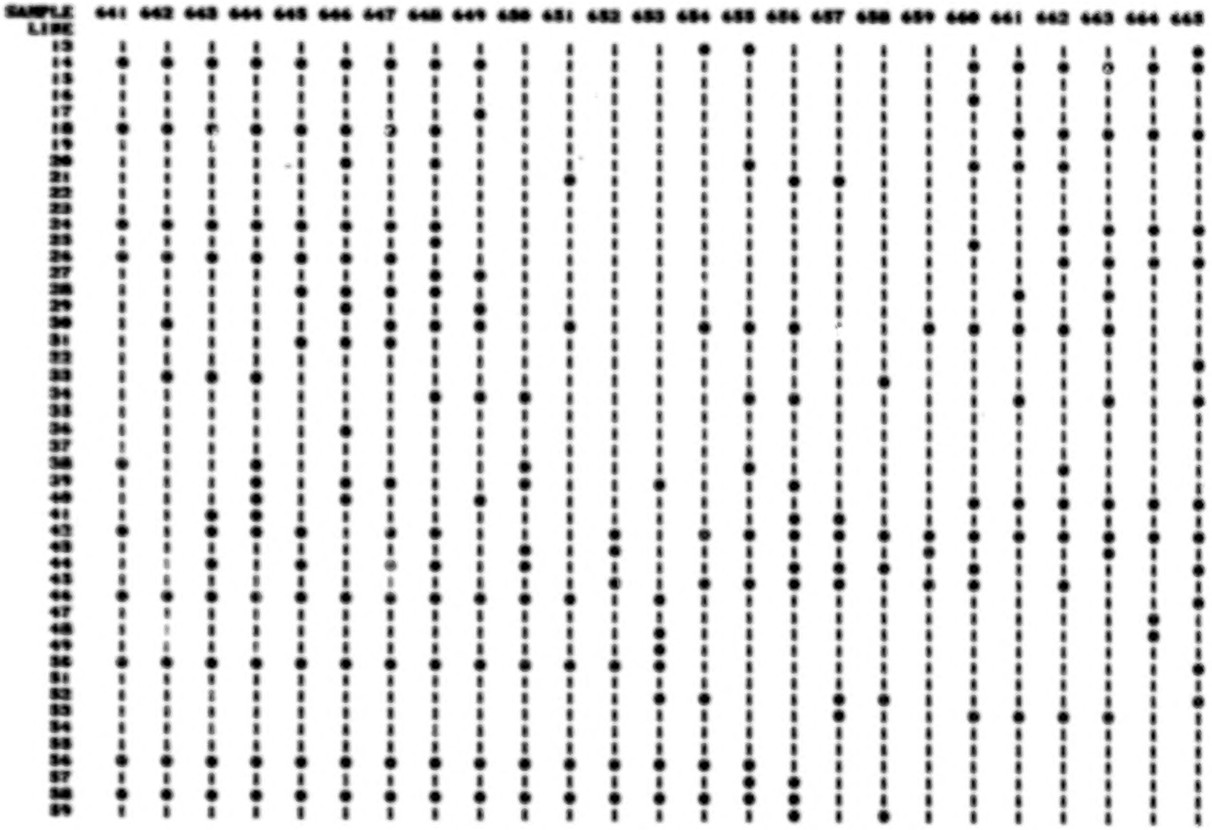

Figure 2-23. An example of the difference image between TM data processed using two different calibration options. Compare with Figures 2-13 and 2-23.

LANDSAT-4 TM — CCT-AT — NOMINAL MINUS IC — BAND 7

MEMPHIS TN (ID = 40037-16033) 22 AUG 1982
START LINE (SL) = 3001, START SAMPLE (SS) = 2001
SCROUNGE ERA (1982-1983)

SAMPLE LINE	641	642	643	644	645	646	647	648	649	650	651	652	653	654	655	656	657	658	659	660	661	662	663	664	665
13	0	0	0	0	0	0	0	0	0	0	0	-1	-1	-1	-1	-1	-1	-1	0	0	0	0	0	0	0
14	0	0	0	0	0	0	0	0	0	0	1	0	0	0	0	0	0	0	0	0	1	0	0	0	0
15	0	0	0	0	0	0	0	0	0	-1	-2	-2	-1	-1	-1	-2	-1	-2	-2	-1	0	0	0	0	0
16	0	0	0	0	0	0	0	0	0	0	0	0	0	0	-1	0	0	0	0	0	0	0	0	0	0
17	0	0	0	0	0	0	0	0	0	0	0	0	0	0	0	0	0	0	0	0	0	0	0	0	0
18	0	0	0	0	0	0	0	0	0	0	0	0	0	-1	-1	0	-1	0	0	-1	0	0	0	0	0
19	0	0	0	0	0	0	0	0	0	0	0	1	0	0	0	0	0	1	0	0	0	0	0	0	0
20	0	0	0	0	0	0	0	0	0	-1	-1	-1	-1	-1	-1	-1	-1	-1	-1	-1	0	0	0	0	0
21	0	0	0	0	0	0	0	0	0	0	0	0	0	1	0	1	1	0	0	0	0	0	0	0	0
22	0	0	0	0	0	0	0	0	0	-1	-1	-1	-1	-1	-1	-1	-1	-1	-1	-1	-1	0	0	0	0
23	0	0	0	0	0	0	0	0	0	-1	0	0	0	0	0	0	0	0	0	0	0	0	0	0	0
24	0	0	0	0	0	0	0	0	0	-1	0	-1	0	0	0	0	0	0	0	0	0	0	0	0	0
25	0	0	0	0	0	0	0	0	-1	-1	0	-1	-1	-1	-1	-1	-1	-1	-1	-1	-1	0	0	0	0
26	0	0	0	0	0	0	0	0	-1	-1	-1	-1	-1	-1	-2	-2	-2	-2	-1	-1	-1	0	0	0	0
27	0	0	0	0	0	0	0	0	0	-1	-1	-1	-1	-1	-1	-1	-1	-1	-1	-1	0	0	0	0	0
28	0	0	0	0	0	0	0	0	1	2	2	2	2	2	2	2	2	2	2	2	2	1	0	0	0
29	0	0	0	0	0	0	0	0	0	0	0	0	0	0	0	0	0	0	0	0	0	0	0	0	0
30	0	0	0	0	0	0	0	0	0	0	0	0	0	0	0	0	0	0	0	0	0	0	0	0	0
31	-1	-1	0	-1	0	0	0	0	0	-1	-1	-1	-1	0	-1	0	-1	-1	0	-1	-1	-1	-1	0	-1
32	0	0	0	0	0	0	0	0	0	0	0	0	0	0	0	0	0	0	0	0	0	0	0	0	0
33	0	0	0	0	0	0	0	0	0	0	0	0	0	0	0	0	0	0	0	0	0	0	0	0	0
34	0	0	0	0	0	0	0	0	0	0	0	0	0	0	0	0	0	0	0	0	0	0	0	0	0
35	0	0	0	0	0	0	-1	0	0	0	0	0	0	0	0	-1	-1	-1	-1	0	0	0	-1	-1	0
36	0	0	0	0	0	0	0	0	0	-1	0	0	0	0	0	0	0	0	0	0	-1	-1	-1	-1	-1
37	0	0	0	0	0	0	0	0	0	0	0	0	0	0	0	0	0	0	0	0	0	0	0	0	0
38	0	0	0	0	0	0	0	0	0	0	0	0	0	0	0	0	0	0	0	0	0	0	0	0	0
39	0	0	0	0	0	0	0	0	0	0	0	0	0	0	0	0	0	0	0	0	0	0	0	0	0
40	0	0	0	0	0	0	0	0	0	0	0	0	0	0	0	0	0	0	0	0	0	0	0	0	0
41	0	0	0	0	0	0	0	0	0	0	0	0	0	0	0	0	0	0	0	0	0	0	0	0	0
42	0	0	0	0	0	0	0	0	0	0	0	0	0	0	0	0	0	0	0	0	0	0	0	0	0
43	0	0	0	0	0	0	0	0	0	0	0	0	0	0	0	0	0	0	0	0	0	0	0	0	0
44	1	1	1	1	1	1	1	1	1	0	0	0	0	0	0	0	0	0	0	1	1	1	1	1	1
45	0	0	0	0	0	0	0	0	0	0	0	0	0	-1	-1	-1	-1	-1	-1	-1	-1	-1	-1	0	0
46	0	0	0	0	0	0	0	0	0	0	0	0	0	0	1	1	1	1	1	1	1	1	1	0	0
47	0	0	0	0	0	0	0	0	0	0	0	0	-1	-2	-1	-1	-1	-1	-1	-1	-2	-2	-1	-1	0
48	0	0	0	0	0	0	0	0	0	0	0	0	0	0	-1	-1	-1	-1	-1	0	-1	-1	-1	0	0
49	0	0	0	0	0	0	0	0	0	0	0	0	0	-1	0	0	0	0	0	0	0	0	0	-1	0
50	0	0	0	0	0	0	0	0	0	0	0	0	0	0	-1	-1	-1	-1	-1	0	0	-1	-1	0	0
51	0	0	0	0	0	0	0	0	0	0	0	0	0	0	0	0	0	0	0	0	1	0	0	1	0
52	0	0	0	0	0	0	0	0	0	0	0	0	0	0	-1	-1	-1	-1	-1	-1	-1	-1	-1	-1	-1
53	0	0	0	0	0	0	0	0	0	0	0	0	0	0	0	0	0	0	0	1	0	0	0	1	0
54	0	0	0	0	0	0	0	0	0	0	0	0	0	0	0	-1	-1	-1	-1	-1	-1	-1	-1	-1	-1
55	0	0	0	0	0	0	0	0	0	0	0	0	0	0	0	0	0	0	0	0	0	0	0	0	0
56	0	0	0	0	0	0	0	0	0	0	0	0	0	0	0	0	0	0	0	0	0	0	0	0	0
57	0	0	0	0	0	0	0	0	0	0	0	0	0	0	0	0	0	-1	-1	-1	-1	-1	-1	-1	-1
58	0	0	0	0	0	0	0	0	0	0	0	0	0	0	0	0	0	-1	-2	-2	-2	-2	-2	-2	-1
59	0	0	0	0	0	0	0	0	0	0	0	0	0	0	0	0	0	0	-1	-1	-1	-1	-1	-1	-1

Figure 2-24. An example of the difference image between TM data processed using two different calibration options. Compare with Figures 2-15 and 2-24.

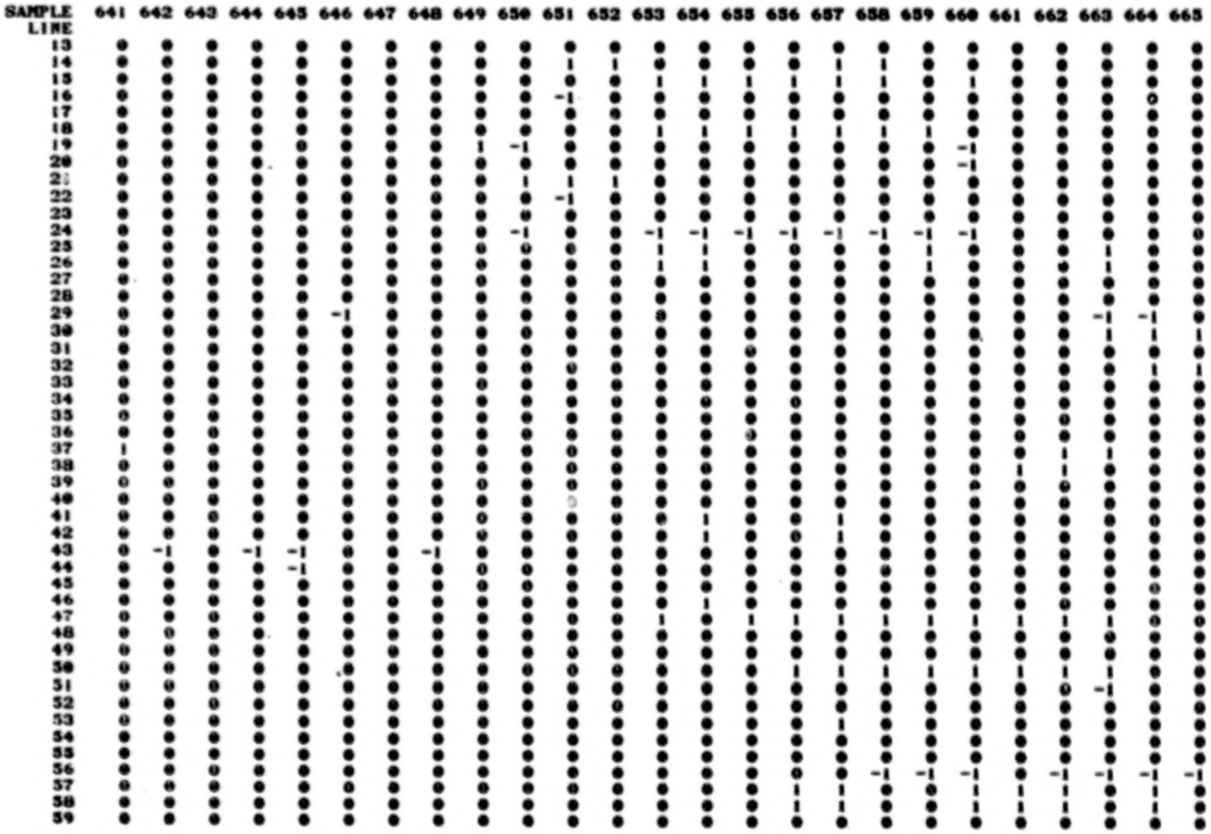

LANDSAT-4 TM — CCT-AT — NOMINAL MINUS IC — BAND 5

MEMPHIS T. (ID = 40037-16033) 22 AUG 1982
START LINE (SL) = 3002, START SAMPLE (SS) = 2001
SCROUNGE ERA (1982-1983)

Figure 2-25. An example of the difference image between TM data processed using two different calibration options.

BAND-AVERAGE COMPARISON OF DIFFERENT CALIBRATION METHODS

LANDSAT-4 TM — CCT-AT — NOMINAL MINUS IC HISTOGRAMS
MEMPHIS TN (ID = 40037-16033) 22 AUG 1982
START LINE (SL) = 3001, START SAMPLE (SS) = 2001 NL = 1024
NS = 1024
SCROUNGE ERA (1982-1983)

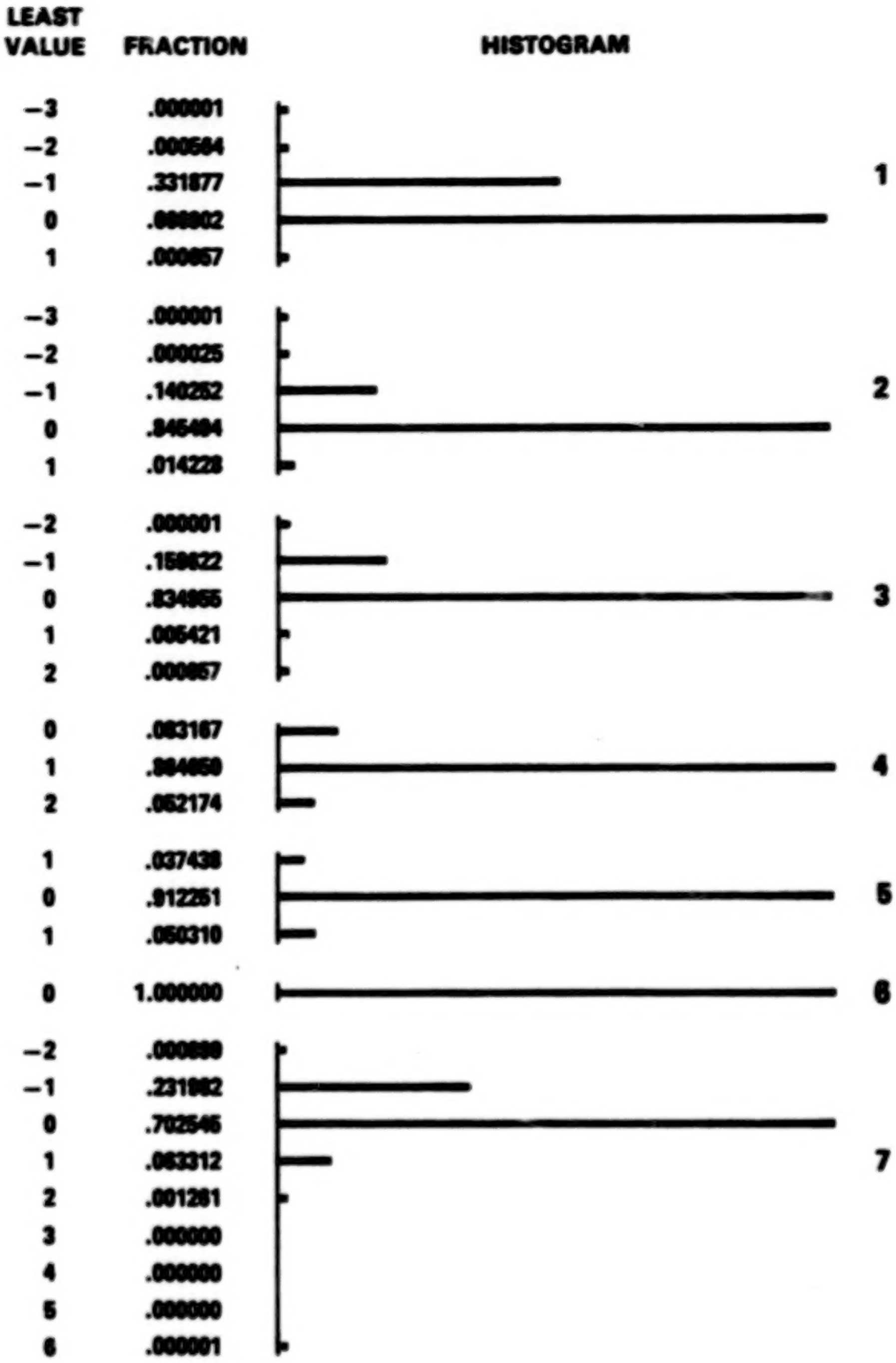

Figure 2-26. Histograms showing the frequency of differences between images produced by two different TM calibration options. Compare with Figures 2-22 to 2-25.

CHANNEL SPECIFIC COMPARISON OF DIFFERENT CALIBRATION METHODS
LANDSAT-4 TM — CCT-AT

BAND 7 NOMINAL — BAND 7 IC
MEMPHIS (ID = 40037-16033) 22 AUG 1982
SL = 3001, SS = 2001, NL = 64, NS = 1024

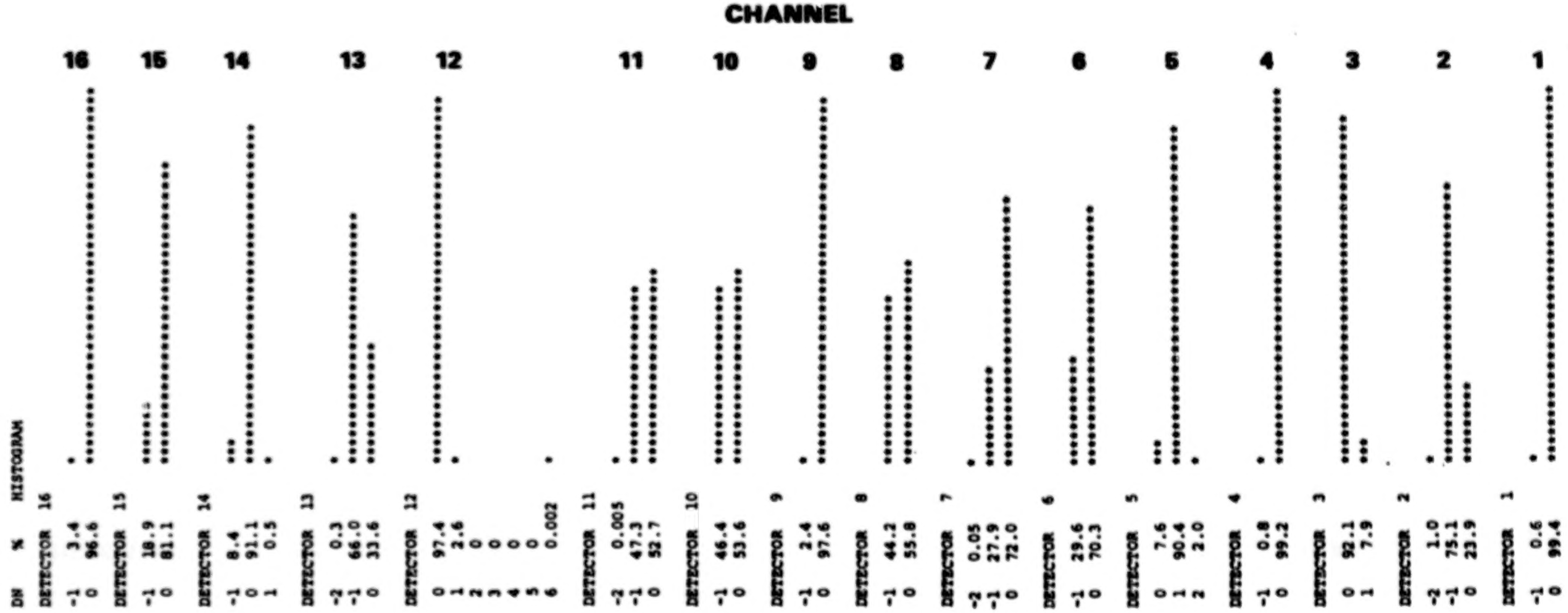

Figure 2-27. Histograms for each channel showing the different frequency of differences between band-7 images produced by two different calibration options. Compare with Figure 2-26.

LANDSAT-4 TM — DIGITAL TAPE CONTENTS — CCT-PT
(4X BLOCKING)

SCROUNGE-ERA (1982—1983)

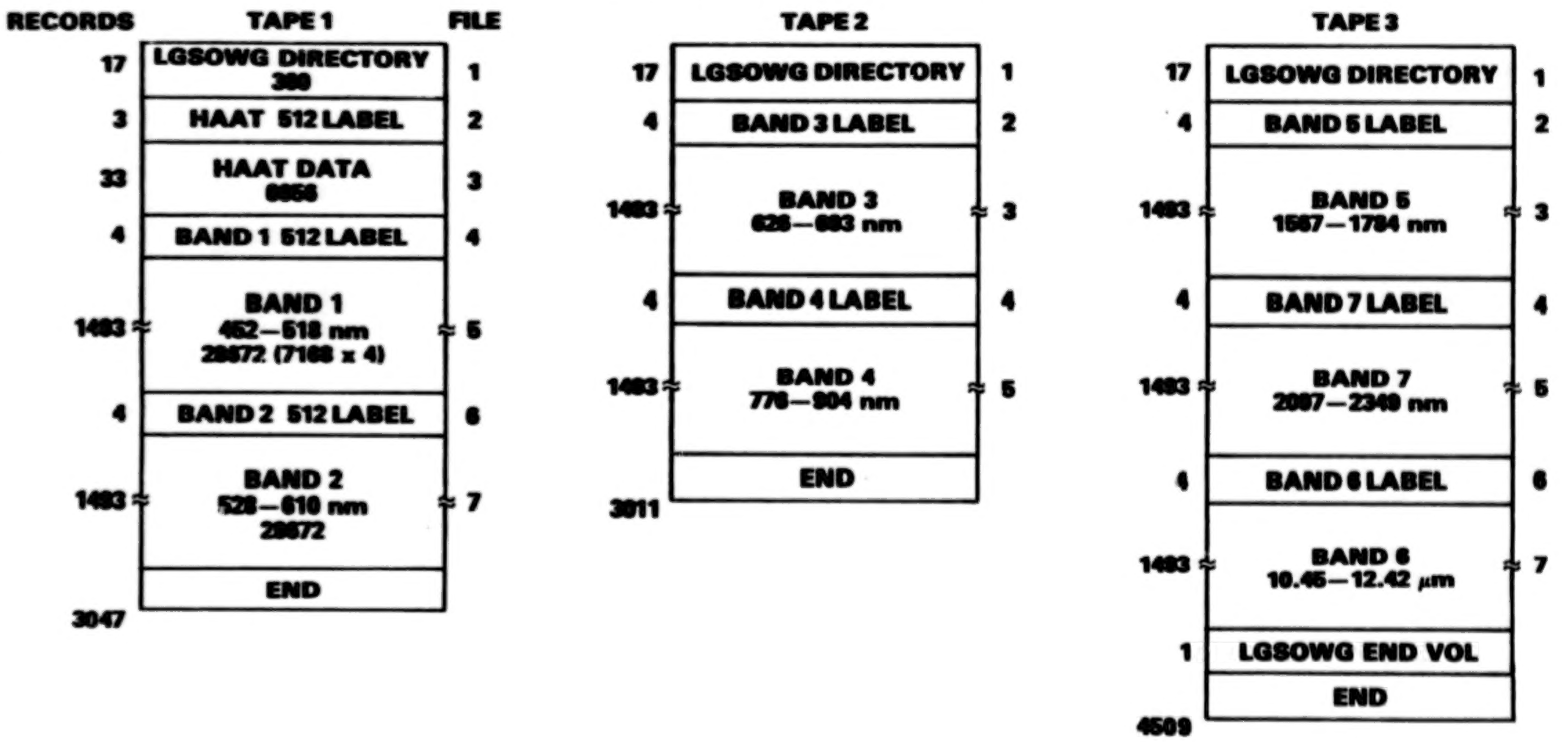
RECORDS
TAPE 1
FILE
17
LGSOWG DIRECTORY
360
1
3
HAAT 512 LABEL
2
33
HAAT DATA
6656
3
4
BAND 1 512 LABEL
4
1493
BAND 1
452—518 nm
28672 (7168 x 4)
5
4
BAND 2 512 LABEL
6
1493
BAND 2
528—610 nm
28672
7
END
3047
TAPE 2
17
LGSOWG DIRECTORY
1
4
BAND 3 LABEL
2
1493
BAND 3
626—693 nm
3
4
BAND 4 LABEL
4
1493
BAND 4
776—904 nm
5
END
3011
TAPE 3
17
LGSOWG DIRECTORY
1
4
BAND 5 LABEL
2
1493
BAND 5
1567—1784 nm
3
4
BAND 7 LABEL
4
1493
BAND 7
2097—2349 nm
5
4
BAND 6 LABEL
6
1493
BAND 6
10.45—12.42 μm
7
1
LGSOWG END VOL
END
4509

Figure 2-28. File organization of TM data and images on the three CCT-PT tapes produced by LAS as final products.

LANDSAT-4 TM CCT-AT IMAGE FILE CONTENTS
SCROUNGE ERA (1982—1983)

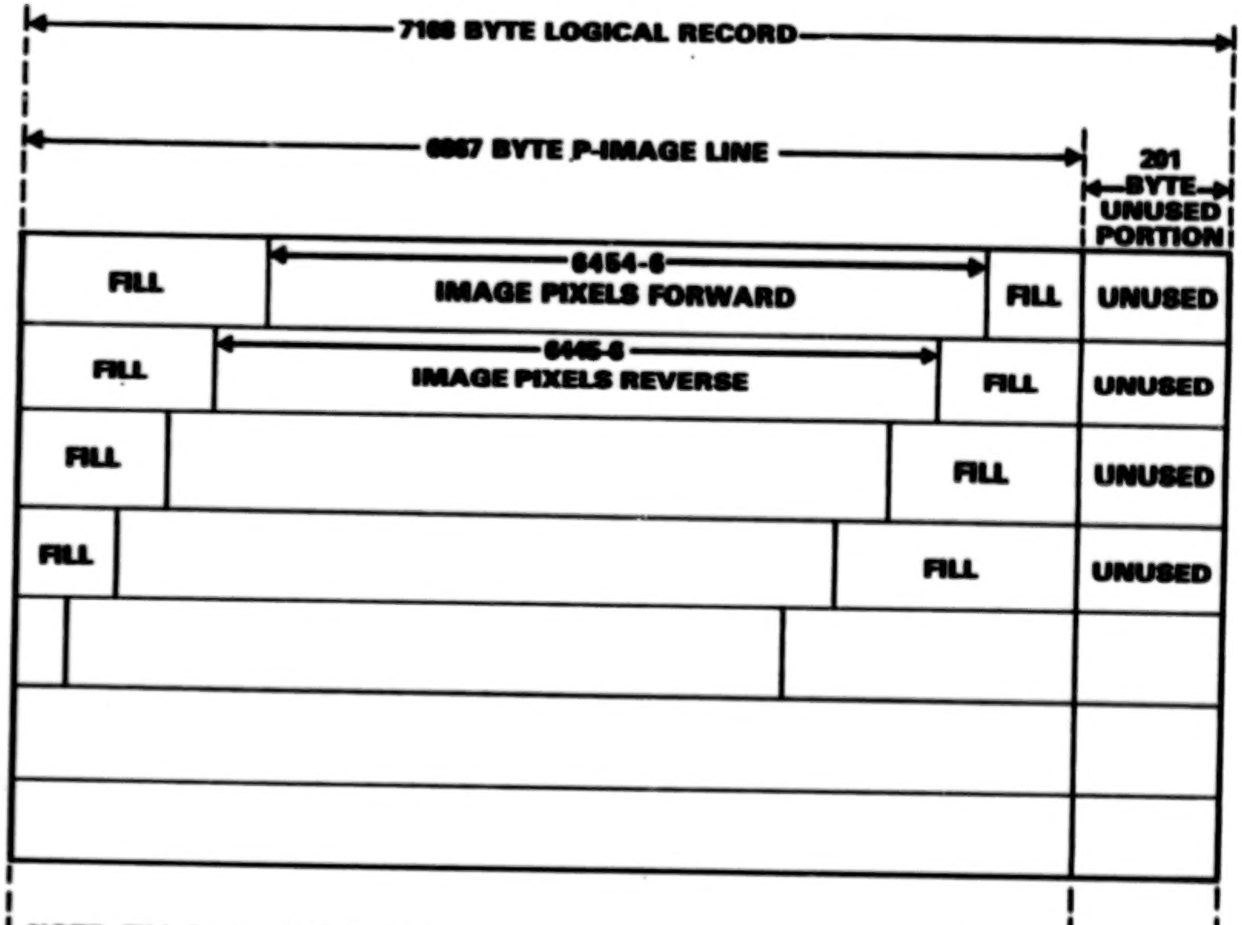
7168 BYTE LOGICAL RECORD
6967 BYTE P-IMAGE LINE
201 BYTE UNUSED PORTION
FILL
6454-6
IMAGE PIXELS FORWARD
FILL
UNUSED
FILL
6445-6
IMAGE PIXELS REVERSE
FILL
UNUSED
FILL
FILL
UNUSED
FILL
FILL
UNUSED

NOTE: FILL DATA ARE ZEROS

Figure 2-29. Image file contents of Landsat-4 TM data in CCT-AT format.

LANDSAT-4 TM APPARENT SPECULAR REFLECTANCE

DETROIT 2 (ID = [illegible] -15413) 25 JULY 1982
SL = 1   SS = 1601

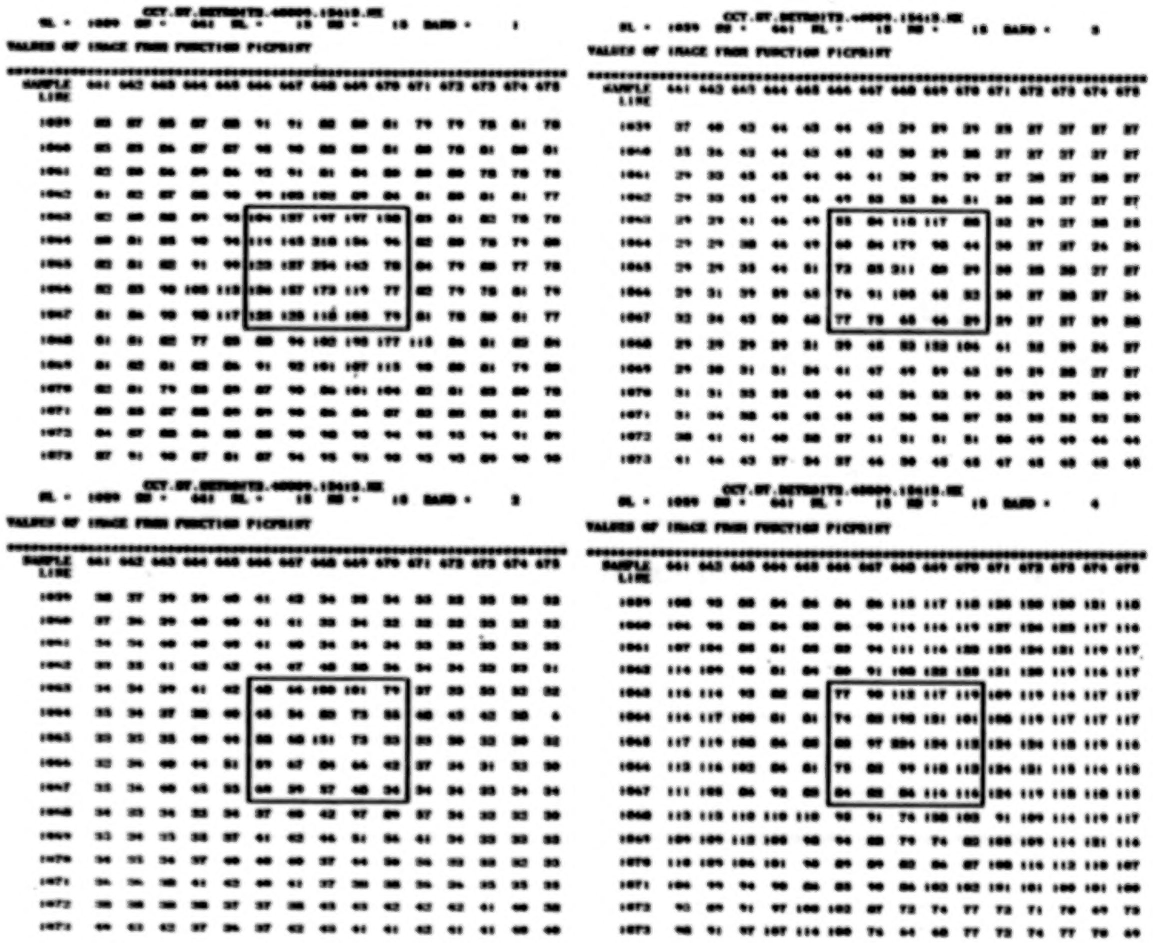

Figure 3-1. An example of spectral reflectivity. The bright pixel is located at relative line number 1065 and sample number 668.

LANDSAT-4 TM-INTERBAND REGISTRATION

PFP

5 x 5 CELL

CCT-BT DETROIT 1

BAND	CENTER	
	l = 2870	s = 1788
1	3.092	2.958
2	3.123	2.933
3	3.155	2.911
4	3.016	3.191
B1—B4	−0.076	0.233

CCT-BT DETROIT 2

BAND	CENTER	
	l = 1065	s = 1768
1	3.088	2.901
2	3.096	2.887
3	3.163	2.767
4	2.946	3.250
B1—B4	0.142	−0.349

Figure 3-2. Interband registration for the primary focal plane.

LANDSAT-4 TM — INTERBAND REGISTRATION — CCT-AT

MEMPHIS TN (ID = 40037-16033) 22 AUG 1982
APPARENT SPECULAR-REFLECTANCE PIXEL
LINE = 3342, SAMPLE = 2519

PRIMARY FOCAL PLANE **7 x 7 CELL**

BAND	CENTER	
	LINE	SAMPLE
1	3.898	3.887
2	3.989	3.954
3	3.821	3.948
4	4.272	4.034
1—4	—0.374	—0.147

COLD FOCAL PLANE

BAND	CENTER	
	LINE	SAMPLE
5	4.077	4.168
7	3.939	4.216
5—7	0.138	—0.048
1—5	—0.179	—0.279

Figure 3-3. Interband registration for a 7-band TM image.

LANDSAT-4 TM—CCT-AT—EMPTY BINS CHANNEL 1 HISTOGRAM

MEMPHIS TN (ID = 40037-16033) 22 AUG 1982

SL = 3001 NL = 63
SS = 2001 NS = 1024

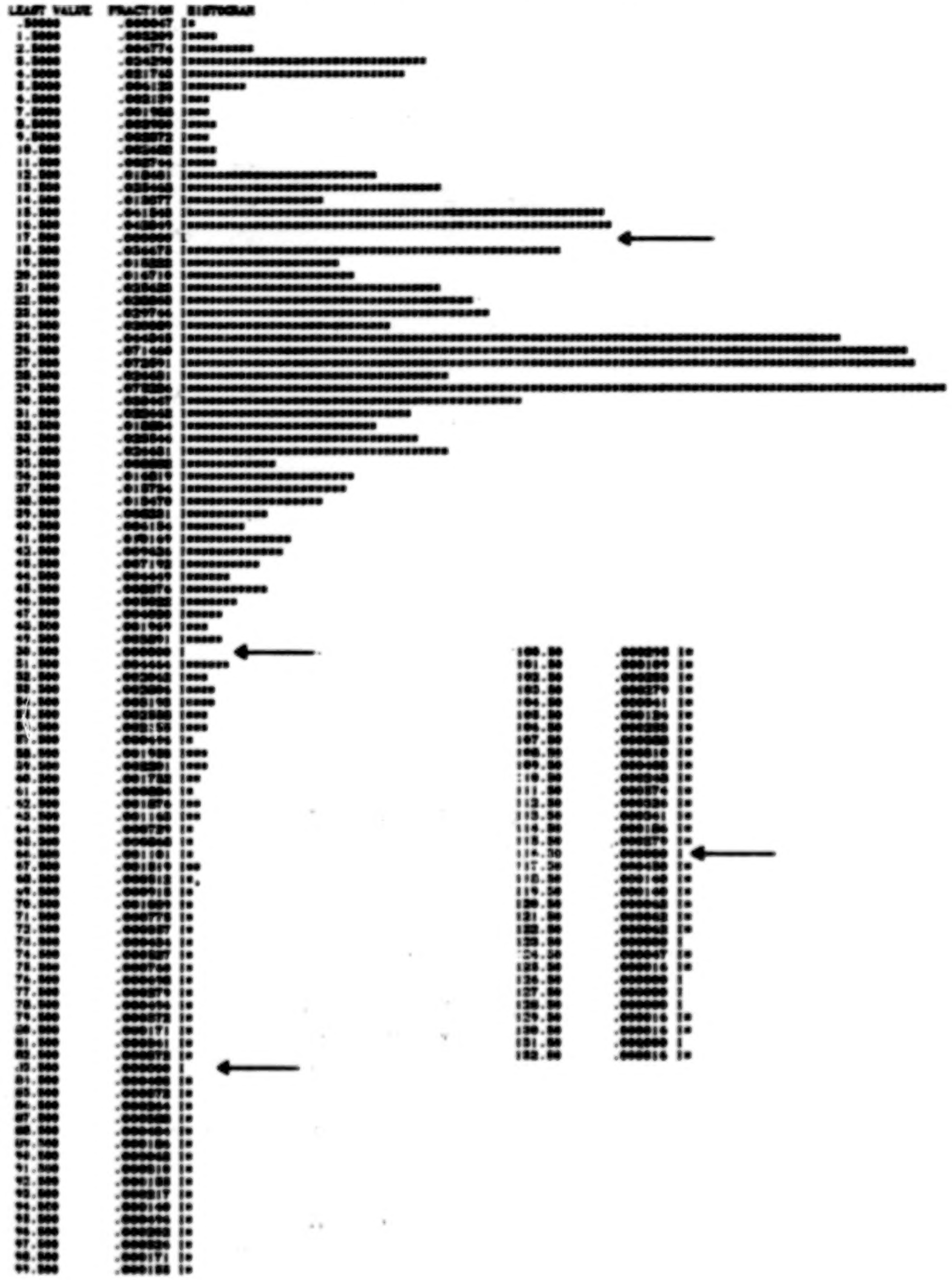

Figure 3-4. An example of a histogram for one data channel showing empty bins at DN values of 18, 51, 84, & 117.

LANDSAT-4 THEMATIC MAPPER
CCT-AT EMPLY BINS

MEMPHIS TN (ID = 40037—16033) 22 AUG 1982
EXAMPLE USING DETECTOR1

BAND	OBSERVED EMPTY BINS	PERIOD
1	79, 132	53
2	29, 74	45
3	39, 94	55
4	39, 117	78
5	47, 99, 151	52
6	—	—
7	18, 51, 84, 117	33

Figure 3-5. An example of empty bin locations and periodicity for data from detector 1, all 7 TM spectral bands.

N85-20513 D5

CANADIAN PLANS FOR THEMATIC MAPPER DATA

W.M. Strome, F.E. Guertin,
A.B. Collins and D.G. Goodenough
Canada Centre for Remote Sensing
2464 Sheffield Road
Ottawa, Ontario, Canada K1A 0Y7

INTRODUCTION

Remote sensing data from satellites are particularly suited for providing information required for resource management and environmental monitoring in a country such as Canada, which has a large geographical area and a relatively low population. Satellite data is especially applicable to remote areas. Because of the importance of this new tool for gathering resource and environmental data, Canada was the first country outside the U.S. to build facilities to receive, record, process and distribute data from the original LANDSAT series. Over the past decade, MSS data have been used extensively to improve the state-of-the-art of resource management and environmental monitoring in Canada for a wide range of application from ice reconnaissance through agriculture and forestry to geological exploration, to name just a few. While the MSS data have been valuable, the limitations of this instrument prevented the achievement of the maximum benefits possible from remote sensing satellite technology in many instances. To improve the quality of data which can be obtained from remote sensing satellites, and thereby improve Canada's resource management capability, it was decided to upgrade our facilities to enable them to receive, record, process, distribute and analyze the Thematic Mapper and MSS data from LANDSAT-4.

LANDSAT-4 MSS

Because of the orbit chosen for LANDSAT-4 as well as changes in the sensor itself, the MSS processing facility required several changes. These were completed in December, 1982. In addition, Canada changed its CCT format to the new Standard Format Family, in order to be compatible with other ground stations, and now supplies all LANDSAT MSS data in that format. The earlier format is no longer supported. However, CCRS has offered to provide assistance to users having difficulty in converting their software in reading the new tape format.

THEMATIC MAPPER RECEPTION

Data from the Thematic Mapper (TM) are transmitted at X-band (compared to S-band for MSS), and have a much higher data rate than that of the MSS. To receive the TM data, the antenna at Prince Albert was modified; an additional feed system installed and a new receiver added. The High Density Digital Tape Recorders (HDDTR) were replaced to permit recording of the higher data rates of TM. These changes were completed in October, 1982. Since that time, the Prince Albert Station has been recording all North American data within its coverage circle (Figure 1). Under an arrangement with NASA, the Prince Albert Station is recording Western U.S. data which cannot be acquired at Greenbelt, MD. In return, NASA is recording Eastern Canadian data which cannot be recorded at Prince Albert. The tapes are exchanged so that each country can process its own data.

TM TRANSCRIPTION SYSTEM

CCRS has developed a transcription system which can convert the HDDT recorded at the receiving station to CCT format. This is required in order to develop the correction algorithms to be used in the TM preprocessing production system. A block diagram of this system is shown in Figure 2. The system, which was completed in December 1982, has limited correction and throughput capabilities. It can transcribe two scenes per week and only provides corrections for detector placements and sampling delays, and for major differences between scan directions. It can also extract the house-keeping data contained in the X-band data stream. At NASA, these data are obtained from a separate low data rate telemetry recorder, which is not used in the Canadian system.

TM BULK PROCESSING SYSTEM

A high throughput (30-40 scenes per day) TM Bulk Processing System (TMBPS) is now under construction to provide system corrected data for distribution to users. This system, for which the block diagram is shown in Figure 3, will be completed by May 1984. The computer used in this system is a DEC VAX-11/780. The data are formatted by a special hardware front end and digital interface. Corrections are performed by an array processor. Curently, a STAR Technology ST-100 is being evaluated for this purpose. There is some concern that this new product may not be available in time to meet our schedule. If this is the case an alternative processor will be considered. A high resolution colour film recorder will be used to generate photographic products. The CCT peripherals are standard 1600/6250 bpi devices.

The design goals of the TMBPS are to provide simple operator interaction instruction; to take data from a HDDT or a CCT; to provide Worldwide Reference System framing; to provide radiometric and along-scan systematic geometric correction; to produce either "raw" or system corrected CCT products in the Standard LANDSAT Ground Station Operators Working Group (LGSOWG) format; to provide black and white or colour film products; and to provide full scene or quarter scene (quadrant) products.

Absolute detector calibration will be provided as well as striping removal and correction for sensor non-linearity. Output to the film recorder will be adjusted for film gamma distortion. Compensation for detector failures will be performed by substitution of data from an adjacent detector. Contrast stretch and corrections for sun angles will also be made.

Corrections will be applied to remove band to band misregistration, detector offsets within a band, forward and reverse scan non-linearity and misregistration and scan line length errors. In addition, geometric errors resulting from earth rotation, altitude changes, panoramic distortion, earth curvature and attitude changes will be corrected to the extent possible with a priori and telemetry data.

MOSAICS

When CCRS began providing users with MSS precision geometrically corrected products, it was decided to adopt a philosophy which differed significantly from that of all other ground station operators. The standard approach was [illegible] produce images which were corrected to match a Space Oblique Mercator Projection, which most closely matched the geometry of the satellite orbit. After a careful survey of Canadian users, it was decided to provide corrected products matching quadrants at standard 1:250,000 scale map sheets, with 50x50 m pixels aligned along the northings and eastings of this projection (Guertin, 1981). This choice made it much easier to combine LANDSAT data with that in existing geocoded data bases. In addition, this choice makes it possible to provide data products which are geometrically independent of the data source. Thus, the geometrically corrected products from LANDSAT-4 MSS match precisely those produced from LANDSAT-1, 2 and 3. Figure 4 depicts the standard platform dependent approach. The MOSAICS system will provide geometrically corrected MSS, TM and SPOT products which match the current MSS data, except for the pixel size, which will be 25x25 m for TM. In this case, four TM pixels cover a single MSS pixel as shown in Figure 5.

A block diagram of MOSAICS is shown in Figure 6. Its configuration is similar to that of the TMBPS with the addition of two work stations which are used for Ground Control Point (GCP) selection and digitizing as well as production control. Indeed, MOSAICS is physically the TMBPS with more hardware and extensive software additions. This system will be completed in 1986.

MOSAICS will provide precision geocoded products which can be corrected for terrain relief where suitable Digital Terrain Models (DTM) are available. Scenes may be corrected using GCPs within the scene or throughout a satellite pass. It will feature extensive quality assessment functions and secure data base archives. Output CCTs will be in the standard LANDSAT Ground Station Operator Working Group (LGSOWG) format. Throughput will be 25 geocoded products per day, 30-40 system corrected products or a mixture of these. In addition, the system will be capable of producing a mosaic using adjacent scenes both along an orbital track and from adjacent orbits. Geometric correction will be to sub-pixel accuracy. In Canada, products will be in the UTM projection and based upon standard map quadrangles. However, the system could be adapted to any standard map projection.

The MOSAICS concept should simplify the task of the user in combining data from different satellites, as well as those from geocoded data bases.

LANDSAT DIGITAL IMAGE ANALYSIS SYSTEM

In order to make effective use of the data from the TM, CCRS is developing a new LANDSAT Digital Image Analysis System (LDIAS). A block diagram of this system is shown in Figure 7. The major design goal of this system is to provide a capability to analyse a full TM scene in the time now required to process a LANDSAT MSS scene on the CCRS Image Analysis System (CIAS), (Goodenough, 1978). This will be achieved using a special pre-processor which will include special hardware functions for image analysis and a powerful array processor as well as image display subsystem with considerable internal processing capabilities. In addition, an Intergraph MAP I[illegible] subsystem will facilitate conversions between raster and vector geocoded data formats to permit effective use of map data in the analysis process, and to provide geocoded data outputs which can be used directly for updating geocoded data bases.

While the hardware and basic software for this system will be completed by the end of 1984, there are several problems which must be solved in order to take full advantage of the higher spatial and spectral resolution as well as the additional bands provided by the TM. Several studies have demonstrated that the application of standard MSS analysis techniques to TM data will often result in poorer classifications than can be achieved with MSS. This is attributed to the reduction of homogeneity with increased spatial resolution. To overcome this difficulty, research and development efforts are required to develop better segmentation algorithms in order to define the areas which contain given materials of interest. Once segments are defined, new algorithms are needed for their classification. Better labelling techniques and methods for use of a *priori* information are also required. Much better use of *textural features* will be required to effectively analyze the higher resolution data from the TM. Also, it will be necessary to determine the level of supervision which is required for different applications.

Research is required to determine effective methods for the integration of multiple pixel data from different satellites and other data sources, and to analyse the resulting high dimensional data sets in an effective manner. More care will be required in correcting the data for geometric and radiometric effects. Appropriate techniques must be developed.

Some of the R&D activities to be undertaken in the LDIAS project will be aimed at improving the geometric and radiometric correction applied to user products from the TMBPS and MOSAICS.

The LDIAS project will not be completed until 1987. However, by early 1984, most of the hardware and standard analysis software will be installed. In addition, the MAP I/O facility will be fully integrated and tested. By early 1985, the high speed processor will be added to the system and plans for incorporating DTM data will be complete. It is expected that the R&D activity leading to the development of effective algorithms for the analysis of high resolution, multidimensional data, such as that obtained with the TM, will be completed by early 1986.

USE OF TM DATA

In preparation for Canada's participation in the LANDSAT-4 program, a cost-benefit study was conducted by A.K. McQuillan (1978) and a Workshop on Canadian Plans for Participation in LANDSAT Follow-On Programs was held (CCRS, 1979). The results of these two reports were summarized by A.K. McQuillan and W.M. Strome (1979).

Most of the advantages of TM data over that for MSS were envisaged to result in improved accuracy in existing applications. However, several applications which are marginal at best with MSS could become practical with TM data. These include, for example, regional land use planning, wetland and intertidal mapping, several geological applications and snow mapping.

At this stage in the evolution of satellite remote sensing technology, it is most important that the users be given high quality products, the analysis tools to take advantage of the increased information in order to offset the costs associated with handling much higher data volumes, and most important of all, the assurance that the data will continue to be available from some source. Without this assurance, operational resource management agencies cannot afford to abandon traditional information gathering methods in favour of the new technology, despite its possible advantages.

REFERENCES

CCRS, (1978) Report on CCRS Workshop on Canadian Plans for Participation in Landsat Follow-on Programs, CCRS, March 1978.

Goodenough, D.G., Strome, W.M., (1978) The Canada Centre for Remote Sensing Image Analysis System (CIAS) CIPS Review, Canada Information Processing Society.

Guertin, F.E., Shaw, E., (1981) Definition and Potential of Geocoded Satellite Imagery Products, 7th Canadian Symposium on Remote Sensing, Winnipeg, pp. 384-394.

McQuillan, A.K., (1978) Application and Potential Benefits of Landsat-D, CCRS Research Report.

McQuillan, A.K., Strome, W.M., (1979) An Evulation of Landsat-D for Canadian Applications, Proceedings of the 13th International Symposium on Remote Sensing of Environment, Ann Arbor, pp. 957-964.

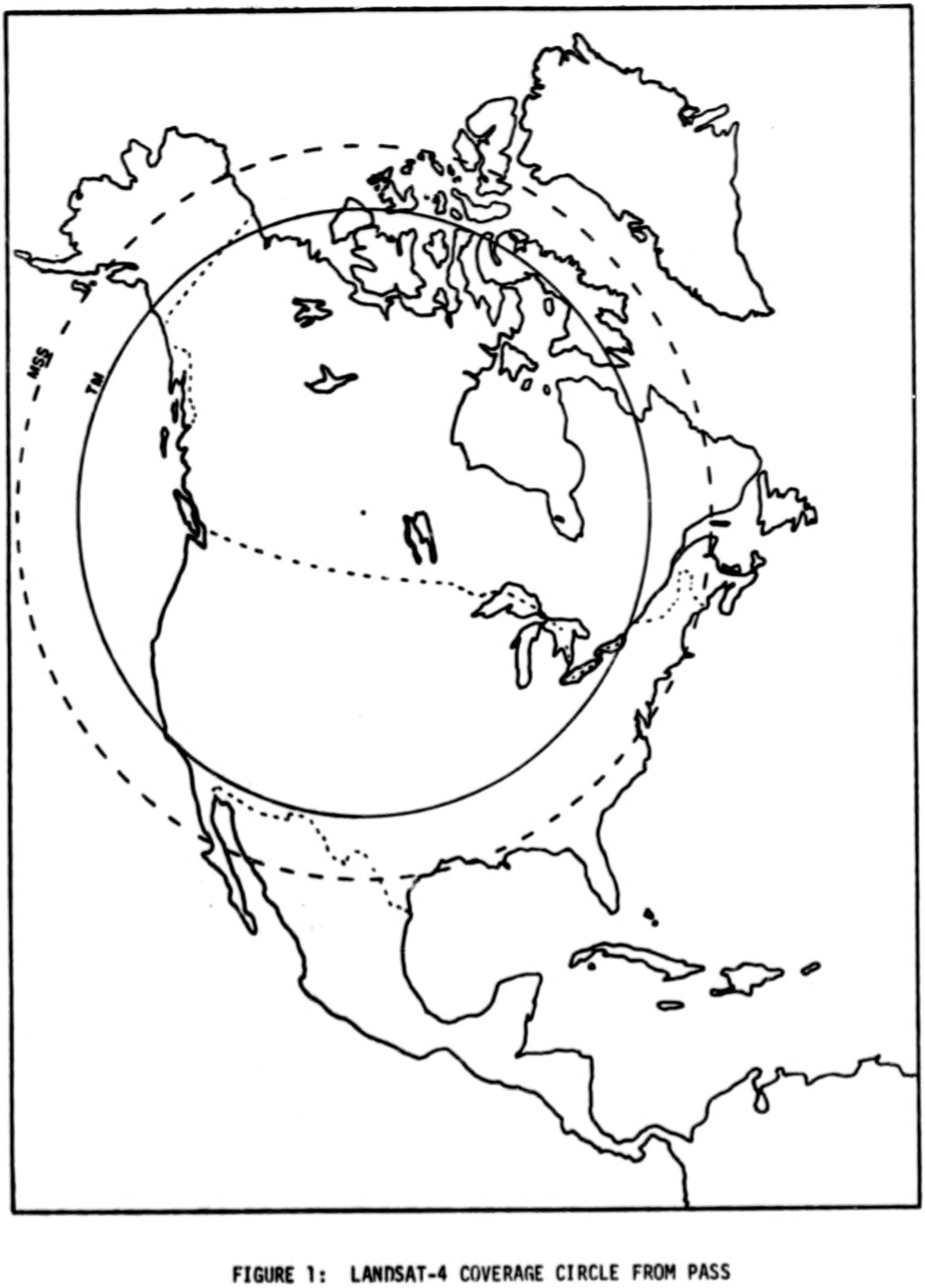

FIGURE 1: LANDSAT-4 COVERAGE CIRCLE FROM PASS

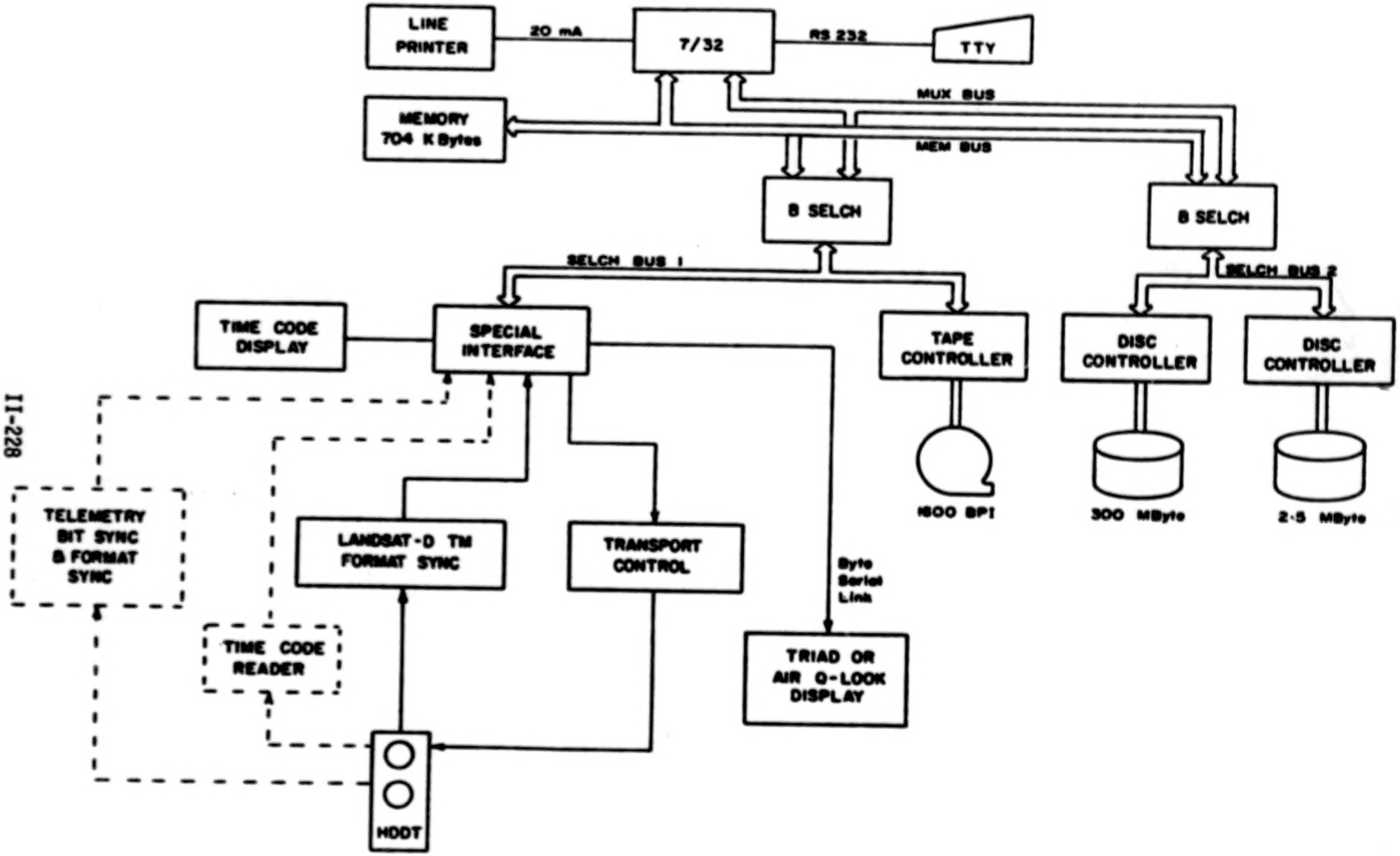
LINE PRINTER
20 mA
7/32
RS 232
TTY
MEMORY 704 K Bytes
MUX BUS
MEM BUS
B SELCH
B SELCH
SELCH BUS 1
SELCH BUS 2
TIME CODE DISPLAY
SPECIAL INTERFACE
TAPE CONTROLLER
DISC CONTROLLER
DISC CONTROLLER
1600 BPI
300 MByte
2·5 MByte
TELEMETRY BIT SYNC & FORMAT SYNC
LANDSAT-D TM FORMAT SYNC
TRANSPORT CONTROL
Byte Serial Link
TIME CODE READER
TRIAD OR AIR Q-LOOK DISPLAY
HDDT

FIGURE 2: THEMATIC MAPPER TRANSCRIPTION SYSTEM

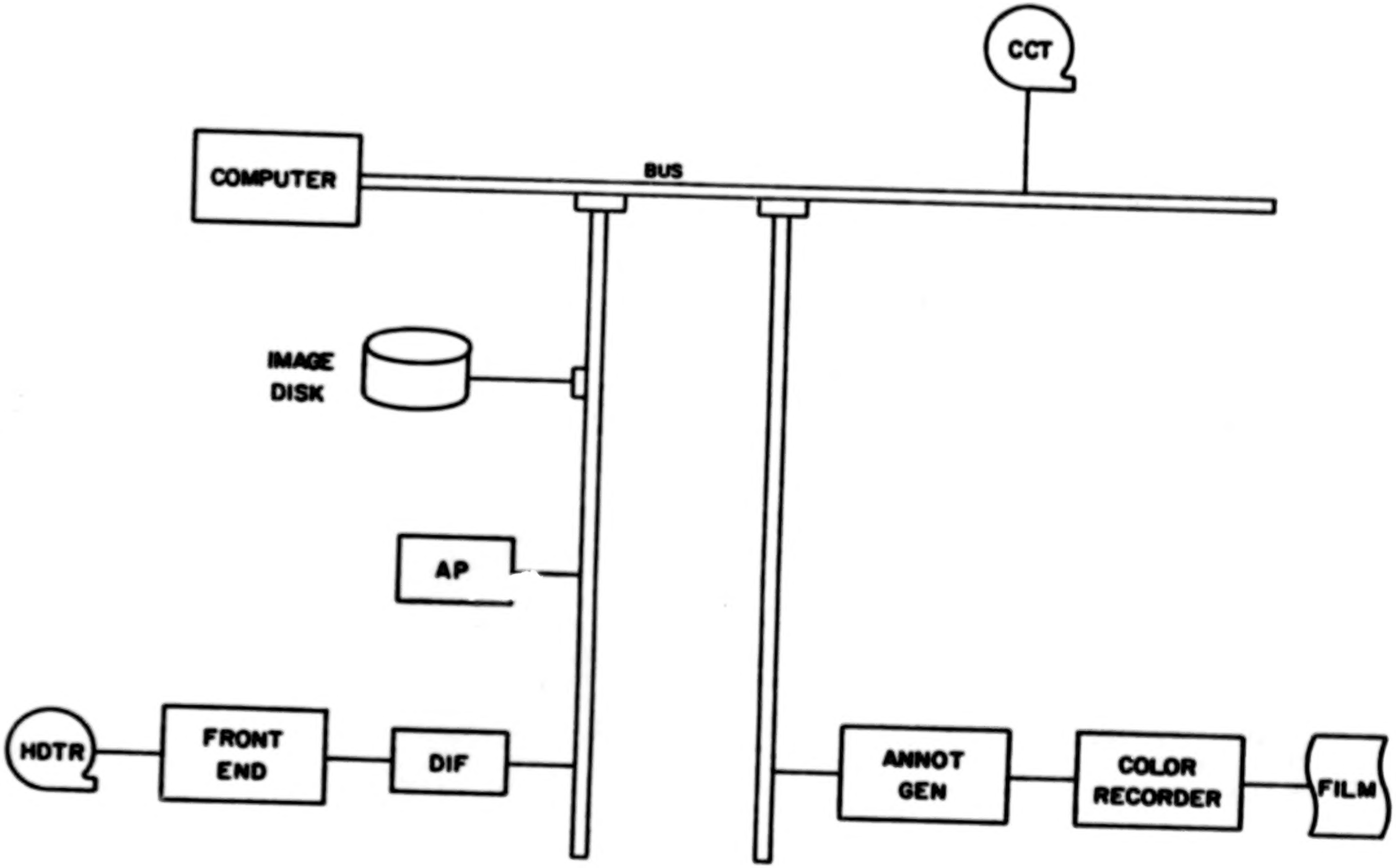
CCT
COMPUTER
BUS
IMAGE DISK
AP
HDTR
FRONT END
DIF
ANNOT GEN
COLOR RECORDER
FILM

FIGURE 3: THEMATIC MAPPER BULK PROCESSING SYSTEM

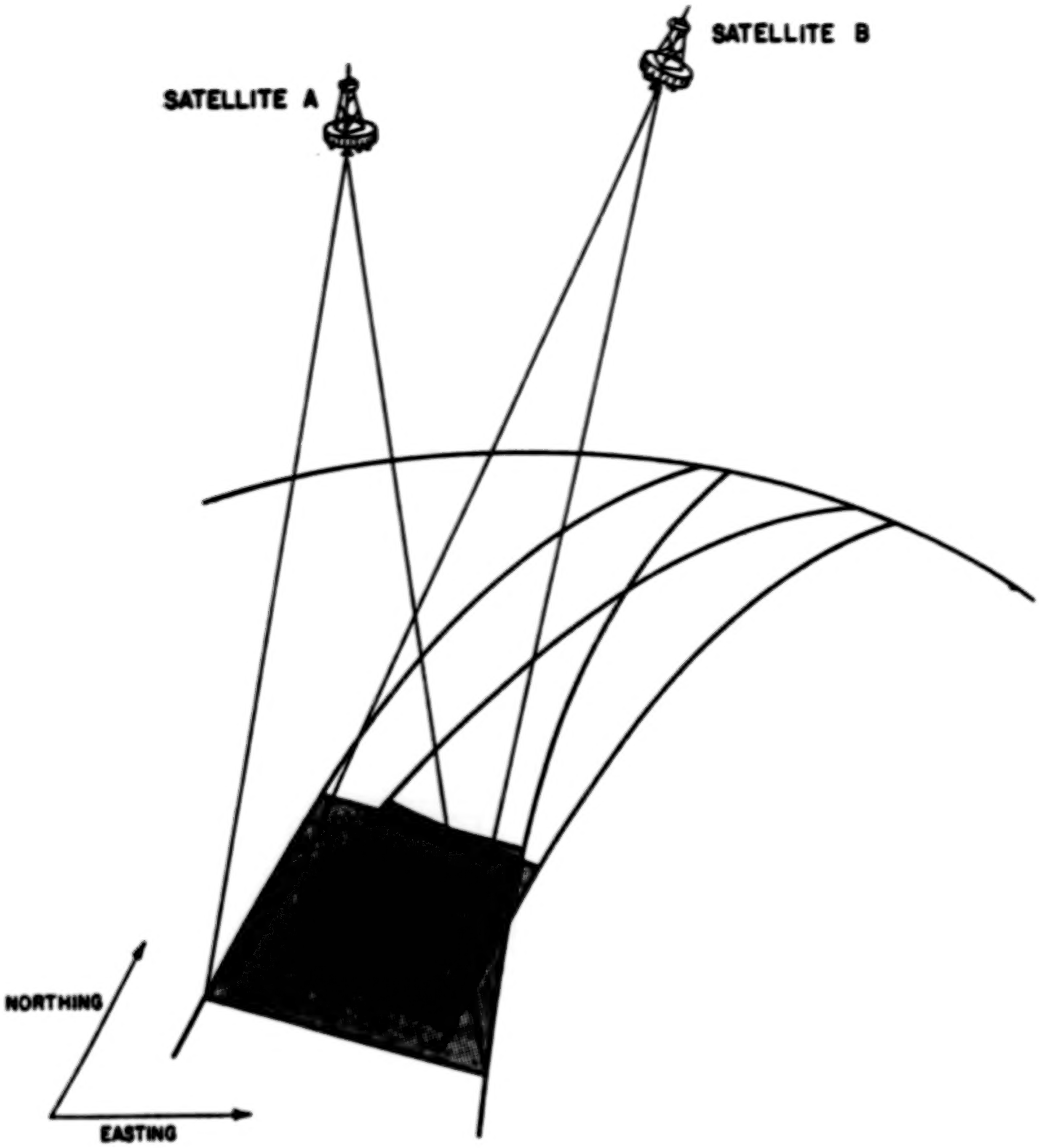
SATELLITE A
SATELLITE B
NORTHING
EASTING

FIGURE 4: MISSION DEPENDENT IMAGERY

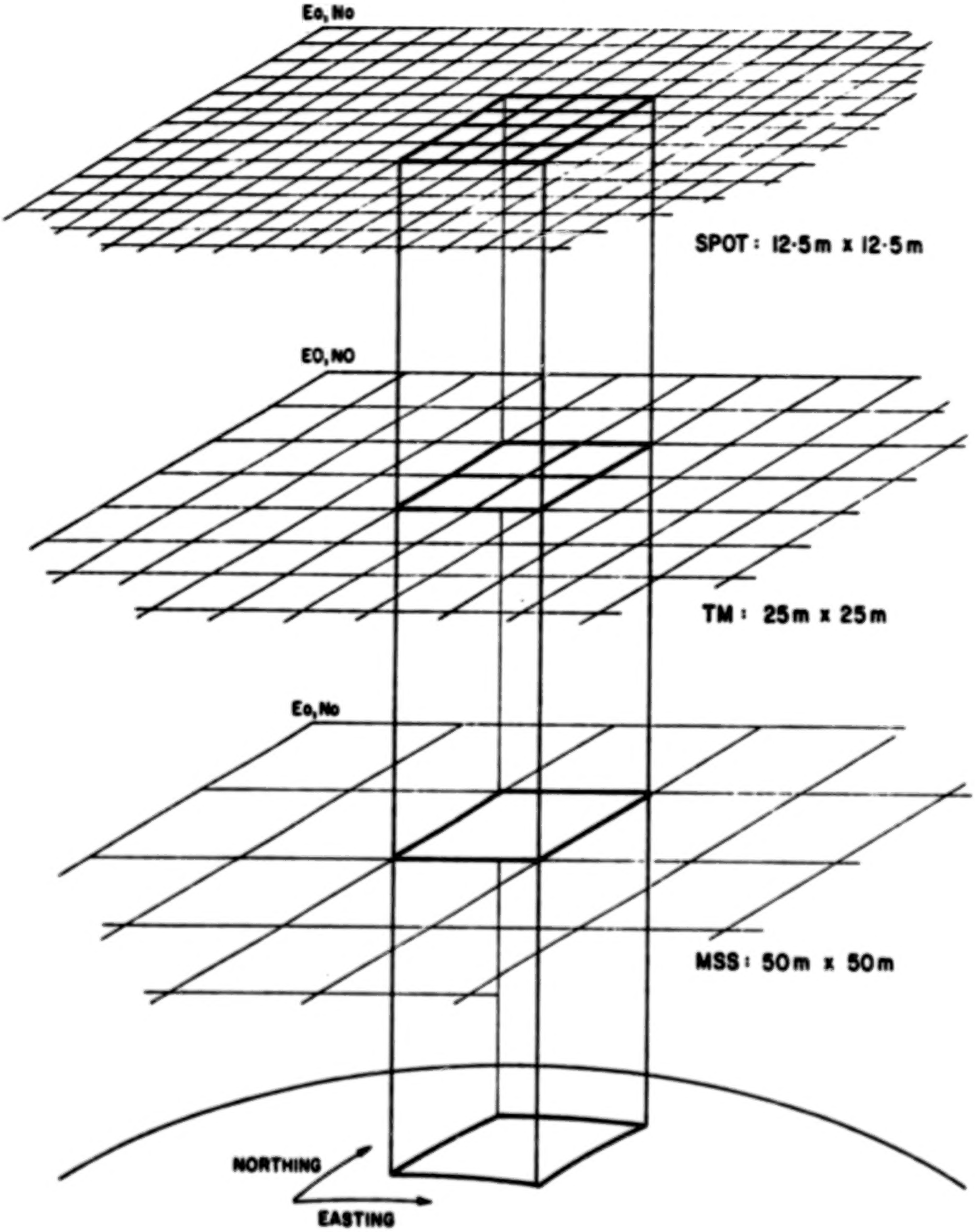
Eo, No
SPOT : 12·5m x 12·5m
EO, NO
TM : 25m x 25m
Eo, No
MSS : 50m x 50m
NORTHING
EASTING

FIGURE 5: GEOCODED IMAGERY

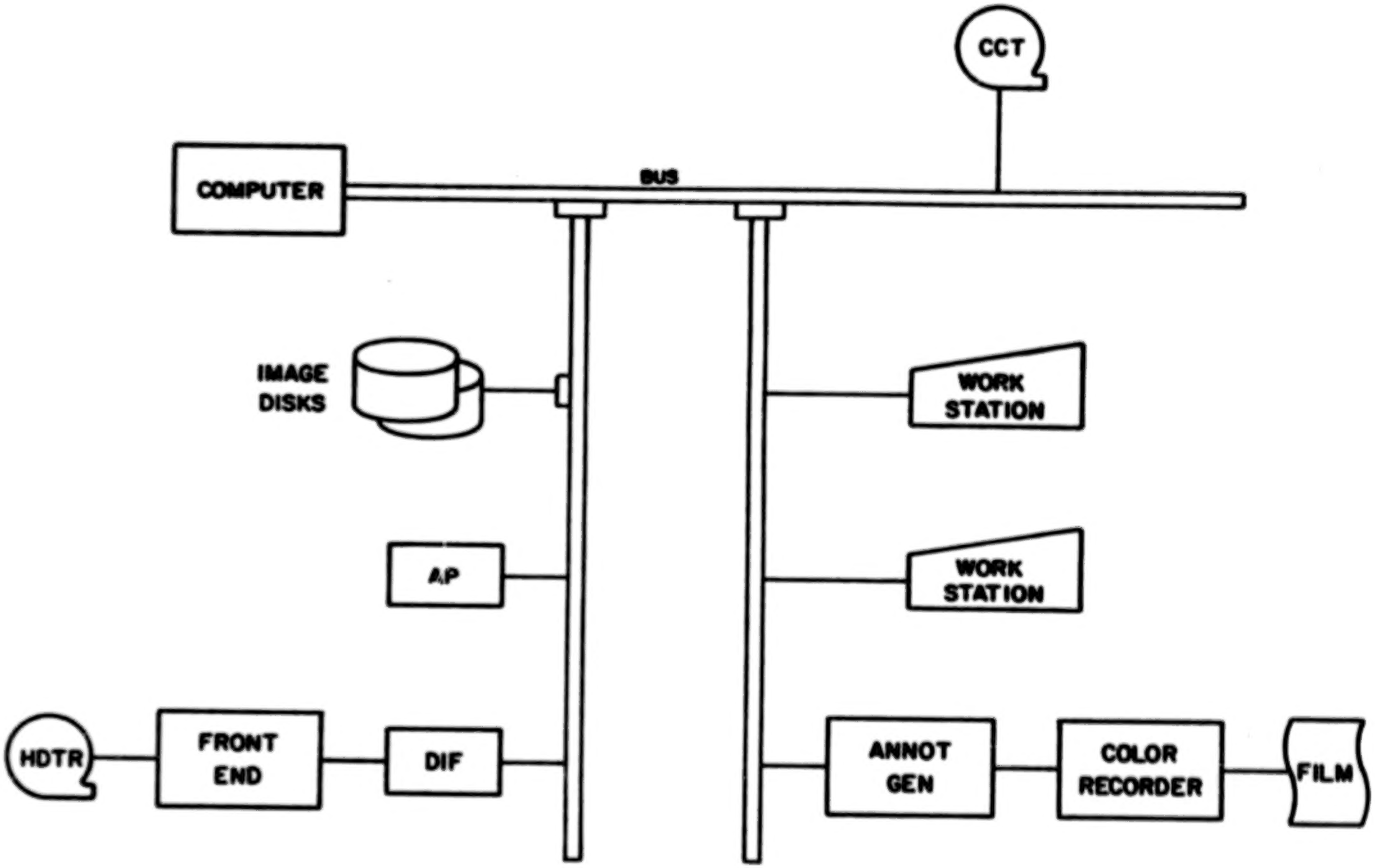
CCT
COMPUTER
BUS
IMAGE DISKS
WORK STATION
AP
WORK STATION
HDTR
FRONT END
DIF
ANNOT GEN
COLOR RECORDER
FILM

FIGURE 6: MOSAICS SYSTEM

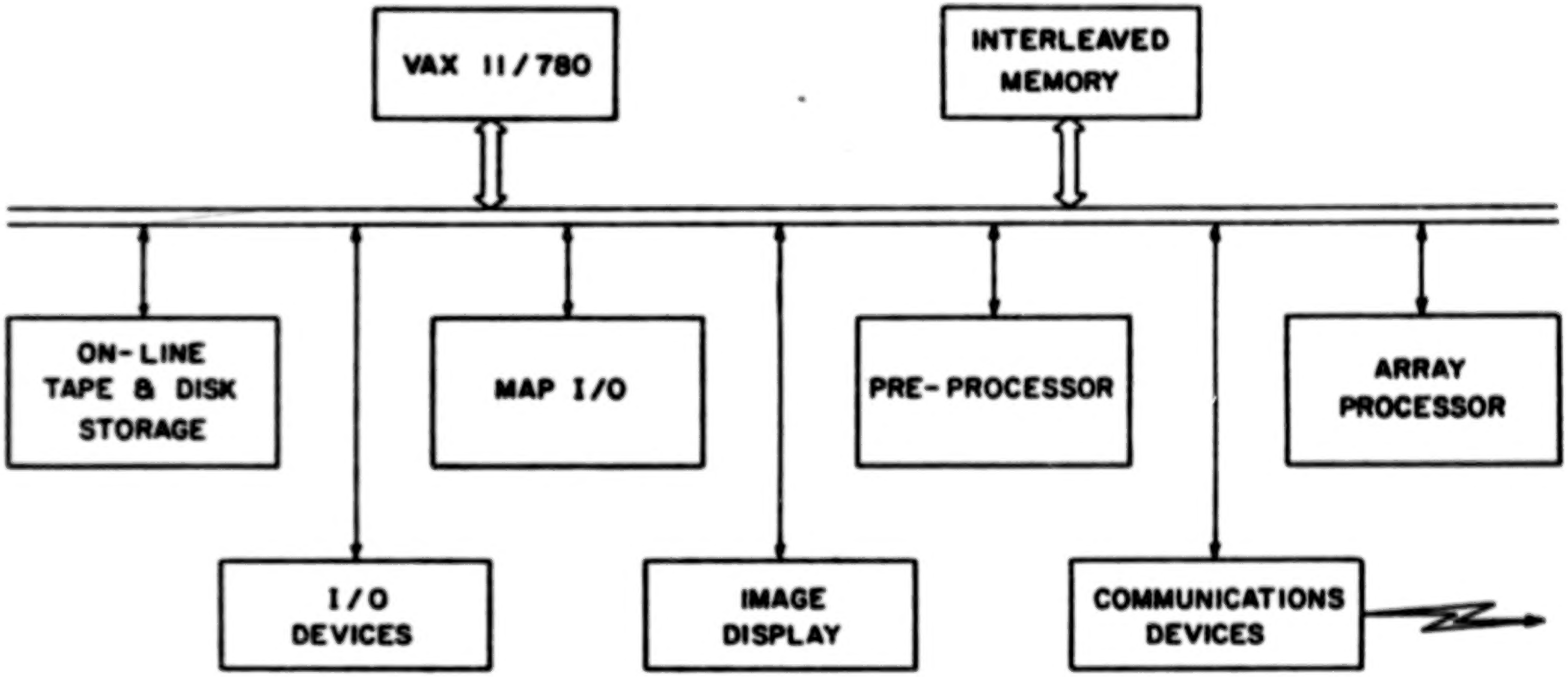
VAX 11/780
INTERLEAVED MEMORY
ON-LINE TAPE & DISK STORAGE
MAP I/O
PRE-PROCESSOR
ARRAY PROCESSOR
I/O DEVICES
IMAGE DISPLAY
COMMUNICATIONS DEVICES

FIGURE 7: LANDSAT DIGITAL IMAGE ANALYSIS SYSTEM

N85-20514 D6

SPECTRAL CHARACTERIZATION OF THE LANDSAT THEMATIC MAPPER SENSORS

Brian L. Markham and John L. Barker
NASA/Goddard Space Flight Center
Earth Resources Branch/Code 923
Greenbelt, MD 20771

INTRODUCTION

The intent of this document is to provide a summary of the information obtained on the spectral characteristics of the two Thematic Mapper (TM) instruments built and tested by Hughes Aircraft Company for the NASA Landsat Program. The first of these two units, the protoflight (TM/PF) model, was integrated into the Landsat-4 satellite, which was launched on 16 July, 1982. The second, the flight (TM/F) unit, has been integrated into the Landsat-4 backup spacecraft, which is scheduled for possible launch in 1985.

Each Thematic Mapper has seven spectral bands. These bands, with their nominal bandpasses are:

1. Blue-green, 450 nm to 520 nm.

2. Green, 520 nm to 600 nm.

3. Red, 630 nm to 690 nm.

4. Near-IR, 760 nm to 900 nm.

5. Mid-IR 1, 1550 nm to 1750 nm.

6. Thermal-IR, 10.4 μm to 12.5 μm.

7. Mid-IR 2, 2080 nm to 2350 nm.

Each reflective band consists of an array of 16 channels; the thermal band consists of four channels. Although there are multiple detectors per band, there is only one filter per band (covering all detectors). This design differs from the MSS where each channel has both an individual detector and

PAGE II-234 INTENTIONALLY BLANK

PRECEDING PAGE BLANK NOT FILMED

filter. The first four bands are located at the primary focal plane of the TM, which is uncooled, and all use monolithic silicon detectors. Bands 5 through 7 are located on the cooled focal plane, which operates at 90°K-105°K. Bands 5 and 7 use monolithic InSb detectors; band 6 uses photoconductive HgCdTe detectors.

NASA placed two sets of specifications related to spectral performance on the instrument. One set of specifications concerned the spectral coverage of the bands. The specifications were on the following parameters (Fig. 1):

1. Lower and upper-band edges--points at 50% of peak relative spectral response (RSR).

2. Lower and upper-edge slopes--widths between specified percentages of maximum spectral response.

3. Spectral flatness--percentage of bandpass within given percentage (10% for reflective bands, 20% for thermal band) of peak response, after dividing out detector slope for silicon detectors.

4. Spurious system response--percentage of response outside 5% RSR points relative to response inside 50% points for solar equivalent input.

The second set of specifications concerned the spectral matching of the channels within each of the reflective bands. It stated that when all channels within a band are calibrated to produce equivalent outputs when viewing the specified flat scene radiances, then the maximum difference in output between channels when all are viewing the specified spectrally sloping scene shall be less than 0.5 percent of the minimum saturation level (Fig. 2).

Hughes developed separate tests to determine compliance with the spectral coverage and spectral matching specifications. In addition, other tests conducted on the TM instruments revealed spectrally related information. Time and program constraints limited the number and detail of the spectral tests conducted, and in general, less spectral data was collected on the TM instruments than on the MSS sensors (Markham and Barker, 1982).

SPECTRAL COVERAGE

Procedures

The primary spectral coverage test* was based on analyses of spectral measurements on the components contributing to the spectral response: filters, detectors and optical surfaces. The overall spectral response for a i^{th} channel was defined as:

$$RSR_{Ai}(\lambda) = \frac{T_{OA}(\lambda)*T_{FA}(\lambda)*R_{Ai}(\lambda)}{K_{Ai}} \quad (1)$$

---

*Hughes Aircraft Company, Santa Barbara Research Center, "TM System Spectral Response," internal memorandum HS236-7213, Jan. 13, 1981; "F-1 TM System Relative Spectral Response," internal memorandum HS236-8162, Nov. 9, 1982.

Where:

$RSR_{Ai}(\lambda)$ = normalized relative spectral response in band A, channel i (percent).

$T_{OA}(\lambda)$ = spectral throughput of the optical system in band A (percent).

$T_{FA}(\lambda)$ = spectral transmission of the filters in band A (percent).

$R_{Ai}(\lambda)$ = relative spectral response of detector i for band A (percent).

K_{Ai} = the normalization factor to bring the peak overall band A, channel i response to 100%.

By measuring the component responses and then calculating the overall spectral response, determination of compliance with the spectral coverage specifications could be facilitated without tying up the TM instrument for the test. Note that the filter and optical responses were band specific, whereas the detector response was channel specific.

The optical system for bands 1-4 consists of five mirror surfaces: the scan mirror, the primary and secondary telescope mirrors and the two mirrors of the scan line corrector (Fig. 3). Bands 5-7 have two additional mirror surfaces and two windows: the relay spherical and folding mirrors and the ambient and dewar windows. The optical components' transmittances and reflectances were measured with a spectrophotometer. Measurements of mirror reflectance were taken on witness samples which were coated concurrently with each mirror. Reflectance measurements were taken at an angle corresponding to use within the system, that is, normal incidence for all but the scan and scan line corrector mirrors, which were measured at a 45 degree angle. Window transmittances were measured on the actual flight parts at a normal angle of incidence. The products of the appropriate set of measurements were used as the optical spectral throughputs for the individual bands.

Each TM band has one filter for all channels within the band (Fig. 4). The small size of each filter made measuring its spectral transmittance difficult, so measurements made on the filter material prior to sizing were used in the calculations of RSR. Filter materials for bands 1-5, 7 were measured at nominal operating temperature. Band 6 filter material could not be measured at operating temperature (90°K-105°K) prior to sizing, and was therefore measured at ambient temperature. Measurements on a piece of witness filter material at ambient and at 90°K were used to determine a factor for converting ambient measurements to 90°K conditions. Both the TM/PF and TM/F used filters cut from the same pieces of filter material, therefore identical filter transmission data were used for both calculations of RSR.

Each TM has 16 silicon photodiode detectors for each of bands 1-4, 16 InSb detectors for bands 5 and 7 and four HgCdTe detectors for band 6 (Fig. 4). The relative spectral responses of three of the TM/PF detectors per band were measured for bands 1-4. Differences between the three detector measurements were deemed to be smaller than the measurement errors, so the average of the three was used to represent all 16 detectors of the TM/PF. As the detector spectral response should theoretically be smooth, a best-fit curve through the averaged measured responses was used in the calculations of RSR. The TM/PF measurements were also used to represent the TM/F detectors as all detector arrays were from the same batch. For bands 5 and 7, one element of "sister" arrays (manufactured from the same wafer as the actual parts) were measured, as the actual parts could not be measured directly. These measurements were used to represent all 16 detectors for both the TM/PF and TM/F. For band 6 in the TM/PF all four detectors were measured and were individually used to make channel-by-channel calculations of RSR. For the TM/F, the odd (1 and 3) channels were similar and the even (2 and 4) channels were similar, and only two calculations were made for band 6.

Thus, with the exception of band 6, RSR's for the TM units were calculated on a band-by-band basis. In addition, again excluding band 6, the same numbers were used for the TM/F as for the TM/PF for the filter and detector responses. In the reflective bands only the differences in the optical surfaces between TM/PF and TM/F affected the calculated RSR's. In band 6, RSR was calculated on a channel-by-channel basis for the TM/PF and with one calculation for the even channels and one for the odd channels for the TM/F.

The one spectral coverage specification not addressed by the RSR calculation was spurious system response. The spurious system response, a measure of out-of-band response, is the integrated response outside the 5% response points relative to inside the 50% response points for solar equivalent input. What was typically used to determine compliance with this specification was the filter vendor's (Optical Coating Laboratory, Inc.) calculations of the integrated spurious filter transmission--with the integration being performed across the nominal range of sensitivity for the detectors, but not considering the detector's response or solar irradiance. For bands 4 and 6, the nominal detector responses and solar irradiances were considered in the calculation and these should give more accurate representations of true out-of-band response.

A limited empirical determination of out-of-band response was also conducted on the TM/F.* Peak responses of the primary focal plane bands to scans of a slit of light passed separately through witness filter pieces of the other bands were recorded.

Results

The results of the RSR calculations are presented in Figures 5-11, along with a comparison of the spectral performance to specifications. In Appendix A the RSR data for TM/PF and TM/F are tabulated (Tables A1-A7). For the reflective bands (1-5, 7) performance was within specifications and near nominal with the following exceptions:

1. Bands 2 and 3 flatnesses were slightly below specifications (<5%), and band 7 flatness was below specifications.

---

*Hughes Aircraft Company, SBRC, "Light Leaks in the Prime Focal Plane Assembly-II," internal memorandum HS236-8163, November 19, 1982.

2. Band 5 upper-band edge was higher than specifications: 1730-1770 nm specified, 1784 nm actual.

3. Band 2 band edges were shifted upward about 9 nm relative to nominal.

4. Band 4, 5 and 7 lower-band edges were 16-18 nm higher than nominal.

The band 5 out-of-specification upper-band edge resulted in the inclusion of a portion of the spectrum affected by atmospheric water absorption. This could contribute to increased sensitivity of the band to atmospheric water content variability. The other variations from specifications are not expected to produce significant data utility impacts. In bands 1-5 and 7 the TM/PF and TM/F responses were similar, with the only differences being apparent in the within-band shape. The differences in within-band shape were due to the only differences in the numbers input to the RSR calculations: optics.

In band 6, the TM/PF and TM/F showed fundamentally different spectral responses. The TM/PF upper-band edge was detector determined at a temperature dependent value of about 11.7 μm; the TM/F upper-band edge was filter determined at 12.43 μm. The TM/PF band 6 was out of specification in terms of the upper band edge, upper-edge slope and flatness. The TM/F band 6 was within specification except for the lower-edge slope which was slightly wide. The principal reason for the 10.4 μm to 12.5 μm bandwidth specification on band 6 was to allow sufficient signal to achieve the 0.5°K radiometric sensitivity requirement. As the TM/PF scanner's band 6 radiometric response was significantly better than specified, the failure to meet the spectral specification was not critical.

The calculated out-of-band responses suggest that all bands are within specifications (Table 1). In most bands the spurious response is simply an indication as to how rapidly the RSR rises from 0% to 5% and drops from 5% to 0%. The bands in general do not contain significant response peaks away from the primary response region. In band 1 there are two minor transmission "peaks" at 800 and 885nm with magnitudes of 0.5% and 0.7%, respectively (Fig. 12). In band 3 there is some transmission in the 950-1100nm range, reaching a peak transmittance of 3% at about 955nm (Fig. 13).

In the empirical test of spurious system response each band gave the highest output to light externally filtered through a piece of its filter material, as expected (Table 2). Also adjacent bands showed some spectral "crosstalk" as their spectral responses overlapped. The only noteworthy out-of-band response occurred in band 1. Band 1 gave a 1.2 count response for a radiance passing through a band 4 filter that produced 115 counts in band 4. This indicates that the two small peaks in the filter transmission of band 1 in the band 4 region result in a 1 count response in band 1 for about every 100 counts in band 4. A comparable impact on band 4 output filtered by a band 1 filter material was not obtained due to the lower gain setting in band 4 and the higher response of silicon in the band 4 region. Note that the impact of the band 3 response at 950-1100 nm was not evaluated in this test as no TM band covered this spectral region. The impact of the band 3 response at 950-1100 nm would be less than the filter transmission indicates, as the relative response of the silicon detectors drops rapidly with increasing wavelength in this region. At 960 nm it is down to about 50% of its peak response at 850 nm and dropping rapidly.

SPECTRAL MATCHING

TM/PF Procedures*

The spectral matching test designed for the TM/PF scanner made use of instrumentation configurations already planned for other tests and data from existing tests, therebylimiting the impact on program scheduling. First, each channel of the TM/PF scanner was calibrated on a 1.22 m integrating sphere of known spectral radiance (Fig. 14). This test, conducted 29-30 June 1981, was a standard calibration test and provided the gainsand offsets for each channel. Then on 8-11 July 1981, a second test, slightly modified to allow for spectral matching data collection, was conducted. In this test, the TM/PF was aligned to the TM calibrator (a collimator and several light sources) (Fig. 14). The output of each channel to the TM calibrator MTF source (a small integrating sphere) was recorded and converted to radiance using the gains and offsets from the first test. The MTF source was filtered for the band 1, 2 and 4 tests. As the large integrating sphere and the MTF light source were spectrally different, this provided a spectral matching test, with the differences in output between channels to the second source indicating the mismatch.

The spectral mismatch was determined as follows:

1. Using the gains and offsets of each channel in a band from the 29-30 June large integrating sphere test, the effective spectral radiance of the calibrator MTF source in each channel was calculated from the 8-11 July test output, e.g. band 1 channel 1:

	Parameter	Units	Value	Source
a.	GAIN	(mux/mw cm^{-2}st$^{-1}\mu$m^{-1})	16.490	29-30 June test
b.	OFFSET	(mux)	1.187	29-30 June test
c.	OUTPUT TO CALIBRATOR	(mux)	146.720	8-11 July test
d.	EFFECTIVE SPECTRAL RADIANCE	(mw/cm^{2}st μm)	8.825	$\frac{(c)-(b)}{(a)}$

2. The channels with the maximum and minimum effective spectral radiances in each band were determined. The difference in their spectral radiances was the spectral mismatch. This difference was expressed as a percentage of the average output of all channels in the band to the calibrator or as a percentage of the minimum saturation level. The first number gave a better measure of the spectral mismatch; the second number was useful for comparing to the specifications.

Although a spectral matching test, this test was not responsive to the original NASA specifications. It somewhat more closely matched a set of spectral matching parameters provided by the Landsat-4 science office (Fig. 15).

---

*Hughes Aircraft Company, SBRC, "Spectral Matching Test Requirement-Supplement to Test BL07," internal memorandum HS236-6922, July 21, 1980.

TM/PF Results

The results of the TM/PF spectral matching tests (Table 3)* showed "spectral mismatches" of up to 6% of signal values (2% of minimum saturation levels), suggesting that either the detectors were poorly matched within bands or the filters had significant local variations in spectral transmittance. Two factors may have caused the indicated spectral mismatches to be greater than the actual values. First, the two tests were conducted about two weeks apart. Although TM detectors are stable relative to MSS photomultipliers, some changes in gains and offsets may have affected the results. Second, measurements of the TM calibrator's MTF spherical integrating source (SIS) indicated significant non-uniformities in illumination. As in the test using the calibrator's SIS, each channel views a different portion of the source, these non-uniformities could have contributed to inflating the spectral mismatches.+ No additional spectral matching tests were performed on the TM/PF to improve the spectral mismatch estimates.

TM/F Procedures†

The spectral matching test was redesigned for the TM/F tests. Data from a 1.22 m integrating sphere test (14 July 1982) were again used to provide the gains and offsets. Then, a new second test, conducted on 15 July 1982 provided the alternate spectral source. In this test a laboratory collimator and a 15 cm integrating sphere replaced the TM calibrator with its spherical integrating source. In addition, a new set of spectral filters was obtained, such that the differences in spectral slopes of the two sources closely approximated the specified differences.

A second modified TM/F spectral matching test was conducted in an attempt to reduce the inflation of the spectral mismatch due to any non-uniformities of this 15 cm integrating sphere. In this test, the same data as before were taken with the filtered source mounted in the collimator and a second set of data was taken with the spectral filter removed. The data, signal levels in MUX, were converted to effective spectral radiance using the 1.22 m sphere calibration. To calculate spectral mismatch, the minimum difference in any channel's output to the two sources was subtracted from the maximum difference in any channels output to give the error quantity, which was then expressed as a percentage of the output or the minimum saturation level. An additional correction was applied to the resultant percentages to account for the fact that the difference in spectra for the collimator with and without filters did not conform to the specified values.

---

*Hughes Aircraft Co., SBRC, "TM PF BL07R Test Result Summary," internal memorandum, HS236-7567, July 23, 1981.

+Hughes Aircraft Co., SBRC, "Protoflight Spectral Matching Performance Revisited," internal memorandum, HS236-7608, August 25, 1981.

†Hughest Aircraft Co., SBRC, "TM Spectral Matching," internal memorandum, HS236-7873, March 1, 1982.

TM/F Results

Results of the first test (Table 4)* were generally "better" than in the TM/PF tests, except in band 4 where the TM/F test was more severe than the TM/PF test. Still, specifications were not indicated as being met in bands 1, 4 and 5. In the second test (Table 5) better performance was indicated, with all but band 4 meeting specifications.

To provide a reference point for the TM/F spectral mismatch results, the spectral mismatches of the five existing MSS sensors were calculated using their measured channel-by-channel relative spectral responses (Norwood et al., 1972; Felkel et al., 1977; Markham and Barker, 1982) for the specified targets (Table 6).+ The TM spectral mismatches fell within the range of MSS mismatches or were somewhat better. Thus, if the TM/F results can also be considered representative of the TM/PF spectral mismatches, no greater spectral striping problems can be expected on the TM than on past MSS's.

---

*Hughes Aircraft Company, SBRC, "Spectral Matching Test Results--Second Revision," internal memorandum, HS236-8084-2, July 21, 1982.

+The output of each MSS channel was calculated as:

$$\mathrm{OUTPUT} = \frac{\sum_{I=a}^{b} SR(I) * RSR(I)}{\sum_{I=a}^{b} RSR(I)}$$

Where:

I - points of RSR measurement
a,b - range of non-zero relative spectral responses for channel
SR(I) - sloped radiance at I for comparable TM Band (mw/cm^2 st μm)
RSR(I) - relative spectral response of channel at I
OUTPUT - output of channel (mw/cm^2 st μm)

The maximum output minus the minimum output equalled the spectral mismatch. This divided by the average output in the band provided the percentage spectral mismatch.

PRIMARY FOCAL PLANT LIGHT LEAKS*

One additional spectrally related characteristic observed on the TM/F was a family of light leaks in the primary focal plane. These leaks were discovered during the spatial coverage testing of the TM/F. The light leaks have the following characteristics:

1. They affect all four bands in the prime focal plane (PFP) and no bands in the cooled focal plane (CFP).
2. They appear as secondary maxima in the scan direction line spread function (Fig. 16).
3. Their position is the same for both the odd and even half bands, (the odd and even detectors are displaced from each other by 2.5 IFOV's) (Table 7). The magnitude of the light leaks is the same for all detectors in a half-band.
4. They are roughly 20 IFOV's (track direction) by 1 IFOV (scan direction) in dimensions.
5. They are white leaks: the light does not pass through the spectral filters, though their relative magnitude does depend on the spectral character of the illumination.

The location and shape of the light leaks suggests they are associated with the gaps between the filter mounts in the primary focal plane (Fig. 4). The gaps between the filter mounts and the slots between the individual band assemblies do not perfectly coincide. This may be allowing light to scatter into the detectors. Note that the PFP diagram is for the TM/PF, whereas the light leak data is the TM/F. It is believed that the TM/PF has comparable leaks, though not exactly at the same locations and of the same magnitudes. Also note that the worst measured light leak was about 1% of the detector's response, though this percentage would be greater when the detector is centered on a dark target and the light leaks are centered on a neighboring bright area.

SUMMARY

Spectral coverage for the TM/PF and TM/F instruments was determined by analyses of spectral measurements of the optics, filters and detectors. Individual channel relative spectral responses were not measured. In the reflective bands, optics accounted for the only differences between the TM/PF and the TM/F, and the calculated spectral responses were similar. The only significant deviation from specifications in the reflective bands was the band 5 upper-band edge which extended to 1784 nm into an atmospheric water absorption region. In band 6 (emissive thermal) the TM/PF and TM/F had fundamentally different spectral responses. The TM/PF upper-band edge was lower than specifications, however the detectors were sufficiently sensitive to exceed the 0.5^{o}K radiometric specification, so the narrower bandwidth was not critical. The TM/F met the upper-band edge specification, as well as the radiometric specification, but was less sensitive overall.

---

*Hughes Aircraft Co., SBRC, "Light Leaks in the Prime Focal Plane Assembly-II," internal memorandum, HS236-8163, November 19, 1982.

Band 1 and band 3 filters had minor transmission peaks in the near-IR region: 0.5% and 0.7% at 800 nm and 885 nm respectively for band 1, 2.8% and 1.2% at 945 nm and 1000 nm respectively for band 3.

Satisfactory spectral matching data for the TM/PF was never obtained. The TM/F spectral matching data indicated within specification performance ($<0.5\%$) for all but band 4 (1.7%). Comparison to MSS performance indicated TM performed comparably or better than MSS's in spectral matching.

Several minor leaks were detected in the TM/F prime focal plane. The odd channels of band 1 (magnitude of the light leaks comparable for all detectors in a half band), had the largest light leaks. In the band 1 odd channels, with the TM calibrator 'white' light source, a light leak at 13.1 IFOV along scan off the detector center made about a 1% contribution to the signal. The location and shape of the light leaks suggests that they are associated with the slots at the sides of the individual band assemblies. It is believed the TM/PF has comparable light leaks.

ACKNOWLEDGEMENTS

This paper is based solely on data obtained from Hughes/SBRC. This data has been provided along with generous assistance in interpretation by R. W. Cline, J. C. Lansing and D. G. Brandshaft. The assistance of Sy Lee and Ronald Achenbach in data entry and presentation is also greatly appreciated.

REFERENCES

Felkel, E. O., K. Brinkman, R. Coon, and J. Stivers, 1977, "Five-Band Multi-Spectral Scanner--Final Report," Hughes Aircraft Co., Final Report for NASA contract NAS5-11255.

Markham, B. L., and J. L. Barker, 1982, "Spectral Characterization of the Landsat-D Multispectral Scanner Subsystems," NASA TM-83955, NASA/GSFC, Greenbelt, MD, 45 pp.

Norwood, V. T., L. R. Fernelia and G. A. Tadler, 1972, "Multispectral Scanner System for ERTS-Four-Band Scanner System, Final Report," NASA CR-132758, NASA/GSFC, Greenbelt, MD.

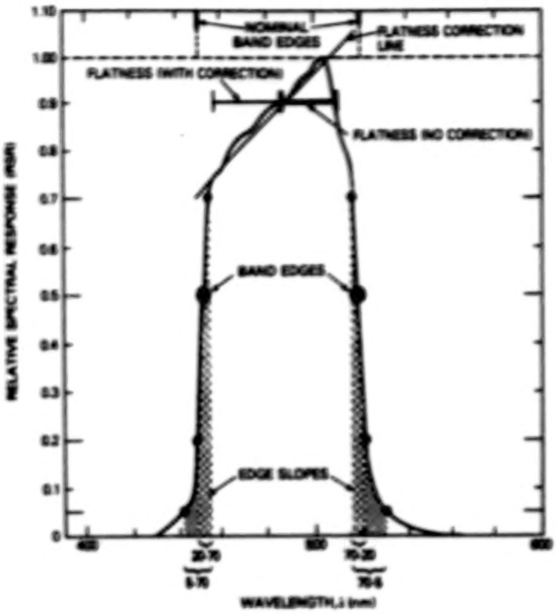

Figure 1. Spectral coverage parameters under specification for TM bands 1-4. The bands 5-7 specifications were on the 5-75% edge slope and the band 6 flatness specification was at 80% RSR.

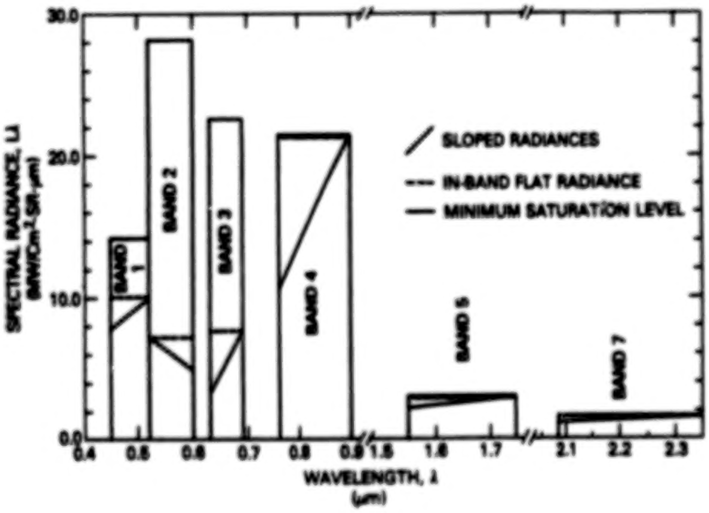

Figure 2. Spectral matching requirements for the Thematic Mapper reflective bands. When all channels within a band are calibrated to produce equivalent outputs when viewing the specified flat scene radiance, then the maximum difference in output between channels when all are viewing the spectrally sloping scene shall be less than 0.5 percent of the minimum saturation level.

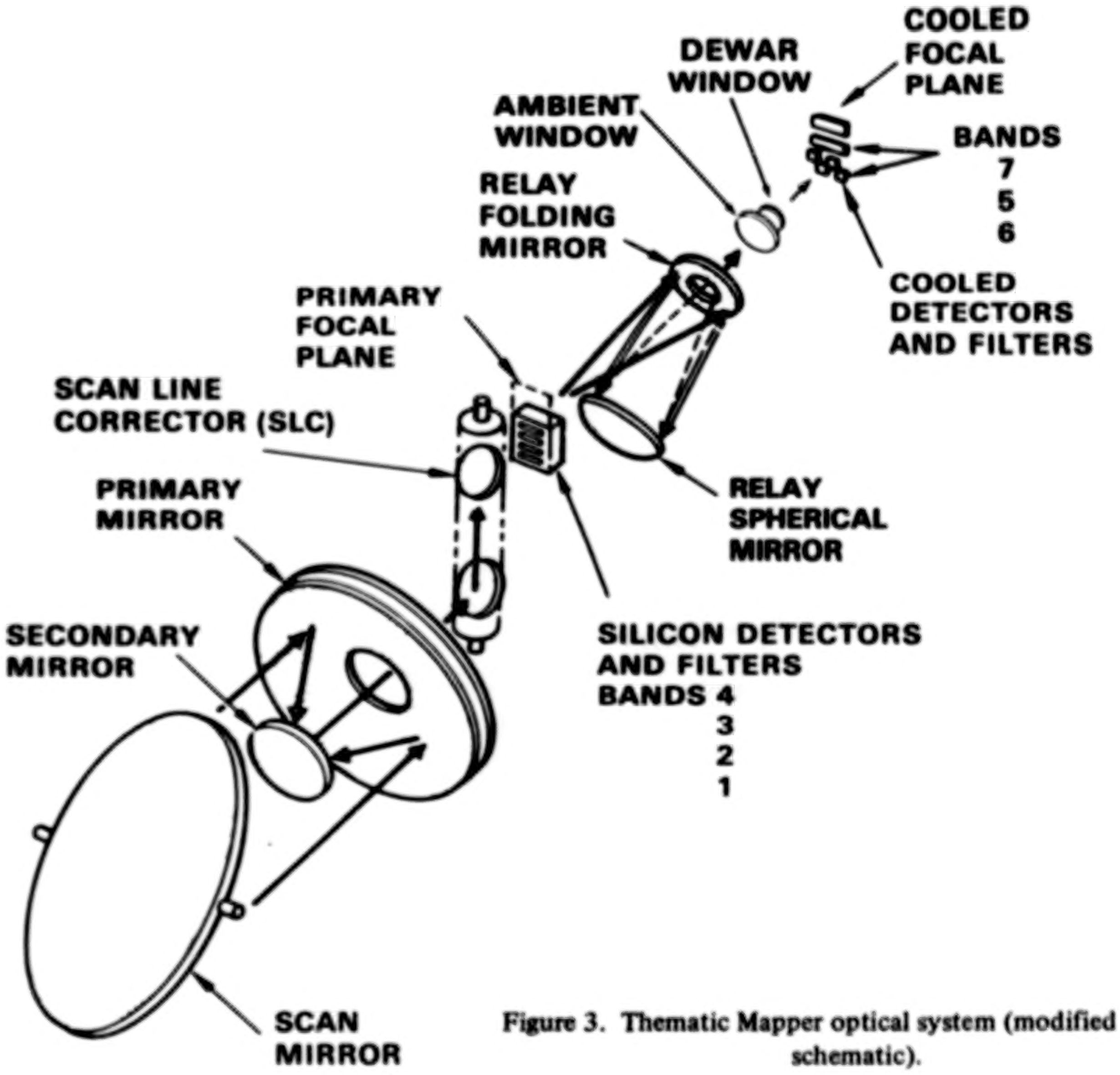
COOLED FOCAL PLANE
DEWAR WINDOW
AMBIENT WINDOW
BANDS 7 5 6
RELAY FOLDING MIRROR
COOLED DETECTORS AND FILTERS
PRIMARY FOCAL PLANE
SCAN LINE CORRECTOR (SLC)
PRIMARY MIRROR
RELAY SPHERICAL MIRROR
SECONDARY MIRROR
SILICON DETECTORS AND FILTERS BANDS 4 3 2 1
SCAN MIRROR

Figure 3. Thematic Mapper optical system (modified Hughes schematic).

ORIGINAL PAGE IS
OF POOR QUALITY

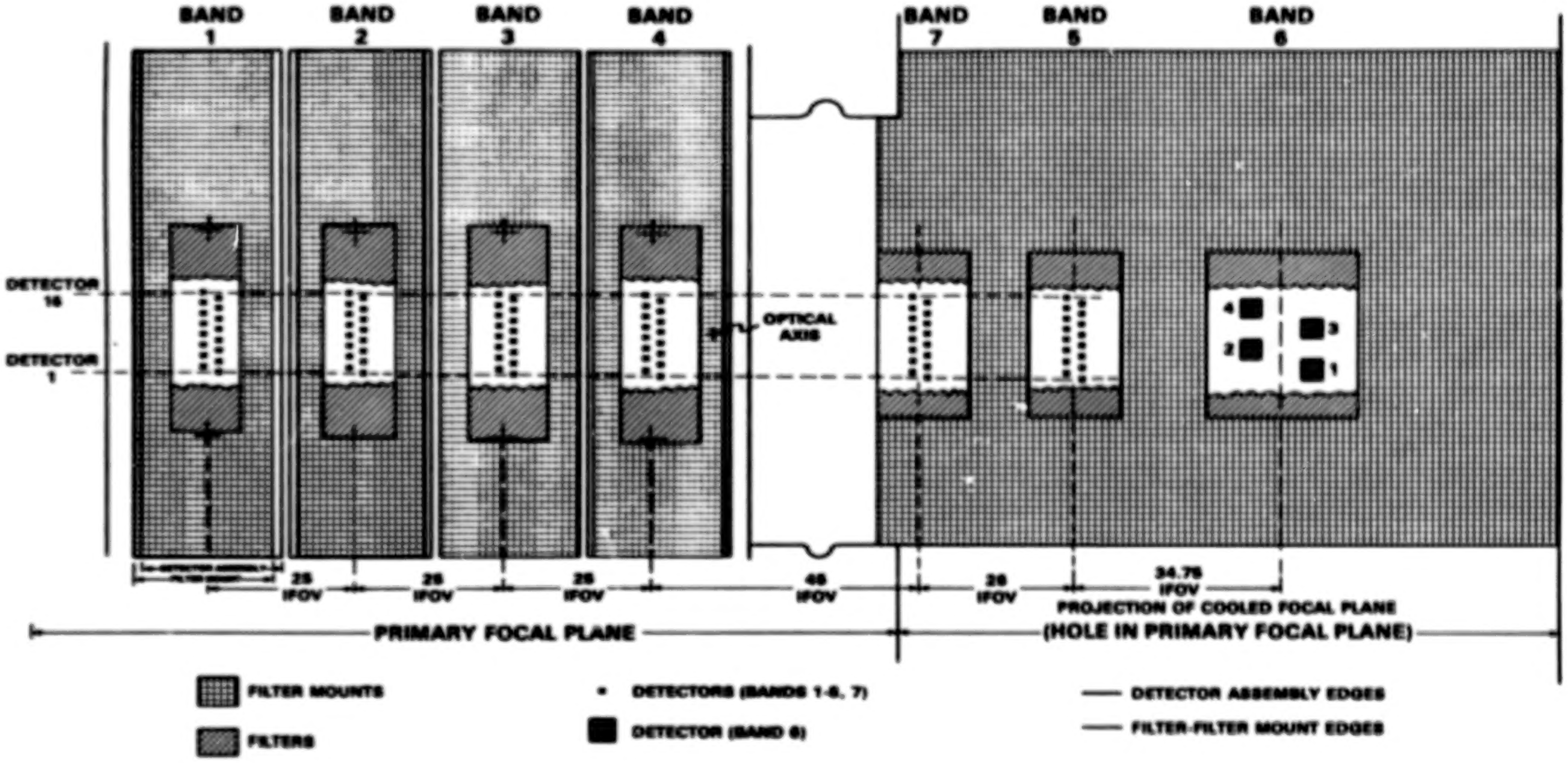
BAND 1
BAND 2
BAND 3
BAND 4
BAND 7
BAND 5
BAND 6
DETECTOR 16
DETECTOR 1
OPTICAL AXIS
1
2
3
4
25 IFOV
25 IFOV
25 IFOV
45 IFOV
25 IFOV
34.75 IFOV
PRIMARY FOCAL PLANE
PROJECTION OF COOLED FOCAL PLANE
(HOLE IN PRIMARY FOCAL PLANE)
FILTER MOUNTS
FILTERS
DETECTORS (BANDS 1-5, 7)
DETECTOR (BAND 6)
DETECTOR ASSEMBLY EDGES
FILTER-FILTER MOUNT EDGES

Figure 4. TM/PF primary focal plane and projection of cooled focal plane at primary focal plane.

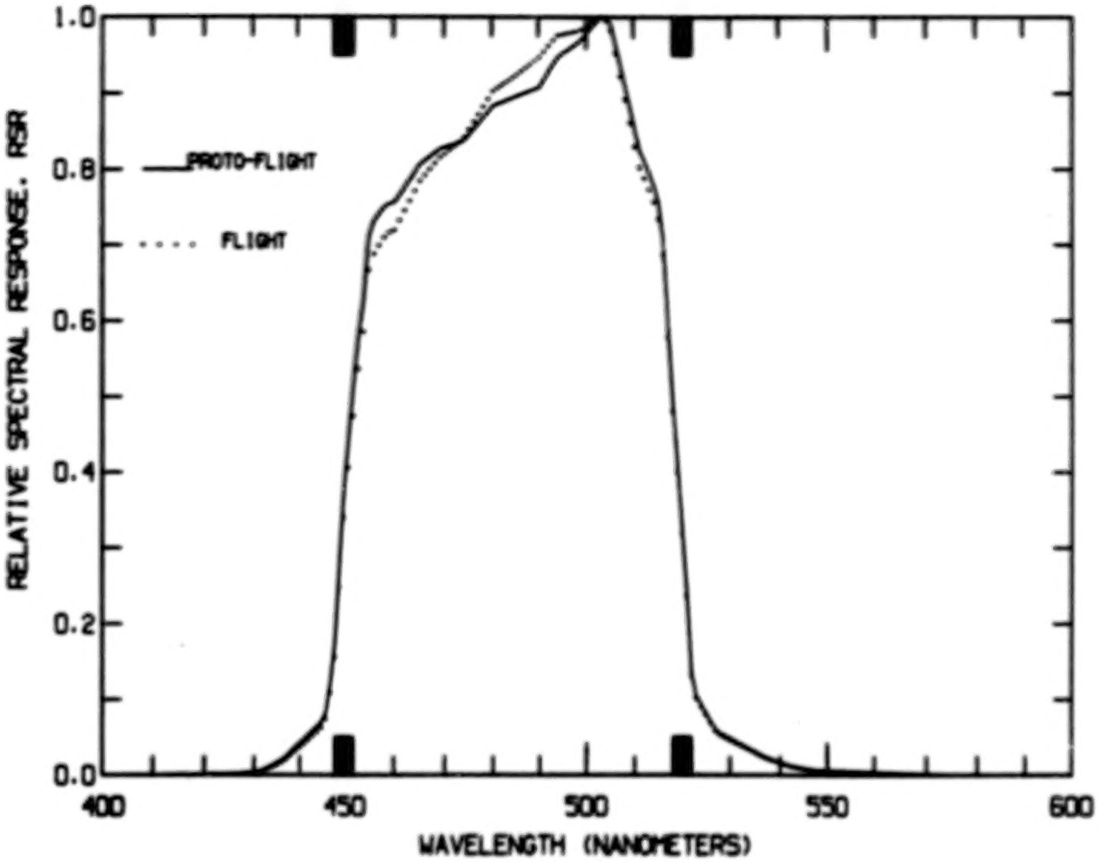

SPECTRAL PARAMETER	SPECIFICATION	PROTOFLIGHT	FLIGHT
LOWER BAND EDGE (nm)	450 ± 10	452	452
UPPER BAND EDGE (nm)	520 ± 10	518	518
LOWER BAND EDGE SLOPE (nm)			
20% TO 70%	20 (MAX)	7	8
5% TO 70%	30 (MAX)	14	15
UPPER BAND EDGE SLOPE (nm)			
70% TO 20%	20 (MAX)	5	6
70% TO 5%	40 (MAX)	14	14
FLATNESS (%)	–	32	42
WITH LINEAR CORRECTION	75 (MIN)	78	76

Figure 5. Thematic Mapper spectral performance – band 1.

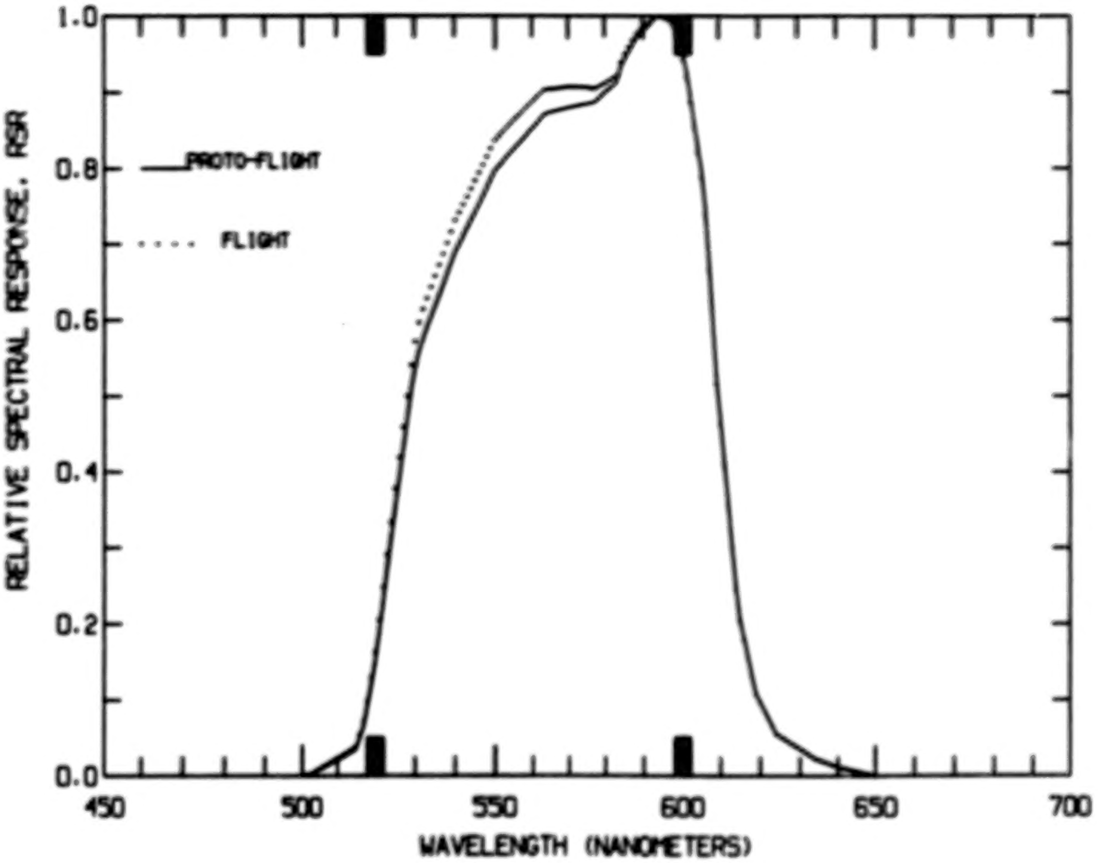

SPECTRAL PARAMETER	SPECIFICATION	PROTOFLIGHT	FLIGHT
LOWER BAND EDGE (nm)	520 ± 10	529	528
UPPER BAND EDGE (nm)	600 ± 10	610	610
LOWER BAND EDGE SLOPE (nm)			
20% TO 70%	20 (MAX)	20	17
5% TO 70%	30 (MAX)	25	22
UPPER BAND EDGE SLOPE (nm)			
70% TO 20%	20 (MAX)	9	9
70% TO 5%	40 (MAX)	19	18
FLATNESS (%)	–	26	48
WITH LINEAR CORRECTION	75 (MIN)	$\boxed{71}$ *	$\boxed{72}$ *

*OUT OF SPECIFICATION

Figure 6. Thematic Mapper spectral performance – band 2.

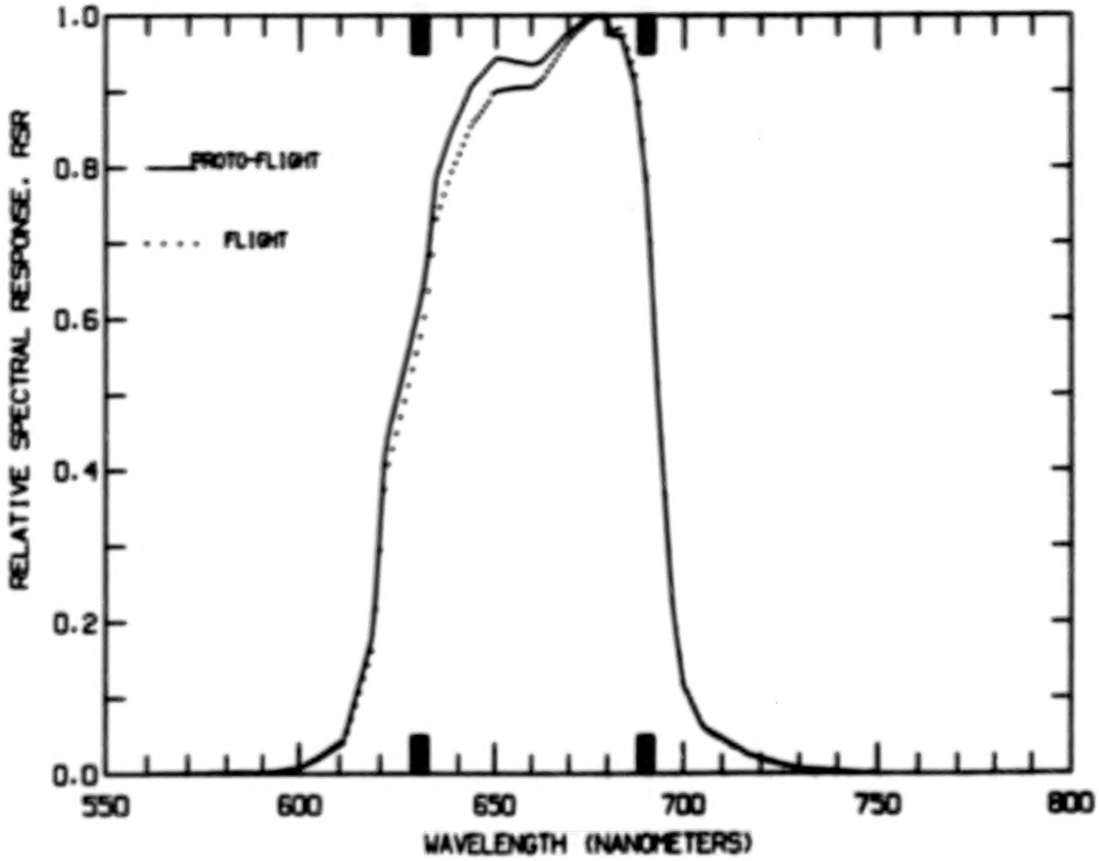

SPECTRAL PARAMETER	SPECIFICATION	PROTOFLIGHT	FLIGHT
LOWER BAND EDGE (nm)	630 ± 20	624	626
UPPER BAND EDGE (nm)	690 ± 10	693	693
LOWER BAND EDGE SLOPE (nm)			
20% TO 70%	20 (MAX)	14	15
5% TO 70%	30 (MAX)	21	22
UPPER BAND EDGE SLOPE (nm)			
70% TO 20%	20 (MAX)	7	6
70% TO 5%	40 (MAX)	18	18
FLATNESS (%)	–	65	56
WITH LINEAR CORRECTION	75 (MIN)	$\boxed{71}$ *	$\boxed{73}$ *

*OUT OF SPECIFICATION

Figure 7. Thematic Mapper spectral performance – band 3.

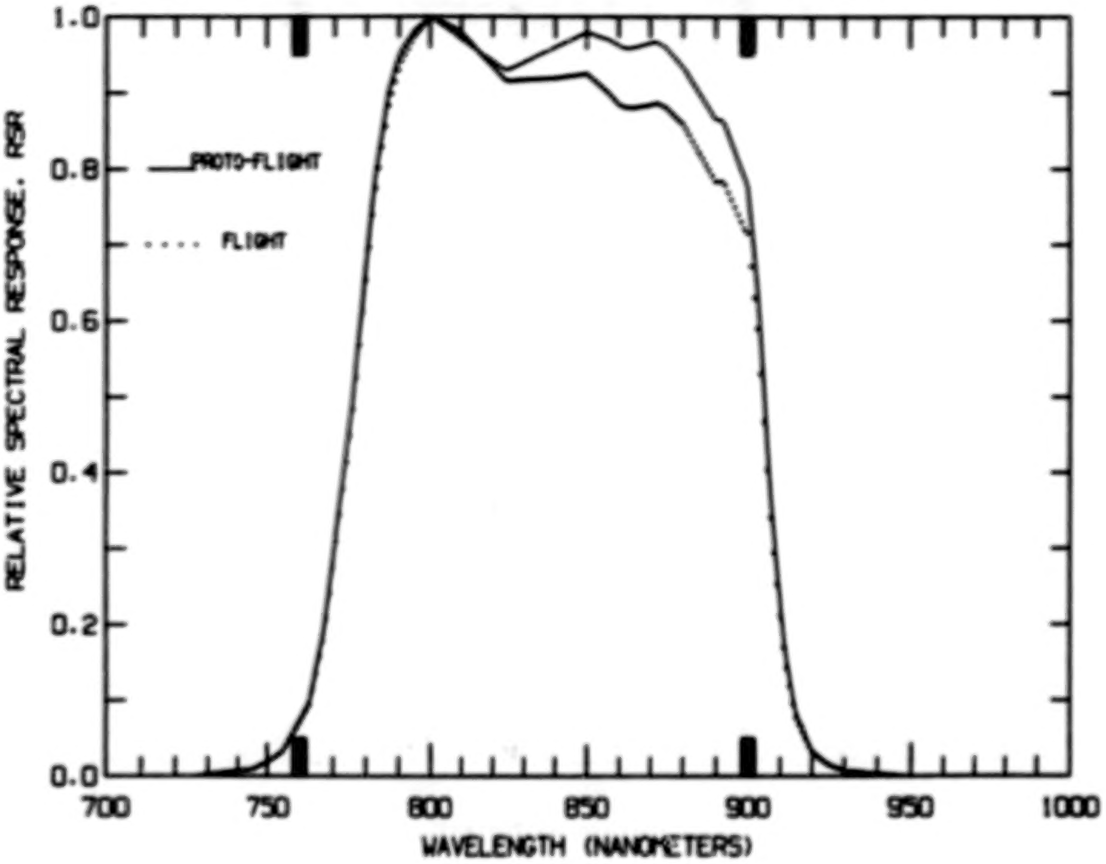

SPECTRAL PARAMETER	SPECIFICATION	PROTOFLIGHT	FLIGHT
LOWER BAND EDGE (nm)	760 ± 20	776	776
UPPER BAND EDGE (nm)	900 ± 10	905	904
LOWER BAND EDGE SLOPE (nm)			
20% TO 70%	20 (MAX)	13	13
5% TO 70%	30 (MAX)	23	24
UPPER BAND EDGE SLOPE (nm)			
70% TO 20%	30 (MAX)	9	10
70% TO 5%	40 (MAX)	17	18
FLATNESS (%)	–	76	53
WITH LINEAR CORRECTION	75 (MIN)	†	81

†NO CORRECTION NEEDED

Figure 8. Thematic Mapper spectral performance – band 4.

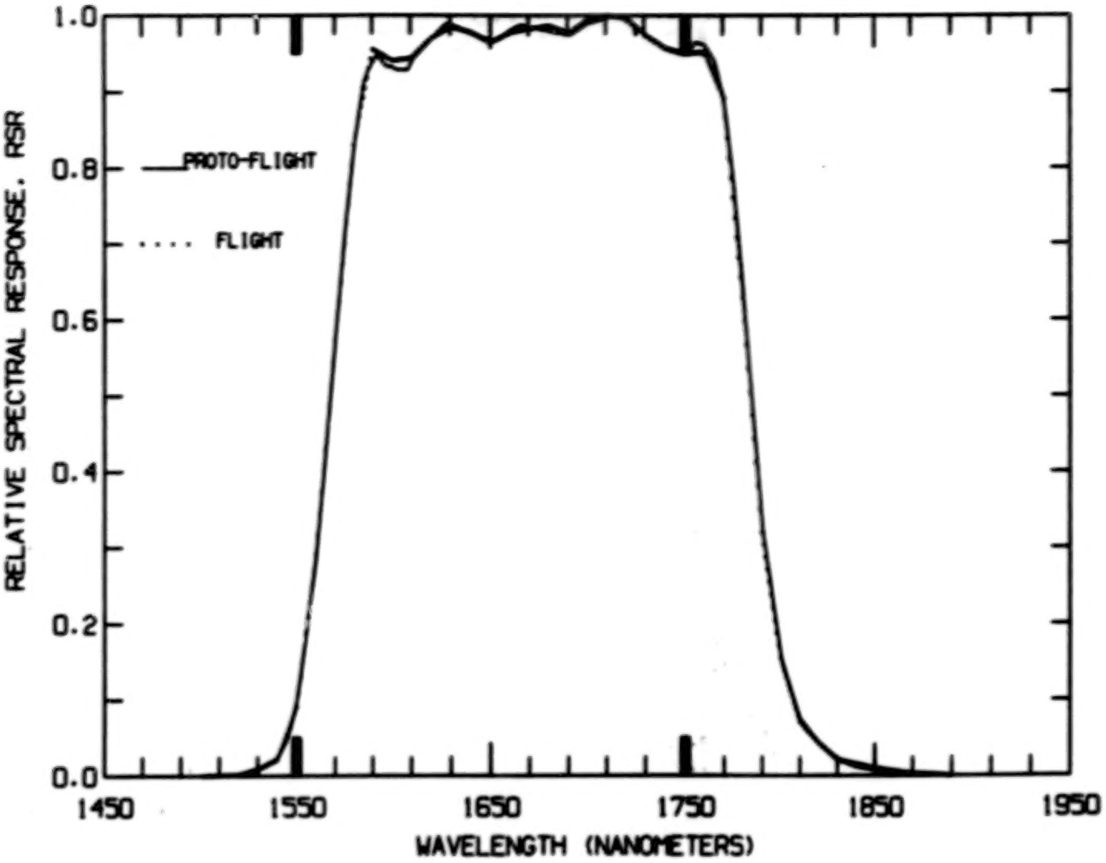

SPECTRAL PARAMETER	SPECIFICATION	PROTOFLIGHT	FLIGHT
LOWER BAND EDGE (nm)	1550 ± 20	1568	1567
UPPER BAND EDGE (nm)	1750 ± 20	$\boxed{1784}$ *	$\boxed{1784}$ *
LOWER BAND EDGE SLOPE (nm) 5% TO 75%	50 (MAX)	32	33
UPPER BAND EDGE SLOPE (nm) 75% TO 5%	50 (MAX)	42	43
FLATNESS (%)	75 (MIN)	84	84

*OUT OF SPECIFICATION

Figure 9. Thematic Mapper spectral performance – band 5.

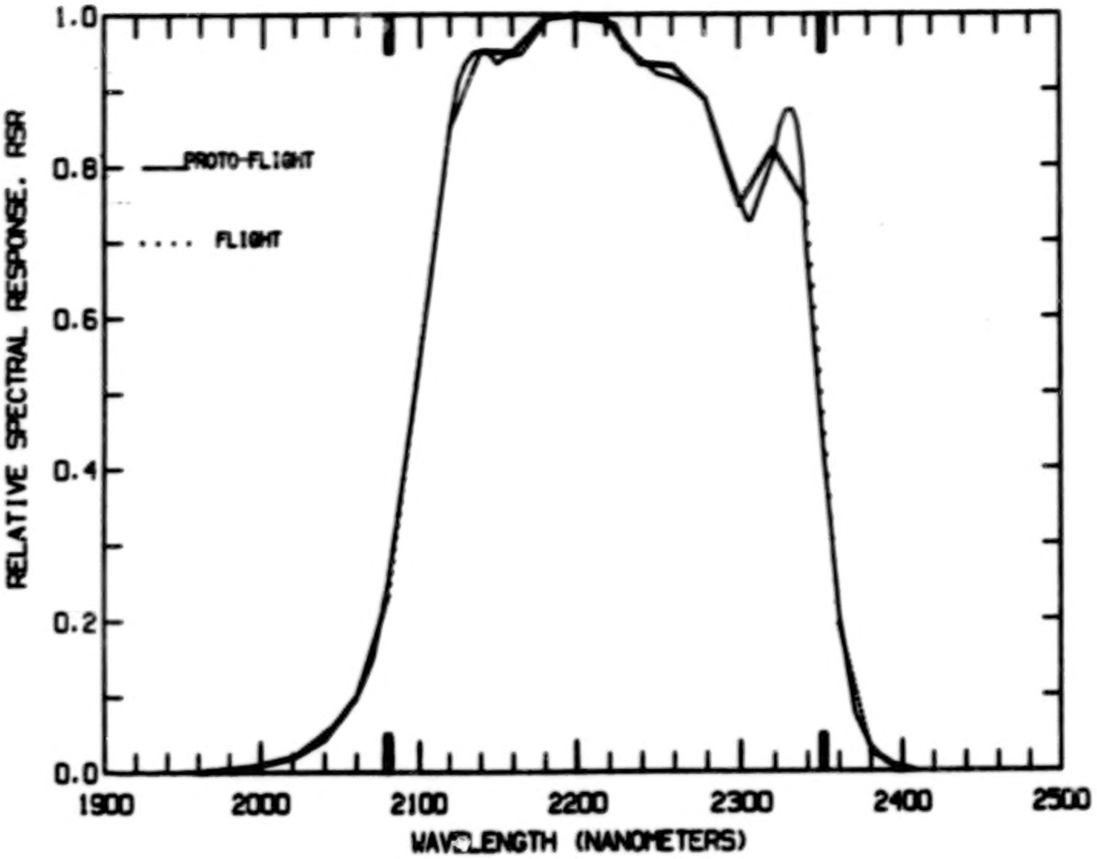

SPECTRAL PARAMETER	SPECIFICATION	PROTOFLIGHT	FLIGHT
LOWER BAND EDGE (nm)	2080 ± 30	2097	2097
UPPER BAND EDGE (nm)	2350 ± 30	2347	2349
LOWER BAND EDGE SLOPE (nm) 5% TO 75%	80	75	71
UPPER BAND EDGE SLOPE (nm) 75% TO 5%	80	37	37
FLATNESS (%)	75	$\boxed{59}$ *	$\boxed{57}$ *

*OUT OF SPECIFICATION

Figure 10. Thematic Mapper spectral performance – band 7.

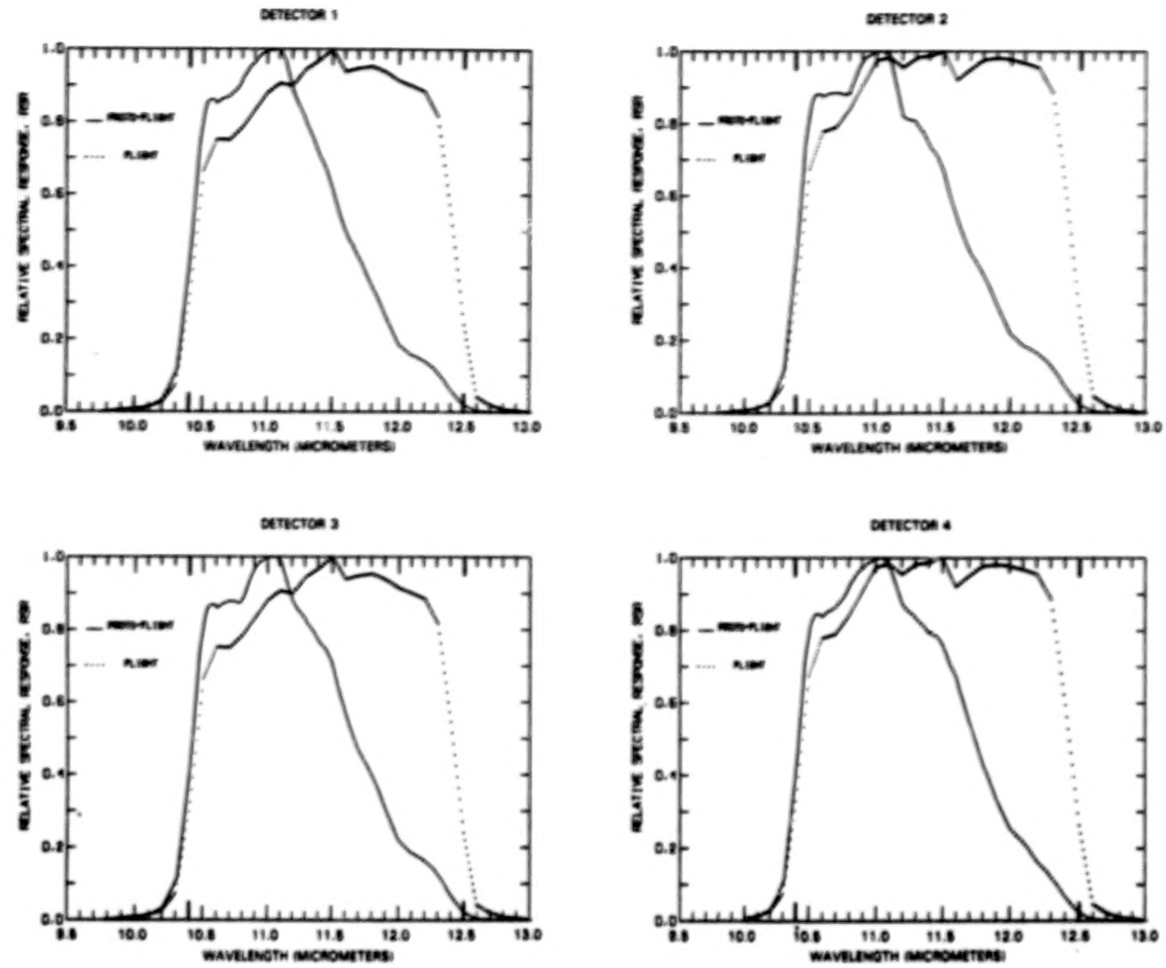

SPECTRAL PARAMETER	SPECIFICATION	PROTOFLIGHT	FLIGHT
LOWER BAND EDGE (μm)	10.4±0.1	10.42	10.45
UPPER BAND EDGE (μm)	12.5±0.1	$\boxed{11.66}$ *	12.43
LOWER BAND EDGE SLOPE (μm) 5% TO 75%	0.3 (MAX)	0.25	$\boxed{0.34}$ *
UPPER BAND EDGE SLOPE (μm) 75% TO 5%	0.3 (MAX)	$\boxed{1.01}$ *	0.26
FLATNESS (%)	75	$\boxed{67}$ *	78

*OUT OF SPECIFICATION

Figure 11. Thematic Mapper spectral performance – band 6.

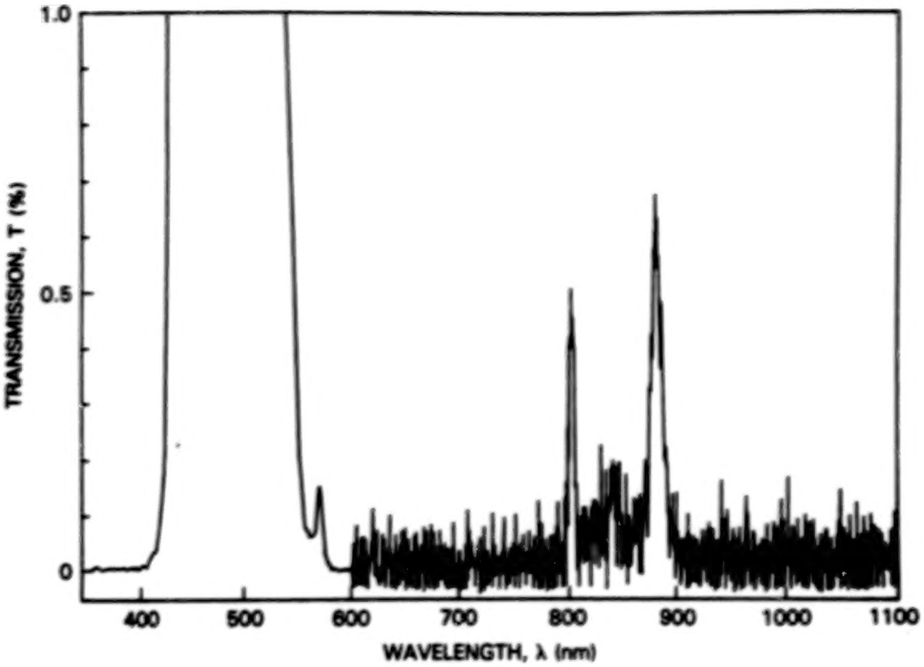

Figure 12. Thematic Mapper band 1 out-of-band filter transmission. Note scale 0-1%.

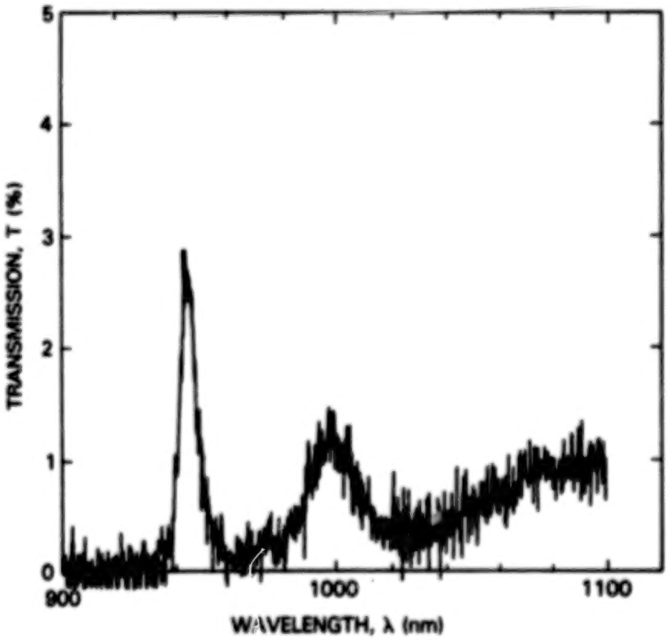

Figure 13. Thematic Mapper band 3 out-of-band filter transmission between 900 & 1100 nm. Note scale 0-5%.

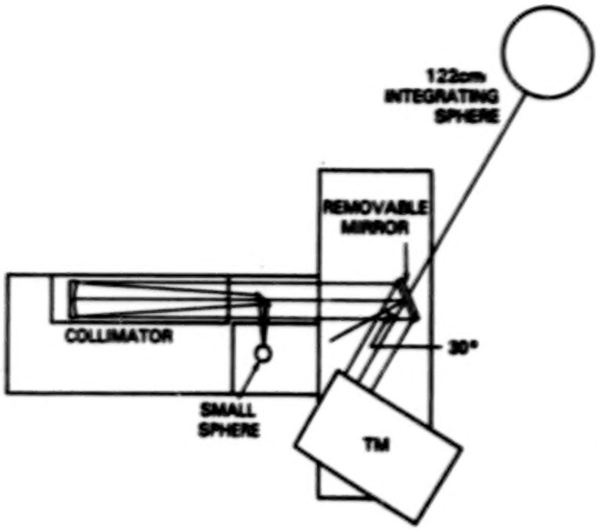
122cm
INTEGRATING
SPHERE
REMOVABLE
MIRROR
COLLIMATOR
30°
SMALL
SPHERE
TM

Figure 14. Spectral matching test schematic. One set of measurements was taken viewing the large integrating sphere (mirror removed). A second set of measurements was taken viewing the small sphere (mirror in place). The TM calibrator with MTF source acted as the collimator/small sphere for the PF tests. A laboratory collimator and a separate small sphere were used for the F tests.

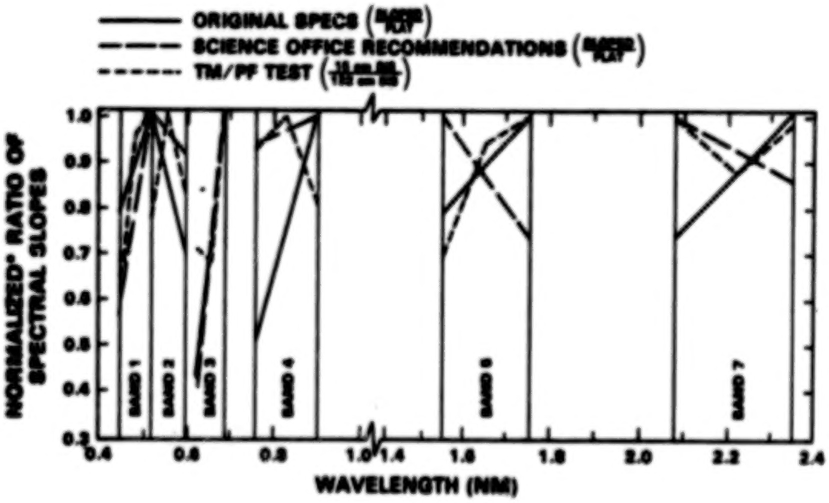

*NORMALIZED TO MAX = 1

Figure 15. Ratio of spectral slopes of Spherical Integration Sources (SIS) used for TM/PF spectral matching tests in relation to specifications and science office recommendations. TM/F tests simulated the original specifications.

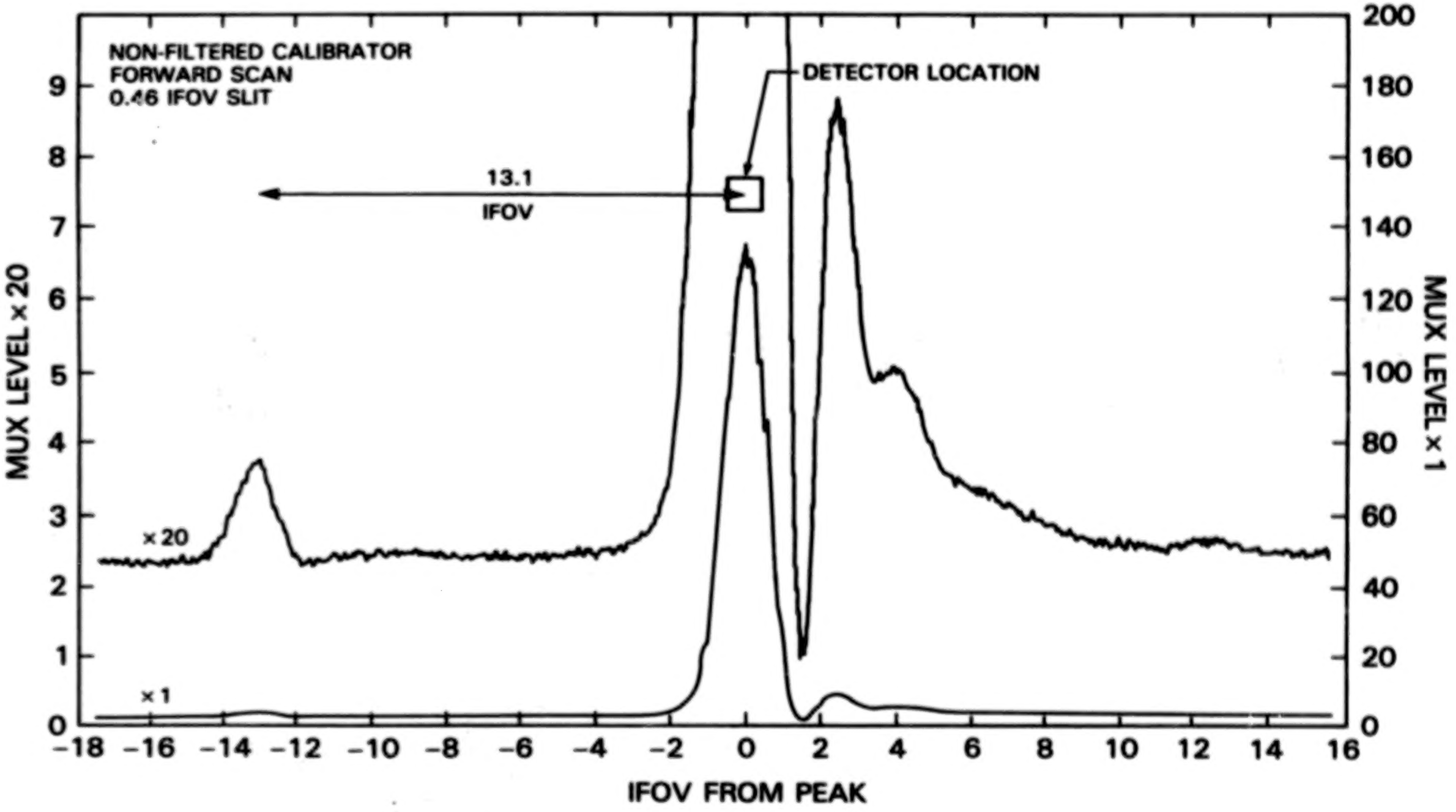

Figure 16. TM/F band 1 odd-channel forward scan line spread function showing location of light leak at 13.1 IFOV off of detector center.

Table 1.
TM Integrated Out-of-Band Responses in Relation to Specifications

	OUT-OF-BAND RESPONSES	
BAND	CALCULATED FROM FILTER TRANSMISSION	(%) SPECIFICATION
1	1.64%	5 (MAX)
2	1.30%	5 (MAX)
3	2.87%	5 (MAX)
4	0.78%*	5 (MAX)
5	0.79%	5 (MAX)
7	1.25%	5 (MAX)
6	0.81%*	5 (MAX)

*DETECTOR RSR AND SOLAR IRRADIANCE CONSIDERED IN CALCULATION

Table 2.
TM/F Peak Responses to Filtered Slit Light Source

BAND IN WHICH OUTPUT MEASURED	SOURCE LIGHT FILTER (BAND #)			
	1	2	3	4
1	120.0	6.6	0.0	1.2
2	2.7	82.0	1.2	0.2
3	<0.2	1.5	105.0	0.2
4	~0.2	~0.2	<0.1	115.0

Table 3.
TM/PF Spectral Matching Results – Large and Filtered Small Integrating Spheres

BAND	MAXIMUM BETWEEN CHANNEL SPECTRAL MISMATCH: PERCENT OF OUTPUT (%)	PERCENT OF MINIMUM SATURATION LEVEL (%)	SPECIFICATION (% MSL)
1	2.9	$\boxed{1.8}$ *	0.5
2	5.9	$\boxed{2.0}$ *	0.5
3	1.3	0.2	0.5
4	0.8	$\boxed{0.6}$ *	0.5
5	1.6	$\boxed{1.2}$ *	0.5
7	2.6	$\boxed{1.2}$ *	0.5

*OUT OF SPECIFICATION

Table 4.
TM/F Spectral Matching Results Test 1 – Large and Filtered Small Integrating Spheres

BAND	MAXIMUM BETWEEN CHANNEL SPECTRAL MISMATCH: PERCENT OF OUTPUT (%)	PERCENT OF MINIMUM SATURATION LEVEL (%)	SPECIFICATION (% MSL)
1	1.67	$\boxed{0.88}$ *	0.50
2	1.20	0.46	0.50
3	1.50	0.35	0.50
4	2.58	$\boxed{1.90}$ *	0.50
5	0.92	$\boxed{0.73}$ *	0.50
7	0.86	0.42	0.50

* OUT OF SPECIFICATION

Table 5.
TM/F Spectral Matching Results Test 2 – Small Integrating Sphere With and Without Filters

BAND	MAXIMUM BETWEEN CHANNEL SPECTRAL MISMATCH: PERCENT OF OUTPUT (%)	PERCENT OF MINIMUM SATURATION LEVEL (%)	SPECIFICATION (% MSL)
1	0.89	0.46	0.50
2	- - - *	- - - *	0.50
3	1.50	0.34	0.50
4	3.00	$\boxed{1.74}$ +	0.50
5	0.09	0.07	0.50
7	0.22	0.11	0.50

* VALID TEST COULD NOT BE CONDUCTED
+OUT OF SPECIFICATION

Table 6.
Comparison of MSS to TM/F Spectral Mismatch

MSS BAND	COMPARABLE TM BAND	RANGE OF MSS* SPECTRAL MISMATCHES (% OF SIGNAL)	FLIGHT MODEL TM SPECTRAL MISMATCH (% OF SIGNAL)
1	2	1–5	1.2
2	3	3–10	1.6
3	4	1–4	3.0
4	4	1–5	3.0

*CALCULATED FROM MSS 1, 2, 3, 4 (PF), F CHANNEL-BY-CHANNEL RELATIVE SPECTRAL RESPONSE MEASUREMENTS USING THE COMPARABLE TM BAND SPECIFIED SLOPING RADIANCE

Table 7.
Principal TM/F Primary Focal Plane Light Leaks (Magnitudes > 0.2 MUX with MTF Slit Source)

HALF-BAND	LEAK POSITION RELATIVE TO CENTRAL MAX (IFOV'S)	LEAK AMPLITUDE (MUX)	LEAK AMPLITUDE (% PEAK RESPONSE)
1-ODD	-13.1	1.3	1.10
1 - EVEN	-15.6	0.45	0.37
	14.7	0.20	0.16
2 - ODD	-12.0	0.20	0.18
2 - EVEN	-	--	-
3 - ODD	-12.0	0.30	0.27
	12.3	0.90	0.80
3 - EVEN	-14.8	0.25	0.21
	9.7	0.30	0.26
4 - ODD	-11.7	0.30	0.24
	12.6	0.20	0.16
4 - EVEN	-14.0	0.60	0.53
	-7.4	0.30	0.26
	10.1	0.20	0.18

APPENDIX A

Table A1

THEMATIC MAPPER RELATIVE SPECTRAL RESPONSE - BAND 1

WAVELENGTH (NM)	PF	F	WAVELENGTH (NM)	PF	F	WAVELENGTH (NM)	PF	F	WAVELENGTH (NM)	PF	F
412	0.0005	*******	453	0.5788	0.5366	494	0.9476	0.9761	535	0.0309	0.0296
413	0.0006	*******	454	0.6282	0.5856	495	0.9519	0.9775	536	0.0273	0.0261
414	0.0006	*******	455	0.7114	0.6667	496	0.9563	0.9788	537	0.0237	0.0227
415	0.0007	*******	456	0.7318	0.6880	497	0.9607	0.9802	538	0.0215	0.0205
416	0.0007	*******	457	0.7415	0.6993	498	0.9651	0.9815	539	0.0192	0.0184
417	0.0008	*******	458	0.7500	0.7095	499	0.9703	0.9837	540	0.0170	0.0162
418	0.0008	*******	459	0.7550	0.7165	500	0.9789	0.9891	541	0.0147	0.0140
419	0.0009	*******	460	0.7564	0.7200	501	0.9866	0.9935	542	0.0125	0.0119
420	0.0009	0.0007	461	0.7663	0.7326	502	0.9943	0.9978	543	0.0110	0.0105
421	0.0010	0.0008	462	0.7763	0.7454	503	1.0000	1.0000	544	0.0098	0.0093
422	0.0010	0.0008	463	0.7864	0.7583	504	0.9986	0.9952	545	0.0086	0.0081
423	0.0011	0.0009	464	0.7965	0.7714	505	0.9897	0.9828	546	0.0073	0.0069
424	0.0012	0.0009	465	0.8067	0.7847	506	0.9629	0.9524	547	0.0061	0.0058
425	0.0012	0.0010	466	0.8117	0.7924	507	0.9358	0.9219	548	0.0059	0.0056
426	0.0016	0.0013	467	0.8168	0.8002	508	0.9085	0.8914	549	0.0057	0.0054
427	0.0020	0.0016	468	0.8219	0.8080	509	0.8806	0.8607	550	0.0055	0.0052
428	0.0024	0.0020	469	0.8266	0.8156	510	0.8519	0.8293	551	0.0053	0.0050
429	0.0028	0.0023	470	0.8288	0.8206	511	0.8244	0.8021	552	0.0051	0.0048
430	0.0032	0.0027	471	0.8309	0.8257	512	0.8101	0.7877	553	0.0048	0.0046
431	0.0051	0.0042	472	0.8331	0.8308	513	0.7956	0.7732	554	0.0046	0.0044
432	0.0072	0.0060	473	0.8351	0.8359	514	0.7788	0.7565	555	0.0044	0.0042
433	0.0103	0.0086	474	0.8383	0.8421	515	0.7559	0.7339	556	0.0042	0.0040
434	0.0134	0.0113	475	0.8457	0.8526	516	0.7068	0.6859	557	0.0040	0.0038
435	0.0166	0.0141	476	0.8532	0.8624	517	0.5964	0.5784	558	0.0038	0.0036
436	0.0199	0.0170	477	0.8607	0.8724	518	0.4966	0.4813	559	0.0036	0.0033
437	0.0252	0.0216	478	0.8682	0.8824	519	0.4132	0.4002	560	0.0034	0.0031
438	0.0310	0.0268	479	0.8758	0.8925	520	0.3292	0.3187	561	0.0031	*******
439	0.0367	0.0321	480	0.8835	0.9026	521	0.2447	0.2367	562	0.0029	*******
440	0.0421	0.0370	481	0.8860	0.9068	522	0.1369	0.1324	563	0.0027	*******
441	0.0476	0.0420	482	0.8885	0.9111	523	0.1054	0.1018	564	0.0025	*******
442	0.0531	0.0471	483	0.8910	0.9154	524	0.0945	0.0911	565	0.0023	*******
443	0.0588	0.0524	484	0.8934	0.9196	525	0.0834	0.0804	566	0.0020	*******
444	0.0645	0.0577	485	0.8959	0.9238	526	0.0723	0.0696	567	0.0018	*******
445	0.0704	0.0633	486	0.8983	0.9285	527	0.0612	0.0588	568	0.0016	*******
446	0.0827	0.0746	487	0.9007	0.9332	528	0.0554	0.0532	569	0.0014	*******
447	0.1213	0.1097	488	0.9031	0.9379	529	0.0520	0.0498	570	0.0011	*******
448	0.1725	0.1564	489	0.9054	0.9425	530	0.0485	0.0465	571	0.0009	*******
449	0.2730	0.2483	490	0.9078	0.9472	531	0.0450	0.0431	572	0.0007	*******
450	0.3718	0.3381	491	0.9179	0.9548	532	0.0415	0.0397	573	0.0005	*******
451	0.4425	0.4058	492	0.9281	0.9623	533	0.0380	0.0364	574	0.0002	*******
452	0.5142	0.4741	493	0.9384	0.9698	534	0.0344	0.0330			

Table A2

THEMATIC MAPPER RELATIVE SPECTRAL RESPONSE - BAND 2

WAVELENGTH (NM)	PF	F	WAVELENGTH (NM)	PF	F	WAVELENGTH (NM)	PF	F	WAVELENGTH (NM)	PF	F
501	0.0006	0.0007	539	0.6754	0.7163	577	0.8869	0.9047	614	0.2487	0.2464
502	0.0019	0.0021	540	0.6899	0.7312	578	0.8914	0.9073	615	0.2057	0.2039
503	0.0032	0.0036	541	0.7003	0.7416	579	0.8958	0.9098	616	0.1810	0.1796
504	0.0065	0.0072	542	0.7107	0.7520	580	0.9003	0.9124	617	0.1562	0.1552
505	0.0089	0.0098	543	0.7213	0.7625	581	0.9047	0.9155	618	0.1313	0.1306
506	0.0114	0.0125	544	0.7319	0.7730	582	0.9092	0.9186	619	0.1078	0.1072
507	0.0139	0.0152	545	0.7426	0.7836	583	0.9136	0.9218	620	0.0873	0.0869
508	0.0164	0.0179	546	0.7533	0.7941	584	0.9323	0.9392	621	0.0868	0.0865
509	0.0190	0.0206	547	0.7642	0.8047	585	0.9444	0.9500	622	0.0763	0.0760
510	0.0215	0.0233	548	0.7751	0.8153	586	0.9536	0.9591	623	0.0657	0.0655
511	0.0241	0.0261	549	0.7861	0.8260	587	0.9630	0.9683	624	0.0550	0.0549
512	0.0268	0.0290	550	0.7971	0.8367	588	0.9715	0.9768	625	0.0518	0.0517
513	0.0295	0.0318	551	0.8031	0.8425	589	0.9768	0.9819	626	0.0486	0.0485
514	0.0322	0.0347	552	0.8091	0.8483	590	0.9820	0.9871	627	0.0454	0.0454
515	0.0349	0.0377	553	0.8152	0.8541	591	0.9875	0.9913	628	0.0422	0.0422
516	0.0504	0.0544	554	0.8206	0.8594	592	0.9941	0.9967	629	0.0390	0.0389
517	0.0662	0.0713	555	0.8261	0.8646	593	0.9986	0.9999	630	0.0357	0.0357
518	0.0912	0.0982	556	0.8316	0.8695	594	1.0000	1.0000	631	0.0324	0.0324
519	0.1205	0.1297	557	0.8371	0.8743	595	0.9991	0.9978	632	0.0291	0.0292
520	0.1520	0.1635	558	0.8427	0.8792	596	0.9984	0.9961	633	0.0258	0.0259
521	0.1912	0.2055	559	0.8482	0.8841	597	0.9953	0.9920	634	0.0225	0.0226
522	0.2309	0.2479	560	0.8538	0.8890	598	0.9799	0.9757	635	0.0207	0.0207
523	0.2711	0.2908	561	0.8593	0.8937	599	0.9644	0.9593	636	0.0188	0.0189
524	0.3117	0.3341	562	0.8650	0.8983	600	0.9488	0.9428	637	0.0170	0.0171
525	0.3529	0.3779	563	0.8706	0.9029	601	0.9265	0.9199	638	0.0151	0.0152
526	0.3917	0.4190	564	0.8731	0.9044	602	0.8941	0.8870	639	0.0132	0.0133
527	0.4299	0.4593	565	0.8743	0.9044	603	0.8616	0.8540	640	0.0114	0.0115
528	0.4685	0.4999	566	0.8754	0.9050	604	0.8288	0.8210	641	0.0102	0.0103
529	0.5075	0.5409	567	0.8766	0.9056	605	0.7959	0.7878	642	0.0091	0.0092
530	0.5372	0.5718	568	0.8777	0.9063	606	0.7466	0.7387	643	0.0080	0.0081
531	0.5606	0.5967	569	0.8788	0.9068	607	0.6721	0.6647	644	0.0069	0.0069
532	0.5772	0.6142	570	0.8799	0.9074	608	0.5970	0.5901	645	0.0057	0.0058
533	0.5909	0.6286	571	0.8809	0.9073	609	0.5215	0.5153	646	0.0046	0.0046
534	0.6046	0.6431	572	0.8820	0.9072	610	0.4674	0.4616	647	0.0034	0.0035
535	0.6186	0.6578	573	0.8830	0.9070	611	0.4131	0.4083	648	0.0023	0.0023
536	0.6326	0.6722	574	0.8840	0.9069	612	0.3586	0.3547	649	0.0012	0.0012
537	0.6467	0.6868	575	0.8850	0.9067	613	0.3038	0.3007	650	******	0.0000
538	0.6610	0.7015	576	0.8860	0.9057						

Table A3

THEMATIC MAPPER RELATIVE SPECTRAL RESPONSE - BAND 3

WAVELENGTH (NM)	PF	F	WAVELENGTH (NM)	PF	F	WAVELENGTH (NM)	PF	F	WAVELENGTH (NM)	PF	F
559	0.0007	*******	607	0.0304	0.0272	655	0.9397	0.9052	703	0.0844	0.0864
560	0.0008	*******	608	0.0341	0.0306	656	0.9388	0.9055	704	0.0737	0.0756
561	0.0009	*******	609	0.0378	0.0340	657	0.9379	0.9058	705	0.0629	0.0646
562	0.0009	*******	610	0.0415	0.0375	658	0.9370	0.9060	706	0.0569	0.0584
563	0.0010	*******	611	0.0453	0.0409	659	0.9360	0.9062	707	0.0539	0.0555
564	0.0011	*******	612	0.0616	0.0555	660	0.9351	0.9064	708	0.0510	0.0525
565	0.0012	*******	613	0.0811	0.0730	661	0.9372	0.9104	709	0.0480	0.0494
566	0.0013	*******	614	0.1007	0.0906	662	0.9394	0.9143	710	0.0450	0.0464
567	0.0014	*******	615	0.1204	0.1082	663	0.9429	0.9195	711	0.0420	0.0433
568	0.0014	*******	616	0.1402	0.1262	664	0.9483	0.9266	712	0.0390	0.0402
569	0.0015	*******	617	0.1602	0.1444	665	0.9537	0.9338	713	0.0360	0.0371
570	0.0016	*******	618	0.1803	0.1626	666	0.9591	0.9412	714	0.0330	0.0340
571	0.0017	*******	619	0.2402	0.2169	667	0.9646	0.9488	715	0.0300	0.0309
572	0.0017	*******	620	0.3271	0.2958	668	0.9700	0.9563	716	0.0270	0.0277
573	0.0017	*******	621	0.4145	0.3759	669	0.9755	0.9640	717	0.0239	0.0246
574	0.0018	*******	622	0.4491	0.4086	670	0.9793	0.9699	718	0.0224	0.0230
575	0.0018	*******	623	0.4706	0.4293	671	0.9831	0.9749	719	0.0210	0.0215
576	0.0019	0.0017	624	0.4921	0.4503	672	0.9869	0.9799	720	0.0195	0.0200
577	0.0019	0.0017	625	0.5138	0.4715	673	0.9904	0.9847	721	0.0180	0.0185
578	0.0020	0.0017	626	0.5354	0.4923	674	0.9969	0.9895	722	0.0164	0.0169
579	0.0020	0.0018	627	0.5572	0.5132	675	0.9964	0.9932	723	0.0151	0.0154
580	0.0021	0.0018	628	0.5790	0.5343	676	0.9982	0.9966	724	0.0136	0.0139
581	0.0021	0.0019	629	0.6010	0.5555	677	1.0000	1.0000	725	0.0121	0.0123
582	0.0022	0.0019	630	0.6235	0.5774	678	0.9977	0.9995	726	0.0109	0.0111
583	0.0022	0.0020	631	0.6504	0.6031	679	0.9957	0.9989	727	0.0097	0.0099
584	0.0023	0.0020	632	0.6866	0.6374	680	0.9936	0.9983	728	0.0085	0.0087
585	0.0023	0.0020	633	0.7366	0.6848	681	0.9725	0.9784	729	0.0073	0.0074
586	0.0024	0.0021	634	0.7869	0.7325	682	0.9734	0.9806	730	0.0061	0.0062
587	0.0024	0.0021	635	0.8027	0.7482	683	0.9742	0.9827	731	0.0058	0.0059
588	0.0025	0.0022	636	0.8185	0.7642	684	0.9635	0.9732	732	0.0055	0.0056
589	0.0025	0.0022	637	0.8345	0.7802	685	0.9451	0.9558	733	0.0052	0.0053
590	0.0026	0.0023	638	0.8485	0.7947	686	0.9265	0.9384	734	0.0049	0.0050
591	0.0029	0.0026	639	0.8598	0.8065	687	0.9078	0.9209	735	0.0046	0.0047
592	0.0033	0.0029	640	0.8711	0.8184	688	0.8710	0.8850	736	0.0043	0.0044
593	0.0037	0.0032	641	0.8826	0.8304	689	0.8220	0.8364	737	0.0040	0.0040
594	0.0040	0.0035	642	0.8941	0.8424	690	0.7727	0.7874	738	0.0037	0.0037
595	0.0044	0.0039	643	0.9056	0.8545	691	0.6869	0.7000	739	0.0034	0.0034
596	0.0053	0.0046	644	0.9116	0.8614	692	0.5940	0.6052	740	0.0031	0.0031
597	0.0062	0.0054	645	0.9170	0.8678	693	0.5049	0.5144	741	0.0028	*******
598	0.0071	0.0062	646	0.9224	0.8743	694	0.4333	0.4413	742	0.0025	*******
599	0.0080	0.0070	647	0.9278	0.8808	695	0.3612	0.3678	743	0.0022	*******
600	0.0089	0.0079	648	0.9332	0.8875	696	0.2888	0.2943	744	0.0019	*******
601	0.0114	0.0101	649	0.9388	0.8971	697	0.2235	0.2277	745	0.0016	*******
602	0.0139	0.0123	650	0.9441	0.9008	698	0.1579	0.1616	746	0.0012	*******
603	0.0165	0.0146	651	0.9433	0.9017	699	0.1522	0.1552	747	0.0009	*******
604	0.0194	0.0173	652	0.9424	0.9026	700	0.1162	0.1186	748	0.0006	*******
605	0.0231	0.0205	653	0.9415	0.9035	701	0.1056	0.1078	749	0.0003	*******
606	0.0267	0.0238	654	0.9406	0.9044	702	0.0850	0.0872			

Table A4

THEMATIC MAPPER RELATIVE SPECTRAL RESPONSE - BAND 4

WAVELENGTH (NM)	PF	F	WAVELENGTH (NM)	PF	F	WAVELENGTH (NM)	PF	F	WAVELENGTH (NM)	PF	F
726	0.0005	******	783	0.7950	0.7745	839	0.9578	0.9194	895	0.8344	0.7592
727	0.0010	******	784	0.8218	0.8017	840	0.9598	0.9196	896	0.8229	0.7495
728	0.0014	******	785	0.8487	0.8290	841	0.9618	0.9202	897	0.8114	0.7398
729	0.0019	******	786	0.8756	0.8564	842	0.9638	0.9208	898	0.8000	0.7302
730	0.0024	0.0023	787	0.9025	0.8838	843	0.9658	0.9214	899	0.7889	0.7206
731	0.0029	0.0028	788	0.9170	0.8992	844	0.9677	0.9220	900	0.7786	0.7152
732	0.0033	0.0032	789	0.9315	0.9146	845	0.9697	0.9226	901	0.7333	0.6710
733	0.0038	0.0037	790	0.9460	0.9300	846	0.9717	0.9232	902	0.6882	0.6299
734	0.0043	0.0042	791	0.9564	0.9418	847	0.9737	0.9237	903	0.6434	0.5891
735	0.0048	0.0046	792	0.9629	0.9499	848	0.9756	0.9243	904	0.5785	0.5299
736	0.0053	0.0051	793	0.9695	0.9580	849	0.9776	0.9248	905	0.5090	0.4664
737	0.0058	0.0056	794	0.9760	0.9661	850	0.9796	0.9254	906	0.4400	0.4033
738	0.0063	0.0060	795	0.9826	0.9743	851	0.9782	0.9217	907	0.3714	0.3405
739	0.0067	0.0065	796	0.9861	0.9794	852	0.9768	0.9179	908	0.3211	0.2945
740	0.0072	0.0070	797	0.9896	0.9845	853	0.9754	0.9141	909	0.2755	0.2528
741	0.0077	0.0074	798	0.9930	0.9897	854	0.9740	0.9104	910	0.2303	0.2114
742	0.0082	0.0079	799	0.9965	0.9948	855	0.9726	0.9067	911	0.1853	0.1702
743	0.0087	0.0084	800	1.0000	1.0000	856	0.9711	0.9029	912	0.1557	0.1430
744	0.0092	0.0088	801	0.9973	0.9982	857	0.9697	0.8992	913	0.1301	0.1195
745	0.0097	0.0093	802	0.9945	0.9964	858	0.9674	0.8947	914	0.1047	0.0962
746	0.0116	0.0112	803	0.9918	0.9946	859	0.9651	0.8901	915	0.0840	0.0772
747	0.0136	0.0130	804	0.9891	0.9928	860	0.9627	0.8856	916	0.0738	0.0679
748	0.0156	0.0149	805	0.9863	0.9910	861	0.9604	0.8831	917	0.0638	0.0587
749	0.0175	0.0168	806	0.9833	0.9889	862	0.9591	0.8815	918	0.0538	0.0495
750	0.0195	0.0186	807	0.9803	0.9868	863	0.9589	0.8810	919	0.0439	0.0404
751	0.0224	0.0214	808	0.9772	0.9846	864	0.9587	0.8804	920	0.0341	0.0314
752	0.0254	0.0242	809	0.9742	0.9825	865	0.9599	0.8811	921	0.0306	0.0281
753	0.0283	0.0270	810	0.9712	0.9804	866	0.9610	0.8818	922	0.0271	0.0249
754	0.0313	0.0298	811	0.9682	0.9758	867	0.9621	0.8824	923	0.0236	0.0217
755	0.0343	0.0326	812	0.9651	0.9712	868	0.9632	0.8831	924	0.0201	0.0186
756	0.0422	0.0402	813	0.9621	0.9666	869	0.9643	0.8838	925	0.0167	0.0154
757	0.0503	0.0478	814	0.9591	0.9620	870	0.9655	0.8844	926	0.0150	0.0138
758	0.0583	0.0554	815	0.9561	0.9574	871	0.9666	0.8858	927	0.0132	0.0122
759	0.0663	0.0630	816	0.9530	0.9529	872	0.9677	0.8871	928	0.0115	0.0106
760	0.0744	0.0706	817	0.9500	0.9483	873	0.9653	0.8853	929	0.0098	0.0090
761	0.0825	0.0784	818	0.9474	0.9442	874	0.9626	0.8832	930	0.0081	0.0075
762	0.0905	0.0862	819	0.9447	0.9400	875	0.9599	0.8810	931	0.0077	0.0071
763	0.0987	0.0940	820	0.9420	0.9359	876	0.9549	0.8768	932	0.0072	0.0067
764	0.1207	0.1152	821	0.9391	0.9313	877	0.9499	0.8725	933	0.0068	0.0063
765	0.1428	0.1364	822	0.9362	0.9268	878	0.9449	0.8683	934	0.0063	0.0059
766	0.1649	0.1577	823	0.9333	0.9223	879	0.9400	0.8641	935	0.0059	0.0055
767	0.1871	0.1791	824	0.9304	0.9178	880	0.9350	0.8599	936	0.0055	0.0051
768	0.2156	0.2069	825	0.9304	0.9161	881	0.9290	0.8530	937	0.0051	0.0047
769	0.2511	0.2409	826	0.9320	0.9160	882	0.9218	0.8451	938	0.0046	0.0043
770	0.2864	0.2752	827	0.9340	0.9164	883	0.9147	0.8372	939	0.0042	0.0039
771	0.3219	0.3095	828	0.9360	0.9167	884	0.9077	0.8294	940	0.0038	0.0035
772	0.3573	0.3440	829	0.9380	0.9170	885	0.9006	0.8217	941	0.0033	0.0032
773	0.3929	0.3786	830	0.9399	0.9173	886	0.8936	0.8139	942	0.0028	0.0028
774	0.4285	0.4133	831	0.9419	0.9176	887	0.8866	0.8063	943	0.0024	0.0024
775	0.4642	0.4482	832	0.9439	0.9178	888	0.8796	0.7986	944	0.0019	0.0021
776	0.5000	0.4833	833	0.9459	0.9181	889	0.8726	0.7910	945	0.0015	0.0017
777	0.5436	0.5259	834	0.9479	0.9183	890	0.8657	0.7835	946	0.0012	0.0014
778	0.5868	0.5683	835	0.9499	0.9185	891	0.8648	0.7835	947	0.0008	0.0010
779	0.6301	0.6108	836	0.9519	0.9188	892	0.8640	0.7836	948	0.0005	0.0007
780	0.6733	0.6534	837	0.9539	0.9190	893	0.8577	0.7787	949	0.0003	0.0003
781	0.7166	0.6963	838	0.9558	0.9192	894	0.8460	0.7690	950	******	0.0000
782	0.7599	0.7393									

Table A5

THEMATIC MAPPER RELATIVE SPECTRAL RESPONSE - BAND 5

WAVELENGTH (NM)	PF	F	WAVELENGTH (NM)	PF	F	WAVELENGTH (NM)	PF	F	WAVELENGTH (NM)	PF	F
1501	0.0000	0.0001	1561	0.3120	0.3179	1621	0.9719	0.9718	1681	0.9788	0.9854
1502	0.0001	0.0002	1562	0.3399	0.3454	1622	0.9747	0.9733	1682	0.9783	0.9844
1503	0.0002	0.0002	1563	0.3680	0.3733	1623	0.9775	0.9747	1683	0.9778	0.9835
1504	0.0002	0.0003	1564	0.3963	0.4012	1624	0.9803	0.9762	1684	0.9772	0.9825
1505	0.0003	0.0004	1565	0.4248	0.4294	1625	0.9831	0.9777	1685	0.9767	0.9815
1506	0.0004	0.0005	1566	0.4536	0.4578	1626	0.9855	0.9791	1686	0.9762	0.9805
1507	0.0005	0.0006	1567	0.4826	0.4865	1627	0.9877	0.9806	1687	0.9757	0.9796
1508	0.0006	0.0006	1568	0.5118	0.5154	1628	0.9894	0.9821	1688	0.9752	0.9786
1509	0.0007	0.0007	1569	0.5412	0.5446	1629	0.9888	0.9835	1689	0.9746	0.9776
1510	0.0008	0.0008	1570	0.5709	0.5739	1630	0.9882	0.9850	1690	0.9741	0.9766
1511	0.0009	0.0009	1571	0.5980	0.5989	1631	0.9871	0.9842	1691	0.9751	0.9784
1512	0.0010	0.0010	1572	0.6252	0.6239	1632	0.9859	0.9835	1692	0.9767	0.9802
1513	0.0010	0.0011	1573	0.6526	0.6492	1633	0.9848	0.9827	1693	0.9784	0.9820
1514	0.0011	0.0012	1574	0.6801	0.6746	1634	0.9836	0.9820	1694	0.9800	0.9838
1515	0.0012	0.0013	1575	0.7077	0.7002	1635	0.9825	0.9813	1695	0.9816	0.9857
1516	0.0013	0.0014	1576	0.7319	0.7260	1636	0.9813	0.9805	1696	0.9833	0.9875
1517	0.0014	0.0014	1577	0.7546	0.7519	1637	0.9802	0.9798	1697	0.9849	0.9893
1518	0.0015	0.0015	1578	0.7775	0.7781	1638	0.9790	0.9790	1698	0.9865	0.9911
1519	0.0016	0.0016	1579	0.8005	0.8044	1639	0.9778	0.9783	1699	0.9882	0.9926
1520	0.0017	0.0017	1580	0.8236	0.8308	1640	0.9767	0.9776	1700	0.9898	0.9947
1521	0.0022	0.0024	1581	0.8417	0.8430	1641	0.9758	0.9763	1701	0.9905	0.9953
1522	0.0029	0.0031	1582	0.8578	0.8553	1642	0.9749	0.9750	1702	0.9912	0.9958
1523	0.0036	0.0039	1583	0.8740	0.8676	1643	0.9740	0.9737	1703	0.9918	0.9963
1524	0.0044	0.0046	1584	0.8903	0.8800	1644	0.9730	0.9724	1704	0.9925	0.9969
1525	0.0051	0.0054	1585	0.9066	0.8925	1645	0.9721	0.9711	1705	0.9932	0.9974
1526	0.0059	0.0061	1586	0.9165	0.9050	1646	0.9712	0.9699	1706	0.9939	0.9979
1527	0.0066	0.0069	1587	0.9236	0.9175	1647	0.9703	0.9686	1707	0.9946	0.9985
1528	0.0074	0.0077	1588	0.9302	0.9301	1648	0.9694	0.9673	1708	0.9953	0.9990
1529	0.0082	0.0085	1589	0.9344	0.9428	1649	0.9685	0.9660	1709	0.9961	0.9995
1530	0.0090	0.0093	1590	0.9387	0.9555	1650	0.9676	0.9648	1710	0.9971	1.0000
1531	0.0102	0.0104	1591	0.9428	0.9540	1651	0.9672	0.9661	1711	0.9978	0.9997
1532	0.0116	0.0116	1592	0.9468	0.9526	1652	0.9668	0.9674	1712	0.9985	0.9994
1533	0.0131	0.0128	1593	0.9459	0.9511	1653	0.9679	0.9687	1713	0.9990	0.9991
1534	0.0146	0.0140	1594	0.9429	0.9497	1654	0.9697	0.9701	1714	0.9995	0.9988
1535	0.0161	0.0152	1595	0.9398	0.9482	1655	0.9715	0.9714	1715	1.0000	0.9984
1536	0.0176	0.0165	1596	0.9368	0.9467	1656	0.9732	0.9727	1716	0.9981	0.9981
1537	0.0191	0.0177	1597	0.9337	0.9453	1657	0.9750	0.9740	1717	0.9976	0.9978
1538	0.0207	0.0190	1598	0.9327	0.9438	1658	0.9768	0.9753	1718	0.9962	0.9975
1539	0.0222	0.0203	1599	0.9326	0.9423	1659	0.9786	0.9767	1719	0.9947	0.9972
1540	0.0238	0.0216	1600	0.9325	0.9409	1660	0.9803	0.9780	1720	0.9932	0.9968
1541	0.0278	0.0283	1601	0.9308	0.9412	1661	0.9819	0.9785	1721	0.9915	0.9945
1542	0.0327	0.0351	1602	0.9290	0.9415	1662	0.9833	0.9790	1722	0.9896	0.9922
1543	0.0378	0.0419	1603	0.9285	0.9418	1663	0.9847	0.9795	1723	0.9878	0.9899
1544	0.0428	0.0488	1604	0.9284	0.9421	1664	0.9861	0.9800	1724	0.9859	0.9877
1545	0.0479	0.0557	1605	0.9283	0.9424	1665	0.9876	0.9805	1725	0.9740	0.9854
1546	0.0566	0.0626	1606	0.9282	0.9428	1666	0.9875	0.9810	1726	0.9821	0.9831
1547	0.0667	0.0695	1607	0.9281	0.9431	1667	0.9867	0.9815	1727	0.9802	0.9808
1548	0.0770	0.0767	1608	0.9280	0.9434	1668	0.9859	0.9820	1728	0.9784	0.9785
1549	0.0873	0.0837	1609	0.9328	0.9437	1669	0.9852	0.9825	1729	0.9765	0.9763
1550	0.0977	0.0909	1610	0.9396	0.9440	1670	0.9844	0.9830	1730	0.9746	0.9740
1551	0.1128	0.1104	1611	0.9436	0.9467	1671	0.9839	0.9833	1731	0.9727	0.9723
1552	0.1325	0.1300	1612	0.9465	0.9493	1672	0.9834	0.9837	1732	0.9709	0.9706
1553	0.1513	0.1497	1613	0.9493	0.9519	1673	0.9829	0.9840	1733	0.9690	0.9688
1554	0.1702	0.1695	1614	0.9521	0.9546	1674	0.9824	0.9844	1734	0.9671	0.9671
1555	0.1893	0.1894	1615	0.9550	0.9572	1675	0.9819	0.9847	1735	0.9652	0.9654
1556	0.2085	0.2094	1616	0.9578	0.9598	1676	0.9813	0.9850	1736	0.9634	0.9637
1557	0.2278	0.2295	1617	0.9606	0.9625	1677	0.9808	0.9854	1737	0.9615	0.9620
1558	0.2473	0.2498	1618	0.9634	0.9651	1678	0.9803	0.9857	1738	0.9597	0.9603
1559	0.2669	0.2701	1619	0.9662	0.9677	1679	0.9798	0.9861	1739	0.9578	0.9586
1560	0.2867	0.2906	1620	0.9691	0.9703	1680	0.9793	0.9864	1740	0.9559	0.9569

Table A5
(CONTINUED)

WAVELENGTH (NM)	PF	F	WAVELENGTH (NM)	PF	F	WAVELENGTH (NM)	PF	F	WAVELENGTH (NM)	PF	F
1741	0.9549	0.9562	1779	0.6658	0.6542	1816	0.0569	0.0546	1853	0.0098	0.0073
1742	0.9541	0.9555	1780	0.6370	0.6277	1817	0.0528	0.0518	1854	0.0094	0.0068
1743	0.9534	0.9549	1781	0.6072	0.5968	1818	0.0507	0.0491	1855	0.0091	0.0064
1744	0.9526	0.9542	1782	0.5769	0.5659	1819	0.0476	0.0463	1856	0.0087	0.0060
1745	0.9519	0.9536	1783	0.5466	0.5350	1820	0.0446	0.0436	1857	0.0083	0.0055
1746	0.9511	0.9529	1784	0.5163	0.5041	1821	0.0421	0.0414	1858	0.0080	0.0051
1747	0.9504	0.9523	1785	0.4860	0.4732	1822	0.0399	0.0392	1859	0.0076	0.0047
1748	0.9496	0.9516	1786	0.4557	0.4423	1823	0.0377	0.0370	1860	0.0073	0.0043
1749	0.9489	0.9509	1787	0.4254	0.4114	1824	0.0355	0.0348	1861	0.0069	0.0041
1750	0.9482	0.9503	1788	0.3950	0.3806	1825	0.0333	0.0326	1862	0.0065	0.0040
1751	0.9505	0.9505	1789	0.3647	0.3497	1826	0.0311	0.0304	1863	0.0062	0.0039
1752	0.9538	0.9507	1790	0.3344	0.3190	1827	0.0290	0.0282	1864	0.0058	0.0038
1753	0.9572	0.9508	1791	0.3134	0.3026	1828	0.0268	0.0260	1865	0.0055	0.0037
1754	0.9605	0.9510	1792	0.2963	0.2862	1829	0.0246	0.0239	1866	0.0051	0.0036
1755	0.9638	0.9512	1793	0.2792	0.2698	1830	0.0224	0.0217	1867	0.0047	0.0035
1756	0.9645	0.9514	1794	0.2621	0.2533	1831	0.0214	0.0208	1868	0.0044	0.0034
1757	0.9635	0.9516	1795	0.2450	0.2369	1832	0.0208	0.0199	1869	0.0040	0.0033
1758	0.9624	0.9517	1796	0.2279	0.2204	1833	0.0202	0.0190	1870	0.0037	0.0032
1759	0.9614	0.9519	1797	0.2108	0.2040	1834	0.0197	0.0182	1871	0.0033	0.0031
1760	0.9604	0.9520	1798	0.1938	0.1875	1835	0.0191	0.0173	1872	0.0030	0.0030
1761	0.9570	0.9460	1799	0.1767	0.1710	1836	0.0186	0.0164	1873	0.0026	0.0028
1762	0.9527	0.9400	1800	0.1596	0.1546	1837	0.0180	0.0155	1874	0.0022	0.0027
1763	0.9483	0.9339	1801	0.1488	0.1462	1838	0.0175	0.0146	1875	0.0019	0.0026
1764	0.9440	0.9279	1802	0.1407	0.1378	1839	0.0169	0.0138	1876	0.0015	0.0025
1765	0.9397	0.9219	1803	0.1327	0.1294	1840	0.0164	0.0129	1877	0.0012	0.0024
1766	0.9307	0.9159	1804	0.1247	0.1210	1841	0.0158	0.0125	1878	0.0008	0.0023
1767	0.9197	0.9098	1805	0.1167	0.1127	1842	0.0153	0.0120	1879	0.0005	0.0022
1768	0.9088	0.9038	1806	0.1087	0.1044	1843	0.0147	0.0116	1880	0.0001	0.0021
1769	0.8978	0.8978	1807	0.1007	0.0960	1844	0.0142	0.0112	1881	*******	0.0019
1770	0.8869	0.8915	1808	0.0927	0.0877	1845	0.0137	0.0107	1882	*******	0.0017
1771	0.8679	0.8651	1809	0.0847	0.0794	1846	0.0131	0.0103	1883	*******	0.0015
1772	0.8457	0.8388	1810	0.0768	0.0712	1847	0.0126	0.0099	1884	*******	0.0013
1773	0.8235	0.8124	1811	0.0723	0.0684	1848	0.0120	0.0094	1885	*******	0.0010
1774	0.8012	0.7861	1812	0.0692	0.0657	1849	0.0115	0.0090	1886	*******	0.0008
1775	0.7790	0.7597	1813	0.0661	0.0629	1850	0.0109	0.0086	1887	*******	0.0006
1776	0.7522	0.7333	1814	0.0630	0.0601	1851	0.0105	0.0081	1888	*******	0.0004
1777	0.7234	0.7069	1815	0.0599	0.0574	1852	0.0102	0.0077	1889	*******	0.0002
1778	0.6946	0.6806									

Table A6

THEMATIC MAPPER RELATIVE SPECTRAL RESPONSE - BAND 7

WAVELENGTH (NM)	PF	F	WAVELENGTH (NM)	PF	F	WAVELENGTH (NM)	PF	F	WAVELENGTH (NM)	PF	F
1951	0.0002	******	2011	0.0148	0.0151	2071	0.1600	0.1732	2131	0.9387	0.9070
1952	0.0003	******	2012	0.0153	0.0156	2072	0.1701	0.1798	2132	0.9414	0.9120
1953	0.0005	******	2013	0.0158	0.0160	2073	0.1802	0.1865	2133	0.9441	0.9170
1954	0.0007	******	2014	0.0163	0.0165	2074	0.1903	0.1931	2134	0.9469	0.9219
1955	0.0009	******	2015	0.0168	0.0170	2075	0.2004	0.1998	2135	0.9496	0.9269
1956	0.0010	******	2016	0.0173	0.0175	2076	0.2106	0.2065	2136	0.9498	0.9319
1957	0.0012	******	2017	0.0178	0.0180	2077	0.2207	0.2132	2137	0.9500	0.9369
1958	0.0014	******	2018	0.0183	0.0185	2078	0.2309	0.2199	2138	0.9502	0.9419
1959	0.0016	******	2019	0.0188	0.0190	2079	0.2410	0.2266	2139	0.9504	0.9469
1960	0.0017	******	2020	0.0193	0.0194	2080	0.2512	0.2333	2140	0.9506	0.9519
1961	0.0019	0.0001	2021	0.0209	0.0207	2081	0.2654	0.2486	2141	0.9503	0.9519
1962	0.0021	0.0002	2022	0.0225	0.0219	2082	0.2797	0.2640	2142	0.9500	0.9518
1963	0.0023	0.0003	2023	0.0241	0.0231	2083	0.2940	0.2794	2143	0.9497	0.9517
1964	0.0025	0.0004	2024	0.0258	0.0244	2084	0.3084	0.2949	2144	0.9494	0.9517
1965	0.0026	0.0004	2025	0.0274	0.0256	2085	0.3227	0.3103	2145	0.9491	0.9516
1966	0.0028	0.0005	2026	0.0290	0.0269	2086	0.3371	0.3258	2146	0.9464	0.9515
1967	0.0030	0.0006	2027	0.0307	0.0281	2087	0.3515	0.3413	2147	0.9437	0.9515
1968	0.0032	0.0007	2028	0.0323	0.0294	2088	0.3659	0.3568	2148	0.9411	0.9514
1969	0.0034	0.0008	2029	0.0340	0.0306	2089	0.3803	0.3723	2149	0.9384	0.9513
1970	0.0036	0.0009	2030	0.0356	0.0319	2090	0.3947	0.3878	2150	0.9357	0.9512
1971	0.0037	0.0010	2031	0.0373	0.0331	2091	0.4092	0.4034	2151	0.9373	0.9512
1972	0.0039	0.0011	2032	0.0389	0.0344	2092	0.4237	0.4190	2152	0.9389	0.9511
1973	0.0041	0.0012	2033	0.0406	0.0356	2093	0.4382	0.4346	2153	0.9405	0.9510
1974	0.0043	0.0013	2034	0.0423	0.0367	2094	0.4528	0.4502	2154	0.9421	0.9509
1975	0.0045	0.0014	2035	0.0439	0.0381	2095	0.4673	0.4658	2155	0.9437	0.9509
1976	0.0047	0.0015	2036	0.0456	0.0394	2096	0.4819	0.4814	2156	0.9442	0.9508
1977	0.0049	0.0016	2037	0.0473	0.0407	2097	0.4965	0.4971	2157	0.9447	0.9507
1978	0.0050	0.0017	2038	0.0489	0.0419	2098	0.5111	0.5128	2158	0.9453	0.9506
1979	0.0052	0.0018	2039	0.0506	0.0432	2099	0.5257	0.5285	2159	0.9458	0.9505
1980	0.0054	0.0018	2040	0.0523	0.0445	2100	0.5404	0.5442	2160	0.9463	0.9505
1981	0.0056	0.0022	2041	0.0540	0.0472	2101	0.5557	0.5593	2161	0.9466	0.9526
1982	0.0058	0.0026	2042	0.0557	0.0500	2102	0.5710	0.5744	2162	0.9470	0.9548
1983	0.0060	0.0030	2043	0.0574	0.0527	2103	0.5864	0.5896	2163	0.9473	0.9570
1984	0.0062	0.0034	2044	0.0591	0.0555	2104	0.6018	0.6048	2164	0.9476	0.9592
1985	0.0064	0.0037	2045	0.0608	0.0583	2105	0.6172	0.6200	2165	0.9480	0.9614
1986	0.0066	0.0041	2046	0.0625	0.0611	2106	0.6327	0.6353	2166	0.9507	0.9636
1987	0.0068	0.0045	2047	0.0642	0.0638	2107	0.6482	0.6506	2167	0.9534	0.9658
1988	0.0070	0.0049	2048	0.0659	0.0666	2108	0.6637	0.6659	2168	0.9562	0.9680
1989	0.0072	0.0053	2049	0.0676	0.0694	2109	0.6792	0.6813	2169	0.9589	0.9702
1990	0.0074	0.0057	2050	0.0693	0.0722	2110	0.6948	0.6967	2170	0.9617	0.9724
1991	0.0076	0.0061	2051	0.0723	0.0750	2111	0.7104	0.7121	2171	0.9646	0.9747
1992	0.0078	0.0065	2052	0.0753	0.0778	2112	0.7261	0.7276	2172	0.9675	0.9769
1993	0.0080	0.0069	2053	0.0783	0.0806	2113	0.7418	0.7431	2173	0.9704	0.9791
1994	0.0082	0.0073	2054	0.0813	0.0834	2114	0.7576	0.7587	2174	0.9733	0.9813
1995	0.0084	0.0077	2055	0.0843	0.0862	2115	0.7733	0.7743	2175	0.9762	0.9835
1996	0.0086	0.0081	2056	0.0874	0.0891	2116	0.7891	0.7899	2176	0.9792	0.9857
1997	0.0088	0.0085	2057	0.0904	0.0919	2117	0.8050	0.8056	2177	0.9821	0.9880
1998	0.0090	0.0089	2058	0.0934	0.0947	2118	0.8209	0.8213	2178	0.9850	0.9902
1999	0.0092	0.0093	2059	0.0964	0.0975	2119	0.8368	0.8370	2179	0.9879	0.9924
2000	0.0094	0.0097	2060	0.0995	0.1004	2120	0.8527	0.8528	2180	0.9909	0.9947
2001	0.0099	0.0102	2061	0.1045	0.1070	2121	0.8641	0.8578	2181	0.9936	0.9949
2002	0.0104	0.0107	2062	0.1095	0.1136	2122	0.8755	0.8627	2182	0.9964	0.9952
2003	0.0109	0.0112	2063	0.1146	0.1201	2123	0.8869	0.8676	2183	0.9968	0.9955
2004	0.0114	0.0117	2064	0.1196	0.1267	2124	0.8983	0.8725	2184	0.9971	0.9957
2005	0.0118	0.0121	2065	0.1247	0.1334	2125	0.9098	0.8774	2185	0.9975	0.9960
2006	0.0123	0.0126	2066	0.1297	0.1400	2126	0.9150	0.8823	2186	0.9979	0.9963
2007	0.0128	0.0131	2067	0.1348	0.1466	2127	0.9202	0.8873	2187	0.9982	0.9966
2008	0.0133	0.0136	2068	0.1398	0.1532	2128	0.9255	0.8922	2188	0.9986	0.9968
2009	0.0138	0.0141	2069	0.1449	0.1599	2129	0.9307	0.8971	2189	0.9989	0.9971
2010	0.0143	0.0146	2070	0.1500	0.1665	2130	0.9359	0.9021	2190	0.9993	0.9974

Table A6
(CONTINUED)

WAVELENGTH (NM)	PF	F	WAVELENGTH (NM)	PF	F	WAVELENGTH (NM)	PF	F	WAVELENGTH (NM)	PF	F
2191	0.9996	0.9976	2246	0.9300	0.9348	2301	0.7514	0.7523	2356	0.2964	0.3060
2192	1.0000	0.9979	2247	0.9281	0.9347	2302	0.7455	0.7561	2357	0.2738	0.2781
2193	0.9994	0.9982	2248	0.9261	0.9345	2303	0.7396	0.7598	2358	0.2512	0.2502
2194	0.9989	0.9984	2249	0.9242	0.9343	2304	0.7337	0.7636	2359	0.2286	0.2223
2195	0.9983	0.9987	2250	0.9223	0.9342	2305	0.7278	0.7673	2360	0.2060	0.1943
2196	0.9977	0.9989	2251	0.9217	0.9340	2305	0.7278	0.7710	2361	0.1930	0.1856
2197	0.9972	0.9992	2252	0.9211	0.9338	2307	0.7279	0.7748	2362	0.1801	0.1774
2198	0.9966	0.9995	2253	0.9205	0.9336	2308	0.7343	0.7785	2363	0.1672	0.1692
2199	0.9960	0.9997	2254	0.9198	0.9335	2309	0.7407	0.7822	2364	0.1542	0.1609
2200	0.9954	1.0000	2255	0.9192	0.9333	2310	0.7471	0.7860	2365	0.1413	0.1526
2201	0.9952	0.9996	2256	0.9186	0.9331	2311	0.7536	0.7897	2366	0.1283	0.1444
2202	0.9949	0.9991	2257	0.9180	0.9329	2312	0.7600	0.7935	2367	0.1153	0.1361
2203	0.9946	0.9987	2258	0.9174	0.9328	2313	0.7660	0.7972	2368	0.1023	0.1278
2204	0.9943	0.9983	2259	0.9168	0.9326	2314	0.7721	0.8009	2369	0.0893	0.1195
2205	0.9940	0.9978	2260	0.9162	0.9324	2315	0.7781	0.8047	2370	0.0763	0.1112
2206	0.9937	0.9974	2261	0.9153	0.9302	2316	0.7841	0.8084	2371	0.0720	0.1028
2207	0.9934	0.9970	2262	0.9145	0.9280	2317	0.7902	0.8121	2372	0.0676	0.0945
2208	0.9931	0.9965	2263	0.9136	0.9258	2318	0.7962	0.8159	2373	0.0633	0.0862
2209	0.9928	0.9961	2264	0.9128	0.9235	2319	0.8022	0.8196	2374	0.0590	0.0778
2210	0.9925	0.9956	2265	0.9119	0.9213	2320	0.8083	0.8233	2375	0.0546	0.0694
2211	0.9922	0.9952	2266	0.9110	0.9191	2321	0.8191	0.8199	2376	0.0503	0.0611
2212	0.9919	0.9948	2267	0.9102	0.9169	2322	0.8300	0.8162	2377	0.0459	0.0527
2213	0.9916	0.9943	2268	0.9093	0.9147	2323	0.8408	0.8126	2378	0.0416	0.0443
2214	0.9913	0.9939	2269	0.9077	0.9125	2324	0.8517	0.8089	2379	0.0372	0.0359
2215	0.9910	0.9934	2270	0.9061	0.9103	2325	0.8572	0.8053	2380	0.0329	0.0274
2216	0.9907	0.9930	2271	0.9045	0.9081	2326	0.8627	0.8016	2381	0.0307	0.0259
2217	0.9904	0.9926	2272	0.9028	0.9059	2327	0.8683	0.7980	2382	0.0285	0.0245
2218	0.9901	0.9921	2273	0.9012	0.9037	2328	0.8738	0.7943	2383	0.0263	0.0232
2219	0.9898	0.9917	2274	0.8996	0.9015	2329	0.8740	0.7907	2384	0.0241	0.0218
2220	0.9895	0.9912	2275	0.8980	0.8993	2330	0.8743	0.7870	2385	0.0219	0.0205
2221	0.9891	0.9885	2276	0.8964	0.8971	2331	0.8745	0.7834	2386	0.0197	0.0191
2222	0.9886	0.9857	2277	0.8948	0.8949	2332	0.8747	0.7797	2387	0.0175	0.0178
2223	0.9882	0.9829	2278	0.8932	0.8927	2333	0.8678	0.7761	2388	0.0153	0.0164
2224	0.9877	0.9802	2279	0.8916	0.8906	2334	0.8609	0.7724	2389	0.0132	0.0150
2225	0.9872	0.9774	2280	0.8900	0.8884	2335	0.8540	0.7688	2390	0.0110	0.0137
2226	0.9811	0.9746	2281	0.8832	0.8814	2336	0.8364	0.7651	2391	0.0104	0.0123
2227	0.9749	0.9718	2282	0.8764	0.8744	2337	0.8188	0.7615	2392	0.0099	0.0110
2228	0.9687	0.9691	2283	0.8696	0.8673	2338	0.8012	0.7578	2393	0.0093	0.0096
2229	0.9625	0.9663	2284	0.8627	0.8603	2339	0.7480	0.7542	2394	0.0088	0.0082
2230	0.9563	0.9635	2285	0.8560	0.8532	2340	0.6947	0.7505	2395	0.0082	0.0069
2231	0.9548	0.9608	2286	0.8492	0.8462	2341	0.6686	0.7233	2396	0.0077	0.0055
2232	0.9533	0.9580	2287	0.8424	0.8392	2342	0.6424	0.6955	2397	0.0071	0.0041
2233	0.9519	0.9552	2288	0.8357	0.8322	2343	0.6162	0.6678	2398	0.0066	0.0028
2234	0.9504	0.9525	2289	0.8290	0.8252	2344	0.5899	0.6400	2399	0.0060	0.0014
2235	0.9490	0.9497	2290	0.8222	0.8182	2345	0.5636	0.6122	2400	0.0055	0.0000
2236	0.9475	0.9470	2291	0.8157	0.8112	2346	0.5372	0.5845	2401	0.0049	******
2237	0.9460	0.9442	2292	0.8092	0.8043	2347	0.5108	0.5567	2402	0.0044	******
2238	0.9446	0.9414	2293	0.8027	0.7973	2348	0.4844	0.5288	2403	0.0038	******
2239	0.9431	0.9387	2294	0.7961	0.7904	2349	0.4579	0.5010	2404	0.0033	******
2240	0.9416	0.9359	2295	0.7896	0.7834	2350	0.4313	0.4732	2405	0.0027	******
2241	0.9397	0.9357	2296	0.7832	0.7765	2351	0.4089	0.4454	2406	0.0022	******
2242	0.9377	0.9355	2297	0.7767	0.7695	2352	0.3864	0.4175	2407	0.0016	******
2243	0.9358	0.9354	2298	0.7702	0.7626	2353	0.3640	0.3896	2408	0.0011	******
2244	0.9339	0.9352	2299	0.7637	0.7557	2354	0.3415	0.3618	2409	0.0005	******
2245	0.9319	0.9350	2300	0.7573	0.7488	2355	0.3189	0.3339			

Table A7a

THEMATIC MAPPER RELATVE SPECTRAL RESPONSE - BAND 6 *** DETECTOR 1

WAVELENGTH (NM)	PF	F	WAVELENGTH (NM)	PF	F	WAVELENGTH (NM)	PF	F	WAVELENGTH (NM)	PF	F
9760	0.0004	*******	10360	0.2821	0.2209	10960	0.9874	0.8613	11560	0.5421	0.9636
9770	0.0008	*******	10370	0.3157	0.2461	10970	0.9896	0.8661	11570	0.5311	0.9575
9780	0.0011	*******	10380	0.3495	0.2715	10980	0.9918	0.8709	11580	0.5203	0.9515
9790	0.0015	*******	10390	0.3835	0.2971	10990	0.9941	0.8758	11590	0.5095	0.9454
9800	0.0019	*******	10400	0.4184	0.3230	11000	0.9963	0.8806	11600	0.5003	0.9393
9810	0.0023	*******	10410	0.4535	0.3566	11010	0.9966	0.8832	11610	0.4912	0.9403
9820	0.0027	*******	10420	0.4920	0.3903	11020	0.9968	0.8859	11620	0.4820	0.9412
9830	0.0031	*******	10430	0.5378	0.4241	11030	0.9970	0.8885	11630	0.4740	0.9422
9840	0.0035	*******	10440	0.5839	0.4581	11040	0.9973	0.8912	11640	0.4673	0.9431
9850	0.0038	*******	10450	0.6306	0.4922	11050	0.9975	0.8938	11650	0.4606	0.9440
9860	0.0042	*******	10460	0.6777	0.5263	11060	0.9984	0.8965	11660	0.4538	0.9449
9870	0.0046	*******	10470	0.7252	0.5606	11070	0.9992	0.8991	11670	0.4471	0.9458
9880	0.0050	*******	10480	0.7532	0.5950	11080	1.0000	0.9018	11680	0.4402	0.9467
9890	0.0054	*******	10490	0.7760	0.6295	11090	0.9992	0.9044	11690	0.4326	0.9476
9900	0.0058	*******	10500	0.7990	0.6641	11100	0.9985	0.9071	11700	0.4253	0.9485
9910	0.0062	*******	10510	0.8225	0.6726	11110	0.9957	0.9064	11710	0.4188	0.9491
9920	0.0066	*******	10520	0.8405	0.6812	11120	0.9883	0.9056	11720	0.4106	0.9496
9930	0.0070	*******	10530	0.8531	0.6898	11130	0.9807	0.9049	11730	0.4024	0.9502
9940	0.0074	*******	10540	0.8568	0.6985	11140	0.9731	0.9042	11740	0.3942	0.9507
9950	0.0078	*******	10550	0.8604	0.7072	11150	0.9656	0.9034	11750	0.3860	0.9513
9960	0.0082	*******	10560	0.8618	0.7160	11160	0.9505	0.9026	11760	0.3778	0.9518
9970	0.0086	*******	10570	0.8617	0.7248	11170	0.9355	0.9019	11770	0.3695	0.9523
9980	0.0090	*******	10580	0.8615	0.7338	11180	0.9207	0.9011	11780	0.3610	0.9528
9990	0.0094	*******	10590	0.8570	0.7427	11190	0.9059	0.9003	11790	0.3525	0.9533
10000	0.0098	0.0056	10600	0.8514	0.7507	11200	0.8913	0.8995	11800	0.3441	0.9538
10010	0.0101	0.0063	10610	0.8542	0.7516	11210	0.8821	0.9089	11810	0.3371	0.9522
10020	0.0105	0.0071	10620	0.8571	0.7515	11220	0.8730	0.9083	11820	0.3301	0.9506
10030	0.0109	0.0078	10630	0.8599	0.7514	11230	0.8638	0.9128	11830	0.3230	0.9490
10040	0.0113	0.0085	10640	0.8625	0.7513	11240	0.8553	0.9172	11840	0.3152	0.9474
10050	0.0117	0.0093	10650	0.8639	0.7512	11250	0.8480	0.9217	11850	0.3069	0.9468
10060	0.0121	0.0100	10660	0.8652	0.7511	11260	0.8405	0.9262	11860	0.2986	0.9442
10070	0.0125	0.0108	10670	0.8665	0.7509	11270	0.8330	0.9307	11870	0.2901	0.9426
10080	0.0129	0.0116	10680	0.8678	0.7507	11280	0.8254	0.9352	11880	0.2815	0.9409
10090	0.0132	0.0123	10690	0.8690	0.7505	11290	0.8177	0.9398	11890	0.2729	0.9394
10100	0.0136	0.0131	10700	0.8710	0.7503	11300	0.8072	0.9443	11900	0.2647	0.9378
10110	0.0154	0.0146	10710	0.8745	0.7537	11310	0.7967	0.9468	11910	0.2564	0.9354
10120	0.0172	0.0160	10720	0.8780	0.7571	11320	0.7891	0.9493	11920	0.2482	0.9331
10130	0.0190	0.0175	10730	0.8812	0.7605	11330	0.7808	0.9518	11930	0.2401	0.9307
10140	0.0208	0.0189	10740	0.8844	0.7639	11340	0.7725	0.9542	11940	0.2323	0.9284
10150	0.0225	0.0204	10750	0.8876	0.7673	11350	0.7641	0.9567	11950	0.2245	0.9260
10160	0.0243	0.0219	10760	0.8911	0.7707	11360	0.7556	0.9591	11960	0.2168	0.9236
10170	0.0262	0.0234	10770	0.8946	0.7741	11370	0.7457	0.9616	11970	0.2091	0.9212
10180	0.0280	0.0249	10780	0.9002	0.7776	11380	0.7350	0.9640	11980	0.2014	0.9189
10190	0.0298	0.0264	10790	0.9079	0.7810	11390	0.7255	0.9664	11990	0.1932	0.9165
10200	0.0316	0.0280	10800	0.9156	0.7845	11400	0.7160	0.9688	12000	0.1851	0.9141
10210	0.0369	0.0325	10810	0.9233	0.7892	11410	0.7064	0.9719	12010	0.1827	0.9127
10220	0.0445	0.0371	10820	0.9285	0.7940	11420	0.6992	0.9751	12020	0.1797	0.9113
10230	0.0522	0.0417	10830	0.9337	0.7988	11430	0.6917	0.9782	12030	0.1767	0.9099
10240	0.0599	0.0464	10840	0.9389	0.8037	11440	0.6839	0.9813	12040	0.1737	0.9085
10250	0.0677	0.0511	10850	0.9440	0.8085	11450	0.6760	0.9844	12050	0.1708	0.9072
10260	0.0756	0.0558	10860	0.9497	0.8134	11460	0.6663	0.9875	12060	0.1678	0.9058
10270	0.0834	0.0606	10870	0.9552	0.8182	11470	0.6548	0.9907	12070	0.1649	0.9044
10280	0.0914	0.0654	10880	0.9581	0.8231	11480	0.6434	0.9938	12080	0.1621	0.9030
10290	0.0994	0.0702	10890	0.9610	0.8280	11490	0.6319	0.9969	12090	0.1592	0.9016
10300	0.1074	0.0751	10900	0.9638	0.8330	11500	0.6196	1.0000	12100	0.1564	0.9002
10310	0.1172	0.0988	10910	0.9689	0.8376	11510	0.6063	0.9939	12110	0.1553	0.8986
10320	0.1498	0.1228	10920	0.9739	0.8423	11520	0.5932	0.9879	12120	0.1541	0.8970
10330	0.1825	0.1470	10930	0.9788	0.8470	11530	0.5802	0.9818	12130	0.1525	0.8955
10340	0.2155	0.1714	10940	0.9820	0.8518	11540	0.5673	0.9758	12140	0.1507	0.8939
10350	0.2487	0.1960	10950	0.9852	0.8565	11550	0.5546	0.9697	12150	0.1490	0.8923

Table A7a
(CONTINUED)

WAVELENGTH (NM)	PF	F	WAVELENGTH (NM)	PF	F	WAVELENGTH (NM)	PF	F	WAVELENGTH (NM)	PF	F
12160	0.1472	0.8907	12380	0.0707	0.5991	12600	0.0034	0.0422	12820	0.0005	0.0076
12170	0.1454	0.8891	12390	0.0656	0.5721	12610	0.0032	0.0400	12830	0.0005	0.0073
12180	0.1437	0.8875	12400	0.0606	0.5451	12620	0.0030	0.0377	12840	0.0004	0.0070
12190	0.1419	0.8859	12410	0.0561	0.5149	12630	0.0028	0.0356	12850	0.0004	0.0067
12200	0.1396	0.8843	12420	0.0517	0.4846	12640	0.0026	0.0334	12860	0.0004	0.0064
12210	0.1371	0.8774	12430	0.0473	0.4543	12650	0.0024	0.0312	12870	0.0004	0.0061
12220	0.1346	0.8706	12440	0.0430	0.4238	12660	0.0022	0.0291	12880	0.0004	0.0058
12230	0.1320	0.8638	12450	0.0389	0.3934	12670	0.0020	0.0270	12890	0.0003	0.0055
12240	0.1295	0.8571	12460	0.0349	0.3628	12680	0.0018	0.0248	12900	0.0003	0.0051
12250	0.1269	0.8503	12470	0.0311	0.3322	12690	0.0016	0.0228	12910	0.0003	0.0047
12260	0.1244	0.8435	12480	0.0274	0.3015	12700	0.0015	0.0207	12920	0.0002	0.0043
12270	0.1219	0.8368	12490	0.0238	0.2708	12710	0.0014	0.0194	12930	0.0002	0.0039
12280	0.1177	0.8301	12500	0.0205	0.2400	12720	0.0013	0.0182	12940	0.0002	0.0035
12290	0.1134	0.8234	12510	0.0186	0.2197	12730	0.0012	0.0170	12950	0.0002	0.0031
12300	0.1092	0.8166	12520	0.0167	0.1996	12740	0.0011	0.0157	12960	0.0001	0.0026
12310	0.1051	0.7893	12530	0.0149	0.1795	12750	0.0010	0.0145	12970	0.0001	0.0022
12320	0.1006	0.7620	12540	0.0130	0.1596	12760	0.0009	0.0132	12980	0.0001	0.0018
12330	0.0963	0.7347	12550	0.0112	0.1397	12770	0.0008	0.0120	12990	0.0001	0.0014
12340	0.0921	0.7075	12560	0.0095	0.1200	12780	0.0007	0.0107	13000	0.0001	******
12350	0.0872	0.6803	12570	0.0077	0.1004	12790	0.0006	0.0095	13010	0.0000	******
12360	0.0815	0.6532	12580	0.0061	0.0808	12800	0.0005	0.0083	13020	0.0000	******
12370	0.0760	0.6261	12590	0.0047	0.0614	12810	0.0005	0.0079			

Table A7b

THEMATIC MAPPER RELATVE SPECTRAL RESPONSE - BAND 6 *** DETECTOR 2

WAVELENGTH (NM)	PF	F	WAVELENGTH (NM)	PF	F	WAVELENGTH (NM)	PF	F	WAVELENGTH (NM)	PF	F
9760	0.0004	*******	10360	0.2893	0.2256	10960	0.9914	0.9479	11560	0.5876	0.9524
9770	0.0008	*******	10370	0.3237	0.2511	10970	0.9933	0.9547	11570	0.5761	0.9446
9780	0.0002	*******	10380	0.3585	0.2769	10980	0.9951	0.9614	11580	0.5649	0.9368
9790	0.0015	*******	10390	0.3934	0.3029	10990	0.9969	0.9683	11590	0.5537	0.9290
9800	0.0019	*******	10400	0.4290	0.3292	11000	0.9988	0.9751	11600	0.5422	0.9213
9810	0.0023	*******	10410	0.4648	0.3633	11010	0.9990	0.9759	11610	0.5309	0.9243
9820	0.0027	*******	10420	0.5042	0.3974	11020	0.9992	0.9768	11620	0.5197	0.9272
9830	0.0031	*******	10430	0.5506	0.4317	11030	0.9995	0.9776	11630	0.5087	0.9302
9840	0.0035	*******	10440	0.5974	0.4661	11040	0.9997	0.9784	11640	0.4994	0.9332
9850	0.0039	*******	10450	0.6447	0.5005	11050	1.0000	0.9793	11650	0.4900	0.9361
9860	0.0043	*******	10460	0.6923	0.5350	11060	0.9978	0.9801	11660	0.4807	0.9391
9870	0.0047	*******	10470	0.7403	0.5696	11070	0.9956	0.9809	11670	0.4715	0.9420
9880	0.0051	*******	10480	0.7683	0.6043	11080	0.9934	0.9818	11680	0.4623	0.9450
9890	0.0055	*******	10490	0.7915	0.6391	11090	0.9878	0.9828	11690	0.4539	0.9480
9900	0.0059	*******	10500	0.8147	0.6739	11100	0.9823	0.9834	11700	0.4460	0.9509
9910	0.0083	*******	10510	0.8384	0.6839	11110	0.9724	0.9806	11710	0.4388	0.9536
9920	0.0067	*******	10520	0.8574	0.6940	11120	0.9547	0.9778	11720	0.4331	0.9562
9930	0.0071	*******	10530	0.8709	0.7042	11130	0.9370	0.9750	11730	0.4273	0.9589
9940	0.0075	*******	10540	0.8753	0.7145	11140	0.9195	0.9721	11740	0.4215	0.9615
9950	0.0080	*******	10550	0.8797	0.7248	11150	0.9023	0.9633	11750	0.4156	0.9642
9960	0.0084	*******	10560	0.8818	0.7353	11160	0.8852	0.9665	11760	0.4096	0.9688
9970	0.0088	*******	10570	0.8823	0.7458	11170	0.8683	0.9637	11770	0.4033	0.9694
9980	0.0092	*******	10580	0.8828	0.7584	11180	0.8518	0.9608	11780	0.3968	0.9721
9990	0.0096	*******	10590	0.8788	0.7671	11190	0.8354	0.9580	11790	0.3902	0.9747
10000	0.0100	0.0058	10600	0.8737	0.7779	11200	0.8193	0.9552	11800	0.3836	0.9773
10010	0.0104	0.0066	10610	0.8761	0.7793	11210	0.8173	0.9579	11810	0.3765	0.9778
10020	0.0108	0.0073	10620	0.8784	0.7806	11220	0.8153	0.9608	11820	0.3693	0.9782
10030	0.0112	0.0081	10630	0.8806	0.7820	11230	0.8131	0.9635	11830	0.3621	0.9787
10040	0.0116	0.0088	10640	0.8826	0.7833	11240	0.8116	0.9661	11840	0.3541	0.9792
10050	0.0120	0.0096	10650	0.8834	0.7846	11250	0.8110	0.9688	11850	0.3456	0.9797
10060	0.0124	0.0104	10660	0.8842	0.7859	11260	0.8104	0.9716	11860	0.3370	0.9801
10070	0.0128	0.0112	10670	0.8849	0.7872	11270	0.8098	0.9743	11870	0.3281	0.9806
10080	0.0132	0.0120	10680	0.8856	0.7884	11280	0.8090	0.9771	11880	0.3192	0.9810
10090	0.0136	0.0128	10690	0.8862	0.7896	11290	0.8081	0.9798	11890	0.3103	0.9815
10100	0.0140	0.0136	10700	0.8845	0.7908	11300	0.8016	0.9826	11900	0.3018	0.9819
10110	0.0158	0.0150	10710	0.8852	0.7958	11310	0.7950	0.9832	11910	0.2932	0.9816
10120	0.0176	0.0165	10720	0.8859	0.8008	11320	0.7913	0.9838	11920	0.2847	0.9813
10130	0.0194	0.0018	10730	0.8847	0.8058	11330	0.7855	0.9844	11930	0.2764	0.9809
10140	0.0213	0.0195	10740	0.8835	0.8108	11340	0.7797	0.9849	11940	0.2683	0.9805
10150	0.0231	0.0210	10750	0.8822	0.8158	11350	0.7789	0.9855	11950	0.2603	0.9801
10160	0.0250	0.0226	10760	0.8809	0.8209	11360	0.7679	0.9860	11960	0.2524	0.9797
10170	0.0268	0.0241	10770	0.8797	0.8260	11370	0.7606	0.9866	11970	0.2444	0.9793
10180	0.0287	0.0256	10780	0.8803	0.8311	11380	0.7525	0.9871	11980	0.2365	0.9788
10190	0.0305	0.0272	10790	0.8862	0.8362	11390	0.7456	0.9876	11990	0.2280	0.9784
10200	0.0324	0.0288	10800	0.8921	0.8413	11400	0.7387	0.9881	12000	0.2196	0.9779
10210	0.0378	0.0334	10810	0.8974	0.8479	11410	0.7317	0.9893	12010	0.2167	0.9769
10220	0.0456	0.0381	10820	0.9068	0.8544	11420	0.7271	0.9905	12020	0.2130	0.9759
10230	0.0535	0.0428	10830	0.9162	0.8610	11430	0.7224	0.9917	12030	0.2094	0.9749
10240	0.0614	0.0476	10840	0.9257	0.8677	11440	0.7174	0.9929	12040	0.2057	0.9739
10250	0.0693	0.0524	10850	0.9352	0.8743	11450	0.7123	0.9941	12050	0.2022	0.9729
10260	0.0774	0.0572	10860	0.9448	0.8810	11460	0.7052	0.9953	12060	0.1986	0.9719
10270	0.0854	0.0621	10870	0.9543	0.8877	11470	0.6963	0.9965	12070	0.1951	0.9708
10280	0.0936	0.0670	10880	0.9612	0.8945	11480	0.6875	0.9977	12080	0.1916	0.9698
10290	0.1018	0.0719	10890	0.9681	0.9013	11490	0.6786	0.9989	12090	0.1881	0.9688
10300	0.1100	0.0769	10900	0.9750	0.9081	11500	0.6689	1.0000	12100	0.1846	0.9677
10310	0.1201	0.1011	10910	0.9787	0.9146	11510	0.6549	0.9920	12110	0.1832	0.9665
10320	0.1535	0.1256	10920	0.9824	0.9212	11520	0.6412	0.9840	12120	0.1818	0.9653
10330	0.1871	0.1502	10930	0.9859	0.9278	11530	0.6276	0.9761	12130	0.1797	0.9640
10340	0.2209	0.1751	10940	0.9878	0.9345	11540	0.6141	0.9682	12140	0.1775	0.9627
10350	0.2550	0.2002	10950	0.9896	0.9412	11550	0.6008	0.9603	12150	0.1754	0.9615

Table A7b
(CONTINUED)

WAVELENGTH (NM)	PF	F	WAVELENGTH (NM)	PF	F	WAVELENGTH (NM)	PF	F	WAVELENGTH (NM)	PF	F
12160	0.1732	0.9602	12380	0.0814	0.6523	12600	0.0038	0.0458	12820	0.0005	0.0081
12170	0.1710	0.9589	12390	0.0754	0.6232	12610	0.0036	0.0433	12830	0.0005	0.0078
12180	0.1688	0.9577	12400	0.0696	0.5940	12620	0.0033	0.0409	12840	0.0005	0.0074
12190	0.1665	0.9564	12410	0.0643	0.5614	12630	0.0031	0.0385	12850	0.0004	0.0071
12200	0.1638	0.9551	12420	0.0591	0.5286	12640	0.0028	0.0361	12860	0.0004	0.0068
12210	0.1607	0.9481	12430	0.0540	0.4957	12650	0.0026	0.0337	12870	0.0004	0.0064
12220	0.1576	0.9412	12440	0.0490	0.4627	12660	0.0024	0.0314	12880	0.0004	0.0061
12230	0.1545	0.9343	12450	0.0442	0.4296	12670	0.0022	0.0291	12890	0.0003	0.0058
12240	0.1514	0.9274	12460	0.0396	0.3964	12680	0.0020	0.0268	12900	0.0003	0.0054
12250	0.1483	0.9205	12470	0.0352	0.3631	12690	0.0018	0.0245	12910	0.0003	0.0050
12260	0.1452	0.9136	12480	0.0309	0.3297	12700	0.0016	0.0223	12920	0.0003	0.0045
12270	0.1422	0.9067	12490	0.0269	0.2962	12710	0.0015	0.0209	12930	0.0002	0.0041
12280	0.1372	0.8999	12500	0.0230	0.2627	12720	0.0014	0.0195	12940	0.0002	0.0037
12290	0.1320	0.8930	12510	0.0209	0.2403	12730	0.0013	0.0182	12950	0.0002	0.0032
12300	0.1270	0.8861	12520	0.0187	0.2181	12740	0.0012	0.0168	12960	0.0002	0.0028
12310	0.1220	0.8568	12530	0.0166	0.1960	12750	0.0011	0.0155	12970	0.0001	0.0023
12320	0.1168	0.8275	12540	0.0146	0.1741	12760	0.0010	0.0141	12980	0.0001	0.0019
12330	0.1116	0.7982	12550	0.0126	0.1523	12770	0.0009	0.0128	12990	0.0001	0.0015
12340	0.1066	0.7690	12560	0.0106	0.1307	12780	[illegible]	0.0115	13000	0.0001	******
12350	0.1009	0.7398	12570	0.0086	0.1092	12790	0.0007	0.0101	13010	0.0000	******
12360	0.0941	0.7136	12580	0.0068	0.0879	12800	0.0005	0.0088	13020	0.0000	******
12370	0.0877	0.6814	12590	0.0053	0.0667	12810	0.0006	0.0085			

Table A7c

THEMATIC MAPPER RELATVE SPECTRAL RESPONSE · BAND 6 *** DETECTOR 3

WAVELENGTH (NM)	PF	F	WAVELENGTH (NM)	PF	F	WAVELENGTH (NM)	PF	F	WAVELENGTH (NM)	PF	F
9760	0.0004	******	10360	0.2830	0.2209	10960	0.9906	0.8613	11560	0.6197	0.9636
9770	0.0008	******	10370	0.3167	0.2461	10970	0.9927	0.8661	11570	0.6072	0.9575
9780	0.0011	******	10380	0.3507	0.2715	10980	0.9947	0.8709	11580	0.5950	0.9515
9790	0.0015	******	10390	0.3849	0.2971	10990	0.9967	0.8758	11590	0.5829	0.9454
9800	0.0019	******	10400	0.4203	0.3230	11000	0.9988	0.8806	11600	0.5706	0.9393
9810	0.0023	******	10410	0.4561	0.3566	11010	0.9990	0.8832	11610	0.5583	0.9403
9820	0.0027	******	10420	0.4954	0.3903	11020	0.9992	0.8859	11620	0.5462	0.9412
9830	0.0031	******	10430	0.5415	0.4241	11030	0.9995	0.8885	11630	0.5344	0.9422
9840	0.0035	******	10440	0.5880	0.4581	11040	0.9997	0.8912	11640	0.5242	0.9431
9850	0.0038	******	10450	0.6350	0.4922	11050	1.0000	0.8938	11650	0.5141	0.9440
9860	0.0042	******	10460	0.6825	0.5263	11060	0.9988	0.8965	11660	0.5040	0.9449
9870	0.0046	******	10470	0.7304	0.5606	11070	0.9976	0.8991	11670	0.4940	0.9458
9880	0.0050	******	10480	0.7586	0.5950	11080	0.9964	0.9018	11680	0.4840	0.9467
9890	0.0054	******	10490	0.7816	0.6295	11090	0.9936	0.9044	11690	0.4748	0.9476
9900	0.0058	******	10500	0.8047	0.6641	11100	0.9908	0.9071	11700	0.4663	0.9485
9910	0.0062	******	10510	0.8286	0.6726	11110	0.9835	0.9064	11710	0.4584	0.9491
9920	0.0066	******	10520	0.8468	0.6812	11120	0.9717	0.9056	11720	0.4521	0.9496
9930	0.0070	******	10530	0.8596	0.6898	11130	0.9597	0.9049	11730	0.4457	0.9502
9940	0.0074	******	10540	0.8633	0.6985	11140	0.9478	0.9042	11740	0.4392	0.9507
9950	0.0078	******	10550	0.8670	0.7072	11150	0.9360	0.9034	11750	0.4326	0.9513
9960	0.0082	******	10560	0.8685	0.7160	11160	0.9243	0.9026	11760	0.4260	0.9518
9970	0.0086	******	10570	0.8684	0.7248	11170	0.9126	0.9019	11770	0.4199	0.9523
9980	0.0090	******	10580	0.8683	0.7338	11180	0.9010	0.9011	11780	0.4119	0.9528
9990	0.0094	******	10590	0.8688	0.7427	11190	0.8895	0.9003	11790	0.4046	0.9533
10000	0.0098	0.0056	10600	0.8582	0.7507	11200	0.8781	0.8995	11800	0.3973	0.9538
10010	0.0102	0.0063	10610	0.8613	0.7516	11210	0.8722	0.9039	11810	0.3895	0.9522
10020	0.0106	0.0071	10620	0.8645	0.7515	11220	0.8662	0.9083	11820	0.3816	0.9506
10030	0.0108	0.0078	10630	0.8677	0.7514	11230	0.8602	0.9128	11830	0.3737	0.9490
10040	0.0111	0.0085	10640	0.8705	0.7513	11240	0.8549	0.9172	11840	0.3650	0.9474
10050	0.0115	0.0093	10650	0.8722	0.7512	11250	0.8507	0.9217	11850	0.3557	0.9458
10060	0.0118	0.0100	10660	0.8738	0.7511	11260	0.8465	0.9262	11860	0.3463	0.9442
10070	0.0121	0.0108	10670	0.8754	0.7509	11270	0.8422	0.9307	11870	0.3367	0.9426
10080	0.0124	0.0116	10680	0.8770	0.7507	11280	0.8379	0.9352	11880	0.3270	0.9409
10090	0.0127	0.0123	10690	0.8786	0.7505	11290	0.8335	0.9398	11890	0.3174	0.9394
10100	0.0131	0.0131	10700	0.8777	0.7503	11300	0.8262	0.9443	11900	0.3081	0.9378
10110	0.0148	0.0146	10710	0.8784	0.7537	11310	0.8190	0.9468	11910	0.2988	0.9354
10120	0.0165	0.0160	10720	0.8792	0.7571	11320	0.8147	0.9493	11920	0.2896	0.9331
10130	0.0183	0.0175	10730	0.8779	0.7605	11330	0.8098	0.9518	11930	0.2805	0.9307
10140	0.0202	0.0189	10740	0.8767	0.7639	11340	0.8048	0.9542	11940	0.2717	0.9284
10150	0.0220	0.0204	10750	0.8755	0.7673	11350	0.7988	0.9567	11950	0.2630	0.9260
10160	0.0239	0.0219	10760	0.8742	0.7707	11360	0.7947	0.9591	11960	0.2543	0.9236
10170	0.0258	0.0234	10770	0.87[illegible]	0.7741	11370	0.7882	0.9616	11970	0.2457	0.9212
10180	0.0278	0.0249	10780	0.8736	0.7776	11380	0.7808	0.9640	11980	0.2370	0.9189
10190	0.0297	0.0264	10790	0.8794	0.7810	11390	0.7747	0.9664	11990	0.2278	0.9165
10200	0.0316	0.0280	10800	0.8853	0.7845	11400	0.7686	0.9688	12000	0.2187	0.9141
10210	0.0370	0.0325	10810	0.8912	0.7892	11410	0.7625	0.9719	12010	0.2158	0.9127
10220	0.0447	0.0371	10820	0.9011	0.7940	11420	0.7589	0.9751	12020	0.2121	0.9113
10230	0.0524	0.0417	10830	0.9109	0.7988	11430	0.7551	0.9782	12030	0.2085	0.9099
10240	0.0601	0.0464	10840	0.9209	0.8037	11440	0.7510	0.9813	12040	0.2050	0.9085
10250	0.0678	0.0511	10850	0.9309	0.8085	11450	0.7468	0.9844	12050	0.2014	0.9072
10260	0.0757	0.0558	10860	0.9406	0.8134	11460	0.7406	0.9875	12060	0.1979	0.9058
10270	0.0836	0.0606	10870	0.9502	0.8182	11470	0.7325	0.9907	12070	0.1944	0.9044
10280	0.0916	0.0654	10880	0.9571	0.8231	11480	0.7244	0.9938	12080	0.1909	0.9030
10290	0.0996	0.0702	10890	0.9641	0.8280	11490	0.7163	0.9969	12090	0.1875	0.9016
10300	0.1077	0.0751	10900	0.9711	0.8330	11500	0.7072	1.0000	12100	0.1841	0.9002
10310	0.1175	0.0988	10910	0.9754	0.8376	11510	0.6922	0.9939	12110	0.1827	0.8986
10320	0.1502	0.1228	10920	0.9797	0.8423	11520	0.6774	0.9879	12120	0.1813	0.8970
10330	0.1830	0.1470	10930	0.9838	0.8470	11530	0.6627	0.9818	12130	0.1793	0.8955
10340	0.2161	0.1714	10940	0.9862	0.8518	11540	0.6482	0.9758	12140	0.1771	0.8939
10350	0.2495	0.1960	10950	0.9886	0.8565	11550	0.6338	0.9697	12150	0.1750	0.8923

Table A7c
(CONTINUED)

WAVELENGTH (NM)	PF	F	WAVELENGTH (NM)	PF	F	WAVELENGTH (NM)	PF	F	WAVELENGTH (NM)	PF	F
12160	0.1728	0.8907	12380	0.0817	0.5991	12600	0.0038	0.0422	12820	0.0005	0.0076
12170	0.1707	0.8891	12390	0.0757	0.5721	12610	0.0036	0.0400	12830	0.0005	0.0073
12180	0.1685	0.8875	12400	0.0699	0.5451	12620	0.0033	0.0377	12840	0.0005	0.0070
12190	0.1663	0.8859	12410	0.0646	0.5149	12630	0.0031	0.0356	12850	0.0004	0.0067
12200	0.1636	0.8843	12420	0.0595	0.4846	12640	0.0028	0.0334	12860	0.0004	0.0064
12210	0.1606	0.8774	12430	0.0544	0.4543	12650	0.0026	0.0312	12870	0.0004	0.0061
12220	0.1575	0.8706	12440	0.0494	0.4238	12660	0.0024	0.0291	12880	0.0004	0.0058
12230	0.1544	0.8638	12450	0.0446	0.3934	12670	0.0022	0.0270	12890	0.0003	0.0055
12240	0.1514	0.8571	12460	0.0399	0.3628	12680	0.0020	0.0248	12900	0.0003	0.0051
12250	0.1483	0.8503	12470	0.0355	0.3322	12690	0.0018	0.0228	12910	0.0003	0.0047
12260	0.1453	0.8435	12480	0.0312	0.3015	12700	0.0016	0.0207	12920	0.0003	0.0043
12270	0.1422	0.8368	12490	0.0272	0.2708	12710	0.0015	0.0194	12930	0.0002	0.0039
12280	0.1373	0.8301	12500	0.0233	0.2400	12720	0.0014	0.0182	12940	0.0002	0.0035
12290	0.1322	0.8234	12510	0.0211	0.2187	12730	0.0013	0.0170	12950	0.0002	0.0031
12300	0.1271	0.8166	12520	0.0189	0.1986	12740	0.0012	0.0157	12960	0.0001	0.0026
12310	0.1222	0.7893	12530	0.0168	0.1785	12750	0.0011	0.0145	12970	0.0001	0.0022
12320	0.1170	0.7620	12540	0.0147	0.1586	12760	0.0010	0.0132	12980	0.0001	0.0018
12330	0.1119	0.7347	12550	0.0127	0.1387	12770	0.0009	0.0120	12990	0.0001	0.0014
12340	0.1068	0.7075	12560	0.0107	0.1200	12780	0.0008	0.0107	13000	0.0001	******
12350	0.1012	0.6803	12570	0.0087	0.1004	12790	0.0007	0.0095	13010	0.0000	******
12360	0.0945	0.6532	12580	0.0068	0.0808	12800	0.0006	0.0083	13020	0.0000	******
12370	0.0880	0.6261	12590	0.0053	0.0614	12810	0.0005	0.0079			

Table A7d

THEMATIC MAPPER RELATVE SPECTRAL RESPONSE - BAND 6 *** DETECTOR 4

WAVELENGTH (NM)	PF	F	WAVELENGTH (NM)	PF	F	WAVELENGTH (NM)	PF	F	WAVELENGTH (NM)	PF	F
10000	0.0094	0.0058	10600	0.8375	0.7779	11200	0.8728	0.9552	11800	0.4297	0.9773
10010	0.0097	0.0066	10610	0.8411	0.7793	11210	0.8682	0.9579	11810	0.4215	0.9778
10020	0.0100	0.0073	10620	0.8447	0.7806	11220	0.8637	0.9606	11820	0.4133	0.9782
10030	0.0103	0.0081	10630	0.8483	0.7820	11230	0.8591	0.9635	11830	0.4050	0.9787
10040	0.0107	0.0088	10640	0.8516	0.7833	11240	0.8552	0.9661	11840	0.3958	0.9792
10050	0.0110	0.0096	10650	0.8538	0.7846	11250	0.8524	0.9688	11850	0.3858	0.9797
10060	0.0113	0.0104	10660	0.8559	0.7859	11260	0.8496	0.9716	11860	0.3751	0.9801
10070	0.0116	0.0112	10670	0.8579	0.7872	11270	0.8468	0.9743	11870	0.3659	0.9806
10080	0.0119	0.0120	10680	0.8600	0.7884	11280	0.8439	0.9771	11880	0.3557	0.9810
10090	0.0122	0.0128	10690	0.8620	0.7896	11290	0.8410	0.9798	11890	0.3455	0.9815
10100	0.0126	0.0136	10700	0.8647	0.7908	11300	0.8358	0.9826	11900	0.3357	0.9819
10110	0.0142	0.0150	10710	0.8694	0.7958	11310	0.8294	0.9832	11910	0.3274	0.9816
10120	0.0158	0.0165	10720	0.8742	0.8008	11320	0.8266	0.9838	11920	0.3190	0.9813
10130	0.0177	0.0018	10730	0.8786	0.8058	11330	0.8232	0.9844	11930	0.3109	0.9809
10140	0.0194	0.0195	10740	0.8830	0.8108	11340	0.8197	0.9849	11940	0.3030	0.9805
10150	0.0212	0.0210	10750	0.8875	0.8158	11350	0.8162	0.9855	11950	0.2953	0.9801
10160	0.0230	0.0226	10760	0.8919	0.8209	11360	0.8126	0.9860	11960	0.2876	0.9797
10170	0.0249	0.0241	10770	0.8964	0.8260	11370	0.8075	0.9866	11970	0.2799	0.9793
10180	0.0267	0.0256	10780	0.9029	0.8311	11380	0.8017	0.9871	11980	0.2722	0.9788
10190	0.0286	0.0272	10790	0.9115	0.8362	11390	0.7971	0.9876	11990	0.2639	0.9784
10200	0.0305	0.0288	10800	0.9202	0.8413	11400	0.7925	0.9881	12000	0.2556	0.9779
10210	0.0357	0.0334	10810	0.9285	0.8479	11410	0.7904	0.9893	12010	0.2524	0.9769
10220	0.0431	0.0381	10820	0.9342	0.8544	11420	0.7889	0.9905	12020	0.2484	0.9759
10230	0.0506	0.0428	10830	0.9398	0.8610	11430	0.7884	0.9917	12030	0.2444	0.9749
10240	0.0581	0.0476	10840	0.9455	0.8677	11440	0.7875	0.9929	12040	0.2404	0.9739
10250	0.0607	0.0524	10850	0.9512	0.8743	11450	0.7865	0.9941	12050	0.2335	0.9729
10260	0.0733	0.0572	10860	0.9569	0.8810	11460	0.7834	0.9953	12060	0.2326	0.9719
10270	0.0811	0.0621	10870	0.9625	0.8877	11470	0.7784	0.9965	12070	0.2287	0.9708
10280	0.0888	0.0670	10880	0.9654	0.8945	11480	0.7733	0.9977	12080	0.2248	0.9698
10290	0.0967	0.0717	10890	0.9682	0.9013	11490	0.7683	0.9989	12090	0.2210	0.9688
10300	0.10[illegible]	0.0765	10900	0.9711	0.9081	11500	0.7622	1.0000	12100	0.2172	0.9677
10310	0.1141	0.1011	10910	0.9752	0.9146	11510	0.7521	0.9920	12110	0.2126	0.9665
10320	0.1459	0.1256	10920	0.9793	0.9212	11520	0.7421	0.9840	12120	0.2080	0.9653
10330	0.1780	0.1502	10930	0.9832	0.9278	11530	0.7322	0.9761	12130	0.2026	0.9640
10340	0.2103	0.1751	10940	0.9854	0.9345	11540	0.7223	0.9682	12140	0.1971	0.9627
10350	0.2428	0.2002	10950	0.9876	0.9412	11550	0.7126	0.9603	12150	0.1915	0.9615
10360	0.2755	0.2256	10960	0.9898	0.9479	11560	0.7029	0.9524	12160	0.1859	0.9602
10370	0.3085	0.2511	10970	0.9921	0.9547	11570	0.6951	0.9446	12170	0.1803	0.9589
10380	0.3417	0.2769	10980	0.9943	0.9614	11580	0.6875	0.9368	12180	0.1747	0.9577
10390	0.3752	0.3029	10990	0.9965	0.9683	11590	0.6799	0.9290	12190	0.1690	0.9564
10400	0.4095	0.3292	11000	0.9988	0.9751	11600	0.6743	0.9213	12200	0.1629	0.9551
10410	0.4438	0.3633	11010	0.9990	0.9759	11610	0.6592	0.9243	12210	0.1581	0.9481
10420	0.4815	0.3874	11020	0.9992	0.9768	11620	0.6442	0.9272	12220	0.1554	0.9412
10430	0.5262	0.4317	11030	0.9995	0.9776	11630	0.6306	0.9302	12230	0.1517	0.9343
10440	0.5713	0.4661	11040	0.9997	0.9784	11640	0.6188	0.9333	12240	0.1479	0.9274
10450	0.6168	0.5005	11050	1.0000	0.9793	11650	0.6070	0.9361	12250	0.1442	0.9205
10460	0.6629	0.5350	11060	0.9968	0.9801	11660	0.5951	0.9391	12260	0.1405	0.9136
10470	0.7093	0.5696	11070	0.9936	0.9809	11670	0.5831	0.9420	12270	0.1368	0.9067
10480	0.7365	0.6043	11080	0.9903	0.9818	11680	0.5711	0.9450	12280	0.1313	0.8999
10490	0.7588	0.6391	11090	0.9855	0.9828	11690	0.5579	0.9480	12290	0.1256	0.8930
10500	0.7812	0.6739	11100	0.9807	0.9834	11700	0.5454	0.9508	12300	0.1201	0.8861
10510	0.8047	0.6839	11110	0.9739	0.9806	11710	0.5358	0.9536	12310	0.1156	0.8568
10520	0.8228	0.6940	11120	0.9625	0.9778	11720	0.5241	0.9562	12320	0.1107	0.8275
10530	0.8307	0.7042	11130	0.9510	0.9750	11730	0.5124	0.9589	12330	0.1059	0.7982
10540	0.8398	0.7145	11140	0.9396	0.9721	11740	0.5008	0.9615	12340	0.1013	0.7690
10550	0.8439	0.7248	11150	0.9283	0.9693	11750	0.4891	0.9642	12350	0.0960	0.7398
10560	0.8458	0.7353	11160	0.9170	0.9665	11760	0.4775	0.9668	12360	0.0897	0.7136
10570	0.8461	0.7459	11170	0.9059	0.9637	11770	0.4656	0.9694	12370	0.0836	0.6814
10580	0.8464	0.7584	11180	0.8948	0.9608	11780	0.4536	0.9721	12380	0.0778	0.6523
10590	0.8425	0.7671	11190	0.8837	0.9340	11790	0.4417	0.9747	12390	0.0721	0.6232

Table A7d
(CONTINUED)

WAVELENGTH (NM)	PF	F	WAVELENGTH (NM)	PF	F	WAVELENGTH (NM)	PF	F	WAVELENGTH (NM)	PF	F
12400	0.0667	0.5840	12560	0.0105	0.1307	12720	0.0014	0.0195	12880	0.0004	0.0061
12410	0.0617	0.5614	12570	0.0086	0.1092	12730	0.0013	0.0182	12890	0.0004	0.0058
12420	0.0570	0.5286	12580	0.0067	0.0879	12740	0.0012	0.0168	12900	0.0003	0.0054
12430	0.0522	0.4957	12590	0.0052	0.0667	12750	0.0011	0.0155	12910	0.0003	0.0050
12440	0.0475	0.4627	12600	0.0038	0.0458	12760	0.0010	0.0141	12920	0.0003	0.0045
12450	0.0430	0.4296	12610	0.0035	0.0433	12770	0.0009	0.0128	12930	0.0002	0.0041
12460	0.0386	0.3964	12620	0.0033	0.0409	12780	0.0008	0.0115	12940	0.0002	0.0037
12470	0.0344	0.3631	12630	0.0031	0.0385	12790	0.0007	0.0101	12950	0.0002	0.0032
12480	0.0304	0.3297	12640	0.0028	0.0361	12800	0.0006	0.0088	12960	0.0002	0.0028
12490	0.0265	0.2962	12650	0.0026	0.0337	12810	0.0006	0.0085	12970	0.0001	0.0023
12500	0.0228	0.2627	12660	0.0024	0.0314	12820	0.0005	0.0081	12980	0.0001	0.0019
12510	0.0206	0.2403	12670	0.0022	0.0291	12830	0.0005	0.0078	12990	0.0001	0.0015
12520	0.0185	0.2181	12680	0.0020	0.0268	12840	0.0005	0.0074	13000	0.0001	*******
12530	0.0165	0.1960	12690	0.0018	0.0245	12850	0.0005	0.0071	13010	0.0000	*******
12540	0.0145	0.1741	12700	0.0016	0.0223	12860	0.0004	0.0068	13020	0.0000	*******
12550	0.0125	0.1523	12710	0.0015	0.0209	12870	0.0004	0.0064			

N85-20515 D7

PRELAUNCH ABSOLUTE RADIOMETRIC CALIBRATION OF THE REFLECTIVE BANDS ON THE LANDSAT-4 PROTOFLIGHT THEMATIC MAPPER

J. L. Barker

National Aeronautics and Space Administration
Goddard Space Flight Center
Greenbelt, Maryland 20771

D. L. Ball and K. C. Leung

Computer Sciences Corporation
8728 Colesville Road
Silver Spring, Maryland 20910

J. A. Walker

Santa Barbara Research Center
75 Coromar Drive
Goleta, California 93017

ABSTRACT

The results on the absolute radiometric calibration of the Landsat-4 Thematic Mapper (TM), as determined during prelaunch tests with a 122-centimeter Integrating Sphere (IS), are presented. Detailed results for the best calibration of the protoflight TM are presented, as well as summaries of other tests performed on the sensor from June 1981 to March 1983. The dynamic range of the TM is within a few percent of that required in all bands, except bands 1 and 3. Three detectors failed to pass the minimum SNR specified for their respective bands: band 5, channel 3 (dead), and band 2, channels 2 and 4 (noisy or slow response). Estimates of the absolute calibration accuracy for the TM show that the detectors are typically calibrated to 5-percent absolute error for the reflective bands; 10-percent full-scale accuracy was specified. Ten tests performed to transfer the detector absolute calibration to the internal calibrator show a 5-percent range at full scale in the transfer calibration; however, in two cases band 5 showed a 10-percent difference and a 7-percent difference. These errors are given under the assumption of identical operating conditions for all transfer tests; known temperature sensitivities for the TM have not yet been included.

KEYWORDS: absolute radiometric calibration, dynamic range, noise, signal to noise, gain, offset.

CONTENTS

Introduction II-279

Absolute Calibration of the Reflective Bands II-280
    Calibration of the Detectors II-280
        Gain and Offset Determination and Dynamic Range . . II-280
        Signal-to-Noise Determination II-302
    Calibration of the IC II-304
    Estimated Errors in the TM/PF Calibration II-309

Discussion of Results II-313
    Radiometric Performance Requirements II-313
    Calibration of the Detectors II-315
    Calibration of the IC II-323

Recommendations II-327
    Protoflight TM II-327
    Flight Unit TM II-328

Appendix - Spectral Radiances for the IC II-329

References II-370

INTRODUCTION

Since the 1972 launch of the Landsat-1 satellite, views of natural and manmade features on the surface of the Earth have been routinely provided to data users at a relatively coarse resolution (<150 meters) on a repeating basis (once every 18 days). These images have had a profound effect in many areas, including agricultural production; water resource, rangeland, and forestry management; land use and urban and regional planning; geologic survey and mineral resource management; oceanography; cartography; and disaster warning and relief. Landsat data have been used in many studies involving hydrology, agriculture, geology, forestry, and land resources in addition to urban area delineation.

The latest in the series of Landsat platforms (Landsat-4) was launched from Vandenberg Air Force Base, California, on July 16, 1982. It carried a new sensor, the Thematic Mapper (TM), that will observe the Earth through atmospheric windows in the visible, near-infrared, middle-infrared, and thermal-infrared portions of the electromagnetic spectrum. Although this sensor will return new information to users of Landsat data, its value will depend critically on how well the TM can be calibrated.

Absolute calibration of a satellite instrument (or absolute radiometry) may be defined as the ability to relate the voltage or digital output of the sensor to the input radiance. It includes the determination of the accuracy to which that conversion is made. Absolute calibration demands the use of a carefully controlled and monitored standard source that can be directly related to absolute standards maintained by the National Bureau of Standards (NBS). In a system like Landsat, the calibration must provide the relationship between the digital counts output by the sensor to the radiance input to the detectors in each spectral band. Achieving absolute accuracy to some specified value allows the determination of relative scene spectral radiance. With known solar irradiance at the ground and known atmospheric characteristics, the scene reflectance may be determined. Understanding the sensor characteristics and how they may change with time allows the accurate detection and analysis of temporally varying features and comparison with other sensors such as the Multispectral Scanner (MSS).

This paper discusses the prelaunch absolute calibration of the protoflight TM reflective band detectors and the onboard internal calibrator that will be used to correct observed scene radiance values and to monitor the health of the sensor. The results of the calibration and estimates of its

C-4

accuracy are presented. The TM thermal band requires a different approach to calibration and is discussed in Lansing and Barker (1983). The procedures and the standard source used to calibrate the sensor and the internal calibrator are discussed in Barker et al. (1983a). In-orbit characterization of the TM is presented in Barker et al. (1983b). An excellent summary of the TM instrument and its major subsystems is given in Engel (1980).

ABSOLUTE CALIBRATION OF THE REFLECTIVE BANDS

CALIBRATION OF THE DETECTORS

Gain and Offset Determination and Dynamic Range

Six different detector calibration tests were performed on the Thematic Mapper (TM) with the 122-centimeter (diameter) Integrating Sphere [IS(122)] to determine gain, offset, and the resulting measured dynamic range of the instrument. The dates and test designations for the six calibration tests are given in Barker et al. (1983a). Certain key assumptions must be made to interpret the data from the IS(122) calibrations of the TM:

- Radiance output from the IS(122) in each TM band and at each level is known; that is, the sphere has not changed characteristics from the time of its calibration until the TM calibration is performed.
- Due to alignment and TM operating mode, the detectors are seeing the peak output from the IS(122).
- The TM voltage response to radiance is linear and uniform.

Some of these assumptions may not be true for certain calibration tests.

During each test, TM data were acquired as the lamps in the IS(122) were switched off according to the test sequences described in Barker et al. (1983a). The test sequences used in the detector calibration give 20 different radiance levels. These data were analyzed to determine the characteristics of the 96 detectors in the reflective bands. Selection of the proper gain resistors to establish the dynamic range of the individual detectors was performed only once (test A in Barker et al., 1983a).

Sample results for band 3, channel 9, from test C2 are shown in Figure 1; the residuals for that data are shown in Figure 2. Gain, offset, dynamic range, and signal-to-noise

ILLUSTRATIVE TM/PF RADIOMETRIC ABSOLUTE DETECTOR CALIBRATION FOR CHANNEL 9 OF BAND 3 (624-693 nm)

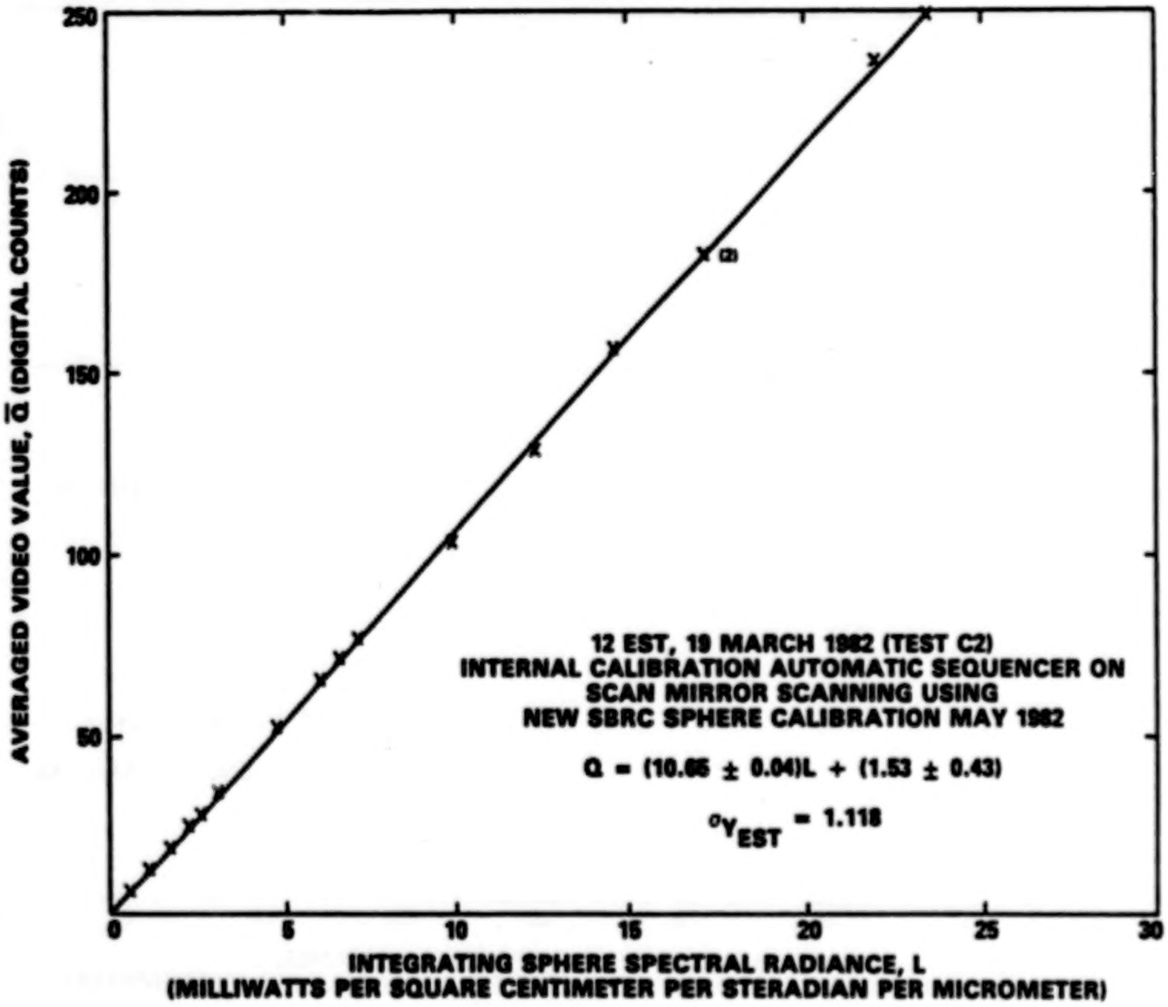

12 EST, 19 MARCH 1982 (TEST C2)
INTERNAL CALIBRATION AUTOMATIC SEQUENCER ON
SCAN MIRROR SCANNING USING
NEW SBRC SPHERE CALIBRATION MAY 1982

$$Q = (10.65 \pm 0.04)L + (1.53 \pm 0.43)$$

$$\sigma_{Y_{EST}} = 1.118$$

FIGURE 1

ILLUSTRATIVE TM/PF RADIOMETRIC ABSOLUTE DETECTOR CALIBRATION RESIDUALS FOR CHANNEL 9 OF BAND 3 (624-693 nm)

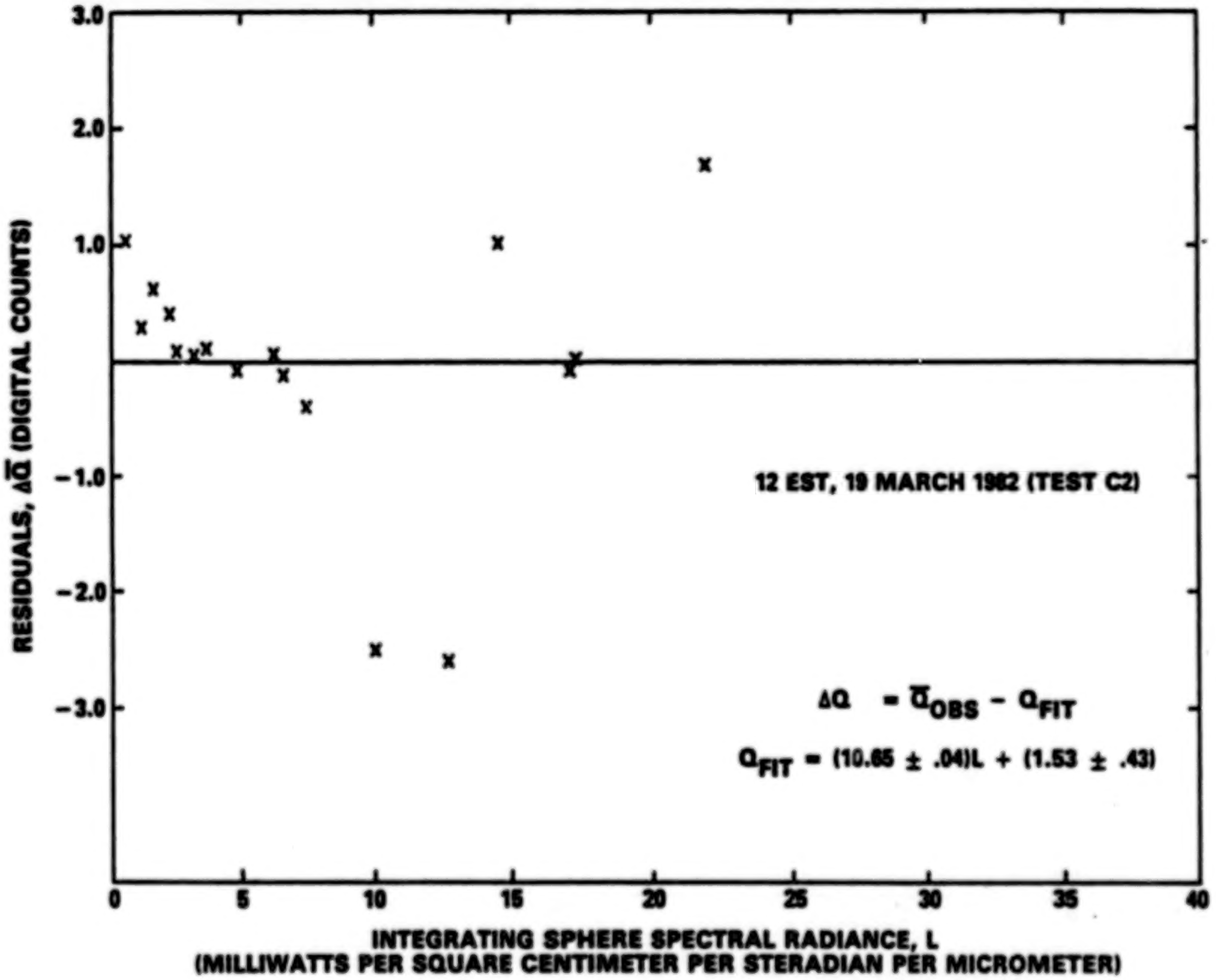

FIGURE 2

ratio (SNR) for these parameters for test C2 are given in Tables 1 through 7; statistics for these parameters are given in Tables 8 through 13 for the same test. Results for the other tests are given in Barker et al. (1983c). The gain and offset are calculated by a least-squares fit to data, such as shown in Figures 1 and 2. The calibration equation is as follows:

$$\bar{Q}_{ijk} = g_{ik} L_{ijk} + O_{ik}$$

where Q_{ijk} is the averaged digital count TM output for detector i (1 to 16) in band k (1 to 5 and 7) and radiance level j (1 to 20), L_{ijk} is the corresponding spectral radiance (milliwatts per square centimeter per steradian per micrometer), and g_{ik} and O_{ik} are the derived gain and offset for the ith detector in band k. The least-squares fit gives values of g_{ik} and O_{ik} as well as their standard errors. The band-averaged gain and offset, the band-averaged SNR, and the derived dynamic range for each band are summarized in Table 14.

The information presented in Tables 1 through 14 should be considered estimates of the best results possible from the TM calibration, not examples of actual calibrations of the TM with the IS(122). A complete set of derived calibration parameters from all six tests has been obtained. A summary of average gains and offsets for three of the tests is given in Table 15. Table 16 shows average gain changes between tests in percent for odd-numbered, even-numbered, and all detectors by band compared to test C2. Although all gains are lower in the March 1982 tests than they were during the initial radiometric calibration, all bands and detectors appear to be within specified values for accuracy and dynamic range. Calculated offset values increased in nearly all bands; values for test C2 are nearly those expected for the background level of two or three digital counts, while those for test A were not.

The apparent systematic nature of the residuals shown in Figure 2 is probably due to the integrating sphere calibration and not to the TM detectors. Other sources of information, such as the sphere calibration of the flight unit TM in July 1982 and the analog-to-digital test measurements on both the protoflight and flight units, show that the TM detectors are extremely linear. Special care was taken in the sphere calibration for the flight unit tests in July 1982, and preliminary results from those tests indicate no such systematic effects.

Table 1

EXPLANATORY INFORMATION FOR DERIVED RADIOMETRIC CALIBRATION PARAMETER TABLES

1. **CALIBRATION EQUATION:**

   COUNTS = GAIN*RADIANCE + OFFSET ($Q = G*L + O$)

2. **UNITS FOR QUANTITIES:**

   A. **DIGITAL COUNTS**

   B. **RADIANCE — MILLIWATTS PER SQUARE CENTIMETER PER STERADIAN PER MICROMETER (i.e., SPECTRAL RADIANCE)**

   C. **GAIN — DIGITAL COUNTS PER "RADIANCE UNITS"**

   D. **OFFSET — DIGITAL COUNTS**

3. **SNR IS SIGNAL TO NOISE RATIO AT:**

   LSR — LOWER SCENE RADIANCE (SPECIFIED)

   MSL — MINIMUM SATURATION LEVEL RADIANCE (SPECIFIED)

4. **RADIANCE IS GIVEN AT:**

   MIN — RADIANCE AT MINIMUM (ZERO COUNTS)

   MSL — RADIANCE AT MINIMUM SATURATION LEVEL (243 COUNTS)

   MAX — RADIANCE AT MAXIMUM (255 COUNTS)

Table 2

TM/PF BAND 1 DERIVED RADIOMETRIC CALIBRATION PARAMETERS

CHAN	GAIN	OFFSET	SNR		RADIANCES			COMMENTS
			LSR	MSL	MIN	MSL	MAX	
1	15.647	3.18	47.	147.	−0.204	15.327	16.094	
2	15.763	2.40	43.	138.	−0.152	15.264	16.026	
3	15.929	2.65	51.	157.	−0.166	15.089	15.842	
4	15.928	2.59	37.	122.	−0.163	15.094	15.847	
5	15.810	2.67	53.	168.	−0.169	15.201	15.960	
6	15.734	2.51	51.	160.	−0.160	15.285	16.048	
7	15.685	2.58	53.	165.	−0.165	15.327	16.092	
8	15.755	2.66	47.	150.	−0.169	15.254	16.016	
9	15.824	2.64	53.	168.	−0.167	15.190	15.948	
10	15.859	2.47	49.	155.	−0.156	15.166	15.923	
11	15.686	2.53	50.	160.	−0.161	15.330	16.095	
12	15.815	2.51	42.	137.	−0.159	15.207	15.966	
13	15.694	2.56	53.	170.	−0.163	15.320	16.085	
14	15.758	2.43	48.	152.	−0.154	15.266	16.027	
15	15.782	2.59	48.	154.	−0.164	15.234	15.994	
16	15.873	2.37	43.	137.	−0.149	15.159	15.915	
SNR COMPUTED AT SPECTRAL RADIANCE			4.00	14.29	[AT 0 COUNTS]	[AT 243 COUNTS]	[AT 255 COUNTS]	
SPECIFIED VALUE OF SNR			32.	85.				

Table 3

TM/PF BAND 2 DERIVED RADIOMETRIC CALIBRATION PARAMETERS

CHAN	GAIN	OFFSET	SNR		RADIANCES			COMMENTS
			LSR	MSL	MIN	MSL	MAX	
1	8.174	2.99	58.	295.	−0.308	29.393	30.831	
2	8.117	2.33	24.	178.	−0.297	23.048	31.127	NOISY
3	8.014	2.41	53.	298.	−0.301	30.021	31.519	
4	8.144	2.44	40.	151.	−0.300	29.538	31.011	SLOW RESPONSE
5	8.196	2.43	59.	293.	−0.297	29.353	30.817	
6	8.183	2.54	61.	302.	−0.311	29.394	30.851	
7	8.057	2.32	51.	303.	−0.288	29.873	31.383	
8	8.079	2.52	51.	317.	−0.312	29.768	31.253	
9	8.075	2.39	53.	308.	−0.298	28.797	31.283	
10	8.093	2.35	53.	298.	−0.290	29.737	31.220	
11	7.998	2.36	57.	304.	−0.296	30.087	31.537	
12	8.014	2.33	55.	311.	−0.291	30.032	31.529	
13	8.117	2.32	51.	285.	−0.285	29.853	31.132	
14	8.141	2.47	58.	278.	−0.304	29.546	31.020	
15	8.195	2.38	59.	283.	−0.290	29.393	30.828	
16	7.979	2.43	55.	304.	−0.304	30.150	31.054	
SNR COMPUTED AT SPECTRAL RADIANCE			3.00	29.12	[AT 0 COUNTS]	[AT 243 COUNTS]	[AT 255 COUNTS]	
SPECIFIED VALUE OF SNR			35.	170.				

Table 4

TM/PF BAND 3 DERIVED RADIOMETRIC CALIBRATION PARAMETERS

CHAN	GAIN	OFFSET	SNR		RADIANCES			COMMENTS
			LSR	MSL	MIN	MSL	MAX	
1	10.777	2.13	47.	204.	−0.197	22.350	23.483	
2	10.802	1.57	50.	247.	−0.148	22.772	23.904	
3	10.590	1.89	48.	236.	−0.179	22.768	23.901	
4	10.531	1.46	47.	253.	−0.139	22.936	24.075	
5	10.624	1.59	47.	229.	−0.149	22.723	23.852	
6	10.663	1.62	47.	229.	−0.152	22.637	23.762	
7	10.582	1.55	49.	241.	−0.146	22.818	23.952	
8	10.535	1.51	47.	256.	−0.144	22.922	24.061	
9	10.645	1.53	44.	246.	−0.144	22.693	23.811	
10	10.567	1.49	47.	240.	−0.141	22.856	23.992	
11	10.556	1.24	45.	240.	−0.117	22.903	24.040	
12	10.643	1.49	45.	229.	−0.140	22.692	23.819	
13	10.695	1.44	42.	218.	−0.135	22.608	23.731	
14	10.640	1.66	45.	239.	−0.156	22.693	23.811	
15	10.769	1.53	44.	209.	−0.142	22.422	23.536	
16	10.484	1.63	43.	239.	−0.156	23.022	24.168	
SNR COMPUTED AT SPECTRAL RADIANCE			1.86	19.29	[AT 0 COUNTS]	[AT 243 COUNTS]	[AT 255 COUNTS]	
SPECIFIED VALUE OF SNR			26.	143.				

Table 5

TM/PF BAND 4 DERIVED RADIOMETRIC CALIBRATION PARAMETERS

CHAN	GAIN	OFFSET	SNR		RADIANCES			COMMENTS
			LSR	MSL	MIN	MSL	MAX	
1	10.972	2.53	76.	359.	−0.231	21.917	23.010	
2	10.817	1.94	74.	306.	−0.179	22.286	23.395	
3	11.019	1.96	70.	380.	−0.178	21.876	22.965	
4	10.831	1.82	76.	310.	−0.168	22.267	23.374	
5	10.812	1.75	69.	348.	−0.162	22.313	23.422	
6	10.832	1.95	63.	344.	−0.179	22.049	23.148	
7	10.813	2.22	78.	328.	−0.205	22.267	23.377	
8	10.881	1.76	76.	315.	−0.162	22.170	23.273	
9	10.860	1.89	84.	304.	−0.174	22.201	23.308	
10	11.291	1.73	63.	356.	−0.153	21.369	22.432	
11	10.753	1.93	67.	400.	−0.179	22.419	23.535	
12	10.901	1.79	60.	320.	−0.164	22.128	23.229	
13	11.055	1.67	79.	368.	−0.151	21.829	22.915	
14	10.911	1.92	61.	385.	−0.176	22.095	23.195	
15	10.771	1.69	65.	348.	−0.157	22.403	23.517	
16	10.828	2.00	65.	303.	−0.184	22.257	23.365	
SNR COMPUTED AT SPECTRAL RADIANCE			1.36	21.43	[AT 0 COUNTS]	[AT 243 COUNTS]	[AT 255 COUNTS]	
SPECIFIED VALUE OF SNR			32.	240.				

Table 6

TM/PF BAND 5 DERIVED RADIOMETRIC CALIBRATION PARAMETERS

CHAN	GAIN	OFFSET	SNR		RADIANCES			COMMENTS
			LSR	MSL	MIN	MSL	MAX	
1	76.569	3.28	42.	184.	−0.043	3.131	3.288	
2	76.830	2.94	43.	198.	−0.038	3.125	3.281	
3	—	—	—	—	—	—	—	DEAD DETECTOR
4	77.698	2.85	43.	182.	−0.037	3.091	3.245	
5	76.906	3.00	37.	172.	−0.039	3.125	3.281	
6	76.888	3.03	38.	190.	−0.039	3.121	3.277	
7	77.412	3.01	33.	158.	−0.039	3.100	3.255	
8	77.166	3.14	43.	193.	−0.041	3.108	3.264	
9	76.966	3.02	40.	184.	−0.039	3.118	3.274	
10	76.969	2.92	40.	183.	−0.038	3.119	3.275	
11	77.665	3.04	42.	175.	−0.039	3.090	3.244	
12	77.755	2.88	44.	179.	−0.037	3.088	3.242	
13	77.555	3.11	45.	177.	−0.040	3.093	3.248	
14	77.242	2.95	45.	183.	−0.038	3.108	3.263	
15	77.309	3.14	44.	177.	−0.041	3.103	3.258	
16	77.742	2.97	48.	185.	−0.038	3.087	3.242	
SNR COMPUTED AT SPECTRAL RADIANCE			0.40	3.00	[AT 0 COUNTS]	[AT 243 COUNTS]	[AT 255 COUNTS]	
SPECIFIED VALUE OF SNR			13.	75.				

Table 7

TM/PF BAND 7 DERIVED RADIOMETRIC CALIBRATION PARAMETERS

CHAN	GAIN	OFFSET	SNR		RADIANCES			COMMENTS
			LSR	MSL	MIN	MSL	MAX	
1	148.235	2.95	30.	169.	−0.020	1.619	1.700	
2	146.770	2.38	25.	172.	−0.016	1.640	1.721	
3	147.693	2.37	31.	194.	−0.016	1.629	1.711	
4	147.723	2.42	26.	172.	−0.016	1.629	1.710	
5	147.729	2.26	29.	192.	−0.015	1.630	1.711	
6	146.698	2.45	27.	176.	−0.017	1.640	1.722	
7	147.815	2.28	13.	99.	−0.015	1.629	1.710	
8	145.350	2.37	28.	198.	−0.016	1.655	1.738	
9	147.910	2.34	27.	178.	−0.016	1.627	1.708	
10	144.747	2.45	25.	166.	−0.017	1.662	1.745	
11	146.976	2.31	26.	185.	−0.016	1.638	1.719	
12	147.933	2.49	27.	171.	−0.017	1.626	1.707	
13	146.146	2.15	30.	200.	−0.015	1.648	1.730	
14	147.462	2.69	25.	156.	−0.018	1.630	1.711	
15	146.199	2.15	31.	204.	−0.015	1.647	1.729	
16	148.492	2.57	29.	169.	−0.017	1.619	1.700	
SNR COMPUTED AT SPECTRAL RADIANCE			0.17	1.59	[AT 0 COUNTS]	[AT 243 COUNTS]	[AT 255 COUNTS]	
SPECIFIED VALUE OF SNR			5.	45.				

Table 8

TM/PF BAND 1

AVERAGE, STANDARD DEVIATION AND COEFFICIENT OF VARIATION FOR DERIVED RADIOMETRIC CALIBRATION PARAMETERS

CHAN	GAIN	OFFSET	SNR		RADIANCES		
			LSR	MSL	MIN	MSL	MAX
MEAN:							
ODD	15.757	2.67	51.	161.	−0.170	15.252	16.014
EVEN	15.811	2.49	45.	144.	−0.158	15.212	15.971
ALL	15.784	2.58	48.	152.	−0.164	15.232	15.992
SIGMA:							
ODD	0.096	0.21	3.	8.	0.014	0.090	0.094
EVEN	0.071	0.10	4.	13.	0.006	0.068	0.071
ALL	0.086	0.18	5.	13.	0.012	0.079	0.083
COEF. VAR. (%):							
ODD	0.61	7.9	6.	5.	−8.2	0.6	0.6
EVEN	0.45	4.0	29.	9.	−3.8	0.4	0.4
ALL	0.54	7.0	10.	9.	−7.3	0.5	0.5

Table 9

TM/PF BAND 2

AVERAGE, STANDARD DEVIATION AND COEFFICIENT OF VARIATION FOR DERIVED RADIOMETRIC CALIBRATION PARAMETERS

CHAN	GAIN	OFFSET	SNR		RADIANCES		
			LSR	MSL	MIN	MSL	MAX
MEAN:							
ODD	8.104	2.45	55.	295.	−0.302	29.689	31.170
EVEN	8.094	2.43	50.	267.	−0.300	29.725	31.208
ALL	8.098	2.44	52.	281.	−0.301	29.707	31.189
SIGMA:							
ODD	0.080	0.22	3.	10.	0.026	0.301	0.316
EVEN	0.070	0.08	12.	65.	0.010	0.256	0.268
ALL	0.072	0.16	9.	47.	0.019	0.276	0.291
COEF. VAR. (%):							
ODD	0.99	8.9	5.	3.	−8.6	1.0	1.0
EVEN	0.86	3.3	24.	24.	−3.3	0.9	0.9
ALL	0.89	6.6	17.	17.	−6.3	0.9	0.9

Table 10

TM/PF BAND 3
AVERAGE, STANDARD DEVIATION AND COEFFICIENT OF VARIATION FOR DERIVED RADIOMETRIC CALIBRATION PARAMETERS

CHAN	GAIN	OFFSET	SNR		RADIANCES		
			LSR	MSL	MIN	MSL	MAX
MEAN:							
ODD	10.654	1.61	46.	228.	−0.151	22.659	23.786
EVEN	10.583	1.55	46.	241.	−0.147	22.815	23.949
ALL	10.618	1.58	46.	235.	−0.149	22.737	23.867
SIGMA:							
ODD	0.084	0.28	2.	16.	0.025	0.190	0.199
EVEN	0.064	0.08	2.	10.	0.007	0.138	0.146
ALL	0.081	0.20	2.	14.	0.018	0.181	0.194
COEF. VAR. (%):							
ODD	0.79	17.4	4.	7.	−16.6	0.8	0.8
EVEN	0.60	5.2	4.	4.	−4.8	0.6	0.6
ALL	0.76	12.7	4.	6.	−12.1	0.8	0.8

Table 11

TM/PF BAND 4

AVERAGE, STANDARD DEVIATION AND COEFFICIENT OF VARIATION FOR DERIVED RADIOMETRIC CALIBRATION PARAMETERS

CHAN	GAIN	OFFSET	SNR		RADIANCES		
			LSR	MSL	MIN	MSL	MAX
MEAN:							
ODD	10.882	1.95	73.	351.	−0.180	22.153	23.256
EVEN	10.924	1.86	67.	330.	−0.171	22.077	23.176
ALL	10.903	1.91	70.	341.	−0.175	22.115	23.216
SIGMA:							
ODD	0.117	0.29	7.	28.	0.027	0.242	0.254
EVEN	0.154	0.10	7.	29.	0.299	0.299	0.313
ALL	0.134	0.22	7.	30.	0.020	0.268	0.280
COEF. VAR. (%):							
ODD	1.08	14.9	10.	8.	−15.0	1.1	1.1
EVEN	1.41	5.4	10.	9.	−174.8	1.4	1.4
ALL	1.23	11.5	10.	9.	−11.4	1.2	1.2

Table 12

TM/PF BAND 5
AVERAGE, STANDARD DEVIATION AND COEFFICIENT OF VARIATION FOR DERIVED RADIOMETRIC CALIBRATION PARAMETERS

CHAN	GAIN	OFFSET	SNR		RADIANCES		
			LSR	MSL	MIN	MSL	MAX
MEAN:							
ODD	77.183	3.08	40.	175.	−0.040	3.108	3.164
EVEN	77.286	2.96	43.	187.	−0.038	3.106	3.261
ALL	77.238	3.02	42.	181.	−0.039	3.107	3.262
SIGMA:							
ODD	0.418	0.10	4.	9.	0.001	0.016	0.017
EVEN	0.404	0.09	4.	7.	0.001	0.016	0.017
ALL	0.406	0.11	4.	10.	0.002	0.016	0.017
COEF. VAR. (%):							
ODD	0.54	3.2	10.	5.	−2.5	0.5	0.5
EVEN	0.52	3.0	9.	4.	−2.6	0.5	0.5
ALL	0.53	3.6	10.	6.	−5.1	0.5	0.5

Table 13

TM/PF BAND 7
AVERAGE, STANDARD DEVIATION AND COEFFICIENT OF VARIATION FOR DERIVED RADIOMETRIC CALIBRATION PARAMETERS

CHAN	GAIN	OFFSET	SNR		RADIANCES		
			LSR	MSL	MIN	MSL	MAX
MEAN:							
ODD	147.338	2.35	27.	178.	−0.016	1.633	1.715
EVEN	146.897	2.47	26.	173.	−0.017	1.637	1.719
ALL	147.117	2.41	27.	175.	−0.016	1.635	1.717
SIGMA:							
ODD	0.807	0.25	6.	34.	0.002	0.010	0.010
EVEN	1.299	0.11	2.	12.	0.001	0.015	0.015
ALL	1.063	0.20	4.	25.	0.001	0.013	0.013
COEF. VAR. (%):							
ODD	0.55	10.6	22.	19.	−12.5	0.6	0.6
EVEN	0.88	4.5	8.	7.	−5.9	0.9	0.9
ALL	0.72	8.3	15.	14.	−6.2	0.8	0.8

Table 14

SUMMARY OF TM/PF CALIBRATION PARAMETERS

BAND	DYNAMIC RANGE		GAIN (counts/(mWcm^{-2}sr^{-1}μm^{-1})	OFFSET (counts)	SIGNAL-TO-NOISE RATIO	
	RMIN[a] (mWcm^{-2}sr^{-1}μm^{-1})	RMAX[b]			SPEC (MSL)[c]	OBS (MSL)[c]
1	−0.152	15.842	15.78 ± 0.54%	2.58 ± 0.18	85	152 ± 9%
2	−0.284	30.817	8.10 ± 0.89%	2.44 ± 0.16	170	281 ± 17%
3	−0.117	23.463	10.62 ± 0.76%	1.58 ± 0.20	143	235 ± 6%
4	−0.151	22.432	10.90 ± 1.23%	1.91 ± 0.22	240	341 ± 9%
5	−0.037	3.242	77.24 ± 0.53%	3.02 ± 0.11	75	180 ± 6%
7	−0.015	1.700	147.12 ± 0.72%	2.41 ± 0.20	45	175 ± 14%

[a] RMIN IS THE LARGEST MINIMUM RADIANCE OBSERVED IN THE BAND (0 COUNTS).

[b] RMAX IS THE SMALLEST MAXIMUM RADIANCE OBSERVED IN THE BAND (255 COUNTS)

[c] MSL IS THE MINIMUM SATURATION LEVEL RADIANCE FOR THE BAND.

Table 15

TM/PF CALCULATED DETECTOR GAINS AND OFFSETS

BAND	A1: CALCULATED[b, c]		B: CALCULATED[b, c]		C2: CALCULATED[b, c]	
	GAIN[a]	OFFSET[a]	GAIN[a]	OFFSET[a]	GAIN[a]	OFFSET[a]
1	16.59 ± 0.09	0.44 ± 0.34	15.97 ± 0.09	---[e]	15.78 ± 0.09	2.58 ± 0.18
2	8.14 ± 0.07	0.89 ± 0.07	7.93 ± 0.07	---[e]	8.10 ± 0.07	2.44 ± 0.16
3	10.66 ± 0.09	0.81 ± 0.20	10.38 ± 0.09	---[e]	10.62 ± 0.08	1.58 ± 0.20
4	11.32 ± 0.13	0.92 ± 0.22	11.31 ± 0.14	---[e]	10.90 ± 0.13	1.91 ± 0.22
5	81.45 ± 0.38[d]	1.53 ± 1.08[d]	---[d]	---[d, e]	77.24 ± 0.40[d]	3.02 ± 0.11[d]
7	152.31 ± 1.48	2.57 ± 0.74	---	---[e]	147.12 ± 1.06	2.41 ± 0.20

[a] ALL GAINS ARE IN UNITS OF DIGITAL COUNTS/(mW cm^{-2} sr^{-1} μ^{-1}), OFFSETS IN DIGITAL COUNTS. DATA GIVEN ARE MEANS ± STANDARD DEVIATION FOR 16 DETECTORS.

[b] IS(122) TESTS DESIGNATION FROM TABLE 2: A—JUNE, 1981; B—NOVEMBER 1981; C—MARCH 1982.

[c] SOURCES: TEST A FROM OSGOOD AND LANSING (1981), TABLES III AND IV.
TEST B FROM YOUNG (1982), TABLES III, IV, V, AND VI.
TEST C FROM UNPUBLISHED COMPUTER PRINTOUTS, WITH NEW IS(122) RADIANCE LEVELS.
(SPHERE WAS RECALIBRATED IN MAY 1982.)

[d] BAND 5 DATA EXCLUDE DETECTOR 3 (DEAD).

[e] TEST B DATA WERE TAKEN FOR BANDS 1 THROUGH 4 ONLY. YOUNG (1982) REPORTS GAINS ONLY (NO OFFSETS).

Table 16

SUMMARY OF AVERAGE GAIN CHANGES IN PERCENT BY TEST REFERENCED TO TEST C2

BAND		TEST					
		A1	A2	B	C1	C2	C3
1	ODD	5.28	5.22	1.17	0.82	—	−0.03
	EVEN	4.91	4.83	1.13	0.91	—	−0.02
	ALL	5.09	5.03	1.15	0.86	—	−0.02
2	ODD	0.48	0.24	−1.95	−0.29	—	−0.63
	EVEN	0.45	0.21	−2.01	−0.32	—	−0.67
	ALL	0.47	0.22	−1.98	−0.30	—	−0.65
3	ODD	0.45	0.20	−2.22	−0.32	—	−0.55
	EVEN	0.23	−0.01	−2.29	−0.23	—	−0.51
	ALL	0.34	−0.09	−2.25	−0.28	—	−0.53
4	ODD	3.91	4.00	3.75	0.62	—	0.08
	EVEN	3.78	3.88	3.69	0.61	—	0.06
	ALL	3.85	3.94	3.72	0.62	—	0.07
5	ODD	5.45	4.75	—[b]	−0.17	—	−0.02
	EVEN	5.45	4.78	—	−0.28	—	−0.18
	ALL	5.45	4.77	—	−0.23	—	−0.11
7	ODD	3.59	3.09	—[b]	0.01	—	−0.12
	EVEN	3.47	4.77	—	0.06	—	−0.09
	ALL	3.53	3.93	—	0.03	—	−0.11

[a] GAIN CHANGE DEFINED AS: VALUE = 100% x (CURRENT − REFERENCE) + REFERENCE.

[b] NO BANDS 5 AND 7 DATA TAKEN DURING TEST B.

Our choice of test C2 as the best calibration of the TM for use during postlaunch activities was dictated by several considerations:

- The IS(122) was recalibrated in May 1982; these output radiances were used to obtain the results presented in Tables 2 through 7 and are not affected by any significant use of the IS(122) from March to May 1982. Tests A and B, however, are well removed in time and sphere usage from both May (and February) 1982 and June 1980 sphere calibrations.

- A change in IS(122) output in the blue wavelengths from the June 1980 to the February and May 1982 sphere calibrations (2 to 4 percent or worse at some wavelengths according to Walker (1982a, b)) may in particular affect TM band 1.

- The cooled focal plane assembly (CFPA) (bands 5, 6, and 7) was removed from the TM in August 1981 for repair. This invalidates the band 5 and 7 calibrations during the A tests.

- Alignment of the IS(122) and the TM was questionable during test B; in addition, no CFPA data were taken during that test.

- One 25-watt lamp burned out after the February 1982 sphere calibration check; the new lamp was calibrated during May 1982.

Changes made in the CFPA in August 1981 may explain most of the observed differences in bands 5 and 7 between tests A and C. Changes in sphere output from June 1980 to February and May 1982 should also be considered for bands 5 and 7 as well as band 1. It is not clear, however, that changes in the sphere can account for more than 1 or 2 percent of the observed differences in band 4 (see Table 16).

To further evaluate the accuracy of the calibration of the TM with the IS(122), errors have been computed for detectors 1, 8, 9, and 16 in each band. These are based on computed errors in gain and offset from the least-squares fit and standard deviations for the averaged digital counts from the highest observed sphere radiance level in each band that does not saturate. The errors are part of the transfer error in the calibration from the IS(122) to the TM. These results are listed in Table 17. The error, in percent, in

Table 17

COMPUTED ERRORS IN SPECTRAL RADIANCE FOR CALIBRATION OF TM/PF DETECTORS WITH IS (122)

CHANNEL	BAND					
	1	2	3	4	5	7
1	1.11	0.76	0.68	0.69	0.65	0.81
8	1.06	0.58	0.59	0.70	0.62	0.70
9	0.95	0.64	0.57	0.70	0.62	0.80
16	1.10	0.70	0.60	0.70	0.66	0.81

VALUE IS FRACTIONAL ERROR IN SPECTRAL RADIANCE AT HIGHEST UNSATURATED SPHERE BRIGHTNESS LEVEL IN BAND, IN PERCENT:

$$\frac{\Delta L}{L}(\%) = 100^{*} \sqrt{\frac{(\Delta\overline{Q})^2 + (\Delta O)^2}{(\overline{Q} - O)^2} + \left(\frac{\Delta G}{G}\right)^2}$$

$\overline{Q}, \Delta\overline{Q}$	AVERAGED VIDEO DIGITAL COUNT AND ITS STANDARD DEVIATION
$O, \Delta O$	OFFSET AND ITS STANDARD DEVIATION
$G, \Delta G$	GAIN AND ITS STANDARD DEVIATION

radiance for the highest unsaturated sphere level is computed as follows, based on the calibration curve $Q = GL + O$:

$$\frac{\Delta L}{L}\ (\%) = 100 * \sqrt{\frac{(\Delta Q)^2 + (\Delta O)^2}{(Q - O)^2} + \left(\frac{\Delta G}{G}\right)^2}$$

These values provide a measure of the full-scale precision of the calibration of the TM. Other sources of error in the calibration, such as errors in the radiance output by the IS(122) in a TM band and the relative spectral response in the band, are also contributing to the transfer error from the IS(122) to the TM. The estimated error in the TM calibration is discussed in a later section.

The measured dynamic range, minimum saturation level (MSL), and maximum radiances for each detector were presented in Tables 1 through 13. They are computed from the inverted calibration curve $L = (Q - O)/G$ at digital count values of zero, 243, and 255. The MSL radiance is computed at 95 percent of full scale. This level was chosen by Santa Barbara Research Center (SBRC) as a measure of both full-scale SNR and dynamic range and allowed for possible errors in the calibration as well as in setting the detector gain. The measured dynamic range of the TM is summarized in Table 18 for the full-scale values. The table gives the average MSL radiance, its standard deviation, and the minimum MSL radiance, which is computed as follows:

$$\mathrm{RMIN}_i = \mathrm{Minimum}\ (\mathrm{RMSL}_{ij})$$

where RMIN_i is the minimum MSL in band i and RMSL_{ij} are the MSL radiances for all j detectors in band i. For example, the RMIN value for band 1 occurs in detector 3 (see Table 2). (Similar values are given in Table 14 for the lowest maximum observable radiance and the highest minimum observable radiance in each band.) The minimum MSL values given in Table 18 have also been compared to the specified dynamic range for each TM band. Each band saturates at a higher level than specified, up to 15 percent for band 3. The within-band variability of the measured dynamic range is about 1 percent. Although this would lead to minimal stripping in a TM scene, it should be compared to the specified relative accuracy level of one digital count. The range of variability by bands is from 1.3 to 3.0 digital counts.

Signal-to-Noise Determination

The SNR ratio for each detector was calculated at two standard radiance levels for each test. First, the mean (signal)

Table 18

AVERAGE DYNAMIC RANGE OF THE TM FROM COMPUTED RADIANCE LEVELS

	BAND					
	1	2	3	4	5	7
AVERAGE MSL	15.232	29.707	22.737	22.115	3.107	1.635
STANDARD DEV OF MSL	0.079	0.276	0.181	0.268	0.016	0.013
MINIMUM MSL	15.089	29.353	22.350	21.369	3.087	1.619
SPECIFICATION	14.29	29.12	19.29	21.43	3.00	1.59
RATIO $\frac{\text{SPEC.}}{\text{AVER.}}$ (%)	93.8	98.0	84.8	96.9	96.6	97.2
RATIO $\frac{\text{S. DEV}}{\text{AVER.}}$ (%)	0.5	0.9	0.8	1.2	0.5	0.8

NOTES:

MSL IS MINIMUM SATURATION LEVEL SPECTRAL RADIANCE (mWcm^{-2} sr^{-1} μm^{-1})

COMPARING OBSERVED MSL WITH SPECIFICATION

1. **SATURATES AT A HIGHER LEVEL (UP TO 15%) THAN SPECIFICATION.**
2. **WITHIN-BAND VARIABILITY IS ABOUT 1%.**

and standard deviation (noise) for each detector were calculated from a large number of scans at each standard source radiance level. The resulting SNR values at each radiance level were then fit by a linear function of spectral radiance. Finally, the fitted straight lines were evaluated at two reference levels, and the high and low SNRs shown in Tables 1 through 7 resulted. Only three channels do not meet the specifications: 5/3 (dead), 2/4 (slow response), and 2/2 (noisy). When band 2/channel 2 data were examined, it was noticed that the SNR-versus-radiance curve showed a pronounced trend typical of a Schott-noise square root curve (Osgood and Lansing, 1981). Detector 2/4 does not show a significant problem until rapidly changing intensities are presented to it. Thus, the gain/offset determinations from the largely static IS(122) radiance levels show no appreciable difference when compared to other detectors in band 2. The 2/4 detector does, however, have a much slower response time to changing radiance values, particularly those characteristic of the TM internal calibrator (IC) light pulse. Under these conditions, the detector is sluggish but still useful.

CALIBRATION OF THE IC

The purpose of the calibration transference was to determine the radiance value for each detector in each band for each IC lamp configuration. As the TM was viewing the eight radiance levels provided by the IC lamps, its output was monitored. By the procedure outlined in Barker et al. (1983a,b), an average integrated calibration pulse value in digital counts was determined for each lamp configuration for each detector. These values were then converted to spectral radiance using calibration coefficients (gains and offsets) determined during the absolute calibration test with the IS(122). The IC data are nominally taken between the two radiance level series that make up the IS(122) test (Barker et al., 1983a), with the IC automatic sequencer on and the lamps operating in normal mode. Some data have also been collected for the backup mode of IC operation. Because the data collection for the calibration transference is a part of the calibration of the TM with the IS(122), this test is always performed in an ambient environment, not in a vacuum test chamber; the IS(122) is too big to fit inside a vacuum chamber. To obtain data taken during in-orbit-like conditions (in vacuum), it is necessary to transfer the results to a set of data taken in these conditions and as close in time and instrument operating conditions to the absolute calibration test as may be feasible; even so, differences due to so-called vacuum shift may still be noted. Several tests have been performed to transfer the IS(122) calibration of the TM detectors to the IC and are listed in Table 19. Three additional sets of IC data taken in vacuum

Table 19

DATES OF TRANSFERS OF CALIBRATION TO THE TM/PF INTERNAL CALIBRATOR

TEST DESIGNATION	DATA COLLECT		LOCATION	TEST ENVIRONMENT	IC MODE	REMARKS
	DATE	TIME				
1	30 JUNE 1981	02:29:56	HAC/SBRC	AMBIENT	NORMAL	T_{CFPA} = 95K
2	30 JUNE 1981	03:03:05	HAC/SBRC	AMBIENT	BACKUP	T_{CFPA} = 95K
3	30 JUNE 1981	04:28:44	HAC/SBRC	AMBIENT	NORMAL	T_{CFPA} = 105K
4	30 JUNE 1981	06:55:33	HAC/SBRC	AMBIENT	NORMAL	T_{CFPA} = 105K
5	30 JUNE 1981	07:20:49	HAC/SBRC	AMBIENT	BACKUP	T_{CFPA} = 105K
6	3 NOV 1981	–	GE/VF	AMBIENT	NORMAL	BANDS 5, 6, 7 OFF
7[a]	20 MAR 1982	21:29:00	GE/VF	AMBIENT	NORMAL	REFERENCE
8[b]	18 SEPT 1981	–	HAC/EL SEGUNDO	VACUUM	NORMAL	
9[b]	9 MAR 1982	12:43:00	GE/VF	VACUUM	NORMAL	SPECIAL TEST 1, PASS 2
10[b]	9 MAR 1982	12:48:30	GE/VF	VACUUM	NORMAL	SPECIAL TEST 1, PASS 3

[a] TEST NUMBER 7 IS THE REFERENCE TEST.

[b] TESTS 8, 9, AND 10 ARE DATA SETS OBTAINED IN VACUUM AND HAVE BEEN INCLUDED FOR COMPARISON.

chamber tests have been included. Some comments on these tests are in order.

First, although any set of IC data may potentially be used to establish the calibration transference, data collected as close in time and environmental conditions to the TM detector absolute calibration as possible are to be preferred to minimize effects of environmental changes on the transfer. Although the March 1982 test (test 7 in Table 19) was performed 1 day after the three IS(122) calibrations (tests C), this test has been selected as the reference for intercomparison of transfer test results as well as for postlaunch operations. This is because it is closest to the date of launch, a large volume of IS(122) data is available, and continuity of absolute calibration of the CFPA detectors with postlaunch operational activities exists.

Second, four data sets have been included for comparison purposes: the November 1981 test, which lacks CFPA detector data, and three sets taken from vacuum chamber testing. Tests 9 and 10 were special tests performed in vacuum at General Electric and designed to mimic expected in-orbit operational conditions (E. Beyer, General Electric, private communication, 1982).

Third, there are only two tests for the backup mode of IC operation; none was performed during the March 1982 test series. If the backup mode is to be used during postlaunch operations, a set of transference data for the backup mode will have to be constructed from other sources. Internal lamp self-consistency problems have been noted with these data sets taken in backup mode.

The results of the calibration transference for test 7 of Table 19, which was selected as the reference transference data set for the TM, are presented in the appendix along with the results of test 9. For each IC lamp configuration and each detector, the averaged observed digital count output obtained with the Hughes pulse integration scheme and the corresponding spectral radiance are given. The spectral radiances were computed using the observed digital counts and gains and offsets given in Tables 2 through 7 for tests 7 and 9. An illustrative plot of average calibration pulse value against lamp radiance is shown in Figure 3 for the reference test (test 7).

To evaluate the repeatability of the calibration transfer from the IS(122) to the IC lamps, a straight-line, least-squares fit was performed for each detector using all eight IC lamp levels between a given test and the reference test. An example of one such comparison is shown in Figure 4. The

Figure 3

TM/PF GAIN AND OFFSET FROM INTERNAL CALIBRATION DATA

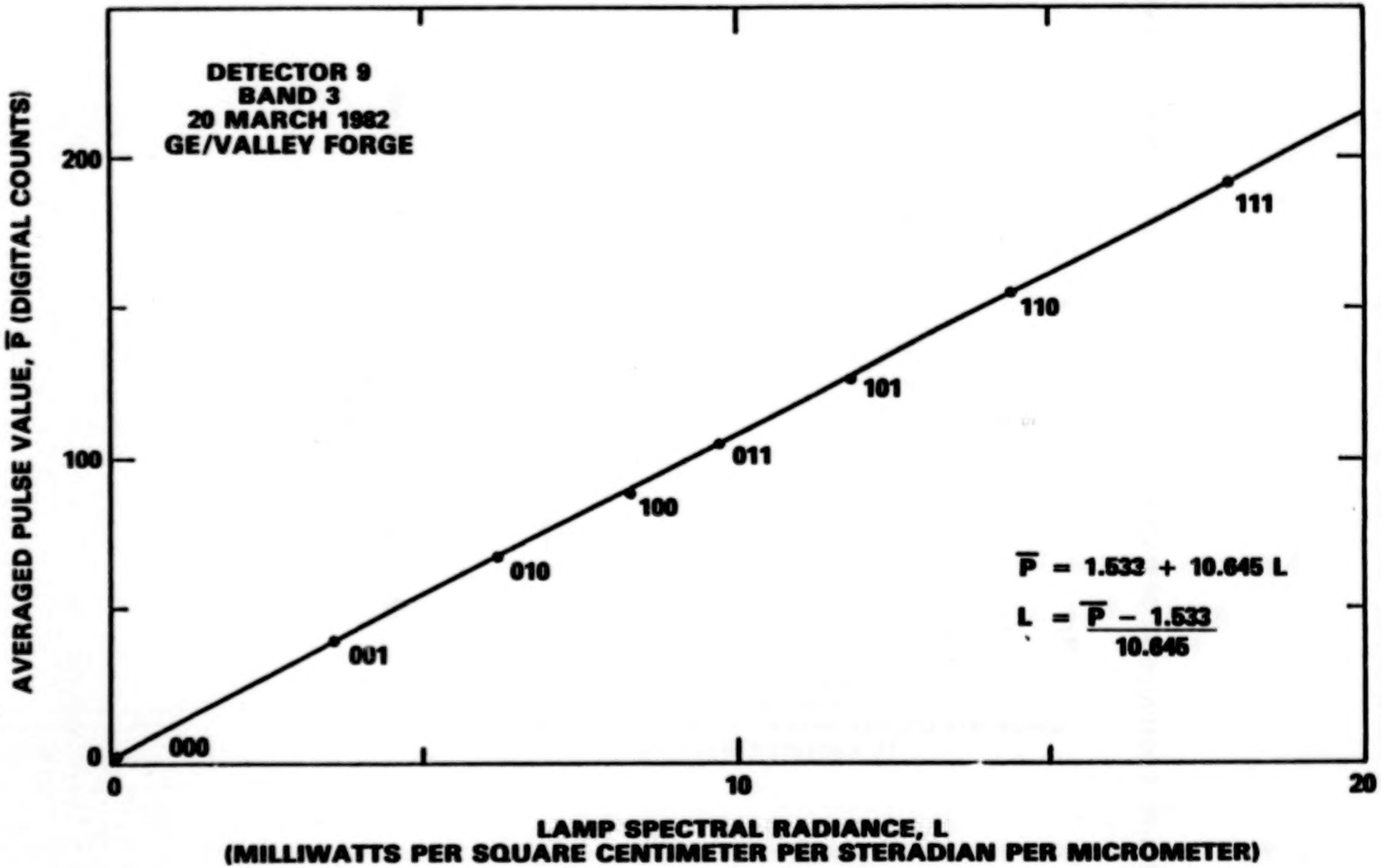

Figure 4

TM/PF: COMPARISON OF CALIBRATION TRANSFER RESULTS, BAND 3/CHANNEL 9

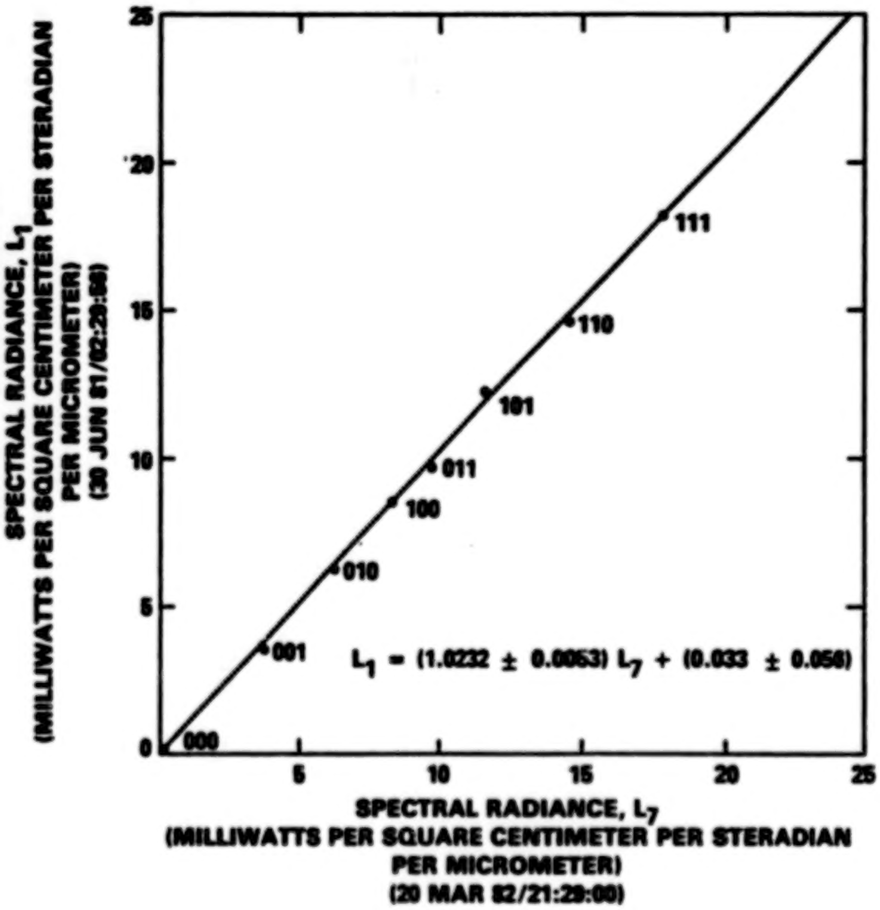

fit was computed two ways, one using radiance value comparisons and one with digital counts. The result of these comparisons is given in detail elsewhere (Barker et al., 1983d) and will only be briefly summarized here. For each test comparison, a slope and intercept and their respective standard deviations and a figure of merit for the overall fit were computed by the method of least squares for each detector. For the data shown in Figure 4, the results are summarized in Table 20. The figure of merit used is the standard error of the estimate. For either radiance or digital count comparison, the figure of merit is less than 0.45 percent of full-scale IC lamp output (lamp configuration 111). These values are typical, not best estimates.

To evaluate the error involved in the transfer of the absolute calibration to the IC, the error in the calibration of the detectors must be determined, as shown in Table 17. Because the detectors are calibrated first and the calibration is then transferred to the IC, this error is twice that given in Table 17. Thus, the error in the transfer is typically 1 to 2 percent, depending on the band. This estimate is included in the error propagation analysis discussed in the next section.

ESTIMATED ERRORS IN THE TM/PF CALIBRATION

It was noted in Barker et al. (1983a) that the IS(122) is calibrated against a secondary standard that is related to standards set by the National Bureau of Standards (NBS). The overall sequence of calibrations is shown in Figure 5. Each standard lamp has a rated lifetime during which its output will not change. For example, the Optronics Laboratories, Inc., standard (NBS) used by SBRC has a rating of 50 hours of use with the calibration holding to within 1 percent for that period. The IS(122) is used for long periods of time in calibrating the TM and, if the sphere were calibrated directly against the SBRC standard, the standard calibration would quickly degrade. Thus, the SBRC standard is used to calibrate secondary standards similar in design and characteristics to the SBRC standard (for example, see Campbell, 1980 and Walker, 1982c). In Figure 5, the lamp filament symbol labeled "PRI" on the upper left represents an Optronics standard quartz-halogen 1000-watt lamp that has been calibrated against an NBS standard lamp. The vendor-stated uncertainty in the transfer of calibration from the NBS lamp to the Optronics standard (SBRC lamp S466) is 1.3 percent at a wavelength of 450 nanometers, 0.9 percent at 1600 nanometers, and 3.1 percent for 1600 to 2500 nanometers. These errors are mainly due to uncertainty

Table 20

TM/PF INTERNAL CALIBRATOR
DERIVED COMPARISON FOR BAND 3, CHANNEL 9 BETWEEN TEST 1 (JUNE 1981) AND TEST 7 (MARCH 1982)

	COMPARISON OF RADIANCE VALUES			
	EXPECTED VALUE	DERIVED VALUE	STANDARD DEVIATION	FIGURE OF MERIT[a]
INTERCEPT	0.0	0.0334	0.05594	0.0815
SLOPE	1.0	1.0232	0.00534	

	COMPARISON OF DIGITAL COUNTS			
	EXPECTED VALUE	DERIVED VALUE	STANDARD DEVIATION	FIGURE OF MERIT[a]
INTERCEPT	0.0	−0.6114	0.6057	0.8724
SLOPE	1.0	1.0288	0.00537	

[a] FIGURE OF MERIT IS

$$\sigma_{Y_{est}} = \sqrt{\frac{\sum_{I=1}^{N} (Y_I - a - bX_I)^2}{N-2}}$$

WHERE I = 1, 2, . . . 8 IS THE IC LAMP CONFIGURATION, a AND b ARE THE INTERCEPT AND SLOPE OF THE FIT, RESPECTIVELY.

in the NBS scale of irradiance. The cumulative root sum of square error at each step in the calibration is then given by

$$\sigma_{cum} = \left(\sigma^2_{cal} + \sigma^2_{trans}\right)^{1/2}$$

where σ_{cum} is the cumulative standard error, σ_{cal} is the source calibration error at the previous step, and σ_{trans} is the transfer error or source-to-source measurement error. Thus, at 450 nanometers, the known error in the calibration of the IS(122) is 1.9 percent. The IS(122) must be recalibrated periodically to ensure that the output of the sphere has not changed significantly due to lamp aging or spectral changes in the surface of the sphere. For example, study of data from June 1980, February 1982, and May 1982 (Walker, 1982b) has shown a decreased output from the IS(122) in the blue wavelengths. The overall change is a net decrease by 2 to 4 percent for the brighter radiance levels.

The transfer error associated with the spectral calibration of the IS(122) by the secondary standards has been specified to be less than or equal to 2.0 percent. This error is the standard deviation obtained when comparing spectral radiance values at 50-nanometer intervals between 450 and 2500 nanometers for two separate measurements at each lamp level setting. Values are typically between 1 and 2 percent. These are higher than those for the transfer from the standard lamp S466 to the secondary standards, primarily because the signal levels differ more in the IS(122) calibration. This standard deviation is an indicator of the consistency and precision of the IS(122) calibration. The absolute accuracy of the calibration is not so clearly defined. Campbell (1980) points out that two different measurement techniques used at SBRC gave results that differed by as much as 7 to 8 percent at some wavelengths; typical values are 2 to 3 percent. There is presently no known reason why either of the two methods should give results that are any more, or less, correct than the other. The method selected is the one that provides a higher signal level and, therefore, a better SNR. The other method provides a good SNR at certain wavelength and lamp level combinations, but still gives different results.

Thus, the precision of measurement of the transfer of the NBS calibration to the IS(122) calibration is typically 2 percent but depends on wavelength (5 percent in the infrared). Due to the differences noted above between methods of calibrating the IS(122) with the secondary standards and uncertainties in the NBS scale of irradiance, the absolute accuracy of the calibration of the IS(122) is no better than 5 percent. In Figure 5, the cumulative errors are given for

Figure 5

ESTIMATED ABSOLUTE RADIOMETRIC CALIBRATION ACCURACY FOR THE LANDSAT THEMATIC MAPPER SENSOR

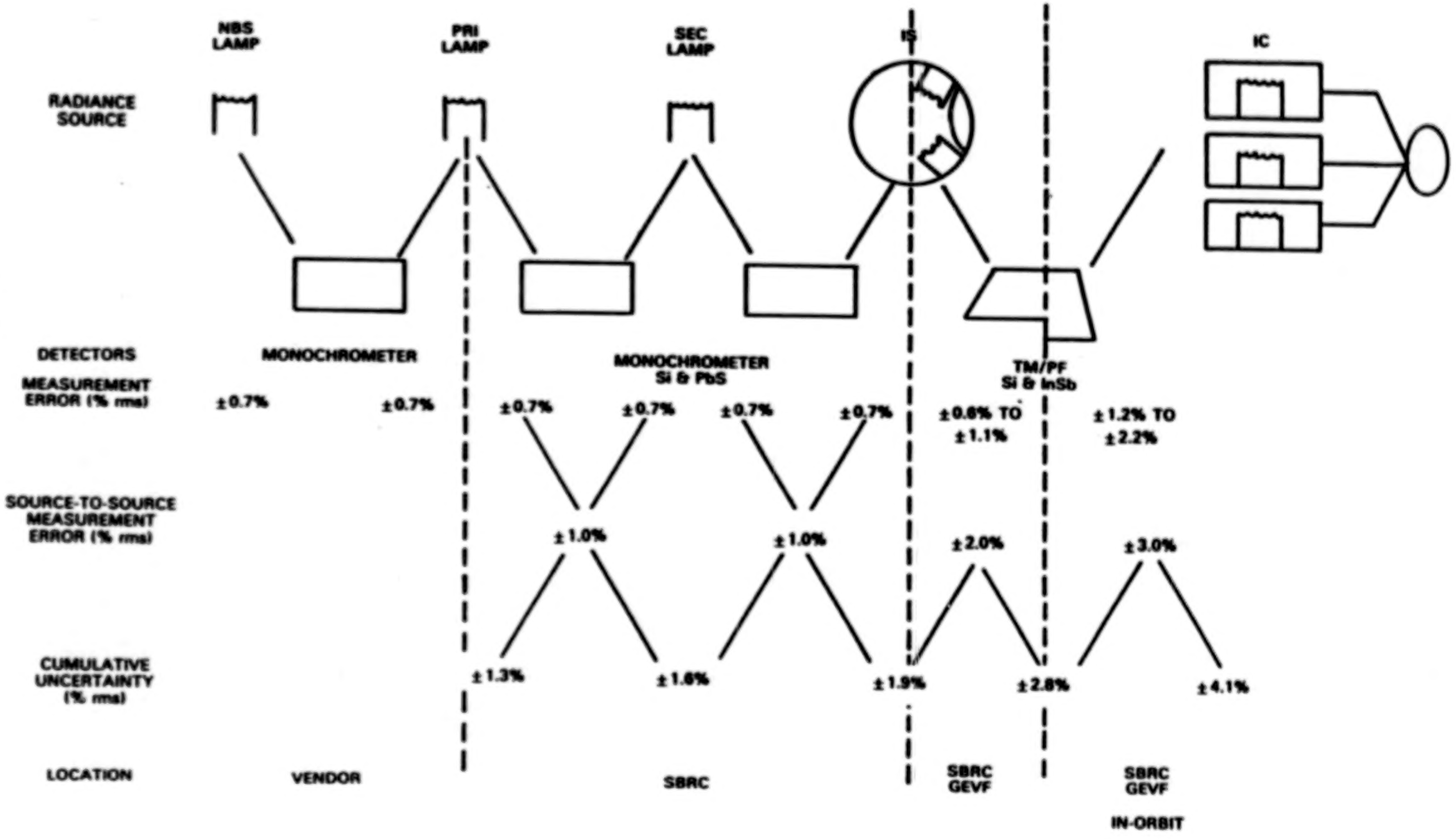
NBS LAMP
PRI LAMP
SEC LAMP
IS
IC
RADIANCE SOURCE
DETECTORS
MONOCHROMETER
MONOCHROMETER Si & PbS
TM/PF Si & InSb
MEASUREMENT ERROR (% rms)
±0.7%
±0.7%
±0.7%
±0.7%
±0.7%
±0.7%
±0.8% TO ±1.1%
±1.2% TO ±2.2%
SOURCE-TO-SOURCE MEASUREMENT ERROR (% rms)
±1.0%
±1.0%
±2.0%
±3.0%
CUMULATIVE UNCERTAINTY (% rms)
±1.3%
±1.6%
±1.9%
±2.8%
±4.1%
LOCATION
VENDOR
SBRC
SBRC GEVF
SBRC GEVF
IN-ORBIT

a wavelength of 450 nanometers; these are typical values and are higher in the infrared and lower in the red. The precision of calibration of the TM with the IS(122) is 2.8 percent (at 450 nanometers). The absolute accuracy based on the above discussion is then no better than 5 percent, due to a typical difference of 2 to 3 percent between IS(122) calibration methods and to uncertainties in the NBS scale of irradiance. The transfer of the detector calibration to the IC is then no better than 6 percent.

To summarize, the absolute calibration of the TM reflective band detectors is affected by

- Uncertainty in the NBS irradiance scale (typically 1.2 percent)
- Transfer errors between lamp standards (typically 1.0 percent)
- Differences between methods used to calibrate the IS(122) with a secondary standard (typically 2 to 3 percent)
- Changes in IS(122) lamps and interior surface between calibrations of the IS(122) with the secondary standard (2 to 4 percent between June 1980 and May 1982)

In Figure 5, the cumulative percent error given for the calibration of the protoflight (PF) TM and the IC are for the March TM calibration and the May IS calibration. Due to other uncertainties mentioned earlier, these are lower than the estimated absolute accuracy quoted.

DISCUSSION OF RESULTS

RADIOMETRIC PERFORMANCE REQUIREMENTS

The prelaunch radiometric calibration procedures are designed to ensure that the TM meets its performance requirements. The radiometric specifications can be divided into three groups: dynamic range, sensitivity, and accuracy. The requirements are listed in Table 21.

The TM is designed for land observations; the reflective bands are therefore designed for maximum dynamic range for the expected land radiance levels (Fraser, 1975; Duck, 1977). This range can be tested using a well-calibrated external source. The radiometric sensitivity is expressed in terms of SNR for reflective bands. The relative accuracy requirements are quite stringent: about 1 quantum level for

Table 21

TM RADIOMETRIC SPECIFICATIONS FOR REFLECTIVE BANDS

BAND	WAVELENGTH[b]		SPECIFICATION[a]					
			CONSTANT		SNR[f]	MSL[e]		SNR[f]
	RANGE	BAND WIDTH	IN-BAND RADIANCE[c]	SPECTRAL RADIANCE[d]		IN-BAND RADIANCE[c]	SPECTRAL RADIANCE[d]	
1	0.45-0.52	0.07	0.28	4.00	32	1.00	14.29	85
2	0.52-0.60	0.08	0.24	3.00	35	2.33	29.12	170
3	0.63-0.69	0.07	0.13	1.86	26	1.35	19.29	143
4	0.76-0.90	0.14	0.19	1.36	32	3.00	21.43	240
5	1.55-1.75	0.20	0.08	0.40	13	0.60	3.00	75
7	2.08-2.35	0.27	0.046	0.17	5	0.43	1.59	45

[a] SOURCE: GSFC SPECIFICATION: THEMATIC MAPPER SYSTEM AND ASSOCIATED TEST EQUIPMENT, GSFC 400-8-D-210, REVISION B, APRIL 1978, SECTION 3.2.9, TABLES IV AND V.

[b] WAVELENGTH IN MICROMETERS (μm).

[c] IN-BAND RADIANCE (mW cm^{-2} sr^{-1}).

[d] SPECTRAL RADIANCE (mW cm^{-2} sr^{-1} μm^{-1}) = IN-BAND RADIANCE DIVIDED BY WAVELENGTH BANDWIDTH.

[e] MINIMUM SATURATION LEVEL (DIGITAL COUNTS = 243) RADIANCE (EITHER IN-BAND OR SPECTRAL).

[f] MINIMUM SIGNAL-TO-NOISE RATIO AT GIVEN INPUT RADIANCE.

between-detector accuracy and 2 percent for between-band accuracy. The overall absolute accuracy specified for the TM is 10 percent.

While in orbit, the TM must rely on its IC to convert individual channel voltages into correct scene radiance values and to monitor the health of the individual detectors, because there are no provisions for performing an external calibration with the Sun or other extraterrestrial body. It is thus very important that the prelaunch absolute calibration of the detectors be accurately transferred to the IC lamps. The absolute accuracy actually attained during the calibration of the TM was stated earlier to be no better than 5 percent for the detectors and 6 percent for the IC. This requirement has thus been met. The relative band-to-band accuracy of the IC is discussed in Barker et al. (1983b).

CALIBRATION OF THE DETECTORS

Gain and Offset Variability

Long-Term Gain Stability

The long-term stability of TM radiometry is quite good. Measurements of its absolute calibration over 9 months (from June 1981 to March 1982) showed that the variations are between 3 and 5 percent (Table 16), well within the required 10-percent accuracy. Variability of individual channels is also within specification.

The within-band variability is quite good. Table 22 summarizes the within-band standard deviations of all the tests. While the band-averaged gain values change by 3 to 5 percent, there is no appreciable change in the within-band spread of individual channel gain values. This indicates that the observed absolute calibration variations are due to changes affecting the whole system, and that the relative accuracy within a single TM band has not deteriorated. The small within-band variability implies that there will be very little striping in an image, even if no calibration by the IC is performed.

Short-Term Reproducibility of Channel Gain

The short-term reproducibility can be established by repeated measurements. The three sets of tests performed in March 1982 were used to obtain an estimate. Although they were different because of mirror scanning mode and IC sequencing mode, they were still the best and most complete set of repeated measurements available. Table 23 shows the

Table 22

STANDARD DEVIATIONS OF TM/PF AVERAGE GAINS

TEST	BAND					
	1	2	3	4	5	7
A1	0.090	0.071	0.092	0.134	(0.378)[a]	(1.487)[a]
A2	0.093	0.071	0.091	0.135	(0.551)[a]	(4.369)[a]
B	0.092	0.068	0.086	0.137	—	—
C1	0.087	0.073	0.079	0.132	0.384	1.059
C2	0.086	0.072	0.081	0.134	0.408	1.063
C3	0.091	0.073	0.080	0.133	0.380	1.047
MEAN	0.092	0.071	0.084	0.134	0.380	1.056
STANDARD DEVIATION	0.00382	0.00886	0.0057	0.0016	0.0055	0.0083

[a] VALUES FOR COOLED FOCAL PLANE BANDS FOR TEST A ARE NOT TO BE TRUSTED DUE TO REPAIR OF CFPA IN SEPTEMBER 1981. THESE VALUES WERE NOT INCLUDED IN MEANS AND STANDARD DEVIATION FOR BANDS 5 AND 7.

mean and standard deviations for the three band-averaged gain values. The short-term reproducibility is excellent, indicating the TM to be a very good instrument. However, noticing the small standard deviations of all the band-averaged gain values, it is obvious that the short-term reproducibility of individual channels is also very good. As an example, Table 24 shows the short-term reproducibility of channel 16. This channel was selected because of the somewhat large coherent noise component observed (Barker et al., 1983b). The reproducibility is good. Good within-band variability and stable short-term performance guarantee that the raw image of the TM will show little stripping and that neighboring scenes will show similar radiance levels. Postlaunch observations lead to similar conclusions (Barker et al., 1983b).

Offset Stability

The value of individual channel offsets is closely tied to the corresponding gain value. They are obtained through a least-squares linear fit to the IS(122) radiance measurements. Because of this, change in gain and offset values cannot be totally separated. However, some interesting conclusions can still be drawn:

- Channel 1 offset values for all reflective bands are high. Table 25 gives a comparison of the channel 1 offset and the mean offset for the same band. In most cases, these channel 1 values are the largest positive numbers for that band. No corresponding trend in the gain values is observed.

- There was a very strong odd-even effect for the cooled focal plane bands for test A. After the assembly was repaired, this effect disappeared.

- The offset values for all channels within a single TM band are close to one another. From Table 25, it can be seen that the standard deviations for all bands for both tests A1 and C2 are small, on the order of 0.25 digital count. These numbers can be further reduced if channel 1 is removed from the computation of the mean. This improvement will not affect the data analysis, because the offset values are treated individually in the radiometric correction algorithm. The smallness of the standard deviations does, however, indicate that the channels are well balanced within a band.

- The offset values are quite stable for all the absolute calibration tests. Table 26 shows the mean offset values for all bands and all tests. All mean offset values are positive.

Table 23

THE MEAN AND STANDARD DEVIATIONS OF GAINS DURING THE THREE MARCH ABSOLUTE CALIBRATION TESTS

TM/PF GAIN (BAND-AVERAGED)						
TESTS	BAND					
	1	2	3	4	5	7
C1	15.92	8.06	10.59	10.97	77.06	147.17
C2	15.78	8.10	10.62	10.90	77.24	147.12
C3	15.78	8.04	10.56	10.91	77.16	146.96
MEAN	15.83	8.07	10.59	10.93	77.15	147.08
STANDARD DEVIATION	0.081	0.031	0.030	0.038	0.090	0.110

Table 24

THE MEAN AND STANDARD DEVIATIONS OF THE GAIN VALUES OF CHANNEL 16 DURING THE THREE MARCH ABSOLUTE CALIBRATION TESTS, SHOWING EXCELLENT SHORT-TERM REPRODUCIBILITY

TM/PF GAIN (CHANNEL 16)						
TESTS	BAND					
	1	2	3	4	5	7
C1	15.99	7.96	10.46	10.89	77.52	148.51
C2	15.87	[illegible].98	10.48	10.83	77.74	148.49
C3	15.83	7.92	10.43	10.84	77.60	148.28
MEAN	15.90	7.95	10.47	10.85	77.62	148.43
STANDARD DEVIATION	0.083	0.031	0.025	0.032	0.111	0.172

Table 25

TM/PF OBSERVED OFFSET VALUES SHOWING THE MEAN, STANDARD DEVIATION, MINIMUM, MAXIMUM, AND CHANNEL 1 VALUES FOR ALL BANDS AND FOR TEST A1 AND C2

TEST	BAND	MEAN	σ^b	MIN	MAX	CHANNEL 1
A1	1	0.44	0.34	0.31	1.19	1.19
	2	0.89	0.16	0.72	1.36	1.36
	3	0.81	0.20	0.53	1.22	1.22
	4	0.92	0.22	0.54	1.41	1.41
	5	1.53[a]	1.09[a]	0.79[a]	5.19[a]	1.84[a]
	7	2.57[a]	0.74[a]	1.35[a]	3.89[a]	3.83[a]
C2	1	2.58	0.18	2.37	3.18	3.18
	2	2.44	0.16	2.32	2.99	2.99
	3	1.58	0.20	1.24	2.13	2.13
	4	1.91	0.22	1.67	2.53	2.53
	5	3.02	0.11	2.85	3.28	3.28
	7	2.41	0.20	2.15	2.95	2.95

[a] COOLED FOCAL PLANE VALUES ARE NOT TO BE USED BECAUSE THE PLANE WAS REMOVED AND SERVICED AFTER THE A TEST.

[b] STANDARD DEVIATION.

Table 26

TM/PF MEAN OFFSET VALUES FOR ALL BANDS FOR ALL TESTS

BAND	TEST					
	1	2	3	4	5	6
1	0.44	0.46	—	2.45	2.58	2.54
2	0.89	0.92	—	2.39	2.44	2.45
3	0.81	0.86	—	1.48	1.58	1.57
4	0.91	0.96	—	1.78	1.91	1.89
5	1.53[a]	1.77[a]	—	2.83	3.02	2.94
7	2.54[a]	2.68[a]	—	2.32	2.41	2.43

[a] COOLED FOCAL PLANE VALUES ARE NOT TO BE USED BECAUSE THE PLANE WAS REMOVED AND SERVICED AFTER THE A TEST.

Signal-to-Noise Ratio

The computed SNRs for all bands for test C2 are presented in Tables 2 through 7. All but five detectors satisfied the specifications by significant amounts; two of the five passed, but barely (1/4 and 7/7). Channel 3 of band 5 is dead, and channels 2 and 4 of band 2 are bad, one due to noise (2/2) and the other due to slow response (2/4). The 5/3 detector is the only one for which no usable data are obtainable, and this should be treated as dead in the postlaunch data processing. Most TM detectors satisfied the specifications although the error in the computed SNR values is somewhat high (typically 4 to 5 for all bands) due to the large scatter.

Dynamic Range

Table 18 gives the ratio of the specified to the average MSL radiance by band, the minimum observed MSL radiance, and the ratio of the standard deviation of the average to the average value. All detectors are within 1 percent of the average, except in band 4 (1.2 percent). The larger standard deviation there is due largely to detector 10, which is an outlier and is less sensitive than the other band 4 detectors. All bands have somewhat poorer dynamic range than specified; band 3 is the worst case, with band 1 next. Bands 2, 4, 5, and 7 are only slightly different from the required values. Whether this will adversely affect TM image data for these bands is not presently known.

A stated requirement for the archived radiometrically corrected data produced by the Landsat-4 Scrounge data processing system for the TM has been that the original raw data must be retrievable. To guarantee this, the radiometric lookup tables used to generate the corrected data should expand or leave the same any raw digital count value. For example, if the original value is 100, the specified dynamic range for the corrected data may give a value slightly greater than 100 by some fraction. The minimum saturation level radiance given in Table 21 for each band is thus appropriate for this requirement because the TM gains have already been set to give a saturation value 5 percent higher than the MSL. However, the postlaunch performance of the TM must also be considered. Data presented in Barker et al. (1983b) show that the gains determined with IC data have shown an expotential-like decline for bands 1 through 4 and have stabilized at approximately 3 to 6 percent below prelaunch values presented here. Bands 5 and 7, however, have shown an oscillatory behavior. Band 7 seems to show no change overall, except for the 2-month oscillation. Band 5 has shown an increase after launch and then the oscillation and possibly some decrease. The largest change was an increase of 8 percent in band 5. If we recommended using the prelaunch MSL radiances as the upper limit to the dynamic range for the data processing corrections, we would risk loss of some image data in bands 5 and 7. Hence, for bands 5 and 7, we recommend using radiance values 10 percent lower than the maximum possible values for RMAX. Table 27 gives the upper and lower radiance limits for each band that we recommend for use in the postlaunch data processing systems.

CALIBRATION OF THE IC

The two most important parameters derived from these test comparisons are the slope, which measures the relative change between tests, and the standard error of the estimates, which is a measure of the goodness of fit. The major contributor to the latter is noise due to the IC pulse integration and averaging procedure.

To determine to what extent the IC lamp levels may vary due to differences in environment or operating conditions, other IC lamp data are presently being studied. The standard deviation of the average calibration pulse for a lamp state is typically 0.5 digital count. The average difference between forward and reverse mirror sweep scans is typically 0.5 digital count; both values are band dependent. The forward-reverse differences are uncorrected for dark background. These problems are related to overall IC stability under a variety of operating and environmental conditions and are discussed in more detail by Barker et al. (1983b). Present estimates of repeatability with the transfer data indicate that the IC gives calibration radiances repeatable to the 5-percent level or better, except for band 5; band 5 is better than 7 percent. Table 28 shows figure-of-merit values for the comparisons between transfer tests 1 and 7 and between tests 9 and 7. The latter is a comparison of ambient to vacuum calibration transfer. Table 29 shows results for the derived slope for the same test comparisons. Differences noted particularly in band 5 may be attributed to slight differences in operating conditions. The other bands typically show changes of 5 percent or less. The differences between tests 1 and 7 for bands 5 and 7 should be ignored due to changes made in the CFPA in September 1981; these changes introduced a discontinuity between previous calibrations and those performed in March 1982.

Typically, the radiance comparisons between tests have shown more variability than the digital count comparisons (see Table 20). This may be understood by noting that there are slight differences in environment or operating conditions

Table 27

TM/PF DYNAMIC RANGE RECOMMENDED RADIANCE VALUES FOR RADIOMETRIC LOOKUP TABLE GENERATION IN DATA PROCESSING SYSTEMS

DYNAMIC RANGE ($mWcm^{-2}sr^{-1}\mu m^{-1}$)	BAND					
	1	2	3	4	5	7
RMAX	15.089	29.353	22.350	21.369	2.925	1.534
RMIN	−0.152	−0.284	−0.117	−0.151	−0.037	−0.015

Table 28

TM/PF INTERNAL CALIBRATOR AVERAGE COMPARISON SLOPE VALUES BY BAND

TEST 1 TO TEST 7						
	BAND					
	1	2	3	4	5	7
DIGITAL COUNTS	1.0256	1.0311	1.0278	1.0363	0.9450	1.0058
RADIANCE	0.9758	1.0262	1.0244	0.9979	0.8962	0.9715

TEST 9 TO TEST 7						
	BAND					
	1	2	3	4	5	7
DIGITAL COUNTS	0.9879	0.9988	1.0365	1.0451	0.9657	0.9812
RADIANCE	0.9884	1.0074	1.0412	1.0487	0.9374	0.9675

Table 29

TM/PF INTERNAL CALIBRATOR
AVERAGE GOODNESS OF A FIT ($^{\sigma}Y_{est}$) VALUES BY BAND

TEST 1 TO TEST 7

	BAND					
	1	2	3	4	5	7
DIGITAL COUNTS	1.35	0.79	0.93	0.79	0.27	0.44
RADIANCE	0.081	0.097	0.087	0.069	0.0033	0.0029

TEST 9 TO TEST 7

	BAND					
	1	2	3	4	5	7
DIGITAL COUNTS	0.79	0.75	1.04	1.26	0.23	0.62
RADIANCE	0.050	0.093	0.098	0.116	0.0028	0.0042

[a] σY_{est} UNITS ARE DIGITAL COUNTS OR MILLIWATTS CM^{-2} $STER^{-1}$ μm^{-1} (RADIANCE).

between the different transfer tests that have not been accounted for. In particular, Clemann et al. (1982) has noted a linear correlation between various temperature parameters, particularly the calibration shutter flag temperature, and the digital output of the TM. Thus, the sensitivity of the TM (gain and offset) changes slightly with these internal temperatures; we are presently studying these effects with these and other TM IC data to firmly establish the correlation and the overall degree of stability of the IC (Barker et al., 1983d). Even so, the results of the transfer test comparisons show good repeatability (5 percent or better for all bands except band 5) without including operational differences; when they are included in the analysis, we can expect to see a significant improvement. The results for tests 1, 3, and 4 that were taken during the June 1981 absolute calibration show that the above considerations are valid. The variation in slope values among these three tests is less than 0.7 percent in all bands.

RECOMMENDATIONS

Our study of the prelaunch absolute radiometric calibration of the protoflight TM reflective bands has shown several areas where improvements in the calibration can be realized, particularly when applied to the flight unit TM. Accordingly, we have separated our recommendations into two categories: protoflight and flight.

PROTOFLIGHT TM

The best calibration of the protoflight TM reflective bands prior to launch was performed in March 1982. The test designated C2 in this paper is to be preferred due to the operating configuration and the state of calibration of the IS(122) afterwards. Tables 1 through 13 summarize the important parameters for this test for all detectors. Additional evaluation of the TM absolute detector calibration is still in progress and is concentrating on the areas of temperature dependence and the effect of nonuniform analog-to-digital conversions on the calibration of the TM. In addition, the raw data from the IS(122) calibration is being examined to ensure that the peak output of the IS(122) was seen by all TM detectors and to evaluate the impact of a non-flat (IS(122) output (if any) on the detector calibration. We are also evaluating the feasibility of recollecting prelaunch calibration data to study the effect of a drifting background (DC restore of offset voltage to a nominal reference corresponding to 2 or 3 digital counts) during an image scan. In-orbit data are also being obtained to study this effect.

The calibrations of the IC that best characterize the transfer from the IS(122) to the IC are the March 20 transfer (test 7 in this paper) for determining the ambient characteristics of the IC and the March 9 transfer (test 9 in this paper) for referencing the vacuum characteristics and transferring the calibration from ambient to vacuum (by comparison with text 7). The use of these data sets as a reference for in-orbit data is discussed in Barker et al. (1983c). Additional studies of protoflight TM data, both prelaunch and in-orbit, to study temperature dependencies of the IC (particularly due to the calibration shutter flag) are needed. (See Clemann et al., 1982). The dependence of the IC calibration on such parameters as the number of minor frames centered on the pulse to average, number of scans to average, etc., are discussed in Barker et al. (1983b).

FLIGHT UNIT TM

Recommendations for the calibration of the flight unit TM have been developed through experience with the protoflight calibration and application of the calibration while radiometrically correcting in-orbit protoflight data. Changes to the calibration procedures and to the type and quantity of data collected should be made as follows:

- Cross-calibration of all Landsat integrating spheres (one for TM and two for MSS) directly at NBS rather than more than one step (lamp source) removed from NBS as is presently the case; include the thermal band in the calibration if possible

- Operation of the IS(122) in scanning mode for all tests (already done; see Lansing 1981) and, increase the size of the video data window collected in each scan

- Use of multiple IC data collects during sphere calibration to improve statistics of the calibration transfer to the IC and to allow for correction of temperature dependencies

- Use of a linear ramp for system-level measurement of analog-to-digital conversion and inclusion of these measurements in the IS(122) calibration

- Calibration of a lamp source small enough to use during thermal vacuum chamber testing to measure change in TM detectors and IC due to so-called "vacuum shift" (compared to the ambient IS(122) calibration)

- Collection and study of sufficient background data to characterize changes in reference level during an image scan

APPENDIX - SPECTRAL RADIANCES FOR THE IC

The averaged digital counts and their corresponding spectral radiance values for each lamp configuration of the TM IC calibration transfer are given in the following tables. Two reference sets are given, March 20, 1982 (test 7 in Table 22) and March 9, 1982 (test 9), representative of ambient and vacuum conditions, respectively. Tables A-1 through A-16 pertain to test 7, Tables A-17 through A-32 pertain to test 9. Tables A-1 through A-8 and A-17 through A-24 give the averaged digital counts, Q, determined by the Hughes averaging procedure (Barker et al., 1983b) for the eight lamp configurations (100, 110, 010, 011, 111, 101, 001, and 000, where 1 indicates lamp on, and 0, lamp off). Using the gains and offsets for each detector given in Tables 2 through 7. The corresponding radiance values are computed as follows:

$$L = \frac{\bar{Q} - O}{G}$$

where L is the resulting radiance, $\bar{Q}$ is the averaged digital count, G the gain, and O is the offset. These values are presented in Tables A-9 through A-16 and A-25 through A-32. Each table gives mean values (MEAN), standard deviations (SDEV), standard deviations of the mean (SMEN), and coefficients of variation (CVAR) for odd-numbered, even-numbered, and all detectors in a band. Values for detector 4, band 2, are not given in Tables A-1 through A-16 because the Hughes computer program treated it as a dead detector (like band 5, channel 3). Values for this detector are presented in the other tables, derived directly from raw data taken in thermal vacuum testing.

Finally, Tables A-33 through A-40 give the ratio of digital counts for test 7 to test 9 for all eight lamp configurations. These tables are presented to aid in evaluating the so-called "vacuum shift" generally noted in the response of a satellite sensor between ambient and vacuum operating conditions. The mean values and standard deviations given have the same meaning as before (e.g., Tables A-1 through A-8).

Table A-1. Lamp 100 for Test 7 in Digital Counts

CHANNEL	BAND					
	TM1	TM2	TM3	TM4	TM5	TM7
1	107.69	102.53	90.99	92.12	47.25	61.09
2	104.79	92.95	91.94	96.76	68.07	57.11
3	108.76	100.11	89.71	92.70	–	59.34
4	106.56	–	91.32	97.34	67.93	57.08
5	107.94	101.71	90.13	91.30	45.82	58.97
6	104.48	92.60	92.85	98.21	68.91	56.85
7	107.01	99.46	89.58	91.40	46.05	58.41
8	104.79	91.23	91.58	97.23	67.23	56.43
9	108.39	100.47	89.79	91.87	45.85	59.19
10	105.29	90.47	92.14	101.11	66.55	56.45
11	107.84	99.53	89.03	90.86	46.10	58.88
12	106.62	90.15	92.78	98.30	67.04	57.83
13	108.10	100.37	89.78	92.82	45.87	58.36
14	105.47	91.46	91.56	97.88	66.46	58.08
15	108.89	100.35	90.60	89.84	46.64	59.46
16	104.98	90.15	91.33	96.57	68.25	59.70
MEAN ODD	107.95	100.56	89.95	91.61	46.23	59.21
MEAN EVEN	105.25	91.29	91.94	97.93	67.30	57.44
MEAN ALL	106.60	96.24	90.94	94.77	57.47	58.33
SDEV ODD	1.04	1.06	0.63	1.00	0.54	0.86
SDEV EVEN	0.65	1.13	0.62	1.44	0.70	1.09
SDEV ALL	1.63	4.91	1.18	3.47	10.90	1.32
SMEN ODD	0.37	0.38	0.22	0.35	0.20	0.30
SMEN EVEN	0.23	0.43	0.22	0.51	0.25	0.39
SMEN ALL	0.41	1.27	0.30	0.87	2.81	0.33
CVAR ODD	0.97	1.06	0.70	1.09	1.16	1.46
CVAR EVEN	0.62	1.25	0.67	1.47	1.04	1.90
CVAR ALL	1.53	5.10	1.30	3.66	18.97	2.27

Table A-2. Lamp 110 for Test 7 in Digital Counts

CHANNEL	BAND					
	TM1	TM2	TM3	TM4	TM5	TM7
1	174.48	180.62	155.73	184.85	87.56	106.21
2	169.00	157.38	160.44	181.46	125.46	110.28
3	178.64	177.00	154.07	185.57	–	103.95
4	170.13	–	159.72	182.28	125.62	110.45
5	175.68	179.49	154.79	183.10	85.77	103.49
6	168.16	156.22	161.91	183.86	123.76	110.07
7	173.85	176.04	153.90	183.26	86.18	103.02
8	167.96	154.04	159.97	182.47	124.25	109.31
9	173.67	177.55	154.65	184.08	85.66	103.88
10	169.03	153.05	160.89	189.43	123.18	109.08
11	175.05	176.01	153.12	182.13	86.23	103.24
12	168.94	152.41	161.79	183.65	123.96	111.73
13	175.89	176.77	154.43	186.13	85.88	102.56
14	169.14	154.57	159.81	183.21	122.85	111.96
15	177.06	177.64	155.56	180.49	87.00	103.83
16	168.91	152.51	159.10	180.90	125.52	114.47
MEAN ODD	175.54	177.64	154.53	183.70	86.33	103.77
MEAN EVEN	168.91	154.31	160.45	183.41	124.33	110.92
MEAN ALL	172.22	166.75	157.49	183.55	106.59	107.35
SDEV ODD	1.69	1.63	0.86	1.86	0.71	1.10
SDEV EVEN	0.67	1.91	1.02	2.65	1.10	1.76
SDEV ALL	3.64	12.17	3.19	2.21	19.64	3.95
SMEN ODD	0.60	0.58	0.30	0.66	0.27	0.39
SMEN EVEN	0.24	0.72	0.36	0.94	0.39	0.62
SMEN ALL	0.91	3.14	0.80	0.56	5.07	0.99
CVAR ODD	0.96	0.92	0.56	1.01	0.83	1.06
CVAR EVEN	0.40	1.24	0.63	1.44	0.88	1.59
CVAR ALL	2.11	7.30	2.03	1.21	18.43	3.68

Table A-3. Lamp 010 for Test 7 in Digital Counts

CHANNEL	BAND					
	TM1	TM2	TM3	TM4	TM5	TM7
1	70.42	81.40	68.27	96.56	43.66	48.83
2	65.60	66.63	70.91	87.77	60.54	55.96
3	71.58	79.26	67.14	98.21	–	47.35
4	67.21	–	70.56	87.98	60.37	55.89
5	70.53	80.34	67.35	94.81	42.48	46.98
6	65.64	66.26	71.56	89.00	59.46	55.85
7	69.67	78.67	68.92	95.42	42.53	46.87
8	66.89	65.30	70.66	88.25	59.60	55.36
9	69.46	79.23	67.03	95.64	42.32	47.08
10	66.07	64.70	70.98	91.34	59.09	55.21
11	70.26	78.70	68.45	94.54	42.58	46.87
12	66.70	64.44	71.33	88.75	59.46	56.50
13	70.73	78.61	67.04	96.57	42.41	46.51
14	66.18	65.35	70.55	88.41	58.87	56.66
15	70.92	79.44	67.48	93.67	43.14	47.40
16	65.79	64.21	70.41	87.58	60.54	58.03
MEAN ODD	70.45	79.45	67.21	95.43	42.70	47.24
MEAN EVEN	66.14	65.27	70.87	88.64	59.74	56.18
MEAN ALL	68.29	72.84	69.04	92.03	51.79	51.71
SDEV ODD	0.69	0.97	0.53	1.04	0.51	0.71
SDEV EVEN	0.57	0.92	0.41	1.20	0.66	0.89
SDEV ALL	2.31	7.38	1.96	3.67	8.82	4.69
SMEN ODD	0.24	0.34	0.19	0.37	0.19	0.25
SMEN EVEN	0.20	0.35	0.15	0.42	0.23	0.32
SMEN ALL	0.58	1.91	0.49	0.92	2.28	1.17
CVAR ODD	0.98	1.22	0.79	1.09	1.20	1.50
CVAR EVEN	0.86	1.41	0.58	1.35	1.11	1.59
CVAR ALL	3.38	10.13	2.82	3.99	17.03	9.06

Table A-4. Lamp 011 for Test 7 in Digital Counts

CHANNEL	BAND					
	TM1	TM2	TM3	TM4	TM5	TM7
1	115.88	127.03	105.64	140.70	66.56	80.75
2	109.45	106.48	111.09	135.10	92.42	88.90
3	118.09	124.15	104.29	141.01	–	78.88
4	110.05	–	110.64	135.87	92.30	88.95
5	116.22	126.09	104.81	138.96	64.88	78.42
6	109.28	106.03	112.32	137.14	91.07	88.65
7	115.37	123.45	104.23	139.48	65.10	78.11
8	108.96	104.33	110.83	136.06	91.41	87.95
9	114.88	124.56	104.67	140.23	64.94	78.85
10	109.35	103.49	111.45	141.03	90.68	87.85
11	116.47	123.51	103.68	138.40	65.23	78.28
12	109.44	103.19	112.08	136.84	91.15	90.03
13	116.90	123.79	104.43	141.78	64.95	77.88
14	109.70	104.47	110.77	136.49	90.50	90.04
15	117.38	124.68	105.31	137.29	66.07	78.93
16	109.48	102.90	110.37	134.80	92.67	92.38
MEAN ODD	116.40	124.66	104.63	139.73	65.39	78.76
MEAN EVEN	109.46	104.41	111.19	136.67	91.52	89.34
MEAN ALL	112.93	115.21	107.91	138.20	79.33	84.06
SDEV ODD	1.06	1.29	0.63	1.49	0.67	0.90
SDEV EVEN	0.31	1.38	0.70	1.94	0.84	1.47
SDEV ALL	3.66	10.53	3.45	2.30	13.52	5.59
SMEN ODD	0.37	0.46	0.22	0.53	0.25	0.32
SMEN EVEN	0.11	0.52	0.25	0.69	0.30	0.52
SMEN ALL	0.91	2.72	0.86	0.57	3.49	1.40
CVAR ODD	0.91	1.03	0.60	1.07	1.03	1.15
CVAR EVEN	0.29	1.33	0.63	1.42	0.92	1.65
CVAR ALL	3.24	9.14	3.20	1.66	17.04	6.65

Table A-5. Lamp 111 for Test 7 in Digital Counts

CHANNEL		BAND					
		TM1	TM2	TM3	TM4	TM5	TM7
1		219.59	225.38	192.57	226.49	109.72	137.32
2		211.38	196.39	199.73	227.68	156.74	142.16
3		224.37	220.79	190.43	227.93	–	135.04
4		214.33	–	198.57	228.72	157.23	142.98
5		221.09	223.94	191.50	225.09	107.65	134.49
6		210.74	194.99	201.58	230.68	154.82	142.49
7		219.16	219.61	190.35	225.02	108.17	133.76
8		210.77	192.43	198.81	229.24	155.27	141.49
9		218.43	221.51	191.11	226.80	107.56	136.00
10		212.19	191.17	200.44	236.84	154.19	141.22
11		220.93	219.58	189.53	224.08	108.32	134.29
12		212.93	190.52	201.40	230.66	155.32	144.57
13		221.70	220.78	191.18	229.33	107.86	133.38
14		212.11	192.97	199.06	229.98	153.85	144.86
15		223.27	221.53	192.65	222.79	108.83	134.84
16		211.50	190.28	198.27	227.12	156.80	147.78
MEAN	ODD	221.07	221.64	191.16	225.94	108.30	134.76
MEAN	EVEN	211.99	192.68	199.73	230.12	155.53	143.44
MEAN	ALL	216.53	208.12	195.45	228.03	133.49	139.10
SDEV	ODD	2.04	2.04	1.09	2.13	0.77	1.20
SDEV	EVEN	1.21	2.31	1.29	3.01	1.27	2.19
SDEV	ALL	4.96	15.10	4.57	3.31	24.41	4.80
SMEN	ODD	0.72	0.72	0.39	0.75	0.29	0.42
SMEN	EVEN	0.43	0.87	0.46	1.07	0.45	0.78
SMEN	ALL	1.24	3.90	1.14	0.83	6.30	1.20
CVAR	ODD	0.92	0.92	0.57	0.94	0.71	0.89
CVAR	EVEN	0.57	1.20	0.65	1.31	0.82	1.53
CVAR	ALL	2.29	7.26	2.34	1.45	18.29	3.45

Table A-6. Lamp 101 for Test 7 in Digital Counts

CHANNEL	BAND					
	TM1	TM2	TM3	TM4	TM5	TM7
1	153.06	148.24	128.50	135.88	69.78	92.41
2	148.69	133.10	132.09	143.70	100.07	89.80
3	155.65	145.15	128.91	136.16	–	90.40
4	150.17	–	131.46	144.39	100.00	89.84
5	154.16	147.41	127.63	134.55	68.18	89.84
6	148.24	132.18	133.43	145.53	98.52	89.58
7	152.47	144.44	128.90	134.92	68.55	89.50
8	147.94	130.39	131.62	144.46	98.85	88.91
9	152.23	145.93	127.54	135.57	68.13	90.29
10	148.92	129.57	132.70	150.21	98.05	88.93
11	153.99	144.42	128.30	134.28	68.58	89.91
12	149.02	128.84	133.38	145.49	98.76	91.00
13	154.89	145.64	127.46	136.99	68.28	89.37
14	149.20	130.56	131.85	146.12	97.86	91.25
15	155.82	145.84	128.38	132.70	69.28	90.65
16	148.97	129.03	131.27	143.63	100.21	93.58
MEAN ODD	154.12	145.88	127.46	135.13	68.68	90.30
MEAN EVEN	148.89	130.53	132.23	145.32	99.06	90.36
MEAN ALL	151.51	138.72	129.84	140.22	84.88	90.33
SDEV ODD	1.57	1.36	0.76	1.33	0.62	0.97
SDEV EVEN	0.69	1.61	0.86	2.11	0.92	1.56
SDEV ALL	2.94	8.06	2.58	5.53	15.70	1.25
SMEN ODD	0.55	0.48	0.27	0.47	0.24	0.34
SMEN EVEN	0.24	0.61	0.30	0.75	0.33	0.55
SMEN ALL	0.74	2.08	0.65	1.38	4.05	0.31
CVAR ODD	1.02	0.93	0.60	0.99	0.91	1.07
CVAR EVEN	0.46	1.23	0.65	1.45	0.93	1.72
CVAR ALL	1.94	5.81	1.99	3.94	18.50	1.38

Table A-7. Lamp 001 for Test 7 in Digital Counts

CHANNEL	BAND					
	TM1	TM2	TM3	TM4	TM5	TM7
1	48.61	48.53	40.67	47.30	25.73	34.96
2	45.38	42.04	42.38	49.78	34.81	35.42
3	49.27	47.20	39.85	47.17	–	33.80
4	46.65	–	42.10	49.96	34.63	35.31
5	48.47	47.88	39.97	46.35	24.71	33.46
6	45.52	41.91	42.94	50.54	34.28	35.25
7	48.13	46.89	39.65	46.80	24.94	33.39
8	45.80	41.38	42.48	50.06	34.35	35.06
9	47.80	47.24	39.73	46.79	24.73	33.77
10	45.94	40.91	42.62	51.77	33.89	35.07
11	48.37	46.93	39.40	46.31	24.83	33.59
12	46.40	40.80	42.75	50.56	34.24	35.77
13	48.57	47.17	39.81	47.35	24.87	33.19
14	45.93	41.39	42.46	50.44	34.00	36.04
15	48.92	47.38	40.22	45.89	25.27	33.88
16	45.61	40.98	42.35	49.88	34.96	37.01
MEAN ODD	48.52	47.40	39.91	46.74	25.01	33.75
MEAN EVEN	45.90	41.34	42.48	50.37	34.39	35.62
MEAN ALL	47.21	44.57	41.20	48.56	30.01	34.68
SDEV ODD	0.46	0.58	0.39	0.53	0.37	0.54
SDEV FVEN	0.44	0.49	0.27	0.65	0.38	0.66
SDEV ALL	1.42	3.17	1.37	1.98	4.86	1.13
SMEN ODD	0.16	0.20	0.14	0.19	0.14	0.19
SMEN EVEN	0.15	0.18	0.10	0.23	0.13	0.23
SMEN ALL	0.38	0.82	0.34	0.49	1.25	0.28
CVAR ODD	0.95	1.18	0.98	1.13	1.47	1.59
CVAR EVEN	0.95	1.18	0.64	1.28	1.11	1.84
CVAR ALL	3.01	7.12	3.32	4.04	16.18	3.25

Table A-8. Lamp 000 for Test 7 in Digital Counts

CHANNEL	BAND					
	TM1	TM2	TM3	TM4	TM5	TM7
1	2.71	2.68	2.61	2.70	2.92	2.84
2	2.20	2.21	2.18	2.22	2.57	2.39
3	2.34	2.28	2.39	2.33	–	2.38
4	1.69	–	2.32	2.22	2.57	2.42
5	2.35	2.12	2.16	2.08	2.69	2.19
6	2.26	2.26	2.22	2.27	2.73	2.44
7	2.28	2.09	2.16	2.06	2.64	2.56
8	2.15	2.20	2.39	2.33	2.84	2.39
9	2.34	2.10	2.19	2.05	2.60	2.31
10	1.85	2.10	2.14	2.04	2.60	2.47
11	2.25	2.17	2.07	2.05	2.63	2.28
12	1.68	2.10	2.12	2.01	2.58	2.35
13	2.19	2.12	2.01	2.04	2.69	2.13
14	2.17	2.16	2.25	2.05	2.59	2.52
15	2.21	2.10	1.99	2.04	2.80	2.15
16	2.25	2.24	2.28	2.04	2.63	2.50
MEAN ODD	2.33	2.21	2.20	2.17	2.71	2.35
MEAN EVEN	2.03	2.18	2.23	2.15	2.64	2.44
MEAN ALL	2.18	2.20	2.22	2.16	2.67	2.39
SDEV ODD	0.16	0.20	0.21	0.24	0.12	0.24
SDEV EVEN	0.25	0.06	0.09	0.13	0.10	0.06
SDEV ALL	0.26	0.15	0.16	0.18	0.11	0.18
SMEN ODD	0.06	0.07	0.07	0.08	0.04	0.09
SMEN EVEN	0.09	0.02	0.03	0.04	0.04	0.02
SMEN ALL	0.06	0.04	0.04	0.05	0.03	0.04
CVAR ODD	6.99	9.09	9.48	10.88	4.25	10.31
CVAR EVEN	12.53	2.83	4.09	5.87	3.78	2.35
CVAR ALL	11.89	6.75	7.06	8.48	4.08	7.34

Table A-9. Lamp 100 for Test 7 in Radiance Units

CHANNEL	BAND					
	TM1	TM2	TM3	TM4	TM5	TM7
1	6.679	12.177	8.246	8.165	0.574	0.392
2	6.496	11.163	8.523	8.766	0.848	0.373
3	6.724	12.191	8.292	8.235	–	0.386
4	6.528	–	8.533	8.819	0.838	0.370
5	6.658	12.114	8.334	8.282	0.557	0.384
6	6.481	11.006	8.556	8.806	0.831	0.371
7	6.657	12.057	8.319	8.248	0.556	0.380
8	6.482	10.981	8.549	8.774	0.830	0.372
9	6.566	12.146	8.290	8.286	0.556	0.384
10	6.483	10.889	8.579	8.802	0.827	0.373
11	6.714	12.148	8.317	8.271	0.564	0.385
12	6.520	10.959	8.577	8.854	0.825	0.374
13	6.724	12.081	8.268	8.245	0.561	0.385
14	6.538	10.932	8.449	8.795	0.822	0.376
15	6.736	11.956	8.271	8.184	0.563	0.392
16	6.463	10.986	8.556	8.734	0.840	0.385
MEAN ODD	6.681	12.109	8.292	8.239	0.569	0.386
MEAN EVEN	6.499	10.989	8.540	8.794	0.833	0.374
MEAN ALL	6.590	11.586	8.416	8.516	0.705	0.380
SDEV ODD	0.060	0.078	0.031	0.045	0.008	0.004
SDEV EVEN	0.028	0.087	0.043	0.037	0.009	0.005
SDEV ALL	0.104	0.584	0.133	0.289	0.141	0.007
SMEN ODD	0.021	0.027	0.011	0.016	0.003	0.002
SMEN EVEN	0.010	0.033	0.015	0.013	0.003	0.002
SMEN ALL	0.026	0.151	0.033	0.072	0.037	0.002
CVAR ODD	0.893	0.642	0.370	0.551	1.357	1.111
CVAR EVEN	0.436	0.792	0.503	0.425	1.027	1.252
CVAR ALL	1.580	5.036	1.582	3.393	20.072	1.966

Table A-10. Lamp 110 for Test 7 in Radiance Units

CHANNEL	BAND					
	TM1	TM2	TM3	TM4	TM5	TM7
1	10.947	21.731	14.252	16.617	1.101	0.697
2	10.570	19.101	14.984	16.596	1.595	0.735
3	11.048	21.786	14.370	16.664	–	0.688
4	10.519	–	15.028	16.660	1.580	0.731
5	10.943	21.604	14.420	16.773	1.078	0.685
6	10.528	18.779	15.032	16.639	1.570	0.734
7	10.919	21.582	14.398	16.743	1.074	0.682
8	10.492	18.756	15.040	16.607	1.569	0.736
9	10.808	21.691	14.384	16.776	1.074	0.687
10	10.502	18.622	15.085	16.624	1.562	0.737
11	10.998	21.710	14.388	16.758	1.071	0.687
12	10.524	18.727	15.061	16.683	1.557	0.738
13	11.044	21.494	14.318	16.685	1.067	0.687
14	10.578	18.683	14.864	16.615	1.552	0.741
15	11.056	21.387	14.302	16.599	1.085	0.696
16	10.492	18.809	15.019	16.522	1.576	0.754
MEAN ODD	10.970	21.621	14.354	16.702	1.079	0.688
MEAN EVEN	10.526	18.783	15.014	16.618	1.570	0.738
MEAN ALL	10.748	20.296	14.684	16.660	1.341	0.713
SDEV ODD	0.085	0.134	0.058	0.070	0.011	0.005
SDEV EVEN	0.033	0.153	0.068	0.048	0.013	0.007
SDEV ALL	0.238	1.472	0.346	0.074	0.254	0.026
SMEN ODD	0.030	0.047	0.021	0.025	0.004	0.002
SMEN EVEN	0.012	0.058	0.024	0.017	0.005	0.002
SMEN ALL	0.059	0.380	0.087	0.018	0.066	0.007
CVAR ODD	0.775	0.621	0.405	0.418	1.036	0.749
CVAR EVEN	0.317	0.816	0.454	0.287	0.857	0.934
CVAR ALL	2.214	7.253	2.368	0.444	18.962	3.701

Table A-11. Lamp 010 for Test 7 in Radiance Units

CHANNEL	BAND					
	TM1	TM2	TM3	TM4	TM5	TM7
1	4.297	9.582	6.137	8.570	0.527	0.310
2	4.010	7.921	6.540	7.935	0.750	0.365
3	4.328	9.589	6.161	8.553	–	0.306
4	4.057	–	6.562	7.955	0.740	0.302
5	4.292	9.506	6.190	8.606	0.511	0.303
6	4.012	7.787	6.559	7.062	0.734	0.364
7	4.277	9.477	6.178	8.619	0.511	0.302
8	4.013	7.771	6.564	7.948	0.732	0.365
9	4.223	9.515	6.153	8.633	0.511	0.302
10	4.010	7.705	6.577	7.936	0.730	0.365
11	4.318	9.544	6.178	8.613	0.509	0.303
12	4.059	7.750	6.562	7.978	0.728	0.365
13	4.343	9.400	6.140	8.584	0.507	0.303
14	4.045	7.724	6.475	7.927	0.724	0.366
15	4.330	9.404	6.124	8.540	0.517	0.310
16	3.995	7.743	6.560	7.904	0.741	0.373
MEAN ODD	4.301	9.503	6.158	8.590	0.513	0.306
MEAN EVEN	4.025	7.772	6.550	7.943	0.735	0.366
MEAN ALL	4.163	8.695	6.354	8.266	0.631	0.335
SDEV ODD	0.039	0.075	0.024	0.034	0.007	0.003
SDEV EVEN	0.026	0.072	0.032	0.024	0.008	0.003
SDEV ALL	0.146	0.897	0.204	0.335	0.115	0.032
SMEN ODD	0.014	0.026	0.009	0.012	0.003	0.001
SMEN EVEN	0.009	0.027	0.011	0.009	0.003	0.001
SMEN ALL	0.036	0.232	0.051	0.084	0.030	0.008
CVAR ODD	0.911	0.786	0.395	0.395	1.363	1.039
CVAR EVEN	0.637	0.921	0.494	0.307	1.138	0.947
CVAR ALL	3.506	10.317	3.216	4.053	18.143	9.441

Table A-12. Lamp 011 for Test 7 in Radiance Units

CHANNEL	BAND					
	TM1	TM2	TM3	TM4	TM5	TM7
1	7.202	15.175	9.606	12.593	0.827	0.525
2	6.791	12.830	10.330	12.310	1.166	0.590
3	7.247	15.190	9.669	12.620	–	0.518
4	6.747	–	10.367	12.376	1.151	0.586
5	7.182	15.089	9.716	12.690	0.806	0.515
6	7.766	12.646	10.382	12.366	1.145	0.588
7	7.190	15.036	9.703	12.694	0.802	0.513
8	6.747	12.603	10.376	12.342	1.144	0.589
9	7.093	15.128	9.669	12.739	0.804	0.517
10	6.739	12.498	10.406	12.338	1.140	0.590
11	7.264	15.146	9.705	12.692	0.801	0.517
12	6.762	12.586	10.391	12.389	1.136	0.592
13	7.265	14.966	9.639	12.673	0.797	0.518
14	6.807	12.529	10.256	12.344	1.133	0.592
15	7.274	14.925	9.636	12.589	0.814	0.525
16	6.748	12.591	10.371	12.266	1.164	0.606
MEAN ODD	7.217	15.082	9.670	12.661	0.807	0.519
MEAN EVEN	6.766	12.612	10.360	12.340	1.148	0.591
MEAN ALL	6.992	13.929	10.015	12.500	0.988	0.555
SDEV ODD	0.064	0.098	0.040	0.056	0.010	0.004
SDEV EVEN	0.026	0.108	0.048	0.041	0.010	0.006
SDEV ALL	0.238	1.279	0.359	0.172	0.175	0.038
SMEN ODD	0.023	0.035	0.014	0.020	0.004	0.002
SMEN EVEN	0.009	0.041	0.017	0.014	0.004	0.002
SMEN ALL	0.059	0.330	0.090	0.043	0.045	0.009
CVAR ODD	0.885	0.652	0.419	0.440	1.237	0.836
CVAR EVEN	0.390	0.858	0.460	0.332	0.900	0.987
CVAR ALL	3.400	9.185	3.580	1.379	17.731	6.824

Table A-13. Lamp 111 for Test 7 in Radiance Units

CHANNEL	BAND					
	TM1	TM2	TM3	TM4	TM5	TM7
1	13.830	27.208	17.671	20.412	1.390	0.907
2	13.258	23.907	18.691	20.870	2.002	0.952
3	13.919	27.250	17.803	20.508	–	0.898
4	13.294	–	18.717	20.948	1.987	0.952
5	13.815	27.028	17.876	20.656	1.383	0.895
6	13.236	23.517	18.752	20.922	1.974	0.955
7	13.808	26.970	17.842	20.604	1.358	0.890
8	13.209	23.508	18.727	20.905	1.971	0.957
9	13.637	27.135	17.809	20.710	1.358	0.897
10	13.224	23.333	18.828	20.823	1.965	0.959
11	13.923	27.158	17.837	20.680	1.356	0.898
12	13.305	23.483	18.783	20.998	1.961	0.960
13	13.983	26.916	17.758	20.593	1.351	0.898
14	13.308	23.400	18.553	20.902	1.964	0.964
15	13.884	26.743	17.746	20.527	1.367	0.908
16	13.175	23.542	18.756	20.790	1.979	0.978
MEAN ODD	13.860	27.051	17.793	20.584	1.363	0.899
MEAN EVEN	13.251	23.527	18.726	20.894	1.974	0.960
MEAN ALL	13.556	25.407	18.259	20.739	1.689	0.929
SDEV ODD	0.113	0.169	0.064	0.096	0.013	0.006
SDEV EVEN	0.049	0.183	0.081	0.065	0.015	0.008
SDEV ALL	0.326	1.828	0.487	0.183	0.316	0.032
SMEN ODD	0.040	0.060	0.023	0.034	0.005	0.002
SMEN EVEN	0.017	0.069	0.029	0.023	0.005	0.003
SMEN ALL	0.081	0.472	0.122	0.046	0.082	0.008
CVAR ODD	0.817	0.624	0.361	0.468	0.949	0.656
CVAR EVEN	0.370	0.777	0.431	0.312	0.770	0.865
CVAR ALL	2.403	7.196	2.668	0.880	18.693	3.469

Table A-14. Lamp 101 for Test 7 in Radiance Units

CHANNEL	BAND					
	TM1	TM2	TM3	TM4	TM5	TM7
1	9.579	17.770	11.728	12.154	0.888	0.604
2	9.281	16.110	12.311	13.108	1.264	0.596
3	9.698	17.812	11.805	12.180	–	0.596
4	9.266	–	12.344	13.162	1.250	0.592
5	9.581	17.689	11.863	12.282	0.849	0.593
6	9.282	16.842	12.381	13.133	1.242	0.594
7	9.556	17.640	11.848	12.272	0.847	0.590
8	9.221	16.828	12.349	13.114	1.240	0.595
9	9.453	17.775	11.837	12.309	0.846	0.595
10	9.234	16.721	12.418	13.150	1.236	0.597
11	9.656	17.761	11.848	12.307	0.844	0.598
12	9.264	16.788	12.382	13.183	1.233	0.598
13	9.687	17.657	11.795	12.240	0.840	0.597
14	9.313	16.734	12.236	13.126	1.230	0.601
15	9.709	17.807	11.779	12.163	0.855	0.605
16	9.236	16.867	12.385	13.080	1.251	0.613
MEAN ODD	9.611	17.701	11.812	12.238	0.860	0.597
MEAN EVEN	9.260	16.841	12.347	13.132	1.243	0.598
MEAN ALL	9.436	16.833	12.080	12.685	1.060	0.598
SDEV ODD	0.085	0.089	0.047	0.065	0.009	0.005
SDEV EVEN	0.031	0.131	0.057	0.036	0.011	0.007
SDEV ALL	0.192	0.967	0.281	0.464	0.203	0.006
SMEN ODD	0.030	0.035	0.016	0.023	0.004	0.002
SMEN EVEN	0.011	0.049	0.020	0.013	0.004	0.002
SMEN ALL	0.048	0.250	0.070	0.116	0.053	0.001
CVAR ODD	0.886	0.559	0.394	0.529	1.113	0.866
CVAR EVEN	0.331	0.824	0.459	0.274	0.906	1.093
CVAR ALL	2.031	5.744	2.323	3.658	19.194	0.959

Table A-15. Lamp 001 for Test 7 in Radiance Units

CHANNEL	BAND					
	TM1	TM2	TM3	TM4	TM5	TM7
1	2.903	5.571	3.577	4.080	0.293	0.216
2	2.728	4.891	3.849	4.423	0.415	0.225
3	2.927	5.589	3.584	4.103	–	0.213
4	2.766	–	3.859	4.445	0.409	0.223
5	2.897	5.546	3.613	4.125	0.283	0.211
6	2.734	4.811	3.875	4.444	0.406	0.224
7	2.904	5.532	3.601	4.123	0.283	0.210
8	2.738	4.808	3.870	4.439	0.404	0.225
9	2.854	5.585	3.588	4.135	0.282	0.212
10	2.741	4.785	3.883	4.432	0.402	0.225
11	2.922	5.572	3.615	4.128	0.281	0.213
12	2.775	4.800	3.877	4.474	0.403	0.225
13	2.932	5.526	3.591	4.131	0.281	0.212
14	2.760	4.781	3.836	4.447	0.402	0.228
15	2.936	5.492	3.583	4.103	0.286	0.217
16	2.724	4.832	3.894	4.422	0.411	0.232
MEAN ODD	2.909	5.548	3.595	4.116	0.284	0.213
MEAN EVEN	2.745	4.812	3.867	4.441	0.407	0.228
MEAN ALL	2.827	5.206	3.731	4.278	0.349	0.219
SDEV ODD	0.027	0.032	0.014	0.020	0.004	0.002
SDEV EVEN	0.019	0.041	0.020	0.018	0.006	0.003
SDEV ALL	0.088	0.381	0.142	0.169	0.063	0.007
SMEN ODD	0.010	0.011	0.005	0.007	0.002	0.001
SMEN EVEN	0.007	0.016	0.007	0.006	0.002	0.001
SMEN ALL	0.022	0.098	0.036	0.042	0.016	0.002
CVAR ODD	0.928	0.576	0.398	0.477	1.578	1.082
CVAR EVEN	0.707	0.850	0.508	0.400	1.152	1.248
CVAR ALL	3.102	7.326	3.798	3.942	18.158	3.152

Table A-16. Lamp 000 for Test 7 in Radiance Units

CHANNEL	BAND					
	TM1	TM2	TM3	TM4	TM5	TM7
1	−0.030	−0.038	0.045	0.015	−0.005	−0.001
2	−0.012	−0.015	0.058	0.028	−0.005	0.000
3	−0.019	−0.016	0.047	0.034	−	−0.000
4	−0.057	−	0.082	0.037	−0.004	−0.000
5	−0.020	−0.038	0.064	0.029	−0.004	−0.001
6	−0.016	−0.035	0.056	0.029	−0.004	−0.070
7	−0.019	−0.028	0.057	−0.014	−0.005	0.002
8	−0.032	−0.040	0.083	0.053	−0.004	0.000
9	−0.019	−0.035	0.082	0.015	−0.006	−0.000
10	−0.039	−0.030	0.081	0.027	−0.004	0.000
11	−0.018	−0.025	0.079	0.012	−0.005	−0.000
12	−0.064	−0.029	0.089	0.020	−0.004	−0.001
13	−0.023	−0.024	0.084	0.033	−0.005	−0.000
14	−0.017	−0.038	0.055	0.012	−0.005	−0.001
15	−0.024	−0.034	0.043	0.032	−0.004	−0.000
16	−0.008	−0.023	0.059	0.004	−0.004	−0.000
MEAN ODD	−0.022	−0.030	0.065	0.019	−0.005	0.000
MEAN EVEN	−0.029	−0.030	0.094	0.026	−0.004	−0.000
MEAN ALL	−0.025	−0.030	0.080	0.023	−0.004	−0.000
SDEV ODD	0.004	0.008	0.012	0.016	0.001	0.001
SDEV EVEN	0.019	0.009	0.011	0.015	0.000	0.001
SDEV ALL	0.014	0.008	0.012	0.016	0.001	0.001
SMEN ODD	0.001	0.003	0.004	0.006	0.000	0.000
SMEN EVEN	0.007	0.003	0.004	0.005	0.000	0.000
SMEN ALL	0.003	0.002	0.003	0.004	0.000	0.000
CVAR ODD	−19.167	−28.384	21.086	84.395	−10.838	4520.822
CVAR EVEN	−65.269	−29.657	17.791	57.237	−10.501	−203.816
CVAR ALL	−54.693	−28.931	20.288	68.283	−13.204	−581.405

Table A-17. Lamp 100 for Test 9 in Radiance Units

CHANNEL	BAND					
	TM1	TM2	TM3	TM4	TM5	TM7
1	106.94	101.19	95.56	97.12	44.79	59.30
2	104.91	94.71	96.49	101.32	63.93	57.87
3	106.22	98.77	94.37	97.07	–	58.36
4	106.25	89.04	95.69	102.31	65.29	58.27
5	106.89	100.55	94.90	95.69	44.64	57.93
6	104.68	94.81	97.00	103.31	64.44	58.09
7	105.65	98.42	93.88	98.09	45.27	49.95
8	105.12	93.05	95.67	102.04	65.06	57.65
9	105.53	99.40	94.06	95.71	44.77	58.20
10	105.32	92.75	96.10	106.10	64.31	57.08
11	106.57	98.38	93.01	95.19	45.52	58.08
12	105.55	92.13	96.75	102.62	65.47	58.53
13	107.19	99.16	94.19	97.26	44.83	57.84
14	105.67	93.53	98.04	102.29	64.13	58.77
15	107.56	99.71	94.93	93.97	44.86	57.90
16	105.71	91.89	95.12	101.56	64.80	59.33
MEAN ODD	106.69	99.45	94.38	96.01	44.96	57.19
MEAN EVEN	105.39	92.74	96.11	102.69	64.65	58.20
MEAN ALL	106.04	96.09	95.23	99.35	55.46	57.70
SDEV ODD	0.95	1.01	0.79	1.14	0.32	2.97
SDEV EVEN	0.52	1.84	0.64	1.51	0.57	0.70
SDEV ALL	1.00	3.75	1.13	3.68	10.18	2.15
SMEN ODD	0.34	0.36	0.28	0.40	0.12	1.05
SMEN EVEN	0.18	0.65	0.23	0.53	0.20	0.25
SMEN ALL	0.25	0.94	0.28	0.92	2.63	0.54
CVAR ODD	0.90	1.01	0.84	1.19	0.71	5.18
CVAR EVEN	0.49	1.98	0.67	1.47	0.88	1.21
CVAR ALL	0.94	3.90	1.19	3.71	18.36	3.72

Table A-18. Lamp 110 for Test 9 in Radiance Units

CHANNEL	BAND					
	TM1	TM2	TM3	TM4	TM5	TM7
1	170.75	177.91	162.38	193.28	82.93	103.02
2	167.12	160.01	168.06	192.33	118.07	110.37
3	175.02	173.94	160.55	193.89	–	102.11
4	169.15	150.33	164.91	194.38	120.73	111.24
5	172.62	176.84	161.74	191.45	83.14	101.19
6	166.78	159.73	166.85	195.71	119.28	110.96
7	170.93	173.35	159.92	191.17	84.12	87.38
8	167.39	156.98	164.75	193.55	120.10	109.84
9	170.84	175.08	160.27	191.42	83.30	101.81
10	167.78	156.42	165.38	201.24	118.92	108.82
11	172.42	173.41	158.52	190.04	84.60	101.38
12	168.12	155.61	166.39	194.19	121.26	111.67
13	173.45	174.29	160.39	194.49	83.20	101.09
14	168.09	157.59	166.05	193.62	118.56	112.04
15	173.79	175.61	161.70	188.38	83.26	101.10
16	168.55	154.92	163.36	192.14	119.26	112.99
MEAN ODD	172.48	175.06	160.68	191.76	83.51	99.88
MEAN EVEN	167.87	156.45	165.34	194.65	119.52	110.99
MEAN ALL	170.18	165.75	163.01	193.21	102.71	105.44
SDEV ODD	1.57	1.66	1.24	2.06	0.62	5.09
SDEV EVEN	0.78	3.06	1.11	2.90	1.09	1.32
SDEV ALL	2.66	9.90	2.66	2.85	18.62	6.77
SMEN ODD	0.56	0.59	0.44	0.73	0.24	1.80
SMEN EVEN	0.28	1.08	0.39	1.03	0.39	0.47
SMEN ALL	0.67	2.47	0.66	0.71	4.81	1.69
CVAR ODD	0.91	0.95	0.77	1.07	0.75	5.10
CVAR EVEN	0.47	1.96	0.67	1.49	0.92	1.19
CVAR ALL	1.56	5.97	1.63	1.47	18.13	6.42

Table A-19. Lamp 010 for Test 9 in Radiance Units

CHANNEL	BAND					
	TM1	TM2	TM3	TM4	TM5	TM7
1	68.40	80.37	70.06	100.35	41.21	46.78
2	64.76	68.17	72.18	93.79	56.96	54.98
3	69.59	78.25	69.19	99.99	–	46.09
4	65.93	64.10	71.59	94.84	58.15	55.36
5	68.53	79.68	69.49	98.54	41.03	45.60
6	64.81	68.13	72.53	95.59	57.21	55.21
7	67.88	77.79	68.71	98.87	41.62	39.36
8	64.87	66.76	71.53	94.49	57.91	54.79
9	67.85	78.68	68.81	98.61	41.07	45.90
10	65.25	66.66	71.93	98.18	57.22	54.16
11	68.30	77.95	68.00	98.05	41.77	45.70
12	65.34	66.07	72.25	94.99	58.38	56.58
13	68.71	78.09	68.88	100.10	41.16	45.67
14	65.43	67.13	71.75	94.68	57.15	55.67
15	69.03	79.16	69.39	96.83	41.24	45.56
16	65.20	65.93	71.06	93.82	57.54	56.16
MEAN ODD	68.54	78.75	69.07	98.92	41.30	45.08
MEAN EVEN	65.20	66.62	71.86	95.06	57.57	55.24
MEAN ALL	66.87	72.68	70.46	96.98	49.98	50.16
SDEV ODD	0.59	0.92	0.62	1.20	0.28	2.36
SDEV EVEN	0.40	1.32	0.48	1.40	0.53	0.61
SDEV ALL	1.79	6.36	1.53	2.36	8.41	5.50
SMEN ODD	0.21	0.33	0.22	0.42	0.11	0.83
SMEN EVEN	0.14	0.47	0.17	0.50	0.19	0.22
SMEN ALL	0.45	1.59	0.38	0.59	2.17	1.38
CVAR ODD	0.86	1.17	0.90	1.21	0.68	5.21
CVAR EVEN	0.61	1.98	0.66	1.48	0.92	1.11
CVAR ALL	2.68	8.75	2.18	2.43	16.83	10.97

Table A-20. Lamp 011 for Test 9 in Radiance Units

CHANNEL	BAND					
	TM1	TM2	TM3	TM4	TM5	TM7
1	112.53	123.71	108.14	144.70	62.60	77.36
2	107.35	107.63	112.79	142.32	86.73	87.14
3	114.65	121.03	106.91	144.96	–	76.60
4	108.34	101.08	111.97	143.79	88.68	87.86
5	113.11	123.08	107.69	143.14	62.53	75.89
6	107.10	107.58	113.42	144.90	87.72	87.64
7	111.86	120.53	108.40	143.23	63.35	65.91
8	107.67	105.53	112.03	143.50	88.30	86.83
9	111.88	121.63	106.68	143.20	62.79	76.41
10	107.77	105.31	112.33	149.02	87.60	85.93
11	112.80	120.71	105.48	142.34	63.80	76.25
12	107.76	104.67	113.21	143.94	89.04	88.19
13	113.65	121.13	106.76	145.53	62.74	75.93
14	107.90	106.05	112.29	143.51	87.12	88.48
15	114.20	122.31	107.59	140.46	62.76	75.96
16	108.24	104.31	111.36	142.46	87.82	89.35
MEAN ODD	113.08	121.77	106.96	143.44	62.94	75.04
MEAN EVEN	107.77	105.27	112.43	144.18	87.87	87.68
MEAN ALL	110.42	113.52	109.69	143.81	76.24	81.36
SDEV ODD	1.03	1.16	0.85	1.64	0.47	3.72
SDEV EVEN	0.41	2.09	0.68	2.12	0.78	1.06
SDEV ALL	2.85	8.67	2.92	1.87	12.89	7.04
SMEN ODD	0.36	0.41	0.30	0.58	0.18	1.32
SMEN EVEN	0.15	0.74	0.24	0.75	0.28	0.38
SMEN ALL	0.71	2.17	0.73	0.47	3.33	1.76
CVAR ODD	0.91	0.96	0.79	1.14	0.75	4.96
CVAR EVEN	0.38	1.98	0.61	1.47	0.89	1.21
CVAR ALL	2.58	7.64	2.66	1.30	16.91	8.65

Table A-21. Lamp 111 for Test 9 in Radiance Units

CHANNEL	BAND					
	TM1	TM2	TM3	TM4	TM5	TM7
1	214.74	221.32	200.09	234.37	104.35	133.54
2	209.67	199.49	206.57	238.14	147.81	142.50
3	219.99	216.62	198.11	235.75	–	132.44
4	211.31	187.01	205.11	240.52	151.31	143.58
5	217.21	220.22	199.69	233.37	104.78	131.50
6	208.94	199.24	207.51	241.50	149.45	143.20
7	214.87	215.63	197.28	232.73	105.90	113.39
8	209.67	195.56	204.97	239.95	150.38	141.79
9	214.77	218.09	198.08	233.63	105.07	132.29
10	210.34	195.37	206.62	245.47	149.08	140.40
11	217.01	215.97	195.85	232.59	106.67	131.72
12	210.09	193.76	207.13	240.64	151.93	144.17
13	218.09	217.41	198.15	236.82	104.92	131.41
14	210.57	196.79	205.28	240.33	148.43	144.53
15	219.30	218.78	199.72	230.85	104.92	131.41
16	211.19	193.16	203.31	238.70	149.35	145.80
MEAN ODD	217.00	218.01	198.37	233.76	105.23	129.71
MEAN EVEN	210.22	195.06	205.69	240.68	149.71	143.25
MEAN ALL	213.61	206.53	202.03	237.21	128.95	136.48
SDEV ODD	2.08	2.02	1.43	1.89	0.79	6.64
SDEV EVEN	0.83	3.98	1.36	2.24	1.40	1.69
SDEV ALL	3.82	12.24	4.01	4.08	23.00	8.41
SMEN ODD	0.74	0.71	0.51	0.67	0.30	2.35
SMEN EVEN	0.30	1.41	0.48	0.79	0.50	0.60
SMEN ALL	0.95	3.06	1.00	1.02	5.94	2.10
CVAR ODD	0.96	0.93	0.72	0.81	0.75	5.12
CVAR EVEN	0.40	2.04	0.66	0.93	0.94	1.18
CVAR ALL	1.79	5.93	1.99	1.72	17.83	6.16

Table A-22. Lamp I01 for Test 9 in Radiance Units

CHANNEL	BAND					
	TM1	TM2	TM3	TM4	TM5	TM7
1	149.49	144.50	133.46	141.60	66.21	89.88
2	146.97	133.92	136.62	149.32	93.72	90.21
3	152.87	141.22	131.86	141.57	–	88.94
4	148.41	125.76	135.85	151.56	95.83	90.88
5	151.08	143.72	132.90	139.93	66.28	88.23
6	146.58	134.06	137.50	152.33	94.55	90.62
7	149.39	140.72	131.24	140.18	67.03	76.48
8	147.15	131.48	135.84	150.37	95.32	89.81
9	149.40	142.22	131.68	140.06	66.37	88.82
10	147.45	131.35	136.35	156.69	94.47	88.92
11	150.79	140.83	130.22	139.40	67.40	88.51
12	147.50	130.25	137.08	151.52	96.19	91.28
13	151.75	141.96	131.76	142.11	66.43	88.30
14	147.74	132.34	136.10	150.92	94.09	91.65
15	152.41	142.65	132.94	137.44	66.48	88.33
16	148.25	129.91	134.90	149.85	94.74	92.48
MEAN ODD	150.90	142.23	132.00	140.28	66.60	87.19
MEAN EVEN	147.51	131.13	136.28	151.57	94.86	90.73
MEAN ALL	149.20	136.68	134.14	145.93	81.67	88.96
SDEV ODD	1.38	1.35	1.05	1.51	0.45	4.36
SDEV EVEN	0.63	2.65	0.81	2.30	0.86	1.12
SDEV ALL	2.04	6.08	2.39	6.12	14.61	3.58
SMEN ODD	0.49	0.48	0.37	0.53	0.17	1.54
SMEN EVEN	0.22	0.94	0.29	0.81	0.30	0.40
SMEN ALL	0.51	1.52	0.60	1.53	3.77	0.89
CVAR ODD	0.92	0.95	0.79	1.08	0.68	5.00
CVAR EVEN	0.42	2.02	0.59	1.51	0.91	1.24
CVAR ALL	1.38	4.45	1.78	4.20	17.89	4.02

Table A-23. Lamp 001 for Test 9 in Radiance Units

CHANNEL	BAND					
	TM1	TM2	TM3	TM4	TM5	TM7
1	46.23	46.46	40.84	47.71	24.25	33.67
2	44.08	41.77	42.74	50.87	32.40	34.76
3	46.94	45.09	40.19	47.53	–	33.01
4	44.82	39.39	42.27	51.36	33.03	34.94
5	46.44	45.94	40.31	46.79	24.03	32.69
6	44.22	41.90	42.91	51.87	32.84	34.83
7	45.78	44.85	39.93	47.06	24.45	28.23
8	44.32	40.91	42.32	51.38	33.11	34.59
9	45.85	45.25	39.96	46.84	24.10	32.84
10	44.41	40.79	42.54	53.22	32.64	34.31
11	46.20	44.86	39.47	46.62	24.51	32.80
12	44.63	40.58	42.86	51.64	33.18	35.10
13	46.51	45.18	40.04	47.52	24.10	32.71
14	44.58	41.25	42.59	51.53	32.52	35.24
15	46.65	45.54	40.27	45.96	24.19	32.75
16	44.70	40.54	42.39	51.21	32.92	35.68
MEAN ODD	46.32	45.40	40.13	47.00	24.23	32.34
MEAN EVEN	44.47	40.89	42.58	51.63	32.83	34.93
MEAN ALL	45.40	43.14	41.36	49.32	28.82	33.63
SDEV ODD	0.39	0.57	0.40	0.59	0.18	1.69
SDEV EVEN	0.27	0.80	0.25	0.71	0.29	0.42
SDEV ALL	1.01	2.42	1.31	2.47	4.46	1.79
SMEN ODD	0.14	0.20	0.14	0.21	0.07	0.60
SMEN EVEN	0.09	0.28	0.09	0.25	0.10	0.15
SMEN ALL	0.25	0.61	0.33	0.62	1.15	0.45
CVAR ODD	0.85	1.25	0.99	1.25	0.76	5.23
CVAR EVEN	0.60	1.96	0.58	1.37	0.87	1.20
CVAR ALL	2.23	5.61	3.16	5.02	15.43	5.33

Table A-24. Lamp 000 for Test 9 in Radiance Units

CHANNEL	BAND					
	TM1	TM2	TM3	TM4	TM5	TM7
1	3.19	2.92	2.93	2.80	2.84	2.76
2	2.66	2.38	2.36	2.23	2.66	2.42
3	2.64	2.44	2.53	2.39	–	2.32
4	2.45	2.42	2.31	2.14	2.57	2.38
5	2.73	2.33	2.31	2.17	2.51	2.28
6	2.71	2.53	2.41	2.37	2.66	2.45
7	2.49	2.24	2.28	2.13	2.62	2.94
8	2.78	2.32	2.49	2.47	2.82	2.56
9	2.47	2.21	2.28	2.15	2.48	2.22
10	2.50	2.20	2.33	2.16	2.61	2.53
11	2.42	2.27	2.08	2.12	2.50	2.27
12	2.49	2.23	2.35	2.17	2.59	2.44
13	2.46	2.24	2.20	2.07	2.57	2.09
14	2.70	2.28	2.46	2.19	2.63	2.47
15	2.49	2.22	2.16	2.09	2.54	2.11
16	2.70	2.38	2.57	2.23	2.65	2.56
MEAN ODD	2.61	2.36	2.35	2.24	2.58	2.37
MEAN EVEN	2.62	2.34	2.41	2.25	2.65	2.48
MEAN ALL	2.62	2.35	2.38	2.24	2.62	2.42
SDEV ODD	0.28	0.24	0.27	0.25	0.12	0.31
SDEV EVEN	0.12	0.11	0.09	0.11	0.08	0.07
SDEV ALL	0.20	0.18	0.20	0.19	0.10	0.22
SMEN ODD	0.09	0.08	0.10	0.09	0.05	0.11
SMEN EVEN	0.04	0.04	0.03	0.04	0.03	0.02
SMEN ALL	0.05	0.04	0.05	0.05	0.03	0.06
CVAR ODD	9.86	10.12	11.51	10.98	4.81	12.97
CVAR EVEN	4.76	4.57	3.75	5.11	2.88	2.70
CVAR ALL	7.47	7.61	8.29	8.27	3.96	9.14

Table A-25. Lamp 100 for Test 9 in Radiance Units

CHANNEL	BAND					
	TM1	TM2	TM3	TM4	TM5	TM7
1	6.567	12.014	8.670	8.621	0.542	0.380
2	6.503	11.380	8.953	9.188	0.794	0.378
3	6.627	12.024	8.733	8.631	–	0.379
4	6.509	10.634	8.948	9.277	0.804	0.378
5	6.591	11.972	8.783	8.688	0.542	0.377
6	6.494	11.276	8.945	9.271	0.799	0.379
7	6.571	11.928	8.728	8.681	0.546	0.323
8	6.503	11.206	8.937	9.216	0.802	0.380
9	6.502	12.013	8.692	8.639	0.542	0.378
10	6.485	11.171	8.954	9.244	0.798	0.377
11	6.633	12.005	8.694	8.673	0.547	0.379
12	6.516	11.206	8.951	9.250	0.805	0.379
13	6.686	11.931	8.681	8.647	0.538	0.381
14	6.546	11.185	8.870	9.199	0.792	0.380
15	6.651	11.877	8.673	8.567	0.540	0.381
16	6.510	11.212	8.916	9.194	0.793	0.382
MEAN ODD	6.601	11.971	8.706	8.643	0.542	0.372
MEAN EVEN	6.508	11.159	8.934	9.230	0.798	0.379
MEAN ALL	6.555	11.565	8.820	8.937	0.679	0.376
SDEV ODD	0.054	0.053	0.039	0.039	0.003	0.020
SDEV EVEN	0.020	0.223	0.030	0.035	0.005	0.002
SDEV ALL	0.062	0.447	0.122	0.305	0.132	0.014
SMEN ODD	0.019	0.019	0.014	0.014	0.001	0.007
SMEN EVEN	0.007	0.079	0.010	0.013	0.002	0.001
SMEN ALL	0.015	0.112	0.031	0.076	0.034	0.004
CVAR ODD	0.825	0.444	0.450	0.453	0.593	5.417
CVAR EVEN	0.301	1.997	0.331	0.384	0.646	0.446
CVAR ALL	0.944	3.869	1.387	3.412	19.462	3.804

Table A-26. Lamp 110 for Test 9 in Radiance Units

CHANNEL	BAND					
	TM1	TM2	TM3	TM4	TM5	TM7
1	10.709	21.400	14.869	17.385	1.040	0.675
2	10.450	19.425	15.514	17.601	1.499	0.736
3	10.821	21.404	14.982	17.419	–	0.675
4	10.457	18.159	15.520	17.777	1.517	0.737
5	10.749	21.280	15.075	17.545	1.043	0.670
6	10.441	19.208	15.496	17.723	1.512	0.740
7	10.733	21.228	14.967	17.474	1.048	0.576
8	10.456	19.120	15.494	17.626	1.516	0.739
9	10.629	21.386	14.912	17.452	1.043	0.672
10	10.424	19.039	15.510	17.671	1.507	0.735
11	10.830	21.386	14.900	17.494	1.050	0.674
12	10.472	19.127	15.494	17.650	1.522	0.738
13	10.869	21.188	14.877	17.441	1.033	0.677
14	10.512	19.064	15.356	17.570	1.497	0.742
15	10.848	21.140	14.872	17.332	1.036	0.677
16	10.469	19.111	15.425	17.580	1.496	0.744
MEAN ODD	10.776	21.302	14.932	17.443	1.042	0.662
MEAN EVEN	10.460	19.030	15.476	17.647	1.508	0.739
MEAN ALL	10.618	20.166	15.204	17.545	1.291	0.700
SDEV ODD	0.086	0.106	0.073	0.065	0.006	0.035
SDEV EVEN	0.028	0.372	0.058	0.074	0.010	0.003
SDEV ALL	0.174	1.203	0.286	0.125	0.241	0.046
SMEN ODD	0.030	0.037	0.026	0.023	0.002	0.012
SMEN EVEN	0.010	0.132	0.020	0.026	0.004	0.001
SMEN ALL	0.044	0.301	0.072	0.031	0.062	0.012
CVAR ODD	0.796	0.497	0.486	0.371	0.584	5.278
CVAR EVEN	0.265	1.957	0.374	0.422	0.678	0.403
CVAR ALL	1.643	5.963	1.896	0.712	18.684	6.609

Table A-27. Lamp 010 for Test 9 in Radiance Units

CHANNEL	BAND					
	TM1	TM2	TM3	TM4	TM5	TM7
1	4.168	9.486	6.304	8.915	0.495	0.296
2	3.957	8.111	6.680	8.491	0.703	0.358
3	4.203	9.463	6.355	8.897	–	0.296
4	3.977	7.571	6.659	8.588	0.712	0.358
5	4.185	9.426	6.392	8.952	0.495	0.293
6	3.980	8.014	6.651	8.565	0.705	0.360
7	4.163	9.388	6.347	8.938	0.499	0.251
8	3.948	7.952	6.646	8.522	0.710	0.361
9	4.121	9.448	6.320	8.906	0.494	0.295
10	3.958	7.947	6.698	8.542	0.705	0.357
11	4.193	9.450	6.324	8.939	0.499	0.295
12	3.973	7.954	6.649	8.550	0.714	0.359
13	4.214	9.335	6.312	8.903	0.491	0.298
14	3.987	7.943	6.588	8.502	0.702	0.359
15	4.210	9.370	6.302	8.832	0.493	0.297
16	3.956	7.958	6.622	8.480	0.702	0.361
MEAN ODD	4.180	9.416	6.332	8.910	0.495	0.290
MEAN EVEN	3.966	7.931	6.643	8.530	0.707	0.359
MEAN ALL	4.073	8.673	6.487	8.720	0.608	0.325
SDEV ODD	0.032	0.051	0.032	0.038	0.003	0.016
SDEV EVEN	0.017	0.157	0.027	0.039	0.005	0.001
SDEV ALL	0.113	0.775	0.163	0.200	0.109	0.037
SMEN ODD	0.011	0.018	0.011	0.014	0.001	0.006
SMEN EVEN	0.006	0.056	0.010	0.014	0.002	0.000
SMEN ALL	0.028	0.194	0.041	0.050	0.028	0.009
CVAR ODD	0.764	0.547	0.502	0.430	0.597	5.481
CVAR EVEN	0.421	1.976	0.407	0.454	0.659	0.370
CVAR ALL	2.781	8.935	2.511	2.292	17.967	11.500

Table A-28. Lamp 111 for Test 9 in Radiance Units

CHANNEL	BAND					
	TM1	TM2	TM3	TM4	TM5	TM7
1	6.988	14.769	9.837	12.957	0.776	0.502
2	6.658	12.972	10.490	12.978	1.091	0.578
3	7.031	14.802	9.916	12.977	–	0.503
4	6.639	12.111	10.494	13.107	1.106	0.578
5	6.985	14.721	9.987	13.077	0.776	0.498
6	6.648	12.836	10.485	13.078	1.101	0.581
7	6.967	14.673	9.909	13.041	0.779	0.431
8	6.695	12.751	10.490	13.026	1.104	0.581
9	6.904	14.786	9.877	13.012	0.777	0.501
10	6.639	12.723	10.490	13.046	1.100	0.577
11	7.030	14.797	9.875	13.058	0.782	0.503
12	6.655	12.771	10.497	13.040	1.108	0.579
13	7.078	14.639	9.857	13.013	0.769	0.506
14	6.692	12.723	10.398	12.977	1.090	0.582
15	7.072	14.635	9.849	12.883	0.771	0.506
16	6.670	12.769	10.486	12.971	1.091	0.584
MEAN ODD	7.007	14.725	9.888	13.002	0.775	0.493
MEAN EVEN	6.658	12.707	10.476	13.027	1.099	0.580
MEAN ALL	6.833	13.716	10.182	13.015	0.948	0.537
SDEV ODD	0.058	0.069	0.049	0.063	0.006	0.025
SDEV EVEN	0.020	0.254	0.034	0.051	0.007	0.003
SDEV ALL	0.186	1.058	0.306	0.057	0.167	0.048
SMEN ODD	0.021	0.024	0.017	0.022	0.002	0.009
SMEN EVEN	0.007	0.090	0.012	0.018	0.003	0.001
SMEN ALL	0.046	0.264	0.077	0.014	0.043	0.012
CVAR ODD	0.830	0.468	0.496	0.483	0.597	5.167
CVAR EVEN	0.294	2.001	0.324	0.393	0.648	0.441
CVAR ALL	2.706	7.711	3.007	0.436	17.619	8.948

Table A-29. Lamp 101 for Test 9 in Radiance Units

CHANNEL	BAND					
	TM1	TM2	TM3	TM4	TM5	TM7
1	13.521	28.711	18.388	21.130	1.320	0.881
2	13.150	24.289	19.336	21.836	1.886	0.955
3	13.644	28.729	18.528	21.218	–	0.881
4	13.104	22.883	19.330	22.038	1.911	0.956
5	13.569	28.573	18.647	21.421	1.325	0.875
6	13.121	24.037	19.308	21.912	1.904	0.980
7	13.534	28.476	18.498	21.317	1.329	0.752
8	13.139	23.896	19.312	21.889	1.908	0.959
9	13.406	28.712	18.463	21.338	1.326	0.879
10	13.107	23.851	19.319	21.587	1.889	0.953
11	13.673	28.707	18.436	21.451	1.334	0.881
12	13.126	23.888	19.322	21.911	1.917	0.958
13	13.733	28.501	18.410	21.270	1.313	0.884
14	13.208	23.869	19.138	21.851	1.883	0.962
15	13.732	28.408	18.403	21.275	1.317	0.884
16	13.155	23.903	19.236	21.860	1.883	0.965
MEAN ODD	13.601	28.602	18.469	21.303	1.323	0.864
MEAN EVEN	13.139	23.799	19.289	21.881	1.898	0.958
MEAN ALL	13.370	26.201	18.879	21.592	1.630	0.911
SDEV ODD	0.115	0.127	0.088	0.104	0.007	0.046
SDEV EVEN	0.035	0.481	0.068	0.127	0.013	0.004
SDEV ALL	0.253	1.487	0.431	0.311	0.297	0.058
SMEN ODD	0.041	0.045	0.031	0.037	0.003	0.016
SMEN EVEN	0.012	0.170	0.024	0.045	0.005	0.001
SMEN ALL	0.083	0.372	0.108	0.078	0.077	0.014
CVAR ODD	0.846	0.478	0.475	0.488	0.561	5.294
CVAR EVEN	0.266	2.022	0.360	0.579	0.695	0.402
CVAR ALL	1.890	5.900	2.281	1.440	18.239	6.329

Table A-30. Lamp 001 for Test 9 in Radiance Units

CHANNEL	BAND					
	TM1	TM2	TM3	TM4	TM5	TM7
1	9.351	17.312	12.188	12.674	0.822	0.586
2	9.172	16.211	12.738	13.626	1.182	0.599
3	9.430	17.322	12.272	12.670	–	0.586
4	9.155	15.141	12.761	13.823	1.197	0.599
5	9.387	17.240	12.380	12.780	0.824	0.582
6	9.157	16.072	12.743	13.755	1.190	0.601
7	9.380	17.179	12.257	12.758	0.827	0.502
8	9.171	15.983	12.750	13.658	1.194	0.602
9	9.275	17.316	12.224	12.723	0.823	0.585
10	9.142	15.941	12.763	13.725	1.189	0.597
11	9.452	17.312	12.219	12.784	0.829	0.586
12	9.168	15.962	12.739	13.738	1.200	0.600
13	9.506	17.204	12.197	12.703	0.816	0.589
14	9.221	15.953	12.636	13.656	1.180	0.603
15	9.480	17.118	12.203	12.603	0.819	0.589
16	9.190	15.977	12.711	13.656	1.180	0.606
MEAN ODD	9.407	17.250	12.240	12.712	0.823	0.576
MEAN EVEN	9.172	15.902	12.730	13.704	1.189	0.601
MEAN ALL	9.289	16.576	12.485	13.208	1.018	0.588
SDEV ODD	0.079	0.078	0.068	0.063	0.004	0.030
SDEV EVEN	0.025	0.321	0.043	0.068	0.008	0.003
SDEV ALL	0.134	0.731	0.258	0.516	0.189	0.024
SMEN ODD	0.028	0.027	0.020	0.022	0.002	0.011
SMEN EVEN	0.009	0.113	0.015	0.024	0.003	0.001
SMEN ALL	0.033	0.183	0.084	0.129	0.049	0.008
CVAR ODD	0.840	0.441	0.470	0.494	0.526	5.197
CVAR EVEN	0.273	2.017	0.336	0.493	0.662	0.447
CVAR ALL	1.439	4.412	2.066	3.908	18.583	4.120

Table A-31. Lamp 000 for Test 9 in Radiance Units

CHANNEL	BAND					
	TM1	TM2	TM3	TM4	TM5	TM7
1	2.751	5.318	3.582	4.117	0.274	0.207
2	2.643	4.858	3.883	4.524	0.383	0.221
3	2.781	5.325	3.617	4.138	–	0.207
4	2.652	4.536	3.875	4.574	0.388	0.220
5	2.768	5.309	3.646	4.165	0.274	0.208
6	2.651	4.810	3.873	4.566	0.388	0.221
7	2.754	5.279	3.627	4.146	0.277	0.176
8	2.644	4.753	3.874	4.580	0.388	0.222
9	2.731	5.307	3.610	4.140	0.274	0.208
10	2.645	4.751	3.885	4.580	0.385	0.220
11	2.784	5.313	3.622	4.157	0.276	0.207
12	2.683	4.770	3.887	4.573	0.390	0.220
13	2.800	5.281	3.613	4.147	0.271	0.209
14	2.674	4.763	3.847	4.547	0.383	0.221
15	2.792	5.287	3.597	4.109	0.272	0.209
16	2.687	4.776	3.887	4.545	0.385	0.223
MEAN ODD	2.770	5.300	3.615	4.140	0.274	0.204
MEAN EVEN	2.656	4.752	3.876	4.556	0.386	0.221
MEAN ALL	2.713	5.026	3.746	4.348	0.334	0.212
SDEV ODD	0.024	0.022	0.017	0.020	0.002	0.011
SDEV EVEN	0.012	0.095	0.014	0.017	0.003	0.001
SDEV ALL	0.062	0.291	0.136	0.216	0.058	0.012
SMEN ODD	0.008	0.008	0.006	0.007	0.001	0.004
SMEN EVEN	0.004	0.033	0.005	0.006	0.001	0.000
SMEN ALL	0.016	0.073	0.034	0.054	0.015	0.003
CVAR ODD	0.858	0.423	0.483	0.479	0.817	5.584
CVAR EVEN	0.448	1.991	0.369	0.378	0.656	0.450
CVAR ALL	2.296	5.780	3.624	4.963	17.435	5.606

Table A-32. Lamp 100 for Test 9 in Radiance Units

CHANNEL	BAND					
	TM1	TM2	TM3	TM4	TM5	TM7
1	0.000	−0.009	0.075	0.024	−0.008	−0.001
2	0.017	0.004	0.073	0.027	−0.004	0.000
3	−0.000	0.003	0.080	0.039	–	−0.000
4	−0.009	−0.003	0.081	0.029	−0.004	−0.000
5	0.004	−0.012	0.088	0.039	−0.008	0.000
6	0.013	−0.001	0.074	0.038	−0.005	0.000
7	−0.006	−0.010	0.069	−0.008	−0.005	0.004
8	0.007	−0.024	0.083	0.085	−0.004	0.001
9	−0.011	−0.022	0.070	0.024	−0.007	−0.001
10	−0.001	−0.018	0.080	0.038	−0.004	0.001
11	−0.007	−0.012	0.080	0.018	−0.007	−0.000
12	−0.001	−0.013	0.080	0.035	−0.004	−0.000
13	−0.007	−0.010	0.071	0.036	−0.007	−0.000
14	0.017	−0.024	0.075	0.025	−0.004	−0.001
15	−0.006	−0.020	0.069	0.037	−0.008	−0.000
16	0.021	−0.008	0.089	0.022	−0.004	−0.000
MEAN ODD	−0.004	−0.011	0.069	0.026	−0.007	0.000
MEAN EVEN	0.008	−0.011	0.081	0.035	−0.004	0.000
MEAN ALL	0.002	−0.011	0.075	0.031	−0.006	0.000
SDEV ODD	0.005	0.008	0.007	0.016	0.001	0.002
SDEV EVEN	0.010	0.011	0.007	0.014	0.000	0.001
SDEV ALL	0.010	0.009	0.009	0.015	0.001	0.001
SMEN ODD	0.002	0.003	0.003	0.006	0.000	0.001
SMEN EVEN	0.004	0.004	0.002	0.005	0.000	0.000
SMEN ALL	0.003	0.002	0.002	0.004	0.000	0.000
CVAR ODD	−119.580	−67.327	10.356	61.327	−14.551	1148.270
CVAR EVEN	125.825	−97.003	8.656	38.706	−9.390	6349.908
CVAR ALL	477.553	−80.049	12.152	49.228	−27.988	1590.829

Table A-33. Lamp 100 Ratio of Digital Counts, Ambient to Vacuum

CHANNEL	BAND					
	TM1	TM2	TM3	TM4	TM5	TM7
1	1.01658	1.01319	0.95217	0.94851	1.05498	1.03020
2	0.99891	0.98138	0.95280	0.95502	1.06486	0.98692
3	1.01429	1.01356	0.95056	0.95506	–	1.01677
4	1.00286	–	0.95438	0.95154	1.04038	0.97919
5	1.00988	1.01155	0.94975	0.95417	1.02633	1.01786
6	0.99815	0.97664	0.95723	0.95062	1.03835	0.97861
7	1.01287	1.01058	0.95420	0.95127	1.01713	1.16935
8	0.99688	0.98043	0.95728	0.95283	1.03328	0.97890
9	1.00817	1.01081	0.95456	0.95993	1.02412	1.01701
10	0.99972	0.97540	0.95880	0.95297	1.03472	0.98906
11	1.01187	1.01160	0.95724	0.95450	1.01267	1.01372
12	1.00066	0.97851	0.95894	0.95790	1.02403	0.98808
13	1.00849	1.01223	0.95314	0.95431	1.02320	1.00902
14	0.99900	0.97796	0.95335	0.95692	1.03637	0.98829
15	1.01250	1.00646	0.95442	0.95604	1.03973	1.02740
16	0.99293	0.98113	0.96022	0.95096	1.05655	1.00628
MEAN ODD	1.01183	1.01125	0.95325	0.95422	1.02831	1.03767
MEAN EVEN	0.99864	0.97878	0.95663	0.95358	1.04107	0.98692
MEAN ALL	1.00523	0.99610	0.95494	0.95390	1.03511	1.01229
SDEV ODD	0.00276	0.00209	0.00250	0.00340	0.01448	0.05365
SDEV EVEN	0.00295	0.00252	0.00286	0.00288	0.01323	0.00909
SDEV ALL	0.00741	0.01691	0.00313	0.00306	0.01484	0.04549
SMEN ODD	0.00098	0.00074	0.00089	0.00120	0.00547	0.01897
SMEN EVEN	0.00104	0.00095	0.00101	0.00102	0.00468	0.00322
SMEN ALL	0.00185	0.00437	0.00078	0.00076	0.00383	0.01137
CVAR ODD	0.27298	0.20648	0.26262	0.35663	1.40807	5.17062
CVAR EVEN	0.29569	0.25761	0.29887	0.30231	1.27044	0.92144
CVAR ALL	0.73730	1.69728	0.32767	0.32049	1.43346	4.49350

Table A-34. Lamp 110 Ratio of Digital Counts, Ambient to Vacuum

CHANNEL		BAND					
		TM1	TM2	TM3	TM4	TM5	TM7
1		1.02181	1.01521	0.95905	0.95638	1.05584	1.03098
2		1.01130	0.98356	0.96616	0.94348	1.06257	0.99919
3		1.02064	1.01757	0.95965	0.95708	–	1.01798
4		1.00578	–	0.96857	0.93775	1.04052	0.99294
5		1.01770	1.01498	0.95701	0.95640	1.03167	1.02275
6		1.00828	0.97802	0.97037	0.93946	1.03771	0.99199
7		1.01708	1.01551	0.96235	0.95862	1.02454	1.17889
8		1.00339	0.98126	0.97097	0.94274	1.03449	0.99515
9		1.01657	1.01406	0.96497	0.96170	1.02831	1.02042
10		1.00744	0.97841	0.97284	0.94128	1.03588	1.00240
11		1.01525	1.01496	0.96590	0.95838	1.01928	1.01835
12		1.00484	0.97943	0.97234	0.94569	1.02230	1.00057
13		1.01406	1.01422	0.96279	0.95700	1.03230	1.01459
14		1.00623	0.98086	0.96827	0.94620	1.03630	0.99926
15		1.01885	1.01155	0.96202	0.95811	1.04489	1.02706
16		1.00217	0.98443	0.97392	0.94150	1.05245	1.01308
MEAN	ODD	1.01774	1.01476	0.96172	0.95796	1.03383	1.04138
MEAN	EVEN	1.00618	0.98085	0.97043	0.94226	1.04028	0.99932
MEAN	ALL	1.01196	0.99894	0.96607	0.95011	1.03727	1.02035
SDEV	ODD	0.00250	0.00157	0.00313	0.00188	0.01251	0.05581
SDEV	EVEN	0.00279	0.00261	0.00281	0.00295	0.01220	0.00671
SDEV	ALL	0.00646	0.01762	0.00533	0.00844	0.01235	0.04413
SMEN	ODD	0.00089	0.00055	0.00111	0.00067	0.00473	0.01973
SMEN	EVEN	0.00099	0.00099	0.00099	0.00104	0.00431	0.00237
SMEN	ALL	0.00161	0.00456	0.00133	0.00211	0.00319	0.01103
CVAR	ODD	0.24598	0.15432	0.32566	0.19647	1.20968	5.35921
CVAR	EVEN	0.27696	0.26654	0.28967	0.31338	1.17250	0.67097
CVAR	ALL	0.63818	1.76433	0.55182	0.88816	1.19088	4.32450

Table A-35. Lamp 010 Ratio of Digital Counts, Ambient to Vacuum

CHANNEL	BAND					
	TM1	TM2	TM3	TM4	TM5	TM7
1	1.02984	1.01281	0.97439	0.96220	1.05929	1.04378
2	1.01289	0.97744	0.98236	0.93687	1.06283	1.01786
3	1.02859	1.01290	0.97040	0.96218	–	1.02734
4	1.01947	–	0.98572	0.92774	1.03820	1.00969
5	1.02917	1.00820	0.96920	0.96209	1.03053	1.03032
6	1.01280	0.97268	0.98658	0.93102	1.03939	1.01143
7	1.02643	1.01132	0.97386	0.96507	1.02184	1.19092
8	1.01580	0.97819	0.98785	0.93395	1.02917	1.01042
9	1.02379	1.00890	0.97422	0.96988	1.03030	1.02573
10	1.01270	0.97058	0.98687	0.93037	1.03277	0.01936
11	1.02875	1.00960	0.97726	0.96422	1.01934	1.02559
12	1.02094	0.97527	0.98716	0.93428	1.01840	1.01650
13	1.02946	1.00671	0.97327	0.96471	1.03044	1.01828
14	1.01148	0.97344	0.98325	0.93373	1.03000	1.01774
15	1.02734	1.00352	0.97249	0.96745	1.04607	1.04034
16	1.00908	0.97398	0.99083	0.93356	1.05218	1.03322
MEAN ODD	1.02790	1.00899	0.97313	0.96472	1.03397	1.05029
MEAN EVEN	1.01439	0.97451	0.98633	0.93256	1.03787	1.01702
MEAN ALL	1.02114	0.99290	0.97973	0.94864	1.03605	1.03366
SDEV ODD	0.00188	0.00320	0.00[illegible]58	0.00293	0.01406	0.05742
SDEV EVEN	0.00399	0.00276	0.00281	0.00276	0.01399	0.00752
SDEV ALL	0.00768	0.01804	0.00728	0.01683	0.01366	0.04312
SMEN ODD	0.00067	0.00113	0.00090	0.00104	0.00531	0.02030
SMEN EVEN	0.00141	0.00104	0.00099	0.00098	0.00496	0.00266
SMEN ALL	0.00192	0.00466	0.00182	0.00421	0.00352	0.01078
CVAR ODD	0.18310	0.31681	0.26278	0.30368	1.35941	5.46680
CVAR EVEN	0.39358	0.28344	0.28500	0.29619	1.34815	0.73934
CVAR ALL	0.75221	1.81699	0.74280	1.77429	1.31769	4.17183

Table A-36. Lamp 011 Ratio of Digital Counts, Ambient to Vacuum

CHANNEL	BAND					
	TM1	TM2	TM3	TM4	TM5	TM7
1	1.02977	1.02882	0.97689	0.97238	1.06329	1.04383
2	1.01955	0.98929	0.98488	0.94922	1.06562	1.02023
3	1.03001	1.02570	0.97549	0.97282	–	1.02983
4	1.01586	–	0.98806	0.94495	1.04082	1.01240
5	1.02748	1.02447	0.97329	0.97078	1.03724	1.03323
6	1.02039	0.98555	0.99030	0.94643	1.03825	1.01146
7	1.03136	1.02420	0.97954	0.97380	1.02769	1.18496
8	1.01202	0.98863	0.98932	0.94818	1.03521	1.01299
9	1.02880	1.02405	0.98120	0.97929	1.03421	1.03203
10	1.01468	0.98272	0.99212	0.94642	1.03520	1.02239
11	1.03249	1.02314	0.98297	0.97234	1.02248	1.02663
12	1.01557	0.98583	0.99005	0.95086	1.02372	1.02081
13	1.02865	1.02193	0.97818	0.97422	1.03524	1.02543
14	1.01674	0.98513	0.98850	0.95110	1.03885	1.01765
15	1.02785	1.01945	0.97874	0.97744	1.05288	1.03911
16	1.01139	0.98643	0.99112	0.94629	1.05528	1.03365
MEAN ODD	1.02930	1.02372	0.97829	0.97413	1.03900	1.05188
MEAN EVEN	1.01577	0.98622	0.98904	0.94791	1.04162	1.01895
MEAN ALL	1.02254	1.00822	0.98366	0.96102	1.04040	1.03541
SDEV ODD	0.00192	0.00221	0.00318	0.00284	0.01426	0.05412
SDEV EVEN	0.00313	0.00236	0.00256	0.00236	0.01299	0.00724
SDEV ALL	0.00755	0.01949	0.00821	0.01378	0.01316	0.04101
SMEN ODD	0.00068	0.00078	0.00112	0.00100	0.00539	0.01913
SMEN EVEN	0.00111	0.00089	0.00090	0.00084	0.00459	0.00256
SMEN ALL	0.00189	0.00503	0.00155	0.00344	0.00340	0.01025
CVAR ODD	0.18633	0.21633	0.32456	0.29104	1.37281	5.14487
CVAR EVEN	0.30833	0.23916	0.25856	0.24933	1.24732	0.71077
CVAR ALL	0.73812	1.93888	0.83154	1.43373	1.26530	3.96038

Table A-37. Lamp 111 Ratio of Digital Counts, Ambient to Vacuum

CHANNEL	BAND					
	TM1	TM2	TM3	TM4	TM5	TM7
1	1.02255	1.01834	0.98242	0.96637	1.05149	1.02832
2	1.00817	0.98446	0.98891	0.95610	1.08044	0.99763
3	1.01982	1.01928	0.98123	0.96683	–	1.01958
4	1.01430	–	0.96610	0.95091	1.03912	0.99588
5	1.01787	1.01691	0.95898	0.96453	1.02746	1.02279
6	1.00881	0.97868	0.97143	0.95519	1.03698	0.99504
7	1.01999	1.01846	0.98495	0.96687	1.02137	1.17989
8	1.00524	0.98399	0.96997	0.95537	1.03263	0.99787
9	1.01701	1.01566	0.98481	0.97079	1.02376	1.02061
10	1.00881	0.97852	0.97477	0.96484	1.03440	1.00578
11	1.01809	1.01671	0.96772	0.96343	1.01550	1.01949
12	1.01350	0.98323	0.97233	0.95865	1.02236	1.00283
13	1.01658	1.01550	0.98485	0.96837	1.02798	1.01495
14	1.00731	0.98061	0.96968	0.95694	1.03653	1.00229
15	1.01810	1.01254	0.98460	0.96507	1.03722	1.02607
16	1.00148	0.98509	0.97519	0.95147	1.04985	1.01358
MEAN ODD	1.01876	1.01687	0.98370	0.96653	1.02926	1.04143
MEAN EVEN	1.00843	0.98208	0.97106	0.95617	1.03891	1.00136
MEAN ALL	1.01360	1.00053	0.96737	0.96135	1.03440	1.02139
SDEV ODD	0.00185	0.00199	0.00284	0.00233	0.01185	0.05602
SDEV EVEN	0.00413	0.00287	0.00311	0.00443	0.01153	0.00621
SDEV ALL	0.00630	0.01801	0.00475	0.00634	0.01226	0.04372
SMEN ODD	0.00065	0.00070	0.00100	0.00083	0.00448	0.01980
SMEN EVEN	0.00146	0.00109	0.00110	0.00157	0.00407	0.00220
SMEN ALL	0.00157	0.00465	0.00119	0.00158	0.00317	0.01093
CVAR ODD	0.18115	0.19651	0.29420	0.24153	1.15102	5.37872
CVAR EVEN	0.40922	0.29274	0.32029	0.46323	1.10837	0.62009
CVAR ALL	0.62142	1.80049	0.49111	0.65937	1.18562	4.28040

Table A-38. Lamp 101 Ratio of Digital Counts, Ambient to Vacuum

CHANNEL	BAND					
	TM1	TM2	TM3	TM4	TM5	TM7
1	1.02384	1.02580	0.96283	0.95966	1.05394	1.02811
2	1.01172	0.98391	0.96865	0.96235	1.06773	0.99547
3	1.02477	1.02783	0.96250	0.96179	–	1.01640
4	1.01183	–	0.96769	0.95278	1.04352	0.98855
5	1.02037	1.02564	0.96032	0.96156	1.02955	1.01824
6	1.01134	0.98595	0.97037	0.95535	1.04190	0.98852
7	1.02063	1.02840	0.96892	0.96253	1.02280	1.17014
8	1.00536	0.99171	0.96891	0.96066	1.03705	0.99000
9	1.01882	1.02808	0.96865	0.95792	1.02844	1.01654
10	1.00992	0.98844	0.97325	0.95861	1.03779	1.00018
11	1.02121	1.02549	0.96869	0.96319	1.01749	1.01586
12	1.01025	0.98917	0.97304	0.96020	1.02678	0.99693
13	1.01870	1.02591	0.96740	0.96395	1.02783	1.01208
14	1.00966	0.98854	0.96876	0.96155	1.04103	0.99555
15	1.02236	1.02237	0.96865	0.96557	1.04205	1.02630
16	1.00491	0.98328	0.97309	0.95948	1.05777	1.01192
MEAN ODD	1.02135	1.02570	0.96552	0.96327	1.03130	1.03796
MEAN EVEN	1.00940	0.98957	0.97024	0.95875	1.04420	0.99569
MEAN ALL	1.01537	1.00884	0.96788	0.96101	1.03818	1.01682
SDEV ODD	0.00212	0.00143	0.00340	0.00264	0.01246	0.05368
SDEV EVEN	0.00269	0.00357	0.00266	0.00332	0.01280	0.00776
SDEV ALL	0.00677	0.01882	0.00383	0.00373	0.01389	0.04296
SMEN ODD	0.00075	0.00051	0.00120	0.00093	0.00471	0.01898
SMEN EVEN	0.00095	0.00136	0.00094	0.00117	0.00452	0.00274
SMEN ALL	0.00169	0.00486	0.00096	0.00093	0.00369	0.01074
CVAR ODD	0.20760	0.13937	0.35245	0.27386	1.20833	5.17174
CVAR EVEN	0.26621	0.36036	0.27433	0.34649	1.22552	0.77920
CVAR ALL	0.66634	1.86596	0.39596	0.38828	1.33786	4.22420

Table A-39. Lamp 001 Ratio of Digital Counts, Ambient to Vacuum

CHANNEL	BAND					
	TM1	TM2	TM3	TM4	TM5	TM7
1	1.05146	1.04451	0.99800	0.99148	1.06109	1.03827
2	1.02959	1.00639	0.99150	0.97656	1.07448	1.01892
3	1.04968	1.04698	0.99141	0.99238	–	1.02372
4	1.04080	–	0.99689	0.97282	1.04821	1.01057
5	1.04364	1.04214	0.99154	0.99065	1.02835	1.02383
6	1.02951	1.00013	1.00048	0.97432	1.04336	1.01193
7	1.05134	1.04547	0.99314	0.99457	1.01993	1.18282
8	1.03333	1.01094	0.99906	0.97431	1.03743	1.01379
9	1.04255	1.04413	0.99406	0.99887	1.02633	1.02681
10	1.03431	1.00274	1.00180	0.97279	1.03803	1.02232
11	1.04690	1.04614	0.99828	0.99330	1.01318	1.02414
12	1.03961	1.00589	0.99754	0.97925	1.03199	1.01908
13	1.04438	1.04390	0.99415	0.99640	1.03189	1.01466
14	1.03020	1.00346	0.99696	0.97897	1.04545	1.02254
15	1.04877	1.04043	0.99884	0.99872	1.04440	1.03442
16	1.02039	1.01069	0.99824	0.97401	1.06214	1.03743
MEAN ODD	1.04734	1.04421	0.99468	0.99455	1.03217	1.04608
MEAN EVEN	1.03222	1.00578	0.99781	0.97563	1.04763	1.01959
MEAN ALL	1.03978	1.02627	0.99624	0.98509	1.04042	1.03284
SDEV ODD	0.00346	0.00199	0.00295	0.00326	0.01604	0.05571
SDEV EVEN	0.00646	0.00407	0.00326	0.00286	0.01410	0.00850
SDEV ALL	0.00936	0.02007	0.00339	0.01020	0.01651	0.04087
SMEN ODD	0.00122	0.00070	0.00104	0.00115	0.00606	0.01970
SMEN EVEN	0.00228	0.00154	0.00115	0.00101	0.00498	0.00300
SMEN ALL	0.00234	0.00518	0.00085	0.00255	0.00426	0.01022
CVAR ODD	0.33080	0.19035	0.29686	0.32777	1.55416	5.32574
CVAR EVEN	0.62562	0.40424	0.32670	0.29305	1.34576	0.83342
CVAR ALL	0.89954	1.95558	0.34051	1.03594	1.58657	3.95704

Table A-40. Lamp 000 Ratio of Digital Counts, Ambient to Vacuum

CHANNEL	BAND					
	TM1	TM2	TM3	TM4	TM5	TM7
1	0.84874	0.91923	0.88045	0.96452	1.02899	1.03086
2	0.82790	0.93593	0.93088	0.98516	0.96443	0.98961
3	0.88800	0.93815	0.94493	0.97528	–	1.01958
4	0.68905	–	1.00238	1.03837	0.99856	1.01477
5	0.86007	0.93683	0.93514	0.95015	1.06775	0.98033
6	0.83347	0.89097	0.92072	0.95662	1.02787	0.99853
7	0.91708	0.93409	0.94489	0.98833	1.00852	0.89978
8	0.77547	0.94852	0.96031	0.94695	1.00804	0.93608
9	0.94653	0.95327	0.96037	0.95465	1.04489	1.04369
10	0.74076	0.95858	0.91749	0.94547	0.99882	0.97597
11	0.92982	0.95312	0.98323	0.98037	1.05126	1.00525
12	0.86705	0.94242	0.90272	0.92591	0.99784	0.95587
13	0.89245	0.94876	0.91475	0.98278	1.04554	1.01587
14	0.80438	0.94893	0.91328	0.93833	0.98298	1.02037
15	0.88726	0.94791	0.92152	0.97628	1.10142	1.01589
16	0.83299	0.94940	0.87937	0.91275	0.99882	0.97583
MEAN ODD	0.89599	0.93767	0.93816	0.96767	1.04948	0.99517
MEAN EVEN	0.77139	0.93856	0.92839	0.95719	0.99592	0.95463
MEAN ALL	0.83369	0.93814	0.93328	0.96243	1.02092	0.98990
SDEV ODD	0.03350	0.01647	0.03100	0.01106	0.02982	0.05622
SDEV EVEN	0.08806	0.02200	0.03774	0.04083	0.01853	0.02744
SDEV ALL	0.08186	0.01853	0.03374	0.02939	0.03630	0.04306
SMEN ODD	0.01184	0.00582	0.01096	0.00391	0.01127	0.01988
SMEN EVEN	0.02336	0.00831	0.01334	0.01443	0.00655	0.00970
SMEN ALL	0.02046	0.00478	0.00844	0.00735	0.00937	0.01077
CVAR ODD	3.73879	1.75689	3.30486	1.14304	2.84126	5.64935
CVAR EVEN	8.56443	2.34332	4.06499	4.26516	1.86012	2.78898
CVAR ALL	9.81898	1.97488	3.61549	3.05395	3.55556	4.35184

REFERENCES

Barker, J. L., R. B. Abrams, D. L. Ball, and K. C. Leung, "Radiometric Calibration and Processing Procedures" (paper presented at Landsat-4 Scientific Characterization Early Results Symposium, Goddard Space Flight Center, Greenbelt, Maryland, 1983a)

--, "Characterization of Radiometric Calibration of Landsat-4 TM Reflective Bands" (paper presented at Landsat-4 Scientific Characterization Early Results Symposium, Goddard Space Flight Center, Greenbelt, Maryland, 1983b)

--, D. L. Ball, and K. C. Leung, "TM/PF Engineering Data Evaluation: Prelaunch Absolute Calibration, "NASA/GSFC Technical Memorandum, in preparation, 1983c

--, D. L. Ball, and K. C. Leung, "TM/PF Engineering Data Evaluation: Transfer of the Prelaunch Absolute Calibration to the Internal Calibrator," NASA/GSFC Technical Memorandum, in preparation, 1983d

Campbell, J. C., "Preliminary Radiometric Tests To Determine a Technique for Calibration of NASA's 48-inch Diameter Spherical Integrating Source," Santa Barbara Research Center, HS236-6926, 1980

Clemann, D., J. Lansing, and C. Rodil, "Protoflight Radiance-Temperature Study," Santa Barbara Research Center, HS236-8076, 1982

Duck, K. I., "Revised Thematic Mapper Radiometric Assessment," National Aeronautics and Space Administration/Goddard Space Flight Center (NASA/GSFC) Internal Memorandum, 1977

Engel, J. C., "Thematic Mapper: An Interim Report on Anticipated Performance," Proceedings of AIAA Sensor Systems for the 80's Conference, 1980

Fraser, R. S., "Radiances for Thematic Mapper," NASA/GSFC Internal Memorandum, 1975

Lansing, J. C., "Test Requirement Changes: AC02, BL07, SRT, "Santa Barbara Research Center, HS236-7708, 1981

--, and J. L. Barker, "Thermal Band Characterization of Landsat-4 Thematic Mapper" (paper presented at Landsat-4 Scientific Characterization Early Results Symposium, Goddard Space Flight Center, Greenbelt, Maryland, February 1983)

Osgood, R. L., and J. C. Lansing, "TM AC02R Test Result Summary, Protoflight Model," Santa Barbara Research Center, HS236-7552, 1981

Walker, J. A., "Comparisons of 48SIS Calibrations--NASA and SBRC," Santa Barbara Research Center, HS236-8160, 1982a

--, "48 SIS Calibration Data for GE Post T.V. Test Configuration," Santa Barbara Research Center, HS236-7995, 1982b

--, "Calibration Results of Secondary Standards of Irradiance SS13 and SS14, "Santa Barbara Research Center, NS236-8161, 1982c

Young, J. B., "Apparent PFM Radioactive Calibration Changes at General Electric," Santa Barbara Research Center, HS236-7881, 1982

N85-20516

CHARACTERIZATION OF RADIOMETRIC CALIBRATION OF LANDSAT-4 TM REFLECTIVE BANDS

J. L. Barker

National Aeronautics and Space Administration
Goddard Space Flight Center
Greenbelt, Maryland 20771

R. B. Abrams, D. L. Ball, and K. C. Leung

Computer Sciences Corporation
8728 Colesville Road
Silver Spring, Maryland 20910

ABSTRACT

Absolute radiometric calibration of known accuracy is important for several applications of Landsat-4 Thematic Mapper (TM) data. This paper examines prelaunch and postlaunch internal calibrator, image, and background data to characterize the radiometric performance of the Landsat-4 TM and to recommend improved procedures for radiometric calibration. All but two channels (band 2, channel 4; band 5, channel 3) have behaved normally. Gain changes relative to a postlaunch reference (scene ID 40109-15140) for channels within a band vary within 0.5 percent as a group. The primary focal plane channels show an initial decrease in gain of 6 percent in bands 1 and 2, 8 percent in band 3, and 3 percent in band 4 during the first 70 days following launch, and thereafter show gain changes of 1 percent or less. Instrument gain for channels in the cold focal plane oscillates. In band 5, the maximum peak-to-peak amplitude is 7 percent and the frequency is approximately 55 days, while in band 7 the amplitude is 5 percent and the frequency is 75 days. Noise in background and image data ranges from 0.5 to 1.7 counts. Average differences in forward and reverse image data indicate a need for separate calibration processing of forward and reverse scans. Precision is improved by increasing the pulse integration width from 31 to 41 minor frames, depending on the band.

KEYWORDS: radiometric performance, internal calibrator stability, channel precision, channel stability, noise, parametric adjustments in calibration, Thematic Mapper, and Landsat-4.

PAGE II-372 INTENTIONALLY BLANK

PRECEDING PAGE BLANK NOT FILMED

CONTENTS

Introduction II-375

Analysis of Radiometric Performance II-376
    Stability of the IC System II-376
    Prelaunch Sensor Performance II-377
    Postlaunch Sensor Performance II-384
    Stability With Time II-388
    Noise II-386
    Other Factors Affecting Data Quality II-396
        Location of Calibration Collect Window II-396
        Acquisition II-401
        Nonuniformity in the A/D Converter II-404

Possible Adjustments to Radiometric Calibration Procedures II-404
    Pulse Integration II-404
    Pulse Averaging II-408
    Calibration II-408
    Net Image II-416
    Separate Processing for Forward and Reverse Scans II-422

Conclusions II-432

Recommendations II-433
    Ground Segment Processing System II-433
    Ground Segment Data Analysis II-433
    Software II-434
    Flight Segment Operations II-435
        Scrounge Era II-435
        TIPS Era II-435

Acknowledgment II-435

References II-435

Appendix - Supplemental Data II-437

INTRODUCTION

Scientists concerned with relating ground-measured variables and atmospheric characteristics to measurements of spectral radiance from satellites need absolute radiometric values for Thematic Mapper (TM) Landsat-4 data. Absolute radiometric calibrations of known accuracy are essential to understand and characterize the physical properties and interactions causing radiance variations, to test theoretical models, to perform arithmetic spectral transforms such as those used to determine within-scene atmospheric corrections, and to compare TM data with laboratory and field observations. Furthermore, image applications in areas such as forestry and geology are aided by knowledge of absolute radiance. Such knowledge would lead to an understanding of the innate bidirectional reflectance properties of the target. With absolute radiance values, signatures could be extended between scenes. With absolute radiance values, monitoring and modeling studies could use data covering the same area but collected by instruments on different satellites. This paper characterizes the radiometric performance of the TM.

The emphasis of this paper is on postlaunch radiometric characterization of the Landsat-4 TM sensor system, especially the precision of the internal calibration (IC) system and its variation with time. Only data for the reflective bands are presented here. Lansing and Barker (1984) discuss procedures and results for the thermal band. A description of the TM calibration subsystem and the prelaunch and postlaunch radiometric calibration procedures in Barker, Abrams, et al., 1984, provides background to this paper. Absolute sensitivities and offsets for each of the TM reflective band channels and spectral radiances for the IC states are presented in Barker, Ball, et al., 1984, which describes the results of the prelaunch absolute radiometric calibration. TM digital image products are described and characterized in Barker, Gunther, et al., 1984.

Several methods of calibrating TM sensor data are available (Barker, 1984). If the sensor channels are more stable with time than the IC system, prelaunch nominal gains and offsets can be used directly. Alternatively, the IC system can be used to determine gains and offsets. In either case, gains and offsets for channels in a band can be modified by histogram normalization. This paper provides insight as to the best calibration procedure to use.

ANALYSIS OF RADIOMETRIC PERFORMANCE

STABILITY OF THE IC SYSTEM

The separation of IC system stability from channel stability ordinarily requires the observation of a known external source, such as the Sun or Moon. Because the TM does not have access to such an external source, another approach must be used. One possibility in evaluating the stability of the IC system involves comparison of the normalized changes in the band-averaged channel response to the single-lamp IC states (100, 010, and 001[1]). The normalized change in digital counts, NC, is calculated for each combination of single lamp IC state and band using the following equation:

$$NC = \frac{\bar{P}_1 - \bar{P}_2}{\bar{P}_2}$$

where $\bar{P}_1$ is the average count for a given IC state and band on day 1, and $\bar{P}_2$ is the count for the same state and band on the reference day, day 2.

In practice, because the odd-numbered detectors in a band are physically separated from the even-numbered ones, separate band averages are computed for the even-numbered and odd-numbered channels. If the IC system is stable between days 1 and 2, the value of NC should depend only on the band; NC should be independent of the IC state.

NC values for nine postlaunch scenes were calculated using two references: (1) a prelaunch vacuum test conducted by the General Electric Company (GE) on March 9, 1982 and (2) the November 2, 1982, postlaunch scene over Washington, D.C. The results, presented in the Appendix (Tables A-1 through A-10), indicate that the relationship of lamp 2 to lamps 1 and 3 has changed relative to prelaunch. For any given band, the NC values for the three lamps with November 2 as the reference are within 0.5 percent of the same value. When prelaunch March 9 data are used as a reference, the NC values for lamps 1 (state 100) and 3 (state 001) have a change in counts within 0.8 percent, and on the average, lamp 2 differs from lamp 1 by 2.2 percent.

---

[1] In this paper, the configuration of the IC is represented by three binary numbers that indicate the status of the three IC lamps, e.g., IC state 100 implies that lamp 1 is on and that lamps 2 and 3 are off.

C-5

Another approach to evaluating the IC system performance that is essentially independent of the channels is to determine the internal consistency of the IC system. Calibration pulse averages collected from the same channel and scene should be consistent; that is, the following sums should be less than 1 digital count:

$$S_{(1)} = P_{(110,C)} - P_{(100,C)} - P_{(010,C)}$$

$$S_{(2)} = P_{(101,C)} - P_{(100,C)} - P_{(001,C)}$$

$$S_{(3)} = P_{(011,C)} - P_{(010,C)} - P_{(001,C)}$$

$$S_{(4)} = P_{(111,C)} - P_{(100,C)} - P_{(010,C)} - P_{(001,C)}$$

where $P_{(1,C)}$ is the average net pulse value in digital counts (background subtracted) for each IC level and $S_{(1,C)}$ is the sum of the IC states. For that channel (C), tables 1 through 4 present values for $S_{(1,C)}$, $S_{(2,C)}$, $S_{(3,C)}$, and $S_{(4,C)}$. It should be noted that, ignoring S_4 for band 4 (where detector saturation in the 111 IC state is a major factor), the values of all but 12 sums are below one digital count; all sums are below 1-1/2 digital counts.

PRELAUNCH SENSOR PERFORMANCE

Prior to launch, nominal gains and offsets for each channel were obtained by external calibration with an integrating sphere under ambient conditions. The Scrounge algorithms for pulse integration, pulse averaging, and regression analysis described in Barker, Abrams, et al. (1984) were used in the external calibration procedure. The detector gains and off-sets were then applied to obtain nominal radiances for each IC state channel combination. The external calibration procedure is described in detail in Barker, Abrams, et al. (1984) and Barker, Ball, et al. (1984).

Prelaunch tests were conducted in February and March of 1982 to compare detector and IC system performance in an ambient environment with performance in a vacuum environment similar to in-orbit conditions. Table 5 lists ambient gain changes relative to vacuum values as measured by the IC system for the primary focal plane channels. It should be noted that the amount and even the direction of the gain shift is different for each bank of detectors (ranging from a 5-percent decrease to a 2-percent increase) and that the gain in ambient conditions decreases relative to the gain in vacuum conditions as the cal-shutter flag temperature increases. Table 6 lists averaged pulse values ($\overline{P}$) in digital counts for the three single-lamp states under ambient and vacuum

TABLE 1

POSTLAUNCH RADIOMETRIC CALIBRATION — TM LANDSAT-4
SACRAMENTO, CALIFORNIA DECEMBER 31, 1982
SUM (S(1,C)) OF NET IC STATES (110-100-010)

CHANNEL	TM 1	TM 2	TM 3	TM 4	TM 5	TM 7
1	−0.75	−0.72	−0.39	−1.03	−0.59	−0.62
2	−0.71	−0.54	−0.25	−0.51	−0.45	−0.60
3	−0.73	−0.78	−0.58	−0.93	—	−0.04
4	−0.38	−0.49	−0.25	−0.56	−0.05	0.00
5	−0.73	−1.13	−0.47	−0.89	−0.05	−0.06
6	−0.70	−0.76	−0.42	−0.97	−0.07	−0.10
7	−0.57	−0.94	−0.59	−1.32	−0.08	0.09
8	−0.48	−0.44	−0.19	−0.55	0.09	−0.17
9	−0.67	−0.96	−0.53	−0.83	−0.19	−0.02
10	−0.71	−0.50	−0.36	−0.81	−0.05	−0.10
11	−0.70	−0.95	−0.38	−0.98	−0.11	−0.12
12	−0.54	−0.41	−0.44	−0.97	−0.01	−0.06
13	−0.56	−1.05	−0.57	−0.96	−0.17	−0.11
14	−0.64	−0.85	−0.43	−1.49	0.05	−0.05
15	−0.85	−0.99	−0.67	−0.41	−0.76	−0.61
16	−0.44	−0.43	−0.28	−0.97	−0.56	−0.85
MEANODD	−0.69	−0.94	−0.52	−0.92	−0.28	−0.19
MEANEVN	−0.58	−0.55	−0.33	−0.85	−0.13	−0.24
MEANALL	−0.64	−0.75	−0.42	−0.88	−0.20	−0.21
MEANODD SD	0.09	0.13	0.10	0.25	0.27	0.27
MEANEVN SD	0.13	0.16	0.09	0.32	0.24	0.31
MEANALL SD	0.12	0.24	0.13	0.28	0.26	0.28

TABLE 2

POSTLAUNCH RADIOMETRIC CALIBRATION — TM LANDSAT-4
SACRAMENTO, CALIFORNIA DECEMBER 31, 1982
SUM (S(2,C)) OF NET IC STATES (101-100-001)

		TM 1	TM 2	TM 3	TM 4	TM 5	TM 7
CHANNEL	1	0.09	−0.01	−0.09	−0.55	−0.22	−0.52
	2	−0.12	−0.05	−0.23	−0.16	−0.01	−0.45
	3	−0.19	−0.27	−0.18	−0.67	—	−0.18
	4	−0.07	−0.02	−0.14	−0.24	−0.26	0.00
	5	−0.05	−0.39	−0.22	−0.50	0.00	−0.04
	6	0.00	−0.34	−0.26	−0.68	0.08	−0.13
	7	0.01	−0.46	−0.25	−0.75	0.19	−0.06
	8	0.07	−0.23	−0.06	−0.40	0.22	−0.03
	9	0.02	−0.39	−0.10	−0.45	−0.01	−0.07
	10	0.08	−0.31	−0.24	−0.55	0.14	−0.09
	11	−0.12	−0.42	−0.11	−0.48	0.10	−0.10
	12	−0.00	−0.21	−0.34	−0.64	0.12	0.02
	13	0.04	−0.22	−0.25	−0.46	−0.02	−0.07
	14	−0.16	−0.58	−0.24	−0.94	0.14	−0.01
	15	0.03	−0.41	−0.27	−0.10	−0.22	−0.38
	16	−0.04	−0.29	−0.15	−0.75	−0.09	−0.48
	MEANODD	−0.01	−0.32	−0.18	−0.50	−0.02	−0.18
	MEANEVN	−0.03	−0.25	−0.21	−0.54	0.10	−0.14
	MEANALL	−0.02	−0.29	−0.20	−0.52	0.04	−0.16
	MEANODD SD	0.09	0.15	0.07	0.19	0.15	0.17
	MEANEVN SD	0.08	0.17	0.08	0.26	0.11	0.20
	MEANALL SD	0.09	0.16	0.07	0.22	0.14	0.18

TABLE 3

POSTLAUNCH RADIOMETRIC CALIBRATION — TM LANDSAT-4
SACRAMENTO, CALIFORNIA DECEMBER 31, 1982
SUM (S(3,C)) OF NET IC STATES (011-010-001)

		TM 1	TM 2	TM 3	TM 4	TM 5	TM 7
CHANNEL	1	0.29	0.14	−0.04	−0.35	−0.28	−0.42
	2	0.41	0.07	0.02	−0.26	−0.14	−0.40
	3	0.32	−0.11	−0.16	−0.23	—	−0.23
	4	0.34	0.04	0.18	−0.07	0.08	−0.09
	5	0.28	−0.16	−0.15	−0.26	0.04	−0.10
	6	0.44	−0.08	−0.05	−0.18	−0.00	−0.21
	7	0.33	−0.34	−0.21	−0.88	−0.01	−0.10
	8	0.31	−0.24	0.16	−0.28	0.02	−0.17
	9	0.20	−0.20	−0.20	−0.40	−0.08	−0.19
	10	0.18	−0.35	−0.01	−0.51	0.00	−0.14
	11	0.06	−0.33	−0.17	−0.40	−0.03	−0.10
	12	0.30	−0.11	−0.08	−0.37	−0.06	−0.14
	13	0.32	−0.32	−0.10	−0.37	−0.10	−0.19
	14	0.10	−0.35	−0.03	−0.54	0.01	−0.12
	15	0.23	−0.24	−0.29	−0.24	−0.28	−0.46
	16	0.41	−0.19	0.27	−0.42	−0.21	−0.40
	MEANODD	0.25	−0.19	−0.17	−0.39	−0.11	−0.22
	MEANEVN	0.31	−0.15	0.06	−0.33	−0.03	−0.21
	MEANALL	0.28	−0.17	−0.05	−0.36	−0.07	−0.22
	MEANODD SD	0.09	0.16	0.07	0.20	0.12	0.14
	MEANEVN SD	0.11	0.16	0.13	0.16	0.09	0.12
	MEANALL SD	0.10	0.15	0.15	0.18	0.11	0.12

TABLE 4

POSTLAUNCH RADIOMETRIC CALIBRATION — TM LANDSAT-4
SACRAMENTO, CALIFORNIA DECEMBER 31, 1982
SUM (S(4,C)) OF NET IC STATES (111-100-010-001)

		TM 1	TM 2	TM 3	TM 4	TM 5	TM 7
CHANNEL	1	−0.197	−0.481	−0.713	−3.034	−1.035	−1.689
	2	−0.039	−0.297	−0.563	−1.594	−0.792	−1.643
	3	−0.439	−0.854	−0.806	−2.598	—	−0.445
	4	−0.106	−0.188	−0.071	−1.644	0.153	−0.360
	5	−0.385	−1.220	−0.716	−2.333	0.019	−0.361
	6	0.005	−0.962	−0.436	−2.397	−0.051	−0.463
	7	0.085	−1.409	−0.697	−3.466	0.169	−0.005
	8	0.027	−0.829	−0.054	−1.469	0.108	−0.512
	9	−0.226	−1.068	−0.666	−1.972	−0.011	−0.345
	10	−0.156	−0.967	−0.379	−3.898	0.160	−0.468
	11	0.054	−1.420	−0.606	−2.117	−0.020	−0.409
	12	−0.144	−0.696	−0.665	−2.135	0.037	−0.554
	13	−0.100	−0.869	−0.631	−2.624	−0.206	−0.495
	14	−0.377	−1.087	−0.549	−2.586	0.018	−0.490
	15	−0.095	−1.392	−0.751	−0.836	−1.022	−1.522
	16	−0.010	−0.796	−0.311	−2.264	−1.008	−1.907
	MEANODD	−0.163	−1.089	−0.698	−2.373	−0.301	−0.659
	MEANEVN	−0.100	−0.727	−0.378	−2.248	−0.159	−0.800
	MEANALL	−0.132	−0.908	−0.538	−2.310	−0.225	−0.729
	MEANODD SD	0.188	0.337	0.065	0.787	0.509	0.604
	MEANEVN SD	0.131	0.324	0.225	0.781	0.464	0.609
	MEANALL SD	0.160	0.370	0.230	0.760	0.473	0.590

TABLE 5

POSTLAUNCH RADIOMETRIC CALIBRATION — TM LANDSAT-4

COMPARISON OF AMBIENT AND VACUUM PULSE VALUES FOR SINGLE LAMP STATES (DIGITAL COUNTS)

BAND[a]	LAMP 100			LAMP 010			LAMP 001		
	VAC[b]	VAC[c]	AMB[d]	VAC[b]	VAC[c]	AMB[d]	VAC[b]	VAC[c]	AMB[d]
1O	108.69	108.67	107.95	68.54	68.47	70.45	46.32	46.22	48.52
1E	105.30	105.25	105.25	65.29	65.08	66.14	44.47	44.32	45.90
2O	98.45	98.15	100.56	78.75	78.40	79.45	45.40	45.23	47.40
2E	93.27	93.02	91.29	68.98	68.71	65.27	41.10	40.95	41.34
3O	94.38	94.01	89.95	68.87	68.76	67.21	40.13	39.95	39.91
3E	96.11	95.75	91.94	71.85	71.52	70.87	42.58	42.38	42.48
4O	96.01	95.89	91.61	98.92	98.66	95.43	47.00	46.94	46.74
4E	102.89	102.53	97.93	95.65	94.85	88.64	51.63	51.58	50.37
5O	44.96	44.87	48.23	41.39	41.19	42.70	24.23	24.14	25.01
5E	64.65	64.59	67.39	57.57	57.49	59.74	32.83	32.74	34.39
7O	57.19	57.10	58.21	45.08	44.95	47.24	32.34	32.27	33.75
7E	58.29	58.18	57.44	55.24	55.22	56.18	34.93	34.87	35.62

NOTES:

[a] O – ODD DETECTORS; E – EVEN DECTORS.

[b] VACUUM, MARCH 9, 1982, 12:43 P.M.

[c] VACUUM, MARCH 9, 1982, 12:46 P.M.

[d] AMBIENT, APRIL 27, 1982, 1:33 P.M.

TABLE 6

POSTLAUNCH RADIOMETRIC CALIBRATION — TM LANDSAT-4
AMBIENT GAIN CHANGES (ppt) RELATIVE TO MARCH 9,1982, VACUUM

BAND[a]	DATE			
	JANUARY 13[b]	FEBRUARY 28[b]	MARCH 12[c]	MARCH 23[b]
1O	28.63	31.38	21.62	30.88
1E	15.75	17.25	8.00	16.63
2O	25.12	28.25	19.75	24.38
2E	−9.40	−4.20	−13.90	−10.90
3O	−23.50	−23.50	−50.00	−18.25
3E	−18.63	−18.63	−46.25	−15.00
4O	−15.00	−15.00	−30.75	−10.13
4E	−27.38	−27.38	−47.00	−27.00

[a] O = ODD DETECTORS; E = EVEN DETECTORS.

[b] CAL SHUTTER FLAG TEMPERATURE, 18.11 C°.

[c] CAL SHUTTER FLAG TEMPERATURE, 22.85 C°, SAME AS VACUUM RUN ON MARCH 9, 1982.

conditions. The exact causes of the differences between ambient and vacuum measurements are not well understood, but are thought to be related to changes in optical surfaces or the filters caused by the deposit of thin water vapor films in ambient conditions.

After final prelaunch adjustments to the TM, several tests were conducted under vacuum conditions in early March to estimate instrument precision. The results (Table 7) indicate that variability in gain for repeated measurements over a timespan of a few days is generally less than 1 percent, but can occasionally be as high as 2 percent.

POSTLAUNCH SENSOR PERFORMANCE

A comparison of within-band relative gain changes yields a measure of TM precision that is somewhat insensitive to changes in the IC system. Table 8 shows the means and standard deviations of in-orbit gain changes in parts per thousand (ppt) relative to the 12:46 p.m. prelaunch vacuum test on March 9, 1982, for five dates ranging from August to December 1982. In the primary focal plane, channels in a band are internally consistent in gain change, varying up to only 0.6 percent (except for the 1-percent spread between even- and odd-numbered channels in band 2). In contrast, the cold focal plane channels demonstrate large within-band variability, up to 5 percent in band 5 and up to 3 percent in band 7 (excluding channel 7, which differs from the other channels in the band by up to 20 percent). Tables A-11 through A-13 in the appendix show the gain changes for each channel in bands 2, 5, and 7 relative to March 9. When a postlaunch data set (Washington, D.C., November 2, 1982) is used as a reference, within-band variability of gain change in the cold focal plane is substantially reduced. Table 9 shows that within-band gain changes relative to November 2 vary only up to 1.5 percent in band 5 and up to 0.7 percent in band 7 (channel 7 included). The divergence between even- and odd-numbered channels in band 2 has decreased to 0.5 percent. The reason for the inconsistency between prelaunch and postlaunch gain changes is unclear, but there are two possible causes: (1) the cold focal plane temperature during prelaunch is different from the in-orbit temperature and (2) the apparent postlaunch shift of the cold focal plane location, as indicated by band-to-band geometric registration studies, affects the shape of the IC calibration pulse.

The below-average performance of four channels needs to be singled out. Channel 3 in band 5 is dead, and channel 4 in band 2 has a very poor modulation transfer function. In the image product, data from both of these channels is replaced

TABLE 7

PRELAUNCH RADIOMETRIC CALIBRATION — TM LANDSAT-4

CHANGE IN GAIN (ppt) RELATIVE TO MARCH 9, 1982, 12:46 P.M. PRELAUNCH VACUUM

BAND[a] \ DATE TIME TEMP°C[b]	FEB. 23[c] 19:57 10.10	FEB. 24[c] 10:00 22.85	MAR. 6 21:54 10.10	MAR. 7 2:55 22.85	MAR. 7 9:50 22.85	MAR. 9 7:25 22.85	MAR. 9 12:41 22.85	MAR. 9 12:50 10.10	MAR. 9 12:55 10.10	MAR. 9 20:21 22.85
1O	−6	−28	−8	−6	−5	−11	7	−4	−8	−7
1E	−3	−27	−12	−11	−9	−12	7	−4	−8	−10
2O	−8	−27	−3	−3	−1	−10	8	−3	−6	−5
2E	9	−15	−14	−13	−10	−12	8	−3	−7	−10
3O	34	15	−12	−10	−C	−15	10	−4	−8	−10
3E	27	6	−10	−9	−7	−15	9	−4	−9	−9
4O	48	38	−2	−1	−1	−2	5	0	−1	−1
4E	50	47	−4	−4	−4	−3	5	−1	−2	−2
5O				−21	−16	−5	5	−1	−2	0
5E				−18	−14	−6	4	−1	−2	1
7O				13	10	−1	3	0	−1	1
7E				12	10	−1	2	−1	0	1

NOTES:

[a] O = ODD DETECTORS; E = EVEN DETECTORS.

[b] CAL SHUTTER FLAG TEMPERATURE.

[c] EARLY VACUUM CHAMBER TESTING WITH UNSTABILIZED PROTOFLIGHT INSTRUMENT.

TABLE 8

POSTLAUNCH RADIOMETRIC CALIBRATION—TM LANDSAT-4 CHANGE IN GAIN (ppt) RELATIVE TO MARCH 9, 1982

BAND		1982 DATE (DAY OF YEAR)				
		AUGUST 22 (234)	SEPTEMBER 10 (253)	OCTOBER 24 (297)	NOVEMBER 24 (328)	DECEMBER 8 (342)
1	MEAN	−35.2	−40.6	−52.0	−52.6	−51.6
	SD	2.5	2.4	2.5	2.0	1.6
2	MEAN	−28.6	−30.3	−30.0	−34.1	−34.6
	SD	7.7	7.3	6.3	6.3	6.3
3	MEAN	−27.8	−35.7	−48.0	−47.5	−40.3
	SD	1.2	0.9	1.4	1.0	0.5
4	MEAN	−8.6	−14.6	−25.0	−27.3	−28.7
	SD	1.6	1.1	1.6	1.4	1.4
5	MEAN	3.7	73.3	28.0	29.3	1.08
	SD	10.4	11.4	10.2	10.2	10.8
7	MEAN	18.9	−2.6	34.0	−0.5	7.9
	SD	45.2	45.6	40.1	43.6	44.4

TABLE 9

POSTLAUNCH RADIOMETRIC CALIBRATON — TM LANDSAT-4 CHANGE IN GAIN (ppt) RELATIVE TO D.C., NOVEMBER 2, 1982

BAND		1982 DATE (DAY OF YEAR)				
		AUGUST 22 (234)	SEPTEMBER 10 (253)	OCTOBER 24 (297)	NOVEMBER 24 (328)	DECEMBER 8 (342)
1	MEAN	10.5	11.1	−1.5	−0.8	0.3
	SD	1.5	2.1	1.5	1.3	0.8
2	MEAN	9.6	6.0	−0.4	2.0	1.7
	SD	2.1	1.3	1.7	1.4	0.6
3	MEAN	21.5	13.4	0.6	2.1	0.1
	SD	0.8	1.9	1.1	0.8	0.7
4	MEAN	10.6	10.7	−0.2	−2.1	−3.1
	SD	1.0	0.9	0.8	0.8	0.8
5	MEAN	54.6	14.9	32.1	−29.5	−55.7
	SD	3.6	3.5	1.5	8.6	5.1
7	MEAN	−8.2	−28.7	8.4	−25.6	10.6
	SD	0.8	1.8	1.5	2.0	1.9

with data from a neighboring channel (channel 4 in band 5 and channel 5 in band 2). Channel 2 in band 2 and channel 7 in band 7 are twice as noisy as the other channels in their respective bands; however, data collected from these channels are not replaced.

STABILITY WITH TIME

Study of the in-orbit gain changes with time characterizes the combined radiometric stability of the channels and the IC system. Table 10 lists the 26 scenes from which in-orbit gain data were collected. Figure 1 shows the location of these scenes. Figures 2 and 3 show gain change relative to prelaunch versus time for the six reflective bands. Figures A-1 through A-6 in the appendix show gain versus time for these bands. From launch through October 1982, gain decreased in the primary focal planes (6 percent in bands 1 and 2, 8 percent in band 3, and 3 percent in band 4), and then stabilized. In the cold focal plane bands, gain oscillates with time (up to 7 percent in band 5, and 5 percent in band 7). If the IC system itself were changing, an apparent decrease in gain in the cold focal plane channels as well as the primary focal plane channels should be observed. This is not the case, however, especially in band 7. The oscillation in bands 5 and 7 is difficult to explain since the oscillation periods of the two bands are not the same (55 days for band 5, and 75 days for band 7). Possible explanations such as temperature effects (arising from orbit precessions) on channel sensitivity or even relative position of the cold focal plane are apparently ruled out by the difference in frequency.

Although gain changes over a period of days are significant, the gain changes in all the reflective channels for successive rows of the same path are 1 ppt or less, except for band 1, channels 7, 10, and 11 (2 ppt); band 1, channel 12 (3 ppt); band 1, channel 4 (4 ppt); and band 4, channel 14 (2 ppt). Table 11 gives the differences between gains from the Kingston and Ottawa scenes. In all cases, the gain changes for scenes from successive rows in the same path are statistically insignificant (see percentage coefficients of variance, Table 12).

NOISE

To ensure positive detector readings at all times, the onboard electronics strives to maintain a constant background of about 2 counts. Table 13 and Tables A-14 and A-15 in the appendix give typical standard deviations in the background for each channel. The magnitude of background noise depends

TABLE 10

LANDSAT-4 TM SCENE IDENTIFICATION

ACQUISITION DATE	SCENE ID	WRS PATH/ROW	AREA
20 JUL 82	40004-15401	020/031	DETROIT, MICHIGAN
29 JUL 82	40011-31525	015/033	WASHINGTON, D.C.
7 AUG 82	40022-15061	014/032	NEW YORK/PHILADELPHIA
17 AUG 82	40032-15425	020/031	TOLEDO, OHIO
22 AUG 82	40037-16031	023/035	NORTHEAST ARKANSAS
25 AUG 82	40040-16321	028/030	FT. DODGE, IOWA
30 AUG 82	40045-15151	015/038	ATLANTIC OCEAN
10 SEP 82	40058-14541	012/031	BOSTON, MASSACHUSETTS
24 SEP 82	40070-16442	030/028	FORMAN, NORTH DAKOTA
26 SEP 82	40072-16325	028/030	NORTHWEST IOWA
27 SEP 82	40073-15400	019/037	ATLANTA, GEORGIA
24 OCT 82	40100-15182	016/028	OTTAWA, CANADA
24 OCT 82	40100-15184	016/029	KINGSTON, CANADA
2 NOV 82	40109-15140	015/033	WASHINGTON, D.C.
9 NOV 82	40116-18350	048/025	VANCOUVER, BRITISH COLUMBIA
17 NOV 82	40124-17495	040/035	DEATH VALLEY, CALIFORNIA
24 NOV 82	40131-17533	041/028	MT. HAMILTON, MONTANA
8 DEC 82	40145-18092	043/034	MODESTO, CALIFORNIA
20 DEC 82	40157-15174	015/041	FT. PIERCE, FLORIDA
22 DEC 82	40159-15032	013/036	CAPE HATTERAS, NORTH CAROLINA
31 DEC 82	40168-18141	044/033	SACRAMENTO, CALIFORNIA
3 JAN 83	40171-	033/037	WHITE SANDS, NEW MEXICO
3 JAN 83	40171-	033/038	WHITE SANDS, NEW MEXICO
6 JAN 83	40174-17372	038/033	MARYSVILLE, UTAH
15 JAN 83	40183-17332	037/038	LUKEVILLE, ARIZONA
29 JAN 83	40197-02267	112/211	WEST WASHINGTON, D.C., PM

The U.S. With
WRS Path/Row Scenes Indicated

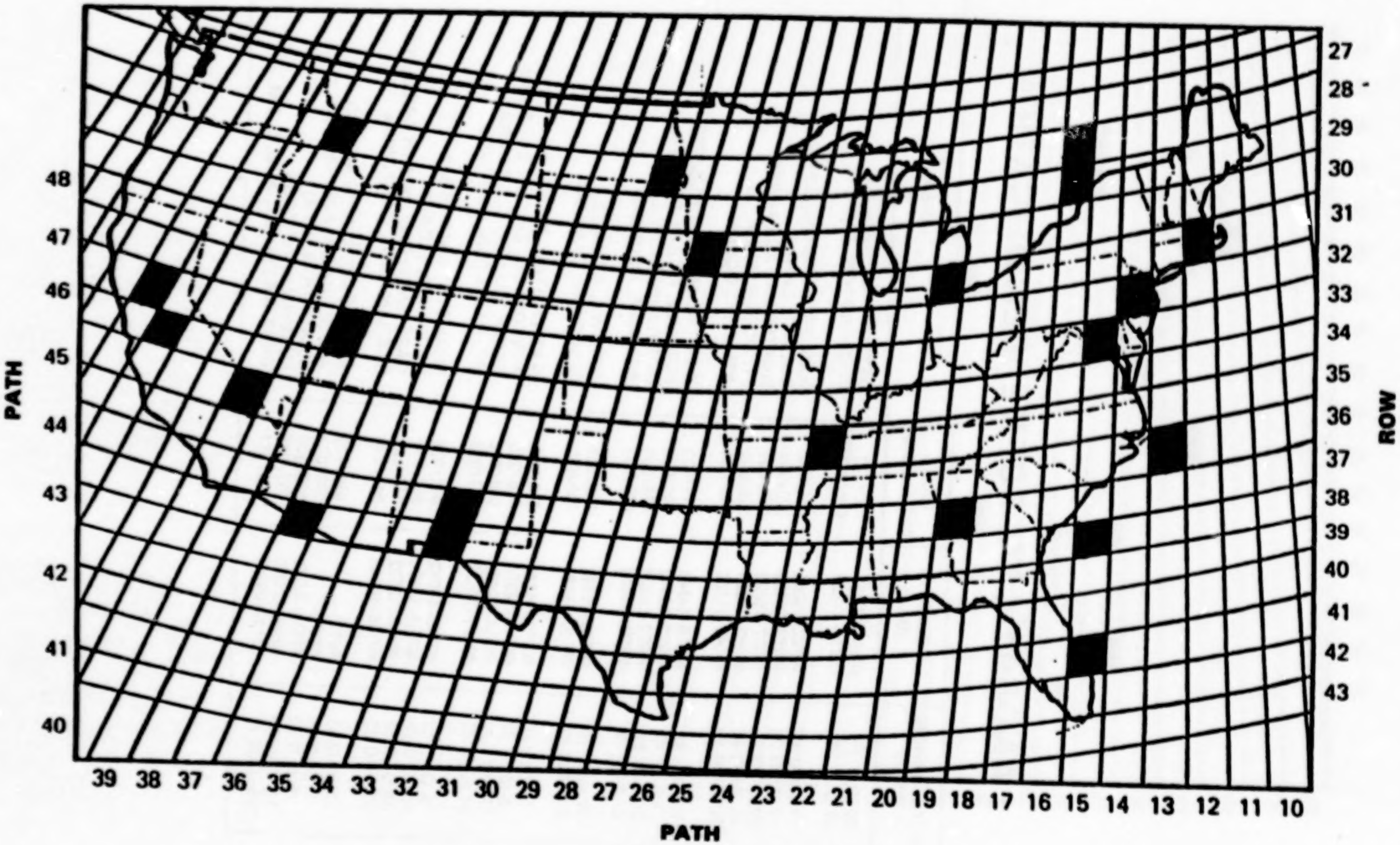
PATH
48
47
46
45
44
43
42
41
40
39 38 37 36 35 34 33 32 31 30 29 28 27 26 25 24 23 22 21 20 19 18 17 16 15 14 13 12 11 10
PATH
ROW
27
28
29
30
31
32
33
34
35
36
37
38
39
40
41
42
43

FIGURE 1

ORIGINAL PAGE IS
OF POOR QUALITY

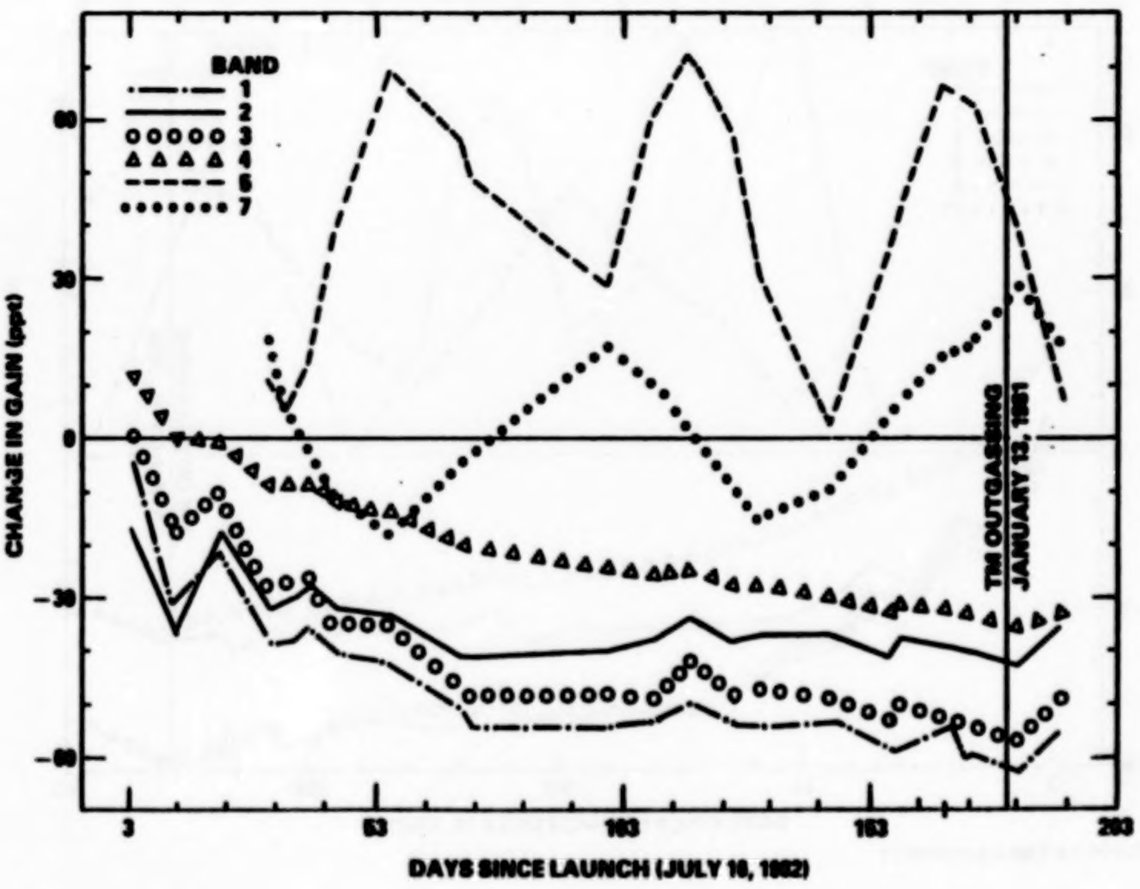
POSTLAUNCH RADIOMETRIC CALIBRATION—TM LANDSAT-4

CHANGE IN GAIN (ppt) EVEN DETECTORS RELATIVE TO MARCH 9, 1982

FIGURE 2

POSTLAUNCH RADIOMETRIC CALIBRATION—TM LANDSAT-4
CHANGE IN GAIN (ppt) ODD DETECTORS RELATIVE TO MARCH 9, 1982

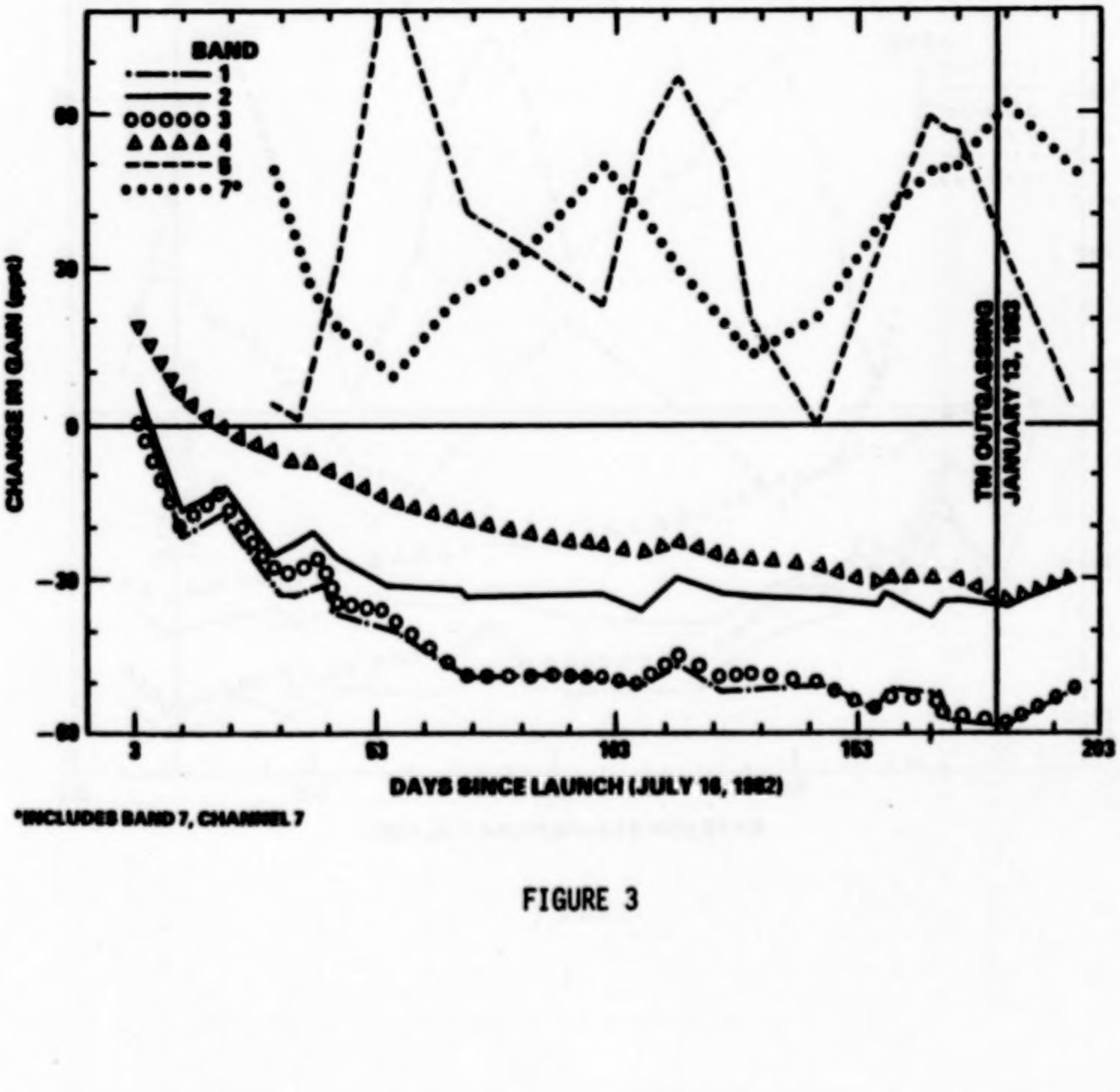

*INCLUDES BAND 7, CHANNEL 7

FIGURE 3

TABLE 11

STABILITY OF THE IC WITH TIME

GAIN DIFFERENCES BETWEEN KINGSTON (40100—15184) AND OTTAWA (40100—15182) IN COUNTS/MW cm^{-2} sr^{-2} μm^{-1}

CHANNEL	TM1	TM2	TM3	TM4	TM5	TM7
1	0.017	0.005	0.010	0.014	−0.033	0.105
2	0.000	−0.004	0.000	0.006	0.021	0.067
3	0.005	−0.002	0.006	−0.001	—	0.149
4	0.059	0.000	0.000	0.001	0.097	0.120
5	0.003	0.005	−0.005	0.000	0.015	0.077
6	0.009	0.008	0.006	0.006	−0.019	−0.053
7	0.025	−0.001	0.010	0.013	0.093	0.070
8	0.020	−0.002	−0.007	−0.007	0.002	0.104
9	−0.005	0.005	0.002	0.010	−0.014	−0.066
10	0.037	0.008	0.006	0.003	−0.008	0.133
11	0.024	0.000	0.001	−0.001	−0.038	0.002
12	0.049	−0.003	0.003	0.013	0.057	0.063
13	0.009	0.002	0.003	−0.012	0.012	0.038
14	−0.002	0.001	0.001	0.019	0.007	0.019
15	0.020	0.000	0.011	0.015	−0.102	−0.014
16	0.003	−0.004	0.004	−0.001	0.009	0.189
MEANODD	0.012	0.002	0.006	0.005	−0.013	−0.046
MEANEVEN	0.022	0.000	0.002	0.004	0.020	0.093
MEAN	0.018	0.001	0.004	0.005	0.005	0.077

TABLE 12

STABILITY OF THE IC WITH TIME

PERCENTAGE COEFFICIENT OF VARIANCE OF GAIN
KINGSTON, CANADA (40100—15184)

		TM1	TM2	TM3	TM4	TM5	TM7
CHANNEL	1	0.477	0.614	0.535	0.772	0.285	0.472
	2	0.513	0.521	0.530	1.197	0.352	0.463
	3	0.456	0.647	0.497	0.722	–	0.512
	4	0.524	0.488	0.574	1.247	0.321	0.443
	5	0.473	0.675	0.545	0.778	0.220	0.450
	6	0.549	0.549	0.573	1.171	0.342	0.426
	7	0.525	0.661	0.516	0.823	0.282	0.498
	8	0.494	0.522	0.553	1.167	0.336	0.435
	9	0.499	0.701	0.557	0.874	0.286	0.474
	10	0.462	0.544	0.568	1.213	0.355	0.448
	11	0.548	0.631	0.539	0.797	0.225	0.506
	12	0.531	0.471	0.531	1.223	0.352	0.429
	13	0.532	0.698	0.518	0.770	0.280	0.463
	14	0.474	0.521	0.551	1.157	0.407	0.432
	15	0.506	0.640	0.542	0.803	0.309	0.485
	16	0.483	0.511	0.572	1.205	0.380	0.451
	MEANODD	0.502	0.658	0.531	0.792	0.261	0.480
	MEANEVN	0.504	0.516	0.557	1.199	0.353	0.441
	MEANALL	0.503	0.587	0.544	0.996	0.310	0.460

$$CV = \frac{N \cdot 100}{\Sigma X_i} \sqrt{\frac{(N/N-2) \cdot \sum_i (Y_i - GX_i - B)}{N\Sigma X_i^2 - (\Sigma X_i)^2}}$$

WHERE CV = PERCENT COEFFICIENT OF VARIANCE
N = NUMBER OF MEASUREMENTS
Y_i = DIGITAL COUNTS
G = GAIN (DIGITAL COUNT/RADIANCE)
X_i = RADIANCE (MW cm^{-2} sr^{-1} μm^{-1})
B = OFFSET IN DIGITAL COUNTS

TABLE 13

POSTLAUNCH RADIOMETRIC CALIBRATION — TM LANDSAT-4 STANDARD DEVIATION OF WATER IMAGE, BOSTON, SEPTEMBER 10, 1982 (DIGITAL COUNTS)

		TM1	TM2	TM3	TM4	TM5	TM7
CHANNEL	1	1.51	0.67	0.96	0.38	0.88	1.02
	2	1.77	1.06	0.85	0.48	0.82	1.04
	3	1.46	0.57	0.83	0.35	—	0.93
	4	1.77	0.80	1.06	0.52	0.90	1.07
	5	1.42	0.58	0.88	0.49	0.97	0.99
	6	1.76	0.62	0.82	0.38	0.94	1.05
	7	1.58	0.52	0.84	0.49	1.21	1.91
	8	1.67	0.48	1.15	0.56	0.88	0.94
	9	1.46	0.56	0.77	0.45	0.83	1.09
	10	1.49	0.55	0.88	0.38	0.86	1.12
	11	1.59	0.54	0.71	0.49	0.89	1.06
	12	1.60	0.53	0.78	0.50	0.82	1.09
	13	1.48	0.61	0.86	0.50	0.84	0.98
	14	1.68	0.57	0.87	0.42	0.76	1.15
	15	1.56	0.61	0.87	0.51	0.81	0.97
	16	1.95	0.59	1.11	0.43	0.73	1.00
MEANODD		1.51	0.58	0.84	0.46	0.92	1.12
MEANEVN		1.71	0.65	0.94	0.46	0.84	1.06
MEANALL		1.61	0.62	0.89	0.46	0.87	1.09
MEANODD SD		0.06	0.04	0.07	0.06	0.13	0.32
MEANEVN SD		0.13	0.18	0.14	0.07	0.06	0.06
MEANALL SD		0.14	0.13	0.12	0.06	0.11	0.22
MEANALL CV		9.11	22.13	13.67	13.68	12.67	20.74

primarily on the band and secondarily on whether the detector is in the even or the odd bank. Band 1 is noisiest at 1.2 counts, followed by band 7. Bands 2 and 4 are quietest, with noise of up to 0.5 count. In the primary focal plane, the even-numbered detectors are 0.1 to 0.2 count noisier than the odd-numbered detectors. In the cold focal plane, the odd-numbered detectors are slightly (less than 0.1 count) noisier than the even-numbered detectors. Noise in the image is of comparable magnitude to background noise and follows the same pattern, indicating that noise in the image arises primarily from noise in the background. Table 14 gives the standard deviation by channel of the image with a flooding lamp target. The image area is 24 midscan pixels by 400 scans. An estimate of the upper limit of postlaunch noise in the image was obtained by examining a water scene in Boston harbor (September 10, 1982). The image area was 512 pixels by 32 scans (512 lines). Table 15 gives the standard deviation of the signal for each channel. The results are consistent with the prelaunch pattern.

The only significant coherent noise peaks appear at 32.7 kilohertz (kHz). Table 16 gives the peak-to-peak amplitudes (background subtracted) at 32.7 kHz derived from fast Fourier transforms of the first scan (1024 samples per detector) of video data in the August 22, 1982, Memphis scene. It should be noted that the largest amplitude occurs in band 1, channel 16, and is 1.43 counts. The first scan of background data from the August 22, 1982, Missouri scene showed a similar peak-to-peak amplitude of 1.58 counts in band 1, channel 16, at 32.7 kHz. Both of these data sets were collected while the Multispectral Scanner (MSS) was turned on. In contrast, the scene of White Sands, New Mexico, on January 3, 1983, which was collected when the MSS was turned off, showed no coherent noise. Table 17 shows the coherent noise pattern from the first reverse scan of prelaunch, March 9, 1982, flooding lamp image data (52 samples per detector). In general, the pattern is similar to postlaunch data, although the amplitudes are somewhat smaller.

OTHER FACTORS AFFECTING DATA QUALITY

Location of Calibration Collect Window

The Scrounge ground system hardware can only extract 200 minor frames of the 1115 minor frames generated during scan minor turnaround. Fifty-two minor frames are selected from the background region; the remaining 148 minor frames contain calibration pulse data. The location of the 148-frame window is fixed relative to line start and depends

TABLE 14

POSTLAUNCH RADIOMETRIC CALIBRATION — TM LANDSAT-4 STANDARD DEVIATION OF FLOODING LAMP IMAGE, MARCH 9, 1982 (DIGITAL COUNTS)

		TM1	TM2	TM3	TM4	TM5	TM7
CHANNEL	1	1.53	0.65	0.82	0.52	1.28	1.33
	2	1.73	1.06	0.81	0.49	1.11	1.30
	3	1.44	0.57	0.85	0.55	—	1.42
	4	1.21	0.63	0.90	0.58	1.04	1.33
	5	1.39	0.62	0.86	0.44	1.09	1.31
	6	1.63	0.64	0.83	0.50	1.45	1.45
	7	1.32	0.56	0.76	0.51	1.32	3.82
	8	1.53	0.57	1.23	0.62	1.10	1.40
	9	1.35	0.57	0.90	0.37	1.04	1.35
	10	1.18	0.57	1.03	0.65	1.41	1.59
	11	1.56	0.56	1.03	0.39	1.16	1.45
	12	1.17	0.60	0.95	0.46	1.12	1.27
	13	1.41	0.52	0.80	0.57	1.09	1.31
	14	1.53	0.58	1.01	0.49	1.10	1.39
	15	1.53	0.75	0.81	0.49	1.33	1.32
	16	1.94	0.79	0.81	0.43	1.12	1.43
MEANODD		1.44	0.60	0.85	0.48	1.19	1.66
MEANEVN		1.49	0.68	0.95	0.53	1.18	1.40
MEANALL		1.47	0.64	0.90	0.50	1.18	1.53
MEANODD SD		0.08	0.07	0.08	0.07	0.12	0.87
MEANEVN SD		0.28	0.16	0.14	0.08	0.15	0.10
MEANALL SD		0.20	0.13	0.12	0.07	0.13	0.61
MEANALL CV		13.85	20.42	13.61	15.38	11.43	40.21

TABLE 15

POSTLAUNCH RADIOMETRIC CALIBRATION — TM LANDSAT-4 STANDARD DEVIATION OF BACKGROUND, BOSTON, SEPTEMBER 10, 1982 (DIGITAL COUNTS)

		TM1	TM2	TM3	TM4	TM5	TM7
CHANNEL	1	1.21	0.47	0.74	0.58	0.80	0.99
	2	1.38	1.00	0.58	0.52	0.75	0.99
	3	1.11	0.48	0.55	0.59	—	0.85
	4	1.40	0.70	0.70	0.52	0.81	1.03
	5	1.03	0.43	0.52	0.51	0.7[illegible]	0.92
	6	1.34	0.52	0.53	0.58	0.8[illegible]	1.00
	7	1.21	0.37	0.48	0.47	1.07	1.96
	8	1.24	0.43	0.86	0.69	0.[illegible]2	0.92
	9	1.01	0.30	0.42	0.48	0.82	0.95
	10	1.11	0.30	0.57	0.52	0.87	1.03
	11	1.14	0.35	0.38	0.44	0.89	0.91
	12	1.30	0.37	0.51	0.63	0.84	1.00
	13	1.05	0.37	0.52	0.39	0.82	0.81
	14	1.30	0.38	0.61	0.54	0.79	1.08
	15	1.16	0.34	0.52	0.48	0.80	0.79
	16	1.56	0.45	0.87	0.56	0.77	0.96
MEANODD		1.11	0.39	0.51	0.49	0.87	1.02
MEANEVN		1.33	0.52	0.65	0.57	0.81	1.00
MEANALL		1.22	0.45	0.58	0.53	0.84	1.01
MEANODD SD		0.08	0.06	0.11	0.06	0.09	0.38
MEANEVN SD		0.12	0.22	0.14	0.06	0.04	0.04
MEANALL SD		0.15	0.17	0.14	0.07	0.07	0.28
MEANALL CV		12.27	38.37	24.35	13.76	8.87	25.98

TABLE 16

IN-ORBIT LANDSAT-4 TM RADIOMETRIC COHERENT NOISE (DIGITAL COUNTS)

Channel No.	Peak-to-Peak Coherent Noise at 32 KHz (DN)					
	Band 1	Band 2	Band 3	Band 4	Band 5	Band 7
1	.54	.08	.09	.28	.25	.16
2	.98	.13	.13	.39	.50	.28
3	.74	.07	.07	.42	—	.20
4	.03	.15	.86	.77	.19	.37
5	.83	.15	.20	.76	.33	.35
6	1.02	.16	.19	.49	.25	.21
7	.39	.10	.15	.58	.59	.46
8	.93	.00	.80	.70	.34	.29
9	.44	.08	.16	.43	.38	.25
10	.33	.14	.08	.35	.19	.28
11	.54	.13	.17	.37	.29	.18
12	.47	.13	.10	.35	.41	.31
13	.52	.05	.21	.43	.20	.26
14	.76	.00	.12	.28	.25	.34
15	.57	.06	.09	.34	.32	.18
16	1.43	.06	.35	.37	.49	.20

Data Measured Peak-to-Peak, With Background Subtracted in Digital Counts
Data from Scene W023036 ID = 40037-16033 (22 Aug 82) Memphis, TN

TABLE 17

PRELAUNCH LANDSAT-4 TM COHERENT NOISE (DIGITAL COUNTS)

CHANNEL NUMBER	PEAK-TO-PEAK COHERENT NOISE AT 32.7 KHz (COUNTS)					
	BAND 1	BAND 2	BAND 3	BAND 4	BAND 5	BAND 7
1	0.75					
2	0.69					
3	0.75					
4	–		0.23	0.22		
5	0.56		0.41		0.44	
6	1.06			0.31	0.50	
7	0.38					
8	0.72		0.63	0.47		
9	0.56					
10	0.69				0.44	
11	1.00					
12	0.25					
13	0.56			0.50		
14	0.50					
15	0.50				0.50	
16	1.00		0.53			

NOTES:

DATA MEASURED PEAK TO PEAK WITH BACKGROUND SUBTRACTED IN DIGITAL COUNTS.

DATA FROM FIRST REVERSE SCAN OF FLOODING LAMP DATA (52 SAMPLES PER CHANNEL) MARCH 9, 1982.

9121-ABR-(10)

only on scan direction. The location of the pulse within the window depends on the channel number, the band number, and the line length (varies up to 10 minor frames), as well as on the scan direction. In the forward scan direction, the pulse leading-edge minor frame number increases for a given scan as the channel number decreases. Band number is considerably less important than channel number in determining pulse location. With TM protoflight band 1, channel 1 is the farthest to the right (starts at the highest minor frame number), followed by bands 2 and 3. Using the Hughes method, pulse width varies from 42 to 44 minor frames in the primary focal plane band and 40 to 41 frames in bands 5 and 7. A more detailed description of the scan timeline is given in Barker, Abrams, et al. (1984).

For scene data processed by the Scrounge system before December 22, 1982, the beginning of the 148-frame window was located at minor frame 7009 for forward scans and 6525 for reverse scans. The location of the forward scan calibration pulse window caused part of the calibration pulse to fall outside the window in channel 1 on all bands, and in channel 2 on bands 1, 2, and 3. Figure 4 shows a raw data dump of a truncated pulse. As a result of pulse truncation, gain was underestimated by 3.8 percent in channel 1 of band 1; 0.6 percent in channel 1 of band 2; 0.2 percent in channel 1 of band 5 and channel 2 of bands 1 and 2; and 0.1 percent in channel 1 of bands 3, 4, and 7 and channel 2 of band 3. On December 22, the calibration window was reset to begin at minor frame 7029 in the forward direction and minor frame 6517 in the reverse direction. This adjustment eliminated truncation, but it occasionally introduced a new problem. The new positions of the collect windows were such that data from the transition region (from full obscuration of the optical axis by the shutter to full imaging) were occasionally included in the collect window. This happened primarily for channels 16, 15, and 14 in both forward and reverse scans. Because the transition data had a higher count level than the lamps-off 000 IC state, "pulse" averages for the 000 state had an abnormally high digital count level. The offset values for channels 16, 15, and 14 resulting from the linear regression analysis also tended to be high (up to 18 digital counts). A compromise set of calibration windows that will eliminate this problem is currently being proposed. Table 18 gives the history of the calibration collect window location.

Acquisition

Two scenes collected via the Prince Albert ground station have been examined in detail: Hamilton, Montana, on November 24, 1982, and Vancouver, British Columbia, on

RAW DATA DUMP OF TRUNCATED PULSE

```
TRAPP PROGRAM     SCN ID/ PATHROW : 4010815140/ DCGFSC  RUN ON DATE: 12-APR-83 AT TIME: 12:34:29                    PAGE NO.  17

SORTED AND SIGN CORRECTED CALIBRATION DATA, FORWARD DIRECTION, SCAN #   1,  DET #  1
   5   4   2   4   4   2   2   5   4   1   4   2   5   4   4   5   3   5   4   2   4   3   2   5   3   3   4   2   2   4   4   2
   3   5   2   4   5   3   2   5   2   4   4   4   2   4   3   3   2   5   3   3   5   3   4   3   5   2   4   3   4   3   5   2
   4   3   5   2   5   4   3   5   4   1   5   4   2   4   5   3   3   4   5   4   5   6   3   5   6   3   5   6   4   4   6   4
   5   8   8   6  10   9  12  17  25  33  42  54  60  68  75  81  46  91  93  98  99  99  99  98 104 103 105 108 109 108 116 112
 115 117 117 117 119 121 120 125 125 128 125 130 130 131 134 130 125 122 112  99
```

FIGURE 4

TABLE 18

IN-ORBIT 148-mf CALIBRATION COLLECT WINDOWS

PERIOD	FORWARD SCAN (mf)	REVERSE SCAN (mf)
LAUNCH TO DECEMBER 22, 1982	7009	6525
DECEMBER 22, 1982, TO PRESENT	7029	6517
PROPOSED COMPROMISE	7017	6525
PROPOSED CENTERED	7037	6513

November 9, 1982. Background noise (standard deviation) in the Vancouver scene was about 0.1 count larger in bands 1, 2, and 3 than is typical for scenes collected via the transportable ground station. The data from these two scenes were otherwise comparable to data collected via the transportable ground station.

Nonuniformity in the A/D Converter

The conversion from voltage to digital counts by the analog-to-digital (A/D) converter is linear, but the cutoff (threshold) voltages are not spaced uniformly (Barker, 1984). The voltage range allocated to a digital count level varies anywhere from 3 to 22 millivolts. The least two significant bits in the digital count value are closely correlated with the size of the allocated range. A higher digital count level still implies a higher radiance, but the precision of the radiance value depends on the count level of the raw data. Table A-16 in the appendix lists the threshold voltage and bin size for each count level for band 1, channel 1. The pattern for the other channels is similar but not identical.

As a result of the nonuniformity in the A/D converter, histograms of raw scene data are saw-toothed. When the raw histogram is normalized using the following equation, the resulting histogram is smoother:

$$C'(n) = \frac{C(n) \cdot \bar{b}}{b(n)}$$

where $C(n)$ = number of pixels at digital level n
$C'(n)$ = normalized count for digital level n
$\bar{b}$ = average bin size in millivolts
$b(n)$ = bin size for level n

Figure 5 shows the raw histogram collected by band 1, channel 1, on January 3, 1983, over White Sands, New Mexico. Figure 6 shows the same histogram after normalization to remove the effects of A/D nonuniformity.

POSSIBLE ADJUSTMENTS TO RADIOMETRIC CALIBRATION PROCEDURES

PULSE INTEGRATION

The standard deviation of integrated pulse values is sensitive to pulse integration width. In general, the larger the integration width, the lower the variability in the integrated pulse value for a given channel and IC state. Figure 7 shows the change in standard deviation with pulse integration width for channel 9, IC state 110, in all bands. The rise in standard deviation when the integration width

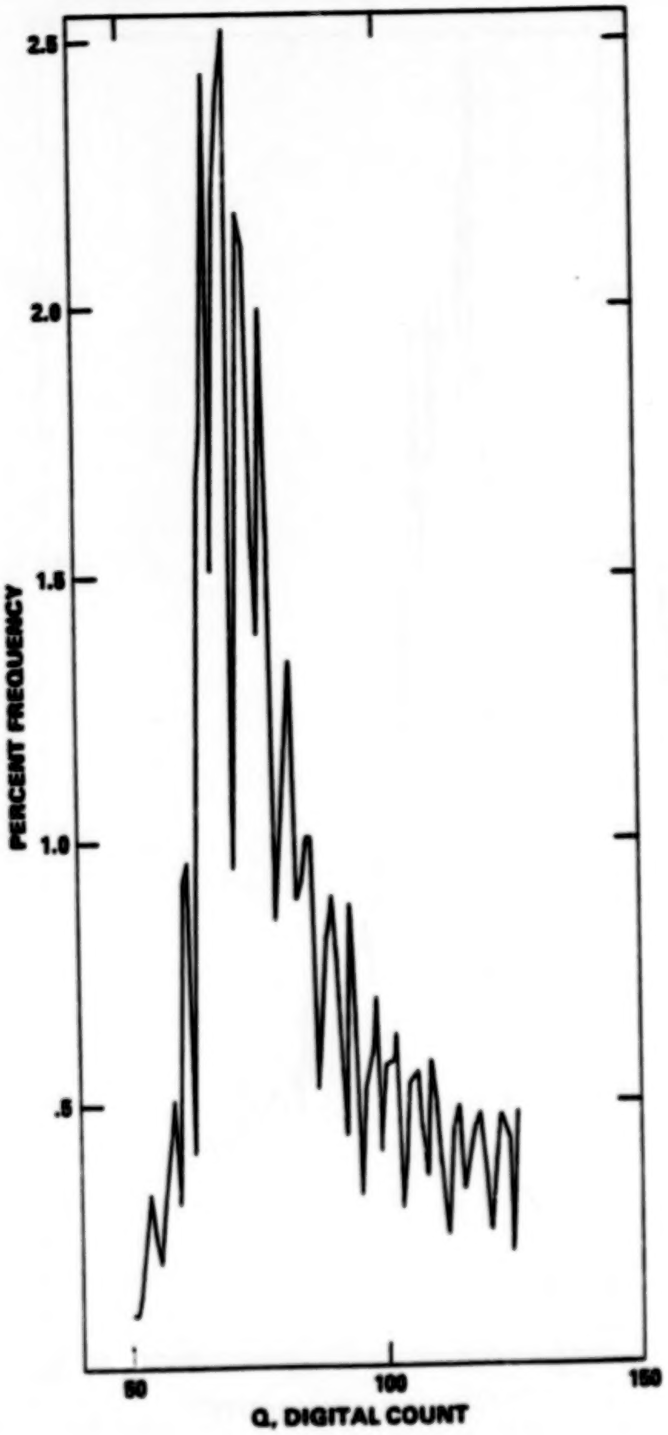

POSTLAUNCH RADIOMETRIC CALIBRATION — TM LANDSAT-4
HISTOGRAM TM1, CHANNEL 1, RAW DATA
WHITE SANDS, NEW MEXICO, JANUARY 3, 1983

FIGURE 5

POSTLAUNCH RADIOMETRIC CALIBRATION — LANDSAT-4
HISTOGRAM TM1, CHANNEL 1, NORMALIZED
WHITE SANDS, NEW MEXICO, JANUARY 3, 1983

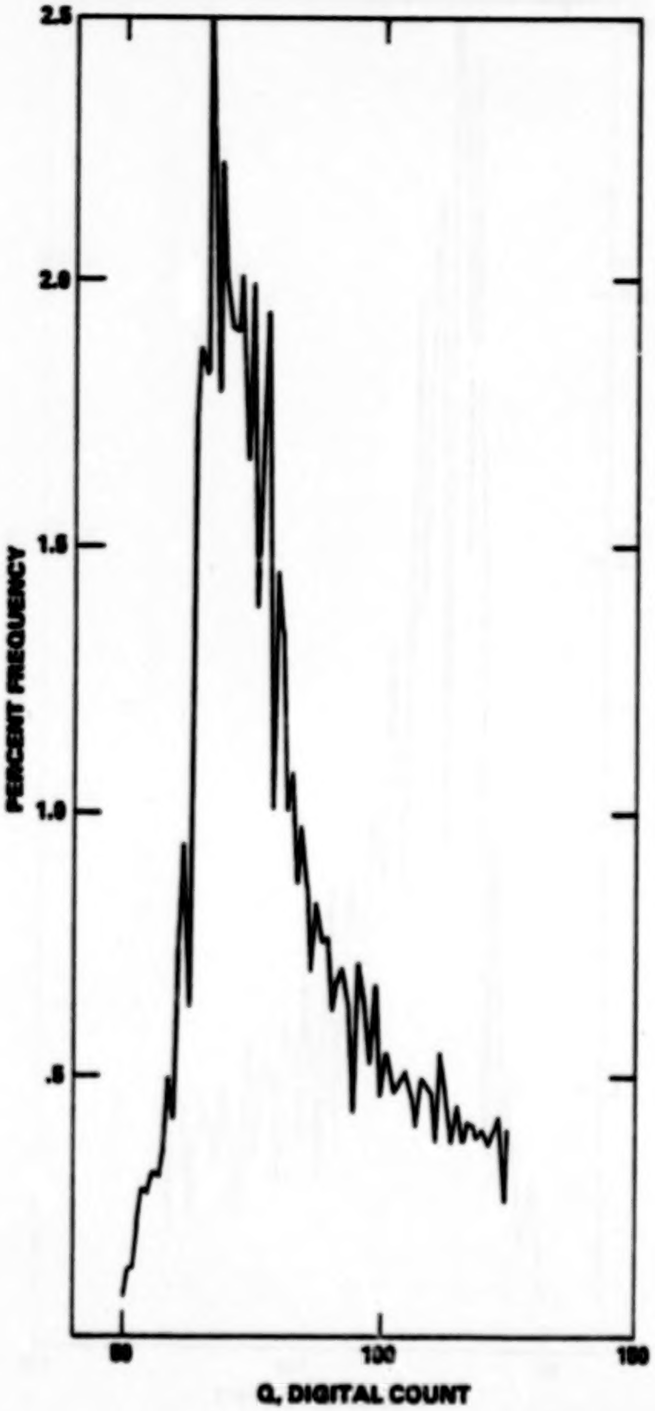

FIGURE 6

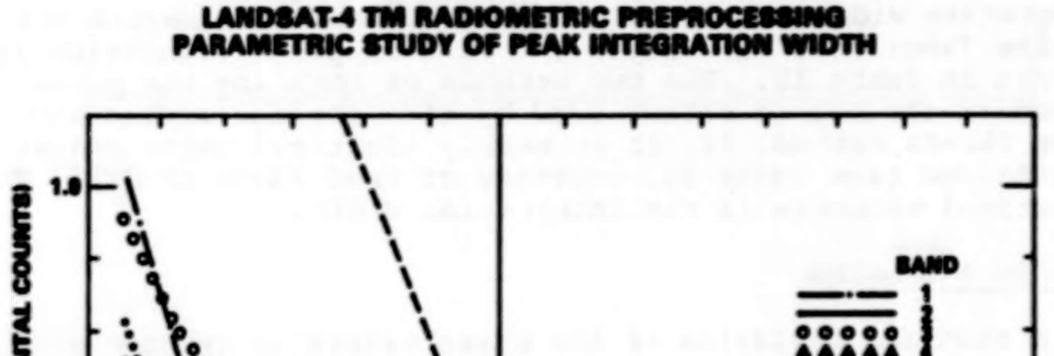
LANDSAT-4 TM RADIOMETRIC PREPROCESSING
PARAMETRIC STUDY OF PEAK INTEGRATION WIDTH
σ, STANDARD DEVIATION OF PULSE (DIGITAL COUNTS)
1.0
0.5
0
0
30
70
PULSE INTEGRATION WIDTH (MINOR FRAMES)
BAND
1
2
3
4
5
7
CHANNEL 9
LAMPSTATE 110
2 NOV 82, D.C.

FIGURE 7

cuts the pulse at the "shoulder" should be noted. As a result of line length variation ($\pm$10 minor frames) and a channel-dependent variation of pulse location of approximately 80 minor frames, pulse truncation cannot be safely avoided with a pulse integration width larger than 45. Integration widths that reduce standard deviation, avoid the pulse "shoulder," and avoid the risk of pulse truncation are given in Table 19. The two methods of locating the pulse center, the Hughes method used by the Scrounge system and the Thresh method, result in nearly identical pulse center locations (see Table 20, courtesy of Fred Alyea of GE). The critical variable is the integration width.

PULSE AVERAGING

The standard deviation of the pulse values is reduced when scans surrounding an IC state transition are eliminated from the pulse average. Tables 21 and 22 give the standard deviations when 2 to 20 scans are excluded from the average following the two types of transition, lamp turn-on and lamp turn-off. After lamp turn-on, there is an initial overshoot involving 1 to 3 scans, followed by a small undershoot involving 1 scan (Figures 8 and A-7 to A-17) before the count level stabilizes. Following lamp turn-off, the heat radiation from the still-hot lamp contributes to the radiance measured in the mid-infrared (IR) (cold focal plane) bands. The heat radiation persists at measurable levels for about 10 scans. Table 23 gives the standard deviations when up to six scans preceding a transition are eliminated from the average. It should be noted that improved results are obtained for cold focal plane channels (1) when four scans are excluded before the sensing of a condition indicating a lamp turn-off transition and (2) when two scans are excluded before the sensing of a lamp turn-on transition. No clear physical explanation for these empirical results is available. Table 24 gives the standard deviations at all eight IC levels obtained using the improved parameters and those obtained using the original parameters to analyze the scene from November 2, 1982, of Washington, D.C.

CALIBRATION

The authors tested a least-square regression analysis using a quadratic relationship between digital counts and radiance:

$$Q = a + bR + dR^2$$

TABLE 19

POSTLAUNCH RADIOMETRIC CALIBRATION
TM LANDSAT-4

IMPROVED PARAMETERS

BAND[a]	PULSE WIDTH (MINOR FRAMES)	SCANS[b] AT END (MINOR FRAMES)	SCANS[c] AT BEGINNING (MINOR FRAMES)
1O	39	2	4
1E	41	2	4
2O	41	2	4
2E	41	2	4
3O	37	2	4
3E	35	2	4
4O	39	2	4
4E	41	2	4
5O	39	4	10
5E	39	4	8
7O	33	4	14
7E	33	4	12

NOTES:

[a] O = ODD DETECTORS; E = EVEN DETECTORS.

[b] SCANS TO DROP FROM AVERAGE AT END OF PLATEAU, i.e., BEFORE A TRANSITION.

[c] SCANS TO DROP FROM AVERAGE AT BEGINNING OF PLATEAU, i.e., AFTER A TRANSITION

TABLE 20

CENTER INDICES FOR FORWARD SCANS USING THRESH AND HUGHES ALGORITHMS[a]

THRESH (RELATIVE mf)	HUGHES (RELATIVE mf)
115.000	115.500
116.000	116.500
116.000	116.500
115.000	115.500
116.000	116.500
115.500	116.000
115.000	115.500
115.500	116.000
116.000	116.500
116.000	116.500
116.000	116.500
116.500	117.000
117.000	117.000
116.500	116.500
116.500	116.500
116.000	116.500
115.000	116.500
116.000	116.500
116.500	117.000

[a] INFORMATION USED IN THIS TABLE WAS GENERATED BY FRED ALYEA AND ERIC BEYER OF GENERAL ELECTRIC COMPANY.

TABLE 21

POSTLAUNCH RADIOMETRIC CALIBRATION — TM LANDSAT-4 STANDARD DEVIATION vs. NUMBER OF SCANS DROPPED AFTER A LAMP TURN-ON TRANSITION

STATE 110, D.C., NOVEMBER 2, 1982

BAND[a]	SCAN									
	2	4	6	8	10	12	14	16	18	20
1O	0.53	0.53	0.53	0.53	0.53	0.53	0.53	0.54	0.51	0.52
1E	0.53	0.55	0.55	0.56	0.55	0.55	0.55	0.52	0.52	0.53
2O	0.28	0.28	0.28	0.28	0.27	0.27	0.27	0.27	0.27	0.28
2E	0.32	0.31	0.31	0.31	0.31	0.31	0.31	0.30	0.30	0.31
3O	0.42	0.41	0.41	0.41	0.39	0.40	0.39	0.40	0.40	0.42
3E	0.32	0.30	0.30	0.30	0.30	0.29	0.30	0.30	0.30	0.30
4O	1.14	1.13	1.12	1.12	1.12	1.11	1.09	1.12	1.12	1.13
4E	0.6[illegible]	0.59	0.58	0.58	0.59	0.59	0.60	0.60	0.60	0.61
5O	0.58	0.35	0.28	0.27	0.27	0.26	0.26	0.27	0.27	0.27
5E	0.81	0.46	0.38	0.36	0.34	0.34	0.34	0.34	0.34	0.34
7O	1.04	0.66	0.51	0.47	0.47	0.44	0.45	0.46	0.46	0.45
7E	1.23	0.74	0.54	0.47	0.43	0.43	0.40	0.40	0.39	0.40

NOTE:

[a] O – ODD DETECTORS; E – EVEN DETECTORS.

TABLE 22

POSTLAUNCH RADIOMETRIC CALIBRATION — TM LANDSAT-4 STANDARD DEVIATION vs. NUMBER OF SCANS DROPPED AFTER A LAMP TURN-OFF TRANSITION

STATE 110, D.C., NOVEMBER 2, 1982

BAND[a]	SCAN									
	2	4	6	8	10	12	14	16	18	20
1O	0.57	0.57	0.57	0.58	0.59	0.60	0.60	0.61	0.61	0.62
1E	0.70	0.69	0.70	0.70	0.71	0.71	0.68	0.69	0.67	0.62
2O	0.83	0.63	0.63	0.63	0.62	0.63	0.64	0.63	0.61	0.61
2E	0.70	0.60	0.61	0.60	0.60	0.61	0.61	0.60	0.61	0.62
3O	0.45	0.34	0.34	0.34	0.35	0.34	0.32	0.32	0.33	0.30
3E	0.41	0.31	0.31	0.30	0.30	0.30	0.29	0.28	0.28	0.28
4O	1.26	1.28	1.29	1.29	1.14	1.15	1.15	1.14	1.15	1.15
4E	0.68	0.62	0.62	0.62	0.63	0.61	0.61	0.61	0.62	0.62
5O	0.43	0.42	0.42	0.43	0.43	0.44	0.45	0.46	0.45	0.44
5E	0.58	0.57	0.57	0.57	0.57	0.55	0.56	0.55	0.56	0.57
7O	0.49	0.49	0.50	0.49	0.49	0.50	0.50	0.49	0.50	0.50
7E	0.48	0.46	0.45	0.45	0.46	0.46	0.46	0.46	0.46	0.45

NOTE:

[a] O – ODD DETECTORS; E – EVEN DETECTORS.

POSTLAUNCH RADIOMETRIC CALIBRATION — TM LANDSAT-4
TM1 CHANNEL 9 ID = 40109—15140 PULSE VALUES

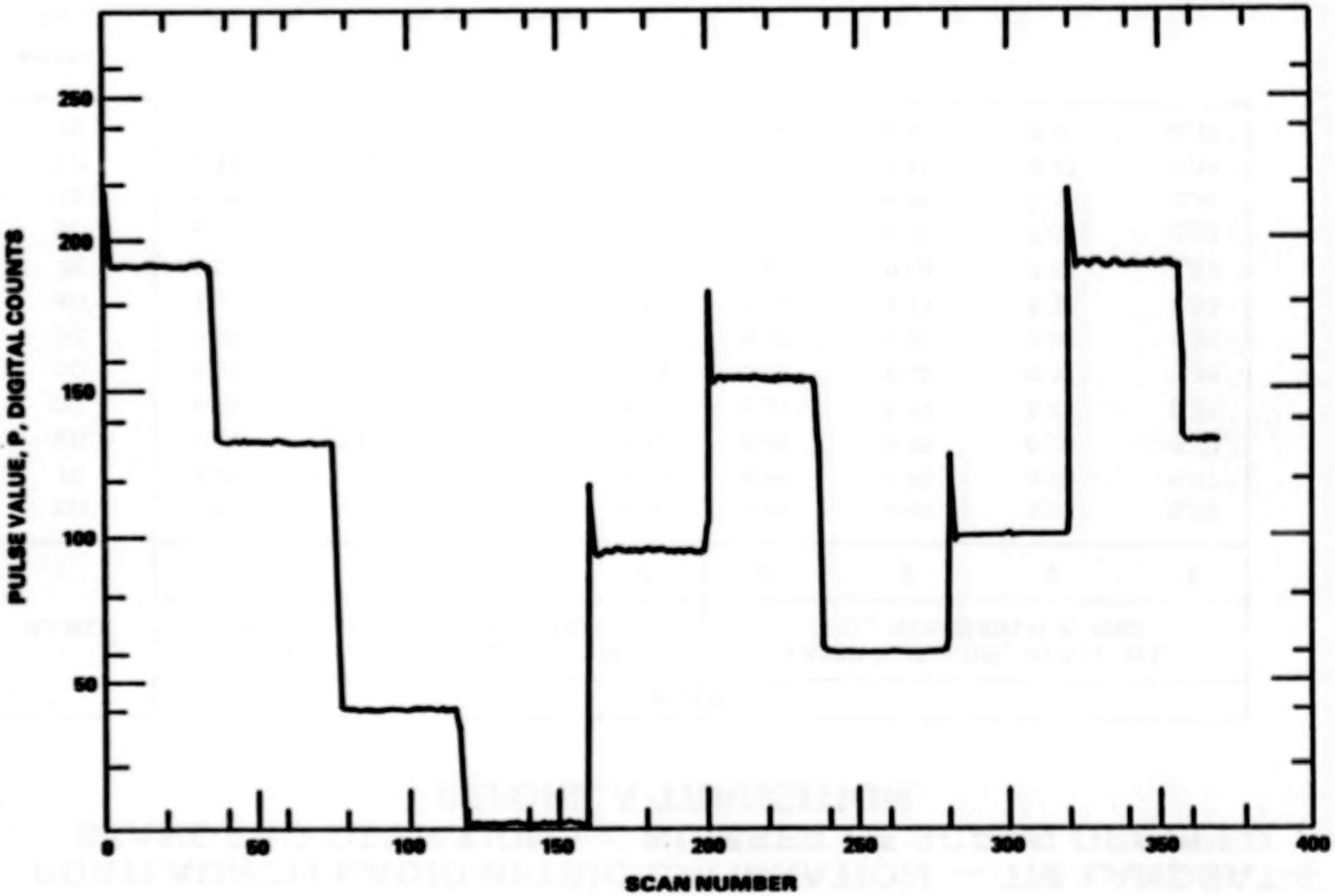

FIGURE 8

TABLE 23

POSTLAUNCH RADIOMETRIC CALIBRATION — TM LANDSAT-4 STANDARD DEVIATION vs. NUMBER OF SCANS DROPPED BEFORE A TRANSITION

BAND[a]	SCAN							
	LAMP TURN-OFF, STATE 110, D.C., NOVEMBER 2, 1982				LAMP TURN-ON, STATE 011, D.C., NOVEMBER 2, 1982			
	0	2	4	6	0	2	4	6
1O	0.58	0.58	0.58	0.55	0.55	0.54	0.53	0.53
1E	0.69	0.69	0.70	0.70	0.56	0.55	0.56	0.57
2O	0.63	0.63	0.63	0.64	0.28	0.28	0.28	0.27
2E	0.59	0.59	0.60	0.59	0.31	0.32	0.31	0.31
3O	0.34	0.34	0.34	0.34	0.40	0.40	0.41	0.41
3E	0.30	0.30	0.30	0.30	0.30	0.30	0.30	0.31
4O	1.30	1.30	1.29	1.28	1.13	1.11	1.12	1.13
4E	0.62	0.62	0.62	0.62	0.60	0.58	0.58	0.57
5O	0.71	0.71	0.43	0.43	0.65	0.27	0.27	0.27
5E	0.93	0.93	0.57	0.57	0.87	0.36	0.36	0.36
7O	0.82	0.82	0.49	0.50	0.77	0.46	0.47	0.47
7E	0.74	0.74	0.45	0.46	0.76	0.47	0.47	0.47

NOTE:

[a] O – ODD DETECTORS, E – EVEN DETECTORS.

TABLE 24

COMPARISON OF INITIAL PARAMETERS WITH IMPROVED PARAMETERS

STANDARD DEVIATION OF PULSE VALUES, P

IC STATE[b] \ BAND[a]		1		2		3		4		5		7	
		O^1	I^2	O^1	I^2	O^1	I^2	O^1	I^2	O^1	I^2	O^1	I^2
100	O	0.480	0.224	0.205	0.230	0.291	0.262	0.838	0.244	0.280	0.170	0.235	0.327
	E	0.539	0.524	0.203	0.173	0.222	0.107	0.610	0.171	0.203	0.251	0.207	0.780
	A	0.510	0.424	0.229	0.208	0.267	0.229	0.724	0.208	0.233	0.217	0.301	0.297
110	O	0.582	0.347	0.631	0.283	0.348	0.335	1.289	0.734	0.432	0.379	0.480	0.483
	E	0.703	0.540	0.601	0.348	0.306	0.270	0.623	0.733	0.678	0.480	0.458	0.489
	A	0.642	0.448	0.616	0.316	0.327	0.302	0.958	0.733	0.600	0.417	0.470	0.478
010	O	0.551	0.248	0.472	0.211	0.252	0.278	0.301	0.238	0.294	0.213	0.342	0.271
	E	0.580	0.498	0.435	0.238	0.255	0.242	0.290	0.101	0.324	0.243	0.289	0.289
	A	0.565	0.373	0.453	0.221	0.253	0.260	0.308	0.211	0.298	0.228	0.316	0.281
011	O	0.587	0.253	0.529	0.214	0.304	0.294	0.508	0.244	0.351	0.273	0.305	0.305
	E	0.604	0.475	0.495	0.247	0.201	0.217	0.387	0.101	0.404	0.318	0.308	0.304
	A	0.600	0.364	0.512	0.230	0.282	0.251	0.446	0.218	0.380	0.293	0.301	0.300
111	O	0.642	2.052	0.531	0.321	0.370	1.292	0.884	1.020	0.686	0.329	0.557	0.643
	E	0.918	1.702	0.688	1.498	0.405	1.135	0.634	1.140	0.682	0.518	0.584	0.587
	A	0.780	1.907	0.614	0.908	0.388	0.721	0.780	0.780	0.680	0.428	0.570	0.605
101	O	0.537	0.381	0.280	0.285	0.410	0.280	1.117	0.243	0.270	0.280	0.471	0.437
	E	0.565	0.580	0.311	0.219	0.308	0.214	0.588	0.105	0.308	0.323	0.477	0.433
	A	0.551	0.434	0.295	0.252	0.358	0.298	0.582	0.219	0.322	0.293	[illegible]	0.435
001	O	0.482	0.585	0.227	0.220	0.280	0.244	0.440	0.341	0.174	0.145	0.310	0.274
	E	0.628	0.616	0.188	0.167	0.295	0.283	0.471	0.313	0.220	0.280	0.253	0.218
	A	0.545	0.580	0.280	0.193	0.292	0.284	0.455	0.327	0.190	0.170	0.282	0.248
000	O	0.428	0.413	0.142	0.141	0.218	0.219	0.197	0.198	0.120	0.112	0.108	0.105
	E	0.585	0.575	0.121	0.118	0.208	0.201	0.230	0.235	0.162	0.147	0.107	0.100
	A	0.508	0.494	0.131	0.129	0.211	0.210	0.218	0.218	0.137	0.131	0.110	0.102

[a] O - ORIGINAL PARAMETERS, I - IMPROVED PARAMETERS.

[b] O - ODD CHANNELS, E - EVEN CHANNELS, A - ALL CHANNELS.

where R represents spectral radiance and Q represents digital counts. The resulting error of estimate (Table 25) was about 30 percent higher in every band than the error of estimate obtained using the linear relationship:

$$Q = a + bR$$

Because the relationship of input spectral radiance (R) to the output digital count (Q) is linear, gain can be calculated using only a single lamp state and background data. Table 26 gives the change in gain (in ppt) using only a single lamp state and background relative to using all eight IC lamp states for March 9, 1982, prelaunch data. Table 27 gives the results for postlaunch data collected over Washington, D.C., on November 2, 1982. In both data sets, gain changes associated with lamp 3 are significantly higher than those associated with lamps 1 and 2. These data point to inaccuracies in the prelaunch radiometric calibration of lamp 3.

An examination of pulse values shows that the channels in band 4 saturate in IC state 111. Radiance values for IC state 111 in band 4 obtained in the prelaunch calibration are thus in error, and IC state 111 should not be included in the linear regressions for the band 4 channels.

NET IMAGE

Because the upper limits of noise in the image are comparable to background noise, it was hoped that more precise image radiance measurements could be obtained by using net values. Background readings, however, are available only during scan mirror turnaround. Experimentation with net images based on background readings at two different places in the cycle showed net images in both instances to be as noisy as the overall uncorrected image. Tables 28 and 29 compare the standard deviations, over a scene, of net and gross image readings from prelaunch flooding lamp data and postlaunch data over the Boston harbor (September 10, 1982). Other workers have found, however, that the use of a separate background for each image line, as opposed to a scene-averaged bias for each channel in the calibration process, reduces striping (private communication, D. Fischel, GSFC, and J. Kogut, Research Data Corporation). Of course, the background sample applied to the image needs to be approximately the same as the actual background level present during imaging. To obtain the best estimate of actual background, it is desirable to select background from two regions, one on each side of the image. Because the background level is adjusted during DC restore, the background collect windows need to be located so that DC restore

TABLE 25

POSTLAUNCH RADIOMETRIC CALIBRATION — TM LANDSAT-4

REGRESSION ANALYSIS ERROR OF ESTIMATE

	TM 1	TM 2	TM 3	TM 4	TM 5	TM 7
LINEAR[a]	0.60	0.67	0.65	0.97	0.22	0.35
QUADRATIC[a]	0.95	1.06	1.01	1.53	0.34	0.54

NOTE:

[a] D.C., NOVEMBER 2, 1982, ID = 4010915140.

TABLE 26

PRELAUNCH RADIOMETRIC CALIBRATION — TM LANDSAT-4

CHANGE IN GAIN (ppt)* FOR CALIBRATION WITH A SINGLE LAMP PRELAUNCH DATA, MARCH 9, 1982

IC STATE USED	BAND	1	2	3	4	5	7
001	ODD	37	31	38	36	−0.7	9
	EVEN	41	27	33	32	12	22
010	ODD	16	−5.4	14	6.2	2	12
	EVEN	17	−6.1	19	−14	0.1	17
100	ODD	−2.6	−3.8	−8.0	−4.4	3.7	−1.3
	EVEN	−3.2	−2.4	−13	8.7	3.0	−13

*REFERENCE: MARCH 9, 1982, PRELAUNCH DATA USING ALL EIGHT IC STATES.

TABLE 27

POSTLAUNCH RADIOMETRIC CALIBRATION — TM LANDSAT-4

CHANGE IN GAIN (ppt)* FOR CALIBRATION WITH A SINGLE LAMP D.C., NOVEMBER 2, 1982

IC STATE USED	BAND	1	2	3	4	5	7
001	ODD	37	41	43	47	8.6	20
	EVEN	38	28	36	40	20	27
010	ODD	5.1	−14	0.6	−1.9	−3.2	−7.1
	EVEN	4.6	−14	6.2	−2.3	−4.9	−0.7
100	ODD	−4.4	−2.2	−5.4	1.2	−4.1	3.2
	EVEN	−5.1	−1.7	−8.6	13	3.6	−4.7

*REFERENCE: D.C., NOVEMBER 2, 1982, WITH ALL EIGHT IC STATES USED IN CALIBRATION.

TABLE 28

PRELAUNCH RADIOMETRIC CALIBRATION — TM LANDSAT-4

STANDARD DEVIATION OF IMAGE DATA (FLOODING LAMP)
(DIGITAL COUNTS)

BAND[a]	GROSS ALL SCANS	GROSS FORWARD SCANS	NET[b] ALL SCANS	NET[c] FORWARD SCANS
1O	1.45	1.44	1.28	1.48
1E	1.50	1.49	1.41	1.51
2O	0.61	0.60	0.59	0.62
2E	0.68	0.69	0.67	0.69
3O	0.86	0.88	0.83	0.89
3E	0.95	0.96	0.93	0.98
4O	0.48	0.48	0.48	0.48
4E	0.53	0.53	0.52	0.53
5O	1.19	1.19	1.19	1.20
5E	1.19	1.19	1.18	1.21
7O	1.40	1.66	1.66	1.68
7E	1.53	1.40	1.40	1.56

NOTES:

[a] O = ODD DETECTORS; E = EVEN DETECTORS.

[b] IMAGE SCAN N – BACKGROUND SCAN N.

[c] IMAGE FORWARD SCAN N – BACKGROUND REVERSE SCAN N–1.

TABLE 29

POSTLAUNCH RADIOMETRIC CALIBRATION — TM LANDSAT-4

STANDARD DEVIATION OF IMAGE DATA, BOSTON WATER SCENE, SEPTEMBER 10, 1982 (DIGITAL COUNTS)

BAND[a]	GROSS ALL SCANS	GROSS FORWARD SCANS	NET[b] ALL SCANS	NET[c] FORWARD SCANS
1O	1.51	1.46	1.47	1.46
1E	1.72	1.68	1.60	1.67
2O	0.59	0.58	0.58	0.58
2E	0.66	0.65	0.65	0.65
3O	0.84	0.81	0.80	0.83
3E	0.94	0.96	0.93	0.98
4O	0.46	0.46	0.47	0.46
4E	0.46	0.46	0.47	0.46
5O	0.92	0.93	0.93	0.93
5E	0.84	0.85	0.84	0.86
7O	1.13	1.12	1.11	1.16
7E	1.06	1.05	1.05	1.08

NOTES:

[a] O = ODD DETECTORS; E = EVEN DETECTORS.

[b] IMAGE SCAN N – BACKGROUND SCAN N.

[c] IMAGE FORWARD SCAN N – BACKGROUND REVERSE SCAN N–1.

does not occur between the background window and the image to which the background is applied. Table 30 gives the present collect windows and proposed windows for achieving this goal. The locations for the proposed windows were derived using information from the scan timeline presented in Barker, Abrams, et al. (1984).

SEPARATE PROCESSING FOR FORWARD AND REVERSE SCANS

Differences in forward and reverse calibration data arise primarily from calibration pulse shape and pulse integration techniques (Barker, Abrams, et al., 1984). The pulse in band 4 (Figure 9) is shaped like a right triangle on top of a rectangle. The pulse center is located so far from the pulse peak that a small variation in pulse shape could cause some of the minor frames near the pulse peak to fall outside the pulse integration region. The use of a wider pulse integration width reduces differences in forward and reverse calibration pulse values (Tables 31 and 32). The magnitude of forward-reverse differences in calibration pulse in band 4 (from 0 to 4 counts) is highly variable as a result of sensitivity to small changes in pulse shape. Figures 10 and 11 show the forward-reverse pulse differences for the 100 IC state, band 4, channel 9, in the March 9, 1982, prelaunch data and the D.C., November 2, 1982, postlaunch data. A secondary cause of calibration pulse forward-reverse differences possibly results from a gradual drift in the background counts during a scan.

Differences in forward and reverse background values, averaged over a scene, tend to vary widely (Table 33) but are occasionally as high as a count. The source of the differences must be investigated. One possible explanation is the gradual drift in the background mentioned above. Another explanation is that background data were collected from the section of the scan cycle where background levels are unstable. This region, known as DC restore, is the region in which the TM restores the background toward the nominal value of 2 digital counts.

Prelaunch flooding lamp data collected from 52 minor frames in the middle of the scan show, as expected, only small (less than 0.35 digital count) forward and reverse differences (Table 34). Forward-reverse differences in postlaunch image data arise from variations in the background discussed above. Table 35 gives forward-reverse differences taken from 512 minor frames of B data (Barker, Gunther, et al., 1984).

TABLE 30

BACKGROUND COLLECT WINDOWS (52 MINOR FRAMES WIDE)

PERIOD	FIRST COLLECT		SECOND COLLECT	
	FORWARD SCAN (MINOR FRAMES)	REVERSE SCAN (MINOR FRAMES)	FORWARD SCAN (MINOR FRAMES)	REVERSE SCAN MINOR FRAMES)
LAUNCH TO PRESENT	6543 (52)	7069 (52)	—	—
PROPOSED	6469 (24)	6749 (28)	6925 (28)	7205 (24)

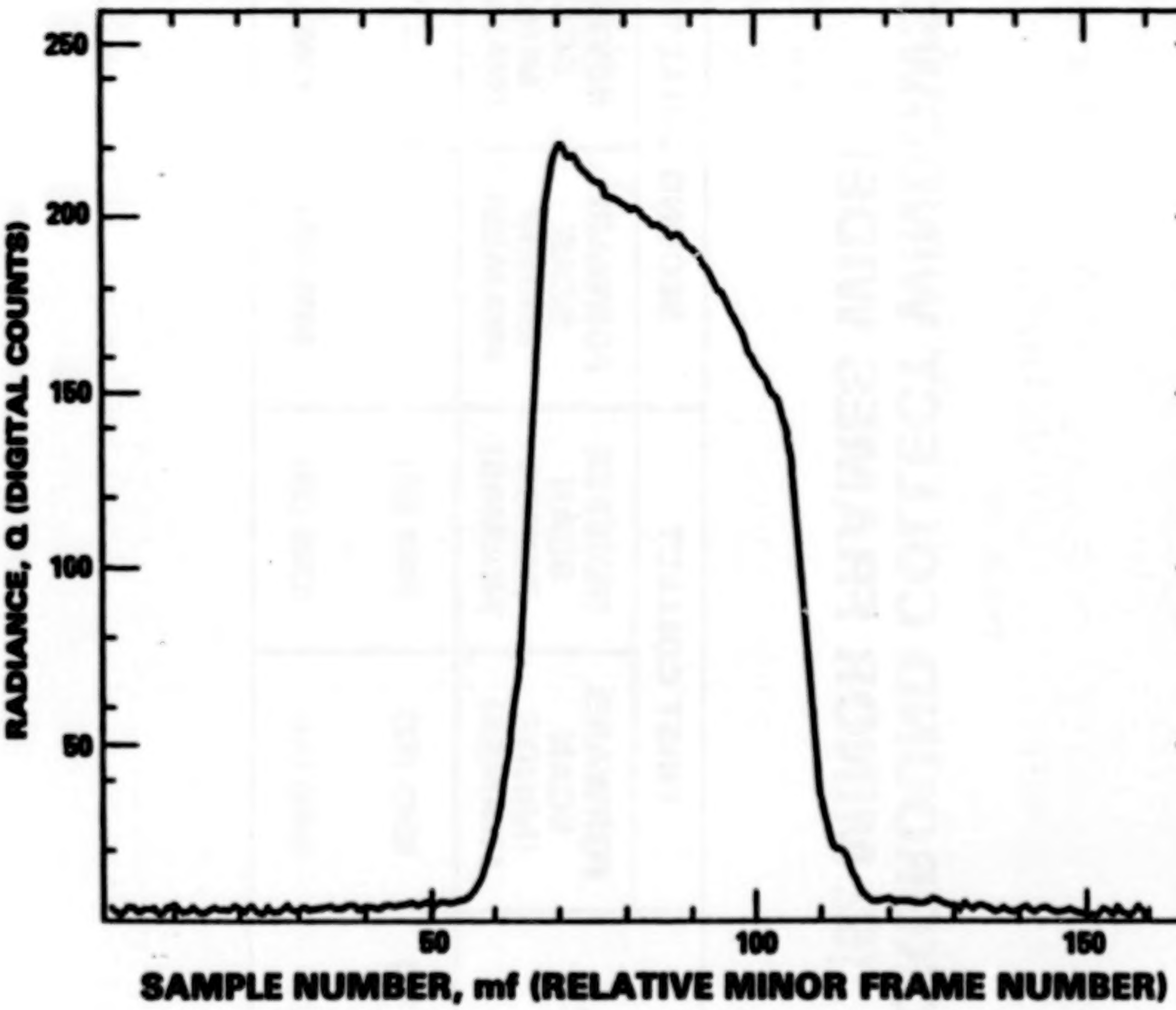

RADIOMETRIC CALIBRATION — TM LANDSAT-4
TM4 CHANNEL 8 FORWARD SCAN, MARCH 9, 1982, VACUUM

FIGURE 9

TABLE 31

DIFFERENCE BETWEEN FORWARD AND REVERSE AVERAGES (DIGITAL COUNTS)

D.C., NOVEMBER 2, 1982 — USING STANDARD PARAMETERS

		TM 1	TM 2	TM 3	TM 4	TM 5	TM 7
CHANNEL	1	—	−0.74	0.62	1.86	0.67	0.96
	2	−0.06	−0.13	0.10	0.08	0.83	0.91
	3	0.28	0.29	0.30	1.88	—	−0.03
	4	0.29	−0.09	0.13	0.38	0.06	0.12
	5	0.25	0.15	0.22	1.49	−0.09	—
	6	0.29	−0.06	−0.06	0.67	−0.12	0.03
	7	0.37	0.15	0.30	1.30	−0.14	0.54
	8	0.20	0.13	0.12	0.54	−0.10	−0.06
	9	0.29	0.22	0.13	1.36	−0.08	−0.09
	10	0.32	−0.18	0.09	0.18	−0.23	−0.07
	11	0.37	0.13	0.19	1.45	−0.10	−0.08
	12	0.01	0.04	0.00	0.36	−0.26	−0.06
	13	0.27	0.04	0.15	1.52	−0.17	−0.21
	14	0.11	−0.32	−0.02	0.70	−0.41	−0.18
	15	0.62	0.04	0.04	1.24	−0.22	−0.49
	16	0.11	−0.20	0.01	0.62	−0.34	−0.21
	MEANODD	0.04	0.03	0.24	1.53	−0.02	0.07
	MEANEVN	0.15	−0.10	0.04	0.52	−0.07	0.05
	MEANALL	0.10	−0.03	0.14	1.02	−0.05	0.06
	MEANODD SD	0.88	0.32	0.17	0.26	0.30	0.46
	MEANEVN SD	0.14	0.14	0.07	0.18	0.39	0.36
	MEANALL SD	0.61	0.25	0.16	0.58	0.34	0.40
	MEAN SPSD	0.15	0.06	0.04	0.14	0.09	0.10

TABLE 32

DIFFERENCE BETWEEN FORWARD AND REVERSE AVERAGES (DIGITAL COUNTS)

D.C., NOVEMBER 2, 1982 — USING OPTIMIZED PARAMETERS

		TM 1	TM 2	TM 3	TM 4	TM 5	TM 7
CHANNEL	1	—	−0.06	−0.05	0.00	0.01	0.00
	2	0.36	0.04	0.03	0.23	0.00	0.06
	3	0.55	0.27	0.17	0.47	—	−0.06
	4	0.40	−0.30	0.10	0.17	0.12	0.07
	5	0.41	0.11	0.10	0.23	−0.06	−0.04
	6	0.00	0.04	−0.01	0.12	−0.10	0.02
	7	0.52	0.06	0.10	0.23	−0.15	0.42
	8	0.38	0.01	0.05	0.05	−0.10	−0.08
	9	0.48	0.00	0.13	0.38	−0.14	−0.13
	10	0.44	−0.15	−0.02	0.04	−0.28	−0.14
	11	0.48	—	—	0.05	−0.16	−0.14
	12	0.07	−0.06	−0.03	0.03	0.26	−0.09
	13	0.51	−0.04	−0.02	−0.03	−0.23	−0.23
	14	0.16	−0.33	−0.15	−0.05	−0.45	−0.23
	15	0.54	−0.07	−0.04	0.08	−0.14	−0.43
	16	0.11	−0.29	−0.09	−0.15	−0.29	−0.27
	MEANODD	0.44	−0.06	0.04	0.19	−0.04	0.03
	MEANEVN	0.33	−0.13	−0.01	0.05	−0.05	0.01
	MEANALL	0.38	−0.10	0.01	0.12	−0.05	0.02
	MEANODD SD	0.18	0.38	0.09	0.17	−0.29	0.42
	MEANEVN SD	0.29	0.16	0.08	0.12	0.42	0.36
	MEANALL SD	0.19	0.28	0.08	0.16	0.35	0.38
	MEAN SPSD	0.04	0.07	0.02	0.04	0.09	0.09

PRELAUNCH TM LANDSAT-4 RADIOMETRIC CALIBRATION

BETWEEN-LINE VARIABILITY OF IC PULSE
TM4, CHANNEL 9, LAMP 100, MARCH 5, 1982

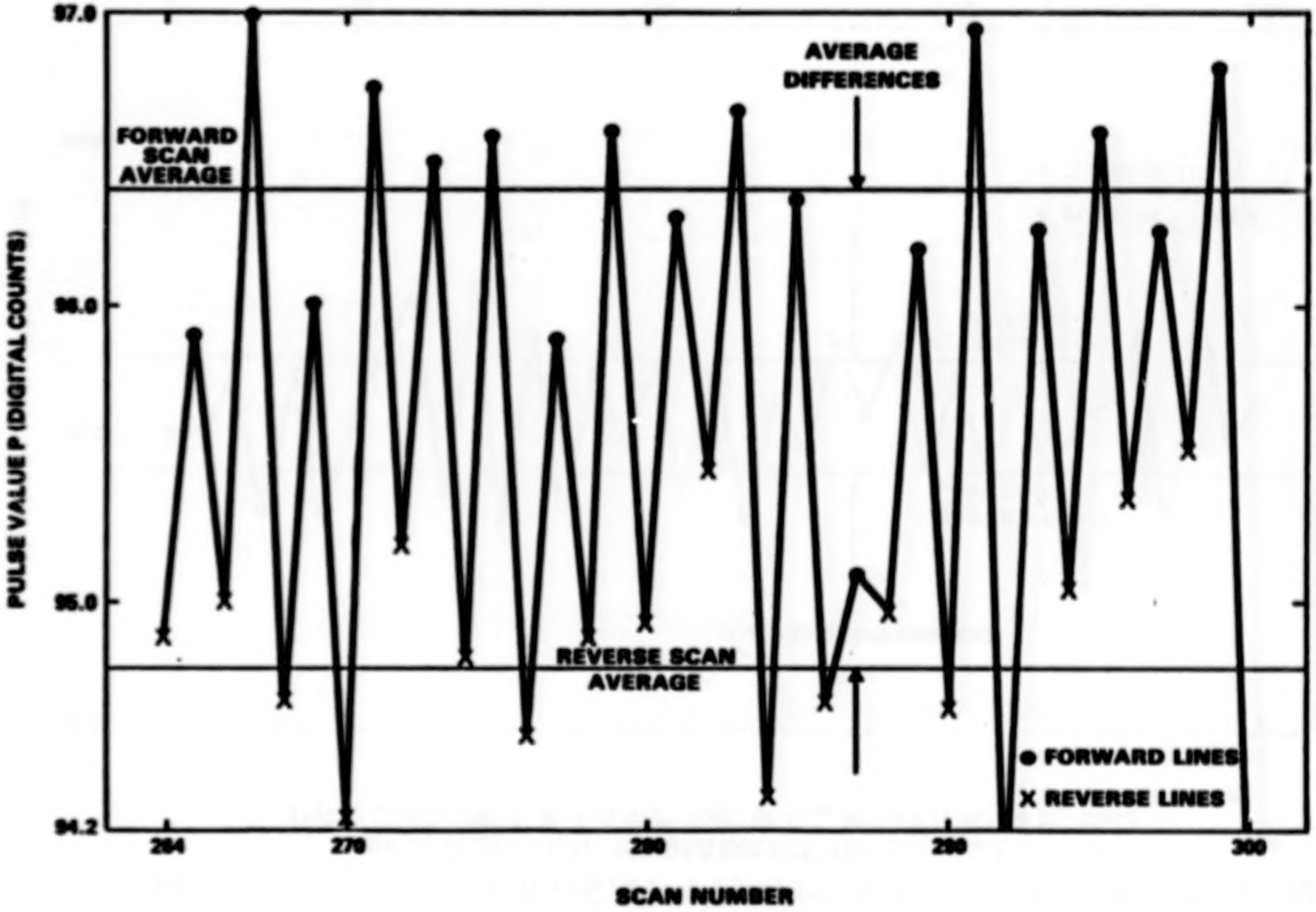

FIGURE 10

POSTLAUNCH TM LANDSAT-4 RADIOMETRIC CALIBRATION

BETWEEN-LINE VARIABILITY OF IC PULSE
TM4, CHANNEL 9, LAMP 100, D.C., NOVEMBER 2, 1982

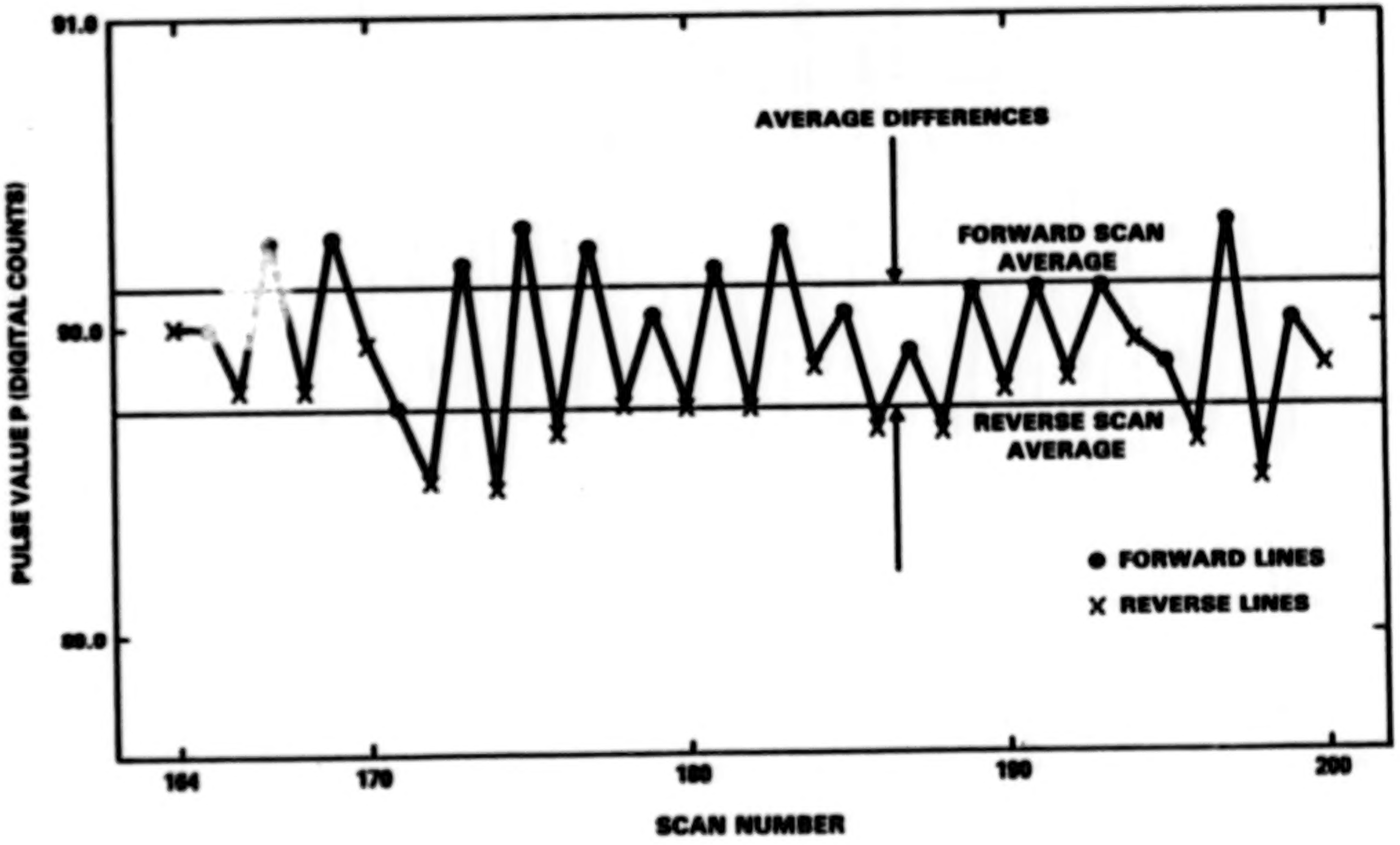

FIGURE 11

TABLE 33

POSTLAUNCH RADIOMETRIC CALIBRATION — TM LANDSAT-4 DIFFERENCE BETWEEN FORWARD AND REVERSE (F-R) BACKGROUND DATA (DIGITAL COUNTS)

BAND[a]	FLOODING LAMP	WATER	NE ARKANSAS	FT. DODGE	D. C.	HAMILTON, MONTANA	FT. PIERCE, FLORIDA
1O	0.08	−0.07	−0.16	−0.54	−1.04	−0.87	−0.56
1E	0.10	−0.04	−0.11	−0.50	−1.01	−0.81	−0.50
2O	0.11	−0.03	0.01	−0.08	−0.22	−0.19	−0.09
2E	0.08	−0.03	0.03	−0.08	−0.22	−0.19	0.02
3O	0.10	−0.00	0.01	−0.04	−0.25	−0.24	0.04
3E	0.13	−0.02	0.07	−0.04	−0.27	−0.27	0.09
4O	0.12	0.55	−0.50	−0.59	−0.07	−0.20	0.33
4E	0.14	0.04	−0.55	−0.04	−0.06	−0.23	0.41
5O	−0.01	−0.03	−0.04	−0.05	−0.04	−0.03	−0.03
5E	−0.02	−0.02	−0.05	−0.04	−0.04	−0.03	−0.02
7O	−0.09	−0.05	−0.04	−0.05	−0.04	−0.03	−0.02
7E	0.02	0.00	−0.04	−0.02	−0.04	−0.02	0.00

NOTE:

[a] O = ODD DETECTORS; E = EVEN DETECTORS.

TABLE 34

PRELAUNCH TM LANDSAT-4 RADIOMETRIC CALIBRATION

AVERAGE DIFFERENCES BETWEEN FORWARD AND REVERSE VIDEO
MIDSCAN
(DIGITAL COUNTS)

BAND \ DATE	2-22-82	2-23-82	3-3-82	3-4-82	3-6-82	3-7-82	3-9-82	3-17-82	3-17-82	3-22-82	4-23-82
1	−0.038	−0.082	−0.112	−0.190	−0.149	−0.092	−0.119	0.056	0.020	0.041	−0.535
2	−0.041	−0.072	−0.175	−0.189	−0.100	−0.083	−0.091	0.033	0.021	0.013	−0.013
3	−0.105	−0.182	−0.349	−0.337	−0.228	−0.213	−0.226	0.025	0.008	0.021	0.046
4	−0.081	−0.112	−0.142	−0.135	−0.118	−0.108	−0.117	0.023	0.012	0.020	0.241
5	—	—	—	—	—	0.015	0.011	—	—	—	—
7	—	—	—	—	—	0.021	0.010	—	—	—	—

TABLE 35

POSTLAUNCH RADIOMETRIC CALIBRATION — TM LANDSAT-4 DIFFERENCE BETWEEN FORWARD AND REVERSE (F-R) IMAGE DATA (DIGITAL COUNTS)

BAND[a]	SCENE						
	FLOODING LAMP	WATER	NE ARKANSAS	FT. DODGE	BOSTON	D. C.	HAMILTON, MONTANA
1O	−0.06	−0.85	−0.27	−0.40	−1.63	−0.71	4.20
1E	−0.10	−0.90	−0.24	−0.40	−1.61	−0.71	3.80
2O	−0.07	−0.10	−0.08	−0.10	−1.07	−0.24	3.11
2E	−0.10	−0.13	0.10	−0.12	−1.09	−0.25	2.97
3O	−0.17	−0.01	0.20	−0.07	−1.42	−0.05	3.78
3E	−0.24	−0.10	0.26	−0.18	−1.48	−0.05	3.61
4O	−0.10	−0.01	−2.80	0.02	−3.28	0.77	3.09
4E	−0.11	0.00	−2.70	−0.24	−3.21	0.72	2.83
5O	0.01	0.01	−0.12	−0.07	−2.70	1.73	0.54
5E	0.00	0.01	−0.09	−0.43	−2.64	1.09	0.54
7O	−0.03	−0.02	0.20	−0.01	−1.33	0.39	0.20
7E	0.03	0.06	0.30	−0.20	−1.15	0.37	0.29

NOTE:

[a] O = ODD DETECTORS; E = EVEN DETECTORS.

These results suggest that the external calibration data should be examined again to obtain separate nominal gains and offsets for forward and reverse scans. In postlaunch processing, forward and reverse calibration pulse data could then be used to generate separate forward and reverse scan radiometric lookup tables (RLUTs).

CONCLUSIONS

It is difficult to separate changes of the channels with time from changes of the IC system with time. As indicated in this study, the channels within a primary plane band change gain as a self-consistent group (within 0.6 percent). The gains of the cold focal plane channels in a given band change as a group relative to a postlaunch reference (within 1.5 percent), but vary widely relative to a prelaunch reference (up to 5 percent in band 5 and up to 3 percent in band 7). The primary focal plane channels decrease in gain during the first 70 days after launch (6 percent in bands 1 and 2, 8 percent in band 3, and 3 percent in band 4), but stabilize in October 1982. Gain in the cold focal plane channels oscillates with time with a variability of up to 7 percent in band 5 and 5 percent in band 7. When a prelaunch reference is used, lamps 1 and 3 behave consistently, but lamp 2 does not. When a postlaunch reference is used, all three lamps are mutually consistent.

The changed relationship of lamp 2 to the other lamps since prelaunch calibration implies that the lamps are not stable with time. On the other hand, the difference in the gain change pattern of the channels in the cold focal plane and those in the primary focal plane would indicate that the observed gain change is due primarily to the changes in the channels. Perhaps in the future it would be desirable to "burn-in" TM before absolute calibration. The cause of the oscillation in gain in the cold focal plane needs to be better understood.

Variations in the background range from 0.5 to 1.27 digital counts. The degree to which this variation is systematically related to the dark current (DC) restore cycle must be investigated. Coherent noise is strongest in band 1, channels 2, 3, 4, 5, 6, 8, 14, and 16, band 3, channels 4 and 8, and band 4, channels 4 and 5, with peak-to-peak amplitudes ranging from 0.7 to 1.4.

RECOMMENDATIONS

Brief recommendations are given below; extensive recommendations are given in the paper by Barker (1984).

GROUND SEGMENT PROCESSING SYSTEM

At present, the continued use of the IC to calibrate is preferred to the use of prelaunch nominal gains and offsets. Because the channels in a band vary as a group, it would be possible to assess the time changes in sensitivity of all the channels in a given band by monitoring a single representative channel with the IC. To improve the use of the IC system in determining gains and offsets, the following procedural changes are recommended:

- Improvement of windows for background extraction to obtain a better estimate of background applicable to an image
- Improvement of the pulse location algorithm so that a few minor frames of partial image data at the edge of the calibration window do not affect results
- Use of a wider, band-dependent pulse integration width
- Exclusion from the averaged pulse value, Q, of the four scans preceding an IC state transition
- Elimination in the regression analysis of the four states involving lamp 3 (001, 101, 011, 111) until calibration data from lamps 1 and 2 can be used to estimate new spectral radiances for these states
- Separate processing of forward and reverse scans

The first five suggestions would be implemented during the Scrounge era; the last is a major change, best implemented under the TM Image Processing System (TIPS).

GROUND SEGMENT DATA ANALYSIS

The degree of uniformity in the shutter flag movement could be evaluated by monitoring the minor frame separation of the channel 1 and channel 16 calibration pulse centers. The separation in minor frames of the calibration pulse centers of the cold focal plane (CFP) channels from the end of the scan line signal would be a sensitive indicator of slight movements in the cold focal plane. IC data could be used to investigate movements of the CFP. IC pulse shape is particularly sensitive to movement of the CFP along the axis defined by the following two planes: (1) the plane of the shutter movement and (2) the plane containing the shutter arm and optical axis of the TM. The location of the pulse (in minor frames) relative to shutter obscuration of the image indicates movement of the CFP in the direction parallel to the shutter movement. Movement of the CFP along the optical axis would be difficult to detect with IC data.

Variations in image data can be used to study variations in the background over a scan. Target variation is removed by computing, for several images, scene-wide averages for each channel in each direction for each horizontal position in the scan. Part of the variation along the scan arises from differences in solar zenith angles for the eastern and western parts of an image. However, because background drift depends on scan direction, and solar illumination is independent of scan direction, these two effects can be separated.

SOFTWARE

A software tool for automatically monitoring Landsat-4 TM data needs to be developed. Quantities to be monitored should include channel gains and offsets, background noise, digital count differences between forward and reverse scans in background and integrated calibration pulse values, and self-consistency checks of the IC states. A suitable program to use as a basis for the TM monitor would be TRAPP, the software analysis tool designed and developed by the authors, which was used to obtain the data presented in this paper. TRAPP also needs to be enhanced to generate a history file. The history file should include the above-mentioned quantities plus additional pertinent data such as instrument temperatures and pulse and background window locations. Further study both to better characterize the radiometric performance of the TM and to determine methods for improving the calibration procedures will increase knowledge of the absolute radiometric values in TM scenes.

FLIGHT SEGMENT OPERATIONS

Scrounge Era

The temperature of various parts of the TM affects channel sensitivity and IC system output. The indium antimonide detectors in the mid-IR bands are sensitive to the shutter flag temperature as well as the temperature of the cold focal plane itself. The IC system output shifts to shorter wavelength with higher lamp filament temperatures. An increase in temperature at the regulatory photodiode in the lamp circuit tends to make the photodiode more sensitive to lamp output and hence to reduce the output of the lamp. To assess the magnitude of the effect of temperature variations on the protoflight TM, the duration of the TM duty cycle should be varied, so that data at different operating temperatures can be collected.

TIPS Era

Gain measured using only lamp 1 and background data agrees with gain measured using all eight IC states within 0.9 percent. The possibility of lamp burnout can be reduced while accuracy is preserved by doing the following: Every pass, leave lamp 1 on and the automatic sequencer off; once a week, turn the automatic sequencer on, and check lamp 1 against the other two lamps.

ACKNOWLEDGMENT

The authors extend a special thanks to Barbara Jeffe for her assistance in programming the TRAPP software package and for supervising the data processing team.

REFERENCES

Barker, J. L., "Relative Radiometric Calibration of Landsat TM Reflective Bands," PROCEEDINGS, LANDSAT-4 SCIENTIFIC CHARACTERIZATION, EARLY RESULTS SYMPOSIUM, Goddard Space Flight Center, Greenbelt, Maryland, April 1984

Barker, J. L., R. B. Abrams, D. L. Ball, and K. C. Leung, "Radiometric Calibration and Processing Procedures," PROCEEDINGS, LANDSAT-4 SCIENTIFIC CHARACTERIZATION EARLY RESULTS SYMPOSIUM, Goddard Space Flight Center, Greenbelt, Maryland, April 1984

--, D. L. Ball, K. C. Leung, and J. A. Walker, "Prelaunch Absolute Radiometric Calibration of the Reflective Band on Landsat-4 Protoflight Thematic Mapper," PROCEEDINGS, LANDSAT-4 SCIENTIFIC CHARACTERIZATION EARLY RESULTS SYMPOSIUM, Goddard Space Flight Center, Greenbelt, Maryland, April 1984

--, F. J. Gunther, R. B. Abrams, and D. L. Ball, "TM Digital Products for Applications," PROCEEDINGS, LANDSAT-4 SCIENTIFIC CHARACTERIZATION EARLY RESULTS SYMPOSIUM, Goddard Space Flight Center, Greenbelt, Maryland, April 1984

Lansing, J. C., and J. L. Barker, "Thermal Band Characterization of Landsat-4 Thematic Mapper," PROCEEDINGS, LANDAST-4 SCIENTIFIC CHARACTERIZATION EARLY RESULTS SYMPOSIUM, Goddard Space Flight Center, Greenbelt, Maryland, April 1984

APPENDIX - SUPPLEMENTAL DATA

The figures and tables presented here provide detailed information that was summarized in the paper. Figures A-1 through A-6 show channel sensitivity as a function of time. Figures A-7 through A-17 show pulse averages versus scan number. Tables A-1 through A-5 give the changes in the pulse averages of the single-lamp states relative to the March 9, 1982, prelaunch reference. Tables A-6 through A-10 provide similar information using the Washington, D.C., November 2, 1982, postlaunch reference. Changes in gain (parts per thousand) on five separate dates relative to March 9, 1982, are given for each channel in bands 2, 5, and 7 in Tables A-11, A-12, and A-13, respectively. Tables A-14 and A-15 give typical background noise in postlaunch and prelaunch data. Table A-16 lists analog-to-digital convertor bin sizes for each digital level in band 1, channel 1.

POSTLAUNCH RADIOMETRIC CALIBRATION—TM LANDSAT-4
TM1 GAIN IN COUNTS/SPECTRAL RADIANCE AS A FUNCTION OF TIME

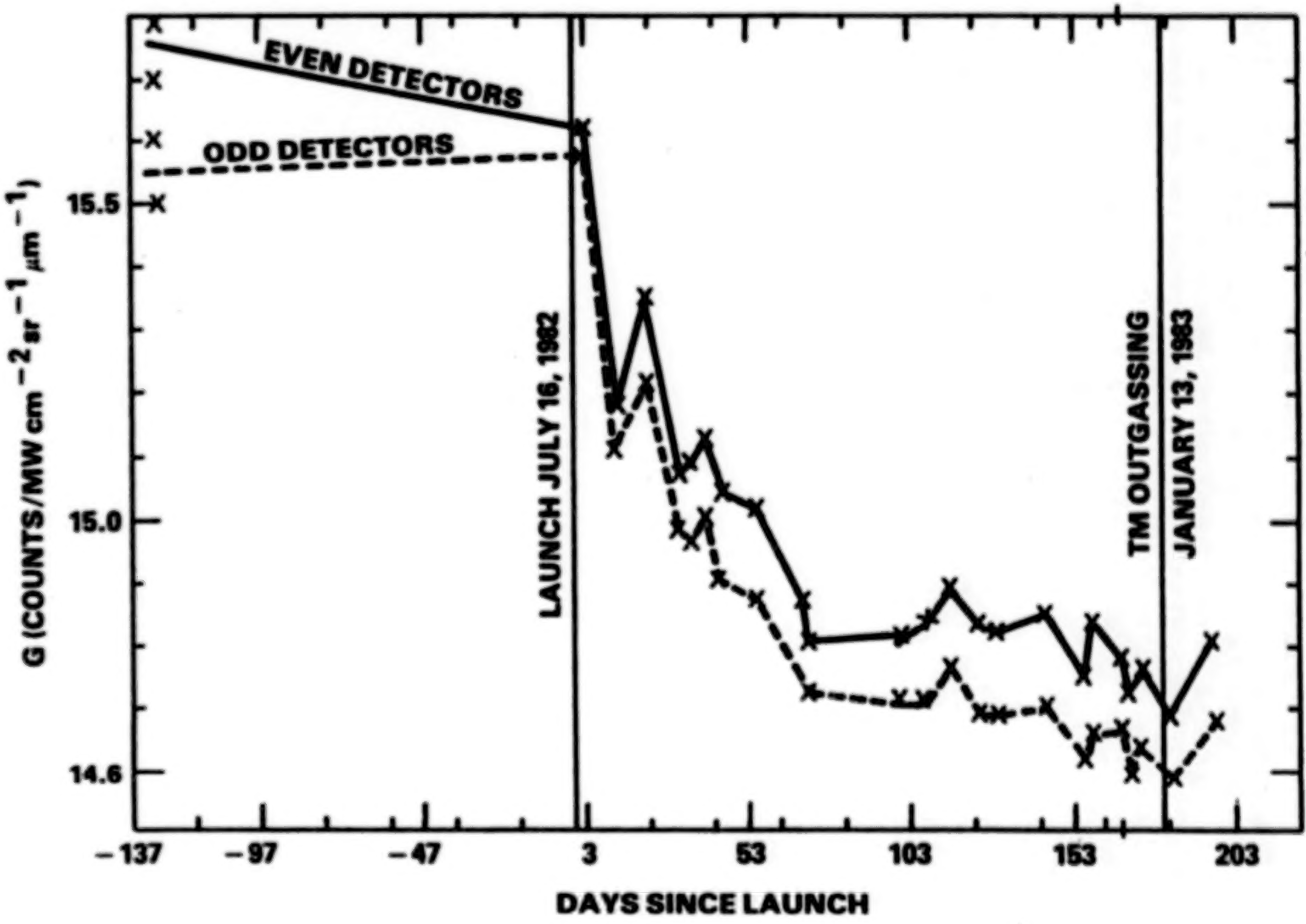

FIGURE A-1

POSTLAUNCH RADIOMETRIC CALIBRATION—TM LANDSAT-4
TM2 GAIN IN COUNTS/SPECTRAL RADIANCE AS A FUNCTION OF TIME

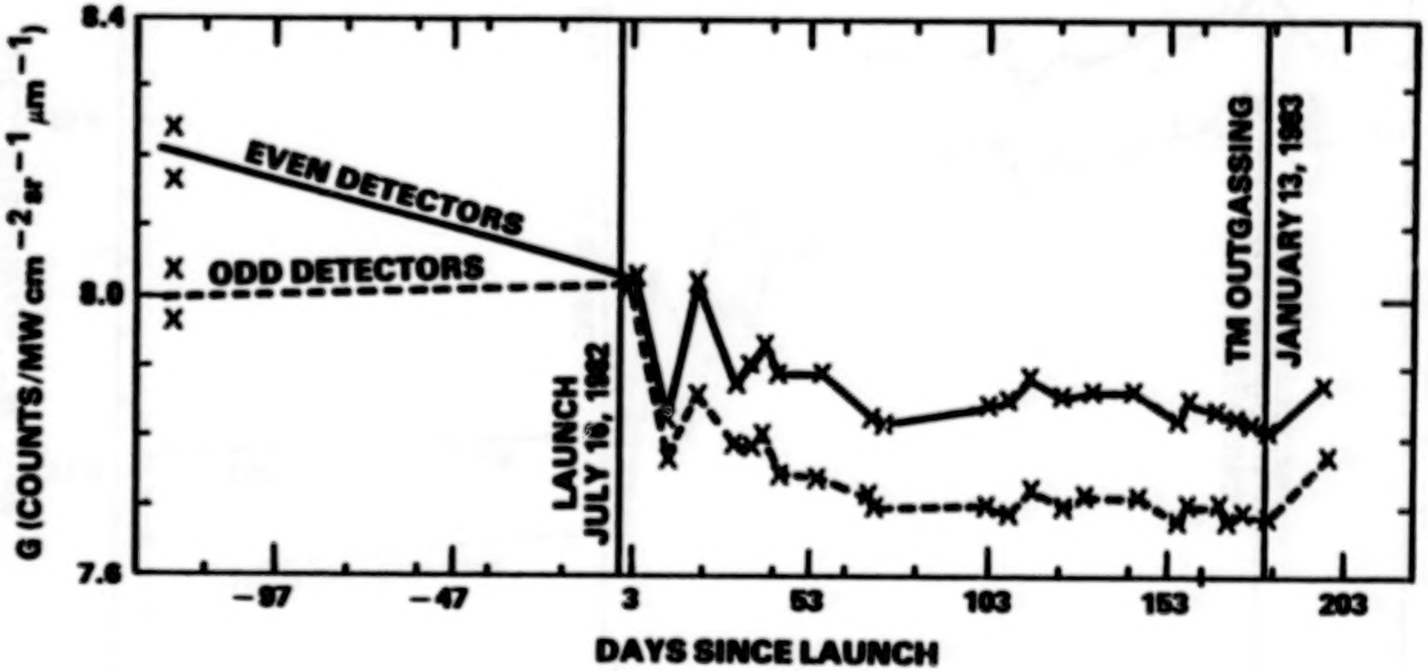

FIGURE A-2

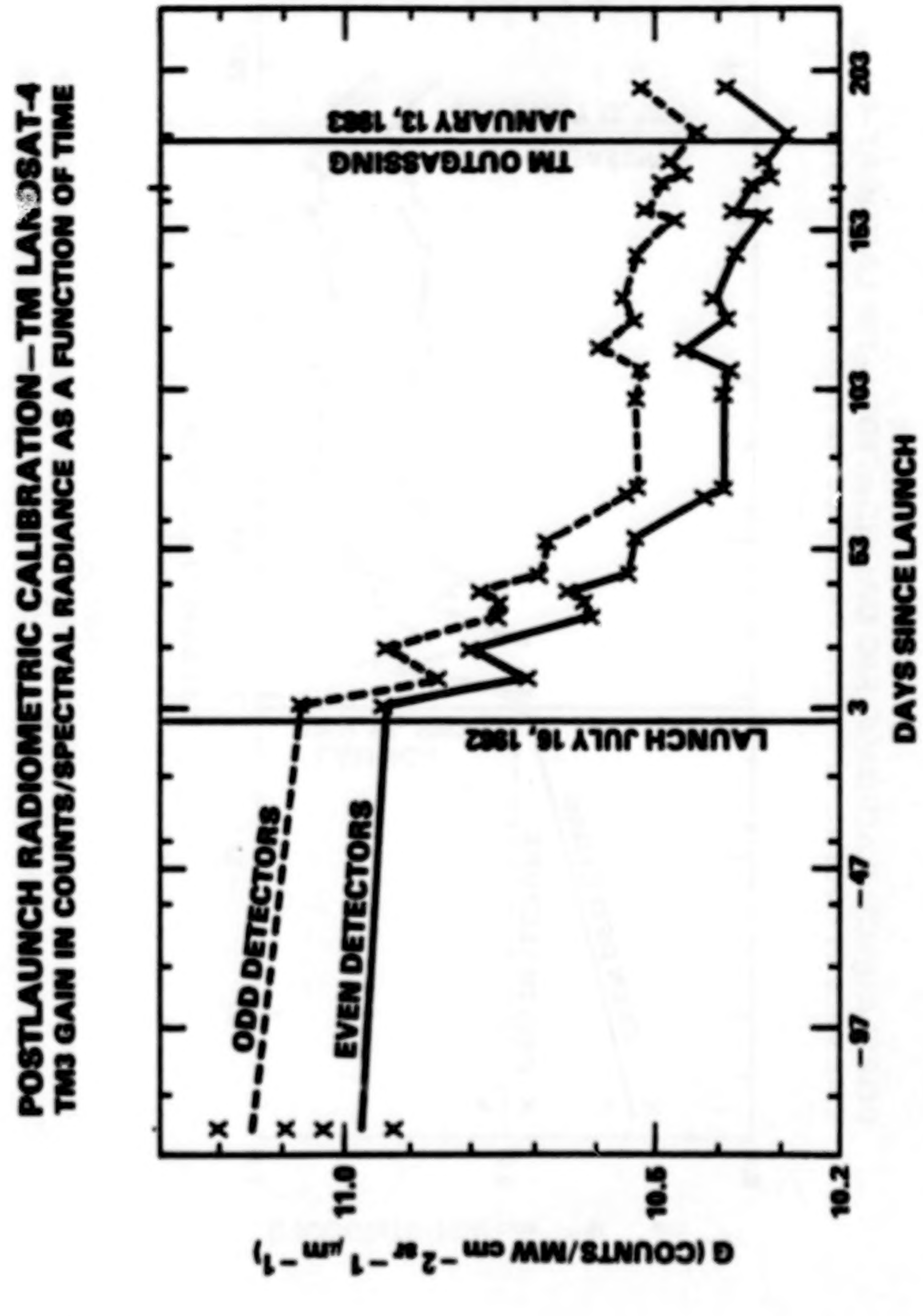
POSTLAUNCH RADIOMETRIC CALIBRATION—TM LANDSAT-4
TM3 GAIN IN COUNTS/SPECTRAL RADIANCE AS A FUNCTION OF TIME
G (COUNTS/MW cm^{-2}sr^{-1}μm^{-1})
11.0
10.5
10.2
ODD DETECTORS
EVEN DETECTORS
LAUNCH JULY 16, 1982
TM OUTGASSING
JANUARY 13, 1983
−97
−47
3
53
103
153
203
DAYS SINCE LAUNCH

FIGURE A-3

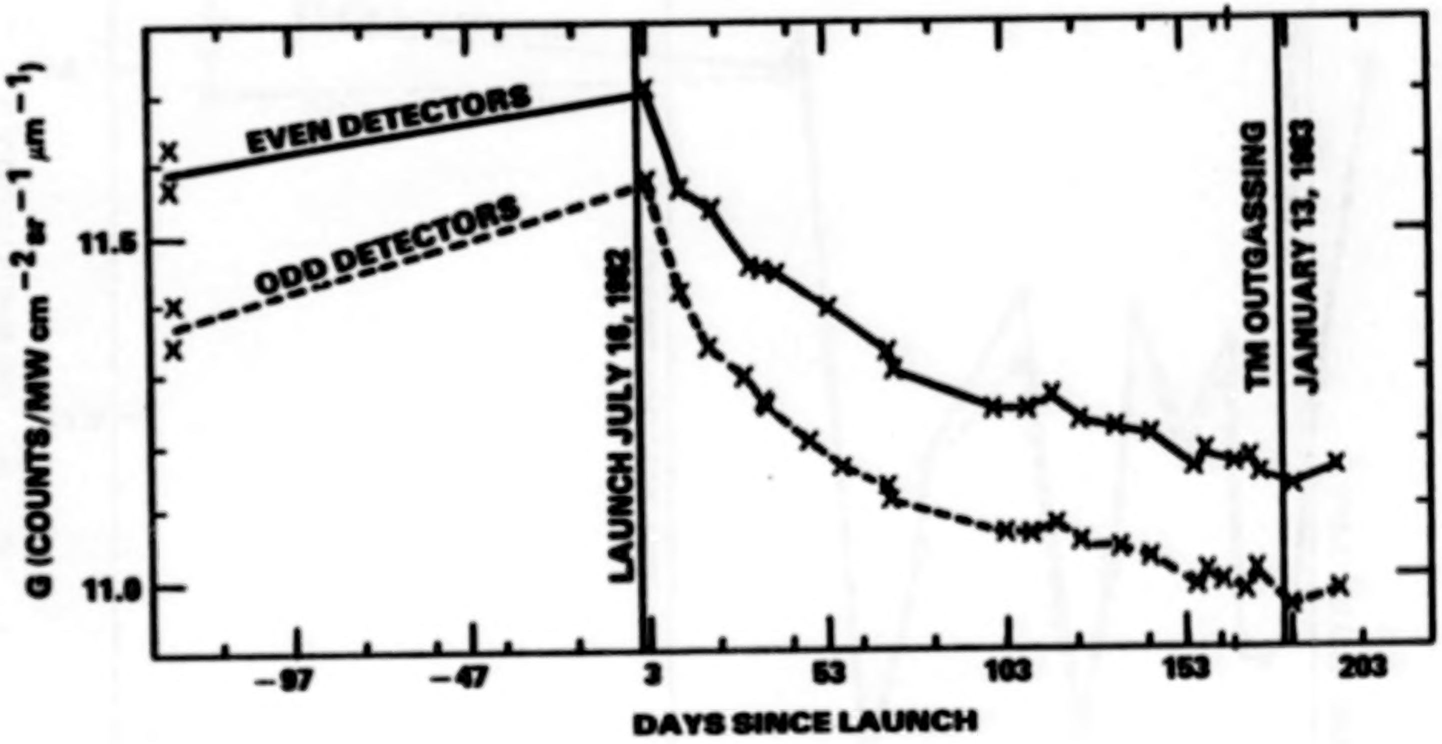

POSTLAUNCH RADIOMETRIC CALIBRATION—TM LANDSAT-4

TM4 GAIN IN COUNTS/SPECTRAL RADIANCE AS A FUNCTION OF TIME

FIGURE A-4

POSTLAUNCH RADIOMETRIC CALIBRATION—TM LANDSAT-4

TM5 GAIN IN COUNTS/SPECTRAL RADIANCE AS A FUNCTION OF TIME

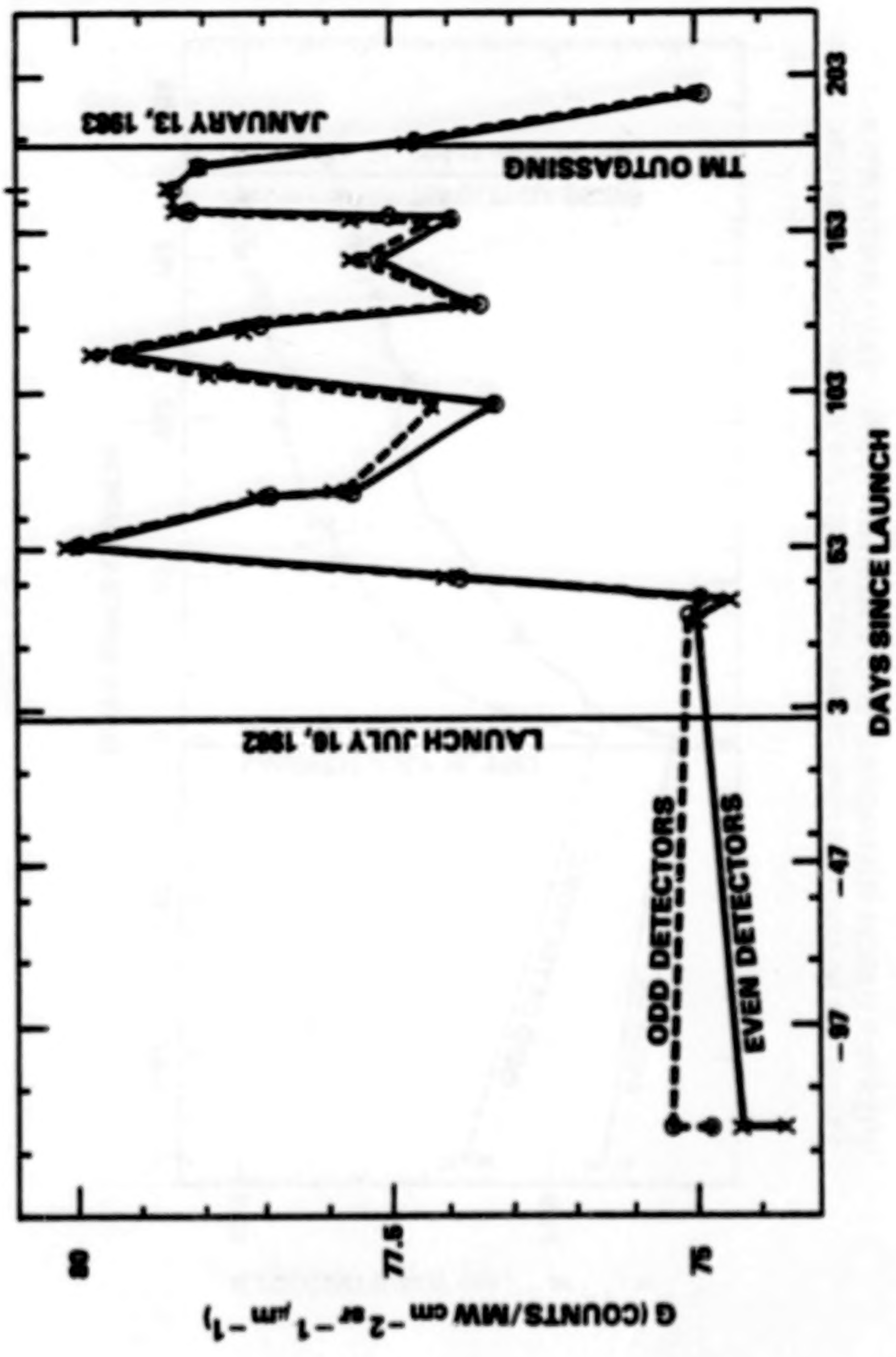

FIGURE A-5

POSTLAUNCH RADIOMETRIC CALIBRATION—TM LANDSAT-4
TM7 GAIN IN COUNTS/SPECTRAL RADIANCE AS A FUNCTION OF TIME

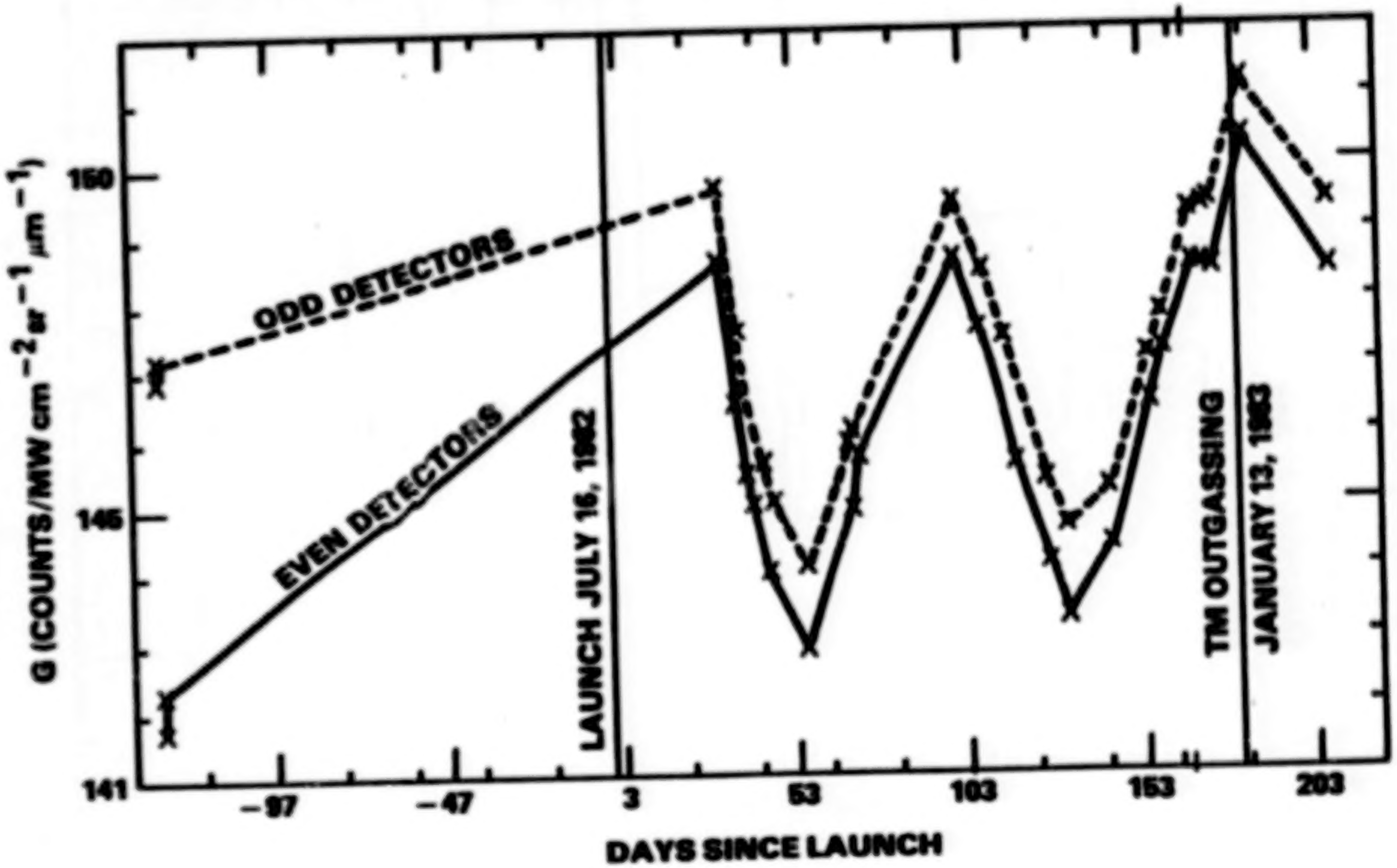

FIGURE A-6

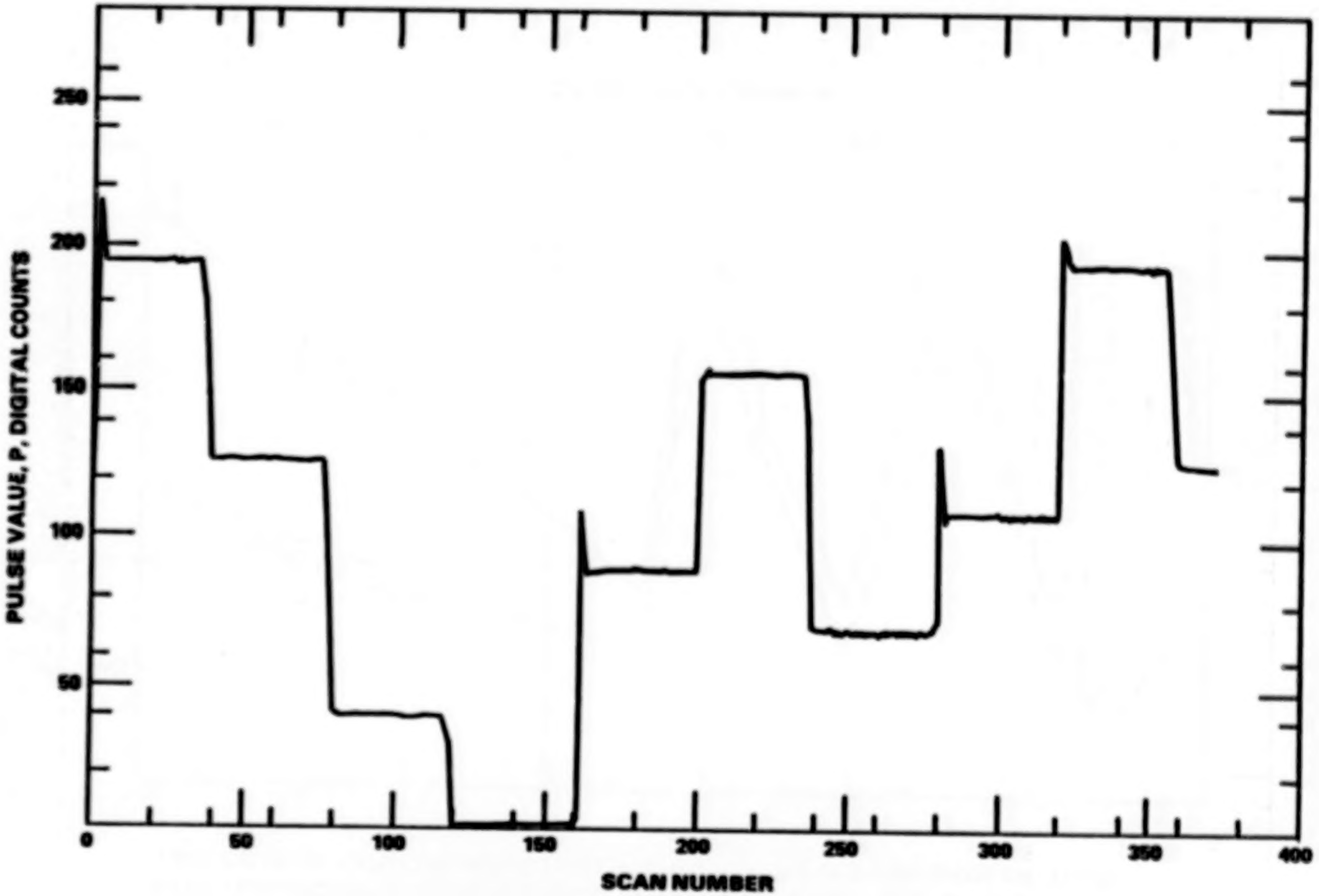
POSTLAUNCH RADIOMETRIC CALIBRATION — TM LANDSAT-4
TM2 CHANNEL 9 ID = 40109—15140 PULSE VALUES

FIGURE A-7

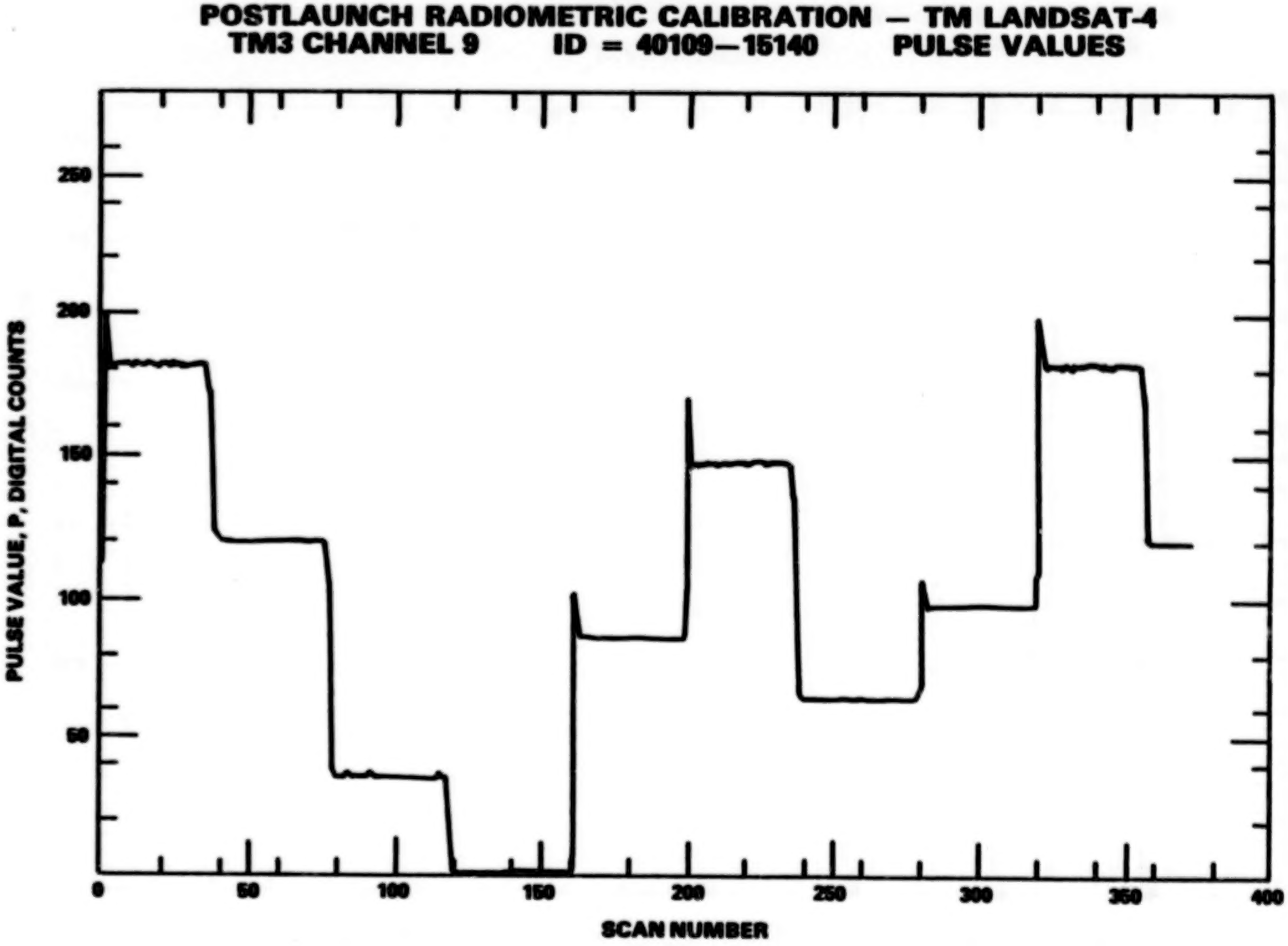
POSTLAUNCH RADIOMETRIC CALIBRATION — TM LANDSAT-4
TM3 CHANNEL 9 ID = 40109—15140 PULSE VALUES

FIGURE A-8

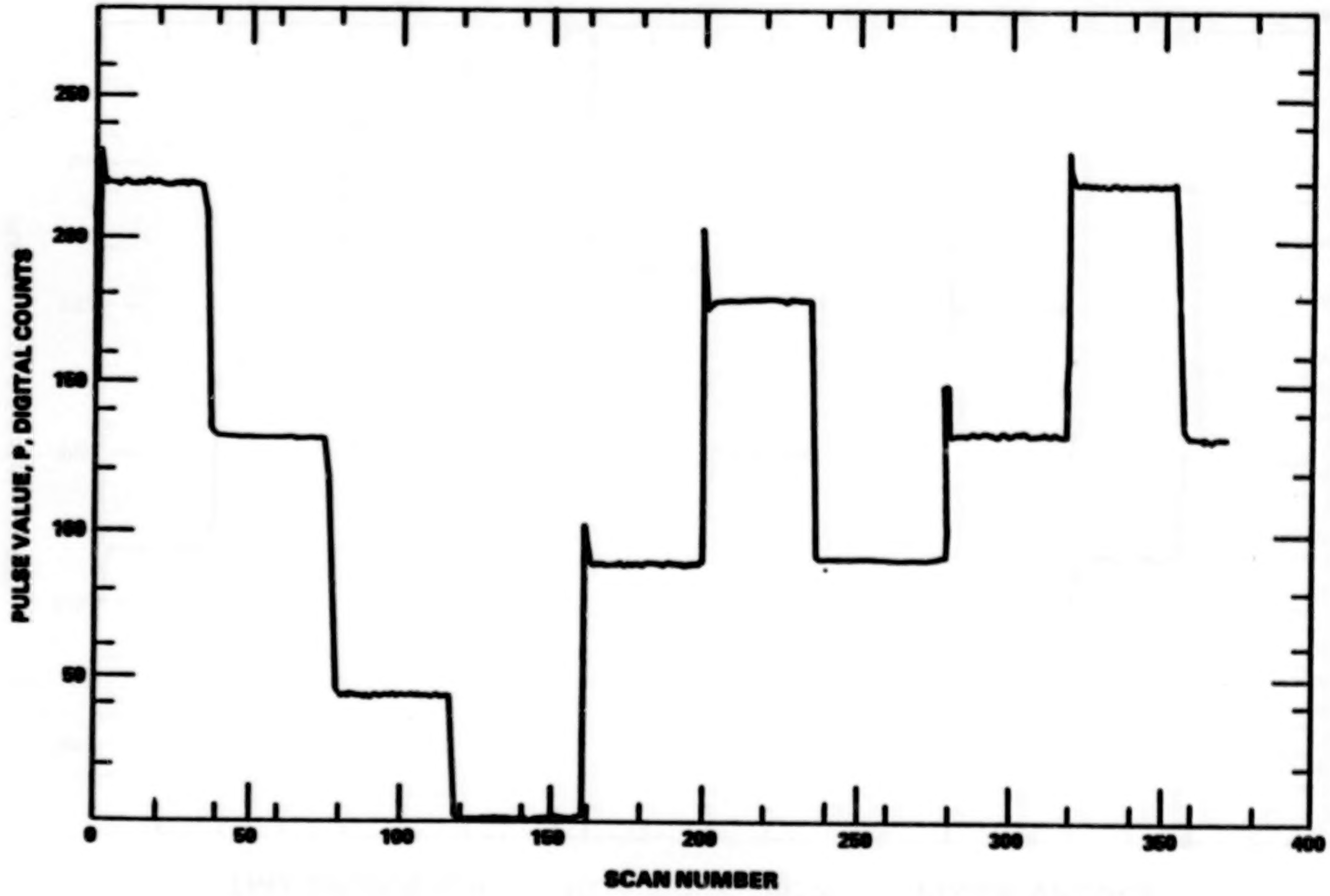

POSTLAUNCH RADIOMETRIC CALIBRATION — TM LANDSAT-4
TM4 CHANNEL 9 ID = 40109—15140 PULSE VALUES

FIGURE A-9

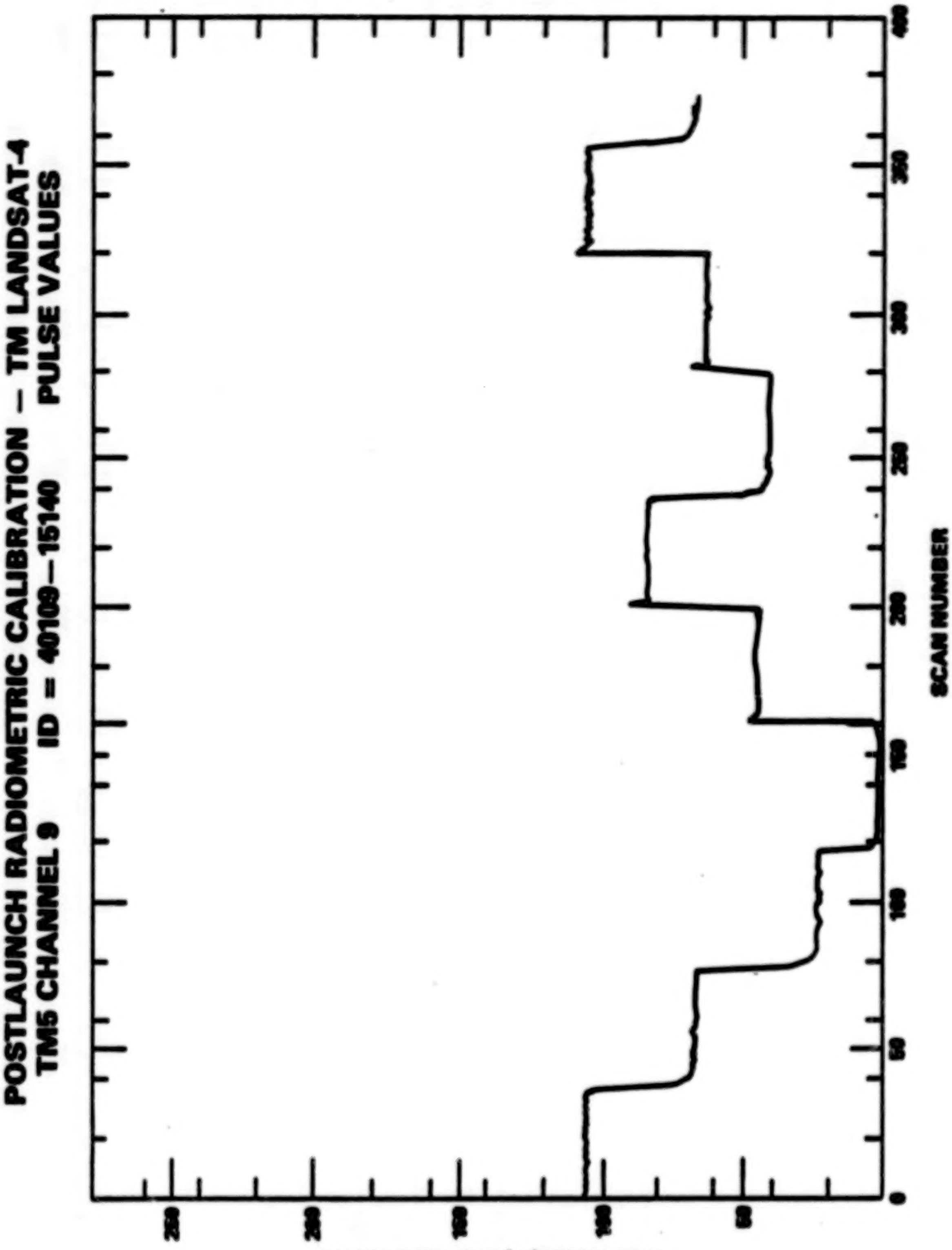
POSTLAUNCH RADIOMETRIC CALIBRATION — TM LANDSAT-4
TM5 CHANNEL 9 ID = 40109—15140 PULSE VALUES
PULSE VALUE, P, DIGITAL COUNTS
250
200
150
100
50
SCAN NUMBER
0
50
100
150
200
250
300
350
400

FIGURE A-10

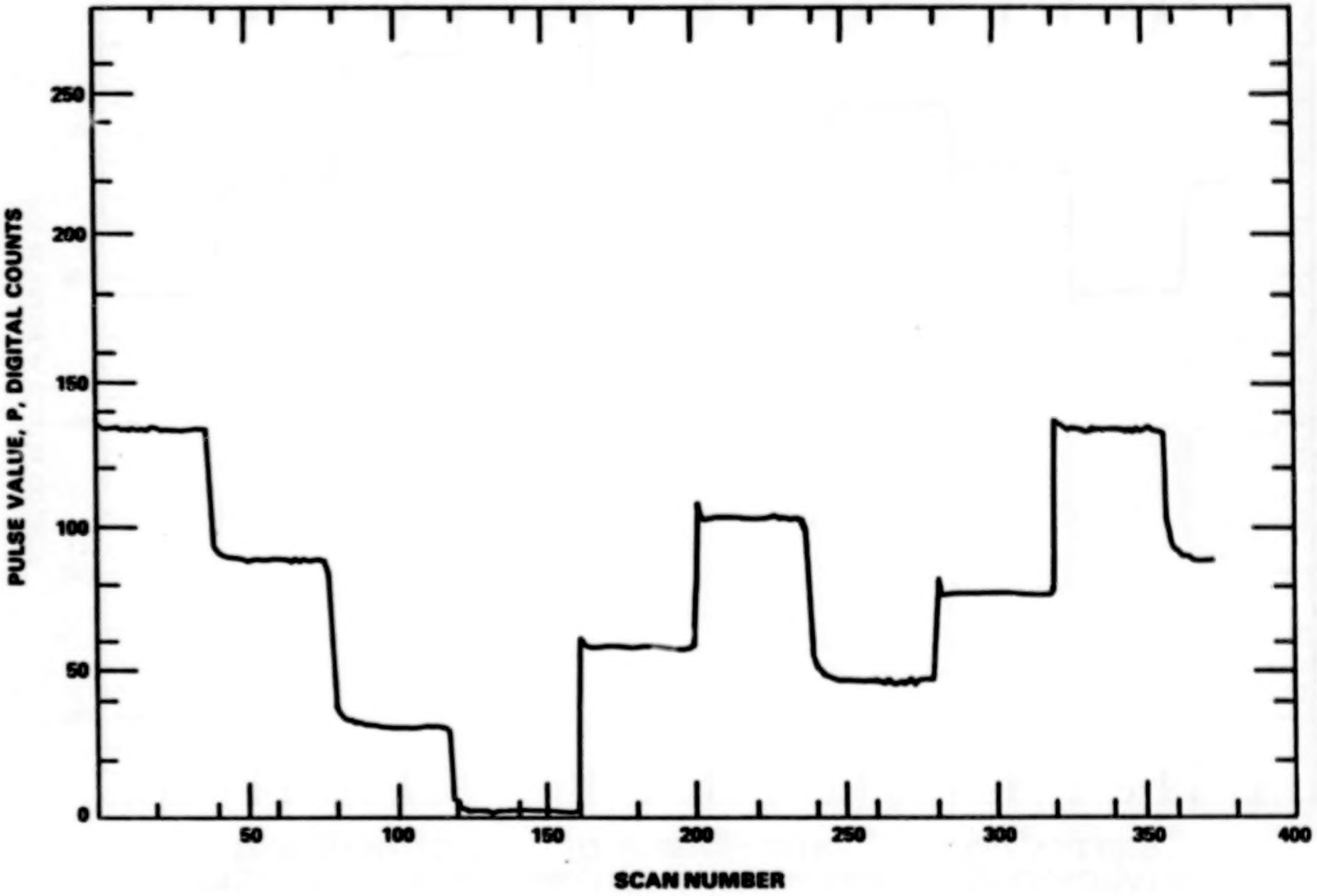

POSTLAUNCH RADIOMETRIC CALIBRATION — TM LANDSAT-4
TM7 CHANNEL 9, ID = 40109—15140 PULSE VALUES

FIGURE A-11

PRELAUNCH RADIOMETRIC CALIBRATION — TM LANDSAT-4
TM1 CHANNEL 9, MARCH 9, 1982, PULSE VALUES

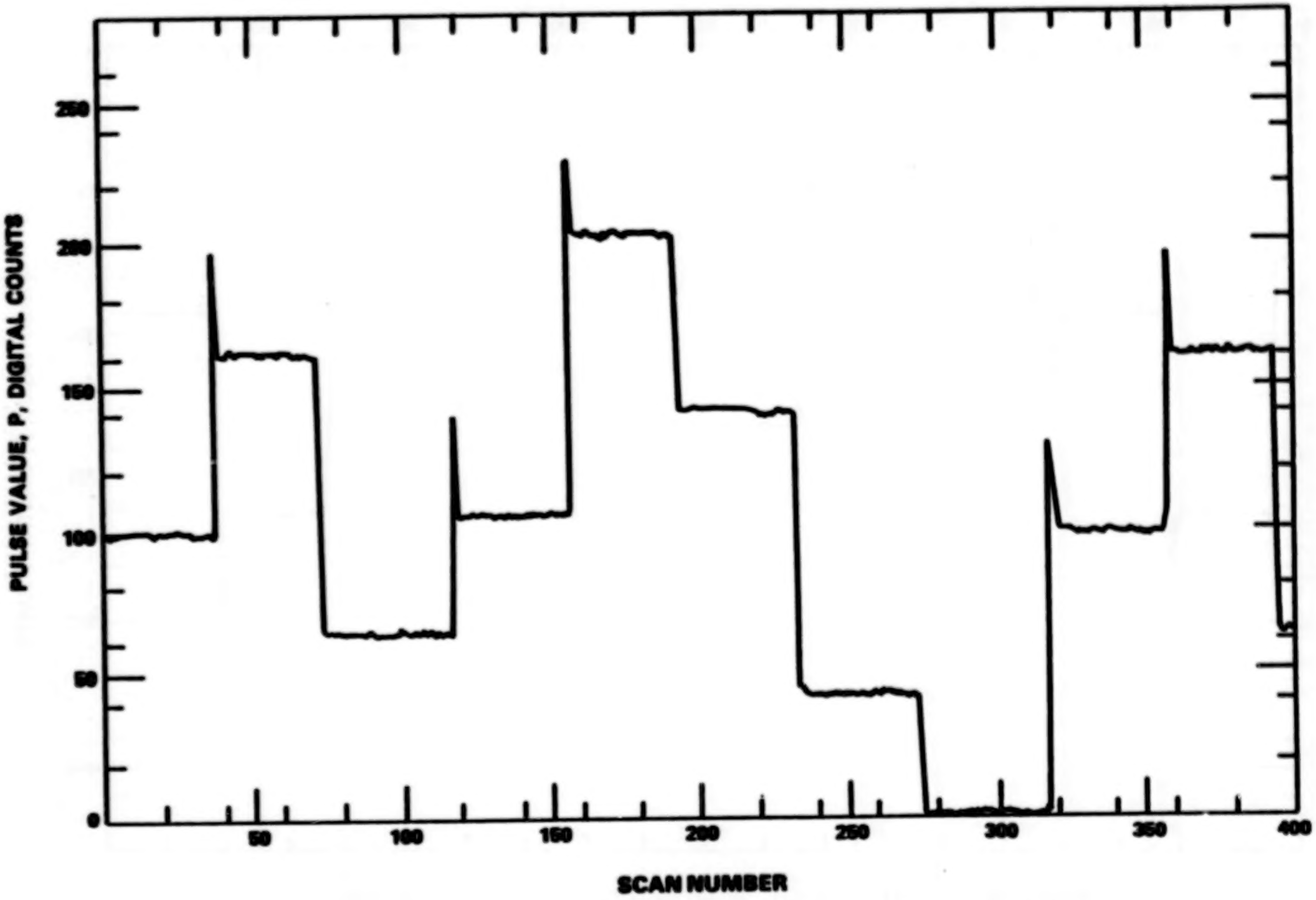

FIGURE A-12

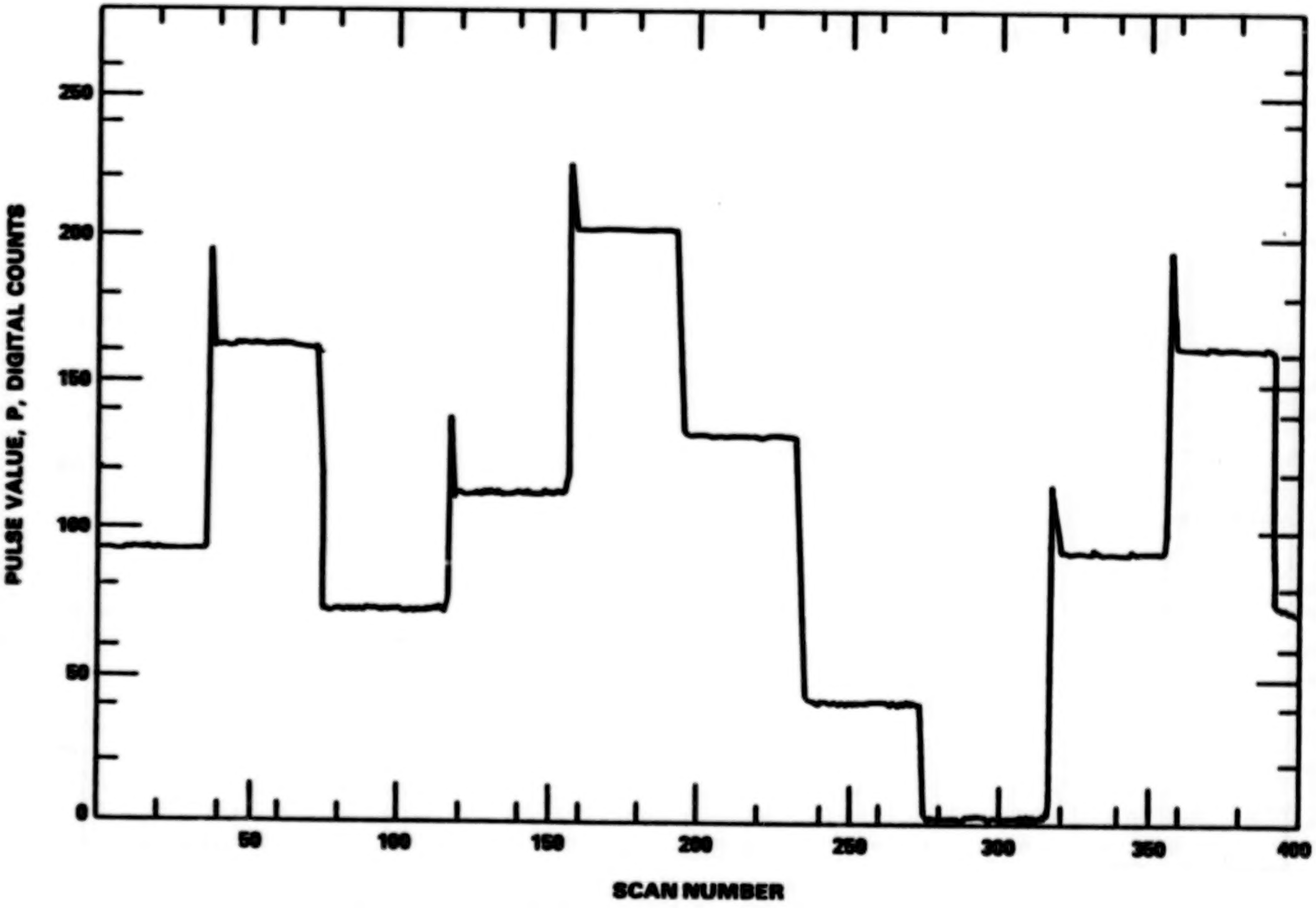

PRELAUNCH RADIOMETRIC CALIBRATION — TM LANDSAT-4
TM2 CHANNEL 9, MARCH 9, 1982, PULSE VALUES

FIGURE A-13

PRELAUNCH RADIOMETRIC CALIBRATION — TM LANDSAT-4
TM3 CHANNEL 9, MARCH 9, 1982, PULSE VALUES

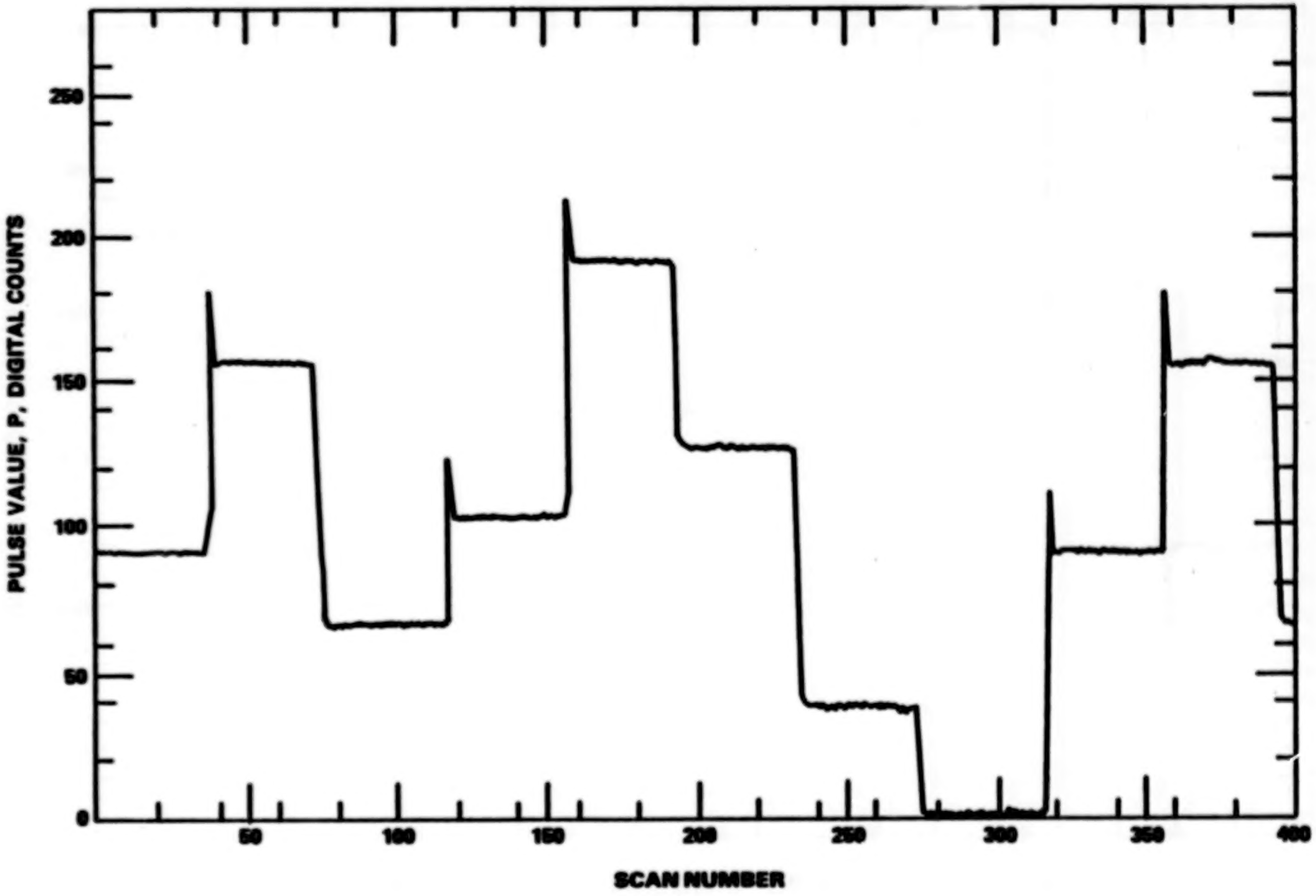

FIGURE A-14

PRELAUNCH RADIOMETRIC CALIBRATION — TM LANDSAT-4
TM4 CHANNEL 9, MARCH 9, 1982, PULSE VALUES

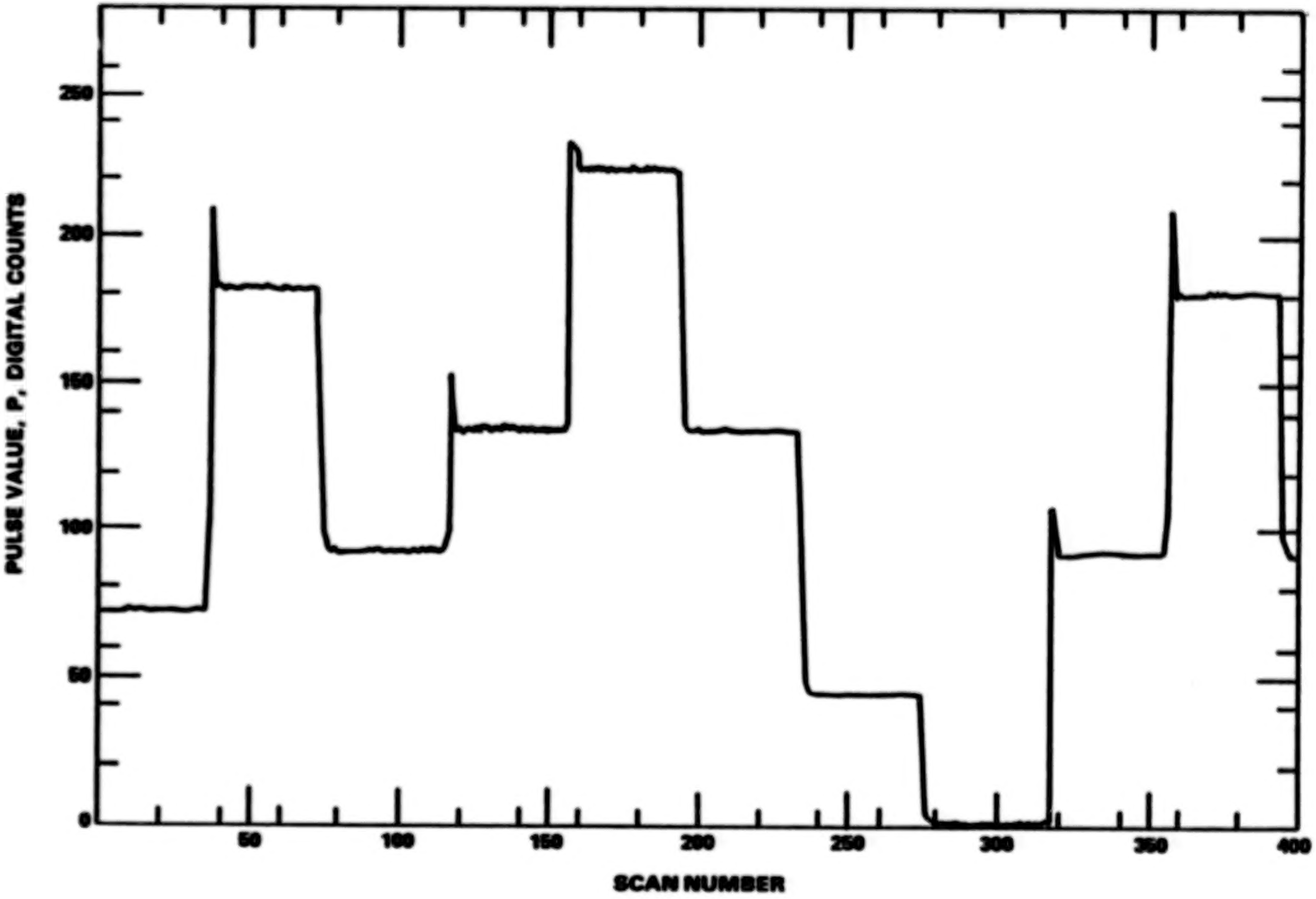

FIGURE A-15

PRELAUNCH RADIOMETRIC CALIBRATION — TM LANDSAT-4
TM5 CHANNEL 9, MARCH 9, 1982, PULSE VALUES

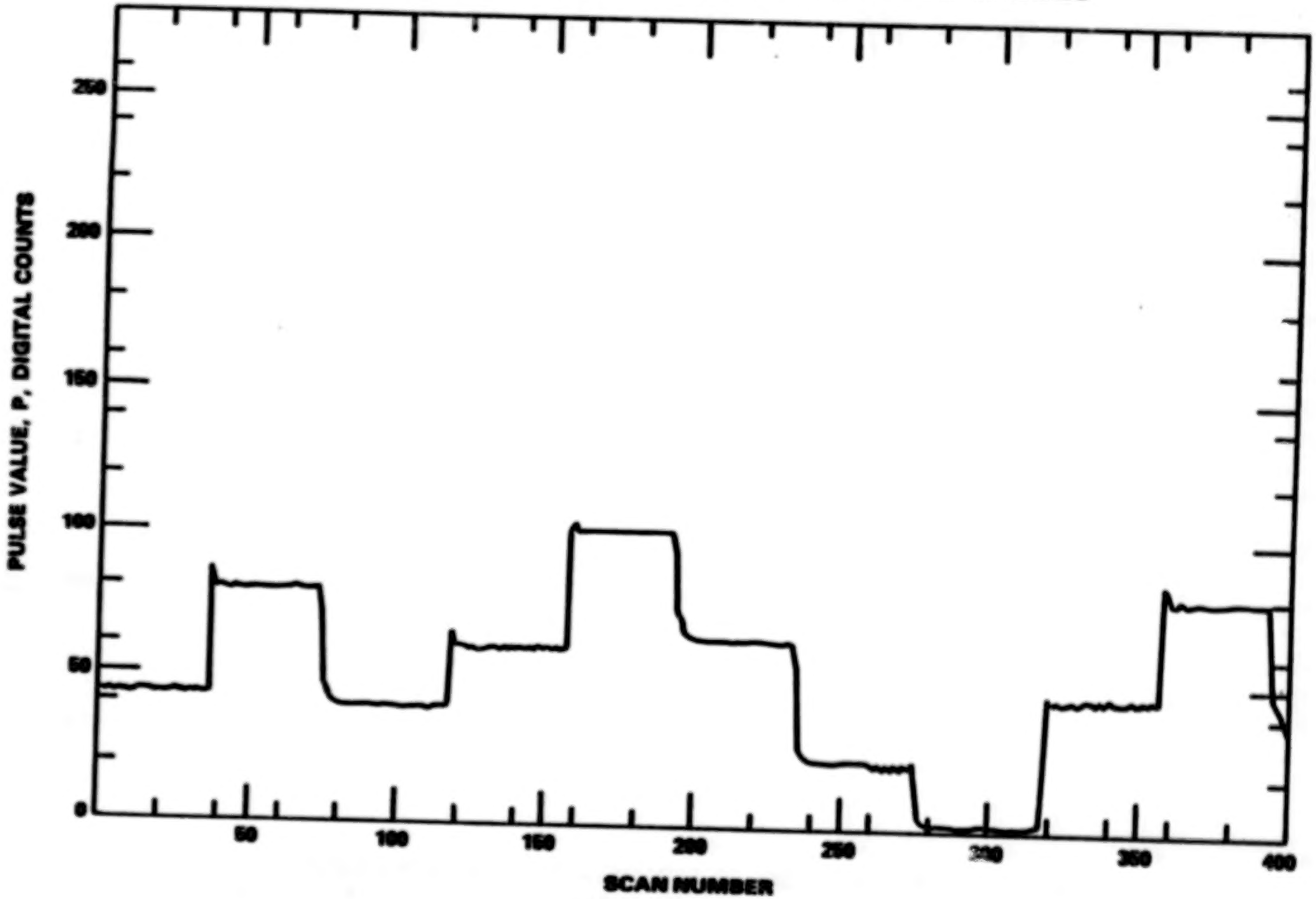

FIGURE A-16

PRELAUNCH RADIOMETRIC CALIBRATION — TM LANDSAT-4
TM7 CHANNEL 9, MARCH 9, 1982, PULSE VALUES

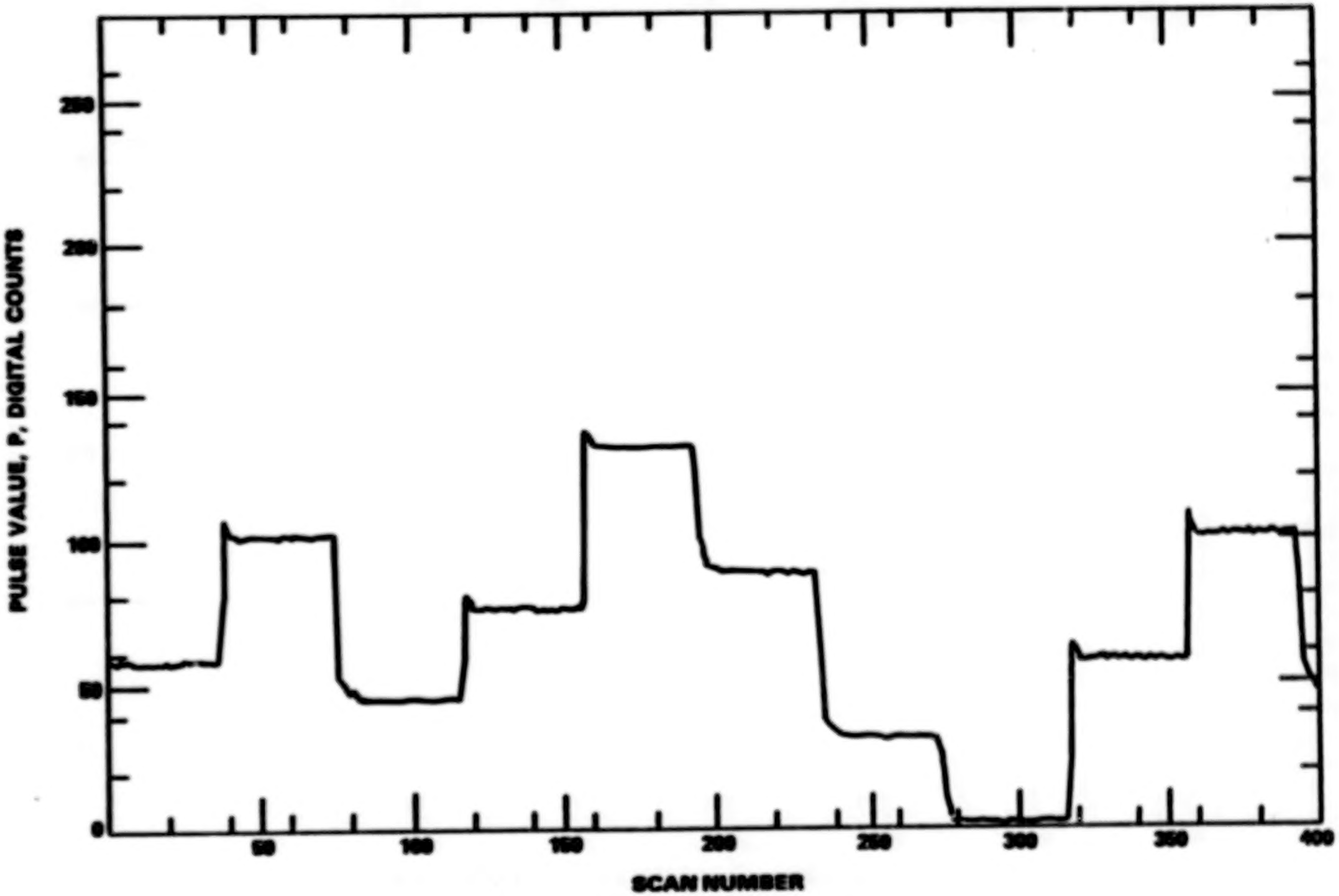

FIGURE A-17

TABLE A-1

POSTLAUNCH RADIOMETRIC CALIBRATION — TM LANDSAT-4 STABILITY OF INTERNAL CALIBRATION SYSTEM

% $(\overline{P}_1 - \overline{P}_2)/\overline{P}_2$

$\overline{P}_2$ — PRELAUNCH, VACUUM, MARCH 9, 1982

BAND[a]	$\overline{P}_1$ – NE ARKANSAS, AUGUST 22, 1982			$\overline{P}_1$ – BOSTON, SEPTEMBER 10, 1982		
	IC STATE					
	100	010	001	100	010	001
1O	−3.3	−2.9	−3.6	−4.0	−3.3	−4.2
1E	−3.7	−3.0	−4.1	−4.3	−2.7	−4.4
2O	−2.6	−1.5	−3.1	−3.1	−1.9	−3.7
2E	−3.2	−2.5	−3.3	−3.6	−2.7	−3.6
3O	−3.3	−1.6	−3.1	−4.1	−2.5	−4.2
3E	−3.2	−1.5	−3.1	−4.0	−2.3	−3.9
4O	−1.9	0	−1.7	−2.4	−1.1	−3.0
4E	−1.5	−0.2	−1.5	−2.1	−1.3	−3.3
5O	0	0.7	−0.6	6.9	7.8	6.0
5E	0.4	1.2	−0.2	7.5	8.2	6.7
7O	0.5	3.4	0	−1.9	1.0	−2.3
7E	−0.8	2.4	−0.10	−3.1	0	−2.6

NOTE: [a]O = ODD DETECTORS; E = EVEN DETECTORS.

TABLE A-2

POSTLAUNCH RADIOMETRIC CALIBRATION — TM LANDSAT-4 STABILITY OF INTERNAL CALIBRATION SYSTEM

% $(\bar{P}_1 - \bar{P}_2)/\bar{P}_2$

$\bar{P}_2$ — PRELAUNCH, VACUUM, MARCH 9, 1982

BAND[a]	$\bar{P}_1$ – FT. DODGE, AUGUST 25, 1982			$\bar{P}_1$ – WASHINGTON, D.C., NOVEMBER 2, 1982		
	IC STATE			IC STATE		
	100	010	001	100	010	001
1O	−3.1	−2.5	−3.4	−5.0	−4.3	−5.4
1E	−3.5	−2.9	−3.7	−5.1	−4.4	−5.4
2O	−2.5	−1.3	−3.1	−3.8	−2.7	−4.4
2E	−2.9	−2.1	−3.1	−3.9	−3.2	−4.0
3O	−3.2	−1.4	−3.2	−5.2	−3.8	−5.4
3E	−3.0	−1.2	−2.8	−5.1	−3.5	−5.1
4O	−1.8	−0.1	−1.8	−3.1	−1.8	−2.8
4E	−1.5	−0.2	−1.5	−3.0	−2.1	−3.4
5O	0.8	1.7	0.2	5.5	0.2	4.8
5E	1.3	2.0	0.4	5.9	0.6	5.1
7O	6.1	2.7	0.0	1.3	3.7	5.4
7E	−1.4	1.7	−1.0	3.0	2.8	2.3

NOTE: [a]O = ODD DETECTORS; E = EVEN DETECTORS.

TABLE A-3

POSTLAUNCH RADIOMETRIC CALIBRATION – TM LANDSAT-4 STABILITY OF INTERNAL CALIBRATION SYSTEM

% $(\bar{P}_1 - \bar{P}_2)/\bar{P}_2$

$\bar{P}_2$ – PRELAUNCH, VACUUM, MARCH 9, 1982

BAND[a]	$\bar{P}_1$ – HAMILTON, MONTANA, NOVEMBER 24, 1982			$\bar{P}_1$ – FT. PIERCE, FLORIDA, DECEMBER 29, 1982		
	IC STATE			IC STATE		
	100	010	001	100	010	001
1O	−4.3	−4.2	−5.6	−5.5	−4.9	−6.1
1E	−4.6	−4.6	−5.8	−5.8	−5.5	−6.3
2O	−3.1	−2.3	−4.2	−3.7	−2.8	−4.5
2E	−3.6	−3.0	−4.1	−4.3	−3.7	−4.5
3O	−4.8	−3.5	−5.3	−5.8	−4.4	−6.0
3E	−4.7	−3.3	−5.1	−5.7	−4.0	−5.7
4O	−3.4	−1.9	−3.8	−4.0	−2.8	−4.8
4E	−3.2	−2.2	−3.7	−3.8	−3.1	−4.5
5O	−2.5	3.3	1.7	3.1	3.7	2.1
5E	−3.1	2.8	2.1	3.4	3.9	2.3
7O	0.0	3.5	0.4	3.4	6.1	2.8
7E	−2.5	0.3	−2.4	−0.7	2.3	−0.4

NOTE: [a]O – ODD DETECTORS; E – EVEN DETECTORS.

TABLE A-4

POSTLAUNCH RADIOMETRIC CALIBRATION — TM LANDSAT-4 STABILITY OF INTERNAL CALIBRATION SYSTEM

% $(\bar{P}_1 - \bar{P}_2)/\bar{P}_2$

$\bar{P}_2$ — PRELAUNCH, VACUUM, MARCH 9, 1982

BAND[a]	$\bar{P}_1$ — FORMAN, NORTH DAKOTA, SEPTEMBER 24, 1982			$\bar{P}_1$ — OTTAWA, CANADA, OCTOBER 24, 1982		
	IC STATE			IC STATE		
	100	010	001	100	010	001
1O	−4.8	−4.2	−5.1	−5.2	−4.5	−5.4
1E	−5.0	−4.8	−5.4	−5.6	−5.2	−5.7
2O	−3.5	−2.4	−4.1	−3.8	−2.5	−4.2
2E	−4.2	−3.5	−4.2	−4.2	−3.4	−4.1
3O	−5.2	−3.4	−5.1	−5.4	−3.7	−5.4
3E	−5.0	−3.2	−4.9	−5.3	−3.4	−5.0
4O	−2.8	−1.0	−2.7	−3.4	−1.6	−3.4
4E	−2.5	−1.3	−2.0	−3.1	−1.8	−3.2
5O	4.8	5.7	3.9	2.3	3.1	1.5
5E	5.3	6.1	4.5	2.7	3.4	1.8
7O	1.9	5.0	1.5	4.3	7.5	3.0
7E	−1.9	1.4	−1.4	0.5	3.9	1.0

NOTE: [a]O = ODD DETECTORS; E = EVEN DETECTORS.

TABLE A-5

POSTLAUNCH RADIOMETRIC CALIBRATION — TM LANDSAT-4 STABILITY OF INTERNAL CALIBRATION SYSTEM

$\% \, (\overline{P}_1 - \overline{P}_2)/\overline{P}_2$

$\overline{P}_1$ = DETROIT, JULY 20, 1983

$\overline{P}_2$ = MARCH 9, 1982

BAND[a]	IC STATE		
	100	010	001
1O	0.9	1.3	1.3
1E	−0.1	0.3	0.3
2O	0.6	0.9	0.5
2E	−1.5	−1.6	−1.4
3O	−0.6	1.2	0.2
3E	−0.3	1.9	0.5
4O	0.3	2.4	0.2
4E	0.3	1.2	−0.3

NOTE: [a]0 = ODD DETECTORS; E = EVEN DETECTORS.

TABLE A-6

POSTLAUNCH RADIOMETRIC CALIBRATION — TM LANDSAT-4 STABILITY OF INTERNAL CALIBRATION SYSTEM

$\% (\bar{P}_1 - \bar{P}_2)/\bar{P}_2$

$\bar{P}_2$ = D.C., NOVEMBER 2, 1982

BAND[a]	$\bar{P}_1$ = NE ARKANSAS, AUGUST 22, 1982			$\bar{P}_1$ = BOSTON, SEPTEMBER 10, 1982		
	IC STATE			IC STATE		
	100	010	001	100	010	001
1O	1.6	1.5	1.8	1.0	1.0	1.2
1E	1.4	0.8	1.3	0.8	0.6	1.0
2O	1.0	1.3	1.3	0.5	0.8	0.7
2E	0.7	0.8	0.7	0.4	0.8	0.4
3O	1.9	2.2	2.3	1.1	1.3	1.2
3E	1.9	2.1	2.0	1.1	1.2	1.2
4O	1.4	1.8	1.9	0.7	0.7	0
4E	1.6	1.8	1.8	0.9	0.7	0.2
5O	−5.5	−5.5	−5.4	1.4	1.6	1.4
5E	−5.3	−5.2	−5.3	1.5	1.9	1.5
7O	−0.7	−0.3	0.5	−3.1	−2.9	−2.9
7E	−0.8	−0.3	0.1	−3.1	−2.7	−2.7

NOTE:

[a] O = ODD DETECTORS; E = EVEN DETECTORS.

TABLE A-7

POSTLAUNCH RADIOMETRIC CALIBRATION – TM LANDSAT-4 STABILITY OF INTERNAL CALIBRATION SYSTEM

$\% (\bar{P}_1 - \bar{P}_2)/\bar{P}_2$

$\bar{P}_2$ – D.C., NOVEMBER 2, 1982

BAND[a]	$\bar{P}_1$ – FT. DODGE, AUGUST 25, 1982			$\bar{P}_1$ – FOREHAM, NORTH DAKOTA, SEPTEMBER 24, 1982		
	IC STATE			IC STATE		
	100	010	001	100	010	001
1O	1.8	1.9	2.0	0.4	0.1	0.3
1E	1.6	1.5	1.7	0.1	−0.4	−0.1
2O	1.1	1.5	1.3	0.1	0.3	0.2
2E	1.0	1.1	1.0	−0.4	−0.3	−0.2
3O	2.0	2.3	2.2	0.0	−0.3	0.2
3E	2.1	2.3	2.3	0.0	−0.3	0.2
4O	1.5	1.7	1.8	0.3	0.8	0.9
4E	1.5	1.9	1.8	0.5	0.8	0.8
5O	−4.7	−4.9	−4.4	−0.8	−0.5	−0.7
5E	−4.7	−4.4	−4.7	−0.7	−0.5	−0.6
7O	−1.4	−0.9	−1.1	−1.7	−1.0	−1.4
7E	−1.3	−1.0	−1.2	−1.9	−1.3	−1.6

NOTE: [a]O = ODD DETECTORS; E = EVEN DETECTORS.

TABLE A-8

POSTLAUNCH RADIOMETRIC CALIBRATION — TM LANDSAT-4 STABILITY OF INTERNAL CALIBRATION SYSTEM

% $(\bar{P}_1 - \bar{P}_2)/\bar{P}_2$ = D.C., NOVEMBER 2, 1982

BAND[a]	$\bar{P}_1$ – OTTAWA, CANADA, OCTOBER 24, 1982			$\bar{P}_1$ – HAMILTON, MONTANA, NOVEMBER 24, 1982		
	IC STATE			IC STATE		
	100	010	001	100	010	001
1O	−0.2	−0.2	−0.1	0.6	0.2	−0.2
1E	−0.5	−0.9	−0.4	0.5	0.3	−0.4
2O	0.0	0.3	0.2	0.4	0.5	−0.2
2E	−0.3	−0.2	−0.1	0.3	0.2	−0.1
3O	−0.2	0.1	0.0	0.4	0.3	0.0
3E	−0.2	0.1	0.1	0.3	0.3	0.0
4O	−0.3	0.2	0.1	−0.3	0.0	−0.2
4E	−0.1	0.2	0.2	−0.2	−0.1	−0.3
5O	−3.3	−3.0	−3.1	−2.4	−2.9	−2.9
5E	−3.3	−3.1	−3.3	−3.1	−2.8	−3.0
7O	0.7	1.5	1.0	−2.7	−2.5	−2.6
7E	0.5	1.2	0.8	−2.6	−2.5	−2.2

NOTE: [a] O = ODD DETECTORS; E = EVEN DETECTORS.

TABLE A-9

POSTLAUNCH RADIOMETRIC CALIBRATION – TM LANDSAT-4 STABILITY OF INTERNAL CALIBRATION SYSTEM

% $(\bar{P}_1 - \bar{P}_2)/\bar{P}_2$ = D.C., NOVEMBER 2, 1982

BAND[a]	$\bar{P}_1$ – MODESSA, CALIFORNIA, DECEMBER 8, 1982			$\bar{P}_1$ – FT. PIERCE, FLORIDA, DECEMBER 20, 1982		
	IC STATE			IC STATE		
	100	010	001	100	010	001
1O	0.1	0.3	1.1	−0.5	−0.6	−0.7
1E	0.0	0.0	1.0	−0.7	−1.2	−1.0
2O	0.2	0.4	0.3	−0.1	−0.1	−0.2
2E	0.1	0.3	0.3	−0.4	−0.5	−0.5
3O	0.0	0.1	0.1	−0.6	−0.6	−0.6
3E	0.0	0.1	0.5	−0.6	−0.5	−0.7
4O	−0.3	−0.2	−0.2	−0.9	−0.8	−1.0
4E	−0.5	−0.3	−0.2	−0.8	−0.8	−1.1
5O	−5.3	−5.7	−6.4	−2.4	−2.5	−2.5
5E	−5.9	−3.8	−5.0	−2.6	−2.5	−2.8
7O	−2.0	−1.8	−1.7	−0.3	0.1	−0.2
7E	−2.1	−2.1	−2.2	−0.7	−0.4	−0.6

NOTE: [a]O = ODD DETECTORS; E = EVEN DETECTORS.

TABLE A-10

POSTLAUNCH RADIOMETRIC CALIBRATION — TM LANDSAT-4
STABILITY OF INTERNAL CALIBRATION SYSTEM

$\% \, (\bar{P}_1 - \bar{P}_2)/\bar{P}_2$

$\bar{P}_1$ = DETROIT, JULY 20, 1983

$\bar{P}_2$ = D.C., NOVEMBER 1982

BAND[a]	IC STATE		
	100	010	001
1O	5.9	3.0	6.7
1E	5.0	4.1	5.6
2O	4.2	3.7	4.9
2E	2.3	1.6	2.6
3O	4.7	5.0	5.6
3E	4.8	5.4	5.6
4O	2.8	4.1	3.7
4E	2.8	3.3	3.1

NOTE: [a]0 = ODD DETECTORS; E = EVEN DETECTORS.

TABLE A-11

POSTLAUNCH RADIOMETRIC CALIBRATION — TM LANDSAT-4
TM2 CHANGE IN GAIN (ppt) RELATIVE TO MARCH 9, 1982

CHANNEL	DATE				
	AUGUST 22	SEPTEMBER 10	OCTOBER 24	NOVEMBER 24	DECEMBER 8
1	−23	−27	−32	−31	−32
2	−34	−36	−43	−40	−40
3	−22	−27	−32	−31	−31
4	−6	−9	−17	−17	−16
5	−22	−26	−31	−30	−31
6	−33	−36	−42	−39	−40
7	−23	−28	−34	−31	−32
8	−34	−37	−44	−41	−40
9	−23	−28	−33	−32	−33
10	−34	−37	−43	−39	−40
11	−24	−29	−34	−32	−33
12	−34	−37	−43	−40	−39
13	−23	−27	−32	−31	−32
14	−33	−37	−42	−39	−41
15	−23	−28	−34	−32	−33
16	−34	−36	−43	−41	−40
MEAN	−26.6	−30.3	−36.0	−34.1	−34.6
SD	7.7	7.3	7.2	6.3	6.3

TABLE A-12

POSTLAUNCH RADIOMETRIC CALIBRATION — TM LANDSAT-4 TM5 CHANGE IN GAIN (ppt) RELATIVE TO MARCH 9, 1982

CHANNEL	DATE				
	AUGUST 22	SEPTEMBER 10	OCTOBER 24	NOVEMBER 24	DECEMBER 8
1	19	87	36	55	19
2	23	93	42	59	22
3	—	—	—	—	—
4	−9	61	12	20	−11
5	−14	52	6	12	−16
6	6	78	29	32	3
7	2	73	26	27	0
8	8	80	33	33	7
9	0	69	23	22	−2
10	−8	60	16	12	−11
11	1	71	25	23	0
12	6	77	32	28	3
13	2	71	26	24	0
14	7	78	31	30	4
15	−4	62	17	20	−7
16	17	87	40	43	14
MEAN	3.7	73.3	26.0	29.3	1.66
SD	10.4	11.4	10.2	13.8	10.8

TABLE A-13

POSTLAUNCH RADIOMETRIC CALIBRATION — TM LANDSAT-4 TM7 CHANGE IN GAIN (ppt) RELATIVE TO MARCH 9, 1982

CHANNEL	DATE				
	AUGUST 22	SEPTEMBER 10	OCTOBER 24	NOVEMBER 24	DECEMBER 8
1	23	0	39	4	8
2	9	−14	22	−9	−7
3	16	−7	31	−3	1
4	0	−22	14	−19	−15
5	0	−22	16	−19	−12
6	1	−20	15	−18	−12
7	185	158	203	160	170
8	−11	−33	2	−30	−25
9	15	−8	30	−4	4
10	11	−11	25	−8	−2
11	13	−10	29	−7	1
12	11	−11	24	−9	−3
13	12	−11	28	−7	0
14	−6	−28	7	−26	−20
15	6	−17	21	−13	−6
16	18	−3	33	0	4
MEAN	18.9	−2.6	34.0	−0.5	7.9
SD	45.2	45.6	46.1	43.8	44.4

TABLE A-14

POSTLAUNCH RADIOMETRIC CALIBRATION — TM LANDSAT-4 STANDARD DEVIATION OF BACKGROUND, WASHINGTON, D.C., NOVEMBER 2, 1982 (DIGITAL COUNTS)

		TM1	TM2	TM3	TM4	TM5	TM7
CHANNEL	1	1.28	0.50	0.79	0.47	0.80	0.98
	2	1.44	1.00	0.54	0.38	0.75	0.99
	3	1.19	0.49	0.57	0.48	—	0.85
	4	1.44	0.69	0.72	0.38	0.82	1.03
	5	1.08	0.43	0.53	0.30	0.87	0.91
	6	1.43	0.52	0.52	0.48	0.88	1.01
	7	1.26	0.37	0.49	0.25	1.08	1.94
	8	1.31	0.42	0.86	0.53	0.81	0.92
	9	1.09	0.30	0.45	0.24	0.85	0.98
	10	1.18	0.30	0.57	0.32	0.87	1.05
	11	1.24	0.35	0.39	0.25	0.91	0.93
	12	1.32	0.37	0.47	0.41	0.84	1.00
	13	1.14	0.35	0.52	0.20	0.83	0.80
	14	1.35	0.36	0.59	0.26	0.79	1.09
	15	1.26	0.34	0.51	0.25	0.82	0.78
	16	1.60	0.43	0.84	0.41	0.78	0.95
MEANODD		1.19	0.39	0.53	0.31	0.88	1.02
MEANEVN		1.38	0.51	0.64	0.39	0.82	1.00
MEANALL		1.[illegible]9	0.45	0.59	0.35	0.85	1.01
MEANODD SD		0.08	0.07	0.11	0.10	0.09	0.37
MEANEVN SD		0.12	0.23	0.14	0.08	0.04	0.05
MEANALL SD		0.14	0.17	0.14	0.10	0.07	0.26
MEANALL CV		10.86	38.94	23.72	29.21	9.05	25.72

TABLE A-15

POSTLAUNCH RADIOMETRIC CALIBRATION -- TM LANDSAT-4 STANDARD DEVIATION OF BACKGROUND, MARCH 9, 1982 (DIGITAL COUNTS)

		TM1	TM2	TM3	TM4	TM5	TM7
CHANNEL	1	1.37	0.49	0.69	0.45	0.89	1.10
	2	1.44	1.02	0.53	0.41	0.89	1.12
	3	1.23	0.52	0.56	0.49	—	1.03
	4	1.00	0.65	0.77	0.43	0.84	1.14
	5	1.18	0.47	0.54	0.34	0.93	1.01
	6	1.40	0.54	0.53	0.49	1.16	1.12
	7	1.12	0.42	0.52	0.29	1.08	2.85
	8	1.32	0.46	0.88	0.56	0.85	1.05
	9	1.15	0.39	0.50	0.30	0.93	1.09
	10	1.00	0.40	0.58	0.34	0.96	1.20
	11	1.30	0.44	0.42	0.29	0.98	1.05
	12	0.99	0.39	0.53	0.29	0.95	1.14
	13	1.19	0.42	0.54	0.22	0.89	0.92
	14	1.35	0.44	0.64	0.30	0.92	1.17
	15	1.31	0.41	0.52	0.25	0.91	0.90
	16	1.65	0.51	0.86	0.38	0.90	1.08
MEANODD		1.23	0.45	0.53	0.33	0.94	1.24
MEANEVN		1.27	0.56	0.66	0.40	0.93	1.13
MEANALL		1.25	0.50	0.60	0.36	0.94	1.19
MEANODD SD		0.08	0.04	0.07	0.09	0.06	0.65
MEANEVN SD		0.24	0.20	0.14	0.09	0.10	0.04
MEANALL SD		0.18	0.15	0.13	0.09	0.08	0.45
MEANALL CV		14.38	30.99	21.90	26.88	8.95	37.85

TABLE A-16

PROTOFLIGHT TM1, CHANNEL 1 A/D CONVERTER BIN SIZES[a] (1 OF 5)

DIGITAL COUNT LEVEL	MEASURED INPUT (mV)	INCREASE FROM PREVIOUS THRESHOLD (mV)	BEST FIT STRAIGHT LINE		DIGITAL COUNT LEVEL	MEASURED INPUT (mV)	INCREASE FROM PREVIOUS THRESHOLD (mV)	BEST FIT STRAIGHT LINE	
			CALCULATED (mV)	DEVIATION				CALCULATED (mV)	DEVIATION
0	−46.6		−45.3	−1.3	27	387.6	16.5	382.8	4.8
1	−30.9	15.7	−29.4	−1.4	28	400.2	12.6	398.7	1.5
2	−10.2	20.6	−13.6	3.4	29	420.7	20.5	414.5	6.2
3	0.0	10.3	2.3	−2.2	30	436.8	16.1	430.4	6.4
4	19.6	19.5	18.1	1.4	31	441.3	4.4	446.2	−4.9
5	37.5	17.9	34.0	3.5	32	461.0	19.7	462.1	−1.1
6	56.2	18.7	49.8	6.4	33	476.4	15.4	478.0	−1.6
7	63.4	7.1	65.7	−2.3	34	497.5	21.1	493.8	3.7
8	81.0	17.6	81.6	−0.6	35	507.6	10.1	509.6	−2.0
9	98.7	17.7	97.4	1.3	36	526.7	19.1	525.5	1.2
10	117.4	18.6	113.3	4.1	37	544.5	17.7	541.4	3.1
11	131.6	14.3	129.1	2.5	38	563.3	18.8	557.2	6.1
12	146.9	15.2	145.0	1.9	39	573.7	10.3	573.1	0.6
13	167.0	20.1	160.9	6.1	40	587.9	14.2	588.9	−1.0
14	183.2	16.3	176.7	6.5	41	605.5	17.6	604.8	0.7
15	192.7	9.5	192.5	0.2	42	624.6	19.2	620.6	4.0
16	207.5	14.7	208.4	−0.9	43	638.7	14.0	636.5	2.2
17	223.1	15.7	224.2	−1.1	44	653.5	14.8	652.3	1.2
18	243.5	20.4	240.1	3.4	45	673.5	19.9	668.2	5.3
19	256.4	12.9	256.0	0.4	46	690.0	16.5	684.1	5.9
20	273.3	17.0	271.8	1.5	47	702.9	12.9	699.9	3.0
21	291.4	18.0	287.7	3.7	48	713.7	10.7	715.8	−2.1
22	309.8	18.4	303.5	6.3	49	729.5	15.8	731.6	−2.1
23	320.7	10.9	319.4	1.3	50	749.7	20.2	747.5	2.2
24	334.4	13.7	335.2	−0.8	51	762.8	13.0	763.3	−0.5
25	352.5	18.1	351.1	1.4	52	779.2	16.4	779.2	0.0
26	371.1	18.6	366.9	4.1	53	797.3	18.1	795.0	2.3

[a] MEASUREMENT ON NOVEMBER 15, 1980.

TABLE A-16

PROTOFLIGHT TM1, CHANNEL 1 A/D CONVERTER BIN SIZES[a] (2 OF 5)

DIGITAL COUNT LEVEL	MEASURED INPUT (mV)	INCREASE FROM PREVIOUS THRESHOLD (mV)	BEST FIT STRAIGHT LINE		DIGITAL COUNT LEVEL	MEASURED INPUT (mV)	INCREASE FROM PREVIOUS THRESHOLD (mV)	BEST FIT STRAIGHT LINE	
			CALCULATED (mV)	DEVIATION				CALCULATED (mV)	DEVIATION
54	815.7	16.4	810.9	4.8	81	1235.0	15.3	1239.0	-4.0
55	829.7	14.0	826.8	3.0	82	1255.7	20.7	1254.8	0.9
56	840.1	10.4	842.6	-2.5	83	1267.7	12.0	1270.7	-3.0
57	858.0	17.9	858.5	-0.4	84	1284.9	17.2	1286.5	-1.6
58	876.8	18.8	874.3	2.5	85	1302.6	17.7	1302.4	0.2
59	893.3	16.5	890.2	3.1	86	1321.3	18.7	1318.3	3.0
60	905.5	12.2	906.0	-0.5	87	1333.3	12.0	1334.1	-0.8
61	925.7	20.2	921.9	3.8	88	1346.2	12.9	1350.0	-3.8
62	942.0	16.3	937.7	4.3	89	1363.4	17.2	1365.8	-2.4
63	952.1	10.1	953.6	-1.5	90	1381.9	18.5	1381.7	0.2
64	967.4	15.3	969.4	-2.0	91	1401.3	19.4	1397.5	3.8
65	982.3	14.9	985.3	-3.0	92	1411.4	10.1	1413.4	-2.0
66	1003.3	21.1	1001.2	2.2	93	1431.3	19.9	1429.3	2.1
67	1012.8	9.5	1017.0	-4.2	94	1447.8	16.4	1445.1	2.7
68	1033.0	20.2	1032.9	4.2	95	1460.1	12.3	1461.0	-0.9
69	1050.0	17.0	1048.7	1.3	96	1471.9	11.8	1476.8	-4.9
70	1069.1	19.1	1064.6	4.5	97	1486.7	14.8	1492.7	-6.0
71	1077.0	7.9	1080.4	-3.4	98	1507.9	21.2	1508.5	-0.6
72	1094.0	16.9	1096.3	-2.3	99	1517.6	9.7	1524.4	-6.8
73	1111.1	17.1	1112.2	-1.0	100	1537.4	19.8	1540.3	-2.8
74	1130.0	18.9	1128.0	2.0	101	1554.3	16.9	1556.1	-1.8
75	1143.6	13.6	1143.9	-0.3	102	1573.7	19.4	1572.0	1.7
76	1159.5	15.9	1159.7	-0.3	103	1583.8	10.1	1587.8	-4.0
77	1179.0	19.5	1175.6	3.4	104	1598.7	14.9	1603.7	-5.0
78	1195.8	16.8	1191.4	4.4	105	1615.4	16.7	1619.5	-4.2
79	1208.5	12.7	1207.3	1.2	106	1634.6	19.2	1635.4	-0.8
80	1219.6	11.2	1223.1	-3.5	107	1652.0	17.4	1651.2	0.8

TABLE A-16

PROTOFLIGHT TM1, CHANNEL 1 A/D CONVERTER BIN SIZES[a] (3 OF 5)

DIGITAL COUNT LEVEL	MEASURED INPUT (mV)	INCREASE FROM PREVIOUS THRESHOLD (mV)	BEST FIT STRAIGHT LINE		DIGITAL COUNT LEVEL	MEASURED INPUT (mV)	INCREASE FROM PREVIOUS THRESHOLD (mV)	BEST FIT STRAIGHT LINE	
			CALCULATED (mV)	DEVIATION				CALCULATED (mV)	DEVIATION
108	1663.9	11.9	1667.1	−3.2	135	2090.3	5.5	2095.2	−4.9
109	1683.2	19.3	1683.0	0.2	136	2106.1	15.8	2111.0	−5.0
110	1700.3	17.1	1698.8	1.5	137	2124.5	18.4	2126.9	−2.4
111	1716.7	16.4	1714.7	2.0	138	2144.9	20.4	2142.8	2.1
112	1724.0	7.3	1730.5	−6.5	139	2161.9	17.0	2158.6	3.2
113	1739.1	15.1	1746.4	−7.3	140	2171.6	9.7	2174.5	−2.9
114	1760.0	20.9	1762.2	−2.3	141	2196.0	24.4	2190.3	5.7
115	1772.2	12.2	1778.1	−5.9	142	2212.5	16.4	2206.2	6.3
116	1789.4	17.2	1793.9	−4.6	143	2220.8	8.4	2222.0	−1.2
117	1806.8	17.4	1809.8	−3.0	144	2232.1	11.3	2237.9	−5.8
118	1825.7	18.9	1825.7	0.0	145	2248.2	16.1	2253.7	−5.5
119	1840.2	14.5	1841.5	−1.3	146	2269.5	21.3	2269.6	−0.1
120	1850.5	10.3	1857.4	−6.9	147	2281.5	12.0	2285.5	−3.9
121	1867.4	16.9	1873.2	−5.8	148	2297.6	16.0	2301.3	−3.7
122	1886.3	18.9	1889.1	−2.8	149	2319.0	21.4	2317.2	1.8
123	1902.6	16.3	1904.9	−2.3	150	2337.2	18.2	2333.0	4.1
124	1915.9	13.3	1920.8	−4.9	151	2348.0	10.8	2348.9	−0.9
125	1935.3	19.4	1936.6	−1.4	152	2358.5	10.5	2364.7	−6.2
126	1951.8	16.5	1952.5	−0.7	153	2377.1	18.7	2380.6	−3.5
127	1965.2	13.4	1968.4	−3.2	154	2397.2	20.0	2396.4	0.7
128	1979.6	14.4	1984.2	−4.6	155	2417.7	20.5	2412.3	5.4
129	1995.7	16.1	2000.1	−4.3	156	2423.8	6.1	2428.2	−4.3
130	2017.2	21.4	2015.9	1.2	157	2450.0	26.1	2444.0	6.0
131	2031.9	14.7	2031.8	0.1	158	2464.8	14.8	2459.9	4.9
132	2045.2	13.3	2047.6	−2.4	159	2468.1	3.3	2475.7	−7.7
133	2065.4	20.2	2063.5	1.9	160	2484.5	16.4	2491.6	−7.1
134	2084.8	19.4	2079.3	5.5	161	2500.5	16.0	2507.4	−7.0

TABLE A-16

PROTOFLIGHT TM1, CHANNEL 1 A/D CONVERTER BIN SIZES[a] (4 OF 5)

DIGITAL COUNT LEVEL	MEASURED INPUT (mV)	INCREASE FROM PREVIOUS THRESHOLD (mV)	BEST FIT STRAIGHT LINE		DIGITAL COUNT LEVEL	MEASURED INPUT (mV)	INCREASE FROM PREVIOUS THRESHOLD (mV)	BEST FIT STRAIGHT LINE	
			CALCULATED (mV)	DEVIATION				CALCULATED (mV)	DEVIATION
162	2522.3	21.8	2523.3	−1.0	189	2955.5	26.1	2951.4	4.1
163	2531.8	9.5	2539.1	−7.3	190	2970.2	14.7	2967.2	2.9
164	2550.0	18.2	2555.0	−5.0	191	2980.9	10.8	2983.1	−2.2
165	2568.2	18.2	2570.9	−2.7	192	2996.2	15.3	2998.9	−2.7
166	2589.8	21.6	2586.7	3.1	193	3007.2	11.0	3014.8	−7.6
167	2598.6	8.8	2602.6	−4.0	194	3029.3	22.1	3030.7	−1.3
168	2611.1	12.5	2618.4	−7.3	195	3043.3	13.9	3046.5	−3.3
169	2629.1	18.0	2634.3	−5.1	196	3057.7	14.4	3062.4	−4.7
170	2649.8	20.7	2650.1	−0.3	197	3075.2	17.5	3078.2	−3.1
171	2667.5	17.7	2666.0	1.5	198	3097.1	21.9	3094.1	3.0
172	2676.9	9.4	2681.8	−5.0	199	3102.6	5.5	3109.9	−7.4
173	2700.7	23.8	2697.7	3.0	200	3119.0	16.4	3125.8	−6.8
174	2717.4	16.7	2713.6	3.8	201	3136.9	17.9	3141.7	−4.7
175	2729.0	11.6	2729.4	−0.4	202	3157.7	20.8	3157.5	0.2
176	2737.3	8.3	2745.3	−8.0	203	3175.1	17.3	3173.4	1.7
177	2753.1	15.8	2761.1	−8.1	204	3184.9	9.8	3189.2	−4.3
178	2774.6	21.5	2777.0	−2.4	205	3209.2	24.3	3205.1	4.1
179	2786.7	12.2	2792.8	−6.1	206	3225.9	16.7	3220.9	5.0
180	2802.8	16.0	2808.7	−5.9	207	3238.0	12.0	3236.8	1.2
181	2823.9	21.1	2824.5	−0.7	208	3245.8	7.9	3252.6	−6.8
182	2842.3	18.4	2840.4	1.9	209	3261.8	16.0	3268.5	−6.7
183	2858.0	15.7	2856.3	1.7	210	3283.8	22.0	3284.4	−0.6
184	2863.8	5.8	2872.1	−8.3	211	3295.1	11.3	3300.2	−5.1
185	2882.1	18.3	2888.0	−5.8	212	3312.2	17.1	3316.1	−3.9
186	2902.6	20.4	2903.8	−1.3	213	3331.3	19.1	3331.9	−0.7
187	2924.0	21.4	2919.7	4.3	214	3351.9	20.6	3347.8	4.1
188	2929.4	5.4	2935.5	−6.2	215	3364.5	12.6	3363.6	0.9

C-6

TABLE A-16

PROTOFLIGHT TM1, CHANNEL 1 A/D CONVERTER BIN SIZES[a] (5 OF 5)

DIGITAL COUNT LEVEL	MEASURED INPUT (mV)	INCREASE FROM PREVIOUS THRESHOLD (mV)	BEST FIT STRAIGHT LINE		DIGITAL COUNT LEVEL	MEASURED INPUT (mV)	INCREASE FROM PREVIOUS THRESHOLD (mV)	BEST FIT STRAIGHT LINE	
			CALCULATED (mV)	DEVIATION				CALCULATED (mV)	DEVIATION
216	3373.8	9.3	3379.5	−5.7	236	3696.9	9.9	3696.6	0.3
217	3392.0	18.2	3395.3	−3.3	237	3721.1	24.2	3712.5	8.6
218	3412.8	20.8	3411.2	1.6	238	3737.9	16.8	3728.3	9.6
219	3433.4	20.6	3427.1	6.4	239	3752.6	14.7	3744.2	8.5
220	3439.8	6.4	3442.9	−3.1	240	3766.2	13.6	3760.0	6.2
221	3465.7	25.9	3458.8	6.9	241	3773.9	7.7	3775.9	−2.0
222	3481.2	15.5	3474.6	6.6	242	3800.0	26.1	3791.7	8.2
223	3492.1	10.9	3490.5	1.6	243	3807.8	7.8	3807.6	0.2
224	3508.8	16.7	3506.3	2.5	244	3825.0	17.2	3823.4	1.6
225	3517.1	8.3	3522.2	−5.0	245	3846.1	21.1	3839.3	6.8
226	3539.4	22.2	3538.0	1.3	246	3865.0	18.9	3855.2	9.9
227	3548.7	9.3	3553.9	−5.2	247	3882.4	17.4	3871.0	11.4
228	3568.1	19.4	3569.8	−1.7	248	3887.1	4.7	3886.9	0.3
229	3585.6	17.5	3585.6	−0.0	249	3905.2	18.0	3902.7	2.4
230	3607.9	22.4	3601.5	6.5	250	3926.4	21.2	3918.6	7.8
231	3617.2	9.2	3617.3	−0.1	251	3948.1	21.7	3934.4	13.6
232	3630.4	13.2	3633.2	−7.8	252	3954.2	6.1	3950.3	3.9
233	3647.8	17.4	3649.0	−1.2	253	3979.9	25.7	3966.1	13.8
234	3668.9	21.1	3664.9	4.0	254	3994.1	14.1	3982.0	12.1
235	3687.0	18.1	3680.7	6.2					

Index of Authors

Authors	Summary* Volume	Summary* Page	Proceedings** Volume	Proceedings** Page
Abrams, R.	I	90	II	47
	I	116	II	147
			II	373
Abrams, M.			IV	127
Ackleson, S.	II	137	IV	325
Aepli, T.	I	15		
Alford, W.	II	69	I	1
	II	85	I	9
			I	143
Amis, M.	II	60	III	571
Anderson, J.	II	82	I	119
Anderson, W.	II	129	IV	281
Anuta, P.	II	1	III	321
	II	53	III	527
Baker, J.	II	149	IV	369
Ball, D.	I	90	I	25
	I	116		
	I	130	II	47
			II	147
			II	277
			II	373
Balick, L.	II	129	IV	281
Barker, J.	I	90	I	23
	I	116		
	I	127	II	1
	I	130	II	47
	I	140	II	147
	I	186	II	235
	II	73	II	277
			II	373
			III	1
			III	233
Bartolucci, L.	II	1	III	321
Batson, R.	II	59	III	565
Bender, L.	II	35	III	497
Bennett, D.	II	81	I	77
Bernstein, R.	I	108	IV	25
Beyer, E.	I	92	II	87
Bizzell, R.	II	113	IV	153
	II	133	IV	299
Blodget, H.	II	160	IV	403
Boatwright	II	141	IV	337
Borgeson, W.	II	59	III	565
Brooks, J.	I	101	I	177
	II	91		
Brumfield			IV	403
Bryant, N.	II	46		
Butlin, T.	I	190		
Card, D.	II	55	III	553
Carnes, J.	II	113	IV	153
Castle, K.	II	15	III	389
Chavez, P.	II	33	III	471
Cicone, R.	II	28	III	443
Collins, A.			II	221
Colwell, R.	II	98	IV	91
Conel, J.	II	109	IV	127
Crist, E.	II	28	III	443
Dean, E.	II	1	III	321
DeGloria, S.	II	98	IV	91
Deschamps, P.	II	21		
DeVries, D.	II	62	I	133
			III	581
Dickinson, K.	I	189	III	257
Dinguirard, M.	II	15	III	389
Dozier, J.	II	142	IV	349
Duff, P.	I	190		
Duggin, M.	II	64		
Dykstra, J.	II	103	IV	119
Eliason, E.	II	33	III	471
Engel, J.	I	41		
	I	65		
Everett, J.	II	103	IV	119
Ezra, C.	II	15	III	389
Falcone, N.			III	497
Feuquay, J.	II	129	IV	281
Fischel, D.	I	106		
Fitzerald, A.	I	190	II	275
Fleming, E.	I	189	III	257
Friedman, S.	II	46		
Fusco, L.	I	199	III	309
	II	7	III	359
	II	40		
Gayler, J.	II	149	IV	369
Gervin, J.	II	167	IV	415
			IV	421
Gillespie, A.			IV	127
Gokhman, B.	II	46		
Goodenough, D	I	189	II	221
			III	257
Guertin, F.	II	81	I	77
			II	221
Gunther, F.	I	116	II	147
Gurney, C.	II	50	III	513
Haas, R.	II	129		
Hall, J.	II	55	III	553
	II	113	IV	153
Hardisky, M.	II	121	IV	251
Hardy, J.	II	149	IV	369
Haydn, R.	II	116	IV	217
Henderson, K.	II	148	IV	359
Holm, R.	II	15	III	389
Houston, A.	II	148	IV	359

Index of Authors

	Summary*		Proceedings**	
Authors	Volume	Page	Volume	Page
Hovis, W.	II	20	III	411
Imhoff, M.	II	69	I	1
			I	9
			I	143
Irons, J.	I	62	II	15
	II	93	IV	7
	II	116	IV	237
Jackson, M.	II	149	IV	369
Jackson, R.	II	15	III	389
Jones, O.	II	35	III	497
Justice, C.	I	199	III	309
Kahle, A.			IV	127
Kastner, C.	II	15	III	389
Kieffer, H.	II	33	III	471
Kimmer, E.	II	91	I	177
Klemas, V.			IV	251
	II	137	IV	325
Kogut, J.	II	54	III	537
Lang, H.	II	109	IV	127
Lansing, J.	I	186	III	233
Larduinat, E.	II	54	III	537
Latty, R.	II	93	IV	7
	II	116	IV	237
Lauer, D.	II	129	IV	281
Leung, K.	I	90	II	47
	I	130	II	277
			II	373
Likens, W.	II	87	I	159
Logan,	II	46		
Lotspiech, J.	I	108	IV	25
Lozano, F.	II	1		
Lu, Y.	II	167	IV	415
			IV	421
			IV	431
Lyon, J.	I	106		
Malaret, E.	II	1	III	527
	II	53		
Malila, W.	II	23	I	57
	II	76	III	421
Marcell, R.	II	160	IV	403
	II	167	IV	421
Markham, B.	I	127		
	II	73	I	23
	II	93	II	1
	II	116	II	235
	II	135	IV	7
			IV	237
			IV	313
MacDonald, R.	II	113	IV	153
McGillem, C.	II	1	III	527
	II	53		
Mehl, W.	I	199	III	309
			III	359
Mertz, F.	II	55	III	553
Metzler, M.	II	23	III	421
Middleton, E.	II	171	IV	431
Mimms, D.	II	35		
	II	85	I	9
			I	143
Mulligan, P.			IV	415
Murphy, J.	I	190	I	77
	II	81	III	275
Nelson, R.	II	93	IV	7
	II	116	IV	237
Palmer, J.	II	15	III	389
Park, W.			III	275
Paylor, E.	II	109		
Pitts, D.	II	113	IV	153
	II	148	IV	359
Price, J.	II	128	IV	271
Prior, H.	II	133	IV	299
Podwysocki, M.	II	35	III	497
Quattrochi, D.	II	111	IV	131
Rasool, S.	II	21		
Reyna, E.	II	113	IV	153
Rice, D.	II	76	I	57
Ritchie, J.	II	141	IV	337
Sadowski, F.	II	129	IV	281
Salisbury, J.	II	35		
Savage, R.	II	15	III	389
Schiebe, F.	II	141	IV	337
Schoch, L.	II	64		
Schott, J.	I	181	III	221
Schowengerdt, R.	II	32	III	467
Seevers, P.	II	129	IV	281
Sekhon, R.	II	171	IV	431
Sheffield, C.	II	103	IV	119
Short, N.	II	114	IV	163
Slater, P.	II	15	III	389
Sorensen, C.	II	113	IV	153
Stauffer, M.	II	93	IV	7
	II	116	IV	237
Strome, W.	I	120	II	221
Sturdevant, J.	II	129	IV	281
Su, J.	II	91	I	177
Thompson, D.			IV	359
Thormodsgard, J	II	62	I	133
			III	581
Toll, D.	I	93	IV	7
	I	116	IV	237
	I	153	IV	387
Townshend, J.	II	149	IV	369
Trevese, D.	II	7		
Usery, E.	II	83	I	123
Valdes, J.	II	1		

Index of Authors

	Summary*		Proceedings**	
Authors	Volume	Page	Volume	Page
Valenzuela, C.	II	1		
Walker, J.	I	130	II	277
Walker, R.	II	46		
Waltz, F.	II	129	IV	281
Webb, W.	I	1		
Welch, R.	II	83	I	123
Williams, D.	II	93	IV	1
	II	119	IV	7
			IV	237
Witt, R.	II	160	IV	403
	II	171	IV	431
Wrigley, R.	II	55	I	159
	II	87	III	553
Yao, S.	II	60	III	571
	II	113	IV	153
Yu, K.	II	53		
Zobrist, A.	II	46		

* Landsat-4 Science Investigations Summary, John L. Barker, ed., 2 volumes (NASA Conference Publication CP-2326) available through Government Printing Office, National Technical Information Service (NTIS). Accession Numbers N84-30359 and N84-30380 5285 Port Royal, Springfield, VA 22161, Phone 800-336-4700 or (703) 487-4650.

** Landsat-4 Science Characterization Early Results, John L. Barker, ed., 4 volumes NASA Conference Publication.

END

DATE

FILMED

MAY 14 1985